OLLSCOIL NA GAILLIMHE
UNIVERSITY OF GALWAY

The Influence of Collagen Type I Source and Cross-Linking on Cell Function and Phenotype Maintenance

A thesis submitted to the College of Science and Engineering, University of Galway for the degree of Doctor of Philosophy in Biomedical Engineering

By

Anna Sorushanova

Supervisory Team:

Prof. Dimitrios Zeugolis
Dr. Una Fitzgerald

August 2023

Regenerative, Modular & Developmental Engineering Laboratory (REMODEL)

Science Foundation Ireland Centre for Research in Medical Devices (SFI CÚRAM)

University of Galway

Table of contents

Table of figures

Table of supplementary figures

Table of tables

Table of supplementary tables

Supervisory team

Dimitrios Zeugolis was the main supervisor of this work. As Dimitrios Zeugolis moved to University College Dublin, Una FitzGerald joined the supervisory team and became primary supervisor, as per rules and regulations of the University of Galway.

Plagiarism statement

I certify that this thesis is all my own work and I have not obtained a degree in this University, or elsewhere, on the basis of this work.

Anna Sorushanova

List of abbreviations

mM: millimolar

µM: micrometre

PEG: 4-arm poly(ethylene glycol) ether tetrasuccinimidyl glutarate

4SG-PEG: 4-arm poly(ethylene glycol) ether tetrasuccinimidyl glutarate

GTA: glutaraldehyde

EDC: 1-ethyl-3-[3-dimethylaminopropyl] carbodiimide

CTRL: control

PFA: paraformaldehyde

DMEM: Dulbecco's Modified Eagle Medium

BSA: bovine serum albumin

PBS: phosphate buffered saline

BMT: bovine male tendon

BFT: bovine female tendon

BMS: bovine male skin

BFS: bovine female skin

PMT: porcine male tendon

PFT: porcine female tendon

PMS: porcine male skin

PFS: porcine female skin

THP-1: Human derived leukemic monocyte cells

SDS-PAGE: Sodium dodecyl sulphate polyacrylamide gel electrophoresis

DSC: differential scanning calorimetry

ECM: extracellular matrix

TCP: tissue culture plastic

LPS: lipopolysaccharide

PMA: phorbol 12-myristate 13-acetate

SEM: scanning electron microscopy

RT: room temperature

HBSS: Hank's Balanced Salt Solution

hDFs: human adult dermal fibroblasts

hTCs: human tenocytes

NS: no significance

ND: not detected

COL1: collagen type I

COL2: collagen type II

COL3: collagen type III

SCXA: scleraxis

TNMD: tenomodulin

AGAN: aggrecan

BGLAP: osteocalcin

SPP1: secreted phosphoprotein 1; osteopontin

DCN: decorin

BGN: biglycan

TNC: tenascin-c

THBS4: thrombospondin 4

MKX: mohawk homeobox

P4HA1: prolyl 4-hydroxylase subunit alpha-1

P4HA2: prolyl 4-hydroxylase subunit alpha-2

PLOD1: procollagen-Lysine,2-Oxoglutarate 5-Dioxygenase

PLOD2: procollagen-Lysine,2-Oxoglutarate 5-Dioxygenase 2

SERPINH1: serpin H1 precursor; serpin family E member 1

ACTA2: actin alpha 2

FABP4: fatty acid binding protein 4

VCAN: versican

ELN: elastin

RUNX2: runt-related transcription factor 2

ALPP: alkaline phosphatase, placental

BGLAP: bone gamma carboxyglutamate protein

TGFB1: transforming growth factor beta 1

EGR1: early growth response 1

COMP: cartilage oligomeric matrix protein

GAPDH: glyceraldehyde-3-phosphate dehydrogenase

ACTB: actin beta

RN18S1: 18S ribosomal RNA

Acknowledgments

First, I would like to thank my supervisor Prof. Dimitrios Zeugolis for giving me the opportunity of doing the research in his lab, for his guidance and patience. I would also like to thank Dr. Una FitzGerald for her support in the final stretch. I would also like to acknowledge Teagasc, Food Research Centre (ReValueProtein) for financially supporting this project. I would like to acknowledge Dr Oliver Carroll, Ms Tara Cosgrave, Mr Vidoja Kovacevic and Mr Maciej Doczy for their technical support throughout the years.

This work was supported by Teagasc Walsh Fellowship, grant agreement No. 2014045 and Teagasc / Department of Agriculture, Food and the Marine FIRM/RSF/CoFoRD 2011 Call, grant agreement No. 11/F/043. This work has also received funding from the European Union's Horizon 2020 research and innovation programme under the Marie Skłodowska-Curie, grant agreement No. 676338; the European Research Council (ERC) under the European Union's Horizon 2020 research and innovation programme, grant agreement No. 866126; and the Twinning Widespread Coordination and Support Action, grant agreement number 810850. This publication has emanated from research supported by grants from Science Foundation Ireland (SFI) under grant numbers 15/CDA/3629 and 19/FFP/6982 and Science Foundation Ireland (SFI) and European Regional Development Fund (ERDF) under grant number 13/RC/2073_2.

I would like to thank everyone at REMODEL and CURAM for all their help in the lab throughout the years. I would like to thank Dr. Luis Delgado, Dr. Akshay Srivastava, Dr. Zhuning Wu, Dr. Dimitris Tsiapalis and Dr. Kyriakos Spanoudes for helping me with the work through the years and their support. It was a pleasure to work along-side each and every one of you. I would like to extend my gratitude to my lab family who helped me better myself and keep my sanity, in particular Dr. Christina Ryan, Dr. Lígia Bré, Dr. Diana Gaspar, Dr. Kieran Fuller, Dr, Peadar Rooney, Dr. João Coentro, Dr. Joshua Chao, Mr. Alexandre Trotier and Ms. Eugenia Pugliese. Thank you so much for your friendship, all the laughter, great food and great bread, happy and sad tears, all the dancing and singing, all the pep talks and support. My lab and PhD journey would have been much more difficult without you.

I would like to thank my family for their immense support and encouragement. First, I would like to thank my parents, who gave me the platform to stand upon to be able to go on this journey. I would not be here without your guidance, sacrifice, and hard work. I would like to say thank you to my brother, who was always there for me no

matter the time or day and was ready to listen. Thank you for all your technical help when my laptop was miss behaving. Thank you for always cheering me up when things got hard, your support meant a lot. Thank you to my amazing friends, Donna and Emma who lifted me up when I was down. Last but certainly not least, I would like to thank my husband, my rock, my psychologist, who stood by my side through the good and the ugly. Who believed in me and never allowed me to give up. Who gave me the courage to keep going when I wanted to quit. Thank you for always believing in me and pushing me through it all. I wouldn't have been able to make it through this journey without you! To my baby boy Atlan, who was there with me during my viva. Your presence gave me strength, knowing that best things in life are yet to come!
It seems impossible until it's done. Peace out.

Abstract

Collagen is a complex supramolecular structure that occurs in highly diverse morphologies across different tissues, lending them a range of physical and biological functions. Collagens have a long history in both evolution and biotechnology and continue to offer both challenges and exciting opportunities in biomedicine as nature's biomaterial of choice. Despite the significant advancement in the development of collagen-based devices, clinical data clearly demonstrate an inconsistent therapeutic efficiency, even when collagen devices are used that were produced from collagen extracted from the same species, using the same extraction protocol. These observations clearly illustrate that there are other factors at play, when one considers collagen as a raw material for medical device development. To this end, herein the properties of collagen-derived biomaterials and their effect on the behaviour and phenotype of permanently differentiated cells (human adult dermal fibroblasts and human tenocytes) as a function of collagen origin (e.g. species, tissue, gender) and cross-linking type [e.g. 4-star poly(ethylene glycol) ether tetrasuccinimidyl glutarate, glutaraldehyde, carbodiimide] were investigated.

Although collagen type I is extensively used in biomedicine, no study to-date has assessed how the properties of the produced scaffolds are affected as a function of species, gender and tissue from which the collagen was extracted. Herein, collagen from porcine and bovine, male and female and skin and tendon tissues was extracted and characterised and subsequently collagen sponges were fabricated and their structural, biophysical, biochemical and biological properties were assessed. All collagen preparations were of similar purity and free amine content. In general, the porcine groups yielded more collagen; had higher denaturation temperature and resistance to enzymatic degradation; and lower swelling ratio and compression stress and modulus than the bovine groups of the same gender and tissue. All collagen preparations supported growth of human dermal fibroblasts and exhibited similar biological response to human THP-1 monocytes. These results further illustrate the need for standardisation of collagen preparations for the development of reproducible collagen-based devices.

Recent data suggest that collagen retains memory from the tissue that derives from and therefore affecting the properties of the produced devices. With this in mind, collagen (from bovine skin and tendon tissues) sponges were fabricated with different crosslinking densities of 4-arm polyethylene glycol succinimidyl glutarate and their

physicochemical and biological properties were assessed. Structural analysis revealed that crosslinking significantly reduced % porosity of both skin- and tendon- derived collagen sponges. In general, as the crosslinking density was increased, the resistance to enzymatic degradation, denaturation temperature, compressive stress and compressive modulus were significantly increased and the free amine content, % swelling and cytocompatibility (using human dermal fibroblasts) were significantly reduced. The tendon-derived collagen scaffolds exhibited significantly higher compressive stress and compressive modulus values and induced significantly higher human tenocyte DNA concentration and metabolic activity than the skin-derived collagen scaffolds. In human tenocyte cultures at day 14, the 1 mM 4-arm polyethylene glycol succinimidyl glutarate tendon-derived collagen sponges induced significantly higher collagen type III synthesis (as expected at early stages of physiological tendon healing) and downregulated actin alpha 2 (associated with myofibroblast differentiation) and the skin-derived collagen sponges induced significantly higher collagen type IV synthesis (found primarily at the dermal-epidermal junction) and upregulated prolyl 4-hydroxylase subunit alpha-1 (associated with collagen biosynthesis and constitutes a target for antifibrotic compounds). Data obtained indicate that the tissue from which collagen is extracted should be considered in the development of medical devices.

Various chemical, natural, or synthetic in origin, crosslinking methods have been proposed over the years to stabilise collagen fibres. However, an optimal method has yet to be identified. Herein, the potential of 4-star poly(ethylene glycol) ether tetrasuccinimidyl glutarate, as opposed to glutaraldehyde and carbodiimide, on the structural, physical and biological properties of collagen fibres was assessed. The 0.0475 mM 4-star poly(ethylene glycol) ether tetrasuccinimidyl glutarate induced an intermedium surface smoothness, denaturation temperature and swelling. The 4-star poly(ethylene glycol) ether tetrasuccinimidyl glutarate fibres had significantly higher stress at break values than the carbodiimide fibres, but significantly lower than the glutaraldehyde fibres. With respect to strain at break, no significant difference was observed among the crosslinking treatments. 4-star poly(ethylene glycol) ether tetrasuccinimidyl glutarate of 1 mM significantly reduced the amount of free amines and significantly increased resistance to degradation and denaturation temperature. Moreover, mechanical properties of 4-star poly(ethylene glycol) ether tetrasuccinimidyl glutarate collagen fibres were significantly higher compared to

glutaraldehyde, independent of concentration. The 4-star poly(ethylene glycol) ether tetrasuccinimidyl glutarate fibres exhibited significantly higher cell metabolic activity and DNA concentration that all other crosslinking treatments, promoted consistently cellular elongation along the longitudinal fibre axis and by day 7 they were completely covered by cells. This work clearly demonstrates the potential of 4-star poly(ethylene glycol) ether tetrasuccinimidyl glutarate as collagen crosslinker.

Collectively, this work provides further knowledge on the importance of collagen source and cross-linker type and concentration for the development and use of collagen-derived biomaterials.

Chapter 1 - Introduction

This chapter has been published:

The collagen suprafamily - From biosynthesis to advanced biomaterial development. **A. Sorushanova**, L.M. Delgado, Z. Wu, N. Shologu, A. Kshirsagar, R. Raghunath, A.M. Mullen, Y. Bayon, A. Pandit, M. Raghunath, D.I. Zeugolis. Advanced Materials. 2019, 31, 1801651.

1.1 Introduction

The term ‘collagen’ derives from the Greek words for ‘glue’ and ‘to produce’ and as such it was first known as the component of tissues that when boiled produces glue. The word ‘collagen’ was coined in the 19th century to designate the constituent of connective tissues that yields gelatin after boiling [1]. It has also been considered as the biological glue that holds cells in place [2]. The more modern view is that collagen is the major extracellular matrix (ECM) molecule that self-assembles into cross-striated fibrils, provides support for cell growth and is responsible for the mechanical resilience of connective tissues.

The prevalence of collagen in human tissues and various inherent properties (e.g. cell recognition signals, ability to form three-dimensional scaffolds of various physical conformations, controllable mechanical properties, and biodegradability) makes it a natural choice as raw material for tissue-engineered scaffolds for various clinical indications. The desirability of collagen as a biomaterial depends principally on the fact that it is a naturally abundant extracellular matrix (ECM) component and, as such, it is perceived as an endogenous constituent of the body and not as foreign matter.

Collagen is a complex supramolecular structure and occurs in highly diverse morphologies across different tissues, thus lending them a range of biological functions. Collagen components interact sequentially with each other and with other ECM constituents to produce higher order structures with numerous hierarchical levels of association and specific functions. Further, collagen, as the fundamental structural component of connective tissues, plays a pivotal role in maintaining their structural and biological integrity. Advanced understanding of these properties has paved the path for the development of novel biomaterials that mimic both the structural and biological properties of native tissues, particularly tissues primarily comprised of collagen type I or collagen type II.

To fully exploit the potential of this unique biopolymer in biomedicine, it is essential to understand its fundamental characteristics, key processing modes and application features. To this end, we provide an overview of the suprafamily of collagens and their biosynthesis, assembly and native cross-linking. We also critically discuss current various sources of collagen, natural to synthetic, along with collagen-based device fabrication, cross-linking and characterisation methods. We further highlight significant new knowledge on collagen as a biopolymer that will effectively drive innovation in reparative therapies in the years to come.

1.2 Collagen family

The collective term ‘collagen’ encapsulates a whole family of glycoproteins that are characterized by three signature features. First among these is the amino acid repeating sequence $[Gly\text{-}X\text{-}Y]_n$, both with and without interruptions. The second characteristic feature is the occupation of the X and Y positions by proline and its hydroxylated form, hydroxyproline, respectively. Thirdly, the right-handed triple helix is formed from three left-handed polyproline *α* chains of identical length, which gives collagen a unique quaternary structure.

The ubiquity of collagen and collagenous structures throughout the animal kingdom serves as an indication of their importance in biological viability. Sponges, the simplest known multicellular organisms, express genes for at least two types of a prototypic collagen [3, 4]. In vertebrates, collagen is the major component of specialized and non-specialized connective tissues, making up almost ¼ of total body protein in humans, ¾ of the dry weight of human skin, over 90 % of human tendon and corneal tissues and almost 80 % of the organic matter in bones [5, 6].

It is interesting to note that the triple helical blueprint has been partially carried over into the structures of other complex molecules that have evolved in air-breathing animals with advanced immune and nervous systems. A data bank search (Source: www.uniprot.org; Term searched: collagen-like domains; Species: human) yielded 42 glycoproteins that are not *bona fide* collagens. These include all three subunits of complement component C1q, 13 proteins related to them, as well as adiponectin, collectins, EMILINs, gliomedin, neurogranin, otolin-1, macrophage scavenger receptors, mannose-binding protein, pulmonary surfactant proteins A1/A2 and D and the collagenic tail peptide associated with acetyl cholinesterase.

Evolutionary branching, partially by reduplication of chromosome parts, has led to a multitude of genetically distinct collagen types; 29 have been described to date [7]. Notably, these collagen types were discovered through their homologies to other collagen genes and their characteristic $[Gly\text{-}X\text{-}Y]_n$ sequences. Although the tissue distribution and function of many collagen types still remains obscure, along with confirmation of their existence on the protein level, it is clear that collagens occur in many places throughout the body, with collagen types I, II and III representing the lion’s share; together they make up around 80-90 % of total body collagen.

1.2.1 Collagen structure and conformation

The collagen molecule is comprised of a triple helical region and two non-helical regions at either end of the helix. The triple helical conformation is the defining structural element of all collagens (**Figure 1.1a**). The collagen triple helix (tertiary structure) has a coiled-coil structure made of three parallel α polypeptide chains (secondary structure) that are wound around each other in a regular helix to generate a rope-like structure of approximately 300,000 g/mole molecular weight and 280 nm in length and 1.4 nm in diameter. Intramolecular hydrogen bonds between glycines in adjacent chains stabilize the triple helix. The hydroxyl groups of hydroxyproline residues also form hydrogen bonds and stabilize the triple helix. Two hydrogen bonds per triplet are found: one between the amine-group of a glycyl residue and the carboxyl-group of the residue in the second position of the triplet in the adjacent chain and one via the water molecule participating in the formation of additional hydrogen bonds with the help of the hydroxyl group of hydroxyproline in the third position (**Figure 1.1b**). Each α-chain is left-handed, but when they are staggered by one residue relative to each other around a central axis, they form a right-handed super-helix (**Figure 1.1c**). This super-helix is due to the twisting of the chain helices around the central axis by about +30 ° at every turn. Thus, every third amino acid is in the centre of the helix and, for steric reasons, only glycine, with a side chain limited to a single hydrogen atom, can occupy this position without altering the triple helical conformation. The Gly-Pro-Hyp sequence is the most common (about 12 %), sequences of the form Gly-Pro-Y and Gly-X-Hyp represent about 44 % and Gly-X-Y sequences constitute the remaining 44 %. Proline and hydroxyproline stabilize the collagen molecule and because of their alicyclic nature, they stiffen the α chain, where they occur by preventing rotation around the C-N bond. During or following secretion in the extracellular space, the propeptides are removed at either end of the triple helical molecule by specialized enzymes, leaving the triple helix with short, non-triple helical regions, measuring 9-26 amino acids in length at the N- and C- termini. These non-helical domains, referred to as telo-peptides, play a crucial role in the registering (the alignment of the three pro-α-chains) and cross-linking of collagen α chains and they also add flexibility to the otherwise rigid molecule. The removal of the propeptides is prerequisite to the self-assembly of collagen molecules into a quarter-staggered

arrangement by lateral and head-to-tail fashion, ultimately resulting in the formation of cross-striated fibrils.

Collagen type I, the most abundant collagen type, is present in the form of elongated fibrils that can be greater than 500 μm in length, 500 nm in diameter and contain more than 10^7 molecules. The collagen fibrils exhibit a high degree of axial alignment, which results in a characteristic D banding / periodicity, due to the alternating overlap (two adjacent triple helices) and gap (triple helices lined up head-to-tail with some space in between) zones, produced by the specific packing arrangement of the 300 nm long and 1.5 nm in diameter collagen molecules. This produces an average periodicity of 67 nm in the native hydrated state (**Figure 1.1d**), although dehydration and shrinkage during conventional sample preparation for electron microscopy results in lower values of around 55 to 65 nm. The *in vitro* fibrillogenesis of collagen type I is dependent on temperature, pH and ionic strength. Under appropriate conditions, collagen molecules will spontaneously self-assemble to form microscopic fibrils, fibril bundles and macroscopic fibres that exhibit D periodicity banding virtually indistinguishable from native collagen fibres. This feature was first described in the late 1940s with transmission electron microscopy (TEM) [8] and is absolutely typical of collagen. Topographical analysis of the surface of large collagen fibres by atomic force microscopy (AFM) confirmed ridges alternating with 5-15 nm deep grooves with a 60-70 nm period [9-11].

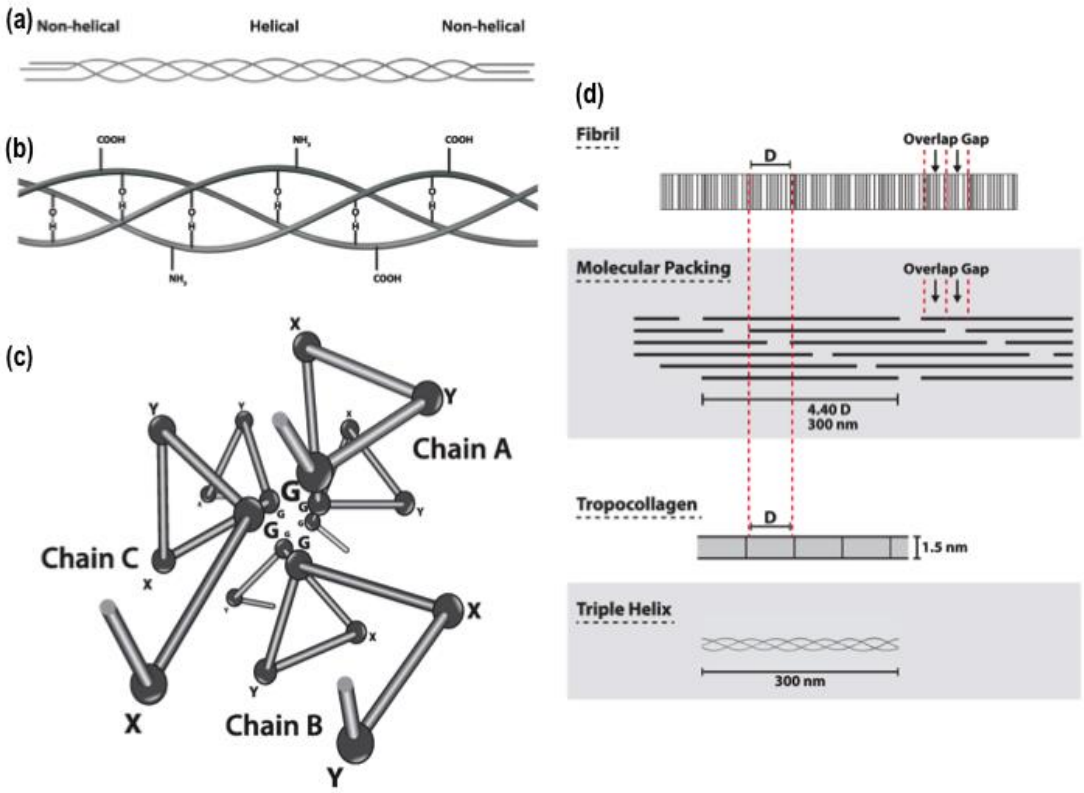

Figure 1.1: (a) The triple-helical collagen structure. (b) Hydrogen bonds within the collagen triple helix. (c) Cross-section of collagen triple helix. (d) Schematic representation of the arrangement of collagen molecules within fibrils.

1.2.2 Collagen types

To date, 40 vertebrate collagen genes have been identified that form 29 distinct homo- and/or hetero- trimeric molecules (**Table 1.1**) [12-18]. Roman numerals are used to indicate the type and Greek letters are used to identify the chains, bands and higher molecular weight components. The trimeric nature of a collagen molecule allows for the combination of three identical pro α chains or of two identical chains and one other with fitting length and registration of C-propeptide, or even of three different chains to form a complete triple helix. The fit of the respective pro α chains, as defined by their length, corresponding interruptions (if any), the correct registration of the C-propeptides and their combination, delineates different collagen types. However, isoforms within individual collagen type do exist. For example, most collagen type I exists as heterotrimer of two α1 chains and one α2 chain, but also as homotrimer of three α1 chains. Many collagen types, such as collagen type II, type III or type VII, exist exclusively as homotrimers. At the other end of the spectrum is collagen IV, where six different α chains are available for combination to yield a considerable number of isoforms that form tissue-specific basement membranes.

While some of the 29 currently identified collagen types show highly unique features, most of them appear highly interrelated, but confined to specific tissue locations. This variety points to diverse biological functions is reflected by a multitude of physical structures. Based on their primary structure, the length of the triple helical domain, the molecular weight, the charge profile along the helix, the triple helix interruptions, the size and shape of the terminal domains, the cleavage or retention of the latter in the supramolecular aggregate and variation in the post-translation modifications, four overarching collagen groups can be identified [19-27]:

Group 1 hosts the fibril-forming collagen type I, type II, type III, type V, type XI, type XXIV and type XXVII. They all possess triple helices with uninterrupted Gly-X-Y stretches approximately 300 nm in length. However, XXI and XXVII show imperfections in these Gly-X-Y stretches, suggesting very short interruptions of triple helical structure. Collagen fibrils in the dermis, tendon and other tissues are often mixtures of different collagen types, usually type I, type III and type V. These mixed fibres are referred to as heterotypic fibrils, contrasting with homotypic fibrils that are composed of only one collagen type (e.g. collagen VII in anchoring fibrils of the dermo-epidermal junction).

Group 2 hosts the basement membrane collagen type IV, type VII and type XXVIII. While collagen type IV forms a fibrillar meshwork, collagen type VII is created through antiparallel dimer association and forms cross-striated fibrils with a different banding pattern.

Group 3 contains the short-chain collagen type VI, type VIII and type X. They are named after their triple helical regions, which extend up to 100 nm and 150 nm, respectively. Collagen type VI forms beaded microfilaments, whilst collagen type VIII and type X form hexagonal lattices. Collagen type XXIX has a short and uninterrupted triple helical region that is flanked by several von Willebrand factor A domains.

Group 4 contains collagens with multiple interruptions of their triple-helical Gly-X-Y stretches. Collagen type IX, type XII, type XIV, type XVI and types XIX to XXII comprise the fibril-associated collagens with interrupted triple-helices (FACIT collagens). These collagens fulfil specific roles by association with collagen fibrils and adding functionality to them. They may also play a role in controlling the diameter of collagen fibres in various tissues by limiting lateral appositional growth, as has been described for collagen type IX [28], but also for the fibrillar collagen type V [29]. The term MULTIPLEXINs (multiple triple-helix domains and interruptions) has been created for collagen type XV and type XVIII, as they present the highest number of interruptions. A remarkable subgroup of the non-fibrillar collagens is the transmembrane collagens (type XIII, type XVII, type XXIII and type XXV), which possess transmembrane domains that allow these molecules to be inserted into cell membranes, whilst projecting the (interrupted) triple-helical domains outwards into the extracellular space.

At supramolecular assembly level, admixtures of fibrillar collagen types that lead to heterotypic fibrils are identified. A typical extract of dermis will show a combination of collagen type I, type III and type V in varying proportions, as will biochemical analysis of matrix that has been deposited by cultured dermal fibroblasts isolated from this tissue. On top of these heterotypic fibrils, non-fibrillar collagens and other ligands, such as proteoglycans, are identified. Major advances have been made in identifying fibrillar composition using highly sensitive techniques, such as infrared matrix-assisted laser desorption / ionization time-of-flight mass spectrometry (IR-MALDI-TOF-MS) [30-32]. Thus, the composition of triple-helices, the supramolecular heterogeneity of fibrils and finally the admixture of non-fibrillar ligands generates the biological versatility and functionality of the collagens.

Table 1.1: Collagen family characteristics and tissue distribution (adopted with modifications from [17, 18]).

Collagen Type	Chains	Molecular Assembly	Supramolecular Structure	Mw (kDa) / α chain	Tissue Distribution
I (Heterotrimer)	$[\alpha 1(I)]_2\alpha 2(I)]$	Monomers staggered by 67 nm	Large-diameter, 67 nm banded fibrils	95	Skin, tendon, ligament, cornea, organ capsules, dura mater of brain and spinal cord, the main organic component of bone
I (Homotrimer)	$[\alpha 1(I)]_3$		67 nm banded fibrils		Tumours, dermis, bone
II	$[\alpha 1(II)]_3$	Monomers staggered by 67 nm	67 nm banded fibrils	95	Cartilage, vitreous, cartilagenous zones of tendon, intervertebral disc

III	$[\alpha 1(III)]_3$	Monomers staggered by 67 nm	Small-diameter, 67 nm banded fibrils	95	Dermis, aorta, uterus, admixture in tendon, intestine, blood vessels, in the reticular connective tissue of liver, spleen and surrounding internal organs
IV	$[\alpha 1(IV)_2 \alpha 2(IV)]$; $\alpha 3(IV)$, $\alpha 4(IV)$, $\alpha 5(IV)$, α 6(IV)	Association of 4N- and 2C-termini	Non-fibrillar meshwork	170-180	Basement membranes
V	$[\alpha 1(V)]_2$ $\alpha 2(V)$ $[\alpha 1(V)$ $\alpha 2(V)$ $\alpha 3(V)]$ $[\alpha 1(V)]_3$	Monomers staggered by 67 nm	9 nm diameter banded fibrils	120-145	Placental/embryonic tissue, dermis, bone, cornea, cell surfaces

VI	[α1(VI) α2(VI) $\alpha\alpha$3(VI)]	Association into tetramers that aggregate end to end	5-10 nm diameter	αl(VI) 140	Uterus, dermis, cartilage
			beaded micro-fibrils	α2(VI) 140	Muscle
			100-nm periodicity	α(VI) 340	
VII	[α1(VII)]$_3$	Lateral aggregation of antiparallel dimers	Anchoring fibrils	170	Skin, amniotic membrane, Cornea, mucosal epithelium

VIII	[α1(VIII)]$_2$ α2(VIII)	Interrupted helical structure	Non-fibrillar, hexagonal lattice	61	Descemet's membrane, endothelial cells
IX	[α1(IX) α 2(IX) $\alpha\alpha$3(IX)]	Covalently cross-linked to surface of collagen II fibrils	FACIT; non-fibrillar	68-115	Cartilage, vitreous, admixture in tendon, co-distributes with collagen II
X	[α1(X)]$_3$	Assemble a mat-like structure	Non-fibrillar, hexagonal lattice	59	Calcifying cartilage (including parts of tendons)
XI	[α1(XI) α 2(XI) $\alpha\alpha$3(XI)]	Monomers staggered by 67 nm	Fine fibrils similar to those of collagen V	110-145	Cartilage, intervertebral disc

XII	[α 1(XII)]$_3$	Associates with surface of collagen fibrils	FACIT; non-fibrillar	220,340	Dermis, tendon, cartilage
XIII	[α1(XIII)]$_3$	150 nm rod with two flexible hinges	Trans-membrane	62-67	Endothelial cells, epidermis
XIV	[α1(XIV)]$_3$	Disulphide-linked cross-shape	FACIT; non-fibrillar	220	Dermis, tendon, cartilage
XV	[α1(XV)]$_3$	Figure eight knot configuration	MULTIPLEXIN; non-fibrillar	125	Placenta, kidney, heart, ovary, testis

XVI	$[\alpha 1(XVI)]_3$	Associates with dermal fibrillin; associates with banded collagen in cartilage	FACIT; non-fibrillar	150-160	Heart, kidney, muscle
XVII	$[\alpha 1\ (XVII)]_3$	Shed from cell surface into shorter soluble form	Membrane-intercalated	180	Hemidesmosomes (skin), specialized epithelia
XVIII	$[\alpha 1(XVIII)]_3$		MULTIPLEXIN; non-fibrillar	200	Kidney, liver
XIX	$[\alpha 1(XIX)]_3$	Sharply kinked and higher order complexes	FACIT; non-fibrillar	165	Transitory embryonic expression, interneurons and formation of hippocampal synapses**,** basement membranes,

					muscle cell, rhabdomyosarcoma
XX	$[\alpha 1(XX)]_3$	Binds to collagen fibrils with amino terminal domains away from fibrillar surface	FACIT	185, 170, and 135	Corneal epithelium, embryonic skin, sternal cartilage, tendon
XXI	$[\alpha 1(XXI)]_3$		FACIT		Blood vessel walls, secreted by smooth-muscle cells.
XXII	$[\alpha 1(XXII)]_3$	Associates with cartilage micro-fibrils	FACIT	200	Tissue junctions

XXIII	[α1(XXIII)]$_3$		Trans-membrane		Tumors (prostate)
XXIV	[α1(XXIV)]$_3$	Associates with vertebrate fibrillar	Fibrillar, fibril associated		Regulation of collagen I fibrillogenesis, osteoblast differentiation marker
XXV	[α1(XXV)]$_3$	Binds to fibrillized Aβ	Trans-membrane	50 / 100	Interaction with β amyloid plaques in Alzheimer's disease
XXVI	[α1(XXVI)]$_3$		FACIT	~ 80	Ovary and testis
XXVII	[α1(XXVII)]$_3$	10 nm network organization	Thin non-striated fibrils		Hypertrophic cartilage

XXVIII	[α1(XXVIII)]$_3$	Associates with non-myelinated regions	Beaded filament forming	~ 50	Basement membrane of Schwann cells, peripheral nervous system
XXIX	[α1(XXIX)]$_3$		Non-fibrillar		Supra-basal cells in epidermis, lung, small intestine, colon and testis

1.3 Collagen biosynthesis

1.3.1 Intracellular events and triple-helix formation

The pathway of collagen biosynthesis, from gene transcription to secretion and aggregation of collagen monomers into functional fibrils, is a complex multi-step process, requiring the coordination of numerous temporally and spatially coordinated biochemical events (**Figure 1.2**). Depending on the collagen type and isoform, the initial step of the intracellular biosynthesis of collagen involves transcription of mRNA molecules encoded by various three-chain combinations of different α chain genes. The nascent collagen α chain enters the lumen of the endoplasmic reticulum with the N-terminus first as pre-procollagen, which is converted into procollagen by the removal of the signal peptide. A remarkable feature of collagen biosynthesis is the fact that synthesis starts at the N-terminus, while triple-helix formation starts at the C-terminus [33]. This requires the pro α chains to remain untangled for the timespan taken to complete the α chain translation, upon which three pro α chains align precisely at the C-terminus before triple-helix formation begins. Several chaperone proteins protect α chains from getting tangled, including prolyl 4-hydroxylase (P4-H), protein disulphide isomerase (PDI), a homologue of heat shock protein 70 of the endoplasmic reticulum (BiP/Grp78), various peptidyl-prolyl cis-trans isomerases (PPIases), and heat shock protein 47 (hsp47) [34].

For collagen type I, the most abundant collagen type, the alignment of the three pro α chains is called registration and is driven by the C-telo-peptides. The C-propeptides contain cysteines, which form disulphide bonds (the only covalent bonds in the procollagen trimer) that will disappear with the removal of the propeptides upon secretion. Intracellularly, this allows for a firm alignment, preventing any slippage of α chains against each other. The triple helical formation then propagates in a zipper-like manner from the C- to the N- terminus [35]. It takes an average of 14 minutes for a procollagen type I triple helix to fold, a considerable time span for a single molecule. hsp47 has been shown preferentially bind to procollagen after triple helical folding has taken place, attaching to Gly-X-Y repeats with Arg in the Y position and thereby lending stability to the triple helix and preventing the premature aggregation of procollagen [34, 36]. However, hsp47 detaches after procollagen transfers to the Golgi apparatus from the endoplasmic reticulum, probably due to pH change. Interestingly, for collagen type I, trimers consisting of [pro α1(I)]3 and [(pro α1(I))2, pro α2(I)] can

be formed, but [pro α2(I)]3 trimers have never been retrieved from cell culture or intact tissues.

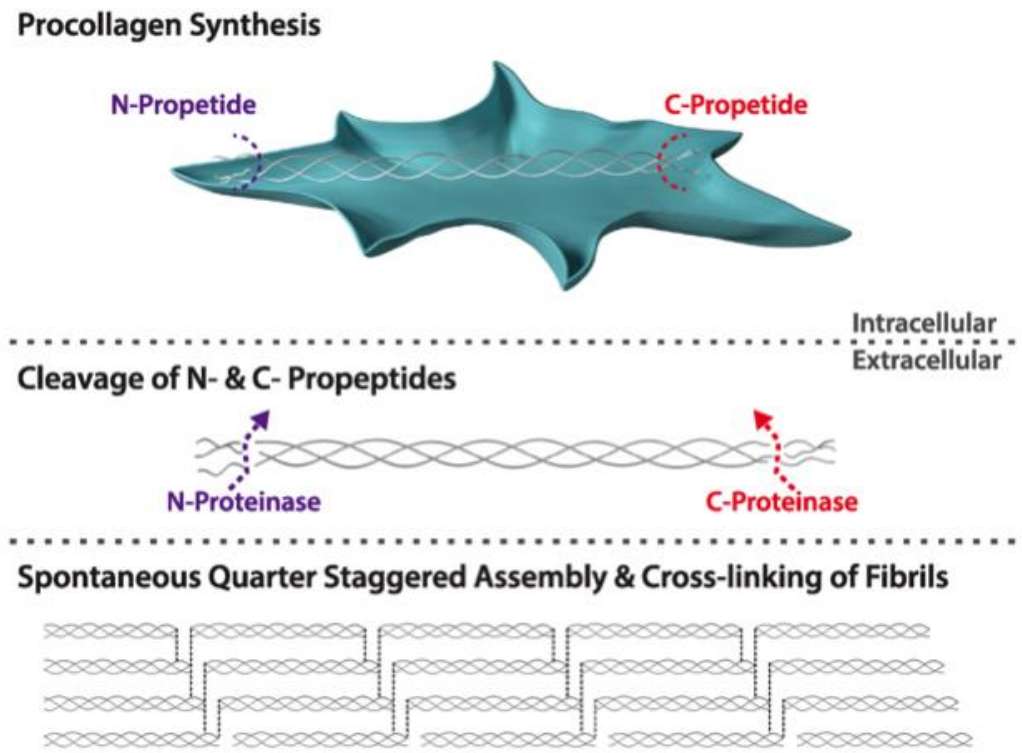

Figure 1.2: Biosynthesis and processing of collagen. Procollagen is synthesized intracellularly with intact pro-peptide extensions. Following or during secretion in the extracellular space, specific cleavage of the *N*- and *C*- propeptide extensions, by the *N*- and *C*- proteinases respectively, takes place. This triggers the spontaneous quarter staggered assembly of collagen into fibrils, which are stabilized through various cross-linking pathways.

1.3.2 Post-translational modification of collagens

Two major post-translational modifications (PTMs) of collagen, hydroxylation and glycosylation, occur in the endoplasmic reticulum, which contribute to the thermal and mechanical stability of collagen in triple helical and assembled form, respectively. Pathological conditions that interfere with these PTMs, either by genetic alteration (e.g. Alport Syndrome) or by nutritional deficiencies, have also been reported.

1.3.2.1 Prolyl hydroxylation

The signature amino acid of collagen, hydroxyproline (Hyp), is derived from Pro by catalytic activity of prolyl 4-hydroxylase (procollagen-proline dioxygenase; E.C. 1.14.11.2), an enzyme resident in the lumen of the endoplasmic reticulum of fibrogenic cells. Hyp represents ~ 10 % of the amino acid composition of collagen and is usually present at the Y position in the Gly-X-Y repeat domains. It therefore can be regarded as a molecular fingerprint of collagen. The content of Hyp is critical for the formation of intra-molecular H-bonds within the triple helix, which in turn confer thermal stability (at body temperature) to the trimer. In mammals with a body temperature of around 37 °C, a minimum of 100 Pro residues per pro α chain must be converted to Hyp to achieve thermal stability, whilst in cold blooded species (e.g. arctic cod) much less hydroxylation is evident [37]. Although this correlation between increased body temperature and Hyp content in multicellular organisms is non-linear [38], it points to a remarkable enzymatic flexibility of collagen's thermal stability, which allowed collagens to accommodate different body temperatures across the evolution of fish, amphibians, reptiles and mammals [39]. The role of 3-prolyl hydroxylase has been less clear, but it seems to be associated with modifications of the C-termini of the α chains of collagen type I and type III. These regions contain stretches of $[GPP]_5$ and $[GPP]_7$, respectively, that are rich in Hyp and appear to particularly increase local thermal stability [40]. These $[GPP]_n$ regions seem to be preferentially modified by 3-prolyl hydroxylase. While the significance of this PTM remains unclear, it is a particular feature of tendon and appears to have contributed to the structural evolution of this connective tissue [41].

The role of Hyp in stabilizing the triple helix via hydrogen bonds was contested in the late 1990s by studies using synthetic halogen-substituted peptides, like $[ProFlpGly]_{10}$, where Flp was a 4(R)-fluoroproline residue, with Flp being the most electronegative element and incapable of forming H-bonds [42, 43]. The resulting hyper-stability in

the absence of H-bonds and water networks was attributed to exopyrrolidine ring pucker and trans/cis preferences mediated by its electronegative inductive effect; this has led to further investigations of the puckering states of the proline pyrrolidine ring [44]. It is currently debated whether Flp and Hyp stabilise the collagen triple helix in the same way. As an additional explanation for the formation of hyper-stable triple helices with halogen-substituted Pro, inter-strand dipole-dipole interaction have been proposed to take effect, as compensating forces between electronegative substituents of Pro derivatives in the X and Y positions [45]. Therefore, inductive effects and H-bonding of Hyp through hydration networks are now both accepted mechanism of triple helix stabilization [46].

Interestingly, there are alternatives to prolyl hydroxylation to stabilize collagenous polyproline coils in invertebrates and bacteria. The cuticle collagen of the deep-sea hydrothermal vent worm *Riftia pachyptila* has thermal stability at 37 °C, despite a very low Pro content (5%) and therefore a low Hyp content. Thr occupies the Y position of Hyp in the Y position, representing 18% of total amino acid content and showing O-glycosylation. This PTM is required for the triple helix stability in this species [47]. The cell surface protein Scl2 of *Streptococcus pyogenes* contains a sizeable collagenous domain of 79 Gly-X-Y triplets, resulting in melting temperatures of 36 °C at neutral pH, thus matching human body temperature. The reason for this stability seems to be the relative abundance of Gly-Lys-Asp triplets, contributing to considerable electrical charge; thus allowing for electrostatic interactions between α chain equivalents, including a hydration network in the absence of Hyp [48]. The new understanding of Hyp-free stability of collagenous domains in bacterial species, which act as a pathogens to mammals, points to a co-evolution of stabilizing strategies for polyproline triple helices at mammalian body temperatures and underlines the feasibility of producing and applying bacterial collagens for biomaterial purposes [49].

1.3.2.2 Enzymatic glycosylation and lysyl hydroxylation

As a glycoprotein, collagen type I has a relatively low carbohydrate content (< 1 %). The sugar components in collagen are either a single galactose unit or a disaccharide of galactose and glucose, O-glycosidically attached via hydroxylysine residues. Collagen also contains hydroxylysine (Hyl), a PTM compound of lysine that is produced via lysyl hydroxylase (E.C. 1.14.11.4) activity. The formation of Hyl residues and subsequent attachment of sugar components appears to be an important

modulator of fibrillogenesis and is associated with covalent cross-linking and fibril stabilization. O-linked glycosylation of Hyl residues has long been known to be a unique PTM for collagens and proteins with collagenous sequences. It is interesting that human lysyl hydroxylase isoform 3 (LH3) possesses both lysyl hydroxylase and glucosyl transferase (GGT) activities [50]. Transfections studies with LH3 in osteoblast cultures revealed five glycosylation sites in type I collagen, one of them including a major helical cross-linking site. Manipulation of LH3-mediated glycosylation resulted in different collagen cross-linking, fibrillogenesis and mineralization [51]. N-linked glycosylation has been shown to be restricted to propeptide regions of some mammalian collagens [52] and adjoined regions of collagenous domains of some invertebrates [53]. In mammals, potentially N-glycosylated regions are lost after the proteolytic conversion of procollagen to collagen.

1.3.3 Proteolytic cleavage of procollagen

The procollagen trimer is released and secreted to the extracellular space, but only if the triple helix is completely folded. The quality-control mechanism measuring triple helicity, along with the sorting mechanism that allocates appropriate α chains to the respective nascent triple helices in precise stoichiometric relationships, is only partially understood. Heat shock protein 47 is a collagen binding chaperone that assists in stabilizing correctly folded procollagen [54]. Protein disulphide isomerase, a subunit of the prolyl hydroxylation complex, also serves as a chaperone during the assembly of procollagen α chains [55] and assists in preventing non-assembled procollagen leaving the endoplasmic reticulum [56]. Upon or during secretion into the extracellular space, procollagen is proteolytically processed. Initially, the N- and C-propeptides are removed enzymatically in the presence of Ca^{2+} by procollagen N-proteinase and procollagen C-proteinase, respectively. In procollagen type I, procollagen N-proteinase cleaves N-terminal propeptides between Pro and Gln residues, while procollagen C-proteinase cleaves between Ala and Asp. The N-proteinases belong to the ADAMTS (a disintegrin and a metalloproteinase with thrombospondin repeats) family, whilst procollagen C-proteinases are now classified as bone morphogenetic protein-1 / Tolloid-like proteinases (BTPs) [57] and simultaneously trigger matrix assembly and boost the synthesis of matrix proteins via a direct effect on growth factors, such as TGF-β and IGFs [58].

Another group of metalloproteinases, meprins, are capable of removing both N- and C- terminal collagen propeptides [59]. In line with this are studies showing that removed propeptides can re-enter the cell to regulate the amount of collagen biosynthesis taking place on the basis of a negative feedback loop [60, 61]. The propeptides of intact procollagen prevent premature intracellular supramolecular assembly and formation of water-insoluble aggregates, but need to be removed in the extracellular space to allow collagen assembly. Thus, procollagen proteinase activity is a rate-limiting step for fibrillogenesis [62].

1.3.4 Extracellular supramolecular assembly

After the enzymatic removal of the propeptides, the resulting collagen triple helices (also described as tropocollagen) are able to form supramolecular aggregates. The debate as to where exactly the procollagen / collagen conversion occurs is not yet settled and two potential models seem plausible with respect to the release of procollagen [63]. The first model proposes that fibril formation begins inside the Golgi-to-plasma membrane carriers (GPCs), where cleavage of procollagen propeptides already occurs, after which GPCs containing newly formed fibrils fuse and form finger-like structures at the cell surface, probably with cytoskeletal contribution. The second model describes collagen fibrillogenesis as a mostly extracellular process, whereby collagen fibril formation occurs at the surface of fibroblasts in deep invaginations of the plasma membranes, where narrow elongated ‘hangars’ formed through the merging of collagen-containing GPCs. Although enveloped partially by the plasma membrane, the interior of these ‘hangars’ is part of the extracellular space. It is here that propeptide removal occurs and after procollagen cleavage of the C- and N-propeptides, the collagen molecules aggregate to form collagen fibril intermediates that grow out of their ‘hangars’. This theory takes into consideration spatial constraints for secreting bulky procollagen molecules, essentially linear rods, via the Golgi apparatus in GPCs.

Fibrillogenesis cannot occur *in vivo* without the mediation of cells that engage nascent and mature fibrils via cell surface receptors (e.g. integrins). The peptide sequence Arg-Gly-Asp is a significant feature of the glycoprotein fibronectin, representing an integrin-binding site, along with a collagen- and gelatin- binding site. Accordingly, integrins and fibronectin have been described as ‘fibril organizers’, whereby fibronectin forms a fibril network which is then engaged by integrins, thus serving as

a template for further collagen fibril assembly [64, 65]. Notably, collagen fibrils assembled *in vivo* and *ex vivo* (in cell culture) are heterotypic [66]. The admixture of minor collagens (e.g. collagen V and XI) forms the side of dermal collagen type I and cartilage collagen type II fibres, respectively, with N-terminal domains at the fibril surface. This suggests a similar nucleating function with a diameter-limiting effect [65]. As such, collagen fibrillogenesis is affected by cell-fibre contact, by the reshuffling fibres resulting from cell movement, by ligands that control the growth of fibres and by proteolytic enzymes that remodel the deposited matrix. For example, studies of the corneal stroma of the developing chick eye have revealed the intricate assembly of the stromal ECM, which is finely controlled to build the correct shape and transparency. The corneal stroma is characterized by homogeneous collagen fibrils of small diameter, the size of which is controlled by accessory molecules, such as FACIT collagens and small leucine-rich proteoglycans [67], and shows a highly ordered hierarchical organization [68].

Molecular packing of collagen molecules then takes place, with certain structural features applying to almost all collagenous fibrillar structures [69]. The fibril-forming collagens are subdivided into type I rich fibrils (containing predominantly collagens II and V) and type II rich fibrils (more typically containing collagen types IX and XI) [69]. Collagen triple helices form longitudinal structures by lateral alignment and with a stagger of roughly one fourth of the molecular length. The pairing occurs between a stretch of 234 amino acids of either helix, a region that ensures maximal electrostatic interaction and hydrophobic interactions. The molecular stagger leads in projection to regions of high and low electron density, namely the overlap (two adjacent triple-helices) and gap (triple-helices lined up head-to-tail, but with some space between them) regions. The key to further axial growth seems to be the interaction of telo-peptide regions of a triple helix with an adjacent trimer. Current models suggest a hook-like back-folding of C-telo-peptides, bringing Tyr residues within the telo-peptide trimer into axial vicinity, while bringing a Lys residue in a position to register with a Hyl residue in a triple helical domain of an adjacent triple helix [69]. Three-dimensional packing of collagen trimers of collagen type I includes five trimers in a pentagonal arrangement forming a micro-fibril [70]. This popular model has been recently revised to a compressed five-stranded micro-fibril that forms a trapezoid and accounts for the degree of crystallinity seen in collagen fibres. This model accommodates both crystallinity and liquid-like disorder, suggesting a concentric and

appositional packing of these structures, where the gap regions represent disordered areas [69]. The packing of molecules deviates by roughly 5 degrees from the longitudinal axis (molecular tilt) in tendons and by up to 18 degrees in dermis. Subsequent modelling and ultrastructural investigation showed that collagen fibrils pack and grow in a helical fashion, reminiscent of winding techniques used in rope-making [71]. The 67 nm axial repeat is the most frequently observed in collagen-containing tissues in animals, although shorter (e.g. 9 nm and 23 nm) and larger [e.g. 150 to 250 nm, named fibrous long spacing (FLS)] periods have been reported. The range of diameters of collagen fibres found in mammalian tissues spans two orders of magnitude. Thus, the enigma of which factors assign particular diameters to specific tissues and keep them in homogenous distribution over a lifespan remains unanswered. Replenishing of molecules, remodelling of structures and age-related changes has been shown to be critical in this process [72].

1.3.5 Natural cross-linking

The hierarchical assembly / packing of collagen molecules provides structural stability, mechanical integrity and enzymatic resilience to collagen-based tissues. This is further enhanced by weak interactions and strong intermolecular cross-links. Collagen type I is stabilized through the action of four cross-links: two in the helical region and one more in each telo-peptide, where the action of lysyl oxidase catalyses the formation of aldehydes from lysine and hydroxylysine residues [73, 74]. The resulting aldehydes react spontaneously with other lysine and hydroxylysine molecules from adjacent chains of the same molecule or from other adjacent molecules. These cross-links between two different molecules result in head-to-tail bonding along fibrils, known as aldimide bridges [75]. During *in vivo* biosynthesis, three main cross-linking pathways take place: the lysyl oxidase cross-linking, the sugar-mediated cross-linking and the transglutaminase cross-linking.

1.3.5.1 Lysyl oxidase cross-linking

Beyond the triple helical structure of individual collagen molecules, collagen assemblies receive additional mechanical and chemical stability from cross-links both between and within component molecules. Intra-molecular cross-links are generated by the action of lysyl oxidase (LO; gene name LOX, EC 1.4.3.13), which engages in PTM of secreted triple helices during fibril formation. While deamidation by LO is

prerequisite for the formation of such cross-links, it merely sets the molecular stage for the spontaneous cross-linking that occurs later. The telo-peptides present at either end of the collagen triple helix are an easy substrate for the enzymes to target, as opposed to the compact triple helix itself. It is here (telo-peptide regions) that LO takes effect, converting selected Lys and Hyl residues to the aldehydes allysine and hydroxyl-allysine, respectively, which can then spontaneously react via aldol condensation during fibrillogenesis (**Figure 1.3**). Thus, α chain dimers are produced from intra-molecular cross-links between the telo-peptide sections of two α chains. These dimers can be observed in SDS-PAGE as β bands.

In contrast, intermolecular cross-links occur between the telo-peptides of one collagen trimer and the helical region of a quarter-staggered adjacent trimer. One potential trimer bond is the formation of aldimine from an aldehyde residue on one trimer and an ε-amino group of either Lys or Hyl on the other, which yields a bivalent inter-chain cross-link that is still reactive. Subsequently, multiple condensations with His, Lys or Hyl residues yield further multivalent cross-links, which are reducible by sodium borohydride ($NaBH_4$). In most tissues, the number of borohydride-reducible cross-links decreases with age, most probably because they mature into stable, non-reducible cross-links [76, 77]. In the case of the Hyl aldehyde pathway, the more mature cross-links appear to be based on trivalent 3-hydroxypyridinium residues – Hyl-pyridinoline (3Hyl) and Lys-pyridinoline (2Hyl and 1Lys). The pyridinoline cross-links withstand proteolytic attack and are released after collagen tissue remodeling. Eventually, they reach the bloodstream and are excreted in the urine, where HPLC or ELISA can be used to quantify this cross-link and consequently assess collagen turnover in the body [78, 79].

Mature cross-links are formed later in life and their local concentration depends on the tissue in which they are formed, age, gender, activity, physical state [80]. In addition to trivalent pyridinolines, another cross-link has been identified in adult cartilage that is formed spontaneously from the initial divalent ketoimines [81]. This arginoline cross-link represents a 3, 4-dihydroxy imidazolidine that is formed by condensation of a free arginine with the oxidised ketoimine cross-link. Arginoline content increases with age and is not reducible with sodium borohydride. These findings not only revealed that cartilage collagen II fibrils are more cross-linked than hitherto assumed, but also highlight the importance of cross-linking for load-bearing tissues.

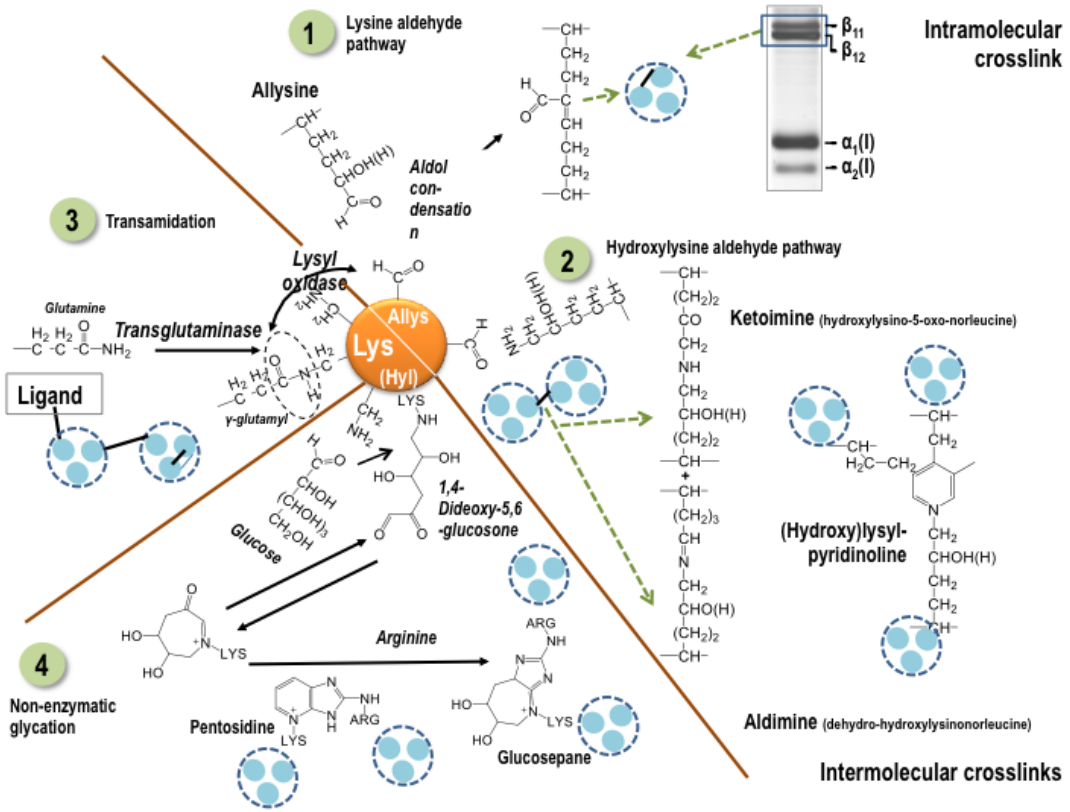

Figure 1.3: (1) Lysyl oxidase-mediated cross-linking. Lysyl oxidase desamidates lysine to allysine and hydroxylysine to hydroxyallysine (not shown). The lysine aldehyde (allysyine) pathway leads to aldol condensation and intra-molecular cross-links within a given triple helix, which are evident in SDS-PAGE gels (here shown after silver staining). (2) The hydroxylysine pathways leads to ketoimine and aldimine cross-links, respectively, which bridge two separate collagen triple helices. With a third partner these cross-links mature to non-reducible hydroxyl pyridinolines. (3) Transglutaminase-mediated isopeptide cross-links affix mainly non-collagen ligands to collagen, but also form intra/intermolecular collagen cross-links, too. (4) Non-enzymatic glycation. Glucose plays role in the formation of intermolecular cross-links by forming a Schiff base with Lys, then an Amadori product. Finally, a ring structure with Arg is formed, resulting in glucosepane; a comparable structure, pentosidine, is formed with ribose.

1.3.5.2 Sugar-mediated cross-linking

The discovery of non-enzymatic glycation of haemoglobin molecules in patients with diabetes mellitus triggered investigations into the role of sugars in modifying connective. Specific to collagen, its prolonged exposure to reducing sugars (e.g. ribose and glucose) produces advanced glycation end products (AGEs) that are implicated in aging and diabetic complications [82]. The non-enzymatic glycosylation reaction, which is accelerated in diabetes, is the first step of the Maillard or non-enzymatic browning reaction that occurs in stored food. The glucose-protein adduct rearranges and dehydrates to form brown and fluorescent pigments, which act as cross-links, resulting in decreased protein solubility and altered mechanical properties. Early studies not only confirmed, but also demonstrated that browning is increased in human collagen over age in a linear fashion and that diabetic patients show accelerated browning, suggesting a correlation between arterial stiffening, decreased joint mobility and severity of microvascular complications in type I diabetes [83]. One should consider that glycation is the major cause of dysfunction of collagenous tissues in old age and the process is significantly accelerated in diabetic patients largely attributed to the higher levels of glucose. Glycation modulates numerous collagen properties, including its biomechanical behaviour and supramolecular aggregate assembly. The most damaging effects are due to glucose-mediated intermolecular cross-links between the triple helices, which decrease flexibility, permeability and turnover. Almost all ECM proteins can react non-enzymatically with a sugar group (frequently glucose) via a free ε-amino group of a Lys or Hyl. This form of glycation is described as Maillard reaction and involves the chemical reaction of a sugar aldehyde or ketone with a free amino group to form Schiff base, which then undergoes rearrangement to form a fairly stable keto-imine (Amadori product). These structures are still reactive and can go on to form AGEs or to degrade into reactive α-dicarbonyl groups, which in turn react with other free amino groups to form cross-linked adducts. These additional (non-LO-facilitated) cross-links influence the resistance of collagen to degradation and remodelling [84-87]. This appears particularly relevant for collagen-rich tissues, such as dermis, cornea, tendons, ligaments and endomysial sheets of muscles. However, the basement membrane function of macro- and micro-vasculature (including the blood-filtering glomeruli of the kidney) largely provided by collagen IV is an obvious target for AGE formation and explains the complications of

diabetes. Certain molecules, including urea, have been described as AGE-breakers and are potential therapeutic targets.

1.3.5.3 Transglutaminase cross-linking

Transglutaminase (TGase) mediated collagen to collagen cross-links were first demonstrated for the highly homologous α1 chains of collagens type V and type XI in cell culture, with an indication that cross-linking occurs in the non-triple helical propeptide domains. TGase activity has also been shown on collagen VIII anchoring fibrils, presumably on cross-linking sites in the NC1 domain of collagen II [88] and on collagen type VII was recently confirmed [89]. In contrast to lysyl oxidase, which facilitates collagen cross-links, TGases (EC 2.3.2.13) can create them directly. TGases are widely distributed and have been found in microorganisms [90, 91], across the animal kingdom [92, 93] and recently also in plants [94]. TGases catalyse the formation of an isopeptide bond between the ε amino group of a Lys and the γ carboxamide group of a glutamine. The reaction (transamidation) also produces an ammonia molecule. Depending on the isoenzyme and species the TGase is derived from, the reaction is Ca^{+2} dependent; microbial TGase (mTGase) does not require Ca^{+2}. The resulting isopeptides [ε-(glutamyl)-lysine dipeptides] are very stable and can be isolated from tissue homogenates only after aggressive proteolytic tissue digest. They can also be detected as separate peaks in HPLC, serving as fingerprints of transamidation [95]. Antibodies are also available against the ε-(glutamyl)-lysine cross-link and used as tools to discover transamidated tissue structures. It should be noted that the primary structure of a given protein does not allow prediction of which Lys or Gln might serve as an amine donor or acceptor, respectively. Determination of actual TGase cross-linking sites still requires a good deal of empirical work and direct biochemical analysis. Also, and in contrast to pyridinolines, the identification of an isopeptide bond is not specific for a collagen-to-collagen cross-link; it could also indicate a non-collagen ligand cross-linked with collagen.

There are currently nine TGases known in humans with distinct functions [96]. Knowledge about the exact biochemical activity of TGases was derived from early studies of coagulation protein factor XIII [97-99]. As stabilizer of fibrin/fibronectin blood clots, FXIIIα has been converted into an industrial product known as fibrin glue (Tisseel™). FXIIIα can cross-link fibronectin to collagen, but evidence for the cross-linking of fibrillar collagens is sparse. FXIIIα has been implicated in the cross-linking

of the non-collagenous domain of collagen type XVI. The activity of different TGase isoforms can be monitored in tissue cryosections, where the enzyme(s) are still active. Biotinylated peptides, serving as either amine donors/acyl acceptors (containing Lys) or amine acceptors/acyl donors (containing Gln), have been successfully employed to localize sites of TGase activity. Conveniently, the offered peptides are irreversibly cross-linked into target structures of the tissue sections or cell cultures and can then be detected with avidin-conjugated probes (enzymes, fluorophores). Thus, TGase activity has been visualized in the cornified envelope of the epidermis [100] and dermis [101], as well as in connective tissue structures of other organs [102]. As these peptides were designed to be fragments of other ECM molecules, such as fibrillin-1 and osteonectin, these localization studies suggest that TGase 2 may be a modifier of collagen assemblies.

1.4 Sources of collagen

To-date, numerous collagen preparations are commercially and clinically available; they have been extracted from animal tissues, including human and fish, or from human or land animal cells grown *in vitro* or have been produced by recombinant expression or direct peptide synthesis. Each of these collagen preparations come with distinct advantages and disadvantages (**Table 1.2**).

Table 1.2: Indicative advantages and disadvantages of collagen preparations from various sources.

Source	Advantages	Disadvantages
Tissue Extracted Collagen	High yield Acid / pepsin extraction removes antigenic p-determinant	Potential of interspecies transmission of disease
Cell Synthesised Collagen	Can be autologous	Low yield
Recombinantly Produced Collagen	Low immune response	Low yield Stability issues
Peptide Synthesis Produced Collagen	Would rule out allogeneic / xenogeneic issues	Low yield Assembly / registration issues

1.4.1 Extracted collagen

For biomedical applications, mammalian skin and tendon tissues (porcine, bovine and ovine in origin) are the primary source of collagen type I, whilst collagen type II is primarily extracted from bovine, porcine and chicken cartilaginous tissues (**Figure 1.4**). Type IV collagen is an important component of Episkin™ (L'Oréal), a reconstituted human epidermis, actively used for the evaluation of the potential toxicity and irritancy of topically applied compounds and as an OECD validated and adopted skin corrosion test [103-106]. It is worth pointing out that the vast majority of the early work in collagen was carried out using rat-tail tendon collagen due to its high purity and relatively easy extraction process. Waste materials of the fish processing industry (fins, scales and bones) have also been used to extract collagen for the fabrication of biomaterials [107-112], but to a smaller extend. Although sponges are the simplest-known multicellular organisms containing collagen, the extraction of collagen from this source is not widely used, though in principle it would be a sustainable source. Pioneering work on the predominantly Mediterranean Sea sponge *Chondrosia reniformis* has shown that collagen from this species is, in contrast to other sources, not soluble in weak acids, but in weak alkaline conditions [113, 114]. The use of sea sponge collagen preparations in tissue engineering is sparse [115].

Despite the species / tissue origin, collagen is particularly notorious for its large, coherent, covalently cross-linked fibrillar meshwork. To this end, different methods (dilute acidic solutions with or without enzymes, neutral salts and alkali treatments) are used to isolate and purify different types and amounts of collagen from various tissues, whilst harsher methods employing heat and acid or alkaline agents (liming) tend to denature collagen to gelatin A or B, respectively, which contain single broken-down triple helices. Dilute acidic solutions effectively disassociate intermolecular aldimine cross-links (between triple helices), however, they are ineffective against more stable and mature cross-links (e.g. ketoimine bonds). In this case, proteolytic enzymes (primarily pepsin) are employed, which also increase the yield by up to 10 times [116-124]. Notably, an even partially or locally unfolded triple helix is vulnerable to proteolytic attack, but a tightly folded and intact triple helix is not [125]. The efficacy of enzymatic treatment therefore arises from selective cleavage in the non-helical N- and C- telo-peptide regions that allows the excision of intact triple helices out of cross-linked fibrillar assemblies [126, 127]. The resulting mono triple helical collagen is named atelocollagen and has been shown to provoke a markedly

lower immune response due the removal of the antigenic sequence P-determinant, located at the telo-peptide regions [128-136].

All advances in extraction and purification procedures aside, collagen is an animal extracted material and therefore raises issues about immunogenicity and interspecies transmission of disease [137-142]. The triple helical domains of bovine and porcine collagens are highly homologous to human collagen, but immunologically relevant differences lay in the telo-peptide regions may provoke an immune response [124, 143]. Although peptic digestion cleaves off the non-helical ends, the immunogenic potential is not completely eliminated. A much greater concern with xenogeneic biological materials is the transfer of infectious pathogens (e.g. prion disease). These concerns, combined with cultural issues stimulated the investigation into cell-produced collagen, human recombinant collagens and collagen-like synthetic peptides.

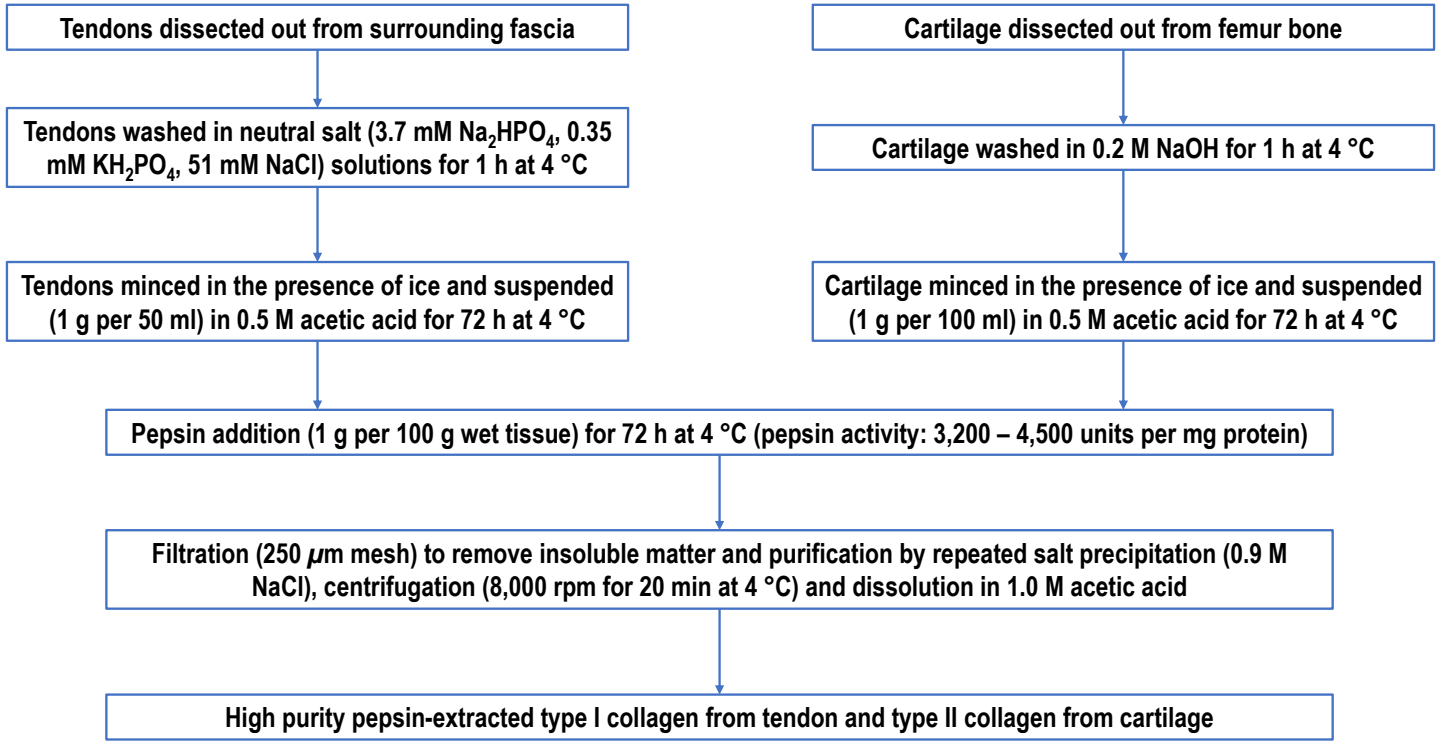

Figure 1.4: Collagen type I and collagen type II extraction and purification protocol.

1.4.2 Cell-produced collagen

As collagens are synthesized by specialized cells, it is plausible to let cells in culture produce these essential ECM molecules and subsequently harvest them either from the media or from the deposited cell-layer. This, however, requires fast- and well-growing cells, with strong biosynthetic activity. Numerous primary and immortalized cells have been used over the years for the production of various collagen types (primarily collagen type I from fibroblasts and collagen type II from chondrocytes) from various species. To enhance collagen synthesis, L-ascorbic acid supplementation is required, given that ascorbate is an essential cofactor in the hydroxylation of collagenous proline and lysine and humans, guinea pigs, primates and other species cannot synthesize ascorbate, due to deficiency in one of the essential enzymes in the liver (gulonolactone oxidase) [144-147]. Low oxygen tension has also been used to increase collagen synthesis up to 5-fold in permanently differentiated cells [148, 149], as hypoxia inducible factor 1 α (HIF 1α) is activated at low oxygen tension cultures and is central regulator of collagen hydroxylation and secretion [150-152]. Further, low oxygen tension has been shown to upregulate the synthesis of TGF-β1, which is a collagen inducer [153, 154]. It is worth pointing out that this increased collagen synthesis at low oxygen tension (2 %) was not mirrored in stem cell cultures, suggesting that activation of HIF-1α alone does not necessarily translate into increased ECM synthesis [155]. Biological factors, in the form of growth factors [156-163] or gene transfection [164, 165], have also been recruited as means to increase collagen synthesis. Insect cells [166] and sarcoma cell lines, as is [167] or in combination with recombinant technologies [168-172], have also been used as means to produce various collagen types. However, the non-mammalian origin of the former and the cancerous origin of the latter restrict or even prohibit their clinical translation. The yield of collagen from human cells is also very low [173, 174], limiting further their clinical potential.

1.4.3 Recombinant collagen

The use of genetically engineered microorganisms, animals and plants appears to be an alternative option for the production of recombinant human collagens that avoids problems related to batch-to-batch variability, interspecies transmission of disease and xenogeneic immune responses, all of which can be induced by animal extracted

collagens [175-177]. The rational of using microorganisms as means to produce recombinant collagen lays on the fact that evolutionary collagens and collagen-like proteins existed in bacteria before they were present in multicellular organisms [178]. *S. cerevisiae* [179-181] and *P. pastoris* [182, 183] yeasts were the first to be investigated, given that as eukaryotes, they are capable of glycosylation. Considering that certain viruses harbour genes encoding prolyl 4-hydroxylase [184] and lysyl hydroxylase [185], the co-expression of a human collagen type III with mimivirus prolyl and lysyl hydroxylases in *E. coli* has recently been reported [186]. However, the yield of such systems is very low (e.g. 15 mg/l for yeast [187], 60 mg/l for baculovirus [166], 90 mg/l in *E. coli* [186]), thus limiting broad commercialization potential. The extraction yield of collagen-like Scl2 protein from *S. pyogenes* was recently improved considerably up to 19 g/l by combining a stirred bank bioreactor, high cell density and adjusting culture time [188]. Although helical conformation of this collagen-like protein was validated, the enzymatic resistance was not studied. Moreover, this collagen-like Scl2 protein was decorated with heparin, integrin binding or discoidin domain receptors to increase cell adhesion, as Scl2 protein lacks cell binding sites [189, 190]. Another disadvantage of bacterial recombinant collagens is the absence of hydroxyproline. Therefore, bacterial recombinant collagen-like proteins show relatively low denaturation temperature (~26 ºC) and when they are stabilised by electrostatic interaction via multiple interpeptide lysine-aspartate and lysine-glutamate salt-bridges [191, 192], they reach denaturation temperature of 35 ºC to 39 ºC [193]. Tyrosine and cysteine residues have been introduced to induce cross-links through oxidation [194]. Further, incorporation of Gly-Pro-Ala or Gly-Pro-Hyp peptides has been shown to reduce bacterial invasion of root dentine [195]. This customisation was also used to modulate chondrogenesis of human mesenchymal stem cells by incorporating heparin-binding, integrin-binding and hyaluronic acid-binding peptide sequences into the collagen-like Scl2 protein [196]. Recombinant collagen-like proteins also demonstrated affinity with fibronectin, when it was incorporated into the protein sequence a minimum of 6 triplets of human collagen type II sequence from residue Gly^{775}-Arg^{792} [197].

While recombinant collagens have been expressed in a thermally stable triple helical form, they may still differ with respect to proteolytic susceptibility in comparison to native fibrillar collagens [198, 199]. These issues (e.g. low yield, low thermal properties, susceptibility to enzymatic degradation) were tackled with a more complex

approach using transgenic animals that secreted procollagen type I trimers into their milk in the mammary glands [200, 201]. Silkworms have also been induced to express a fusion protein of fibroin and collagen [202]. Plants have developed an ECM based on carbohydrate polymers and a variety of them possess PTM machinery that includes membrane-bound protein disulphide isomerase/prolyl 4-hydroxylase [203]. To this end, transgenic corn [204, 205] and tobacco [206-208] plants have successfully been employed to produce human recombinant pro-collagens. Despite the strides that have been made to-date, unicellular organisms do not produce ECM and therefore lack the enzymatic toolbox to post-translationally modify collagen. Thus, in most cases the produced collagens are not stable at peptic digest, suggesting incomplete triple helix formation or thermal instability. Further, the yield is very low for industrial applications, suggesting that a niche area should be identified that would offer opportunities for recombinant technologies to thrive [209, 210].

1.4.4 Synthetic collagens

Trimeric structures of synthetic Gly-X-Y repeats, referred to as collagen-mimicking sequences, collagen-like peptides or collagen-related peptides, are at the forefront of scientific research to address issues associated with animal extracted collagens, cell-produced collagen and recombinantly synthesized collagens [211-217]. Although advances in synthetic strategies and technologies allow synthesis of long chains, all current synthetic triple helices are below 10 nm in length, thereby falling far short of the classical collagen type I α helix length of 300 nm. Thus, such collagen mimicking synthetic analogues have been used as nano-spheres [218], nano-sheets [219] and other micro-structures [220]. The problem of registration of alpha chains to form a triple helical domain has been overcome with a sticky-end approach that is related to the strand invasion feature; three short collagen strands [two $[Gly\text{-}Pro\text{-}Pro]_5$-$[Gly\text{-}Pro\text{-}Pro]_3$-Cys-Gly and one $[Gly\text{-}Hyp\text{-}Pro]_3$-Gly-Cys-Gly-$[Gly\text{-}Hyp\text{-}Pro]_5$] are held in a staggered array by disulphide bonds. The $[Gly\text{-}Y\text{-}Pro]_3$ segment forms an intra-molecular triple helix with a single strand overhang represented by the $[Gly\text{-}Hyp\text{-}Pro]_5$ stretch (sticky end), allowing annealing of further overhangs of identical trimers to a length of nearly 1 μm in length and 1 nm in diameter. Such systems have the ability to produce collagen-like structures from nano- [221] to micro- [222] scale. The electrostatic interaction of these oppositely charged amino acids stabilizes the sticky-ended triple helix by forming salt bridges, which have been calculated to increase

significantly triple helical stability [223]. The limitation of these materials sets with their production costs. We foresee here a very interesting avenue towards building collagenous, yet synthetic, biomaterials, should their safety and efficacy be demonstrated.

Regardless the source, if collagen is to be part of an implantable medical device, the manufacturing process should include a microbiological safety assessment in conformity with regulatory requirements [224-226]. For viral inactivation, WHO recommends low pH, solvent and detergent treatments [227]. Sodium hydroxide treatment (1 M, for 1 hour at 20 °C) has also shown promise [228]; it should be noted that sodium hydroxide affects collagen stability [229]. Chemical and biochemical contaminants should also be identified and quantified and potentially safety hazards should be documented [230]. With no exception, the final product should entirely comply with ISO 10993 [231], with the in force standard [232], directives and regulations related to medical devices [233].

1.5 Exogenous collagen cross-linking

The natural lysyl oxidase-mediated cross-linking of collagen does not occur *in vitro* and therefore reconstituted collagen assemblies lack sufficient strength and may disintegrate upon handling or collapse under the pressure from surrounding tissues *in vivo*. Furthermore, the rate of biodegradation has to be customized for the specific application / clinical indication. Thus, it is often necessary to introduce chemical, physical or biological in nature exogenous cross-links into the molecular structure to tune mechanical properties, to prevent denaturation at 37 °C and to control the degradation rate [234, 235]. The fundamental principle of exogenous collagen cross-linking is the formation of covalent bonds between collagen molecules using chemical or natural reagents, which generally link either to the free amine or carboxyl groups of collagen. Although each method (chemical, physical or biological) provides unique advantages [e.g. tailored to the clinical indication thermal (**Table 1.3**) and mechanical properties], disadvantages [e.g. cytotoxicity at the effective concentration, foreign body response (**Table 1.4**) have also been reported, imposing the question ‘to cross-link or not to cross-link’ [235].

Table 1.3: Denaturation temperature of collagen-based devices as a function of species, tissue, scaffold conformation and cross-linking method employed.

Species	Tissue	Scaffold Conformation	Cross-linking Method	Denaturation Temperature (°C)	References
Human	Dermis	Tissue graft	Non-cross-linked	64-67	[236, 237]
			Glutaraldehyde	87-88	
			Genipin	81	
Bovine	Tendon	Sponge	Non-cross-linked	79	[238]
			Carbodiimide	80-86	
			Non-cross-linked	62-82	[239, 240]
			Dehydrothermal	54-58	
			Carbodiimide	78-91	
		Extruded fibre	Non-cross-linked	45-47	[234, 241, 242]
			Dehydrothermal	42-44	
			Ultra-violet irradiation	51	
			Glutaraldehyde	74-76	
			Carbodiimide	56-63	
			Diphenylphosphoryl azide	65	
			Hexamethylene	66-67	

			diisocyanate		
			Genipin	67-68	
			Poly(ethylene glycol) ether tetrasuccinimidyl glutarate	54	
			Transglutaminase	48	
			Myrica rubra	82	
		Film	Non-cross-linked	48	[243]
			Glutaraldehyde	73	
			Genipin	73	
	Dermis	Sponge	Non-cross-linked	49-52	[244, 245]
			Glutaraldehyde	48-87	[246]
		Gel	Glutaraldehyde	115-130	[247]
			Carbodiimide	56	[248]
		Electro-spun fibre	Non-cross-linked	36-40	[244]
			Carbodiimide	45-60	[249, 250]
Porcine	Tendon	Sponge	Non-cross-linked	53-69	[244, 245, 251]
			Carbodiimide	86	
		Gel	Non-cross-linked	36-37	[252]
			Carbodiimide	47-49	
		Electro-spun fibre	Non-cross-linked	37	[244]

	Dermis	Gel	Non-cross-linked	58	[253]
		Film	Non-cross-linked	36-47	[254]
Fish	Asian sea bass	Sponge	Non-cross-linked	125	[255]
	Asian sea bass	Film	Gamma Irradiation	110-113	[256]
	Jumbo squid	Film	Non-cross-linked	91-108	[257]
	Blue shark	Gel	Non-cross-linked	41	[258]
	Salmon	Film	Ultraviolet irradiation	102	[259]

Table 1.4: Advantages and disadvantages of the most widely used exogenous chemical, physical and biological collagen cross-linking methods.

Cross-linking Method		Advantages	Disadvantages
Chemical	Glutaraldehyde	Very good mechanical properties and resistance to biodegradation	Difficult to control due to self-polymerization capacity Toxicity / Inflammation / Foreign body response issues
	Hexamethylene diisocyanate	Very good mechanical properties and resistance to biodegradation	Toxicity / Inflammation / Foreign body response issues

	Carbodiimide	Water soluble system In general, low toxicity	Low inflammation / foreign body response issues
	Branched polyethylene glycol	Tailored molecular weight and number of functional groups Low toxicity Good mechanical properties and resistance to biodegradation	Very good *in vivo* response
	Genipin	Good mechanical properties and resistance to biodegradation In general, low toxicity	Low inflammation / foreign body response issues

Physical	Dehydrothermal	Non-toxic	Denaturation issues
	Ultraviolet	Non-toxic	Denaturation issues
Biological	Mammalian transglutaminase	Non-toxic	Expensive Low stability
	Microbial transglutaminase	Non-toxic	Expensive Low stability

1.5.1 Chemical methods

The most widely used chemical cross-linking agents are aldehydes (e.g. glutaraldehyde, GTA) [13, 260], isocyanates (e.g. hexamethylene diisocyanate, HMDI) [14, 261], and carbodiimides [e.g. 1-ethyl-3-(3-dimethylaminopropyl)carbodiimide, EDC] [262], with variable degree of efficiency [24]. GTA has been shown to extensively stabilize collagen materials because of its self-polymerization capacity that can even cross-link free amines that are relatively far apart [263, 264]. However, degradation products and unreacted GTA, which may remain non-specifically bound to the matrix, even after exhaustive rinsing with glycine solutions, result in high cytotoxicity [265, 266]. Isocyanates also react with amine groups, forming urea linkages and resulting in superior cytocompatibility to GTA, as no potentially toxic side products are formed [267, 268]. In addition, the short half-life of the isocyanates in physiological solutions further enhances their potential in biomedicine [269, 270]. Nonetheless, such potent cross-linking methods are associated with cytotoxicity [271, 272], calcification [273-275] and foreign body response [235, 276], even at low concentration, imposing the need for alternative strategies.

Carbohydrates (e.g. ribose [277], glucose [85]) and plant extracts (e.g. genipin [278, 279], oleuropein [280], *myrica rubra* [242]) have also been assessed, but to a smaller extent as the former are associated with pathophysiologies (e.g. diabetes), whilst the latter may have to face a complex regulatory framework to reach commercialization or clinical translation. The carboxyl groups of aspartic and glutamic acid residues can be used to cross-link collagen through acyl azide (one step reaction) [70, 281-287] and carbodiimide (two step reaction) [288-290]. EDC/NHS cross-linking involves activation of carboxyl groups, which then spontaneously bond to amine groups of lysine and hydroxylysine residues of collagen. After extensive washing foreign cross-linking molecules are removed, resulting in collagen devices of good cytocompatibility, reduced susceptibility to calcification, but with reduced mechanical properties and resistance to proteolytic attack [291, 292].

Recent data advocate the use of branched polyethylene glycol (PEG) polymers [25, 58, 266, 293-296] but more studies are needed to clearly demonstrate their superiority over conventional chemical approaches.

1.5.2 Physical methods

To avoid cytotoxic effects associated with the chemical cross-linkers, physical methods, such as dehydrothermal (DHT) [297-302] and UV irradiation [302-306] and to a lesser extend photo-reactive agents (e.g. rose Bengal [307], riboflavin [308]) have been assessed. DHT treatment uses high vacuum and temperatures over 100 °C for several hours to promote severe collagen dehydration [309, 310]. Consequently, formation of inter-chain cross-links is induced as a result of condensation reactions either by amide formation or esterification between carboxyl and free amino and hydroxyl groups, respectively [302]. UV cross-linking promotes bonds by free radical formation on tyrosine and phenylalanine residues. The cross-linking mechanism is based on the formation of a hydroxyl radical ($OH^{\bullet}$) from water. The $OH^{\bullet}$ radical attacks the peptide backbone to produce peptide radicals (-NH-$C^{\bullet}$-CO-), which can interact to form a cross-link [303, 304]. The efficiency of the reaction depends mainly on the sample preparation, the irradiation dose and time of exposure [311]. It has been reported that UV irradiation of wet collagen fibres causes rapid insolubility [312] and increases their tensile strength [313]. Nonetheless, all physical methods are a lot weaker than the milder chemical method and are often associated with collagen denaturation (especially the DHT treatment), imposing the need for introduction of chemical cross-links (usually carbodiimide).

1.5.3 Biological methods

Tissue-type and microbial TGase have been utilized to stabilize collagen- and gelatin-based materials mimicking the enzymatic *in vivo* collagen cross-linking pathway. Data to-date demonstrate moderate increase in denaturation temperature, mechanical integrity and biological stability, independently of the TGase origin (mammalian or microbial) and the collagen source (mammalian, fish, type I collagen, type II collagen) [102, 314-327].

It is worth pointing out that both physical and biological methods, despite their superior cytocompatibility to chemical approaches, are very weak, often weaker than the mildest chemical approach. Further, the physical methods are associated with collagen denaturation. As such, the quest for the optimal collagen cross-linker continues.

1.5.4 Collagen properties assessment

Over the years, an array of structural, thermal, mechanical, biochemical and biological assays has been developed to analyse / characterize collagen in tissues, cell culture setting, solutions and three-dimensional scaffold conformations, with variable degree of efficiency, accuracy and capital infrastructure requirement.

1.5.4.1 Structural properties

Collagen molecules self-assemble at nano-scale level to form supramolecular structures (fibrils and then fibres) in the micron range that are visible with various microscopic techniques (**Figure 1.5**). X-ray diffraction studies have been used in conjugation with TEM analysis to assess the crystalline order of collagenous tissues [328, 329]. Advances in TEM and image processing have allowed the reconstruction of 3D images from serial ultrathin sections to determine collagen assemblies in tissue and their spatial relationship to the cells synthesizing them [330]. Scanning electron microscopy is used to study collagen assemblies in tissue context [331] and for imaging collagen-based scaffolds used in the biomaterials field [332]. Time-lapse studies of nano-structures formed by collagen assemblies were conducted [333], culminating in the real-time monitoring of the kinetics of collagen type I fibrillogenesis on atomically flat mica substrates [334]. Further, time-lapse AFM studies have suggested that collagen fibrils assemble in a two-step process. In a first step, collagen molecules assemble with each other, whilst during the second step, these molecules rearrange themselves into micro-fibrils, which are the building blocks of collagen fibres [335]. The *in vitro* self-assembly process of collagen has also been assessed turbidimetrically and with confocal fluorescence microscopy and is characterized by a lag phase, in which nucleation points form, a growth phase, in which lateral and particularly longitudinal extension of these nuclei into fibres occurs, and a plateau phase, during which no further assembly occurs [336-340]. Raman spectroscopy has also been used for surface imaging of Tyr and Phe rings on assembled collagen fibres [341].

The observation of cross-striation is a strong indicator for a regular self-assembly, native state, and minimal denaturation. It should be noted, however, that the absence of cross-striation does not signify the absence of collagens, merely the absence of fibrillar collagens. In crystallographic terms, a collagen triple-helix can be described as a non-centrosymmetric structure, which after self-assembly into higher-order fibres

provides '*an ordered nonlinear medium with a cross-sectional path length comparable to near infrared wavelengths*' [342]. This particular physical feature of collagen fibres allows the observation of optical second-harmonics in multi-photon microscopy [343]. Second harmonic generation (SHG) signals have been shown to depend on the order of the structure under observation. For example, skin, tendon, cornea (highly order tissues rich in collagen types I, III and V) give strong SHG signals, whereas the dermo-epidermal junction (collagen types IV, VII and XVII) does not. Further, tissues give stronger SHG signals that collagen-based biomaterials [244]. Various histological stains have been used over the years to assess collagen structures, primarily post implantation. Picrosirius Red staining, for example, of collagenous tissues has been used in conjunction with polarized light microscope to detect fibre quantity and hue [344]. Picrosirius Red consists of elongated dye molecules that readily react with amino acid-rich collagen molecules [345]. Thus, the dye enhances the natural birefringence of collagen by aligning itself in parallel with each collagen molecule [346]. Differences in the birefringence of constituent molecules can be used to identify collagen in a non-collagenous environment and to differentiate individual collagen types, albeit to a certain degree [347].

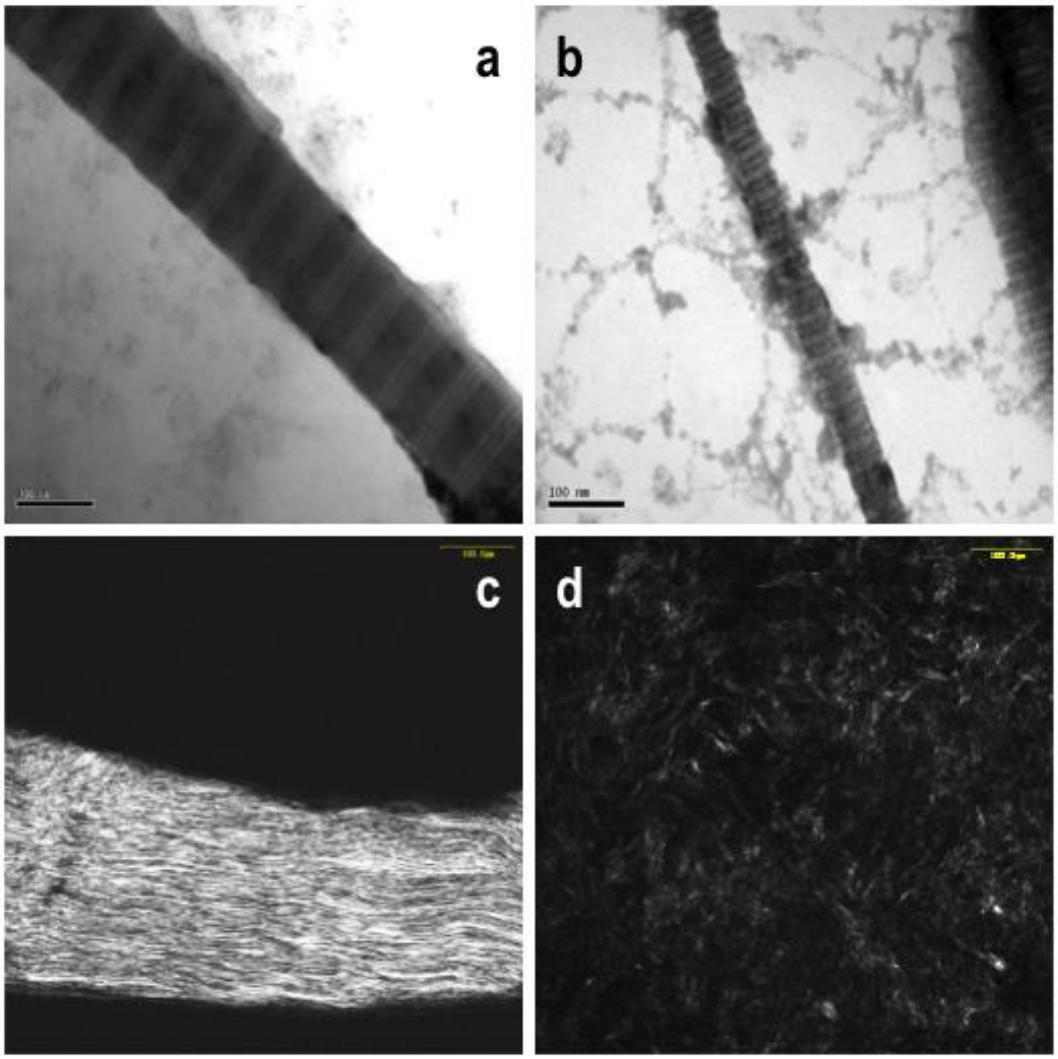

Figure 1.5: TEM analyses of rat-tail tendon (a) and self-assembled collagen scaffolds (b) clearly demonstrate the D periodicity / quarter staggered assembly of collagen molecules. SHG signals of rat-tail tendon (c) are stronger than those of self-assembled collagen hydrogels (d).

1.5.4.2 Thermal properties

The C-propeptide is the only area of the procollagen I molecule that can form covalent disulphide bonds to stabilize the procollagen trimer. These bonds lock the C-telo-peptide-mediated registration adjacent to the triple-helical region, where the folding and insertion process of the Gly-X-Y stretches occurs. In addition, chaperones like hsp47 hold the triple helix in shape. In the extracellular space, the removal of the propeptides from procollagen will deprive the triple-helix of any covalent bonds that would assist in securing the triple helical conformation of the three α chains. The tightly coiled triple-helix is now held together only by hydrogen bonds and inductive forces created via Hyp residues when facing thermal impact.

The melting temperature 50 (Tm50), at which 50 % of a given population of triple-helices is molten, can be determined by probing with proteolytic enzymes [348]. Typically, a solution of triple-helices is gradually heated and periodically probed at 20 °C with trypsin (targeting the triple-helical domain) and other enzymes that remove propeptides (chymotrypsin, pepsin). Each α chain contains over seventy consensus sites (www.uniprot.org), which are positioned at the C-terminally of a Lys or an Arg, except when either is bound to a C-terminal Pro [349]. However, these sites are sterically inaccessible, so trypsin can only attack melting regions of the triple helix. During the thermal ramp, α chains will not loosen progressively, but will melt in cooperative blocks as single structural units. This mode of melting first received attention in micro-calorimetric work [37] and was confirmed via studies of the destabilizing effects of single point mutations [350-352].

The unfolding of the triple helix shows a steep transition upon heating, whereas refolding occurs in more gradual manner [353]. This is exploited for proteolytic probing at 20 °C after heating. The Tm50 for tryptic measurement has been shown to be 41.5 °C for human collagen I and 39.5 °C for human collagen III [33], which was validated with circular dichroism spectroscopy [354]. However, it has emerged that the heating rate has major impact on determining Tm50 values; a very slow heating rate (0.004 °C/min), applied through differential scanning calorimetry (DSC), gave a Tm50 for lung collagen below 36 °C [355]. However, it is worth pointing out that the experiments were carried out in the presence of glycerol, which has been reported not only to inhibit fibril formation of acid and pepsin soluble collagen type I, but also to disassemble already formed fibrils [356, 357].

In general, DSC is traditionally used to assess the denaturation temperature of medical devices. The high-temperature peak corresponds to the melting of the supra-molecular aggregates [358]. Although early studies have assessed the denaturation temperature of various materials in dry state, it has become clear that implants should be incubated overnight in physiological solutions [245]. Given the simplicity of the methods, DSC is extensively used to assess the thermal stability of collagen devices. Data to-date clearly illustrate that denaturation temperature is dependent on species, tissues, scaffold conformation / packing density and the extent of cross-linking [359-362].

1.5.4.3 Mechanical properties

Collagen fibres are responsible for the elastic and viscoelastic properties of the tissues [363, 364]. The primary mechanical strength of collagen results from the self-assembly of collagen molecules into triple helices and collagen fibril which are additionally stabilized by intra- and inter- molecular cross-links [365]. The non-collagenous components are believed to play important roles either through their unique viscoelastic properties (e.g. elastin) or via their interaction with collagen fibres (e.g. glycosaminoglycans and proteoglycans) and allow the tissue to withstand compressive and tensile forces [366-369]. The length and diameter of the collagen fibres, their spatial distribution, the collagen types present, the content of non-collagenous molecules and the cross-linking content determine the functionality of tissues such as skin, tendon, cornea, blood vessel, cartilage, bone and their mechanical properties [370-376].

The deformation mechanism of collagenous structures is similar to those of crystalline polymers that yield and undergo plastic flow and can be divided into four regions: toe or low strain region, heel region, elastic or linear region and failure (**Figure 1.6**) [377-382]. In general, the slope of the stress-strain curve is increased with strain and this is characteristic of connective tissue [301, 383, 384]. The region of low strain corresponds to the gradual removal of a macroscopic crimp in the collagen fibrils and this is visible in the light microscope. The crimp has been shown to act as a buffer or a shock absorber within the tendon, permitting small longitudinal elongation of individual fibrils without damage to the tissue [365], resulting in its low stiffness [385]. The second stage starts at strains typically beyond 2% strain, after which the effective elastic modulus increases progressively. X-ray studies have demonstrated increase in D-period distance and lateral molecular packing of collagen molecules

within fibrils, as a result of the straightening of the collagen kinks. The straightening of the kinks allows fibril elongation and reduction in entropic disorder. The entropic forces increase as the number of kinks decreases, leading to the typical curving upwards stress-strain curve [386-388]. The elastic region starts when collagen is stretched beyond the heel region. Most kinks are now straightened and no further extension is possible by the entropic mechanism [381]. For larger strains, the exact mechanism by which mechanical energy is translated into molecular and fibrillar deformation is still unclear; most probably, large strain rates indicate stretching of the triple helixes and fibre slippage, resulting in lengthening of the gap region with respect to the length of the overlap region, implying a side-by-side gliding of collagen fibrils [381, 389]. During loading at large strains, collagen hierarchical structure is extensively deformed and fibrils can split into individual micro-fibrils. The collagen network ruptures when several micro-fibrils break up, a process termed defibrillation [387, 390-393].

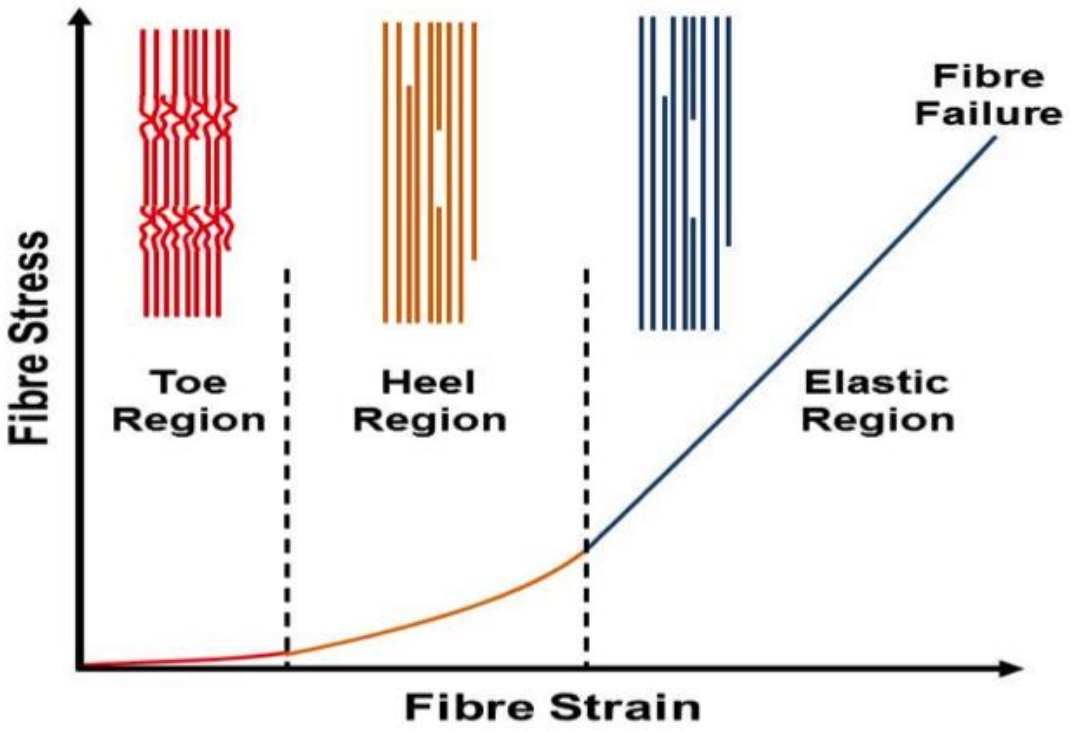

Figure 1.6: Typical stress-strain curve / deformation mechanism of collagen-based devices depicting the four distinct regions: the toe region, the heel region, the elastic region and the failure region.

1.5.4.4 Biochemical and biological properties

Various assays are available to assess the purity, concentration and cross-linking density of collagen-based materials [394]. Collagen extracted from different tissue sources and cell layers (**Figure 1.7**) can be characterized using sodium dodecyl sulphate polyacrylamide gel electrophoresis (SDS-PAGE), which separates proteins according to their molecular weight, charge, size and shape [395-399]. Protein bands are subsequently visualized using Coomassie Brilliant Blue or silver staining (over 40-fold more sensitive than Coomassie Brilliant Blue) and quantified by densitometry [117, 400]. Delayed and reduced electrophoresis can be used to separate α1(III) chains from α1(I) chains [401]. To determine collagen content, hydroxyproline assay is customarily used [402, 403], although metabolic labelling with radioactive amino acids [404-408], high-performance liquid chromatography [409, 410] and colorimetric assays have been proposed [411-419]. A rather simplified colorimetric assay has also been introduced (Sircol Collagen Assay, Biocolor Ltd., Northern Ireland) for the quantification of collagen in cell and tissue culture [420-427]. However, the binding capacity of Sirius Red with the side-chain of basic amino acids overestimates collagen content. To this end, a pepsin digestion step followed by column ultrafiltration purification step has been recommended to increase the accuracy of the assay [428, 429]. Ninhydrin assay is utilized to quantify the amount of free amino acids. Ninhydrin reacts with the primary free amino groups of the protein and a colour change, from yellow to purple (Ruhemann's purple), occurs [430, 431]. 2,4,6-trinitrobenzene sulfonic acid (TNBSA) assay is also used as means to quantify free amino groups. The concentration of N-trinitrophenyl protein derivatives is measured by molecular absorption spectroscopy at 345 nm [432, 433]. *In vitro* enzymatic degradation of collagen-based devices by matrix metalloproteinases, usually MMP-1 [236, 434-436], allows investigation of the stability of the devices [437-444]. However, MMP-1 preferentially cleaves collagen type III, as opposed to MMP-8, which is the predominant collagenase present in normal wound healing and degrades collagen type I more efficiently than MMP-1 [445]. MMP- 1, 2, 8, 13 and 14 are capable of hydrolysing collagen types I, II and III, whilst MMP- 3 and 9 are unable to degrade tropocollagen [446-455].

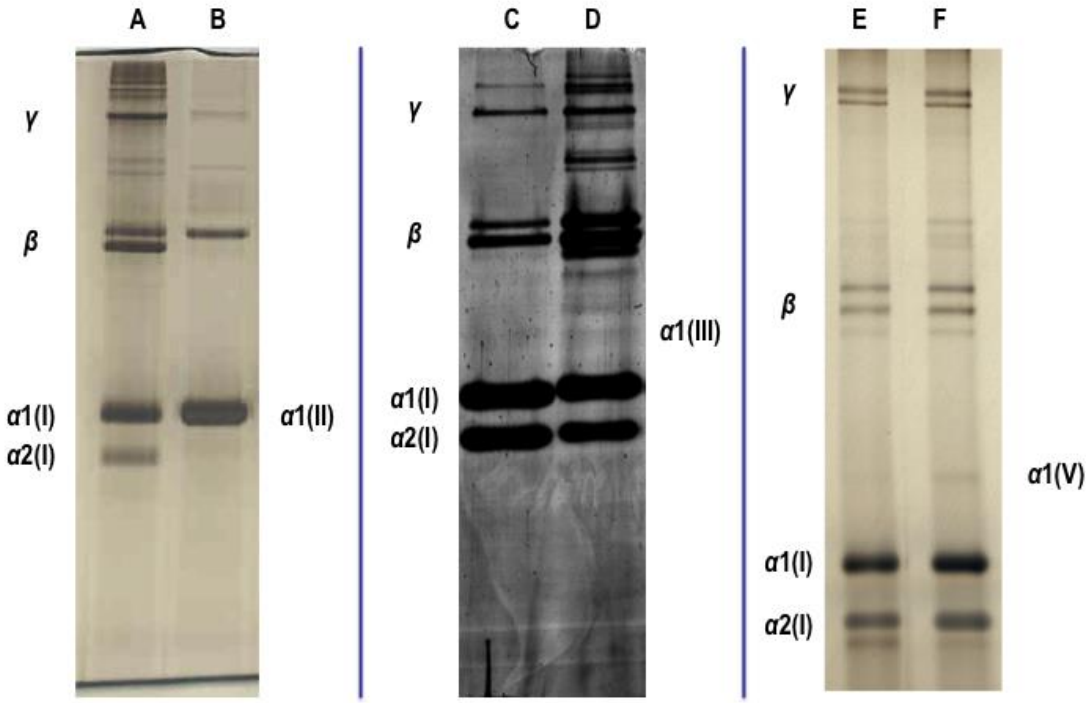

Figure 1.7: SDS-PAGE of collagen preparations from different tissues and cell layers. A: Porcine Achilles tendon collagen. B: Porcine articular cartilage collagen. C: Bovine Achilles tendon collagen. D: Porcine skin collagen. E: Dermal fibroblast deposited collagen. F: Mesenchymal stem cell deposited collagen.

1.6 Collagen scaffolds

Collagen-based devices, in various physical forms, are extensively used in biomedicine (**Figure 1.8**). Current and emerging scaffold fabrication technologies aspire to recapitulate the complex native tissue structural hierarchy and mechanical integrity [456, 457]. Obviously, decellularised tissues achieve maximum structural biomimicry, but suffer from limited availability (autografts) and potential immune response (allografts and xenografts) [458]. Mechanical loading has been used as a means to develop aligned and densified collagen gels, but further optimisation is needed to mimic the complexity of native tissues [458-461]. Electro-spinning has enabled the development of three-dimensional tissue equivalents, however, controlling spatially fibre distribution is still challenging, dense constructs limit cell infiltration and the solvents used induce collagen denaturation [244, 462]. This section provides a short overview on recent advancements in tissue grafts, hydrogels, sponges, fibres, films, hollow spheres and tissue-engineered living substitutes.

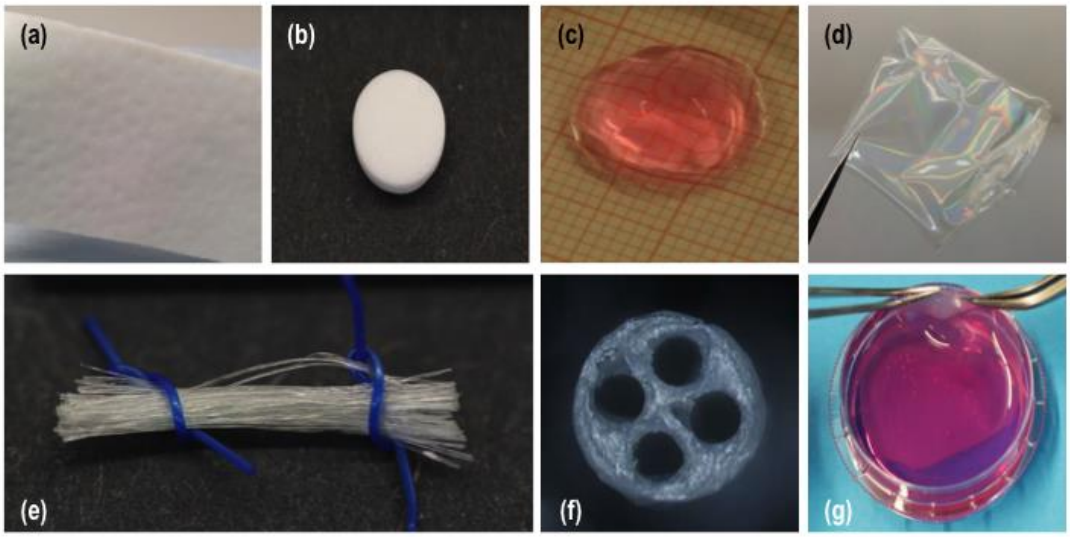

Figure 1.8: Indicative examples of collagen-based devices utilised in biomedicine. (a) Acellular porcine dermal tissue graft. (b) Freeze dried collagen type I sponge. (c) Collagen type II hydrogel loaded with cells. (d) Transparent collagen type I film. (e) A bundle of extruded collagen type I fibres. (f) Multichannel collagen type I neural conduit. (g) ECM-rich living tissue substitutes produced *in vitro* using primary human skin fibroblasts under macromolecular crowding conditions.

1.6.1 Tissue grafts

Autologous, allogeneic or xenogeneic tissue grafts are well established implantable devices due to their similarity with the tissue to be replaced and their complex molecular and biological content that allows cell attachment and promotes spatial cell organization [463-465]. Given the limited availability of autografts, allogeneic and xenogeneic skin [236], small intestine submucosa [466], bladder [467, 468], pericardium [260], skeletal muscle [469], heart valve [470], tendon [471] and ligament [472] grafts are extensively used in clinic and are often considered as the gold standard.

A typical manufacturing process of tissue grafts consists of depilation (for skin), physical isolation of surrounding tissues, decellularization, cross-linking, disinfection, freeze-drying and sterilization. All processing steps should maintain as much as possible of the original composition, structure, mechanical integrity and bioactivity of the tissue [473]. Decellularization is an inherent part of the process aiming to remove cells, DNA, cellular debris and any other molecules that can act as an immunogen or incite an inflammatory response when implanted [474, 475]. Several decellularization methods are available combining chemical, biological and physical treatments with variable degree of efficiency with respect to ECM disruption [476-479].

Although chemical cross-linking methods are extensively used to control mechanical stability and degradation rate, an optimal method has still to be identified [235]. Data to-date demonstrate that chemical cross-linking methods at low concentration alter wound healing, whilst at high concentration are associated with cytotoxicity, pro-inflammatory macrophage response, inhibition of macrophage polarization, reduced cell infiltration and delayed wound healing, often resulting in peri-implantation fibrosis [235, 480, 481]. Lyophilization is frequently used to increase product longevity and to avoid matrix disruption during sterilization [473]. With respect to sterilization, chemical approaches (e.g. ethylene oxide [482]) are associated with cytotoxicity, whilst physical methods (e.g. gamma irradiation [483], e-beam irradiation [484]) are associated with decreased mechanical properties, subject to the device's physical characteristics, suggesting that the sterilization method to be used is device-dependent [485].

Each clinical application requires different material properties and this has encouraged companies to produce several different ECM materials (**Table 1.5**). For example, small intestine submucosa and bladder have been used for applications that require

rapid cell infiltration, matrix degradation and remodelling that lack high mechanical performance, including certain types of hernia [276], rotator cuff tendon repair [486], bladder surgery [487], pelvic organ prolapse repair [488], cardiovascular surgery [489] or general wound healing (ulcer, burns and skin substitute) [467, 490]. On the other hand, skin-derived materials are used for applications that require higher mechanical performance and enzymatic resistance, such as ventral and abdominal hernia repair [276, 491] and infected wounds [492-494]. Recent efforts are directed towards functionalization of tissue grafts to enhance further their biological activity [495-497]. Despite the significant strides that have been achieved in the field, immune response and delayed remodelling [498-500] have stimulated research into scaffold-based approaches.

Table 1.5: Indicative examples of clinically available tissues grafts, for various clinical indications, provided along with their properties.

Product & Company Name	Product Details	Clinical Indication	Properties
AlloDerm™, LifeCell	Acellular non-cross-linked human dermis Sterilization: Electron beam irradiation	Soft tissue repair (e.g. hernia and breast reconstruction)	Degradation temp: 64-67 °C Max tensile strength: 19-21 MPa Ball burst strength: 800-1200 N/cm Degradation profile: > 12 months
Allomax™, Bard-Davol	Acellular non-cross-linked human dermis Sterilization: Gamma irradiation	Soft tissue repair (e.g. hernia, thoracic wall and breast reconstruction)	Degradation temp: 53-55 °C Max tensile strength: 13-15 MPa Ball burst strength: 230-350 N/cm Degradation profile: > 6 months
Collamend™, Bard-Davol	Acellular porcine dermis cross-linked with EDC Sterilization: Ethylene Oxide	Soft tissue repair (e.g. hernia)	Degradation temp: 62-67 °C Max tensile strength: 8-14 MPa Ball burst strength: 64-120 N/cm

			Degradation profile: > 12 months
FlexHD®, Ethicon	Acellular non-cross-linked human dermis Sterilization: Ethanol	Soft tissue repair (e.g. hernia)	Degradation temp: 62-64 °C Max tensile strength: 12-17 MPa Ball burst strength: 730-1130 N/cm Degradation profile: > 12 months
Permacol™, Medtronic	Acellular porcine dermis cross-linked with HMDI Sterilization: Gamma irradiation	Soft tissue repair (e.g. hernia)	Degradation temp: 60-61 °C Max tensile strength: 7-10 MPa Ball burst strength: 55-75 N/cm Degradation profile: > 24 months
PeriGuard™, Synovis Surgical	Acellular bovine pericardium cross-linked with GTA Sterilization: Ethanol and propylene oxide	Soft tissue repair (e.g. thoracic wall, hernia)	Degradation temp: 83-85 °C Max tensile strength: 20-23 MPa Ball burst strength: 85-115 N/cm Degradation profile: > 24

			months
Strattice™, LifeCell	Acellular non-cross-linked porcine dermis Sterilization: Electron beam irradiation	Soft tissue repair (e.g. hernia)	Degradation temp: 60-62 °C Max tensile strength: 9-11 MPa Ball burst strength: 230-320 N/cm Degradation profile: > 6 months
SurgiMend™, TEI Biosciences	Acellular non-cross-linked bovine dermis Sterilization: Ethylene Oxide	Soft tissue repair (e.g. general and plastic reconstruction)	Degradation temp: 57-58 °C Max tensile strength: 26-30 MPa Ball burst strength: 415-445 N/cm Degradation profile: > 6 months
Surgisis™, Cook Medical	Acellular non-cross-linked porcine small intestine submucosa Sterilization: Ethylene Oxide	Soft tissue repair (e.g. pelvic organ prolapse, hernia)	Degradation temp: 61-62 °C Max tensile strength: 2-3 MPa Ball burst strength: 195-205 N/cm Degradation profile: < 6 months

Veritas™, Synovis Surgical	Acellular non-cross-linked bovine pericardium Sterilization: Irradiation	Soft tissue repair (e.g. hernia)	Degradation temp: 44-46 °C Max tensile strength: 7-11 MPa Ball burst strength: 120-130 N/cm Degradation profile: > 6 months
XenMatrix™, Bard-Davol	Acellular non-cross-linked porcine dermis Sterilization: Electron beam irradiation	Soft tissue repair (e.g. hernia)	Degradation temp: 53-55 °C Max tensile strength: 11-12 MPa Ball burst strength: 330-410 N/cm Degradation profile: < 6 months

1.6.2 Self-assembled hydrogels

Hydrogels are water-swollen structures that resemble the properties of soft tissues more closely than any other type of polymeric biomaterial [501-503]. Collagen has the ability to polymerize *in vitro* into a fibrillar hydrogel at physiological pH, ionic strength and temperature, following an entropy-driven process [504-511]. The intertwined fibrillar substructure is held together by electrostatic and hydrophobic bonds [512] and entraps huge amounts of fluids, permitting that way the exchange of ions and metabolites with surrounding tissues [513]. The flowable nature of collagen hydrogels is primarily attributed to this high liquid phase and along with their fast assembly time (< 10 min) at physiological pH and temperature allow them act as injectable systems and ideal carriers for cells and therapeutic / bioactive molecules [514]. Cross-linking offers control over the liquid content and influences the mechanical properties and the degradation profile of the resultant hydrogels [515, 516]. An alternative strategy to improve the mechanical properties of the hydrogels is based on confined and unconfined plastic compression [517-521]. Advances in engineering have also enabled the development of spherical collagen type I [522] and collagen type II [522] micro-gels (**Figure 1.9**).

These unique properties of collagen hydrogels have made them the scaffold of choice for numerous clinical indications. In soft tissue repair, for example, collagen type I hydrogels seeded with fibroblasts exhibited a compact structure similar to that of dermis [523, 524]. Skeletal muscle derived stem cells loaded into a collagen type I hydrogel increased the expression of cardiac genes and similar contractile forces and intracellular calcium ion transients were observed as that of native cardiac cells [525]. When collagen type I hydrogels were subjected to mechanical tension, embryonic stem cells were differentiated to cardiomyocytes [526], whilst cardiomyocytes loaded collagen type I hydrogels resulted in formation of cardiac muscle bundles, resembling adult cardiac tissue [527]. In the neural space, collagen type I hydrogels, alone or in combination with growth factors and polypeptides, have been shown to promote polarity of neurons [528, 529] and to align and improve neural cell adhesion, survival and growth [530, 531]. Glyco-mimetic functionalized collagen type I hydrogels have been shown to encourage sensory and motor neuron outgrowth and enhance Schwann cell proliferation and extension [532]. Growth factor loaded collagen type I hydrogels have also shown potential in central nervous system applications [533]. In the eye space, collagen type I hydrogels (non-compressed and compressed) have been used as

substrates to grow various ocular-specific cell populations [534-538]. In tendon repair and regeneration, collagen type I hydrogels have been used either as a means to expand tenocytes *in vitro* [539, 540] or to improve cell retention of another device with adequate mechanical properties [541, 542]. Collagen type I [543, 544] and collagen type II [545, 546] hydrogels have been used extensively for osteochondral and cartilage defect repair, respectively. Collagen II is a typical cartilage collagen. It therefore makes sense that collagen type II hydrogels, as opposed to collagen type I hydrogels, maintain chondrocyte phenotype [547, 548] and drive mesenchymal stem cell differentiation towards chondrogenic lineage [549-551].

Numerous preclinical data are also available advocating the use of collagen hydrogels for numerous clinical targets. In skin, for example, collagen type I hydrogels have displayed good integration and they were colonized by host cells within 15 days [552, 553]. In the neural field, collagen hydrogels loaded with growth factors have shown promise in rat spinal cord injury models [533, 554] and in rat sciatic nerve models [555, 556]. In a rabbit corneal keratitis model, a collagen type I hydrogel loaded with a drug inhibited bacterial growth and maintained corneal clarity [557]. In a rabbit Achilles tendon gap model (collagen hydrogels are not suitable for large defects due to low mechanical integrity) collagen type I hydrogels were used as carriers of mesenchymal stem cells, resulting in improved structural and functional outcomes [558]. In a cartilage sheep model, collagen type I hydrogels containing autologous mesenchymal stem cells that had been differentiated into chondrocytes resulted in cartilage regeneration, although it us worth pointing out that areas of incomplete integration and cyst formation were observed [543].

Significant have also been the strides with collagen hydrogels in clinical setting. Apligraf® is a living bioengineered system made out of a collagen type I hydrogel and allogeneic fibroblasts and keratinocytes. This system has been used successfully in clinic for skin replacement, burn wounds and diabetic foot ulcers [523, 524, 559, 560]. However, drawbacks such as extensive shrinkage, poor porosity and poor persistence of fibroblasts within the hydrogel have been reported [561]. A collagen type I hydrogel loaded with bone marrow mesenchymal stem cells has also been used successfully in myocardium [562]. Numerous studies have also demonstrated the potential of collagen type I hydrogels loaded with chondrocytes or mesenchymal stem cells for cartilage repair [563-566]. The potential of human recombinant type III collagen has also been demonstrated in clinical setting for corneal repair [567].

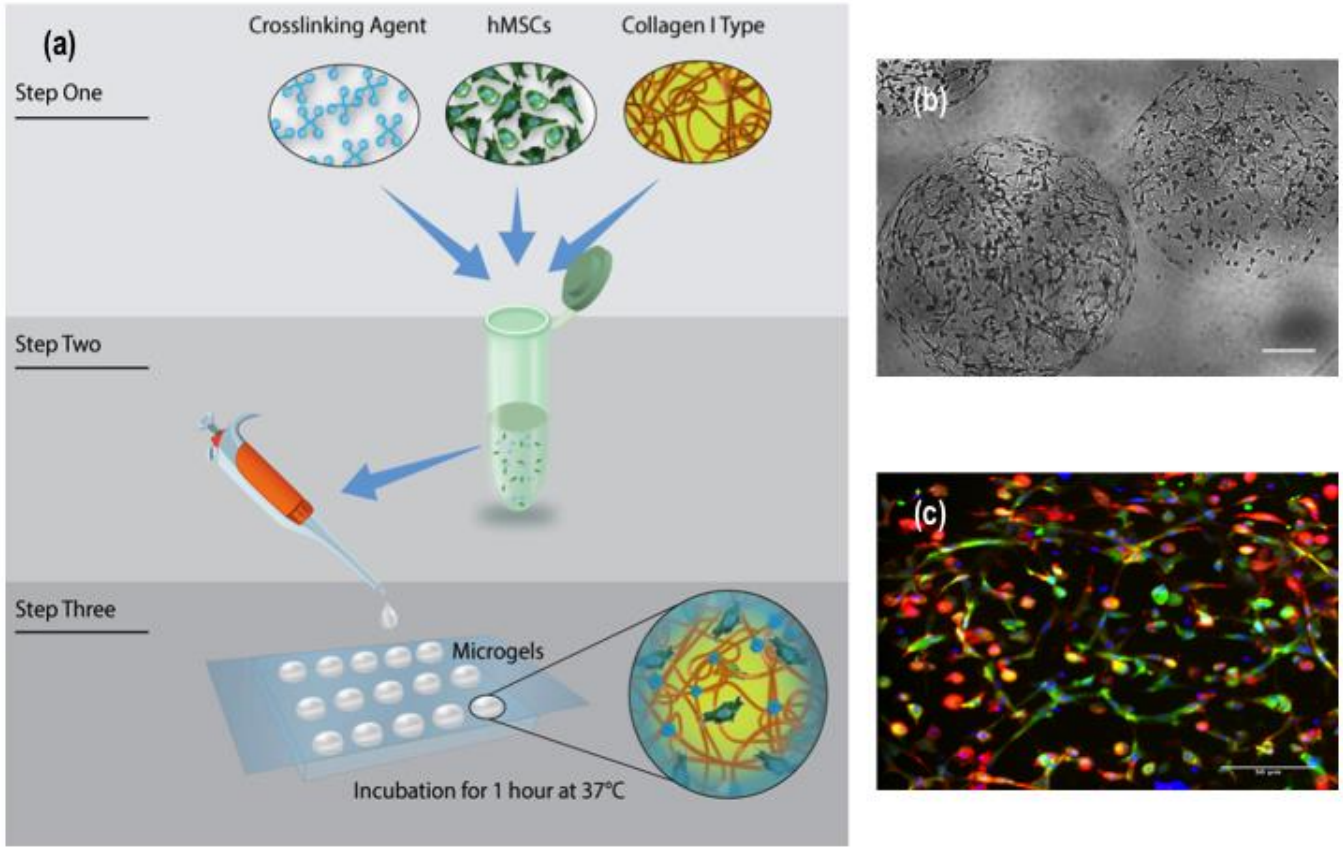

Figure 1.9: (a) Collagen type I microgel fabrication process. (b) Bright-field micrograph of collagen type I microgels loaded with human mesenchymal stem cells after 48 hours in culture (c).

1.6.3 Freeze-dried sponges

Freeze-drying (also known as ice crystal templating or lyophilization or ice-segregation-induced self-assembly) is a dehydration process that can be used for the construction of highly porous implantable devices (**Figure 1.10**) for a diverse range of clinical indications (**Table 1.6**). Upon freezing, collagen is entrapped within the developing ice crystals, which have formed into hexagonal structures. The porosity of the collagen sponge can be controlled by the freeze-drying rate and after sublimation of the ice crystals in the course of the drying phase [568-570]. For optimal bioactivity, the pores should be large enough to permit the migration of cells and diffusion of nutrients and small enough to promote cell attachment [571, 572]. However, too small pores should be avoided, as they restrict cell attachment and differentiation potential [573-575].

Numerous molecules and cell populations have been used to-date to enhance further the bioactivity of collagen sponges with promising results in both *in vitro* and *in vivo* settings. A collagen-glycosaminoglycan scaffold has been shown to enhance *in vitro* osteogenesis in human osteoblast culture [576] and to induce osteogenic and chondrogenic differentiation of adult rat mesenchymal stem cells [577]. Fibrin networks incorporated into a collagen sponge improved osteoblast attachment, proliferation and differentiation [578]. A collagen / hydroxyapatite / chondroitin sulphate sponge has been shown to differentiate stem cells towards chondrogenic lineage and to simulate cartilage-like ECM synthesis [579]. In preclinical models, collagen-glycosaminoglycan and collagen-calcium phosphate scaffolds have been shown to repair rat calvarial defects as effectively as autologous bone materials and more effectively than scaffolds loaded with mesenchymal stem cells [580, 581]. Collagen / recombinant human bone morphogenetic protein 2 scaffolds enhanced osteoclastogenesis, osteoblastogenesis and osteoclast activation and increased bone volume and the expression of bone resorption and formation markers, without adverse healing events (e.g. swelling, excessive bone formation, seroma formation) in a rat calvarial defect model [582, 583]. A collagen-hydroxyapatite sponge loaded with recombinant human bone morphogenetic protein 2 has been shown to increase healing in critical size rat calvarial defect within 8 weeks post-implantation, without provoking bone anomalies or adjacent bone resorption [584]. A collagen / rosuvastatin sponge has been shown to enhance bone formation in critical size proximal tibial cortical bone of New Zealand White rabbits, as evidenced by increased in BMP-2 mRNA levels,

higher bone volume, increased bone mineral density and new bone formation [585]. Collagen sponges, alone [586] or in combination with hyaluronic acid / hydroxyapatite / beta-tricalcium phosphate [587, 588] or with osteogenic protein [589], have been shown regenerative capacity in osteochondral defects of rabbits and mini-pigs, as evidenced by increased gene expression of cartilage molecules (e.g. collagen type II, aggrecan, SOX9) and improved biomechanics. When skin-derived precursors loaded on a collagen sponge and implanted to the wound areas of diabetic mice, accelerated wound healing and enhanced local capillary regeneration was observed by day 14 [590], whilst collagen sponges loaded with adult bone marrow mesenchymal stem cells showed a high density of vascularization in immuno-deficient mice [591]. Collagen / gelatin sponges loaded with basic fibroblast growth factor [592-594] or concentrated platelet lysate [595] have been shown to regenerate full-thickness defects on the backs of normal mice, on the palatal mucosa of dogs and on pressure-induced decubitus ulcer of genetically diabetic mice, as evidenced by neo-epithelium length and total area of newly formed capillaries assessment and accelerated wound healing. Collagen sponges containing latent TGF-β binding protein 4 stimulated elastic fibre growth, when implanted between the dermis and cutaneous muscle on the backs of athymic nude mice [596].

Numerous data have also advocated the use of collagen sponges, with or without functional molecules and / or cells, in clinical (human) setting. Collagen sponges have been shown to induce a substantial increase in the connective tissue thickness of palatal [597]. Collagen sponges have been shown to be more effective than autologous tissues in cranial neurosurgery [598]. Collagen sponges loaded with recombinant human bone morphogenetic protein 12 have been used successfully in rotator cuff surgery [599]. Gentamicin, Cefaclor or Ranalexin loaded collagen sponges have been used successfully in diabetic foot [600], cochlear [601], sternal [602], abdominal [603], thoracic [604] and cardiac [605] infections. A collagen / gelatin / basic fibroblast growth factor has shown promise in chronic skin ulcers treatment [606]. Recombinant human bone morphogenetic protein-2 combined with a collagen sponge resulted in a relatively shorter fusion time, but increased risk of posterior cervical wound complications may rise in posterolateral lumbar spine fusion [607]. A collagen sponge with autologous chondrocytes has shown good short-term clinical and radiological results in large focal chondral and osteochondral defects [608]. A collagen sponge loaded with autologous mesenchymal stem cells has also been used

successfully in intervertebral disc regeneration, as evidenced by radiograph, computed tomography and magnetic resonance imaging analysis [609]. CD34+ cell delivered with a collagen sponge containing recombinant human bone morphogenetic protein 2 achieved mature bone regeneration and increased bone density and mean trabecular bone area [610].

Given that traditional freeze-drying processes produce scaffolds with random architecture, advances in freeze-drying technologies offer control over the ice crystal formation and segregation, enabling the development of highly ordered collagen sponges that closely imitate native supramolecular assemblies [611-617]. Such scaffolds have induced *in vitro* tenocyte [618] and neurite [619] elongation and formation of homogenous cartilage-like tissue [620]. Preliminary *in vivo* data are also promising [575, 590].

Mechanical properties of porous scaffolds have been attributed to a variety of factors which include pore size and porosity, cross-linking density and functionalisation of collagen with molecules or drugs. The balance between pore size, porosity and mechanical properties have been shown to play an important role in the long term success of the implanted scaffold. Pore size can be controlled by adjusting the freezing method and time, as well as increasing the level of cross-linking. As cross-linking density increases, the pore size decreases while making the scaffold denser. Studies showed an increase in mechanical properties following the expression of ECM molecules by cells, given the appropriate pore size. Mechanical properties of sponges have also been shown to be dependent on the source of collagen, including animal age, sex, animal and tissue type. The level of cross-links following the extraction determines mechanical properties of the collagen. Given that collagen does not possess the mechanical properties of a native tissue, a variety of cross-linkers have been used. The type of cross-linker and concentration will depend on the properties of tissue of interest. However, it is important to note that elasticity will differ between tissues and therefore, the cross-linker should reflect this with appropriate young's modulus. This is similar to functionalisation of the collagen sponges with a molecule or a drug of choice. The addition of such molecules will cause modification to the structure of the collagen sponge, and hence the mechanical properties. Many factors influence the mechanical properties of porous scaffolds, therefore, it is important to consider the properties of the native tissues of interest to fabricated scaffold with appropriate properties.

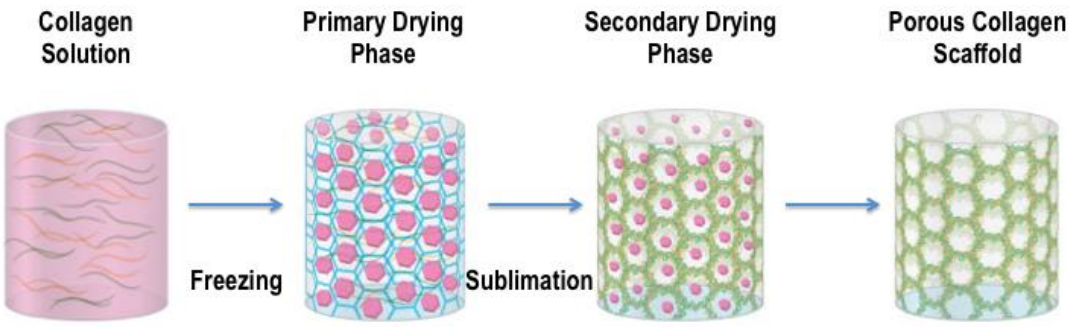

Figure 1.10: Porous collagen scaffolds are fabricated using freeze-drying. By adjusting the freezing rate, the size and the porosity of the sponge can be effectively controlled. Specifically, primary freezing at high temperature increases pore size through the formation of large ice crystals, whereas freezing at low temperature decreases pore size through the formation of small ice-crystals.

Table 1.6: Indicative examples of FDA approved collagen sponges for various clinical indications.

Product & Company Name	Characteristics	Clinical Indication
Avitene™ UltraFoam™, Bard-Davol	Purified bovine corium collagen sponge Sterilization: Dry heat	Haemostasis
CollaGraft®, Zimmer	Bovine collagen sponge containing hydroxyapatite / tricalcium phosphate granules Sterilization: N/A	Bone
COLLARX®, Innocoll	Bovine or equine collagen sponge COLLARX with gentamicin (INL-002) or bupivacaine (INL-001) Sterilization: N/A	Wound healing
CopiOs®, Zimmer Biomet	Bovine collagen sponge containing dibasic calcium phosphate Sterilization: N/A	Bone
GENTA-COLL® resorb, Resorba	Equine collagen sponge containing gentamicin Sterilization: N/A	Soft tissue wounds; Abscess caverns; Joint empyema; Spongioplasty; Osteitis, osteomyelitis; Implant associated infections; Diabetic foot; Extirpation of

		the rectum; Pilonidal sinus; Ano-rectal injuries; Sternotomy; Heart pacemaker replacement
INFUSE®, Medtronic	Collagen sponge containing recombinant human bone morphogenic protein 2 Species: N/A Sterilization: Nano-filtration	Bone
Integra Mozaik®, Integra	Bovine collagen (20 %) and tricalcium phosphate (80 %) sponge Sterilization: Irradiation	Bone
KOLLAGEN resorb™	Equine collagen sponge Sterilization: N/A	General surgery; Gynaecology; Thoracic and cardiovascular surgery; Orthopaedic and trauma surgery; Maxillary surgery and ENT, Haemostasis
Ologen®, Aeon Astron	Porcine collagen (~ 90 %) and glycosaminoglycans (~ 10 %) sponge Sterilization: N/A	Glaucoma surgeries; Glaucoma Drainage; Strabismus; Pterygium; Revision surgeries
OssiMend™, Collagen Matrix	Bovine collagen sponge containing 55 % bone mineral Sterilization: N/A	Bone

Zimmer® Collagen Plug, Tape, Patch, Zimmer Biomet	Bovine collagen sponge Sterilization: Gamma irradiation	Denture sores; Oral ulcers (non-infected nor viral); Periodontal surgical wounds; Suture sites; Burns; Extraction sites; Surgical wounds; Traumatic wounds

1.6.4 Self-assembled fibres

Although the benefits of electro-spinning are well known by now [621], unfortunately, electro-spinning of collagen still remains a challenge, as the current process leads to irreversible denaturation [244, 462]. For this reason, extruded collagen fibres and isoelectric focusing produced fibres are discussed here. Collagen fibres, with structural and mechanical properties similar to native tissues, have been produced through the extrusion of a collagen solution in a series of phosphate buffers maintained at 37 °C [301, 389, 391, 392, 622-624]. Collagen extraction method, collagen concentration, extrusion tube diameter, composition of the phosphate buffers and cross-linking method offer opportunities to tailor the mechanical properties of the fibres to the clinical target of interest [117, 625-630]. Undulation and crevices running parallel to the longitudinal fibre axis (**Figure 1.11**) have been shown to enhance cell attachment and to promote bidirectional cell growth [241, 631] and neotissue formation [632-634]. To enhance further the biological and biophysical properties of these fibres, functionalization strategies with decorin [389] and resilin [635] have been proposed. Such materials have also shown great *in vivo* outcomes in various preclinical models. For example, minor inflammatory reaction and biological degradation within six-weeks post implantation have been reported in a mouse subcutaneous model [636]. In an ovine tendon model, although the collagen fibres were nicely integrated and the tissue was regenerated, the rate of resorption was quite low due to high levels of cross-linking [634]. In rabbit models, carbodiimide and dehydrothermal / carbodiimide cross-linked fibres induced neotendon tissue with mechanical properties and structural characteristics similar to normal tendon tissue within 10 to 52 weeks post implantation, whilst glutaraldehyde cross-linked fibres formed capsule and inflammation [632, 637]. In anterior cruciate ligament rabbit [638] and dog [633] models, these fibres achieved complete regeneration within 12 weeks post-implantation.

An alternative strategy to prepare anisotropic collagen fibres is based on the principles of isoelectric focusing, which induces the collagen monomers to migrate towards and focusing at their isoelectric focusing point, where the overall charge is neutral [639]. The produced fibres have structural and mechanical properties similar to native tissues [640-645]. These aligned collagen fibres have been shown to provide topographical cues for *in vitro* bidirectional axonal guidance (**Figure 1.11**), even in the presence of myelin-associated glycoprotein that is known to inhibit neurite guidance [640]. These

anisotropic substrates have also been shown to induce bidirectional growth of tendon-derived fibroblasts and bone marrow stromal cells [646] and to stimulate tenogenic differentiation of bone marrow stem cells [647, 648]. In a rabbit patellar tendon model, these fibres were gradually degraded over 8 months period [649]. Further, aligned collagen fibres have been demonstrated to improve bone [650] and vascular [651] differentiation.

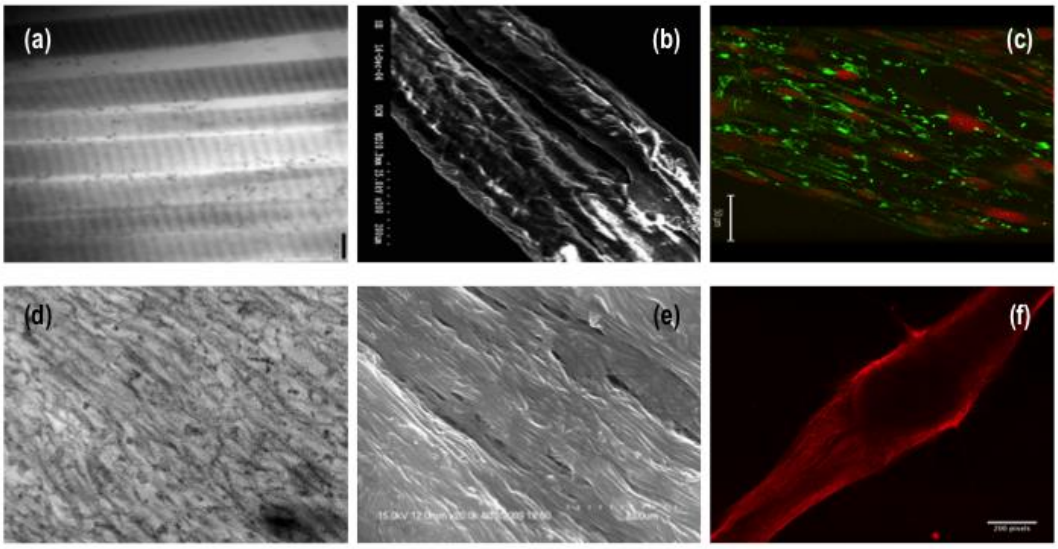

Figure 1.11: (a) TEM analyses of extruded collagen fibres (a) and isoelectric focusing produced fibres (d) illustrate bidirectional sub-fibrillar architecture and the characteristic D-periodicity of collagen. SEM analyses of extruded collagen fibres (b) and isoelectric focusing produced fibres (e) illustrate that the bidirectional sub-fibrillar architecture induces a bidirectional surface topography. This bidirectional surface topography induces bidirectional human tenocyte growth on extruded collagen fibres (c) and bidirectional rat embryonic dorsal root ganglion explants growth on isoelectric collagen fibres (f).

1.6.5 Collagen films and tubes

Isotropic collagen films, produced through evaporation, have been used extensively in biomedicine for cornea repair due to their transparent nature and the low mechanical requirement of the tissue [652]. Indicative *in vitro* data have demonstrated that collagen films with thickness of 2 μm, comparative to Bruch's membrane, supported growth of ARPE-19 cells (a retinal pigment epithelia cell line), maintained physiological cell morphology and the cells developed epithelium characteristics [653]. Collagen films, alone or in combination with gelatin or hyaluronic acid and cross-linked with carbodiimide, exhibited similar diffusion and mechanical properties to human cornea and supported growth of human corneal epithelial cells [654, 655]. Collagen films functionalized with tobramycin and cross-linked with carbodiimide, exhibited prolonged antibiotic release and human corneal epithelial cell adherence and growth [656]. Collagen films, having lamellae-like sub-structure, have been shown to support growth of stromal fibroblasts [657]. In the wound healing area, collagen films, alone [658] or functionalized with Indian Lilac tree extract [659], have been shown to maintain growth of rat epidermal cells, to withheld collagenase degradation and to reduce nitric oxide synthesis in RAW 264.7 culture. In the lung space, collagen films supported pulmonary stem cell attachment and growth [660], whilst collagen films functionalized with Ficoll™ and cross-linked with genipin supported attachment and growth of WI38 fibroblasts [243]. Given that collagen films wrapped in a single channel tubular conformation have resulted in axonal dispersion, multi-channel EDC/NHS cross-linked conduits have been used with *in vitro* data demonstrating high denaturation temperature, resistance to enzymatic degradation, maintenance of structural conformity for up to 30 days in saline solution, superior to single-channel conduits mechanical properties and unaffected neurite outgrowth of dorsal root ganglia explants [661].

In a rabbit model, collagen films functionalized with tobramycin and cross-linked with carbodiimide facilitated wound healing completion within 15 days post implantation and by month 3 neovascularization was observed [656]. Again in a rabbit model, collagen membranes functionalized with citric acid and cross-linked with carbodiimide displayed suitable tensile properties and 6 months post implantation, the implant had degraded and smooth corneal epithelial layer had been created [662]. Collagen films loaded with human growth hormone promoted wound healing in a mouse model [663], whilst when loaded with etoposide, an anticancer drug, they were

used in a liver model [664]. Tubular films, alone [661, 665] or loaded with a neurotrophin-3-encoding gene [666], have demonstrated increased axonal alignment, enhanced neovascularization, axonal regeneration and myelination in rat sciatic models. When these tubes were loaded with collagen fibres, guided Schwann cell migration, decreased axonal dispersion and reduced axonal mismatch in a rat sciatic nerve model were observed [667]. In a rabbit model, the dura was replaced with cyanamide cross-linked collagen films, which displayed very low inflammatory response and increased synthesis of new collagen by connective tissue cells that infiltrated the film by day 56 post-implantation [300].

Collagen films wrapped in form of tube have been extensively used in clinic as nerve guidance conduits (e.g. NeuraWrap™, NeuroMend™, NeuroMatrix™, NeuraGen™) [668], demonstrating limited myofibroblast infiltration, guided Schwann cell migration and axonal regrowth towards their distal targets [669, 670]. Nonetheless, such materials are limited to nerve gaps smaller than 4 cm in length [671]. Tetracycline-immobilized cross-linked collagen films have been used clinically for treatment of periodontitis and have been shown to be successful in reducing the density of microorganisms [672-674]. Collagen calcium-alginate films have been used as wound dressing to treat burn patients, demonstrating significant increase in epithelialization, while patients experienced reduced pain levels [675]. Collagen type IV films have been implanted into patients suffering from tympanic pocket retraction and demonstrated complete healing 6 months post-implantation, a potential alternative to autologous tissue [676]. Collagen films have been implanted and assessed after transvesical prostatectomy, exhibiting no adverse reactions [677]. Despite the overall promising results in multiple clinical indications, the produced films are comprised of isotropic collagen fibrils that fail to imitate the hierarchical architecture of native tissues. To this end, various technologies have been utilized to produce biomimetic anisotropic collagen films.

Subjecting collagen solutions to a magnetic field during fibrillogenesis allows development of films with aligned sub-fibrillar structure [574]. Collagen fibrils align perpendicularly to the magnetic field due to their negative diamagnetic anisotropy of the α chains [678, 679]. In general, magnetic fields of 1.9 to 12 T are applied for 30 to 90 minutes [680-684]. Multilayer magnetically aligned collagen-proteoglycans based scaffolds have been used to align human keratocytes in culture [680], whilst magnetically aligned collagen-hyaluronic acid scaffolds have been used to maintain

primary chondrocytes in culture, albeit the addition of hyaluronic acid decreased the effectiveness of magnetic alignment [681]. In the neural space, magnetically aligned collagen has been shown to orientate Schwann cells and neurons *in vitro* [682, 683] and to promote new nerve fascicle formation in a mouse sciatic nerve model [683]. It is worth pointing out that ribose-cross-linked magnetically aligned collagen scaffolds proved detrimental for regeneration [683]. Plastic compression has been incorporated into the fabrication process to increase mechanical properties and to reduce degradability, resulting in primary murine tenocyte alignment for up to 18 days in culture [684]. Given the high-cost of the superconducting magnets required to induce alignment, the use of iron oxide particles has been proposed, as this method requires magnets of low strength (0.001 T) [685, 686].

Given the complexity of the magnetic field induced alignment, micro-fabrication technologies have been adopted, which have facilitated the generation of structured collagen substrates with precise and reproducible topographical features with nano- and micro- scale resolution. Soft lithography refers to the replication of micro-features on collagen materials using a patterned elastomeric stamp (**Figure 1.12**). Soft lithography has been used for replicating grooves, holes and pillars [687, 688] and for the encapsulation of cells in single forms or multi-arrays [689]. Collagen films, casted on poly(dimethyl siloxane) templates, induced bidirectional elongation of human vascular smooth muscle cells [690-692]. Collagen injection using microfluidics into sacrificial stamps or moulds that precisely contain the structure to be reproduced has also been used as means to produce structures with features of a few microns capable of aligning cells [693, 694]. Aligned collagen films have also been produced via molecular imprinting, through the generation of high and constant shear forces during the collagen deposition on glass substrates [695-697]. Shear force is applied by lateral displacement of the injection needle and orbital spin of the collector. The set of parameters depend on the method; lateral displacement requires thin syringe needles of about 18 to 27 gauge, lateral speed of 100 mm/s and collagen flow of 0.3 ml/min approximately for orienting collagen [696, 698]. The orbital spin method requires high spinning rates of 500 to 3,000 rpm and collagen flow of 0.3 to 1.0 ml/min [697, 699]. Both molecular imprinting methods require fast collagen desiccation, less than 15 minutes, to stabilize the fibril structure and alignment. However, fibril orientation is not stable, fibrils often turn and as such, alignment is slightly altered. This difficulty can be partially solved using collagen at high concentration and reverse dialysis [696,

698]. Given that recent data have questioned the potential of structured substrates for *in vivo* applications, we expect that such structured substrates will be primarily used for *in vitro* applications (maintain cell phenotype and direct stem cell lineage) [700, 701].

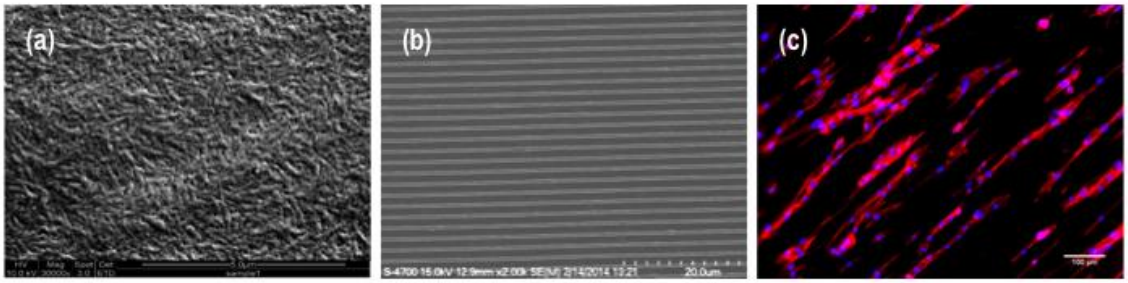

Figure 1.12: (a) SEM analysis reveals the fibrous nature of collagen films. (b) Through soft lithography, anisotropic collagen films can be produced (b), which induce bidirectional human skin fibroblast growth (c).

1.6.6 Template-produced hollow spheres

Hollow microspheres offer several advantages over other carrier systems for delivery of bioactive and therapeutic molecules including: reproducibility, large surface area, large cargo delivery capacity, controllable biodegradability and multi-cargo delivery capacity [702, 703]. In recent years, several methods including emulsion, spray-drying and micro-phase separation have been investigated for the development of collagen reservoir systems for sustained and localized delivery of drugs and biologics [704-706]. However, these techniques offer little control over reproducibility [707], which triggered investigation into the template method [707-710]. With the template method, a natural polymer is deposited on the appropriate template, which afterwards is removed, leaving behind the hollow polymeric shell [702-711]. Polymer-based templates are preferred, as they can be fabricated with controlled size, shape and dispersity [702]. Hollow collagen spheres (**Figure 1.13**) have been produced using sulphonated polystyrene beads as templates [707]. As the coating process is based on an electrostatic interaction between collagen and the negatively charged polystyrene template, polystyrene beads are sulphonated to impart a strong negative charge. The coating process is performed under acidic conditions so that the positively charged collagen forms a thin coat around the negatively charged polystyrene beads. Following sulphonation, the beads are re-suspended in acetic acid and the collagen solution is added to the beads. After formation of the collagenous coating around the polystyrene bead, the collagen is cross-linked. Finally, the polystyrene core is removed with tetrahydrofuran, leaving behind the hollow collagen sphere. To-date, such scaffolds have been used for gene [707, 712], growth factor [713] and drug [714] delivery or ROS scavenging [715, 716].

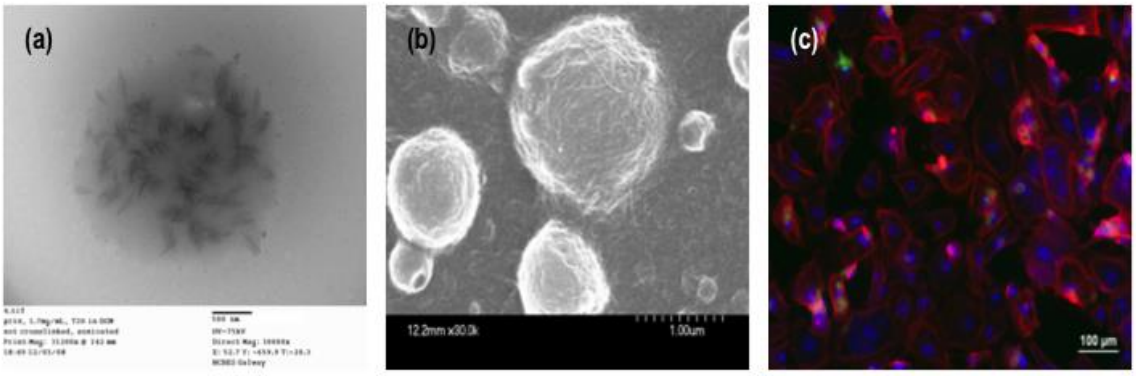

Figure 1.13: TEM (a) and SEM (b) analyses clearly illustrate the fibrous nature of hollow collagen microspheres. (c) Fluorescent microscopy of primary human cardiac fibroblasts up-taking 10 μm FITC-labelled hollow collagen type I microspheres (Red: rhodamine phalloidin, Green: FITC-labelled spheres, Blue: DAPI).

1.6.7 Tissue engineered structures

Advancements in tissue engineering technologies have enabled the development of scaffold-free tissue engineering therapies [717-719], during which a living substitute is formed that is held together with cell-cell and cell-deposited ECM contacts. Such approaches are based on the inherent capacity of cells to synthesize matrix [720-723]. Given that lysyl oxidase is a copper-dependent enzyme [724, 725], it has been suggested to add copper ions into the culture media to increase lysyl oxidase-mediated cross-linking (e.g. hydroxy pyridinoline and pyridinolines) for the mechanical improvement of tissue engineered arteries [726] and cartilage [727]. Although very promising preclinical and clinical data are available for various clinical indications, including skin [728-730], blood vessel [731-735] and cornea [736, 737], only a handful of products have been commercialized (e.g. Epicel®, Genzyme; LifeLine™, Cytograft). The substantial long culture time required to develop an implantable device (e.g. 70 days for lung cell-sheet [738], 84 days for corneal stromal [739, 740] and 196 days for blood vessel [733]) has been recognized as the major limitation for the wide acceptance of this technology. To remedy this, macromolecular crowding has been introduced as means to accelerate ECM deposition (**Figure 1.14**). *In vivo* cells reside in a highly crowded extracellular space, which results in rapid conversion of the *de novo* water soluble procollagen to water insoluble collagen [62]. In the dilute culture media, this procollagen / collagen conversion is very slow. The addition of inert macromolecules into the culture media, by emulating the naturally crowded *in vivo* milieu, amplifies deposition of cell-secreted ECM [741, 742]. Polydispersed macromolecules have been shown to be more effective with respect to ECM deposition, due to more efficient volume exclusion effect [743]. To-date, macromolecular crowding has been shown to enhance ECM deposition in permanently differentiated cell culture [744-748] and in naïve stem cell culture [749-751] and to enhance adipogenesis in adipose-induced stem cell culture [752]. Macromolecular crowding has also been proposed as means to develop *in vitro* pathophysiology models [753-755]. Further, human fibroblast matrices, developed under macromolecular crowding conditions, have been shown to support stable propagation of human embryonic stem cells *ex vivo* [756]. Such system can be used as an alternative to Matrigel®, a cell-produced material (murine in origin, derived from the Engelbreth-Holm-Swarm sarcoma cell line [167]) rich in laminin, collagen IV, heparin sulphate

proteoglycans and a number of growth factors that has been used extensively for optimal *ex vivo* cell growth [757-760].

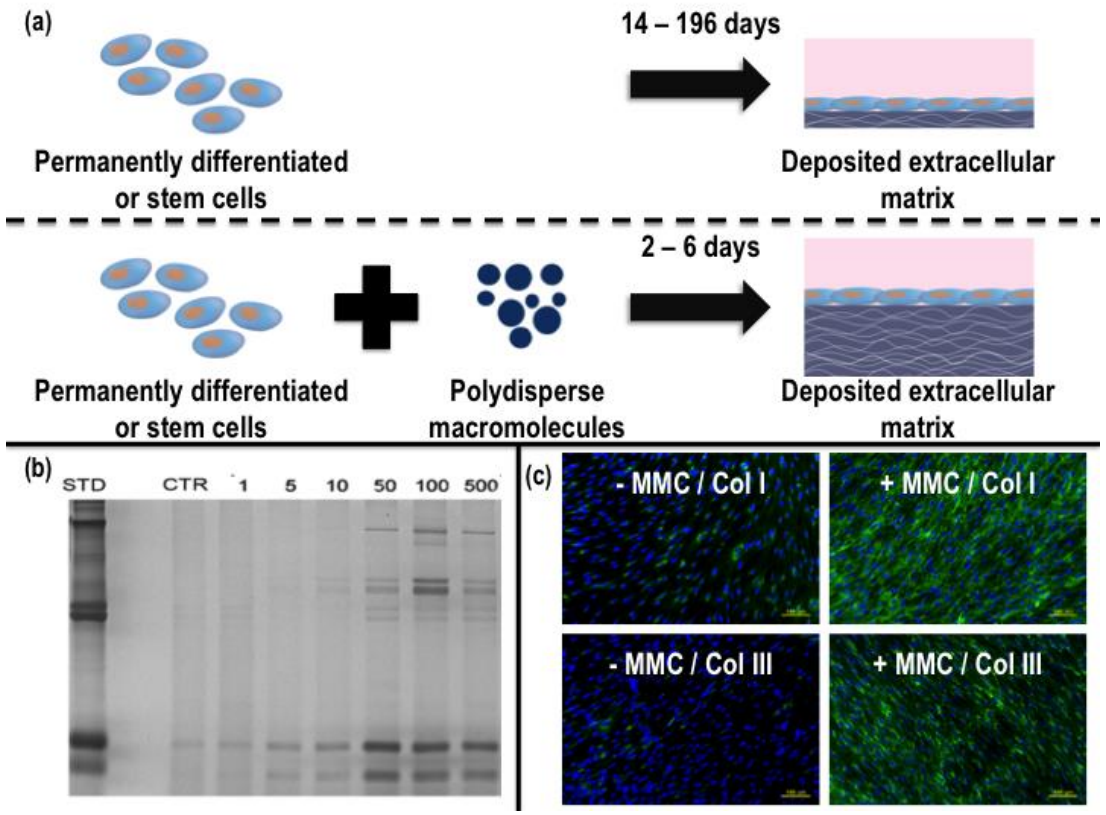

Figure 1.14: (a) In normal permanently differentiated and stem cell culture, ECM deposition is very slow and as such the production of living substitutes can take up to 196 days. The addition of polydispersed macromolecules (macromolecular crowding) in culture media dramatically accelerates ECM deposition and living substitutes can be produced within 6 days in culture. (b) SDS-PAGE analysis of human bone marrow mesenchymal stem cell layers demonstrates that ECM deposition is dramatically enhanced as a function of carrageenan concentration (1, 5, 10, 50, 100 and 500 μg/ml) after 2 days in culture. (c) Immunocytochemistry analysis further corroborates the enhanced collagen type I and collagen type III deposition after 2 days in culture [Cells: human bone marrow mesenchymal stem cells; Macromolecular Crowder (MMC): 100 μg/ml carrageenan].

1.7 Project rationale and hypotheses

Collagen (and in particular collagen type I) for biomedical applications is extracted from a wide range of land and marine animals and tissues. It is interesting to note that resultant collagen type I scaffolds (even when extracted from the same species, using the same extraction protocol) have substantially different structural, biomechanical, biochemical and biological properties. As a direct consequence of this, in clinical practice collagen-based devices exhibit inconsistent therapeutic efficiency. Herein, for very first time, a systematic approach is employed to assess the influence of species, tissue, gender and cross-linking on the properties of collagen type I devices. The work is divided in three phases, as briefly described below.

Phase 1: Chapter 2

Aim: To assess the influence of the extracted collagen type I from different species (porcine and bovine), tissues (skin and tendon) and genders (male and female) on the structural, biophysical, biochemical and biological properties of collagen type I sponges.

Hypothesis: The properties of collagen-based devices are dependent on species / tissue / gender from which the collagen was extracted from.

Objectives:

- To extract, purify and characterise collagen type I from different species, tissues and genders.
- To fabricate collagen type I sponges and to assess structural (scanning electron microscopy), biochemical (ninhydrin), thermal (differential scanning calorimetry), biophysical (mechanical) and biological (collagenase) properties of the produced sponges.
- To assess biological effect of the produced collagen type I sponges on human dermal fibroblasts and human tenocytes.

Phase 2: Chapter 3

Aim: To assess whether collagen retains tissue memory by analysing the influence of tendon and skin extracted collagen type I on the structural, biophysical, biochemical and biological properties of collagen type I sponges.

Hypothesis: Tenogenic phenotype can be maintained in culture for longer on tendon- than skin- derived collagen sponges.

Objectives:

- To optimise the production of collagen type I sponges from bovine female tendon and skin, using different cross-linking densities (4-arm polyethylene glycol succinimidyl glutarate).
- To assess the structural (scanning electron microscopy), biochemical (ninhydrin), thermal (differential scanning calorimetry), biophysical (mechanical) and biological (collagenase) properties of the produced sponges.
- To assess the biological effect of the produced collagen type I sponges on human dermal fibroblasts and human tenocytes.
- To assess the deposition of extracellular matrix molecules (collagen type I, II, III, IV, V, VI, fibronectin, scleraxis, tenomodulin, aggrecan, osteocalcin and osteopontin) by human tenocytes on the produced collagen type I sponges.
- To assess gene expression of tenogenic, chondrogenic and osteogenic markers (qPCR).

Phase 3: Chapter 4

Aim: To develop optimally cross-linked collagen fibres using 4-arm polyethylene glycol succinimidyl glutarate system that will increase the thermal properties, mechanical properties and resistance to enzymatic degradation, without compromising cellular function.

Hypothesis: Optimal 4-arm polyethylene glycol succinimidyl glutarate concentration will provide collagen fibres with increased mechanical, thermal and enzymatic resistance properties, whilst maintaining the anisotropic nano-texture surface topography and cell function.

Objectives:

- To optimise the production of collagen type I fibres, using different cross-linkers and cross-linking densities (4-arm polyethylene glycol succinimidyl glutarate, glutaraldehyde, ethyl-3-[3-dimethylamino-propyl] carbodiimide).
- To assess the structural (scanning electron microscopy, polarised microscopy), biochemical (ninhydrin), thermal (differential scanning calorimetry), biophysical (mechanical) and biological (collagenase) properties of the produced fibres.
- To assess biological effect of the produced collagen type I fibres with human dermal fibroblasts and human tenocytes.

1.8 References

[1] S.D. Gorham, Collagen, in: D. Byrom (Ed.), Biomaterials. Novel materials from biological sources, Macmillan Publishers Ltd and ICI Biological Products Business, New York, 1991, pp. 55-122.

[2] N. Parenteau, Skin: The first tissue-engineered products, Sci Am 280(4) (1999) 83-84.

[3] J. Huxley-Jones, D.L. Robertson, R.P. Boot-Handford, On the origins of the extracellular matrix in vertebrates, Matrix Biol 26(1) (2007) 2-11.

[4] R.N. Granito, M.R. Custodio, A.C.M. Renno, Natural marine sponges for bone tissue engineering: The state of art and future perspectives, J Biomed Mater Res B 105(6) (2017) 1717-1727.

[5] K.A. Piez, Collagens, in: K. JI (Ed.), Encyclopedia of Polymer Science and Engineering, New York: Wiley1985, pp. 699-727.

[6] S. Viguet-Carrin, P. Garnero, P.D. Delmas, The role of collagen in bone strength, Osteoporos Int 17(3) (2006) 319-336.

[7] M.K. Gordon, R.A. Hahn, Collagens, Cell Tissue Res 339(1) (2010) 247-257.

[8] J. Gross, F.O. Schmitt, The structure of human skin collagen as studied with the electron microscope, J Exp Med 88(5) (1948) 555-568.

[9] D.R. Baselt, J.P. Revel, J.D. Baldeschwieler, Subfibrillar structure of type I collagen observed by atomic force microscopy, Biophys J 65(6) (1993) 2644-2655.

[10] M. Gale, M.S. Pollanen, P. Markiewicz, M.C. Goh, Sequential assembly of collagen revealed by atomic force microscopy, Biophys J 68(5) (1995) 2124-2128.

[11] L. Penuela, C. Negro, M. Massa, E. Repaci, E. Cozzani, A. Parodi, S. Scaglione, R. Quarto, R. Raiteri, Atomic force microscopy for biomechanical and structural analysis of human dermis: A complementary tool for medical diagnosis and therapy monitoring, Exp Dermatol 27(2) (2017) 150-155.

[12] M. Koch, J.E. Foley, R. Hahn, P. Zhou, R.E. Burgeson, D.R. Gerecke, M.K. Gordon, α1 (XX) collagen, a new member of the collagen subfamily, fibril-associated collagens with interrupted triple helices, J Biol Chem 276(25) (2001) 23120-23126.

[13] D. Tuckwell, Identification and analysis of collagen α1 (XXI), a novel member of the FACIT collagen family, Matrix Biol 21(1) (2002) 63-66.

[14] J. Fitzgerald, J.F. Bateman, A new FACIT of the collagen family: COL21A1, FEBS Lett 505(2) (2001) 275-280.

[15] K. Sato, K. Yomogida, T. Wada, T. Yorihuzi, Y. Nishimune, N. Hosokawa, K. Nagata, Type XXVI collagen, a new member of the collagen family, is specifically expressed in the testis and ovary, J Biol Chem 277(40) (2002) 37678-37684.

[16] S. Ricard-Blum, F. Ruggiero, The collagen superfamily: From the extracellular matrix to the cell membrane, Pathol Biol 53(7) (2005) 430-442.

[17] C.M. Kielty, M.E. Grant, The collagen family: Structure, assembly, and organization in the extracellular matrix, in: P. Royce, B. Steinmann (Eds.), Connective Tissue and Its Heritable Disorders: Molecular, Genetic, and Medical Aspects, John Wiley & Sons, Inc., Hoboken, NJ, USA, 2002, pp. 159-221.

[18] D.I. Zeugolis, M. Raghunath, Collagen: Materials analysis and implant uses, in: P. Ducheyne, K. Healy, D. Hutmacher, D. Grainger, J. Kirkpatrick (Eds.), Comprehensive Biomaterials, Elsevier, Oxford, 2011, pp. 261-278.

[19] D.J.S. Hulmes, Building collagen molecules, fibrils, and suprafibrillar structures, J Struct Biol 137(1-2) (2002) 2-10.

[20] A.J. Bailey, R.G. Paul, L. Knott, Mechanisms of maturation and ageing of collagen, Mech Ageing Dev 106(1-2) (1998) 1-56.

[21] M. van der Rest, R. Garrone, D. Herbage, Collagen: A family of proteins with many facets, in: H.K. Kleinman (Ed.), Advances in Molecular and Cell Biology, JAI Press Inc1993, pp. 1-67.

[22] J.A.M. Ramshaw, J.A. Werkmeister, V. Glattauer, Collagen-based biomaterials, Biotechnol Genet Eng Rev 13(1) (1995) 335-382.

[23] A.J. Bailey, Procter memorial lecture: Collagen - Nature`s framework in the medical, food and leather industries, J Soc Leath Tech Ch 76(4) (1992) 111-127.

[24] A.J. Bailey, R.G. Paul, Collagen: A not so simple protein, J Soc Leath Tech Ch 82(3) (1998) 104-110.

[25] D.J.S. Hulmes, The collagen superfamily -- Diverse structures and assemblies, Essayes Biochem 27 (1992) 49-67.

[26] J.M. Pace, M. Corrado, C. Missero, P.H. Byers, Identification, characterization and expression analysis of a new fibrillar collagen gene, COL27A1, Matrix Biol 22(1) (2003) 3-14.

[27] E. Jenkins, J.B. Moss, J.M. Pace, L.C. Bridgewater, The new collagen gene COL27A1 contains SOX9-responsive enhancer elements, Matrix Biol 24(3) (2005) 177-184.

[28] U.K. Blaschke, E.F. Eikenberry, D.J. Hulmes, H.J. Galla, P. Bruckner, Collagen XI nucleates self-assembly and limits lateral growth of cartilage fibrils, J Biol Chem 275(14) (2000) 10370-10378.

[29] E. Adachi, T. Hayashi, P.H. Hashimoto, Immunoelectron microscopical evidence that type V collagen is a fibrillar collagen: Importance for an aggregating capability of the preparation for reconstituting banding fibrils, Matrix 9(3) (1989) 232-237.

[30] K. Dreisewerd, A. Rohlfing, B. Spottke, C. Urbanke, W. Henkel, Characterization of whole fibril-forming collagen proteins of types I, III, and V from fetal calf skin by infrared matrix-assisted laser desorption ionization mass spectrometry, Anal Chem 76(13) (2004) 3482-3491.

[31] R. Naffa, G. Holmes, M. Ahn, D. Harding, G. Norris, Liquid chromatography-electrospray ionization mass spectrometry for the simultaneous quantitation of collagen and elastin crosslinks, J Chromatogr A 1478 (2016) 60-67.

[32] L. Mourino-Alvarez, I. Iloro, F. de la Cuesta, M. Azkargorta, T. Sastre-Oliva, I. Escobes, L.F. Lopez-Almodovar, P.L. Sanchez, H. Urreta, F. Fernandez-Aviles, A. Pinto, L.R. Padial, F. Akerstrom, F. Elortza, M.G. Barderas, MALDI-Imaging Mass Spectrometry: a step forward in the anatomopathological characterization of stenotic aortic valve tissue, Sci Rep 6 (2016) 27106.

[33] M. Raghunath, P. Bruckner, B. Steinmann, Delayed triple helix formation of mutant collagen from patients with osteogenesis imperfecta, J Mol Biol 236(3) (1994) 940-949.

[34] T. Koide, K. Nagata, Collagen biosynthesis, Top Curr Chem 247 (2005) 85-114.

[35] J. Engel, D.J. Prockop, The zipper-like folding of collagen triple helices and the effects of mutations that disrupt the zipper, Annu Rev Biophys Biophys Chem 20 (1991) 137-152.

[36] D.J. Hulmes, Collagen diversity, synthesis and assembly, Collagen springer US (2008) 15-47.

[37] P.L. Privalov, E.I. Tiktopulo, V.M. Tischenko, Stability and mobility of the collagen structure, J Mol Biol 127(2) (1979) 203-216.

[38] T.V. Burjanadze, New analysis of the phylogenetic change of collagen thermostability, Biopolymers 53(6) (2000) 523-538.

[39] T. Pihlajaniemi, R. Myllylä, K.I. Kivirikko, Prolyl 4-hydroxylase and its role in collagen synthesis, J Hepatol 13(Suppl3) (1991) S2-S7.

[40] K. Mizuno, S. Boudko, J. Engel, H.P. Bachinger, Vascular Ehlers-Danlos syndrome mutations in type III collagen differently stall the triple helical folding, J Biol Chem 288(26) (2013) 19166-19176.
[41] D.M. Hudson, R. Werther, M. Weis, J.J. Wu, D.R. Eyre, Evolutionary origins of C-terminal (GPP)n 3-hydroxyproline formation in vertebrate tendon collagen, PLoS One 9(4) (2014) e93467.
[42] S.K. Holmgren, K.M. Taylor, L.E. Bretscher, R.T. Raines, Code for collagen's stability deciphered, Nature 392(6677) (1998) 666-667.
[43] S.K. Holmgren, L.E. Bretscher, K.M. Taylor, R.T. Raines, A hyperstable collagen mimic, Chem Biol 6(2) (1999) 63-70.
[44] I. Saha, N. Shamala, Investigating proline puckering states in diproline segments in proteins, Biopolymers 99(9) (2013) 605-610.
[45] M.D. Shoulders, R.T. Raines, Interstrand dipole-dipole interactions can stabilize the collagen triple helix, J Biol Chem 286(26) (2011) 22905-22912.
[46] B. Brodsky, A.V. Persikov, Molecular structure of the collagen triple helix, Adv Protein Chem 70 (2005) 301-339.
[47] J.G. Bann, D.H. Peyton, H.P. Bachinger, Sweet is stable: Glycosylation stabilizes collagen, FEBS Lett 473(2) (2000) 237-240.
[48] A. Mohs, T. Silva, T. Yoshida, R. Amin, S. Lukomski, M. Inouye, B. Brodsky, Mechanism of stabilization of a bacterial collagen triple helix in the absence of hydroxyproline, J Biol Chem 282(41) (2007) 29757-29765.
[49] B. Brodsky, J.A. Ramshaw, Bioengineered Collagens, Subcell Biochem 82 (2017) 601-629.
[50] J. Heikkinen, M. Risteli, C. Wang, J. Latvala, M. Rossi, M. Valtavaara, R. Myllyla, Lysyl hydroxylase 3 is a multifunctional protein possessing collagen glucosyltransferase activity, J Biol Chem 275(46) (2000) 36158-36163.
[51] M. Sricholpech, I. Perdivara, M. Yokoyama, H. Nagaoka, M. Terajima, K.B. Tomer, M. Yamauchi, Lysyl hydroxylase 3-mediated glucosylation in type I collagen: Molecular loci and biological significance, J Biol Chem 287(27) (2012) 22998-3009.
[52] C.C. Clark, The distribution and initial characterization of oligosaccharide units on the COOH-terminal propeptide extensions of the pro-alpha 1 and pro-alpha 2 chains of type I procollagen, J Biol Chem 254(21) (1979) 10798-10802.
[53] J.H. Waite, X.X. Qin, K.J. Coyne, The peculiar collagens of mussel byssus, Matrix Biol 17(2) (1998) 93-106.

[54] M. Tasab, M.R. Batten, N.J. Bulleid, Hsp47: A molecular chaperone that interacts with and stabilizes correctly-folded procollagen, EMBO J 19(10) (2000) 2204-2211.

[55] R. Wilson, J.F. Lees, N.J. Bulleid, Protein disulphide isomerase acts as a molecular chaperone during the assembly of procollagen, J Biol Chem 273(16) (1998) 9637-9643.

[56] M.J. Bottomley, M.R. Batten, R.A. Lumb, N.J. Bulleid, Quality control in the endoplasmic reticulum: PDI mediates the ER retention of unassembled procollagen C-propeptides, Curr Biol 11(14) (2001) 1114-1118.

[57] E. Kessler, K. Takahara, L. Biniaminov, M. Brusel, D.S. Greenspan, Bone morphogenetic protein-1: The type I procollagen C-proteinase, Science 271(5247) (1996) 360-362.

[58] S. Vadon-Le Goff, D.J. Hulmes, C. Moali, BMP-1/tolloid-like proteinases synchronize matrix assembly with growth factor activation to promote morphogenesis and tissue remodeling, Matrix Biol 44 (2015) 14-23.

[59] C. Broder, P. Arnold, S. Vadon-Le Goff, M.A. Konerding, K. Bahr, S. Muller, C.M. Overall, J.S. Bond, T. Koudelka, A. Tholey, D.J. Hulmes, C. Moali, C. Becker-Pauly, Metalloproteases meprin alpha and meprin beta are C- and N-procollagen proteinases important for collagen assembly and tensile strength, Proc Natl Acad Sci U S A 110(35) (2013) 14219-14224.

[60] C.H. Wu, C.B. Donovan, G.Y. Wu, Evidence for pretranslational regulation of collagen synthesis by procollagen propeptides, J Biol Chem 261(23) (1986) 10482-10484.

[61] R.S. Aycock, R. Raghow, G.P. Stricklin, J.M. Seyer, A.H. Kang, Post-transcriptional inhibition of collagen and fibronectin synthesis by a synthetic homolog of a portion of the carboxyl-terminal propeptide of human type I collagen, J Biol Chem 261(30) (1986) 14355-14360.

[62] E.G. Canty, K.E. Kadler, Procollagen trafficking, processing and fibrillogenesis, J Cell Sci 118(7) (2005) 1341-1353.

[63] C.C. Banos, A.H. Thomas, C.K. Kuo, Collagen fibrillogenesis in tendon development: Current models and regulation of fibril assembly, Birth Defects Res C 84(3) (2008) 228-244.

[64] Y. Mao, J.E. Schwarzbauer, Fibronectin fibrillogenesis, a cell-mediated matrix assembly process, Matrix Biol 24(6) (2005) 389-399.

[65] K.E. Kadler, A. Hill, E.G. Canty-Laird, Collagen fibrillogenesis: Fibronectin, integrins, and minor collagens as organizers and nucleators, Curr Opin Cell Biol 20(5) (2008) 495-501.
[66] M. Raspanti, M. Reguzzoni, M. Protasoni, P. Basso, Not only tendons: The other architecture of collagen fibrils, Int J Biol Macromol 107(Pt B) (2018) 1668-1674.
[67] S. Chen, M.J. Mienaltowski, D.E. Birk, Regulation of corneal stroma extracellular matrix assembly, Exp Eye Res 133 (2015) 69-80.
[68] A.J. Quantock, M. Winkler, G.J. Parfitt, R.D. Young, D.J. Brown, C. Boote, J.V. Jester, From nano to macro: Studying the hierarchical structure of the corneal extracellular matrix, Exp Eye Res 133 (2015) 81-99.
[69] T.J. Wess, Collagen fibril form and function, Adv Protein Chem 70 (2005) 341-374.
[70] D.J. Hulmes, T.J. Wess, D.J. Prockop, P. Fratzl, Radial packing, order, and disorder in collagen fibrils, Biophys J 68(5) (1995) 1661-1670.
[71] J. Bohr, K. Olsen, The ancient art of laying rope, EPL 93(6) (2011) 60004.
[72] M.C. Branchet, S. Boisnic, C. Frances, C. Lesty, L. Robert, Morphometric analysis of dermal collagen-fibers in normal human skin as a function of age, Arch Gerontol Geriat 13(1) (1991) 1-14.
[73] L.I. Smith-Mungo, H.M. Kagan, Lysyl oxidase: Properties, regulation and multiple functions in biology, Matrix Biol 16(7) (1998) 387-398.
[74] M. Yamauchi, Y. Taga, S. Hattori, M. Shiiba, M. Terajima, Analysis of collagen and elastin cross-links, Methods Cell Biol 143 (2018) 115-132.
[75] A.J. Bailey, N.D. Light, E.D. Atkins, Chemical cross-linking restrictions on models for the molecular organization of the collagen fibre, Nature 288(5789) (1980) 408-410.
[76] A.J. Bailey, M.S. Shimokomaki, Age related changes in the reducible cross-links of collagen, FEBS Lett 16(2) (1971) 86-88.
[77] H. Oxlund, L. Mosekilde, G. Ortoft, Reduced concentration of collagen reducible cross links in human trabecular bone with respect to age and osteoporosis, Bone 19(5) (1996) 479-484.
[78] S. Ribel-Madsen, S. Christgau, S.T. Gronemann, E.M. Bartels, B. Danneskiold-Samsoe, H. Bliddal, Urinary markers of altered collagen metabolism in fibromyalgia patients, Scand J Rheumatol 36(6) (2007) 470-477.

[79] C.C. Chan, O.S. Tang, W.N. Lau, G.W. Tang, Bone turnover in young hypoestrogenic women on hormonal therapy, Eur J Obstet Gynecol Reprod Biol 124(2) (2006) 204-206.

[80] C.I. Tan, G.N. Kent, A.G. Randall, S.J. Edmondston, K.P. Singer, Age-related changes in collagen, pyridinoline, and deoxypyridinoline in normal human thoracic intervertebral discs, J Gerontol A Biol Sci Med Sci 58(5) (2003) B387-B393.

[81] D.R. Eyre, M.A. Weis, J.J. Wu, Maturation of collagen ketoimine cross-links by an alternative mechanism to pyridinoline formation in cartilage, J Biol Chem 285(22) (2010) 16675-16682.

[82] A. Gautieri, F.S. Passini, U. Silvan, M. Guizar-Sicairos, G. Carimati, P. Volpi, M. Moretti, H. Schoenhuber, A. Redaelli, M. Berli, J.G. Snedeker, Advanced glycation end-products: Mechanics of aged collagen from molecule to tissue, Matrix Biol 59 (2017) 95-108.

[83] V.M. Monnier, R.R. Kohn, A. Cerami, Accelerated age-related browning of human collagen in diabetes mellitus, Proc Natl Acad Sci U S A 81(2) (1984) 583-587.

[84] R.G. Paul, A.J. Bailey, The effect of advanced glycation end-product formation upon cell-matrix interactions, Int J Biochem Cell Biol 31(6) (1999) 653-660.

[85] C.J. Mentink, M. Hendriks, A.A. Levels, B.H. Wolffenbuttel, Glucose-mediated cross-linking of collagen in rat tendon and skin, Clin Chim Acta 321(1-2) (2002) 69-76.

[86] V.M. Monnier, D.R. Sell, X. Wu, K. Rutter, The prospects of health and longevity from the inhibition of the Maillard reaction in vivo, Int Congr Ser 1245(0) (2002) 9-19.

[87] V.M. Monnier, Intervention against the Maillard reaction in vivo, Arch Biochem Biophys 419(1) (2003) 1-15.

[88] M. Raghunath, B. Hopfner, D. Aeschlimann, U. Luthi, M. Meuli, S. Altermatt, R. Gobet, L. Bruckner-Tuderman, B. Steinmann, Cross-linking of the dermo-epidermal junction of skin regenerating from keratinocyte autografts. Anchoring fibrils are a target for tissue transglutaminase, J Clin Invest 98(5) (1996) 1174-1184.

[89] V. Kuttner, C. Mack, C. Gretzmeier, L. Bruckner-Tuderman, J. Dengjel, Loss of collagen VII is associated with reduced transglutaminase 2 abundance and activity, J Invest Dermatol 134(9) (2014) 2381-2389.

[90] P. Strop, Versatility of microbial transglutaminase, Bioconjug Chem 25(5) (2014) 855-862.

[91] M. Kieliszek, A. Misiewicz, Microbial transglutaminase and its application in the food industry. A review, Folia Microbiol 59(3) (2014) 241-250.

[92] D. Aeschlimann, V. Thomazy, Protein crosslinking in assembly and remodelling of extracellular matrices: The role of transglutaminases, Connect Tissue Res 41(1) (2000) 1-27.

[93] S. Beninati, M. Piacentini, The transglutaminase family: An overview: Minireview article, Amino Acids 26(4) (2004) 367-372.

[94] S. Del Duca, E. Verderio, D. Serafini-Fracassini, R. Iorio, G. Cai, The plant extracellular transglutaminase: What mammal analogues tell, Amino Acids 46(3) (2014) 777-792.

[95] G. Wisowski, E.M. Kozma, T. Bielecki, A. Pudelko, K. Olczyk, Dermatan sulfate is a player in the transglutaminase 2 interaction network, PLoS One 12(2) (2017) e0172263.

[96] R.L. Eckert, M.T. Kaartinen, M. Nurminskaya, A.M. Belkin, G. Colak, G.V. Johnson, K. Mehta, Transglutaminase regulation of cell function, Physiol Rev 94(2) (2014) 383-417.

[97] J.J. Pisano, J.S. Finlayson, M.P. Peyton, Y. Nagai, ε-(γ-Glutamyl)lysine in fibrin: Lack of crosslink formation in factor XIII deficiency, Proc Natl Acad Sci U S A 68(4) (1971) 770-772.

[98] J.J. Pisano, J.S. Finlayson, M.P. Peyton, Cross-link in fibrin polymerized by factor XIII: ε-(γ-Glutamyl)lysine, Science 160(3830) (1968) 892-893.

[99] J.J. Pisano, J.S. Finlayson, M.P. Peyton, Chemical and enzymic detection of protein cross-links. Measurement of epsilon-(gamma-glutamyl)lysine in fibrin polymerized by factor XIII, Biochemistry 8(3) (1969) 871-876.

[100] M. Raghunath, H.C. Hennies, F. Velten, V. Wiebe, P.M. Steinert, A. Reis, H. Traupe, A novel in situ method for the detection of deficient transglutaminase activity in the skin, Arch Dermatol Res 290(11) (1998) 621-627.

[101] M. Raghunath, R. Cankay, U. Kubitscheck, J.D. Fauteck, R. Mayne, D. Aeschlimann, U. Schlotzer-Schrehardt, Transglutaminase activity in the eye: Cross-linking in epithelia and connective tissue structures, Invest Ophthalmol Vis Sci 40(12) (1999) 2780-2787.

[102] D.I. Zeugolis, P.P. Panengad, E.S. Yew, C. Sheppard, T.T. Phan, M. Raghunath, An in situ and in vitro investigation for the transglutaminase potential in tissue engineering, J Biomed Mater Res A 92(4) (2010) 1310-1320.

[103] F. Netzlaff, C.M. Lehr, P.W. Wertz, U.F. Schaefer, The human epidermis models EpiSkin, SkinEthic and EpiDerm: An evaluation of morphology and their suitability for testing phototoxicity, irritancy, corrosivity, and substance transport, Eur J Pharm Biopharm 60(2) (2005) 167-178.

[104] N. Alépée, M.H. Grandidier, J. Cotovio, O.f.E.C.-o.a. Development, Sub-categorisation of skin corrosive chemicals by the EpiSkin™ reconstructed human epidermis skin corrosion test method according to UN GHS: Revision of OECD Test Guideline 431, Toxicol In Vitro 28(2) (2014) 131-145.

[105] R. Roguet, C. Cohen, K.G. Dossou, A. Rougier, Episkin, a reconstituted human epidermis for assessing in vitro the irritancy of topically applied compounds, Toxicol In Vitro 8(2) (1994) 283-291.

[106] F. Hao, X. Jin, Q.S. Liu, Q. Zhou, G. Jiang, Epidermal penetration of gold nanoparticles and its underlying mechanism based on human reconstructed 3D Episkin model, ACS Appl Mater Interfaces 9(49) (2017) 42577-42588.

[107] T. Nagai, N. Suzuki, Isolation of collagen from fish waste material - Skin, bone and fins, Food Chem 68(3) (2000) 277-281.

[108] J.H. Hwang, S. Mizuta, Y. Yokoyama, R. Yoshinaka, Purification and characterization of molecular species of collagen in the skin of skate (Raja kenojei), Food Chem 100(3) (2007) 921-925.

[109] E. Song, S.Y. Kim, T. Chun, H.J. Byun, Y.M. Lee, Collagen scaffolds derived from a marine source and their biocompatibility, Biomaterials 27(15) (2006) 2951-2961.

[110] S. Yunoki, N. Nagai, T. Suzuki, M. Munekata, Novel biomaterial from reinforced salmon collagen gel prepared by fibril formation and cross-linking, J Biosci Bioeng 98(1) (2004) 40-47.

[111] D. Arola, S. Murcia, M. Stossel, R. Pahuja, T. Linley, A. Devaraj, M. Ramulu, E.A. Ossa, J. Wang, The limiting layer of fish scales: Structure and properties, Acta Biomater 67 (2017) 319-330.

[112] A.M. Mullen, C. Alvarez, D.I. Zeugolis, M. Henchion, E. O'Neill, L. Drummond, Alternative uses for co-products: Harnessing the potential of valuable compounds from meat processing chains, Meat Sci 132 (2017) 90-98.

[113] D. Swatschek, W. Schatton, J. Kellermann, W.E. Muller, J. Kreuter, Marine sponge collagen: Isolation, characterization and effects on the skin parameters surface-pH, moisture and sebum, Eur J Pharm Biopharm 53(1) (2002) 107-113.

[114] D. Swatschek, W. Schatton, W. Muller, J. Kreuter, Microparticles derived from marine sponge collagen (SCMPs): Preparation, characterization and suitability for dermal delivery of all-trans retinol, Eur J Pharm Biopharm 54(2) (2002) 125-133.
[115] Z. Lin, K.L. Solomon, X. Zhang, N.J. Pavlos, T. Abel, C. Willers, K. Dai, J. Xu, Q. Zheng, M. Zheng, In vitro evaluation of natural marine sponge collagen as a scaffold for bone tissue engineering, Int J Biol Sci 7(7) (2011) 968-977.
[116] W. Friess, Collagen -- Biomaterial for drug delivery, Eur J Pharm Biopharm 45(2) (1998) 113-136.
[117] D.I. Zeugolis, R.G. Paul, G. Attenburrow, Factors influencing the properties of reconstituted collagen fibers prior to self-assembly: Animal species and collagen extraction method, J Biomed Mater Res A 86A(4) (2008) 892-904.
[118] S. Nalinanon, S. Benjakul, W. Visessanguan, H. Kishimura, Use of pepsin for collagen extraction from the skin of bigeye snapper (Priacanthus tayenus), Food Chem 104(2) (2007) 593-601.
[119] E. Skierka, M. Sadowska, The influence of different acids and pepsin on the extractability of collagen from the skin of Baltic cod (Gadus morhua), Food Chem 105(3) (2007) 1302-1306.
[120] C.C. Danielsen, Thermal stability of reconstituted collagen fibrils. Shrinkage characteristics upon in vitro maturation, Mech Ageing Dev 15(3) (1981) 269-278.
[121] B.J. Rigby, Relation between the shrinkage of native collagen in acid solution and the melting temperature of the tropocollagen molecule, Biochim Biophys Acta 133(2) (1967) 272-277.
[122] R.L. Trelstad, Human aorta collagens: Evidence for three distinct species, Biochem Biophys Res Commun 57(3) (1974) 717-725.
[123] D.W. Bannister, A.B. Burns, Pepsin treatment of avian skin collagen. Effects on solubility, subunit composition and aggregation properties, Biochem J 129(3) (1972) 677-681.
[124] L.M. Delgado, N. Shologu, K. Fuller, D.I. Zeugolis, Acetic acid and pepsin result in high yield, high purity and low macrophage response collagen for biomedical applications, Biomed Mater 12(6) (2017) 065009.
[125] P. Bruckner, D.J. Prockop, Proteolytic-enzymes as probes for the triple-helical conformation of procollagen, Anal Biochem 110(2) (1981) 360-368.

[126] G.C. Na, L.J. Butz, D.G. Bailey, R.J. Carroll, In vitro collagen fibril assembly in glycerol solution: Evidence for a helical cooperative mechanism involving microfibrils, Biochemistry 25(5) (1986) 958-966.
[127] R.A. Gelman, D.C. Poppke, K.A. Piez, Collagen fibril formation in vitro. The role of the nonhelical terminal regions, J Biol Chem 254(22) (1979) 11741-11745.
[128] H. Ishikawa, T. Koshino, R. Takeuchi, T. Saito, Effects of collagen gel mixed with hydroxyapatite powder on interface between newly formed bone and grafted achilles tendon in rabbit femoral bone tunnel, Biomaterials 22(12) (2001) 1689-1694.
[129] M.I. Alam, I. Asahina, K. Ohmamiuda, K. Takahashi, S. Yokota, S. Enomoto, Evaluation of ceramics composed of different hydroxyapatite to tricalcium phosphate ratios as carriers for rhBMP-2, Biomaterials 22(12) (2001) 1643-1651.
[130] N. Yamada, N. Shioya, Y. Kuroyanagi, Evaluation of an allogeneic cultured dermal substitute composed of fibroblasts within a spongy collagen matrix as a wound dressing, Scand J Plast Reconstr Surg Hand Surg 29(3) (1995) 211-219.
[131] F.Y. Hsu, S.C. Chueh, Y.J. Wang, Microspheres of hydroxyapatite/reconstituted collagen as supports for osteoblast cell growth, Biomaterials 20(20) (1999) 1931-1936.
[132] C.V. Rodrigues, P. Serricella, A.B. Linhares, R.M. Guerdes, R. Borojevic, M.A. Rossi, M.E. Duarte, M. Farina, Characterization of a bovine collagen-hydroxyapatite composite scaffold for bone tissue engineering, Biomaterials 24(27) (2003) 4987-4997.
[133] J. Rosenblatt, W. Rhee, D. Wallace, The effect of collagen fiber size distribution on the release rate of proteins from collagen matrices by diffusion, J Control Release 9(3) (1989) 195-203.
[134] J. Rosenblatt, B. Devereux, D.G. Wallace, Injectable collagen as a ph-sensitive hydrogel, Biomaterials 15(12) (1994) 985-995.
[135] M.R. Wells, K. Kraus, D.K. Batter, D.G. Blunt, J. Weremowitz, S.E. Lynch, H.N. Antoniades, H.A. Hansson, Gel matrix vehicles for growth factor application in nerve gap injuries repaired with tubes: A comparison of biomatrix, collagen, and methylcellulose, Exp Neurol 146(2) (1997) 395-402.
[136] A.K. Lynn, I.V. Yannas, W. Bonfield, Antigenicity and immunogenicity of collagen, J Biomed Mater Res B 71B(2) (2004) 343-354.
[137] D.E. Trentham, A.S. Townes, A.H. Kang, Autoimmunity to type II collagen an experimental model of arthritis, J Exp Med 146(3) (1977) 857-868.

[138] W.A. Rutala, D.J. Weber, Creutzfeldt-Jakob disease: Recommendations for disinfection and sterilization, Clin Infect Dis 32(9) (2001) 1348-1356.
[139] A. Tiwari, D.P. Patnayak, Y. Chander, M. Parsad, S.M. Goyal, Survival of two avian respiratory viruses on porous and nonporous surfaces, Avian Dis 50(2) (2006) 284-287.
[140] J.S. Joly, V. Nguyen, F. Bourrat, Conservation of the prion proteins in Vertebrates, Prod Anim 14(2) (2001) 91-96.
[141] D. Louz, H.E. Bergmans, B.P. Loos, R.C. Hoeben, Cross-species transfer of viruses: Implications for the use of viral vectors in biomedical research, gene therapy and as live-virus vaccines, J Gene Med 7(10) (2005) 1263-1274.
[142] D. Louz, H.E. Bergmans, B.P. Loos, R.C. Hoeben, Reappraisal of biosafety risks posed by PERVs in xenotransplantation, Rev Med Virol 18(1) (2008) 53-65.
[143] R. Parenteau-Bareil, R. Gauvin, F. Berthod, Collagen-based biomaterials for tissue engineering applications, Materials 3(3) (2010) 1863-1887.
[144] C.I. Levene, Diseases of the collagen molecule, J Clin Path 31(12) (1978) 82-94.
[145] F.L. Stassen, G.J. Cardinale, S. Udenfriend, Activation of prolyl hydroxylase in L-929 fibroblasts by ascorbic acid, Proc Natl Acad Sci U S A 70(4) (1973) 1090-1093.
[146] T.A. Sullivan, B. Uschmann, R. Hough, P.S. Leboy, Ascorbate modulation of chondrocyte gene expression is independent of its role in collagen secretion, J Biol Chem 269(36) (1994) 22500-22506.
[147] J.C. Geesin, D. Darr, R. Kaufman, S. Murad, S.R. Pinnell, Ascorbic acid specifically increases type I and type III procollagen messenger RNA levels in human skin fibroblast, J Invest Dermatol 990(4) (1988) 420-424.
[148] A. Satyam, P. Kumar, D. Cigognini, A. Pandit, D.I. Zeugolis, Low, but not too low, oxygen tension and macromolecular crowding accelerate extracellular matrix deposition in human dermal fibroblast culture, Acta Biomater 44 (2016) 221-231.
[149] P. Kumar, A. Satyam, D. Cigognini, A. Pandit, D.I. Zeugolis, Low oxygen tension and macromolecular crowding accelerate extracellular matrix deposition in human corneal fibroblast culture, J Tissue Eng Regen Med 41 (2016) 221-231.
[150] D.M. Gilkes, S. Bajpai, P. Chaturvedi, D. Wirtz, G.L. Semenza, Hypoxia-inducible factor 1 (HIF-1) promotes extracellular matrix remodeling under hypoxic conditions by inducing P4HA1, P4HA2, and PLOD2 expression in fibroblasts, J Biol Chem 288(15) (2014) 10819-10829.

[151] L. Bentovim, R. Amarilio, E. Zelzer, HIF1α is a central regulator of collagen hydroxylation and secretion under hypoxia during bone development, Development 139(23) (2012) 4473-4483.
[152] E. Aro, R. Khatri, R. Gerard-O'Riley, L. Mangiavini, J. Myllyharju, E. Schipani, Hypoxia-inducible factor-1 (HIF-1) but not HIF-2 is essential for hypoxic induction of collagen prolyl 4-hydroxylases in primary newborn mouse epiphyseal growth plate chondrocytes, J Biol Chem 287(44) (2012) 37134-37144.
[153] V. Falanga, L. Zhou, T. Yufit, Low oxygen tension stimulates collagen synthesis and COL1A1 transcription through the action of TGF-beta1, J Cell Physiol 191(1) (2002) 42-50.
[154] V. Falanga, S.W. Qian, D. Danielpour, M.H. Katz, A.B. Roberts, M.B. Sporn, Hypoxia upregulates the synthesis of TGF-beta 1 by human dermal fibroblasts, J Invest Dermatol 97(4) (1991) 634-637.
[155] D. Cigognini, D. Gaspar, P. Kumar, A. Satyam, S. Alagesan, C. Sanz-Nogués, M. Griffin, T. O'Brien, A. Pandit, D.I. Zeugolis, Macromolecular crowding meets oxygen tension in human mesenchymal stem cell culture - A step closer to physiologically relevant in vitro organogenesis, Sci Rep 6 (2016) 30746.
[156] S. Younai, L.S. Nichter, T. Wellisz, J. Reinisch, M.E. Nimni, T.L. Tuan, Modulation of collagen synthesis by transforming growth factor-beta in keloid and hypertrophic scar fibroblasts, Ann Plast Surg 33(2) (1994) 148-151.
[157] R. Raghow, A.E. Postlethwaite, J. Keski-Oja, H.L. Moses, A.H. Kang, Transforming growth factor-beta increases steady state levels of type I procollagen and fibronectin messenger RNAs posttranscriptionally in cultured human dermal fibroblasts, J Clin Invest 79(4) (1987) 1285-1288.
[158] A. Fine, R.H. Goldstein, The effect of transforming growth factor-beta on cell proliferation and collagen formation by lung fibroblasts, J Biol Chem 262(8) (1987) 3897-3902.
[159] J. Varga, S.A. Jimenez, Stimulation of normal human fibroblast collagen production and processing by transforming growth factor-beta, Biochem Biophys Res Commun 138(2) (1986) 974-980.
[160] E. Canalis, Effect of insulinlike growth factor I on DNA and protein synthesis in cultured rat calvaria, J Clin Invest 66(4) (1980) 709-719.

[161] C. Schmid, H.P. Guler, D. Rowe, E.R. Froesch, Insulin-like growth factor I regulates type I procollagen messenger ribonucleic acid steady state levels in bone of rats, Endocrinology 125(3) (1989) 1575-1580.

[162] R.H. Goldstein, C.F. Poliks, P.F. Pilch, B.D. Smith, A. Fine, Stimulation of collagen formation by insulin and insulin-like growth factor I in cultures of human lung fibroblasts, Endocrinology 124(2) (1989) 964-970.

[163] H. Murata, L. Zhou, S. Ochoa, A. Hasan, E. Badiavas, V. Falanga, TGF-beta3 stimulates and regulates collagen synthesis through TGF-beta1-dependent and independent mechanisms, J Invest Dermatol 108(3) (1997) 258-262.

[164] F.J. Thornton, M.R. Schäffer, M.B. Witte, L.L. Moldawer, S.L. MacKay, A. Abouhamze, C.L. Tannahill, A. Barbul, Enhanced collagen accumulation following direct transfection of the inducible nitric oxide synthase gene in cutaneous wounds, Biochem Biophys Res Commun 246(3) (1998) 654-659.

[165] W. Xia, Z. Szomor, Y. Wang, G.A. Murrell, Nitric oxide enhances collagen synthesis in cultured human tendon cells, J Orthop Res 24(2) (2006) 159-172.

[166] J. Myllyharju, A. Lamberg, H. Notbohm, P.P. Fietzek, T. Pihlajaniemi, K.I. Kivirikko, Expression of wild-type and modified pro alpha chains of human type I procollagen in insect cells leads to the formation of stable [alpha 1(I)](2)alpha 2(I) collagen heterotrimers and [alpha 1(I)](3) homotrimers but not [alpha 2(I)](3) homotrimers, J Biol Chem 272(35) (1997) 21824-21830.

[167] H.K. Kleinman, Isolation of laminin-1 and type IV collagen from the EHS sarcoma, J Tissue Cult Methods 16(3-4) (1994) 231-233.

[168] A.E. Geddis, D.J. Prockop, Expression of human COL1A1 gene in stably transfected HT1080 cells: The production of a thermostable homotrimer of type I collagen in a recombinant system, Matrix 13(5) (1993) 399-405.

[169] A. Fertala, A.L. Sieron, A. Ganguly, S.W. Li, L. Ala-Kokko, K.R. Anumula, D.J. Prockop, Synthesis of recombinant human procollagen II in a stably transfected tumour cell line (HT1080), Biochem J 298 (Pt1) (1994) 31-37.

[170] L. Ala-Kokko, J. Hyland, C. Smith, K.I. Kivirikko, S.A. Jimenez, D.J. Prockop, Expression of a human cartilage procollagen gene (COL2A1) in mouse 3T3 cells, J Biol Chem 266(22) (1991) 14175-14178.

[171] K. Wagner, E. Pöschl, J. Turnay, J. Baik, T. Pihlajaniemi, S. Frischholz, K. von der Mark, Coexpression of alpha and beta subunits of prolyl 4-hydroxylase stabilizes

the triple helix of recombinant human type X collagen, Biochem J 352(3) (2000) 907-911.

[172] H. Wu, M.H. Byrne, A. Stacey, M.B. Goldring, J.R. Birkhead, R. Jaenisch, S.M. Krane, Generation of collagenase-resistant collagen by site-directed mutagenesis of murine pro alpha 1(I) collagen gene, Proc Natl Acad Sci U S A 87(15) (1990) 5888-5892.

[173] A. Fichard, E. Tillet, F. Delacoux, R. Garrone, F. Ruggiero, Human recombinant alpha1(V) collagen chain. Homotrimeric assembly and subsequent processing, J Biol Chem 272(48) (1997) 30083-30087.

[174] S. Frischholz, F. Beier, I. Girkontaite, K. Wagner, E. Pöschl, J. Turnay, U. Mayer, K. von der Mark, Characterization of human type X procollagen and its NC-1 domain expressed as recombinant proteins in HEK293 cells, J Biol Chem 273(8) (1998) 4547-4555.

[175] C. Yang, P.J. Hillas, J.A. Baez, M. Nokelainen, J. Balan, J. Tang, R. Spiro, J.W. Polarek, The application of recombinant human collagen in tissue engineering, BioDrugs 18(2) (2004) 103-119.

[176] J. Baez, D. Olsen, J.W. Polarek, Recombinant microbial systems for the production of human collagen and gelatin, Appl Microbiol Biotechnol 69(3) (2005) 245-252.

[177] W. Liu, K. Merrett, M. Griffith, P. Fagerholm, S. Dravida, B. Heyne, J.C. Scaiano, M.A. Watsky, N. Shinozaki, N. Lagali, R. Munger, F. Li, Recombinant human collagen for tissue engineered corneal substitutes, Biomaterials 29(9) (2008) 1147-1158.

[178] J.A. Ramshaw, J.A. Werkmeister, G.J. Dumsday, Bioengineered collagens: Emerging directions for biomedical materials, Bioengineered 5(4) (2014) 227-233.

[179] P.R. Vaughn, M. Galanis, K.M. Richards, T.A. Tebb, J.A. Ramshaw, J.A. Werkmeister, Production of recombinant hydroxylated human type III collagen fragment in Saccharomyces cerevisiae, DNA Cell Biol 17(6) (1998) 511-518.

[180] D.R. Olsen, S.D. Leigh, R. Chang, H. McMullin, W. Ong, E. Tai, G. Chisholm, D.E. Birk, R.A. Berg, R.A. Hitzeman, P.D. Toman, Production of human type I collagen in yeast reveals unexpected new insights into the molecular assembly of collagen trimers, J Biol Chem 276(26) (2001) 24038-24043.

[181] P.D. Toman, G. Chisholm, H. McMullin, L.M. Giere, D.R. Olsen, R.J. Kovach, S.D. Leigh, B.E. Fong, R. Chang, G.A. Daniels, R.A. Berg, R.A. Hitzeman,

Production of recombinant human type I procollagen trimers using a four-gene expression system in the yeast Saccharomyces cerevisiae, J Biol Chem 275(30) (2000) 23303-23309.

[182] J. Myllyharju, M. Nokelainen, A. Vuorela, K.I. Kivirikko, Expression of recombinant human type I-III collagens in the yeast Pichia pastoris, Biochem Soc Trans 28(4) (2000) 353-357.

[183] I. Keizer-Gunnink, A. Vuorela, J. Myllyharju, T. Pihlajaniemi, K.I. Kivirikko, M. Veenhuis, Accumulation of properly folded human type III procollagen molecules in specific intracellular membranous compartments in the yeast Pichia pastoris, Matrix Biol 19(1) (2000) 29-36.

[184] M. Eriksson, J. Myllyharju, H. Tu, M. Hellman, K.I. Kivirikko, Evidence for 4-hydroxyproline in viral proteins. Characterization of a viral prolyl 4-hydroxylase and its peptide substrates, J Biol Chem 274(32) (1999) 22131-22134.

[185] K.B. Luther, A.J. Hulsmeier, B. Schegg, S.A. Deuber, D. Raoult, T. Hennet, Mimivirus collagen is modified by bifunctional lysyl hydroxylase and glycosyltransferase enzyme, J Biol Chem 286(51) (2011) 43701-43709.

[186] C. Rutschmann, S. Baumann, J. Cabalzar, K.B. Luther, T. Hennet, Recombinant expression of hydroxylated human collagen in Escherichia coli, Appl Microbiol Biotechnol 98(10) (2014) 4445-4455.

[187] A. Vuorela, J. Myllyharju, R. Nissi, T. Pihlajaniemi, K.I. Kivirikko, Assembly of human prolyl 4-hydroxylase and type III collagen in the yeast pichia pastoris: Formation of a stable enzyme tetramer requires coexpression with collagen and assembly of a stable collagen requires coexpression with prolyl 4-hydroxylase, EMBO J 16(22) (1997) 6702-3712.

[188] Y.Y. Peng, L. Howell, V. Stoichevska, J.A. Werkmeister, G.J. Dumsday, J.A.M. Ramshaw, Towards scalable production of a collagen-like protein from Streptococcus pyogenes for biomedical applications, Microbial Cell Factories 11 (2012) 146-146.

[189] Y.Y. Peng, V. Stoichevska, K. Schacht, J.A. Werkmeister, J.A. Ramshaw, Engineering multiple biological functional motifs into a blank collagen-like protein template from Streptococcus pyogenes, J Biomed Mater Res A 102(7) (2014) 2189-2196.

[190] B. An, V. Abbonante, H. Xu, D. Gavriilidou, A. Yoshizumi, D. Bihan, R.W. Farndale, D.L. Kaplan, A. Balduini, B. Leitinger, B. Brodsky, Recombinant collagen

engineered to bind to discoidin domain receptor functions as a receptor inhibitor, J Biol Chem 291(9) (2016) 4343-4355.

[191] A.A. Jalan, B. Demeler, J.D. Hartgerink, Hydroxyproline-free Single Composition ABC Collagen Heterotrimer, Journal of the American Chemical Society 135(16) (2013) 6014-6017.

[192] B. An, D.L. Kaplan, B. Brodsky, Engineered recombinant bacterial collagen as an alternative collagen-based biomaterial for tissue engineering, Front Chem 2 (2014) 40.

[193] Z. Yu, B. An, J.A. Ramshaw, B. Brodsky, Bacterial collagen-like proteins that form triple-helical structures, J Struct Biol 186(3) (2014) 451-461.

[194] V. Stoichevska, B. An, Y.Y. Peng, S. Yigit, A.V. Vashi, D.L. Kaplan, J.A. Werkmeister, G.J. Dumsday, J.A. Ramshaw, Formation of multimers of bacterial collagens through introduction of specific sites for oxidative crosslinking, J Biomed Mater Res A 104(9) (2016) 2369-2376.

[195] J.L. Brittan, S.V. Sprague, S.P. Huntley, C.N. Bell, H.F. Jenkinson, R.M. Love, Collagen-like peptide sequences inhibit bacterial invasion of root dentine, Int Endod J 49(5) (2016) 462-70.

[196] P.A. Parmar, S.C. Skaalure, L.W. Chow, J.P. St-Pierre, V. Stoichevska, Y.Y. Peng, J.A. Werkmeister, J.A. Ramshaw, M.M. Stevens, Temporally degradable collagen-mimetic hydrogels tuned to chondrogenesis of human mesenchymal stem cells, Biomaterials 99 (2016) 56-71.

[197] B. An, V. Abbonante, S. Yigit, A. Balduini, D.L. Kaplan, B. Brodsky, Definition of the native and denatured type II collagen binding site for fibronectin using a recombinant collagen system, J Biol Chem 289(8) (2014) 4941-4951.

[198] I. Majsterek, E. McAdams, E. Adachi, S.T. Dhume, A. Fertala, Prospects and limitations of the rational engineering of fibrillar collagens, Protein Sci 12(9) (2003) 2063-2072.

[199] F. Ruggiero, M. Koch, Making recombinant extracellular matrix proteins, Methods 45(1) (2008) 75-85.

[200] P.D. Toman, F. Pieper, N. Sakai, C. Karatzas, E. Platenburg, I. de Wit, C. Samuel, A. Dekker, G.A. Daniels, R.A. Berg, G.J. Platenburg, Production of recombinant human type I procollagen homotrimer in the mammary gland of transgenic mice, Transgenic Res 8(6) (1999) 415-427.

[201] D.C. John, R. Watson, A.J. Kind, A.R. Scott, K.E. Kadler, N.J. Bulleid, Expression of an engineered form of recombinant procollagen in mouse milk, Nat Biotechnol 17(4) (1999) 385-389.

[202] M. Tomita, H. Munetsuna, T. Sato, T. Adachi, R. Hino, M. Hayashi, K. Shimizu, N. Nakamura, T. Tamura, K. Yoshizato, Transgenic silkworms produce recombinant human type III procollagen in cocoons, Nat Biotechnol 21(1) (2003) 52-56.

[203] K. Yuasa, K. Toyooka, H. Fukuda, K. Matsuoka, Membrane-anchored prolyl hydroxylase with an export signal from the endoplasmic reticulum, Plant J 41(1) (2005) 81-94.

[204] C. Zhang, J. Baez, K.M. Pappu, C.E. Glatz, Purification and characterization of a transgenic corn grain-derived recombinant collagen type I alpha 1, Biotechnol Prog 25(6) (2009) 1660-1668.

[205] C.M. Setina, J.P. Haase, C.E. Glatz, Process integration for recovery of recombinant collagen type I alpha1 from corn seed, Biotechnol Prog 32(1) (2016) 98-107.

[206] F. Ruggiero, J.Y. Exposito, P. Bournat, V. Gruber, S. Perret, J. Comte, B. Olagnier, R. Garrone, M. Theisen, Triple helix assembly and processing of human collagen produced in transgenic tobacco plants, FEBS Lett 469(1) (2000) 132-136.

[207] H. Stein, M. Wilensky, Y. Tsafrir, M. Rosenthal, R. Amir, T. Avraham, K. Ofir, O. Dgany, A. Yayon, O. Shoseyov, Production of bioactive, post-translationally modified, heterotrimeric, human recombinant type-I collagen in transgenic tobacco, Biomacromolecules 10(9) (2009) 2640-2645.

[208] S. Majumdar, Q. Guo, M. Garza-Madrid, X. Calderon-Colon, D. Duan, P. Carbajal, O. Schein, M. Trexler, J. Elisseeff, Influence of collagen source on fibrillar architecture and properties of vitrified collagen membranes, J Biomed Mater Res B 104(2) (2016) 300-307.

[209] N.J. Bulleid, D.C. John, K.E. Kadler, Recombinant expression systems for the production of collagen, Biochem Soc Trans 28(4) (2000) 350-353.

[210] S. Browne, D.I. Zeugolis, A. Pandit, Collagen: Finding a solution for the source, Tissue Eng A 19(13-14) (2013) 1491-1494.

[211] S. Chattopadhyay, C.J. Murphy, J.F. McAnulty, R.T. Raines, Peptides that anneal to natural collagen in vitro and ex vivo, Org Biomol Chem 10(30) (2012) 5892-5897.

[212] J.A. Fallas, L.E. O'Leary, J.D. Hartgerink, Synthetic collagen mimics: Self-assembly of homotrimers, heterotrimers and higher order structures, Chem Soc Rev 39(9) (2010) 3510-3527.
[213] F.W. Kotch, R.T. Raines, Self-assembly of synthetic collagen triple helices, Proc Natl Acad Sci U S A 103(9) (2006) 3028-3033.
[214] L.E. O'Leary, J.A. Fallas, J.D. Hartgerink, Positive and negative design leads to compositional control in AAB collagen heterotrimers, J Am Chem Soc 133(14) (2011) 5432-5443.
[215] V. Gauba, J.D. Hartgerink, Synthetic collagen heterotrimers: Structural mimics of wild-type and mutant collagen type I, J Am Chem Soc 130(23) (2008) 7509-7515.
[216] B. Brodsky, G. Thiagarajan, B. Madhan, K. Kar, Triple-helical peptides: An approach to collagen conformation, stability, and self-association, Biopolymers 89(5) (2008) 345-353.
[217] G.B. Ramirez-Rodriguez, M. Montesi, S. Panseri, S. Sprio, A. Tampieri, M. Sandri, Biomineralized recombinant collagen-based scaffold mimicking native bone enhances mesenchymal stem cell interaction and differentiation, Tissue Eng A 23(23-24) (2017) 1423-1435.
[218] T.Z. Luo, L.R. He, P. Theato, K.L. Kiick, Thermoresponsive self-assembly of nanostructures from a collagen-like peptide-containing diblock copolymer, Macromol Biosci 15(1) (2015) 111-123.
[219] T. Jiang, C.F. Xu, Y. Liu, Z. Liu, J.S. Wall, X.B. Zuo, T.Q. Lian, K. Salaita, C.Y. Ni, D. Pochan, V.P. Conticello, Structurally defined nanoscale sheets from self-assembly of collagen-mimetic peptides, J Am Chem Soc 136(11) (2014) 4300-4308.
[220] M.M. Pires, D.E. Przybyla, C.M.R. Perez, J. Chmielewski, Metal-mediated tandem coassembly of collagen peptides into banded microstructures, J Am Chem Soc 133(37) (2011) 14469-14471.
[221] L.E. O'Leary, J.A. Fallas, E.L. Bakota, M.K. Kang, J.D. Hartgerink, Multi-hierarchical self-assembly of a collagen mimetic peptide from triple helix to nanofibre and hydrogel, Nat Chem 3(10) (2011) 821-828.
[222] S. Rele, Y. Song, R.P. Apkarian, Z. Qu, V.P. Conticello, E.L. Chaikof, D-periodic collagen-mimetic microfibers, J Am Chem Soc 129(47) (2007) 14780-14787.
[223] A.V. Persikov, J.A. Ramshaw, A. Kirkpatrick, B. Brodsky, Electrostatic interactions involving lysine make major contributions to collagen triple-helix stability, Biochemistry 44(5) (2005) 1414-1422.

[224] EMEA, Virus vaidation studies: The design, contribution and interpretation of studies validationg the inactivation and removal of viruses (CPMP/BWP/268/95), UK, 1996.
[225] EEC, Validation of virus removal/inactivation procedures: Choice of viruses (Directive 75/318/EEC; Previous Title: None/III/5543/94), 1995.
[226] EMEA, Quality of biotechnological products: Viral safety evaluation of biotechnology products derived from cell lines of human or animal origin, UK, 2006.
[227] WHO, Guidelines on viral inactivation and removal procedures intended to assure the viral safety of human blood plasma products, 2004, pp. 150-224.
[228] P.O. Forest, F. Morfin, E. Bergeron, J. Dore, S. Bensa, C. Wittmann, S. Picot, F.N. Renaud, J. Freney, C.H. Gagnieu, Validation of a viral and bacterial inactivation step during the extraction and purification process of porcine collagen, Biomed Mater Eng 17(4) (2007) 199-208.
[229] J.R. Whitaker, R.E. Feeney, Chemical and physical modification of proteins by the hydroxide ion, Crit Rev Food Sci Nutr 19(3) (1983) 173-212.
[230] EEC, Council Directive 93/42/EEC of 14 June 1993 concerning medical devices (OJ L 169, 12.7.1993), Belgium, 1993.
[231] FDA, Use of International Standard ISO 10993-1, "Biological evaluation of medical devices - Part 1: Evaluation and testing within a risk management process" Guidance for Industry and Food and Drug Administration Staff, USA, 2016.
[232] ASTM, Standard guide for characterization of type I collagen as starting material for surgical implants and substrates for tissue engineered medical products (TEMPs), ASTM International, West Conshohocken, PA, USA, 2011.
[233] D.B. Kramer, S. Xu, A.S. Kesselheim, Regulation of medical devices in the United States and European Union, N Engl J Med 366(9) (2012) 848-855.
[234] D.I. Zeugolis, G.R. Paul, G. Attenburrow, Cross-linking of extruded collagen fibers - A biomimetic three-dimensional scaffold for tissue engineering applications, J Biomed Mater Res A 89(4) (2009) 895-908.
[235] L. Delgado, Y. Bayon, A. Pandit, D.I. Zeugolis, To cross-link or not to cross-link? Cross-linking associated foreign body response of collagen-based devices, Tissue Eng B 21(3) (2015) 298-313.
[236] A.H. Annor, M.E. Tang, C.L. Pui, G.C. Ebersole, M.M. Frisella, B.D. Matthews, C.R. Deeken, Effect of enzymatic degradation on the mechanical properties of biological scaffold materials, Surg Endosc 26(10) (2012) 2767-2778.

[237] M.C. Bottino, V. Thomas, M.V. Jose, D.R. Dean, G.M. Janowski, Acellular dermal matrix graft: Synergistic effect of rehydration and natural crosslinking on mechanical properties, J Biomed Mater Res B 95(2) (2010) 276-282.

[238] N. Davidenko, J.J. Campbell, E.S. Thian, C.J. Watson, R.E. Cameron, Collagen-hyaluronic acid scaffolds for adipose tissue engineering, Acta Biomater 6(10) (2010) 3957-3968.

[239] A. Yahyouche, X. Zhidao, J.T. Czernuszka, A.J. Clover, Macrophage-mediated degradation of crosslinked collagen scaffolds, Acta Biomater 7(1) (2011) 278-286.

[240] S. Balaji, R. Kumar, R. Sripriya, U. Rao, A. Mandal, P. Kakkar, P.N. Reddy, P.K. Sehgal, Characterization of keratin–collagen 3D scaffold for biomedical applications, Polym Adv Technol 23(3) (2012) 500-507.

[241] M. Sanami, I. Sweeney, Z. Shtein, S. Meirovich, A. Sorushanova, A.M. Mullen, M. Miraftab, O. Shoseyov, C. O'Dowd, A. Pandit, D.I. Zeugolis, The influence of poly(ethylene glycol) ether tetrasuccinimidyl glutarate on the structural, physical, and biological properties of collagen fibers, J Biomed Mater Res B 104(5) (2016) 914-922.

[242] D.I. Zeugolis, R.G. Paul, G. Attenburrow, The influence of a natural cross-linking agent (Myrica rubra) on the properties of extruded collagen fibres for tissue engineering applications, Mater Sci Eng C 30 (2010) 190-195.

[243] A. Satyam, G.S. Subramanian, M. Raghunath, A. Pandit, D.I. Zeugolis, In vitro evaluation of Ficoll-enriched and genipin-stabilised collagen scaffolds, J Tissue Eng Regen Med 8(3) (2014) 233-241.

[244] D.I. Zeugolis, S.T. Khew, E.S. Yew, A.K. Ekaputra, Y.W. Tong, L.Y. Yung, D.W. Hutmacher, C. Sheppard, M. Raghunath, Electro-spinning of pure collagen nano-fibres - just an expensive way to make gelatin?, Biomaterials 29(15) (2008) 2293-2305.

[245] D.I. Zeugolis, M. Raghunath, The physiological relevance of wet versus dry differential scanning calorimetry for biomaterial evaluation: A technical note, Polym Int 59(10) (2010) 1403-1407.

[246] D. Lickorish, J.A. Ramshaw, J.A. Werkmeister, V. Glattauer, C.R. Howlett, Collagen-hydroxyapatite composite prepared by biomimetic process, J Biomed Mater Res A 68(1) (2004) 19-27.

[247] N. Shanmugasundaram, P. Ravichandran, P.N. Reddy, N. Ramamurty, S. Pal, K.P. Rao, Collagen-chitosan polymeric scaffolds for the in vitro culture of human epidermoid carcinoma cells, Biomaterials 22(14) (2001) 1943-1951.

[248] X. Duan, C. McLaughlin, M. Griffith, H. Sheardown, Biofunctionalization of collagen for improved biological response: Scaffolds for corneal tissue engineering, Biomaterials 28(1) (2007) 78-88.

[249] L. Buttafoco, N.G. Kolkman, P. Engbers-Buijtenhuijs, A.A. Poot, P.J. Dijkstra, I. Vermes, J. Feijen, Electrospinning of collagen and elastin for tissue engineering applications, Biomaterials 27(5) (2006) 724-734.

[250] M.V. Jose, V. Thomas, D.R. Dean, E. Nyairo, Fabrication and characterization of aligned nanofibrous PLGA/Collagen blends as bone tissue scaffolds, Polymer 50(15) (2009) 3778-3785.

[251] K. Pietrucha, Changes in denaturation and rheological properties of collagen-hyaluronic acid scaffolds as a result of temperature dependencies, Int J Biol Macromol 36(5) (2005) 299-304.

[252] Y. Liu, M. Griffith, M.A. Watsky, J.V. Forrester, L. Kuffova, D. Grant, K. Merrett, D.J. Carlsson, Properties of porcine and recombinant human collagen matrices for optically clear tissue engineering applications, Biomacromolecules 7(6) (2006) 1819-1828.

[253] S. Chen, T. Ikoma, N. Ogawa, S. Migita, H. Kobayashi, N. Hanagata, In vitro formation and thermal transition of novel hybrid fibrils from type I fish scale collagen and type I porcine collagen, Sci Tech Adv Mater 11(3) (2010) 035001.

[254] C.F. Rousseau, C.H. Gagnieu, In vitro cytocompatibility of porcine type I atelocollagen crosslinked by oxidized glycogen, Biomaterials 23(6) (2002) 1503-1510.

[255] A. Mandal, S. Sekar, K.M.S. Meera, A. Mukherjee, T.P. Sastry, A.B. Mandal, Fabrication of collagen scaffolds impregnated with sago starch capped silver nanoparticles suitable for biomedical applications and their physicochemical studies, Phys Chem Chem Phys 16(37) (2014) 20175-20183.

[256] D.P. Perkasa, E. Erizal, B. Abbas, Polymeric biomaterials film based on poly (vinyl alcohol) and fish scale collagen by repetitive freeze-thaw cycles followed by gamma irradiation, Indo J Chem 13(3) (2013) 221-228.

[257] M.H. Uriarte-Montoya, J.L. Arias-Moscoso, M. Plascencia-Jatomea, H. Santacruz-Ortega, O. Rouzaud-Sández, J.L. Cardenas-Lopez, E. Marquez-Rios, J.M.

Ezquerra-Brauer, Jumbo squid (Dosidicus gigas) mantle collagen: Extraction, characterization, and potential application in the preparation of chitosan–collagen biofilms, Bioresour Technol 101(11) (2010) 4212-4219.

[258] Y. Nomura, S. Toki, Y. Ishii, K. Shirai, The physicochemical property of shark type I collagen gel and membrane, J Agric Food Chem 48(6) (2000) 2028-2032.

[259] S. Yunoki, T. Suzuki, M. Takai, Stabilization of low denaturation temperature collagen from fish by physical cross-linking methods, J Biosci Bioeng 96(6) (2003) 575-577.

[260] J.K. McDade, E.P. Brennan-Pierce, M.B. Ariganello, R.S. Labow, J. Michael Lee, Interactions of U937 macrophage-like cells with decellularized pericardial matrix materials: Influence of crosslinking treatment, Acta Biomater 9(7) (2013) 7191-7199.

[261] N. Bryan, H. Ashwin, N. Smart, Y. Bayon, N. Scarborough, J.A. Hunt, The innate oxygen dependant immune pathway as a sensitive parameter to predict the performance of biological graft materials, Biomaterials 33(27) (2012) 6380-6392.

[262] L.H. Olde Damink, P.J. Dijkstra, M.J. van Luyn, P.B. van Wachem, P. Nieuwenhuis, J. Feijen, Cross-linking of dermal sheep collagen using a water-soluble carbodiimide, Biomaterials 17(8) (1996) 765-773.

[263] K.B. Hey, C.M. Lachs, M.J. Raxworthy, E.J. Wood, Crosslinked fibrous collagen for use as a dermal implant: Control of the cytotoxic effects of glutaraldehyde and dimethylsuberimidate, Biotechnol Appl Biochem 12(1) (1990) 85-93.

[264] J.A. Chapman, M. Tzaphlidou, K.M. Meek, K.E. Kadler, The collagen fibril -- A model system for studying the staining and fixation of a protein, Electron Microsc Rev 3(1) (1990) 143-182.

[265] C.R. Lee, A.J. Grodzinsky, M. Spector, The effects of cross-linking of collagen-glycosaminoglycan scaffolds on compressive stiffness, chondrocyte-mediated contraction, proliferation and biosynthesis, Biomaterials 22(23) (2001) 3145-3154.

[266] L.M. Delgado, K. Fuller, D.I. Zeugolis, Collagen cross-linking: Biophysical, biochemical, and biological response analysis, Tissue Eng A 23(19-20) (2017) 1064-1077.

[267] L.H.H.O. Damink, P.J. Dijkstra, M.J.A. van Luyn, P.B. van Wachem, P. Nieuwenhuis, J. Feijen, Crosslinking of dermal sheep collagen using hexamethylene diisocyanate, J Mater Sci Mater Med 6(7) (1995) 429-434.

[268] M.J.A. van Luyn, P.B. van Wachem, L.H.H. Damink, P.J. Dijkstra, J. Feijen, P. Nieuwenhuis, Secondary cytotoxicity of cross-linked dermal sheep collagens during repeated exposure to human fibroblasts, Biomaterials 13(14) (1992) 1017-1024.

[269] J.L. Panza, W.R. Wagner, H.L. Rilo, R.H. Rao, E.J. Beckman, A.J. Russell, Treatment of rat pancreatic islets with reactive PEG, Biomaterials 21(11) (2000) 1155-1164.

[270] C.R. Deible, P. Petrosko, P.C. Johnson, E.J. Beckman, A.J. Russell, W.R. Wagner, Molecular barriers to biomaterial thrombosis by modification of surface proteins with polyethylene glycol, Biomaterials 19(20) (1998) 1885-1893.

[271] J.E. Gough, C.A. Scotchford, S. Downes, Cytotoxicity of glutaraldehyde crosslinked collagen/poly(vinyl alcohol) films is by the mechanism of apoptosis, J Biomed Mater Res 61(1) (2002) 121-130.

[272] P.B. van Wachem, R. Zeeman, P.J. Dijkstra, J. Feijen, M. Hendriks, P.T. Cahalan, M.J. van Luyn, Characterization and biocompatibility of epoxy-crosslinked dermal sheep collagens, J Biomed Mater Res 47(2) (1999) 270-277.

[273] R.J. Levy, F.J. Schoen, F.S. Sherman, J. Nichols, M.A. Hawley, S.A. Lund, Calcification of subcutaneously implanted type I collagen sponges. Effects of formaldehyde and glutaraldehyde pretreatments, Am J Pathol 122(1) (1986) 71-82.

[274] S.C. Vasudev, T. Chandy, Effect of alternative crosslinking techniques on the enzymatic degradation of bovine pericardia and their calcification, J Biomed Mater Res 35(3) (1997) 357-369.

[275] J.M. McPherson, S. Sawamura, R. Armstrong, An examination of the biologic response to injectable, glutaraldehyde cross-linked collagen implants, J Biomed Mater Res 20(1) (1986) 93-107.

[276] B.N. Brown, R. Londono, S. Tottey, L. Zhang, K.A. Kukla, M.T. Wolf, K.A. Daly, J.E. Reing, S.F. Badylak, Macrophage phenotype as a predictor of constructive remodeling following the implantation of biologically derived surgical mesh materials, Acta Biomater 8(3) (2012) 978-987.

[277] R. Roy, A. Boskey, L.J. Bonassar, Processing of type I collagen gels using nonenzymatic glycation, J Biomed Mater Res A 93(3) (2010) 843-851.

[278] L.L. Huang, H.W. Sung, C.C. Tsai, D.M. Huang, Biocompatibility study of a biological tissue fixed with a naturally occurring crosslinking reagent, J Biomed Mater Res 42(4) (1998) 568-576.

[279] H.W. Sung, Y. Chang, C.T. Chiu, C.N. Chen, H.C. Liang, Mechanical properties of a porcine aortic valve fixed with a naturally occurring crosslinking agent, Biomaterials 20(19) (1999) 1759-1772.

[280] A.P.M. Antunes, G. Attenburrow, A.D. Covington, J. Ding, Utilisation of oleuropein as a crosslinking agent in collagenic films, J Leather Sci 2(2) (2008) 1-12.

[281] P.B. van Wachem, M.J. van Luyn, L.H.O. Damink, P.J. Dijkstra, J. Feijen, P. Nieuwenhuis, Biocompatibility and tissue regenerating capacity of crosslinked dermal sheep collagen, J Biomed Mater Res 28(3) (1994) 353-363.

[282] H. Petite, J.L. Duval, V. Frei, N. Abdul-Malak, M.F. Sigot-Luizard, D. Herbage, Cytocompatibility of calf pericardium treated by glutaraldehyde and by the acyl azide methods in an organotypic culture model, Biomaterials 16(13) (1995) 1003-1008.

[283] S. Zahedi, C. Bozon, G. Brunel, A 2-year clinical evaluation of a diphenylphosphorylazide-cross-linked collagen membrane for the treatment of buccal gingival recession, J Periodontol 69(9) (1998) 975-981.

[284] B. Chevallay, N. Abdul-Malak, D. Herbage, Mouse fibroblasts in long-term culture within collagen three-dimensional scaffolds: Influence of crosslinking with diphenylphosphorylazide on matrix reorganization, growth, and biosynthetic and proteolytic activities, J Biomed Mater Res A 49(4) (2000) 448-459.

[285] S. Roche, M.C. Ronziere, D. Herbage, A.M. Freyria, Native and DPPA cross-linked collagen sponges seeded with fetal bovine epiphyseal chondrocytes used for cartilage tissue engineering, Biomaterials 22(1) (2001) 9-18.

[286] L. Marinucci, C. Lilli, M. Guerra, S. Belcastro, E. Becchetti, G. Stabellini, E.M. Calvi, P. Locci, Biocompatibility of collagen membranes crosslinked with glutaraldehyde or diphenylphosphoryl azide: An in vitro study, J Biomed Mater Res A 67(2) (2003) 504-509.

[287] E. Jorge-Herrero, P. Fernandez, J. Turnay, N. Olmo, P. Calero, R. Garcia, I. Freile, J.L. Castillo-Olivares, Influence of different chemical cross-linking treatments on the properties of bovine pericardium and collagen, Biomaterials 20(6) (1999) 539-545.

[288] J.M. Girardot, M.N. Girardot, Amide cross-linking: An alternative to glutaraldehyde fixation, J Heart Valve Dis 5(5) (1996) 518-525.

[289] J.S. Pieper, T. Hafmans, J.H. Veerkamp, T.H. van Kuppevelt, Development of tailor-made collagen-glycosaminoglycan matrices: EDC/NHS crosslinking, and ultrastructural aspects, Biomaterials 21(6) (2000) 581-593.

[290] H.M. Powell, S.T. Boyce, EDC cross-linking improves skin substitute strength and stability, Biomaterials 27(34) (2006) 5821-5827.
[291] H.W. Sung, W.H. Chang, C.Y. Ma, M.H. Lee, Crosslinking of biological tissues using genipin and/or carbodiimide, J Biomed Mater Res A 64(3) (2003) 427-438.
[292] C.P. Barnes, C.W. Pemble, D.D. Brand, D.G. Simpson, G.L. Bowlin, Cross-linking electrospun type II collagen tissue engineering scaffolds with carbodiimide in ethanol, Tissue Eng 13(7) (2007) 1593-1605.
[293] E.C. Collin, S. Grad, D.I. Zeugolis, C.S. Vinatier, J.R. Clouet, J.J. Guicheux, P. Weiss, M. Alini, A.S. Pandit, An injectable vehicle for nucleus pulposus cell-based therapy, Biomaterials 32(11) (2011) 2862-2870.
[294] E. Cosgriff-Hernandez, M.S. Hahn, B. Russell, T. Wilems, D. Munoz-Pinto, M.B. Browning, J. Rivera, M. Hook, Bioactive hydrogels based on designer collagens, Acta Biomater 6(10) (2010) 3969-3977.
[295] J. Ward, J. Kelly, W. Wang, D.I. Zeugolis, A. Pandit, Amine functionalization of collagen matrices with multifunctional polyethylene glycol systems, Biomacromolecules 11(11) (2010) 3093-3101.
[296] T. Taguchi, L. Xu, H. Kobayashi, A. Taniguchi, K. Kataoka, J. Tanaka, Encapsulation of chondrocytes in injectable alkali-treated collagen gels prepared using poly(ethylene glycol)-based 4-armed star polymer, Biomaterials 26(11) (2005) 1247-1252.
[297] K. Matsumoto, T. Nakamura, Y. Shimizu, H. Ueda, T. Sekine, Y. Yamamoto, T. Kiyotani, Y. Takimoto, A novel surgical material made from collagen with high mechanical strength: A collagen sandwich membrane, ASAIO J 45(4) (1999) 288-292.
[298] M.F. Cote, C.J. Doillon, Wettability of cross-linked collagenous biomaterials: *In vitro* study, Biomaterials 13(9) (1992) 612-616.
[299] M. Koide, K. Osaki, J. Konishi, K. Oyamada, T. Katakura, A. Takahashi, K. Yoshizato, A new type of biomaterial for artificial skin: Dehydrothermally cross-linked composites of fibrillar and denatured collagens., J Biomed Mater Res 27(1) (1993) 79-87.
[300] R.L. Collins, D. Christiansen, G.A. Zazanis, F.H. Silver, Use of collagen film as a dural substitute: Preliminary animal studies, J Biomed Mater Res 25(2) (1991) 267-276.

[301] M.C. Wang, G.D. Pins, F.H. Silver, Collagen fibres with improved strength for the repair of soft tissue injuries, Biomaterials 15(7) (1994) 507-512.
[302] K.S. Weadock, E.J. Miller, L.D. Bellincampi, J.P. Zawadsky, M.G. Dunn, Physical crosslinking of collagen fibers: Comparison of ultraviolet irradiation and dehydrothermal treatment, J Biomed Mater Res 29(11) (1995) 1373-1379.
[303] A. Sionkowska, Modification of collagen films by ultraviolet irradiation, Polym Degrad Stabil 68(2) (2000) 147-151.
[304] A. Sionkowska, T. Wess, Mechanical properties of UV irradiated rat tail tendon (RTT) collagen, Int J Biol Macromol 34(1-2) (2004) 9-12.
[305] N. Metreveli, L. Namicheishvili, K. Jariashvili, G. Mrevlishvili, A. Sionkowska, Mechanisms of the influence of UV irradiation on collagen and collagen-ascorbic acid solutions, Int J Photoenergy 2006 (2006) 1-4.
[306] K. Vizarova, D. Bakos, M. Rehakova, V. Macho, Modification of layered atelocollagen by ultraviolet irradiation and chemical cross-linking: Structure stability and mechanical properties, Biomaterials 15(13) (1994) 1082-1086.
[307] D. Cherfan, E.E. Verter, S. Melki, T.E. Gisel, F.J. Doyle, Jr., G. Scarcelli, S.H. Yun, R.W. Redmond, I.E. Kochevar, Collagen cross-linking using rose bengal and green light to increase corneal stiffness, Invest Ophthalmol Vis Sci 54(5) (2013) 3426-3433.
[308] S. Ibusuki, G.J. Halbesma, M.A. Randolph, R.W. Redmond, I.E. Kochevar, T.J. Gill, Photochemically cross-linked collagen gels as three-dimensional scaffolds for tissue engineering, Tissue Eng 13(8) (2007) 1995-2001.
[309] A. Terzi, E. Storelli, S. Bettini, T. Sibillano, D. Altamura, L. Salvatore, M. Madaghiele, A. Romano, D. Siliqi, M. Ladisa, L. De Caro, A. Quattrini, L. Valli, A. Sannino, C. Giannini, Effects of processing on structural, mechanical and biological properties of collagen-based substrates for regenerative medicine, Sci Rep 8(1) (2018) 1429.
[310] A. Nakada, K. Shigeno, T. Sato, T. Hatayama, M. Wakatsuki, T. Nakamura, Optimal dehydrothermal processing conditions to improve biocompatibility and durability of a weakly denatured collagen scaffold, J Biomed Mater Res B 105(8) (2017) 2301-2307.
[311] A. Sionkowska, T. Wess, Mechanical properties of UV irradiated rat tail tendon (RTT) collagen, International Journal of Biological Macromolecules 34(1-2) (2004) 9-12.

[312] R.G. Paul, A.J. Bailey, Chemical stabilisation of collagen as a biomimetic, Sci World J 24(3) (2003) 138-155.
[313] L.D. Bellincampi, R.F. Closkey, R. Prasad, J.P. Zawadsky, M.G. Dunn, Viability of fibroblast-seeded ligament analogs after autogenous implantation, J Orthop Res 16(4) (1998) 414-420.
[314] H. Sakamoto, Y. Kumazawa, M. Motoki, Strength of protein gels prepared with microbial transglutaminase as related to reaction conditions, J Food Science 59(4) (1994) 866-871.
[315] H.L. Fuchsbauer, U. Gerber, J. Engelmann, T. Seeger, C. Sinks, T. Hecht, Influence of gelatin matrices cross-linked with transglutaminase on the properties of an enclosed bioactive material using beta-galactosidase as model system, Biomaterials 17(15) (1996) 1481-1488.
[316] H. Babin, E. Dickinson, Influence of transglutaminase treatment on the thermoreversible gelation of gelatin, Food Hydrocoll 15(3) (2001) 271-276.
[317] Y. Nomura, S. Toki, Y. Ishii, K. Shirai, Effect of transglutaminase on reconstruction and physicochemical properties of collagen gel from shark type I collagen, Biomacromolecules 2(1) (2001) 105-110.
[318] J.M. Orban, L.B. Wilson, J.A. Kofroth, M.S. El-Kurdi, T.M. Maul, D.A. Vorp, Crosslinking of collagen gels by transglutaminase, J Biomed Mater Res A 68(4) (2004) 756-762.
[319] R.N. Chen, H.O. Ho, M.T. Sheu, Characterization of collagen matrices crosslinked using microbial transglutaminase, Biomaterials 26(20) (2005) 4229-4235.
[320] D.Y. Chau, R.J. Collighan, E.A. Verderio, V.L. Addy, M. Griffin, The cellular response to transglutaminase-cross-linked collagen, Biomaterials 26(33) (2005) 6518-6529.
[321] D.M. O Halloran, R.J. Collighan, M. Griffin, A.S. Pandit, Characterization of a microbial transglutaminase cross-linked type II collagen scaffold, Tissue Eng 12(6) (2006) 1467-1474.
[322] R.J. Collighan, M. Griffin, Transglutaminase 2 cross-linking of matrix proteins: Biological significance and medical applications, Amino Acids 36(4) (2009) 659-670.
[323] I. Stachel, U. Schwarzenbolz, T. Henle, M. Meyer, Cross-linking of type I collagen with microbial transglutaminase: Identification of cross-linking sites, Biomacromolecules 11(3) (2010) 698-705.

[324] W. Schloegl, A. Klein, R. Furst, U. Leicht, E. Volkmer, M. Schieker, S. Jus, G.M. Guebitz, I. Stachel, M. Meyer, M. Wiggenhorn, W. Friess, Residual transglutaminase in collagen - Effects, detection, quantification, and removal, Eur J Pharm Biopharm 80(2) (2012) 282-288.

[325] P.F. Lee, Y. Bai, R.L. Smith, K.J. Bayless, A.T. Yeh, Angiogenic responses are enhanced in mechanically and microscopically characterized, microbial transglutaminase crosslinked collagen matrices with increased stiffness, Acta Biomater 9(7) (2013) 7178-7190.

[326] E. Gebauer, E. Gossla, C. Kwas, D. Salzig, A. Schmiermund, P. Czermak, H.L. Fuchsbauer, Identification of transglutaminase substrates from porcine nucleus pulposus as potential amplifiers in cross-linking cell scaffolds, Biomacromolecules 14(5) (2013) 1564-1571.

[327] D. Fortunati, D.Y. Chau, Z. Wang, R.J. Collighan, M. Griffin, Cross-linking of collagen I by tissue transglutaminase provides a promising biomaterial for promoting bone healing, Amino Acids 46(7) (2014) 1751-1761.

[328] D.J. Hulmes, J.C. Jesior, A. Miller, C. Berthet-Colominas, C. Wolff, Electron microscopy shows periodic structure in collagen fibril cross sections, Proc Natl Acad Sci U S A 78(6) (1981) 3567-3571.

[329] B. Brodsky, D.W. Hukins, D.J. Hulmes, A. Miller, S. White, J. Woodhead-Galloway, Low angle X-ray diffraction studies on stained rat tail tendons, Biochim Biophys Acta 535(1) (1978) 25-32.

[330] M. Tzaphlidou, Measurement of the axial periodicity of collagen fibrils using an image processing method, Micron 32(3) (2001) 337-339.

[331] A. Boyde, S.J. Jones, Scanning electron microscopy of cementum and Sharpey fibre bone, Z Zellforsch Mikrosk Anat 92(4) (1968) 536-548.

[332] M. Stoppato, E. Carletti, D. Maniglio, C. Migliaresi, A. Motta, Functional role of scaffold geometries as a template for physiological ECM formation: Evaluation of collagen 3D assembly, J Tissue Eng Regen Med 7(2) (2013) 161-168.

[333] C.M. Franz, D.J. Muller, Studying collagen self-assembly by time-lapse high-resolution atomic force microscopy, Methods Mol Biol 736 (2011) 97-107.

[334] D.R. Stamov, E. Stock, C.M. Franz, T. Jahnke, H. Haschke, Imaging collagen type I fibrillogenesis with high spatiotemporal resolution, Ultramicroscopy 149 (2015) 86-94.

[335] D.A. Cisneros, C. Hung, C.M. Franz, D.J. Muller, Observing growth steps of collagen self-assembly by time-lapse high-resolution atomic force microscopy, J Struct Biol 154(3) (2006) 232-245.

[336] J.Y. Dewavrin, N. Hamzavi, V.P. Shim, M. Raghunath, Tuning the architecture of three-dimensional collagen hydrogels by physiological macromolecular crowding, Acta Biomater 10(10) (2014) 4351-4359.

[337] J. Zhu, L.J. Kaufman, Collagen I self-assembly: Revealing the developing structures that generate turbidity, Biophys J 106(8) (2014) 1822-1831.

[338] K. Kar, P. Amin, M.A. Bryan, A.V. Persikov, A. Mohs, Y.H. Wang, B. Brodsky, Self-association of collagen triple helic peptides into higher order structures, J Biol Chem 281(44) (2006) 33283-33290.

[339] K.E. Kadler, Y. Hojima, D.J. Prockop, Assembly of type I collagen fibrils de novo. Between 37 and 41 degrees C the process is limited by micro-unfolding of monomers, J Biol Chem 263(21) (1988) 10517-10523.

[340] D.E. Birk, F.H. Silver, Collagen fibrillogenesis in vitro: Comparison of types I, II, and III, Arch Biochem Biophys 235(1) (1984) 178-185.

[341] C. Gullekson, L. Lucas, K. Hewitt, L. Kreplak, Surface-sensitive raman spectroscopy of collagen I fibrils, Biophys J 100(7) (2011) 1837-1845.

[342] A.T. Yeh, B. Choi, J.S. Nelson, B.J. Tromberg, Reversible dissociation of collagen in tissues, J Invest Dermatol 121(6) (2003) 1332-1335.

[343] W.R. Zipfel, R.M. Williams, W.W. Webb, Nonlinear magic: Multiphoton microscopy in the biosciences, Nat Biotechnol 21(11) (2003) 1369-1377.

[344] L. Rich, J. Whittaker, Collagen and picrosirius red staining: A polarized light assessment of fibrillar hue and spatial distribution, Braz J Morphol Sci 22(2) (2005) 97-104.

[345] A. Alves, N. Attik, Y. Bayon, E. Royet, C. Wirth, X. Bourges, A. Piat, G. Dolmazon, G. Clermont, J.P. Boutrand, B. Grosgogeat, K. Gritsch, Devising tissue ingrowth metrics: a contribution to the computational characterization of engineered soft tissue healing, Biomed Mater 13(3) (2018) 035010.

[346] G.S. Montes, L.C. Junqueira, The use of the Picrosirius-polarization method for the study of the biopathology of collagen, Mem Inst Oswaldo Cruz 86(Suppl3) (1991) 1-11.

[347] L.C. Junqueira, W. Cossermelli, R. Brentani, Differential staining of collagens type I, II and III by Sirius Red and polarization microscopy, Arch Histol Jpn 41(3) (1978) 267-274.

[348] P. Bruckner, E.F. Eikenberry, D.J. Prockop, Formation of the triple helix of type I procollagen in cellulo. A kinetic model based on cis-trans isomerization of peptide bonds, Eur J Biochem 118(3) (1981) 607-613.

[349] J. Rodriguez, N. Gupta, R.D. Smith, P.A. Pevzner, Does trypsin cut before proline?, J Proteome Res 7(1) (2008) 300-305.

[350] C.T. Baldwin, C.D. Constantinou, K.W. Dumars, D.J. Prockop, A single base mutation that converts glycine 907 of the alpha 2(I) chain of type I procollagen to aspartate in a lethal variant of osteogenesis imperfecta. The single amino acid substitution near the carboxyl terminus destabilizes the whole triple helix, J Biol Chem 264(5) (1989) 3002-3006.

[351] S.B. Deak, P.M. Scholz, P.S. Amenta, C.D. Constantinou, S.A. Levi-Minzi, L. Gonzalez-Lavin, J.W. Mackenzie, The substitution of arginine for glycine 85 of the alpha 1(I) procollagen chain results in mild osteogenesis imperfecta. The mutation provides direct evidence for three discrete domains of cooperative melting of intact type I collagen, J Biol Chem 266(32) (1991) 21827-21832.

[352] P.L. Privalov, Microcalorimetry of macromolecules: The physical basis of biological structures, John Wiley & Sons2012.

[353] K. Mizuno, S.P. Boudko, J. Engel, H.P. Bachinger, Kinetic hysteresis in collagen folding, Biophys J 98(12) (2010) 3004-3014.

[354] T. Hyashi, S. Curran-Patel, D.J. Prockop, Thermal stability of the triple helix of type I procollagen and collagen. Precautions for minimizing ultraviolet damage to proteins during circular dichroism studies, Biochemistry 18(19) (1979) 4182-4187.

[355] E. Leikina, M.V. Mertts, N. Kuznetsova, S. Leikin, Type I collagen is thermally unstable at body temperature, P Natl Acad Sci 99(3) (2002) 1314-1318.

[356] G.C. Na, L.J. Phillips, E.I. Freire, In vitro fibril assembly: Thermodynamic studies, Biochemistry 28(18) (1989) 7153-7161.

[357] G.C. Na, L.J. Butz, D.G. Bailey, R.J. Carroll, In vitro collagen fibril assembly in glycerol solution: Evidence for a helical cooperative mechanism involving microfibrils, Biochemistry 25 (1986) 958-966.

[358] E.I. Tiktopulo, A.V. Kajava, Denaturation of type I collagen fibrils is an endothermic process accompanied by a noticeable change in the partial heat capacity, Biochemistry 37(22) (1998) 8147-8152.
[359] R. Holmes, S. Kirk, G. Tronci, X. Yang, D. Wood, Influence of telopeptides on the structural and physical properties of polymeric and monomeric acid-soluble type I collagen, Mater Sci Eng C 77 (2017) 823-827.
[360] M. Gauza-Wlodarczyk, L. Kubisz, S. Mielcarek, D. Wlodarczyk, Comparison of thermal properties of fish collagen and bovine collagen in the temperature range 298-670K, Mater Sci Eng C 80 (2017) 468-471.
[361] M. Schroepfer, M. Meyer, DSC investigation of bovine hide collagen at varying degrees of crosslinking and humidities, Int J Biol Macromol 103 (2017) 120-128.
[362] V. Ferraro, B. Gaillard-Martinie, T. Sayd, C. Chambon, M. Anton, V. Sante-Lhoutellier, Collagen type I from bovine bone. Effect of animal age, bone anatomy and drying methodology on extraction yield, self-assembly, thermal behaviour and electrokinetic potential, Int J Biol Macromol 97 (2017) 55-66.
[363] Z.L. Shen, H. Kahn, R. Ballarini, S.J. Eppell, Viscoelastic properties of isolated collagen fibrils, Biophys J 100(12) (2011) 3008-3015.
[364] V.R. Sherman, Y. Tang, S. Zhao, W. Yang, M.A. Meyers, Structural characterization and viscoelastic constitutive modeling of skin, Acta Biomater 53 (2017) 460-469.
[365] T.A.H. Jarvinen, T.L.N. Jarvinen, P. Kannus, L. Jozsa, M. Jarvinen, Collagen fibres of the spontaneously ruptured human tendons display decrease thickness and crimp angle, J Orthop Res 22(6) (2004) 1303-1309.
[366] E. Reichenberger, B.R. Olsen, Collagens as organizers of extracellular matrix during morphogenesis, Semin Cell Dev Biol 7(5) (1996) 631-638.
[367] G.E. Kempson, H. Muir, C. Pollard, M. Tuke, The tensile properties of the cartilage of human femoral condyles related to the content of collagen and glycosaminoglycans, Biochim Biophys Acta 297(2) (1973) 456-472.
[368] H. Oxlund, T.T. Andreassen, The roles of hyaluronic acid, collagen and elastin in the mechanical properties of connective tissues, J Anat 131(4) (1980) 611-620.
[369] F.R. Partington, G.C. Wood, The role of non-collagen components in the mechanical behaviour of tendon fibres, Biochim Biophys Acta 69 (1963) 485-495.
[370] C. Boote, S. Dennis, Y. Huang, A.J. Quantock, K.M. Meek, Lamellar orientation in human cornea in relation to mechanical properties, J Struct Biol 149(1) (2005) 1-6.

[371] E.G. Canty, K.E. Kadler, Collagen fibril biosynthesis in tendon: A review and recent insights, Comp Bioch Physiol A Mol Integ Physiol 133(4) (2002) 979-985.
[372] D.F. Holmes, H.K. Graham, K.E. Kadler, Collagen fibrils forming in developing tendon show an early and abrupt limitation in diameter at the growing tips, J Mol Biol 283(5) (1998) 1049-1058.
[373] E. Yamamoto, K. Hayashi, N. Yamamoto, Mechanical properties of collagen fascicles from the rabbit patellar tendon, J Biomech Eng 121(1) (1999) 124-131.
[374] M. Franchi, A. Trirè, M. Quaranta, E. Orsini, V. Ottani, Collagen structure of tendon relates to function, Sci World J 7 (2007) 404-420.
[375] F. Flandin, C. Buffevant, D. Herbage, Age-related changes in the biochemical and physicochemical properties of rat skin. Collagen synthesis and maturation and mechanical parameters (uniaxial tension), Cell Mol Biol 32(5) (1986) 565-571.
[376] A.K. Williamson, A.C. Chen, K. Masuda, E.J. Thonar, R.L. Sah, Tensile mechanical properties of bovine articular cartilage: Variations with growth and relationships to collagen network components, J Orthop Res 21(5) (2003) 872-880.
[377] N.A. Kurniawan, L.H. Wong, R. Rajagopalan, Early stiffening and softening of collagen: Interplay of deformation mechanisms in biopolymer networks, Biomacromolecules 13(3) (2012) 691-698.
[378] H.S. Gupta, J. Seto, S. Krauss, P. Boesecke, H.R. Screen, In situ multi-level analysis of viscoelastic deformation mechanisms in tendon collagen, J Struct Biol 169(2) (2010) 183-191.
[379] B. Depalle, Z. Qin, S.J. Shefelbine, M.J. Buehler, Influence of cross-link structure, density and mechanical properties in the mesoscale deformation mechanisms of collagen fibrils, J Mech Behav Biomed Mater 52 (2014) 1-13.
[380] M.P. Wenger, L. Bozec, M.A. Horton, P. Mesquida, Mechanical properties of collagen fibrils, Biophys J 93(4) (2007) 1255-1263.
[381] P. Fratzl, K. Misof, I. Zizak, G. Rapp, H. Amenitsch, S. Bernstorff, Fibrillar structure and mechanical properties of collagen, J Struct Biol 122(1-2) (1997) 119-122.
[382] B.J. Rigby, N. Hirai, J.D. Spikes, H. Eyring, The mechanical properties of rat tail tendon, J Gen Physiol 43(2) (1959) 265-283.
[383] V. Arumugam, M.D. Naresh, N. Somanathan, R. Sanjeevi, Effect of strain rate on the fracture behaviour of collagen, J Mater Sci 27(10) (1992) 2649-2652.

[384] P. Fratzl, K. Misof, I. Zizak, G. Rapp, H. Amenitsch, S. Bernstorff, Fibrillar structure and mechanical properties of collagen., Journal of Structural Biology 122(1-2) (1997) 119-22.

[385] R. Puxkandl, I. Zizak, O. Paris, J. Keckes, W. Tesch, S. Bernstorff, P. Purslow, P. Fratzl, Viscoelastic properties of collagen: Synchrotron radiation investigations and structural model, Philos Trans R Soc Lond B 357(1418) (2002) 191-197.

[386] K. Misof, G. Rapp, P. Fratzl, A new molecular model for collagen elasticity based on synchrotron X-ray scattering evidence, Biophys J 72(3) (1997) 1376-1381.

[387] P.P. Purslow, T.J. Wess, D.W.L. Hukins, Collagen orientation and molecular spacing during creep and stress-relaxation in soft connective tissues, J Exp Biol 201(Pt1) (1998) 135-142.

[388] F.H. Silver, D.L. Christiansen, P.B. Snowhill, Y. Chen, Transition from viscous to elastic-based dependancy of mechanical properties of self-assembled type I collagen fibers, J Appl Polym Sci 79(1) (2001) 134-142.

[389] G.D. Pins, D.L. Christiansen, R. Patel, F.H. Silver, Self-assembly of collagen fibers. Influence of fibrillar alignment and decorin on mechanical properties, Biophys J 73(4) (1997) 2164-2172.

[390] N. Sasaki, S. Odajima, Elongation mechanism of collagen fibrils and force-strain relations of tendon at each level of structural hierarchy, J Biomech 29(9) (1996) 1131-1136.

[391] Y.P. Kato, D. Christiansen, R.A. Hahn, S.J. Shieh, J.D. Goldstein, F.H. Silver, Mechanical properties of collagen fibres: A comparison of reconstituted and rat tail tendon fibres, Biomaterials 10(1) (1989) 38-42.

[392] Y.P. Kato, F.H. Silver, Formation of continuous collagen fibres: Evaluation of biocompatibilily and mechanical properties, Biomaterials 11(3) (1990) 169-175.

[393] E. Knorzer, W. Folkhard, W. Geercken, C. Boschert, M.H. Koch, B. Hilbert, H. Krahl, E. Mosler, H. Nemetschek-Gansler, T. Nemetschek, New aspects of the etiology of tendon rupture. An analysis of time-resolved dynamic-mechanical measurements using synchrotron radiation, Arch Orthop Trauma Surg 105(2) (1986) 113-120.

[394] H. Capella-Monsonís, J.Q. Coentro, V. Graceffa, Z. Wu, D.I. Zeugolis, An experimental toolbox for characterization of mammalian collagen type I in biological specimens, Nat Protoc 13(3) (2018) 507-529.

[395] I.P. Griffith, The effect of cross-links on the mobility of proteins in dodecyl sulphate-polyacrylamide gels, Biochem J 126(3) (1972) 553-560.

[396] A.L. Shapiro, E. Vinuela, J.V. Maizel, Molecular weight estimation of polypeptide chains by electrophoresis in SDS-polyacrylamide gels, Biochem Biophys Res Commun 28(5) (1967) 815-820.

[397] A.L. Shapiro, J.V.J. Maizel, Molecular weight estimation of polypeptides by SDS-polyacrylamide gel electrophoresis: Further data concerning resolving power and general considerations, Anal Biochem 29(3) (1969) 505-514.

[398] K. Weber, M. Osborn, The reliability of molecular weight determinations by dodecyl sulfate-polyacrylamide gel electrophoresis, J Biol Chem 244(16) (1969) 4406-4412.

[399] D.M. Smith, Protein separation and characterisation procedures, in: S.S. Nielsen (Ed.), Food Analysis, Aspen Publishers, Inc1998, pp. 251-263.

[400] D.I. Zeugolis, B. Li, R.R. Lareu, C.K. Chan, M. Raghunath, Collagen solubility testing, a quality assurance step for reproducible electro-spun nano-fibres fabrication. A technical note, J Biomater Sci Polym Ed 19(10) (2008) 1307-1317.

[401] B. Sykes, B. Puddle, M. Francis, R. Smith, The estimation of two collagens from human dermis by interrupted gel electrophoresis, Biochem Biophys Res Commun 72(4) (1976) 1472-1480.

[402] N.C. Avery, T.J. Sims, C. Warkup, A.J. Bailey, Collagen cross-linking in porcine m. longissimus lumborum: Absence of a relationship with variation in texture at pork weight, Meat Sci 42(3) (1996) 355-369.

[403] R. Komsa-Penkova, R. Spirova, B. Bechev, Modification of Lowry's method for collagen concentration measurement, J Biochem Biophys Methods 32(1) (1996) 33-43.

[404] M. Raghunath, C.M. Kielty, K. Kainulainen, A. Child, L. Peltonen, B. Steinmann, Analysis of truncated fibrillin caused by a 366 bp deletion in the FBN1 gene resulting in Marfan-Syndrome, Biochem J 302 (Pt3) (1994) 889-896.

[405] M. Raghunath, B. Steinmann, C. Delozierblanchet, P. Extermann, A. Supertifurga, Prenatal-diagnosis of collagen disorders by direct biochemical-analysis of chorionic villus biopsies, Pediatr Res 36(4) (1994) 441-448.

[406] R.J. McAnulty, Methods for measuring hydroxyproline and estimating in vivo rates of collagen synthesis and degradation, in: J. Varga, D.A. Brenner, S.H. Phan (Eds.), Fibrosis Research, Humana Press2005, pp. 189-207.

[407] J.G. Clark, J.N. Hildebran, Fibroblast procollagen production rates in vitro based on [3H]hydroxyproline production and procollagen hydroxyproline specific activity, Anal Biochem 140(2) (1984) 478-485.
[408] E.C. LeRoy, E.D.J. Harris, A. Sjoerdsma, A modified procedure for radioactive hydroxyproline assay in urine and tissues after labeled proline administration Anal Biochem 17(3) (1966) 377-382.
[409] N.P. Stimler, High-performance liquid chromatographic quantitation of collagen biosynthesis in explant cultures, Anal Biochem 142(1) (1984) 103-108.
[410] T.J. Sims, A.J. Bailey, Quantitative analysis of collagen and elastin cross-links using a single-column system, J Chromatogr B 582(1-2) (1992) 49-55.
[411] J.F.J. Woessner, The determination of hydroxyproline in tissue and protein samples containing small proportions of this imino acid, Arch Biochem Biophys 93(2) (1961) 440-447.
[412] D.S. Miyada, A.L. Tappel, Colorimetric determination of hydroxyproline, Anal Biochem 28(5) (1956) 909-910.
[413] K. Kolar, Colorimetric determination of hydroxyproline as measure of collagen content in meat and meat products: NMKL collaborative study, J Assoc Off Anal Chem 73(1) (1990) 54-57.
[414] H. Stegeman, K. Stalder, Determination of hydroxyproline, Clin Chim Acta 18(2) (1967) 267-273.
[415] R.S. Levine, A nanogram method for hydroxyproline, Microchimica Acta 61(5) (1973) 797-800.
[416] I.S. Jamall, V.N. Finelli, S.S. Que-Hee, A simple method to determine nanogram levels of 4-hydroxyproline in biological tissues, Anal Biochem 112(1) (1981) 70-75.
[417] N. Blumenkrantz, G. Asboe-Hansen, An assay for hydroxyproline and proline on one sample and a simplified method for hydroxyproline, Anal Biochem 63(2) (1975) 331-340.
[418] E.A. Popenoe, R.B. Aronson, D.D. van Slyke, Hydroxylysine formation from lysine during collagen biosynthesis, Biochemistry 55(2) (1966) 393-397.
[419] G.K. Reddy, C.S. Enwemeka, A simplified method for the analysis of hydroxyproline in biological tissues, Clin Biochem 29(3) (1996) 225-229.
[420] M.D. Ball, D. O'Connor, A. Pandit, Use of tissue transglutaminase and fibronectin to influence osteoblast responses to tricalcium phosphate scaffolds, J Mater Sci Mater Med 20(1) (2009) 113-122.

[421] D.W. Green, B.J.R.F. Bolland, J.M. Kanczler, S.A. Lanham, D. Walsh, S. Mann, R.O.C. Oreffo, Augmentation of skeletal tissue formation in impaction bone grafting using vaterite microsphere biocomposites, Biomaterials 30(10) (2009) 1918-1927.
[422] J.A. Henry, K. Burugapalli, P. Neuenschwander, A. Pandit, Structural variants of biodegradable polyesterurethane in vivo evoke a cellular and angiogenic response that is dictated by architecture, Acta Biomater 5(1) (2009) 29-42.
[423] A.J. Almarza, G. Yang, S.L.Y. Woo, T. Nguyen, S.D. Abramowitch, Positive changes in bone marrow-derived cells in response to culture on an aligned bioscaffold, Tissue Eng A 14(9) (2008) 1489-1495.
[424] H. Fan, H. Liu, S.L. Toh, J.C.H. Goh, Enhanced differentiation of mesenchymal stem cells co-cultured with ligament fibroblasts on gelatin/silk fibroin hybrid scaffold, Biomaterials 29(8) (2008) 1017-1027.
[425] V. Gupta, J.A. Werdenberg, J.S. Mendez, J.K. Grande-Allen, Influence of strain on proteoglycan synthesis by valvular interstitial cells in three-dimensional culture, Acta Biomater 4(1) (2008) 88-96.
[426] Y. Kanno, A. Kaneiwa, M. Minamida, M. Kanno, K. Tomogane, K. Takeuchi, K. Okada, S. Ueshima, O. Matsuo, H. Matsuno, The absence of uPAR Is associated with the progression of dermal fibrosis, J Invest Dermatol 128(12) (2008) 2792-2797.
[427] H.J. Park, D.H. Cho, H.J. Kim, J.Y. Lee, B.K. Cho, S.I. Bang, S.Y. Song, K. Yamasaki, A. Di Nardo, R.L. Gallo, Collagen synthesis Is suppressed in dermal fibroblasts by the human antimicrobial peptide LL-37, J Invest Dermatol 129(4) (2008) 843-850.
[428] R. Lareu, D.I. Zeugolis, M. Abu-Rub, A. Pandit, M. Raghunath, Essential modification of the Sircol Collagen Assay for the accurate quantification of collagen content in complex protein solutions, Acta Biomater 6(8) (2014) 3146-3151.
[429] J.Q. Coentro, H. Capella-Monsonis, V. Graceffa, Z. Wu, A.M. Mullen, M. Raghunath, D.I. Zeugolis, Collagen quantification in tissue specimens, Methods Mol Biol 1627 (2017) 341-350.
[430] S. Prochazkova, K.M. Varum, K. Ostgaard, Quantitative determination of chitosans by ninhydrin, Carbohyd Polym 38(2) (1999) 115-122.
[431] C.W. Liu, L.C. Chang, K.J. Lin, T.J. Yu, C.C. Tsai, H.K. Wang, T.R. Tsai, Preparation and characterization of gelatin-based mucoadhesive nanocomposites as intravesical gene delivery scaffolds, Biomed Res Int 2014(4) (2014) doi: 10.1155/2014/473823.

[432] R. Kale, A. Bajaj, Ultraviolet spectrophotometric method for determination of gelatin crosslinking in the presence of amino groups, J Young Pharm 2(1) (2010) 90-94.

[433] P. Cayot, G. Tainturier, The quantification of protein amino groups by the trinitrobenzenesulfonic acid method: A reexamination, Anal Biochem 249(2) (1997) 184-200.

[434] V. Charulatha, A. Rajaram, Influence of different crosslinking treatments on the physical properties of collagen membranes, Biomaterials 24(5) (2003) 759-767.

[435] J.S. Pieper, A. Oosterhof, P.J. Dijkstra, J.H. Veerkamp, T.H. van Kuppevelt, Preparation and characterization of porous crosslinked collagenous matrices containing bioavailable chondroitin sulphate, Biomaterials 20(9) (1999) 847-858.

[436] K.E. Williams, D.R. Olsen, Matrix metalloproteinase-1 cleavage site recognition and binding in full-length human type III collagen, Matrix Biol 28(6) (2009) 373-379.

[437] K.G. Lu, C.M. Stultz, Insight into the degradation of type-I collagen fibrils by MMP-8, J Mol Biol 425(10) (2013) 1815-1825.

[438] P.S. Nerenberg, C.M. Stultz, Differential unfolding of alpha1 and alpha2 chains in type I collagen and collagenolysis, J Mol Biol 382(1) (2008) 246-256.

[439] M. Gioia, G.F. Fasciglione, S. Marini, S. D'Alessio, G. De Sanctis, O. Diekmann, M. Pieper, V. Politi, H. Tschesche, M. Coletta, Modulation of the catalytic activity of neutrophil collagenase MMP-8 on bovine collagen I. Role of the activation cleavage and of the hemopexin-like domain, J Biol Chem 277(26) (2002) 23123-23130.

[440] S.W. Manka, F. Carafoli, R. Visse, D. Bihan, N. Raynal, R.W. Farndale, G. Murphy, J.J. Enghild, E. Hohenester, H. Nagase, Structural insights into triple-helical collagen cleavage by matrix metalloproteinase 1, Proc Natl Acad Sci U S A 109(31) (2012) 12461-12466.

[441] L. Chung, D. Dinakarpandian, N. Yoshida, J.L. Lauer-Fields, G.B. Fields, R. Visse, H. Nagase, Collagenase unwinds triple-helical collagen prior to peptide bond hydrolysis, EMBO J 23(15) (2004) 3020-3030.

[442] J.L. Lauer-Fields, T. Broder, T. Sritharan, L. Chung, H. Nagase, G.B. Fields, Kinetic analysis of matrix metalloproteinase activity using fluorogenic triple-helical substrates, Biochemistry 40(19) (2001) 5795-5803.

[443] M. Gioia, S. Monaco, G.F. Fasciglione, A. Coletti, A. Modesti, S. Marini, M. Coletta, Characterization of the mechanisms by which gelatinase A, neutrophil collagenase, and membrane-type metalloproteinase MMP-14 recognize collagen I and enzymatically process the two alpha-chains, J Mol Biol 368(4) (2007) 1101-1113.

[444] S. Marini, G.F. Fasciglione, G. de Sanctis, S. D'Alessio, V. Politi, M. Coletta, Cleavage of bovine collagen I by neutrophil collagenase MMP-8. Effect of pH on the catalytic properties as compared to synthetic substrates, J Biol Chem 275(25) (2000) 18657-18663.

[445] A.L. Helling, E.K. Tsekoura, M. Biggs, Y. Bayon, A. Pandit, D.I. Zeugolis, In vitro enzymatic degradation of tissue grafts and collagen biomaterials by matrix metalloproteinases: Improving the collagenase assay, ACS Biomater Sci Eng 3(9) (2017) 1922-1932.

[446] R.T. Aimes, J.P. Quigley, Matrix metalloproteinase-2 is an interstitial collagenase - inhibitor-free enzyme catalyzes the cleavage of collagen fibrils and soluble native type-I collagen generating the specific 3/4-length and 1/4-length fragments, J Boil Chem 270(11) (1995) 5872-5876.

[447] G.B. Fields, A model for interstitial collagen catabolism by mammalian collagenases, J Theor Biol 153(4) (1991) 585-602.

[448] J.M.P. Freije, I. Diezitza, M. Balbin, L.M. Sanchez, R. Blasco, J. Tolivia, C. Lopezotin, Molecular-cloning and expression of collagenase-3, a novel human matrix metalloproteinase produced by breast carcinomas, J Biol Chem 269(24) (1994) 16766-16773.

[449] V. Knauper, C. LopezOtin, B. Smith, G. Knight, G. Murphy, Biochemical characterization of human collagenase-3, J Biol Chem 271(3) (1996) 1544-1550.

[450] E. Ohuchi, K. Imai, Y. Fujii, H. Sato, M. Seiki, Y. Okada, Membrane type 1 matrix metalloproteinase digests interstitial collagens and other extracellular matrix macromolecules, J Biol Chem 272(4) (1997) 2446-2451.

[451] M.Z. Yang, M. Kurkinen, Cloning and characterization of a novel matrix metalloproteinase (MMP), CMMP, from chicken embryo fibroblasts - CMMP, Xenopus XMMP, and human MMP19 have a conserved unique cysteine in the catalytic domain, J Biol Chem 273(28) (1998) 17893-17900.

[452] J.A. Allan, R.M. Hembry, S. Angal, J.J. Reynolds, G. Murphy, Binding of latent and high Mr-active forms of stromelysin to collagen is mediated by the C-terminal domain, J Cell Sci 99(Pt4) (1991) 789-795.

[453] J.A. Allan, A.J.P. Docherty, P.J. Barker, N.S. Huskisson, J.J. Reynolds, G. Murphy, Binding of gelatinases A and B to type-I collagen and other matrix components, Biochem J 309 (Pt1) (1995) 299-306.

[454] G. Murphy, J.A. Allan, F. Willenbrock, M.I. Cockett, J.P. Oconnell, A.J.P. Docherty, The role of the C-terminal domain in collagenase and stromelysin specificity, J Biol Chem 267(14) (1992) 9612-9618.

[455] J.L. Lauer-Fields, G.B. Fields, Triple-helical peptide analysis of collagenolytic protease activity, Biol Chem 383(7-8) (2002) 1095-1105.

[456] Y. Xu, W. Cui, Y. Zhang, P. Zhou, Y. Gu, X. Shen, B. Li, L. Chen, Hierarchical micro/nanofibrous bioscaffolds for structural tissue regeneration, Adv Healthc Mater 6(13) (2017).

[457] R. Portillo-Lara, E. Shirzaei Sani, N. Annabi, Biomimetic orthopedic materials, in: B. Li, T. Webster (Eds.), Orthopedic biomaterials: Advances and applications, Springer International Publishing, Cham, 2017, pp. 109-139.

[458] J.L. Zitnay, S.P. Reese, G. Tran, N. Farhang, R.D. Bowles, J.A. Weiss, Fabrication of dense anisotropic collagen scaffolds using biaxial compression, Acta Biomaterialia 65 (2018) 76-87.

[459] J.L. Puetzer, E. Koo, L.J. Bonassar, Induction of fiber alignment and mechanical anisotropy in tissue engineered menisci with mechanical anchoring, J Biomech 48(8) (2015) 1436-1443.

[460] U.N.G. Wudebwe, A. Bannerman, P. Goldberg-Oppenheimer, J.Z. Paxton, R.L. Williams, L.M. Grover, Exploiting cell-mediated contraction and adhesion to structure tissues in vitro, Philos Trans R Soc Lond B Biol Sci 370(1661) (2015) 20140200.

[461] H.Y. Tuan-Mu, P.C. Lu, P.Y. Lee, C.C. Lin, C.J. Chen, L.L. Huang, J.H. Lin, J.J. Hu, Rapid fabrication of a cell-seeded collagen gel-based tubular construct that withstands arterial pressure : Rapid fabrication of a gel-based media equivalent, Ann Biomed Eng 44(11) (2016) 3384-3397.

[462] L. Yang, C.F. Fitié, K.O. van der Werf, M.L. Bennink, P.J. Dijkstra, J. Feijen, Mechanical properties of single electrospun collagen type I fibers, Biomaterials 29(8) (2008) 955-962.

[463] J.J. Song, H.C. Ott, Organ engineering based on decellularized matrix scaffolds, Trends Mol Med 17(8) (2011) 424-432.

[464] F.M. Chen, X. Liu, Advancing biomaterials of human origin for tissue engineering, Prog Polym Sci 53 (2015) 86-168.

[465] S.F. Badylak, Xenogeneic extracellular matrix as a scaffold for tissue reconstruction, Transpl Immunol 12(3–4) (2004) 367-377.

[466] M. Sandor, H. Xu, J. Connor, J. Lombardi, J.R. Harper, R.P. Silverman, D.J. McQuillan, Host response to implanted porcine-derived biologic materials in a primate model of abdominal wall repair, Tissue Eng A 14(12) (2008) 2021-2031.

[467] K. Burugapalli, J.C. Chan, J.L. Kelly, A.S. Pandit, Efficacy of crosslinking on tailoring in vivo biodegradability of fibro-porous decellularized extracellular matrix and restoration of native tissue structure: A quantitative study using stereology methods, Macromol Biosci 14(2) (2014) 244-256.

[468] K. Burugapalli, A. Pandit, Characterization of tissue response and in vivo degradation of cholecyst-derived extracellular matrix, Biomacromolecules 8(11) (2007) 3439-3451.

[469] G.H. Borschel, R.G. Dennis, W.M. Kuzon, Jr., Contractile skeletal muscle tissue-engineered on an acellular scaffold, Plast Reconstr Surg 113(2) (2004) 595-602; discussion 603-634.

[470] B. Sanders, S. Loerakker, E.S. Fioretta, D.J. Bax, A. Driessen-Mol, S.P. Hoerstrup, F.P. Baaijens, Improved geometry of decellularized tissue engineered heart valves to prevent leaflet retraction, Ann Biomed Eng 44(4) (2016) 1061-1071.

[471] H. Omae, C. Zhao, Y.L. Sun, K.N. An, P.C. Amadio, Multilayer tendon slices seeded with bone marrow stromal cells: A novel composite for tendon engineering, J Orthop Res 27(7) (2009) 937-942.

[472] T. Woods, P.F. Gratzer, Effectiveness of three extraction techniques in the development of a decellularized bone-anterior cruciate ligament-bone graft, Biomaterials 26(35) (2005) 7339-7349.

[473] E.A. Abou Neel, L. Bozec, J.C. Knowles, O. Syed, V. Mudera, R. Day, J.K. Hyun, Collagen -- Emerging collagen based therapies hit the patient, Adv Drug Deliv Rev 65(4) (2013) 429-456.

[474] S.F. Badylak, T.W. Gilbert, Immune response to biologic scaffold materials, Semin Immunol 20(2) (2008) 109-116.

[475] M. Kawecki, W. Labus, A. Klama-Baryla, D. Kitala, M. Kraut, J. Glik, M. Misiuga, M. Nowak, T. Bielecki, A. Kasperczyk, A review of decellurization methods caused by an urgent need for quality control of cell-free extracellular matrix' scaffolds and their role in regenerative medicine, J Biomed Mater Res B 106(2) (2018) 909-923.

[476] P.M. Crapo, T.W. Gilbert, S.F. Badylak, An overview of tissue and whole organ decellularization processes, Biomaterials 32(12) (2011) 3233-3243.
[477] T.J. Keane, I.T. Swinehart, S.F. Badylak, Methods of tissue decellularization used for preparation of biologic scaffolds and in vivo relevance, Methods 84 (2015) 25-34.
[478] T.W. Gilbert, T.L. Sellaro, S.F. Badylak, Decellularization of tissues and organs, Biomaterials 27(19) (2006) 3675-3683.
[479] C. Fidalgo, L. Iop, M. Sciro, M. Harder, D. Mavrilas, S. Korossis, A. Bagno, G. Palu, P. Aguiari, G. Gerosa, A sterilization method for decellularized xenogeneic cardiovascular scaffolds, Acta Biomater 67 (2017) 282-294.
[480] B.N. Brown, S.F. Badylak, Expanded applications, shifting paradigms and an improved understanding of host-biomaterial interactions, Acta Biomater 9(2) (2013) 4948-4955.
[481] L. Utomo, G.S.A. Boersema, Y. Bayon, J.F. Lange, G. van Osch, Y.M. Bastiaansen-Jenniskens, In vitro modulation of the behavior of adhering macrophages by medications is biomaterial-dependent, Biomed Mater 12(2) (2017) 025006.
[482] G. Monaco, R. Cholas, L. Salvatore, M. Madaghiele, A. Sannino, Sterilization of collagen scaffolds designed for peripheral nerve regeneration: Effect on microstructure, degradation and cellular colonization, Mater Sci Eng C 71 (2017) 335-344.
[483] A.M. Matuska, P.S. McFetridge, The effect of terminal sterilization on structural and biophysical properties of a decellularized collagen-based scaffold; implications for stem cell adhesion, J Biomed Mater Res B 103(2) (2015) 397-406.
[484] A. Herbert, J.H. Edwards, G.L. Jones, E. Ingham, J. Fisher, The effects of irradiation dose and storage time following treatment on the viscoelastic properties of decellularised porcine super flexor tendon, J Biomech 57 (2017) 157-160.
[485] L.M. Delgado, A. Pandit, D.I. Zeugolis, Influence of sterilisation methods on collagen-based devices stability and properties, Expert Rev Med Devices 11(3) (2014) 305-314.
[486] E.T. Ricchetti, A. Aurora, J.P. Iannotti, K.A. Derwin, Scaffold devices for rotator cuff repair, J Shoulder Elbow Surg 21(2) (2012) 251-265.
[487] Y. Wang, L. Liao, Histologic and functional outcomes of small intestine submucosa-regenerated bladder tissue, BMC Urol 14 (2014) 69.

[488] C. Madhu, J. Cooke, P. Harber, D. Holmes, Functional outcomes of posterior vaginal wall repair and prespinous colpopexy with biological small intestinal submucosal (SIS) graft, Arch Gynecol Obstet 290(4) (2014) 711-716.

[489] C. Hodonsky, L. Mundada, S. Wang, R. Witt, G. Raff, S. Kaushal, M.S. Si, Effects of scaffold material used in cardiovascular surgery on mesenchymal stem cells and cardiac progenitor cells, Ann Thorac Surg 99(2) (2015) 605-611.

[490] I.L. Valerio, P. Campbell, J. Sabino, C.L. Dearth, M. Fleming, The use of urinary bladder matrix in the treatment of trauma and combat casualty wound care, Regen Med 10(5) (2015) 611-622.

[491] A.M. Warwick, R. Velineni, N.J. Smart, I.R. Daniels, Onlay parastomal hernia repair with cross-linked porcine dermal collagen biologic mesh: long-term results, Hernia 20(2) (2016) 321-325.

[492] Z. Zhang, L. Lv, M. Mamat, Z. Chen, Z. Zhou, L. Liu, Z. Wang, Xenogenic (porcine) acellular dermal matrix promotes growth of granulation tissues in the wound healing of Fournier gangrene, Am Surg 81(1) (2015) 92-95.

[493] B. Romain, F. Story, N. Meyer, J.B. Delhorme, C. Brigand, S. Rohr, Comparative study between biologic porcine dermal meshes: risk factors of postoperative morbidity and recurrence, J Wound Care 25(6) (2016) 320-325.

[494] M.M. Abdelfatah, N. Rostambeigi, E. Podgaetz, M.G. Sarr, Long-term outcomes (>5-year follow-up) with porcine acellular dermal matrix (Permacol) in incisional hernias at risk for infection, Hernia 19(1) (2015) 135-140.

[495] D. Eberli, L. Freitas Filho, A. Atala, J.J. Yoo, Composite scaffolds for the engineering of hollow organs and tissues, Methods 47(2) (2009) 109-115.

[496] C.C. Roth, F.G. Mondalek, Y. Kibar, R.A. Ashley, C.H. Bell, J.A. Califano, S.V. Madihally, D. Frimberger, H.K. Lin, B.P. Kropp, Bladder regeneration in a canine model using hyaluronic acid-poly(lactic-co-glycolic-acid) nanoparticle modified porcine small intestinal submucosa, BJU Int 108(1) (2011) 148-155.

[497] I. Mencia Castano, C.M. Curtin, G.P. Duffy, F.J. O'Brien, Next generation bone tissue engineering: non-viral miR-133a inhibition using collagen-nanohydroxyapatite scaffolds rapidly enhances osteogenesis, Sci Rep 6 (2016) 27941.

[498] T.J. Keane, R. Londono, N.J. Turner, S.F. Badylak, Consequences of ineffective decellularization of biologic scaffolds on the host response, Biomaterials 33(6) (2012) 1771-1781.

[499] D.D. Cissell, J.C. Hu, L.G. Griffiths, K.A. Athanasiou, Antigen removal for the production of biomechanically functional, xenogeneic tissue grafts, J Biomech 47(9) (2014) 1987-1996.

[500] S.U. Scheffler, T. Schmidt, I. Gangéy, M. Dustmann, F. Unterhauser, A. Weiler, Fresh-frozen free-tendon allografts versus autografts in anterior cruciate ligament reconstruction: Delayed remodeling and inferior mechanical function during long-term healing in sheep, Arthroscopy 24(4) (2008) 448-458.

[501] E.M. Ahmed, Hydrogel: Preparation, characterization, and applications: A review, J Adv Res 6(2) (2015) 105-121.

[502] J. Zhu, R.E. Marchant, Design properties of hydrogel tissue-engineering scaffolds, Expert Rev Med Devices 8(5) (2011) 607-626.

[503] D. Thomas, D. Gaspar, A. Sorushanova, G. Milcovich, K. Spanoudes, A.M. Mullen, T. O'Brien, A. Pandit, D.I. Zeugolis, Scaffold and scaffold-free self-assembled systems in regenerative medicine, Biotechnol Bioeng 113(6) (2016) 1155-1163.

[504] K.E. Kadler, Y. Hojima, D.J. Prockop, Assembly of collagen fibrils de novo by cleavage of the type I pC-collagen with procollagen C-proteinase. Assay of critical concentration demonstrates that collagen self-assembly is a classical example of an entropy-driven process, J Biol Chem 262(32) (1987) 15696-15701.

[505] H. Kuivaniemi, G. Tromp, D.J. Prockop, Mutations in fibrillar collagens (types I, II, III, and XI), fibril-associated collagen (type IX), and network-forming collagen (type X) cause a spectrum of diseases of bone, cartilage, and blood vessels, Hum Mutat 9(4) (1997) 300-315.

[506] K.J. Payne, A. Veis, Fourier transform IR spectroscopy of collagen and gelatin solutions: Deconvolution of the amide I band for conformational studies, Biopolymers 27(11) (1988) 1749-1760.

[507] D.F. Holmes, H.K. Graham, J.A. Trotter, K.E. Kadler, STEM/TEM studies of collagen fibril assembly, Micron 32(3) (2001) 273-285.

[508] J. Parkinson, A. Brass, G. Canova, Y. Brechet, The mechanical properties of simulated collagen fibrils, J Biomech 30(6) (1997) 549-554.

[509] P. Ngo, P. Ramalingam, J.A. Phillips, G.T. Furuta, Collagen gel contraction assay, Methods Mol Biol 341 (2006) 103-109.

[510] G.C. Wood, The formation of fibrils from collagen solutions. 2. A mechanism of collagen-fibril formation, Biochem J 75(3) (1960) 598-605.

[511] F.H. Silver, J.W. Freeman, G.P. Seehra, Collagen self-assembly and the development of tendon mechanical properties, J Biomech 36(10) (2003) 1529-1553.
[512] D.F. Holmes, J.A. Chapman, D.J. Prockop, K.E. Kadler, Growing tips of type I collagen fibrils formed in vitro are near-paraboloidal in shape, implying a reciprocal relationship between accretion and diameter, Proc Natl Acad Sci U S A 89(20) (1992) 9855-9859.
[513] E.A. Abou Neel, U. Cheema, J.C. Knowles, R.A. Brown, S.N. Nazhat, Use of multiple unconfined compression for control of collagen gel scaffold density and mechanical properties, Soft Matter 2(11) (2006) 986-992.
[514] D.G. Wallace, J. Rosenblatt, Collagen gel systems for sustained delivery and tissue engineering, Adv Drug Deliv Rev 55(12) (2003) 1631-1649.
[515] I. Rault, V. Frei, D. Herbage, N. Abdul-Malak, A. Huc, Evaluation of different chemical methods for cros-linking collagen gel, films and sponges, J Mater Sci Mater Med 7(4) (1996) 215-221.
[516] H. Stratesteffen, M. Kopf, F. Kreimendahl, A. Blaeser, S. Jockenhoevel, H. Fischer, GelMA-collagen blends enable drop-on-demand 3D printablility and promote angiogenesis, Biofabrication 9(4) (2017) 045002.
[517] K. Hu, H. Shi, J. Zhu, D. Deng, G. Zhou, W. Zhang, Y. Cao, W. Liu, Compressed collagen gel as the scaffold for skin engineering, Biomed Microdevices 12(4) (2010) 627-635.
[518] G.A. Busby, M.H. Grant, S.P. Mackay, P.E. Riches, Confined compression of collagen hydrogels, J Biomech 46(4) (2013) 837-840.
[519] E. Braziulis, M. Diezi, T. Biedermann, L. Pontiggia, M. Schmucki, F. Hartmann-Fritsch, J. Luginbühl, C. Schiestl, M. Meuli, E. Reichmann, Modified plastic compression of collagen hydrogels provides an ideal matrix for clinically applicable skin substitutes, Tissue Eng C 18(6) (2012) 464-474.
[520] E.M. Engelhardt, E. Stegberg, R.A. Brown, J.A. Hubbell, F.M. Wurm, M. Adam, P. Frey, Compressed collagen gel: A novel scaffold for human bladder cells, J Tissue Eng Regen Med 4(2) (2010) 123-130.
[521] R.A. Brown, M. Wiseman, C.B. Chuo, U. Cheema, S.N. Nazhat, Ultrarapid engineering of biomimetic materials and tissues: Fabrication of nano- and microstructures by plastic compression, Adv Funct Mater 15(11) (2005) 1762-1770.

[522] G. Fontana, D. Thomas, E. Collin, A. Pandit, Microgel microenvironment primes adipose-derived stem cells towards an NP cells-like phenotype, Adv Healthc Mater 3(12) (2014) 2012-2022.
[523] W.H. Eaglstein, M. Iriondo, K. Laszlo, A composite skin substitute (graftskin) for surgical wounds. A clinical experience, Dermatol Surg 21(10) (1995) 839-843.
[524] E. Bell, H.P. Ehrlich, D.J. Buttle, T. Nakatsuji, Living tissue formed in vitro and accepted as skin-equivalent tissue of full thickness, Science 211(4486) (1981) 1052-104.
[525] K.C. Clause, J.P. Tinney, L.J. Liu, B. Gharaibeh, J. Huard, J.A. Kirk, S.G. Shroff, K.L. Fujimoto, W.R. Wagner, J.C. Ralphe, B.B. Keller, K. Tobita, A three-dimensional gel bioreactor for assessment of cardiomyocyte induction in skeletal muscle-derived stem cells, Tissue Eng C 16(3) (2010) 375-385.
[526] N.L. Tulloch, V. Muskheli, M.V. Razumova, F.S. Korte, M. Regnier, K.D. Hauch, L. Pabon, H. Reinecke, C.E. Murry, Growth of engineered human myocardium with mechanical loading and vascular coculture, Circ Res 109(1) (2011) 47-59.
[527] W.H. Zimmermann, K. Schneiderbanger, P. Schubert, M. Didie, F. Munzel, J.F. Heubach, S. Kostin, W.L. Neuhuber, T. Eschenhagen, Tissue engineering of a differentiated cardiac muscle construct, Circ Res 90(2) (2002) 223-230.
[528] J. Xie, K. Pak, A. Evans, A. Kamgar-Parsi, S. Fausti, L. Mullen, A.F. Ryan, Neurotrophins differentially stimulate the growth of cochlear neurites on collagen surfaces and in gels, Neural Regen Res 8(17) (2013) 1541-1550.
[529] A.N. Koppes, K.W. Keating, A.L. McGregor, R.A. Koppes, K.R. Kearns, A.M. Ziemba, C.A. McKay, J.M. Zuidema, C.J. Rivet, R.J. Gilbert, D.M. Thompson, Robust neurite extension following exogenous electrical stimulation within single walled carbon nanotube-composite hydrogels, Acta Biomater 39 (2016) 34-43.
[530] M. Hiraoka, K. Kato, T. Nakaji-Hirabayashi, H. Iwata, Enhanced survival of neural cells embedded in hydrogels composed of collagen and laminin-derived cell adhesive peptide, Bioconjug Chem 20(5) (2009) 976-983.
[531] N. Moriarty, A. Pandit, E. Dowd, Encapsulation of primary dopaminergic neurons in a GDNF-loaded collagen hydrogel increases their survival, re-innervation and function after intra-striatal transplantation, Sci Rep 7(1) (2017) 16033.
[532] S.N. Masand, J. Chen, I.J. Perron, B.C. Hammerling, G. Loers, M. Schachner, D.I. Shreiber, The effect of glycomimetic functionalized collagen on peripheral nerve repair, Biomaterials 33(33) (2012) 8353-8362.

[533] D.A. Houweling, J.T.H. van Asseldonk, A.J. Lankhorst, F.P.T. Hamers, D. Martin, P.R. Bar, E.A.J. Joosten, Local application of collagen containing brain-derived neurotrophic factor decreases the loss of function after spinal cord injury in the adult rat, Neurosci Lett 251(3) (1998) 193-196.

[534] S. Mi, B. Chen, B. Wright, C.J. Connon, Plastic compression of a collagen gel forms a much improved scaffold for ocular surface tissue engineering over conventional collagen gels, J Biomed Mater Res A 95(2) (2010) 447-453.

[535] M. Kato, T. Taguchi, H. Kobayashi, An attempt to construct the stroma of cornea using primary cultured corneal cells, J Nanosci Nanotechnol 7(3) (2007) 748-751.

[536] X. Duan, H. Sheardown, Dendrimer crosslinked collagen as a corneal tissue engineering scaffold: Mechanical properties and corneal epithelial cell interactions, Biomaterials 27(26) (2006) 4608-4617.

[537] S.L. Mi, V.V. Khutoryanskiy, R.R. Jones, X.P. Zhu, I.W. Hamley, C.J. Connon, Photochemical cross-linking of plastically compressed collagen gel produces an optimal scaffold for corneal tissue engineering, J Biomed Mater Res A 99A(1) (2011) 1-8.

[538] H.J. Levis, G.S. Peh, K.P. Toh, R. Poh, A.J. Shortt, R.A. Drake, J.S. Mehta, J.T. Daniels, Plastic compressed collagen as a novel carrier for expanded human corneal endothelial cells for transplantation, PLoS One 7(11) (2012) e50993.

[539] A. Shimada, S. Wada, K. Inoue, H. Ideno, T. Kamiunten, K. Komatsu, A. Kudo, Y. Nakamura, T. Sato, K. Nakashima, A. Nifuji, Efficient expansion of mouse primary tenocytes using a novel collagen gel culture method, Histochem Cell Biol 142(2) (2014) 205-215.

[540] S.A. Abbah, D. Thomas, S. Browne, T. O'Brien, A. Pandit, D.I. Zeugolis, Co-transfection of decorin and interleukin-10 modulates pro-fibrotic extracellular matrix gene expression in human tenocyte culture, Sci Rep 6 (2016) 20922.

[541] L. Sun, X.H. Zhou, B. Wu, M. Tian, Inhibitory effect of synovial fluid on tendon-to-bone healing: An experimental study in rabbits, Arthroscopy 28(9) (2012) 1297-1305.

[542] K. Xu, M.K. Al-Ani, Y. Sun, W. Xu, L. Pan, Y. Song, Z. Xu, X. Pan, L. Yang, Platelet-rich plasma activates tendon-derived stem cells to promote regeneration of Achilles tendon rupture in rats, J Tissue Eng Regen Med 11(4) (2017) 1173-1184.

[543] M. Zscharnack, P. Hepp, R. Richter, T. Aigner, R. Schulz, J. Somerson, C. Josten, A. Bader, B. Marquass, Repair of chronic osteochondral defects using

predifferentiated mesenchymal stem cells in an ovine model, Am J Sports Med 38(9) (2010) 1857-1869.
[544] D. Hu, X. Shan, Effects of different concentrations of type-I collagen hydrogel on the growth and differentiation of chondrocytes, Exp Ther Med 14(6) (2017) 5411-5416.
[545] Z. Lu, B.Z. Doulabi, C. Huang, R.A. Bank, M.N. Helder, Collagen type II enhances chondrogenesis in adipose tissue-derived stem cells by affecting cell shape, Tissue Eng A 16(1) (2010) 81-90.
[546] A. Krouwels, F.P.W. Melchels, M.H.P. van Rijen, C.B.M. Ten Brink, W.J.A. Dhert, F. Cumhur Oner, M.A. Tryfonidou, L.B. Creemers, Focal adhesion signaling affects regeneration by human nucleus pulposus cells in collagen- but not carbohydrate-based hydrogels, Acta Biomater 66 (2018) 238-247.
[547] A. Frazer, R.A. Bunning, M. Thavarajah, J.M. Seid, R.G. Russell, Studies on type II collagen and aggrecan production in human articular chondrocytes in vitro and effects of transforming growth factor-beta and interleukin-1beta, Osteoarthr Cartil 2(4) (1994) 235-245.
[548] L.S. Kontturi, E. Järvinen, V. Muhonen, E.C. Collin, A.S. Pandit, I. Kiviranta, M. Yliperttula, A. Urtti, An injectable, in situ forming type II collagen/hyaluronic acid hydrogel vehicle for chondrocyte delivery in cartilage tissue engineering, Drug Deliv Transl Res 4(2) (2014) 149-158.
[549] D. Bosnakovski, M. Mizuno, G. Kim, S. Takagi, M. Okumura, T. Fujinaga, Chondrogenic differentiation of bovine bone marrow mesenchymal stem cells (MSCs) in different hydrogels: Influence of collagen type II extracellular matrix on MSC chondrogenesis, Biotechnol Bioeng 93(6) (2006) 1152-1163.
[550] M. Lazarini, P. Bordeaux-Rego, R. Giardini-Rosa, A.S.S. Duarte, M.O. Baratti, A.R. Zorzi, J.B. de Miranda, C. Lenz Cesar, A. Luzo, S.T. Olalla Saad, Natural type II collagen hydrogel, fibrin sealant, and adipose-derived stem cells as a promising combination for articular cartilage repair, Cartilage 8(4) (2017) 439-443.
[551] P.A. Parmar, J.P. St-Pierre, L.W. Chow, C.D. Spicer, V. Stoichevska, Y.Y. Peng, J.A. Werkmeister, J.A.M. Ramshaw, M.M. Stevens, Enhanced articular cartilage by human mesenchymal stem cells in enzymatically mediated transiently RGDS-functionalized collagen-mimetic hydrogels, Acta Biomater 51 (2017) 75-88.

[552] C. Helary, I. Bataille, A. Abed, C. Illoul, A. Anglo, L. Louedec, D. Letourneur, A. Meddahi-Pelle, M.M. Giraud-Guille, Concentrated collagen hydrogels as dermal substitutes, Biomaterials 31(3) (2010) 481-490.

[553] C. Helary, M. Zarka, M.M. Giraud-Guille, Fibroblasts within concentrated collagen hydrogels favour chronic skin wound healing, J Tissue Eng Regen Med 6(3) (2012) 225-237.

[554] M.C. Jimenez Hamann, C.H. Tator, M.S. Shoichet, Injectable intrathecal delivery system for localized administration of EGF and FGF-2 to the injured rat spinal cord, Exp Neurol 194(1) (2005) 106-119.

[555] L.J. Chamberlain, I.V. Yannas, H.P. Hsu, G. Strichartz, M. Spector, Collagen-GAG substrate enhances the quality of nerve regeneration through collagen tubes up to level of autograft, Exp Neurol 154(2) (1998) 315-329.

[556] M. Salehi, M. Naseri-Nosar, S. Ebrahimi-Barough, M. Nourani, A. Vaez, S. Farzamfar, J. Ai, Regeneration of sciatic nerve crush injury by a hydroxyapatite nanoparticle-containing collagen type I hydrogel, J Physiol Sci 68(5) (2017) 579-587.

[557] A.K. Riau, D. Mondal, T.T. Aung, E. Murugan, L. Chen, N.C. Lwin, L. Zhou, R.W. Beuerman, B. Liedberg, S.S. Venkatraman, J.S. Mehta, Collagen-based artificial corneal scaffold with anti-infective capability for prevention of perioperative bacterial infections, ACS Biomater Sci Eng 1(12) (2015) 1324-1334.

[558] R.G. Young, D.L. Butler, W. Weber, A.I. Caplan, S.L. Gordon, D.J. Fink, Use of mesenchymal stem cells in a collagen matrix for Achilles tendon repair, J Orthop Res 16(4) (1998) 406-413.

[559] V. Falanga, Wound healing and its impairment in the diabetic foot, Lancet 366(9498) (2005) 1736-1743.

[560] A. Veves, V. Falanga, D.G. Armstrong, M.L. Sabolinski, Graftskin, a human skin equivalent, is effective in the management of noninfected neuropathic diabetic foot ulcers: A prospective randomized multicenter clinical trial, Diabetes Care 24(2) (2001) 290-295.

[561] M. Griffiths, N. Ojeh, R. Livingstone, R. Price, H. Navsaria, Survival of Apligraf in acute human wounds, Tissue Eng 10(7-8) (2004) 1180-1195.

[562] J.C. Chachques, J.C. Trainini, N. Lago, M. Cortes-Morichetti, O. Schussler, A. Carpentier, Myocardial assistance by grafting a new bioartificial upgraded myocardium (MAGNUM trial): Clinical feasibility study, Ann Thorac Surg 85(3) (2008) 901-908.

[563] S. Wakitani, T. Okabe, S. Horibe, T. Mitsuoka, M. Saito, T. Koyama, M. Nawata, K. Tensho, H. Kato, K. Uematsu, R. Kuroda, M. Kurosaka, S. Yoshiya, K. Hattori, H. Ohgushi, Safety of autologous bone marrow-derived mesenchymal stem cell transplantation for cartilage repair in 41 patients with 45 joints followed for up to 11 years and 5 months, J Tissue Eng Regen Med 5(2) (2011) 146-150.

[564] R. Kuroda, K. Ishida, T. Matsumoto, T. Akisue, H. Fujioka, K. Mizuno, H. Ohgushi, S. Wakitani, M. Kurosaka, Treatment of a full-thickness articular cartilage defect in the femoral condyle of an athlete with autologous bone-marrow stromal cells, Osteoarthr Cartil 15(2) (2007) 226-231.

[565] S. Wakitani, T. Mitsuoka, N. Nakamura, Y. Toritsuka, Y. Nakamura, S. Horibe, Autologous bone marrow stromal cell transplantation for repair of full-thickness articular cartilage defects in human patellae: Two case reports, Cell Transplant 13(5) (2004) 595-600.

[566] M. Ochi, Y. Uchio, K. Kawasaki, S. Wakitani, J. Iwasa, Transplantation of cartilage-like tissue made by tissue engineering in the treatment of cartilage defects of the knee, J Bone Joint Surg Brit 84B(4) (2002) 571-578.

[567] P. Fagerholm, N.S. Lagali, D.J. Carlsson, K. Merrett, M. Griffith, Corneal regeneration following implantation of a biomimetic tissue-engineered substitute, Clin Transl Sci 2(2) (2009) 162-164.

[568] M. Chvapil, Collagen sponge: Theory and practice of medical applications, J Biomed Mater Res 11(5) (1977) 721-741.

[569] F.J. O'Brien, B.A. Harley, I.V. Yannas, L.J. Gibson, Influence of freezing rate on pore structure in freeze-dried collagen-GAG scaffolds, Biomaterials 25(6) (2004) 1077-1086.

[570] M.G. Haugh, C.M. Murphy, F.J. O'Brien, Novel freeze-drying methods to produce a range of collagen–glycosaminoglycan scaffolds with tailored mean pore sizes, Tissue Eng C 16(5) (2009) 887-894.

[571] E.M. Byrne, E. Farrell, L.A. McMahon, M.G. Haugh, F.J. O'Brien, V.A. Campbell, P.J. Prendergast, B.C. O'Connell, Gene expression by marrow stromal cells in a porous collagen–glycosaminoglycan scaffold is affected by pore size and mechanical stimulation, J Mater Sci Mater Med 19(11) (2008) 3455-3463.

[572] L. Huang, L. Zhu, X. Shi, B. Xia, Z. Liu, S. Zhu, Y. Yang, T. Ma, P. Cheng, K. Luo, J. Huang, Z. Luo, A compound scaffold with uniform longitudinally oriented

guidance cues and a porous sheath promotes peripheral nerve regeneration in vivo, Acta Biomater 68 (2017) 223-236.

[573] F.J. O'Brien, B.A. Harley, I.V. Yannas, L.J. Gibson, The effect of pore size on cell adhesion in collagen-GAG scaffolds, Biomaterials 26(4) (2005) 433-441.

[574] C.M. Murphy, F.J. O'Brien, Understanding the effect of mean pore size on cell activity in collagen-glycosaminoglycan scaffolds, Cell Adh Migr 4(3) (2010) 377-381.

[575] D. von Heimburg, S. Zachariah, H. Kühling, I. Heschel, H. Schoof, B. Hafemann, N. Pallua, Human preadipocytes seeded on freeze-dried collagen scaffolds investigated in vitro and in vivo, Biomaterials 22(5) (2001) 429-438.

[576] M.B. Keogh, S. Partap, J.S. Daly, F.J. O'Brien, Three hours of perfusion culture prior to 28 days of static culture, enhances osteogenesis by human cells in a collagen GAG scaffold, Biotechnol Bioeng 108(5) (2011) 1203-1210.

[577] E. Farrell, F.J. O'Brien, P. Doyle, J. Fischer, I. Yannas, B.A. Harley, B. O'Connell, P.J. Prendergast, V.A. Campbell, A collagen-glycosaminoglycan scaffold supports adult rat mesenchymal stem cell differentiation along osteogenic and chondrogenic routes, Tissue Eng 12(3) (2006) 459-468.

[578] B.S. Kim, J.S. Kim, J. Lee, Improvements of osteoblast adhesion, proliferation, and differentiation in vitro via fibrin network formation in collagen sponge scaffold, J Biomed Mater Res A 101A(9) (2013) 2661-2666.

[579] Y. Ohyabu, T. Adegawa, T. Yoshioka, T. Ikoma, T. Uemura, J. Tanaka, Cartilage regeneration using a porous scaffold, a collagen sponge incorporating a hydroxyapatite/chondroitinsulfate composite, Mater Sci Eng B 173(1–3) (2010) 204-207.

[580] M. Alhag, E. Farrell, M. Toner, T.C. Lee, F.J. O'Brien, N. Claffey, Evaluation of the ability of collagen-glycosaminoglycan scaffolds with or without mesenchymal stem cells to heal bone defects in Wistar rats, Oral Maxillofac Surg 16(1) (2012) 47-55.

[581] F.G. Lyons, A.A. Al-Munajjed, S.M. Kieran, M.E. Toner, C.M. Murphy, G.P. Duffy, F.J. O'Brien, The healing of bony defects by cell-free collagen-based scaffolds compared to stem cell-seeded tissue engineered constructs, Biomaterials 31(35) (2010) 9232-9243.

[582] R.Y. Kim, J.H. Oh, B.S. Lee, Y.K. Seo, S.J. Hwang, I.S. Kim, The effect of dose on rhBMP-2 signaling, delivered via collagen sponge, on osteoclast activation and in vivo bone resorption, Biomaterials 35(6) (2014) 1869-1881.

[583] M. Pelaez, C. Susin, J. Lee, T. Fiorini, F.C. Bisch, D.R. Dixon, J.C. McPherson, A.N. Buxton, U.M. Wikesjö, Effect of rhBMP-2 dose on bone formation/maturation in a rat critical-size calvarial defect model, J Clin Periodontol 41(8) (2014) 827-836.
[584] E. Quinlan, E.M. Thompson, A. Matsiko, F.J. O'Brien, A. López-Noriega, Long-term controlled delivery of rhBMP-2 from collagen-hydroxyapatite scaffolds for superior bone tissue regeneration, J Control Release 207 (2015) 112-119.
[585] M. Monjo, M. Rubert, J.C. Wohlfahrt, H.J. Rønold, J.E. Ellingsen, S.P. Lyngstadaas, In vivo performance of absorbable collagen sponges with rosuvastatin in critical-size cortical bone defects, Acta Biomater 6(4) (2010) 1405-1412.
[586] Y. Kawaguchi, E. Kondo, N. Kitamura, K. Arakaki, Y. Tanaka, M. Munekata, N. Nagai, K. Yasuda, In vivo effects of isolated implantation of salmon-derived crosslinked atelocollagen sponge into an osteochondral defect, J Mater Sci Mater Med 22(2) (2011) 397-404.
[587] J.H. Ahn, T.H. Lee, J.S. Oh, S.Y. Kim, H.J. Kim, I.K. Park, B.S. Choi, G.I. Im, Novel hyaluronate-atelocollagen/beta-TCP-hydroxyapatite biphasic scaffold for the repair of osteochondral defects in rabbits, Tissue Eng A 15(9) (2009) 2595-2604.
[588] G.I. Im, J.H. Ahn, S.Y. Kim, B.S. Choi, S.W. Lee, A hyaluronate-atelocollagen/beta-tricalcium phosphate-hydroxyapatite biphasic scaffold for the repair of osteochondral defects: A porcine study, Tissue Eng A 16(4) (2010) 1189-1200.
[589] H. Mori, E. Kondo, Y. Kawaguchi, N. Kitamura, N. Nagai, H. Iida, K. Yasuda, Development of a salmon-derived crosslinked atelocollagen sponge disc containing osteogenic protein-1 for articular cartilage regeneration: In vivo evaluations with rabbits, BMC Musculoskelet Disord 14 (2013) 174.
[590] M. Onuma-Ukegawa, K. Bhatt, T. Hirai, H. Kaburagi, S. Sotome, Y. Wakabayashi, S. Ichinose, K. Shinomiya, A. Okawa, M. Enomoto, Bone marrow stromal cells combined with a honeycomb collagen sponge facilitate neurite elongation in vitro and neural restoration in the hemisected rat spinal cord, Cell Transplant 24(7) (2015) 1283-1297.
[591] M. Markowicz, E. Koellensperger, S. Neuss, S. Koenigschulte, C. Bindler, N. Pallua, Human bone marrow mesenchymal stem cells seeded on modified collagen improved dermal regeneration in vivo, Cell Transplant 15(8-9) (2006) 723-732.
[592] N. Kanda, N. Morimoto, S. Takemoto, A.A. Ayvazyan, K. Kawai, Y. Sakamoto, T. Taira, S. Suzuki, Efficacy of novel collagen/gelatin scaffold with sustained release

of basic fibroblast growth factor for dermis-like tissue regeneration, Ann Plast Surg 69(5) (2012) 569-574.

[593] N. Kanda, N. Morimoto, A.A. Ayvazyan, S. Takemoto, K. Kawai, Y. Nakamura, Y. Sakamoto, T. Taira, S. Suzuki, Evaluation of a novel collagen-gelatin scaffold for achieving the sustained release of basic fibroblast growth factor in a diabetic mouse model, J Tissue Eng Regen Med 8(1) (2014) 29-40.

[594] A. Ayvazyan, N. Morimoto, N. Kanda, S. Takemoto, K. Kawai, Y. Sakamoto, T. Taira, S. Suzuki, Collagen-gelatin scaffold impregnated with bFGF accelerates palatal wound healing of palatal mucosa in dogs, J Surg Res 171(2) (2011) e247-e257.

[595] R. Ito, N. Morimoto, L.H. Pham, T. Taira, K. Kawai, S. Suzuki, Efficacy of the controlled release of concentrated platelet lysate from a collagen/gelatin scaffold for dermis-like tissue regeneration, Tissue Eng A 19(11-12) (2013) 1398-1405.

[596] R. Aya, T. Ishiko, K. Noda, S. Yamawaki, Y. Sakamoto, K. Tomihata, Y. Katayama, K. Yoshikawa, H. Kubota, T. Nakamura, M. Naitoh, S. Suzuki, Regeneration of elastic fibers by three-dimensional culture on a collagen scaffold and the addition of latent TGF-β binding protein 4 to improve elastic matrix deposition, Biomaterials 72 (2015) 29-37.

[597] A.L. Rocha, B.K. Shirasu, R.M. Hayacibara, O. Magro-Filho, J.N. Zanoni, M.G. Araújo, Clinical and histological evaluation of subepithelial connective tissue after collagen sponge implantation in the human palate, J Periodontal Res 47(6) (2012) 758-765.

[598] R.A. Brandão, B.S. Costa, M.A. Dellaretti, G.T. de Carvalho, M.P. Faria, A.A. de Sousa, Efficacy and safety of a porcine collagen sponge for cranial neurosurgery: A prospective case-control study, World Neurosurg 79(3–4) (2013) 544-550.

[599] S. Greiner, J. Ide, A. Van Noort, Y. Mochizuki, H. Ochi, S. Marraffino, S. Sridharan, S. Rudicel, E. Itoi, Local rhBMP-12 on an absorbable collagen sponge as an adjuvant therapy for rotator cuff repair— A phase 1, randomized, standard of care control, multicenter study: Part 1. Safety and feasibility, Am J Sports Med 43(8) (2015) 1994-2004.

[600] B.A. Lipsky, M. Kuss, M. Edmonds, A. Reyzelman, F. Sigal, Topical application of a gentamicin-collagen sponge combined with systemic antibiotic therapy for the treatment of diabetic foot infections of moderate severity, J Am Podiatr Med Assoc 102(3) (2012) 223-232.

[601] E.F.M. Buijs, H.J. Theunisse, J.J. Mulder, F.J.A. van den Hoogen, E.F. Offeciers, A.J. Zarowski, E.A.M. Mylanus, The use of gentamicin-impregnated collagen sponges (Garacol®/Duracoll®) in cochlear implant infections: our experience in four cases, Clin Otolaryngol 40(5) (2015) 492-495.

[602] C. Schimmer, M. Özkur, B. Sinha, J. Hain, A. Gorski, B. Hager, R. Leyh, Gentamicin-collagen sponge reduces sternal wound complications after heart surgery: A controlled, prospectively randomized, double-blind study, J Thorac Cardiovasc Surg 143(1) (2012) 194-200.

[603] E.K. Tsekoura, A.L. Helling, J.G. Wall, Y. Bayon, D.I. Zeugolis, Battling bacterial infection with hexamethylene diisocyanate cross-linked and Cefaclor-loaded collagen scaffolds, Biomed Mater 12(3) (2017) 035013.

[604] M. Kowalewski, W. Pawliszak, K. Zaborowska, E.P. Navarese, K.A. Szwed, M.E. Kowalkowska, J. Kowalewski, A. Borkowska, L. Anisimowicz, Gentamicin-collagen sponge reduces the risk of sternal wound infections after heart surgery: Meta-analysis, J Thorac Cardiovasc Surg 149(6) (2015) 1631-1640.

[605] M.B. Formanek, L.A. Herwaldt, E.N. Perencevich, M.L. Schweizer, Gentamicin/Collagen sponge use may reduce the risk of surgical site infections for patients undergoing cardiac operations: A meta-analysis, Surg Infect 15(3) (2014) 244-255.

[606] N. Morimoto, K. Yoshimura, M. Niimi, T. Ito, R. Aya, J. Fujitaka, H. Tada, S. Teramukai, T. Murayama, C. Toyooka, K. Miura, S. Takemoto, N. Kanda, K. Kawai, M. Yokode, A. Shimizu, S. Suzuki, Novel collagen/gelatin scaffold with sustained release of basic fibroblast growth factor: Clinical trial for chronic skin ulcers, Tissue Eng A 19(17-18) (2013) 1931-1940.

[607] L. Yan, Z. Chang, B. He, T. Liu, X. Wang, H. Guo, D. Hao, Efficacy of rhBMP-2 versus iliac crest bone graft for posterior C1-C2 fusion in patients older than 60 years, Orthopedics 37(1) (2014) e51-e57.

[608] L. Zak, C. Albrecht, B. Wondrasch, H. Widhalm, G. Vekszler, S. Trattnig, S. Marlovits, S. Aldrian, Results 2 years after matrix-associated autologous chondrocyte transplantation using the Novocart 3D scaffold: An analysis of clinical and radiological data, Am J Sports Med 42(7) (2014) 1618-1627.

[609] T. Yoshikawa, Y. Ueda, K. Miyazaki, M. Koizumi, Y. Takakura, Disc regeneration therapy using marrow mesenchymal cell transplantation: A report of two case studies, Spine 35(11) (2010) E475-E480.

[610] R.E. Marx, D.B. Harrell, Translational research: The CD34+ cell is crucial for large-volume bone regeneration from the milieu of bone marrow progenitor cells in craniomandibular reconstruction, Int J Oral Maxillofac Implants 29(2) (2014) e201-e209.

[611] H. Schoof, J. Apel, I. Heschel, G. Rau, Control of pore structure and size in freeze-dried collagen sponges, J Biomed Mater Res 58(4) (2001) 352-357.

[612] K.M. Pawelec, A. Husmann, S.M. Best, R.E. Cameron, Altering crystal growth and annealing in ice-templated scaffolds, J Mater Sci 50(23) (2015) 7537-7543.

[613] K.M. Pawelec, A. Husmann, S.M. Best, R.E. Cameron, A design protocol for tailoring ice-templated scaffold structure, J R Soc Interface 11(92) (2014) 20130958.

[614] N. Davidenko, T. Gibb, C. Schuster, S.M. Best, J.J. Campbell, C.J. Watson, R.E. Cameron, Biomimetic collagen scaffolds with anisotropic pore architecture, Acta Biomater 8(2) (2012) 667-676.

[615] K.M. Pawelec, A. Husmann, S.M. Best, R.E. Cameron, Understanding anisotropy and architecture in ice-templated biopolymer scaffolds, Mater Sci Eng C 37 (2014) 141-147.

[616] K.M. Brouwer, P. van Rensch, V.E. Harbers, P.J. Geutjes, M.J. Koens, R.M. Wijnen, W.F. Daamen, T.H. van Kuppevelt, Evaluation of methods for the construction of collagenous scaffolds with a radial pore structure for tissue engineering, J Tissue Eng Regen Med 5(6) (2011) 501-504.

[617] M.W. Pot, K.A. Faraj, A. Adawy, W.J. van Enckevort, H.T. van Moerkerk, E. Vlieg, W.F. Daamen, T.H. van Kuppevelt, Versatile wedge-based system for the construction of unidirectional collagen scaffolds by directional freezing: Practical and theoretical considerations, ACS Appl Mater Interfaces 7(16) (2015) 8495-8505.

[618] S.R. Caliari, B.A. Harley, The effect of anisotropic collagen-GAG scaffolds and growth factor supplementation on tendon cell recruitment, alignment, and metabolic activity, Biomaterials 32(23) (2011) 5330-5340.

[619] K. Fukushima, M. Enomoto, S. Tomizawa, M. Takahashi, Y. Wakabayashi, S. Itoh, Y. Kuboki, K. Shinomiya, The axonal regeneration across a honeycomb collagen sponge applied to the transected spinal cord, J Med Dent Sci 55(1) (2008) 71-79.

[620] H. Lu, Y.G. Ko, N. Kawazoe, G. Chen, Cartilage tissue engineering using funnel-like collagen sponges prepared with embossing ice particulate templates, Biomaterials 31(22) (2010) 5825-5835.

[621] K. Fuller, A. Pandit, D.I. Zeugolis, The multifaceted potential of electro-spinning in regenerative medicine, Pharmac Nanotechn 2(1) (2014) 23-34.
[622] G.D. Pins, E.K. Huang, D.L. Christiansen, F.H. Silver, Effects of static axial strain on the tensile properties and failure mechanisms of self-assembled collagen fibers, J Appl Polym Sci 63(11) (1997) 1429-1440.
[623] D.L. Christiansen, E.K. Huang, F.H. Silver, Assembly of type I collagen: Fusion of fibril subunits and the influence of fibril diameter on mechanical properties, Matrix Biol 19(5) (2000) 409-420.
[624] E. Gentleman, A.N. Lay, D.A. Dickerson, E.A. Nauman, G.A. Livesay, K.C. Dee, Mechanical characterization of collagen fibers and scaffolds for tissue engineering, Biomaterials 24(21) (2003) 3805-3813.
[625] D.I. Zeugolis, R.G. Paul, G. Attenburrow, Post-self-assembly experimentation on extruded collagen fibres for tissue engineering applications, Acta Biomater 4(6) (2008) 1646-1656.
[626] D.I. Zeugolis, R.G. Paul, G. Attenburrow, Engineering extruded collagen fibers for biomedical applications, J Appl Polym Sci 108(5) (2008) 2886-2894.
[627] D.I. Zeugolis, R.G. Paul, G. Attenburrow, Extruded collagen fibres for tissue-engineering applications: Influence of collagen concentration and NaCl amount, J Biomater Sci Polym Ed 20(2) (2009) 219-234.
[628] T.J. Koob, D.J. Hernandez, Material properties of polymerized NDGA–collagen composite fibers: Development of biologically based tendon constructs, Biomaterials 23(1) (2002) 203-212.
[629] K.G. Cornwell, A. Landsman, K.S. James, Extracellular matrix biomaterials for soft tissue repair, Clin Podiatr Med Surg 26(4) (2009) 507-523.
[630] K.G. Cornwell, P. Lei, S.T. Andreadis, G.D. Pins, Crosslinking of discrete self-assembled collagen threads: Effects on mechanical strength and cell–matrix interactions, J Biomed Mater Res A 80(2) (2007) 362-371.
[631] K.G. Cornwell, B.R. Downing, G.D. Pins, Characterizing fibroblast migration on discrete collagen threads for applications in tissue regeneration, J Biomed Mater Res A 71(1) (2004) 55-62.
[632] Y.P. Kato, M.G. Dunn, J.P. Zawadsky, A.J. Tria, F.H. Silver, Regeneration of Achilles tendon with a collagen tendon prosthesis. Results of a one-year implantation study, J Bone Joint Surg Am 73(4) (1991) 561-574.

[633] J.F. Cavallaro, P.D. Kemp, K.H. Kraus, Collagen fabrics as biomaterials, Biotechnol Bioeng 43(8) (1994) 781-791.

[634] D. Enea, J. Gwynne, S. Kew, M. Arumugam, J. Shepherd, R. Brooks, S. Ghose, S. Best, R. Cameron, N. Rushton, Collagen fibre implant for tendon and ligament biological augmentation. In vivo study in an ovine model, Knee Surg, Sports Traumatol, Arthrosc 21(8) (2013) 1783-1793.

[635] M. Sanami, Z. Shtein, I. Sweeney, A. Sorushanova, A. Rivkin, M. Miraftab, O. Shoseyov, C. O'Dowd, A.M. Mullen, A. Pandit, D.I. Zeugolis, Biophysical and biological characterisation of collagen/resilin-like protein composite fibres, Biomed Mater 10(6) (2015) 065005.

[636] J.M. Caves, V.A. Kumar, J. Wen, W. Cui, A. Martinez, R. Apkarian, J.E. Coats, K. Berland, E.L. Chaikof, Fibrillogenesis in continuously spun synthetic collagen fiber, J Biomed Mater Res B 93(1) (2010) 24-38.

[637] J.D. Goldstein, A.J. Tria, J.P. Zawadsky, Y.P. Kato, D. Christiansen, F.H. Silver, Development of a reconstituted collagen tendon prosthesis. A preliminary implantation study, J Bone Joint Surg Am 71(8) (1989) 1183-1191.

[638] M.G. Dunn, A.J. Tria, Y.P. Kato, J.R. Bechler, R.S. Ochner, J.P. Zawadsky, F.H. Silver, Anterior cruciate ligament reconstruction using a composite collagenous prosthesis - A biomechanical and histologic-study in rabbits, Am J Sports Med 20(5) (1992) 507-575.

[639] A.A. Marino, R.O. Becker, The effect of electric current on rat tail tendon collagen in solution, Calcif Tissue Res 4(1) (1969) 330-338.

[640] M.T. Abu-Rub, K.L. Billiar, M.H. van Es, A. Knight, B.J. Rodriguez, D.I. Zeugolis, S. McMahon, A.J. Windebank, A. Pandit, Nano-textured self-assembled aligned collagen hydrogels promote directional neurite guidance and overcome inhibition by myelin associated glycoprotein, Soft Matter 7(6) (2011) 2770-2781.

[641] H.R. Baker, E.F. Merschrod, K.M. Poduska, Electrochemically controlled growth and positioning of suspended collagen membranes, Langmuir 24(7) (2008) 2970-2972.

[642] J.A. Uquillas, V. Kishore, O. Akkus, Effects of phosphate-buffered saline concentration and incubation time on the mechanical and structural properties of electrochemically aligned collagen threads, Biomed Mater 6(3) (2011) 035008.

[643] D. Denning, M.T. Abu-Rub, D.I. Zeugolis, S. Habelitz, A. Pandit, A. Fertala, B.J. Rodriguez, Electromechanical properties of dried tendon and isoelectrically focused collagen hydrogels, Acta Biomater 8(8) (2012) 3073-3079.

[644] X. Cheng, U.A. Gurkan, C.J. Dehen, M.P. Tate, H.W. Hillhouse, G.J. Simpson, O. Akkus, An electrochemical fabrication process for the assembly of anisotropically oriented collagen bundles, Biomaterials 29(22) (2008) 3278-3288.

[645] J.A. Uquillas, V. Kishore, O. Akkus, Genipin crosslinking elevates the strength of electrochemically aligned collagen to the level of tendons, J Mech Behav Biomed Mater 15 (2012) 176-189.

[646] U.A. Gurkan, X. Cheng, V. Kishore, J.A. Uquillas, O. Akkus, Comparison of morphology, orientation, and migration of tendon derived fibroblasts and bone marrow stromal cells on electrochemically aligned collagen constructs, J Biomed Mater Res A 94(4) (2010) 1070-1079.

[647] V. Kishore, W. Bullock, X. Sun, W.S. Van Dyke, O. Akkus, Tenogenic differentiation of human MSCs induced by the topography of electrochemically aligned collagen threads, Biomaterials 33(7) (2012) 2137-2144.

[648] M. Younesi, A. Islam, V. Kishore, J.M. Anderson, O. Akkus, Tenogenic induction of human MSCs by anisotropically aligned collagen biotextiles, Adv Funct Mater 24(36) (2014) 5762-5770.

[649] V. Kishore, J.A. Uquillas, A. Dubikovsky, M.A. Alshehabat, P.W. Snyder, G.J. Breur, O. Akkus, In vivo response to electrochemically aligned collagen bioscaffolds, J Biomed Mater Res B 100(2) (2012) 400-408.

[650] M.P. Nijsure, M. Pastakia, J. Spano, M.B. Fenn, V. Kishore, Bioglass incorporation improves mechanical properties and enhances cell-mediated mineralization on electrochemically aligned collagen threads, J Biomed Mater Res A 105(9) (2017) 2429-2440.

[651] T.U. Nguyen, C.A. Bashur, V. Kishore, Impact of elastin incorporation into electrochemically aligned collagen fibers on mechanical properties and smooth muscle cell phenotype, Biomed Mater 11(2) (2016) 025008.

[652] P. Kumar, A. Pandit, D.I. Zeugolis, Progress in Corneal Stromal Repair: From Tissue Grafts and Biomaterials to Modular Supramolecular Tissue-Like Assemblies, Adv Mater 28(27) (2016) 5381-5399.

[653] J.T. Lu, C.J. Lee, S.F. Bent, H.A. Fishman, E.E. Sabelman, Thin collagen film scaffolds for retinal epithelial cell culture, Biomaterials 28(8) (2007) 1486-1494.

[654] Y. Liu, L. Ren, H. Yao, Y.J. Wang, Collagen films with suitable physical properties and biocompatibility for corneal tissue engineering prepared by ion leaching technique, Mater Lett 87 (2012) 1-4.

[655] Y. Liu, L. Ren, Y. Wang, Crosslinked collagen-gelatin-hyaluronic acid biomimetic film for cornea tissue engineering applications, Mater Sci Eng C 33(1) (2013) 196-201.

[656] Y. Liu, L. Ren, K. Long, L. Wang, Y. Wang, Preparation and characterization of a novel tobramycin-containing antibacterial collagen film for corneal tissue engineering, Acta Biomater 10(1) (2014) 289-299.

[657] R.A. Crabb, E.P. Chau, M.C. Evans, V.H. Barocas, A. Hubel, Biomechanical and microstructural characteristics of a collagen film-based corneal stroma equivalent, Tissue Eng 12(6) (2006) 1565-1575.

[658] K. Yoshizato, A. Nishikawa, T. Taira, Functionally polarized layers formed by epidermal cells on a permeable transparent collagen film, J Cell Sci 91 (Pt4) (1988) 491-499.

[659] S. Viji Chandran, T.S. Amritha, G. Rajalekshmi, M. Pandimadevi, A preliminary in vitro study on the bovine collagen film incorporated with Azadirachta indica plant extract as a potential wound dressing material, Int J PharmTech Res 8(6) (2015) 248-257.

[660] C.J. Huang, Y.L. Chien, T.Y. Ling, H.C. Cho, J. Yu, Y.C. Chang, The influence of collagen film nanostructure on pulmonary stem cells and collagen-stromal cell interactions, Biomaterials 31(32) (2010) 8271-8280.

[661] L. Yao, G.C. de Ruiter, H. Wang, A.M. Knight, R.J. Spinner, M.J. Yaszemski, A.J. Windebank, A. Pandit, Controlling dispersion of axonal regeneration using a multichannel collagen nerve conduit, Biomaterials 31(22) (2010) 5789-5797.

[662] X. Zhao, Y. Liu, W.C. Li, K. Long, L. Wang, S. Liu, Y.J. Wang, L. Ren, Collagen based film with well epithelial and stromal regeneration as corneal repair materials: Improving mechanical property by crosslinking with citric acid, Mater Sci Eng C 55 (2015) 201-208.

[663] M. Maeda, K. Kadota, M. Kajihara, A. Sano, K. Fujioka, Sustained release of human growth hormone (hGH) from collagen film and evaluation of effect on wound healing in db/db mice, J Control Release 77(3) (2001) 261-272.

[664] H. Sato, H. Kitazawa, I. Adachi, I. Horikoshi, Microdialysis assessment of microfibrous collagen containing a P-glycoprotein-mediated transport inhibitor, cyclosporine A, for local delivery of etoposide, Pharm Res 13(10) (1996) 1565-1569.
[665] S.W. Kemp, S. Syed, W. Walsh, D.W. Zochodne, R. Midha, Collagen nerve conduits promote enhanced axonal regeneration, schwann cell association, and neovascularization compared to silicone conduits, Tissue Eng A 15(8) (2009) 1975-1988.
[666] L. Yao, W. Daly, B. Newland, S. Yao, W. Wang, B.K.K. Chen, N. Madigan, A. Windebank, A. Pandit, Improved axonal regeneration of transected spinal cord mediated by multichannel collagen conduits functionalized with neurotrophin-3 gene, Gene Ther 20(12) (2013) 1149-1157.
[667] W.T. Daly, L. Yao, M.T. Abu-rub, C. O'Connell, D.I. Zeugolis, A.J. Windebank, A.S. Pandit, The effect of intraluminal contact mediated guidance signals on axonal mismatch during peripheral nerve repair, Biomaterials 33(28) (2012) 6660-6671.
[668] S.T. Li, S.J. Archibald, C. Krarup, R.D. Madison, Peripheral nerve repair with collagen conduits, Clin Mater 9(3-4) (1992) 195-200.
[669] G. Lundborg, A 25-year perspective of peripheral nerve surgery: Evolving neuroscientific concepts and clinical significance, J Hand Surg Am 25(3) (2000) 391-414.
[670] W. Daly, L. Yao, D. Zeugolis, A. Windebank, A. Pandit, A biomaterials approach to peripheral nerve regeneration: Bridging the peripheral nerve gap and enhancing functional recovery, J R Soc Interface 9(67) (2012) 202-221.
[671] G.C. de Ruiter, M.J. Malessy, M.J. Yaszemski, A.J. Windebank, R.J. Spinner, Designing ideal conduits for peripheral nerve repair, Neurosurg Focus 26(2) (2009) E5.
[672] M. Minabe, K. Takeuchi, T. Nishimura, T. Hori, T. Umemoto, Therapeutic effects of combined treatment using tetracycline-immobilized collagen film and root planing in periodontal furcation pockets, J Clin Periodontol 18(5) (1991) 287-290.
[673] M. Minabe, K. Takeuchi, T. Tamura, T. Hori, T. Umemoto, Subgingival administration of tetracycline on a collagen film, J Periodontol 60(10) (1989) 552-556.
[674] M. Minabe, K. Takeuchi, E. Tomomatsu, T. Hori, T. Umemoto, Clinical effects of local application of collagen film-immobilized tetracycline, J Clin Periodontol 16(5) (1989) 291-294.

[675] V. Fernandes de Carvalho, A.O. Paggiaro, C. Isaac, J. Gringlas, M.C. Ferreira, Clinical trial comparing 3 different wound dressings for the management of partial-thickness skin graft donor sites, J Wound Ostomy Continence Nurs 38(6) (2011) 643-647.

[676] E. Truy, F. Disant, J. Tiollier, P. Froehlich, A. Morgon, A clinical study of human type IV collagen as tympanic membrane grafting material. Preliminary noncomparative study, Arch Otolaryngol Head Neck Surg 120(12) (1994) 1329-1332.

[677] D. Bergqvist, A. Stahl, Evaluation of collagen film implantation for local haemostasis after transvesical prostatectomy, Acta Chir Scand 143(7-8) (1977) 479-482.

[678] J. Torbet, M.C. Ronziere, Magnetic alignment of collagen during self-assembly, Biochem J 219(3) (1984) 1057-1059.

[679] D.L. Worcester, Structural origins of diamagnetic anisotropy in proteins, Proc Natl Acad Sci U S A 75(11) (1978) 5475-5477.

[680] J. Torbet, M. Malbouyres, N. Builles, V. Justin, M. Roulet, O. Damour, Å. Oldberg, F. Ruggiero, D.J.S. Hulmes, Orthogonal scaffold of magnetically aligned collagen lamellae for corneal stroma reconstruction, Biomaterials 28(29) (2007) 4268-4276.

[681] T. Novak, S.L. Voytik-Harbin, C.P. Neu, Cell encapsulation in a magnetically aligned collagen-GAG copolymer microenvironment, Acta Biomater 11 (2015) 274-282.

[682] Y. Eguchi, M. Ogiue-Ikeda, S. Ueno, Control of orientation of rat Schwann cells using an 8-T static magnetic field, Neurosci Lett 351(2) (2003) 130-132.

[683] D. Ceballos, X. Navarro, N. Dubey, G. Wendelschafer-Crabb, W.R. Kennedy, R.T. Tranquillo, Magnetically aligned collagen gel filling a collagen nerve guide improves peripheral nerve regeneration, Exp Neurol 158(2) (1999) 290-300.

[684] Y. Yang, M. Ahearne, I. Wimpenny, J. Torbet, Monitoring the effect of magnetically aligned collagen scaffolds on tendon tissue engineering by PSOCT, SPIE BiOS: Biomedical Optics, International Society for Optics and Photonics, 2009, pp. 717903-717903-7.

[685] C. Guo, L.J. Kaufman, Flow and magnetic field induced collagen alignment, Biomaterials 28(6) (2007) 1105-1114.

[686] B. Xu, M.J. Chow, Y. Zhang, Experimental and modeling study of collagen scaffolds with the effects of crosslinking and fiber alignment, Int J Biomater 2011 (2011) 172389.

[687] M.D. Tang, A.P. Golden, J. Tien, Fabrication of collagen gels that contain patterned, micrometer-scale cavities, Adv Mater 16(15) (2004) 1345-1348.

[688] R.B. Vernon, M.D. Gooden, S.L. Lara, T.N. Wight, Native fibrillar collagen membranes of micron-scale and submicron thicknesses for cell support and perfusion, Biomaterials 26(10) (2005) 1109-1117.

[689] C.M. Nelson, J.L. Inman, M.J. Bissell, Three-dimensional lithographically defined organotypic tissue arrays for quantitative analysis of morphogenesis and neoplastic progression, Nat Protocs 3(4) (2008) 674-678.

[690] P. Zorlutuna, N. Hasirci, V. Hasirci, Nanopatterned collagen tubes for vascular tissue engineering, J Tissue Eng Regen Med 2(6) (2008) 373-377.

[691] P. Zorlutuna, A. Elsheikh, V. Hasirci, Nanopatterning of collagen scaffolds improve the mechanical properties of tissue engineered vascular grafts, Biomacromolecules 10(4) (2009) 814-821.

[692] P. Zorlutuna, P. Vadgama, V. Hasirci, Both sides nanopatterned tubular collagen scaffolds as tissue-engineered vascular grafts, J Tissue Eng Regen Med 4(8) (2010) 628-637.

[693] A.P. Golden, J. Tien, Fabrication of microfluidic hydrogels using molded gelatin as a sacrificial element, Lab Chip 7(6) (2007) 720-725.

[694] P. Lee, R. Lin, J. Moon, L.P. Lee, Microfluidic alignment of collagen fibers for in vitro cell culture, Biomed Microdevices 8(1) (2006) 35-41.

[695] G. Mosser, A. Anglo, C. Helary, Y. Bouligand, M.M. Giraud-Guille, Dense tissue-like collagen matrices formed in cell-free conditions, Matrix Biol 25(1) (2006) 3-13.

[696] J.E. Kirkwood, G.G. Fuller, Liquid crystalline collagen: A self-assembled morphology for the orientation of mammalian cells, Langmuir 25(5) (2009) 3200-3206.

[697] N. Saeidi, E.A. Sander, J.W. Ruberti, Dynamic shear-influenced collagen self-assembly, Biomaterials 30(34) (2009) 6581-6592.

[698] L. Muthusubramaniam, L. Peng, T. Zaitseva, M. Paukshto, G.R. Martin, T.A. Desai, Collagen fibril diameter and alignment promote the quiescent keratocyte phenotype, J Biomed Mater Res A 100(3) (2012) 613-621.

[699] N. Saeidi, E.A. Sander, R. Zareian, J.W. Ruberti, Production of highly aligned collagen lamellae by combining shear force and thin film confinement, Acta Biomater 7(6) (2011) 2437-2447.

[700] A. English, A. Azeem, K. Spanoudes, E. Jones, B. Tripathi, N. Basu, K. McNamara, S.A.M. Tofail, N. Rooney, G. Riley, A. O'Riordan, G. Cross, D. Hutmacher, M. Biggs, A. Pandit, D.I. Zeugolis, Substrate topography: A valuable in vitro tool, but a clinical red herring for in vivo tenogenesis, Acta Biomater 27 (2015) 3-12.

[701] A. Azeem, A. English, P. Kumar, A. Satyam, M. Biggs, E. Jones, B. Tripathi, N. Basu, J. Henkel, C. Vaquette, N. Rooney, G. Riley, A. O'Riordan, G. Cross, S. Ivanovski, D. Hutmacher, A. Pandit, D. Zeugolis, The influence of anisotropic nano- to micro-topography on in vitro and in vivo osteogenesis, Nanomedicine 10(5) (2015) 693-711.

[702] G. Rethore, A. Pandit, Use of templates to fabricate nanoscale spherical structures for defined architectural control, Small 6(4) (2010) 488-498.

[703] X. Shi, S. Wang, X. Chen, S. Meshinchi, J.R. Baker, Jr., Encapsulation of submicrometer-sized 2-methoxyestradiol crystals into polymer multilayer capsules for biological applications, Mol Pharm 3(2) (2006) 144-151.

[704] P.K. Sehgal, A. Srinivasan, Collagen-coated microparticles in drug delivery, Expert Opin Drug Deliv 6(7) (2009) 687-695.

[705] O.C. Chan, K.F. So, B.P. Chan, Fabrication of nano-fibrous collagen microspheres for protein delivery and effects of photochemical crosslinking on release kinetics, J Control Release 129(2) (2008) 135-143.

[706] W.F. Daamen, P.J. Geutjes, H.T.B. van Moerkerk, S.T.M. Nillesen, R.G. Wismans, T. Hafmans, L.P.W. van den Heuvel, A.M.A. Pistorius, J.H. Veerkamp, J.C.M. van Hest, T.H. van Kuppevelt, “Lyophilisomes”: A new type of (bio)capsule, Adv Mater 19(5) (2007) 673-677.

[707] S. Browne, G. Fontana, B.J. Rodriguez, A. Pandit, A protective extracellular matrix-based gene delivery reservoir fabricated by electrostatic charge manipulation, Mol Pharm 9(11) (2012) 3099-3106.

[708] G. Rethore, A. Mathew, H. Naik, A. Pandit, Preparation of chitosan/polyglutamic acid spheres based on the use of polystyrene template as a nonviral gene carrier, Tissue Eng C 15(4) (2009) 605-613.

[709] B.C. Dash, G. Rethore, M. Monaghan, K. Fitzgerald, W. Gallagher, A. Pandit, The influence of size and charge of chitosan/polyglutamic acid hollow spheres on cellular internalization, viability and blood compatibility, Biomaterials 31(32) (2010) 8188-8197.

[710] B.C. Dash, S. Mahor, O. Carroll, A. Mathew, W. Wang, K.A. Woodhouse, A. Pandit, Tunable elastin-like polypeptide hollow sphere as a high payload and controlled delivery gene depot, J Control Release 152(3) (2011) 382-392.

[711] F.Y. Bai, S.J. Fang, Progress in research on hollow polymer particles by vesicles templating, Chin J Colloids Polym 23(4) (2004) 26-30.

[712] C. Helary, S. Browne, A. Mathew, W. Wang, A. Pandit, Transfection of macrophages by collagen hollow spheres loaded with polyplexes: A step towards modulating inflammation, Acta Biomater 8(12) (2012) 4208-4214.

[713] H. Kraskiewicz, B. Breen, T. Sargeant, S. McMahon, A. Pandit, Assembly of protein-based hollow spheres encapsulating a therapeutic factor, ACS Chem Neurosci 4(9) (2013) 1297-1304.

[714] M. Likhitpanichkul, Y. Kim, O.M. Torre, E. See, Z. Kazezian, A. Pandit, A.C. Hecht, J.C. Iatridis, Fibrin-genipin annulus fibrosus sealant as a delivery system for anti-TNFα drug, Spine J 15(9) (2015) 2045-2054.

[715] G. Milcovich, P. Contessotto, G. Marsico, S. Ismail, A. Pandit, Synthetic/ECM-inspired hybrid platform for hollow microcarriers with ROS-triggered nanoporation hallmarks, Sci Rep 7(1) (2017) 13138.

[716] C. Tapeinos, A. Larranaga, J.R. Sarasua, A. Pandit, Functionalised collagen spheres reduce H2O2 mediated apoptosis by scavenging overexpressed ROS, Nanomedicine 14(7) (2017) 2397-2405.

[717] J. Yang, M. Yamato, K. Nishida, T. Ohki, M. Kanzaki, H. Sekine, T. Shimizu, T. Okano, Cell delivery in regenerative medicine: The cell sheet engineering approach, J Control Release 116(2) (2006) 193-203.

[718] J. Yang, M. Yamato, T. Shimizu, H. Sekine, K. Ohashi, M. Kanzaki, T. Ohki, K. Nishida, T. Okano, Reconstruction of functional tissues with cell sheet engineering, Biomaterials 28(34) (2007) 5033-5043.

[719] M. Peck, N. Dusserre, T.N. McAllister, N. L'Heureux, Tissue engineering by self-assembly, Mater Today 14(5) (2011) 218-224.

[720] H. Green, B. Goldberg, Synthesis of collagen by mammalian cell lines of fibroblastic and nonfibroblastic origin, Proc Natl Acad Sci U S A 53(6) (1965) 1360-1365.

[721] B. Goldberg, H. Green, The synthesis of collagen and protocollagen hydroxylase by fibroblastic and nonfibroblastic cell lines, Proc Natl Acad Sci U S A 59(4) (1968) 1110-1115.

[722] B. Goldberg, H. Green, Relation between collagen synthesis and collagen proline hydroxylase activity in mammalian cells, Nature 221(5177) (1969) 267-268.

[723] U. Langness, S. Udenfriend, Collagen biosynthesis in nonfibroblastic cell lines, Proc Natl Acad Sci U S A 71(1) (1974) 50-51.

[724] R.C. Siegel, S.R. Pinnell, G.R. Martin, Cross-linking of collagen and elastin. Properties of lysyl oxidase, Biochemistry 9(23) (1970) 4486-4492.

[725] B. Marelli, D. Le Nihouannen, S.A. Hacking, S. Tran, J. Li, M. Murshed, C.J. Doillon, C.E. Ghezzi, Y.L. Zhang, S.N. Nazhat, J.E. Barralet, Newly identified interfibrillar collagen crosslinking suppresses cell proliferation and remodelling, Biomaterials 54 (2015) 126-135.

[726] S.L. Dahl, R.B. Rucker, L.E. Niklason, Effects of copper and cross-linking on the extracellular matrix of tissue-engineered arteries, Cell Transplant 14(6) (2005) 367-374.

[727] E.A. Makris, R.F. MacBarb, D.J. Responte, J.C. Hu, K.A. Athanasiou, A copper sulfate and hydroxylysine treatment regimen for enhancing collagen cross-linking and biomechanical properties in engineered neocartilage, FASEB J 27(6) (2013) 2421-2430.

[728] J.G. Rheinwatd, H. Green, Seria cultivation of strains of human epidemal keratinocytes: The formation of keratinizing colonies from single cells, Cell 6(3) (1975) 331-343.

[729] H. Green, O. Kehinde, J. Thomas, Growth of cultured human epidermal cells into multiple epithelia suitable for grafting, Proc Natl Acad Sci U S A 76(11) (1979) 5665-5668.

[730] N.E. O'Connor, J.B. Mulliken, S. Banks-Schlegel, O. Kehinde, H. Green, Grafting of burns with cultured epithelium prepared from autologous epidermal cells, Lancet 317(8211) (1981) 75-78.

[731] N. L'Heureux, L. Germain, R. Labbe, F.A. Auger, In vitro construction of a human blood vessel from cultured vascular cells: A morphologic study, J Vasc Surg 17(3) (1993) 499-509.
[732] N. L'Heureux, S. Paquet, R. Labbe, L. Germain, F.A. Auger, A completely biological tissue-engineered human blood vessel, FASEB J 12(1) (1998) 47-56.
[733] N. L'Heureux, N. Dusserre, G. Konig, B. Victor, P. Keire, T.N. Wight, N.A.F. Chronos, A.E. Kyles, C.R. Gregory, G. Hoyt, R.C. Robbins, T.N. McAllister, Human tissue-engineered blood vessels for adult arterial revascularization, Nat Med 12(3) (2006) 361-365.
[734] N. L'Heureux, T.N. McAllister, L.M. de la Fuente, Tissue-engineered blood vessel for adult arterial revascularization, N Engl J Med 357(14) (2007) 1451-1453.
[735] G. Konig, T.N. McAllister, N. Dusserre, S.A. Garrido, C. Iyican, A. Marini, A. Fiorillo, H. Avila, W. Wystrychowski, K. Zagalski, M. Maruszewski, A.L. Jones, L. Cierpka, L.M. de la Fuente, N. L'Heureux, Mechanical properties of completely autologous human tissue engineered blood vessels compared to human saphenous vein and mammary artery, Biomaterials 30(8) (2009) 1542-1550.
[736] M. Griffiths, R. Osborne, R. Munger, X. Xiong, C.J. Doillon, N.L.C. Laycock, M. Hakim, Y. Song, M.A. Watsky, Functional human corneal equivalents constructed from cell lines, Science 286(5447) (1999) 2169-2172.
[737] K. Nishida, M. Yamato, Y. Hayashida, K. Watanabe, K. Yamamoto, E. Adachi, S. Nagai, A. Kikuchi, N. Maeda, H. Watanabe, T. Okano, Y. Tano, Corneal reconstruction with tissue-engineered cell sheets composed of autologous oral mucosal epithelium, N Engl J Med 351(12) (2004) 1187-1196.
[738] M.A. Nandkumar, M. Yamato, A. Kushida, C. Konno, M. Hirose, A. Kikuchi, T. Okano, Two-dimensional cell sheet manipulation of heterotypically co-cultured lung cells utilizing temperature-responsive culture dishes results in long-term maintenance of differentiated epithelial cell functions., Biomaterials 23(4) (2002) 1121-1130.
[739] N.E. Vrana, N. Builles, V. Justin, J. Bednarz, G. Pellegrini, B. Ferrari, O. Damour, D.J.S. Hulmes, V. Hasirci, Development of a reconstructed cornea from collagen–chondroitin sulfate foams and human cell cultures, Invest Ophthalmol Vis Sci 49(12) (2008) 5325-5331.

[740] R. Ren, A.E.K. Hutcheon, X.Q. Guo, N. Saeidi, S.A. Melotti, J.W. Ruberti, J.D. Zieske, V. Trinkaus-Randall, Human primary corneal fibroblasts synthesize and deposit proteoglycans in long-term 3-D cultures, Dev Dyn 237(10) (2008) 2705-2715.
[741] J. Somkuti, Z. Torok, F. Pfalzgraf, L. Smeller, Low crowding agent concentration destabilizes against pressure unfolding, Biophys Chem 231 (2017) 125-134.
[742] P. Dey, A. Bhattacherjee, Role of macromolecular crowding on the intracellular diffusion of DNA binding proteins, Sci Rep 8(1) (2018) 844.
[743] A. Satyam, P. Kumar, X. Fan, A. Gorelov, Y. Rochev, L. Joshi, H. Peinado, D. Lyden, B. Thomas, B. Rodriguez, M. Raghunath, A. Pandit, D. Zeugolis, Macromolecular crowding meets tissue engineering by self-assembly: A paradigm shift in regenerative medicine, Adv Mater 26(19) (2014) 3024-3034.
[744] P. Kumar, A. Satyam, X. Fan, E. Collin, Y. Rochev, B.J. Rodriguez, A. Gorelov, S. Dillon, L. Joshi, M. Raghunath, A. Pandit, D.I. Zeugolis, Macromolecularly crowded in vitro microenvironments accelerate the production of extracellular matrix-rich supramolecular assemblies, Sci Rep 5 (2015) 8729.
[745] P. Benny, C. Badowski, E.B. Lane, M. Raghunath, Making more matrix: Enhancing the deposition of dermal-epidermal junction components in vitro and accelerating organotypic skin culture development, using macromolecular crowding, Tissue Eng A 21(1-2) (2015) 183-192.
[746] J.Y. Dewavrin, M. Abdurrahiem, A. Blocki, M. Musib, F. Piazza, M. Raghunath, Synergistic rate boosting of collagen fibrillogenesis in heterogeneous mixtures of crowding agents, J Phys Chem B 119(12) (2015) 4350-4358.
[747] R.R. Lareu, I. Arsianti, H.K. Subramhanya, Y.X. Peng, M. Raghunath, In vitro enhancement of collagen matrix formation and crosslinking for applications in tissue engineering: A preliminary study, Tissue Eng 13(2) (2007) 385-391.
[748] R.R. Lareu, K.H. Subrainhanya, Y.X. Peng, P. Benny, C. Chen, Z.B. Wang, R. Rajagopalan, M. Raghunath, Collagen matrix deposition is dramatically enhanced in vitro when crowded with charged macromolecules: The biological relevance of the excluded volume effect, Febs Lett 581(14) (2007) 2709-2714.
[749] A.S. Zeiger, F.C. Loe, R. Li, M. Raghunath, K.J. Van Vliet, Macromolecular crowding directs extracellular matrix organization and mesenchymal stem cell behavior, PLoS One 7(5) (2012) e37904.

[750] R. Rashid, N.S. Lim, S.M. Chee, S.N. Png, T. Wohland, M. Raghunath, Novel use for polyvinylpyrrolidone as a macromolecular crowder for enhanced extracellular matrix deposition and cell proliferation, Tissue Eng C 20(12) (2014) 994-1002.
[751] M.C. Prewitz, A. Stißel, J. Friedrichs, N. Träber, S. Vogler, M. Bornhäuser, C. Werner, Extracellular matrix deposition of bone marrow stroma enhanced by macromolecular crowding, Biomaterials 73 (2015) 60-69.
[752] X.M. Ang, M.H. Lee, A. Blocki, C. Chen, L.L. Ong, H.H. Asada, A. Sheppard, M. Raghunath, Macromolecular crowding amplifies adipogenesis of human bone marrow-derived mesenchymal stem cells by enhancing the pro-adipogenic microenvironment, Tissue Eng A 20(5-6) (2014) 966-981.
[753] P. Kumar, A. Satyam, X. Fan, Y. Rochev, B.J. Rodriguez, A. Gorelov, L. Joshi, M. Raghunath, A. Pandit, D.I. Zeugolis, Accelerated development of supramolecular corneal stromal-like assemblies from corneal fibroblasts in the presence of macromolecular crowders, Tissue Eng C 21(7) (2015) 660-670.
[754] C.Z.C. Chen, Y.X. Peng, Z.B. Wang, P.V. Fish, J.L. Kaar, R.R. Koepsel, A.J. Russell, R.R. Lareu, M. Raghunath, The scar-in-a-jar: Studying potential antifibrotic compounds from the epigenetic to extracellular level in a single well, Br J Pharmacol 158(5) (2009) 1196-1209.
[755] G.A. Siddiqui, A. Naeem, Aggregation of globular protein as a consequences of macromolecular crowding: A time and concentration dependent study, Int J Biol Macromol 108 (2017) 360-366.
[756] Y.X. Peng, M.T. Bocker, J. Holm, W.S. Toh, C.S. Hughes, F. Kidwai, G.A. Lajoie, T. Cao, F. Lyko, M. Raghunath, Human fibroblast matrices bio-assembled under macromolecular crowding support stable propagation of human embryonic stem cells, J Tissue Eng Regen Med 6(10) (2012) e74-e86.
[757] C.S. Hughes, L.M. Postovit, G.A. Lajoie, Matrigel: A complex protein mixture required for optimal growth of cell culture, Proteomics 10(9) (2010) 1886-1890.
[758] H.K. Kleinman, G.R. Martin, Matrigel: Basement membrane matrix with biological activity, Semin Cancer Biol 15(5) (2005) 378-386.
[759] T.K. Feaster, A.G. Cadar, L. Wang, C.H. Williams, Y.W. Chun, J. Hempel, N. Bloodworth, W.D. Merryman, C.C. Lim, J.C. Wu, B.C. Knollmann, C.C. Hong, Matrigel mattress: A method for the generation of single contracting human-induced pluripotent stem cell-derived cardiomyocytes, Circ Res 117(12) (2015) 995-1000.

[760] G. Benton, I. Arnaoutova, J. George, H.K. Kleinman, J. Koblinski, Matrigel: From discovery and ECM mimicry to assays and models for cancer research, Adv Drug Deliv Rev 79-80 (2014) 3-18.

Chapter 2 - The influence of animal species, gender and tissue on the structural, biophysical, biochemical and biological properties of collagen sponges

This chapter has been published:

The influence of animal species, gender and tissue on the structural, biophysical, biochemical and biological properties of collagen sponges. **A. Sorushanova**, I. Skoufos, A. Tzora, A.M. Mullen, D.I. Zeugolis. Journal of Materials Science: Materials in Medicine. 2021, 32.

2.1 Introduction

The term collagen encompasses a large family of proteins with 29 subtypes [1]. Among them, collagen type I is the most abundant in mammalian tissues (e.g. 85-90 % in skin [2], 65-80 % in tendon [3]). This prevalence in tissues coupled with numerous inherent properties (e.g. cell recognition signals, physiological biodegradability, low antigenicity) makes it the material of choice for biomedical applications [4]. Further, advancements in scaffold fabrication and functionalisation technologies allow the development of three-dimensional implantable devices with clinical indication-specific properties and capacity to deliver a broad range of cells and bioactive molecules in a controlled and localised fashion [5, 6].

Despite the significant advancements in the field, collagen remains an animal by-product and, as such, variability is frequently encountered between different collagen preparations, as a function of species, tissue and extraction method [7, 8], which subsequently influence the properties and performance of the produced scaffolds [9-11]. For example, the properties of extruded collagen fibres have been shown to be species (bovine Achilles tendon versus rat tail tendon) and extraction method (acid versus pepsin) dependent [12]. Yet again, no study to-date has assessed whether the properties of collagen scaffolds depend on the species, gender and tissue from which the collagen is extracted.

In this study, collagen sponges were fabricated and their properties were correlated to the origin of collagen (porcine versus bovine, male versus female and skin versus tendon tissues). Porcine and bovine skin and tendon tissues were selected, as the vast majority of collagen used in biomedicine is extracted from these species and tissues [13]. Pepsin extraction was used, as it results in high yield (cleavage of even mature cross-links) and with reduced immunogenicity and antigenicity (removal of antigenic p-determinant located at the non-helical ends) collagen preparations [14, 15]. Male and female tissues were selected, as recent data have shown gender-dependant disease and injury disposition and differences in, for example, mechanical, structural and compositional properties of tendon [16-21] and skin [22-26].

2.2 Materials and methods

2.2.1 Materials

Porcine and bovine, male and female and skin and tendon tissues were collected from a local abattoir and transferred to the laboratory on ice. The following abbreviations are used throughout this manuscript: PMS: Porcine male skin, PMT: Porcine male tendon, PFS: Porcine female skin, PFT: Porcine female tendon, BMS: Bovine male skin, BMT: Bovine male tendon, BFS: Bovine female skin, BFT: Bovine female tendon. SilverQuest™ kit was purchased from Thermo Fisher Scientific (UK). Quant-iT™ PicoGreen® dsDNA Reagent was purchased from Invitrogen (Bio Sciences Ltd., Ireland). Human adult dermal fibroblasts (Donor number: PCS-201-012™, UK; Gender: Lot specific; Age: Adult). and human derived leukemic monocytes (THP-1) (Donor number: TIB-202™; Gender: Male; Age: 1 year) were purchased from ATCC All chemicals, cell culture media and reagents were purchased from Sigma-Aldrich (Ireland), unless otherwise stated. Collagen extraction protocol has been standardised in the group. Each step of the extraction has been followed according to the protocol for collagen type I extraction.

2.2.2 Collagen extraction and yield analysis

Collagen type I was extracted using the acetic acid / pepsin protocol from porcine and bovine, male and female and skin and tendon tissues [12, 14]. Briefly, porcine and bovine tissues (200 g) were cut into small pieces (1 x 1 x 1 cm^3) using a scalpel and the weight was recorded. Tissue pieces were washed 3 times for 2 h each in salt solutions (3.7 mM Na_2HPO_4, 0.35 mM KH_2PO_4, 51 mM NaCl). Tissue pieces were then suspended in 0.5 M acetic acid for 48 h under stirring at 4 ºC. During the process, swollen tissue pieces were sieved, blended and re-suspended in the acetic acid solution. 2 g of pepsin (1 g pepsin per 100 g tissue) was added to the acetic acid solution at room temperature for 1 h and then the solution was transferred at 4 ºC for 48 h under stirring. The collagen solution was then filtered through a sieve with pore diameter of 250 µm. 0.9 M NaCl was added to the filtered solution, stirred manually every 2 h for 8 h and then left static overnight. The next day, precipitated collagen was collected from the top of the solution and re-suspended in 1 M acetic acid overnight at 4 ºC. The solution was then centrifuged at 8,000 rpm for 20 min at 4 ºC and the supernatant was collected and subjected to a second salt-precipitation and re-

suspended in minimum required volume of 1 M acetic acid to produce a concentrated collagen solution. Once fully suspended, the collagen solution was dialysed four times (the first 3 times every 2 h and the last time overnight) against 1 mM acetic acid at 4 ºC. The final collagen solutions, at concentration of 5mg/ml, were stored at 4 ºC until use. Yield was calculated as % of original weight (200 gr).

2.2.3 Collagen purity

Sodium dodecyl sulphate polyacrylamide gel electrophoresis (SDS-PAGE) was performed to assess the purity of the extracted collagen [27]. Briefly, collagen samples were freeze-dried and then dissolved in 0.5 M acetic acid at concentration of 0.1 mg/ml. Collagen samples were neutralised by the addition of 1 N NaOH. Collagen samples (40 µl) were transferred to Eppendorf tubes and 10 µl of the sample buffer (x5) and 34 µl distilled water were added. Bovine (calf hide) collagen type I (Symatese, Biomateriaux, France) was used as a standard at a concentration of 0.1 mg/ml. Samples and standard were heated at 95 ºC for 5 min and then loaded onto 3 % stacking and 5 % separation gels. Gels were run (50 V for ~ 30 min for the stacking gel and 120 V for ~ 60 min for the separation gel) using Mini-Protean 3 system (Bio-Rad Laboratories, UK). Gels were stained using SilverQuest™ kit (Thermo Fisher Scientific, UK) following the manufacturer's instructions.

2.2.4 Fabrication of collagen sponges

To fabricate collagen sponges, collagen solutions at 5 mg/ml were pipetted into well plates, frozen at -80 ºC overnight and freeze-dried (Freezone 4.5L, Labconco, USA) for 24 h. 24 well plates were used to fabricate sponges for stability analysis with 2 ml of collagen per well and 48 well plates were used to fabricate sponges for biological analysis with 250 µl per well.

2.2.5 Structural characterisation

The structure of produced collagen type I sponges was visualised using scanning electron microscopy (SEM, Hitachi S-4700, Japan). Adhesive carbon tabs were used on top of SEM specimen stubs. Collagen sponges were cut horizontally and stuck onto carbon tabs. Collagen sponges were gold coated prior to SEM imaging at 25 mA

current for 5 min. Pore diameter was measured using ImageJ software (National Institutes of Health, USA).

2.2.6 Quantification of free amines

Free amine groups were determined using the ninhydrin assay [28]. Briefly, 3 mg of freeze-dried samples were added in 1 ml ninhydrin buffer and incubated at 100 ºC for 10 min. After the samples were cooled down at room temperature, 50 % of isopropanol was added and the absorbance was measured at 570 nm. Free amine groups were quantified by interpolating values from a linear standard curve of known concentrations of glycine.

2.2.7 Enzymatic stability analysis

Enzymatic degradation of collagen sponges was assessed using collagenase type I assay [29]. Briefly, 5 mg of freeze-dried samples were added in 1 ml of collagenase solution. The samples were incubated for 3, 6, 9, 12 and 24 h at 37 ºC. The supernatants were then collected, the samples freeze dried overnight and weighed.

2.2.8 Thermal stability and swelling analyses

Denaturation temperature of the collagen sponges was analysed using differential scanning calorimetry (DSC-60, Shimadzu, Japan) [30]. The collagen sponges were hydrated over night at room temperature in 0.01 M phosphate buffered saline (PBS). The sponges were then removed from the PBS and quickly blotted on a filter paper. The sponges were then hermetically sealed in aluminium pans. Heating was carried out at a raising temperature rate of 10 ºC/min within temperature range of 20 to 70 ºC. An empty aluminium pan was used as reference. The endothermic transition was recorded as a typical peak and denaturation temperature was defined as the temperature of maximum power absorption during denaturation (peak temperature).

For swelling determination, collagen sponges were incubated in PBS overnight and the next day were quickly blotted using filter paper. Swelling ratio was calculated using the following equation: Swelling (%) = [(Ww - Wd) / (Wd)] x 100, where Ww and Wd refer to the average wet weight and dry weight of the sponges, respectively.

2.2.9 Mechanical stability analysis

Compression test was carried out using an electromechanical testing machine (Z2.5, Zwick, Germany). The collagen sponges were tested in the dry state, as wet sponges were collapsing. Compression stress and modulus values were calculated as follows:

compressive stress was defined as the force at 70 % compression divided by the original cross-sectional area and modulus was defined as the slope of the stress-strain (deformation) curve at the elastic deformation region (Young's modulus).

2.2.10 Dermal fibroblast culture and analysis

Human adult dermal fibroblasts (hDFs) were used between passages 3 and 5. Collagen sponges were sterilised prior to seeding with UV for 2 h. The cells were seeded onto collagen sponges at a density of 30,000 cells per cm^2 in 48 well plates. The cells were cultured for 3, 5 and 7 days in Dulbecco's Modified Eagle Medium (DMEM), supplemented with 1 % penicillin streptomycin and 10 % foetal bovine serum at 37 ºC and 5 % CO_2. Media were changed every 2 days. Cell proliferation was assessed using PicoGreen® dsDNA assay kit after 3, 5 and 7 days in culture, according to manufacturer's protocol. Metabolic activity was assessed using the alamarBlue® assay (Thermo Fisher Scientific, UK) after 3, 5 and 7 days in culture, according to manufacturer's protocol. Cell viability was assessed with calcein AM (Thermo Fisher Scientific, UK) and ethidium homodimer I (Thermo Fisher Scientific, UK) staining after 3, 5 and 7 days in culture, according to the manufacturer's protocol. The cells were visualised under Andor Revolution Spinning Disk Confocal Microscope (Olympus IX81, Japan). Nuclei were stained with 4′,6-diamidino-2-phenylindole (DAPI), whilst cytoskeleton was stained with rhodamine phalloidin based on established protocols. Briefly, media were removed and sponges were washed three times with Hank's Balanced Salt Solution (HBSS) prior to staining. Cells were fixed with 2 % paraformaldehyde (PFA), permeabilised with 0.2 % Triton X-100 and then stained with DAPI and rhodamine. The sponges were imaged using Andor Revolution Spinning Disk Confocal Microscope (Olympus IX81, Japan). Cell morphometric analysis was conducted with ImageJ software (National Institutes of Health, USA). The total area and aspect ratio (the ratio of the major axis divided by the minor axis of each nuclei based on a fitted ellipse) of the nuclei were assessed. For cell viability and morphometric analysis, for each experimental group, cells on three sponges were analysed by taking five images per sponge (fifteen images in total were analysed per experimental group).

2.2.11 Monocyte culture and analysis

Human derived leukemic monocyte cells (THP-1) were seeded onto TCP and collagen sponges at a density of 50,000 cells per cm^2 in 48 well plates. Collagen sponges were sterilised prior to seeding with UV for 2 h. Mature macrophage-like state was induced by treating them with phorbol 12-myristate 13-acetate (PMA) at concentration of 100 ng/ml for 24 h, at 37 ºC and 5 % CO_2. The differentiation media was removed and replaced by activation media and the cells were incubated for 48 h, at 37 ºC and 5 % CO_2. Activated control was induced with 100 ng/ml of lipopolysaccharide (LPS). Cell metabolic activity, proliferation and viability was assessed at day 1 and day 2, as described above (Section 2.10).

2.2.12 Statistical analysis

Statistical analysis was performed using SPSS (version 20.0, IBM SPSS Statistics, IBM Corporation, USA). All values are expressed as mean values ± standard deviation (SD). One-way analysis of variance (ANOVA) for multiple comparisons was employed, after confirming the following assumptions: (a) the distribution from which each of the samples was derived was normal; (b) and the variances of the population of the samples were equal to one another. Nonparametric statistics were used when either one or both of the above assumptions were violated and consequently Kruskal-Wallis test for multiple comparisons was carried out. Statistical significance was accepted at $p < 0.05$.

2.3 Results

2.3.1 Collagen purity and yield

SDS-PAGE revealed that all collagen preparations exhibited typical collagen type I electrophoretic mobility and purity (**Figure 2.1A**). The porcine groups yielded more collagen than the bovine groups of the same gender and tissue (**Figure 2.1B**).

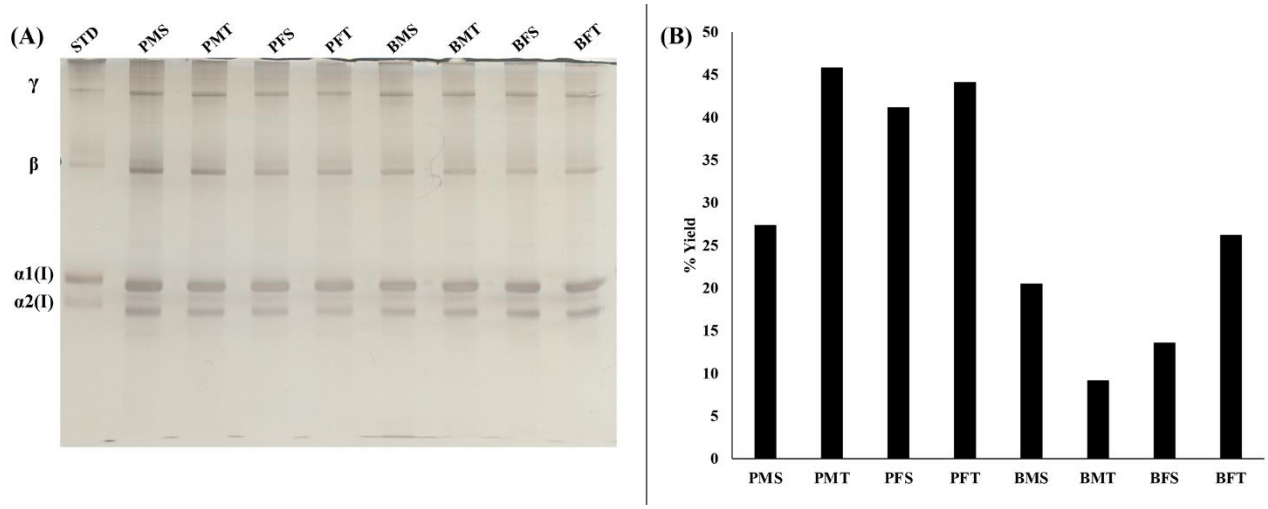

Figure 2.1: (A) SDS-PAGE revealed that all collagen preparations were of similar purity. STD: 0.1 mg/ml bovine (calf hide) collagen type I (Symatese, Biomateriaux, France). **(B)** More collagen was extracted from the porcine than the bovine groups of the same gender and tissue.

2.3.2 Structural analysis

SEM and complementary porosity analysis (**Figure 2.2**) revealed that the bovine groups showed a significantly higher ($p < 0.005$) pore diameter than the porcine groups of the same gender and tissue. No correlation was observed between male and female and skin and tendon tissues across the different species with respect to porosity.

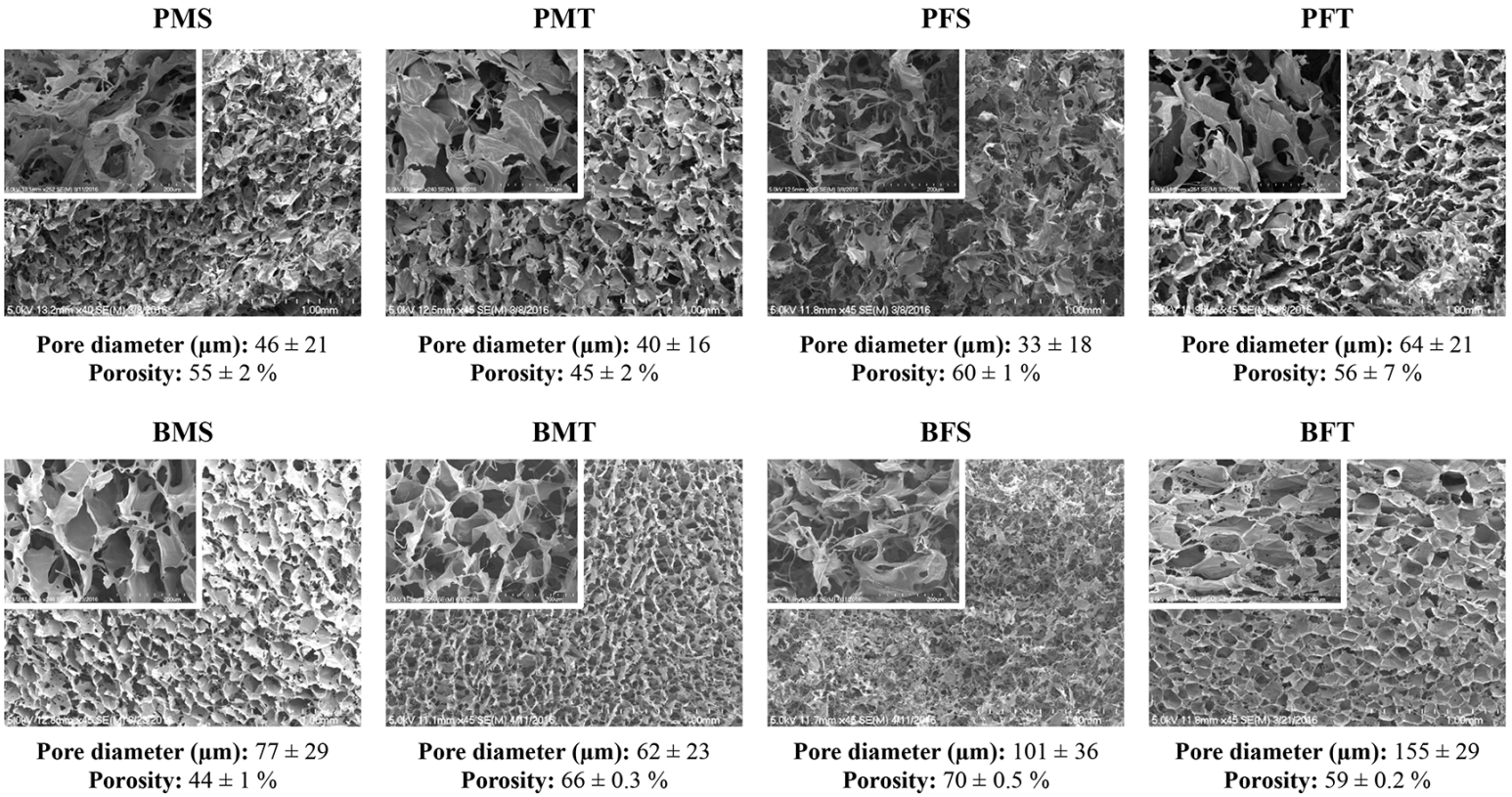

Figure 2.2: SEM and supplementary porosity analysis revealed that the bovine groups exhibited significantly higher ($p < 0.005$) pore diameter than the porcine groups of the same gender and tissue. N=20.

2.3.3 Free amine and resistance to enzymatic degradation analyses

Ninhydrin assay (**Figure 2.3A**) revealed no significant differences ($p > 0.05$) in free amine content as a function of species, gender and tissue. After 24 h, bovine MT, FS and FT exhibited significantly lower ($p < 0.01$) resistance to enzymatic degradation than their porcine counterparts (**Figure 2.3B**).

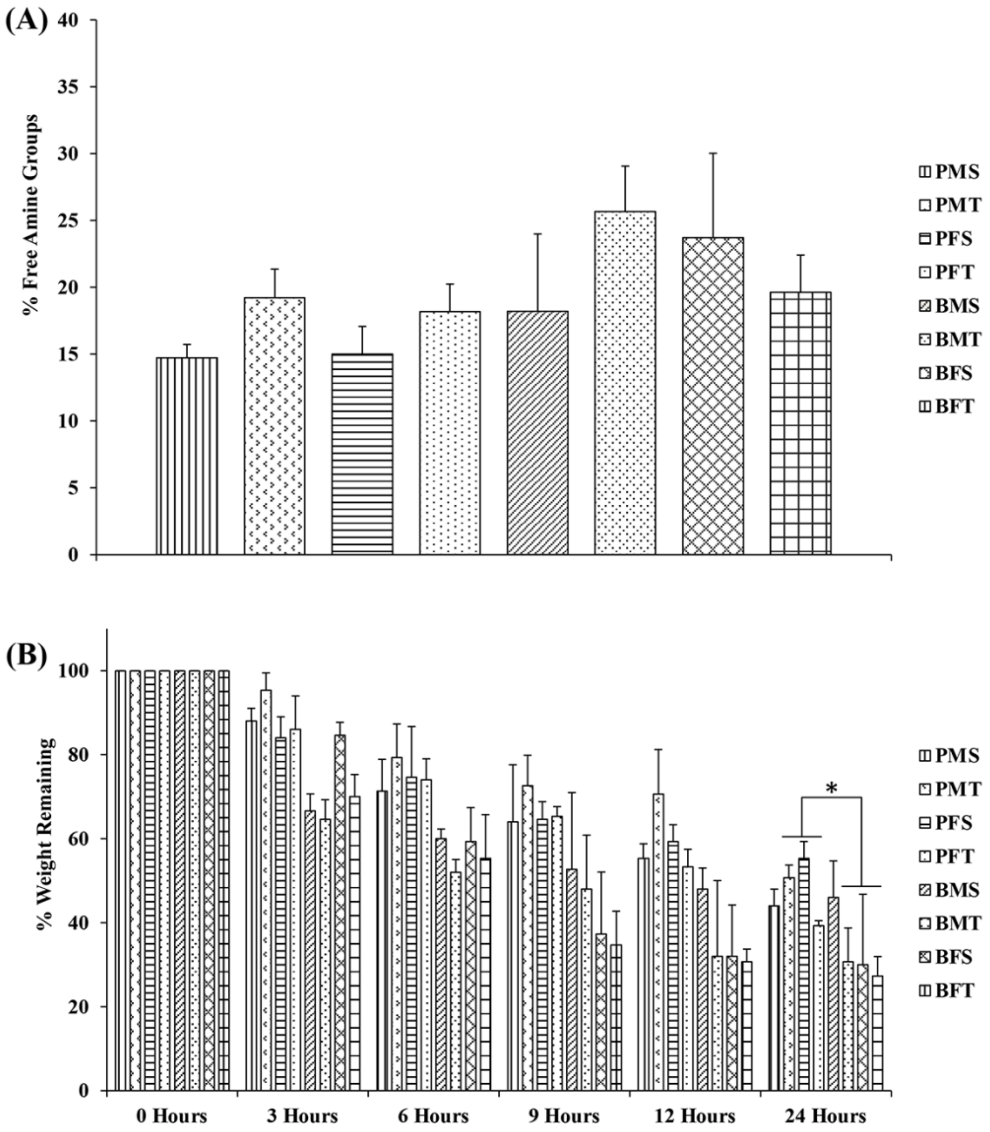

Figure 2.3: (**A**) Species, gender and tissue did not significantly ($p > 0.05$) affect free amine content. N=3. (**B**) Bovine MT, FS and FT exhibited significantly lower ($p < 0.01$) resistance to collagenase degradation than their porcine counterparts after 24 h of enzyme incubation. * indicates statistically significant difference. N=3.

2.3.4 Thermal stability, swelling and mechanical properties analyses

DSC analysis **(Table 2.1)** revealed that sponges produced from porcine collagen exhibited significantly higher ($p < 0.001$) denaturation temperature than the bovine collagen sponges of the same gender and tissue, whilst sponges produced from bovine collagen had significantly higher ($p < 0.001$) PBS absorption capacity (**Table 2.1**) than porcine collagen sponges of the same gender and tissue. Compression test (**Table 2.1**) revealed that sponges produced from porcine collagen exhibited significantly lower ($p < 0.001$) compressive stress and modulus than bovine collagen sponges of the same gender and tissue. Between both species and genders, tendon derived scaffolds exhibited significantly higher ($p < 0.001$) compressive stress and modulus than the skin derived scaffolds.

Table 2.1: Sponges produced from porcine collagen exhibited significantly higher ($p < 0.001$) denaturation temperature and significantly lower ($p < 0.001$) swelling ratio, compressive stress and modulus than bovine collagen sponges of the same gender and tissue. Tendon derived scaffolds exhibited significantly higher ($p < 0.001$) compressive stress and modulus than skin derived scaffolds, independently of the species and gender. Denaturation temperature: N=5; Swelling: N=6; Mechanical properties: N=10.

Group	Peak temperature ± SD (ºC)	Swelling ± SD (%)	Compressive stress at 70 % deformation ± SD (KPa)	Compressive modulus (Young's modulus) ± SD (KPa)
PMS	55.43 ± 1.24	1,603 ± 439	0.75 ± 0.24	0.63 ± 0.29
PMT	54.99 ± 1.08	498 ± 171	1.09 ± 0.13	1.31 ± 0.19
PFS	53.70 ± 1.36	520 ± 109	0.93 ± 0.62	1.07 ± 0.85
PFT	53.08 ± 1.28	771 ± 226	1.56 ± 0.18	2.29 ± 0.30
BMS	51.03 ± 0.46	1,977 ± 463	1.27 ± 0.19	1.78 ± 0.20
BMT	47.65 ± 1.22	7,546 ± 1,736	2.27 ± 0.49	2.84 ± 0.59
BFS	50.55 ± 1.14	2,502 ± 529	1.03 ± 0.21	1.29 ± 0.27
BFT	49.63 ± 1.06	12,031 ± 1,900	3.18 ± 0.66	4.67 ± 1.61

2.3.5 Dermal fibroblast biological analysis

Cytoskeleton and nuclei staining (**Figure 2.4**) demonstrated that both porcine and bovine collagen sponges supported cellular growth, independently of the tissue and gender. Quantitative morphometric analysis (**Figure 2.5**) revealed no apparent differences ($p > 0.05$) in nuclei area and elongation, as a function of species, gender and tissue. Cell viability (**Figure 2.6)** and DNA concentration (**Figure 2.7A**) were not affected as a function of species, gender and tissue, whilst PMS and PFS exhibited the lowest ($p < 0.001$) metabolic (**Figure 2.7B**) activity at day 7; there were no significant differences ($p > 0.05$) in metabolic activity (**Figure 2.7B**) between the other groups.

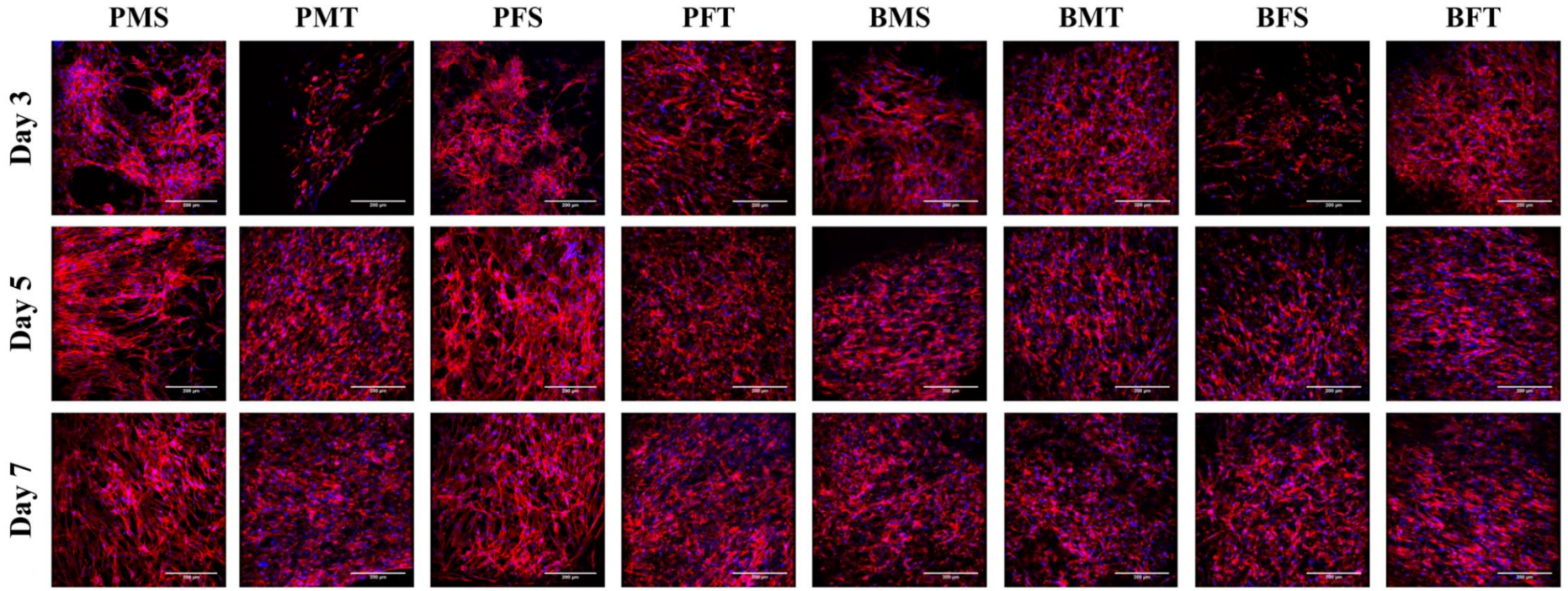

Figure 2.4: Cellular staining (red: cytoskeleton and blue: nuclei) of hDFs at day 3, 5 and 7 demonstrated that all sponges supported cellular growth independently of species, gender and tissue. Scalebar = 200 µm. N=3.

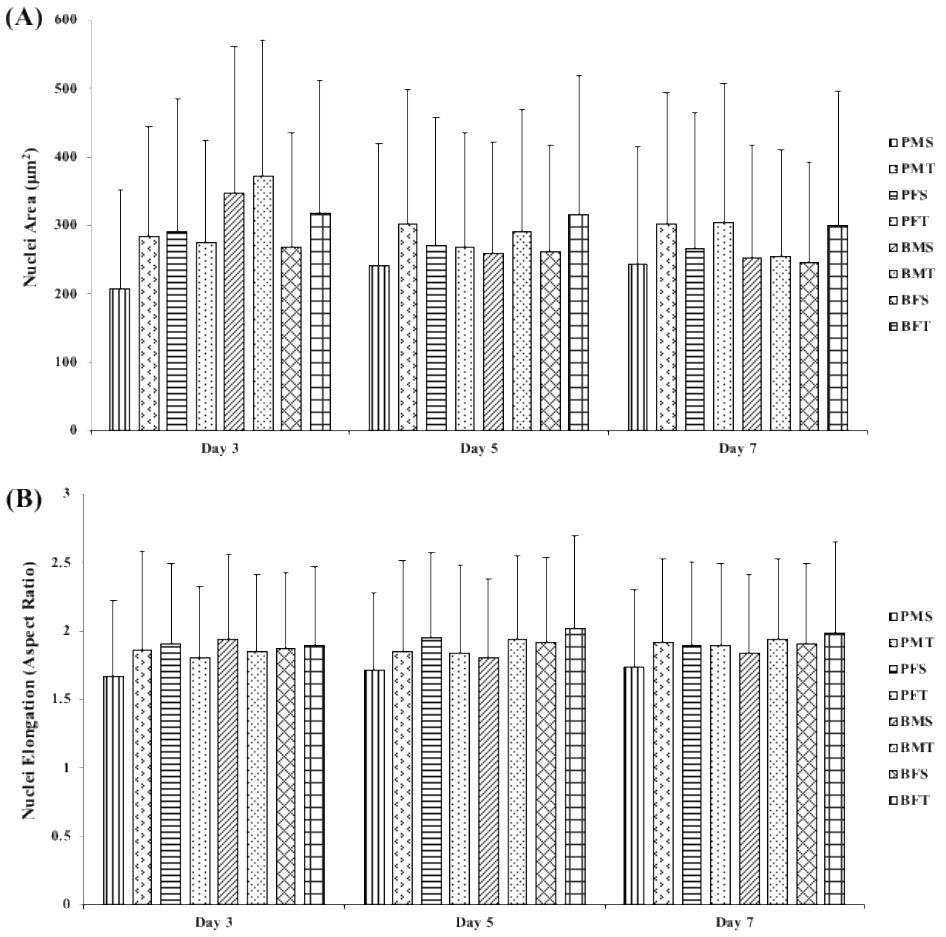

Figure 2.5: Quantitative morphometric analysis of hDFs at day 3, 5 and 7 revealed no apparent significant ($p > 0.05$) differences in (**A**) nuclei area and (**B**) nuclei elongation as a function of species, gender and tissue. N=3.

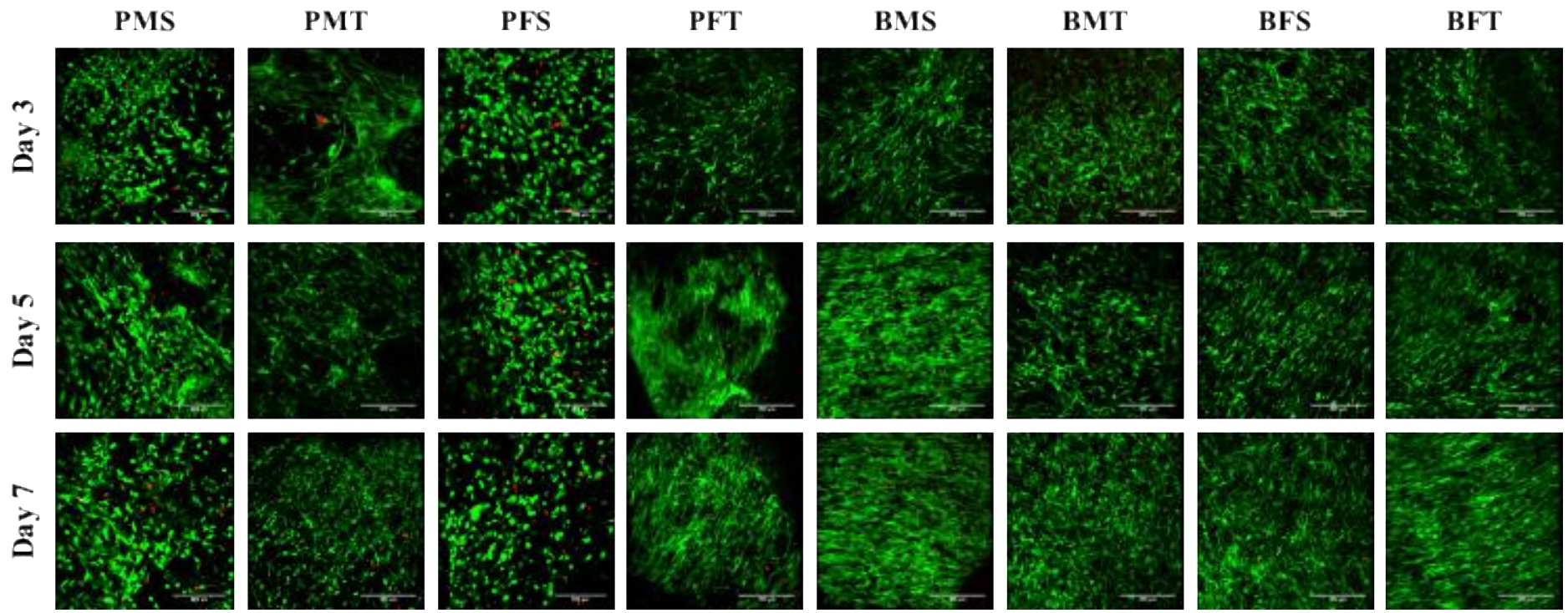

Figure 2.6: Cellular viability of hDFs at day 3, 5 and 7 was affected as a function of species, gender and tissue. Green: live cells, Red: dead cells. Scalebar = 200 µm. N=3.

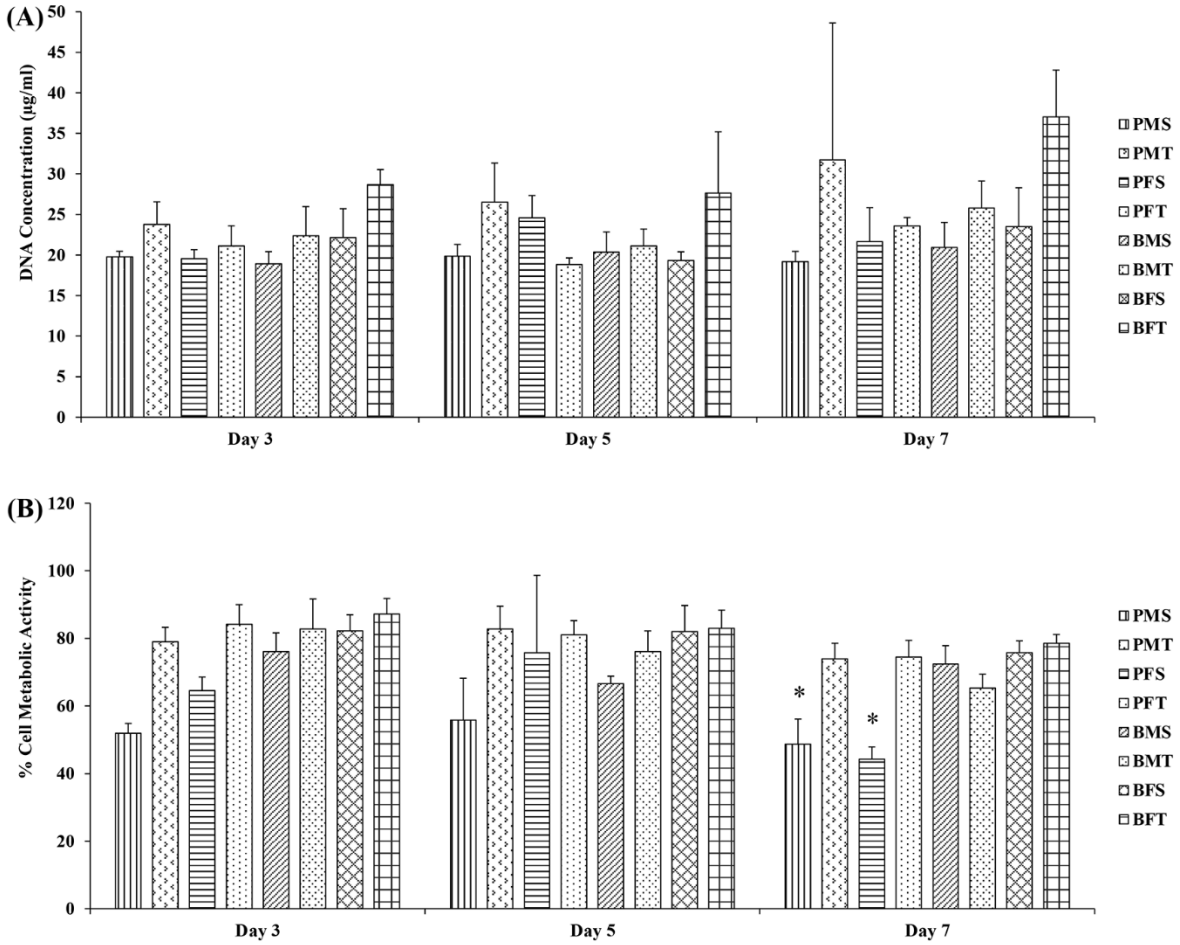

Figure 2.7: (**A**) DNA concentration of hDFs at day 3, 5 and 7 was not significantly ($p > 0.05$) affected as a function of species, gender and tissue. (**B**) By day 7, hDFs grown of PMS and PFS exhibited the lowest ($p < 0.001$) metabolic activity, whilst no significant differences ($p > 0.05$) were observed between the other groups. * indicates statistically significant difference from all other groups. N=3.

2.3.6 Monocyte biological analysis

Qualitative cell morphology analysis via cytoskeleton and nuclei staining (**Figure 2.8**) revealed that most of the THP-1 cells adopted a rounded morphology and formed cell aggregates (5 or more cells) independently of time point, species, gender and tissue. Although some cells grown on TCP and LPS adopted an elongated cell morphology, most cells exhibited a rounded morphology and also formed aggregates (5 or more cells) at both time points.

At day 2, the PMS exhibited the lowest cell viability ($p < 0.001$), whilst no significant differences were observed between the other groups ($p > 0.05$) (**Figure 2.9** and **Figure 2.10A**). Cells on TCP and cells treated with LPS had the highest DNA concentration ($p < 0.001$) and, at day 2, the PMS, BFS and BFT sponges had significantly higher DNA concentration than the other collagen groups ($p < 0.001$) (**Figure 2.10B**). No significant differences were observed in metabolic activity between all groups ($p > 0.05$) (**Figure 2.10C**).

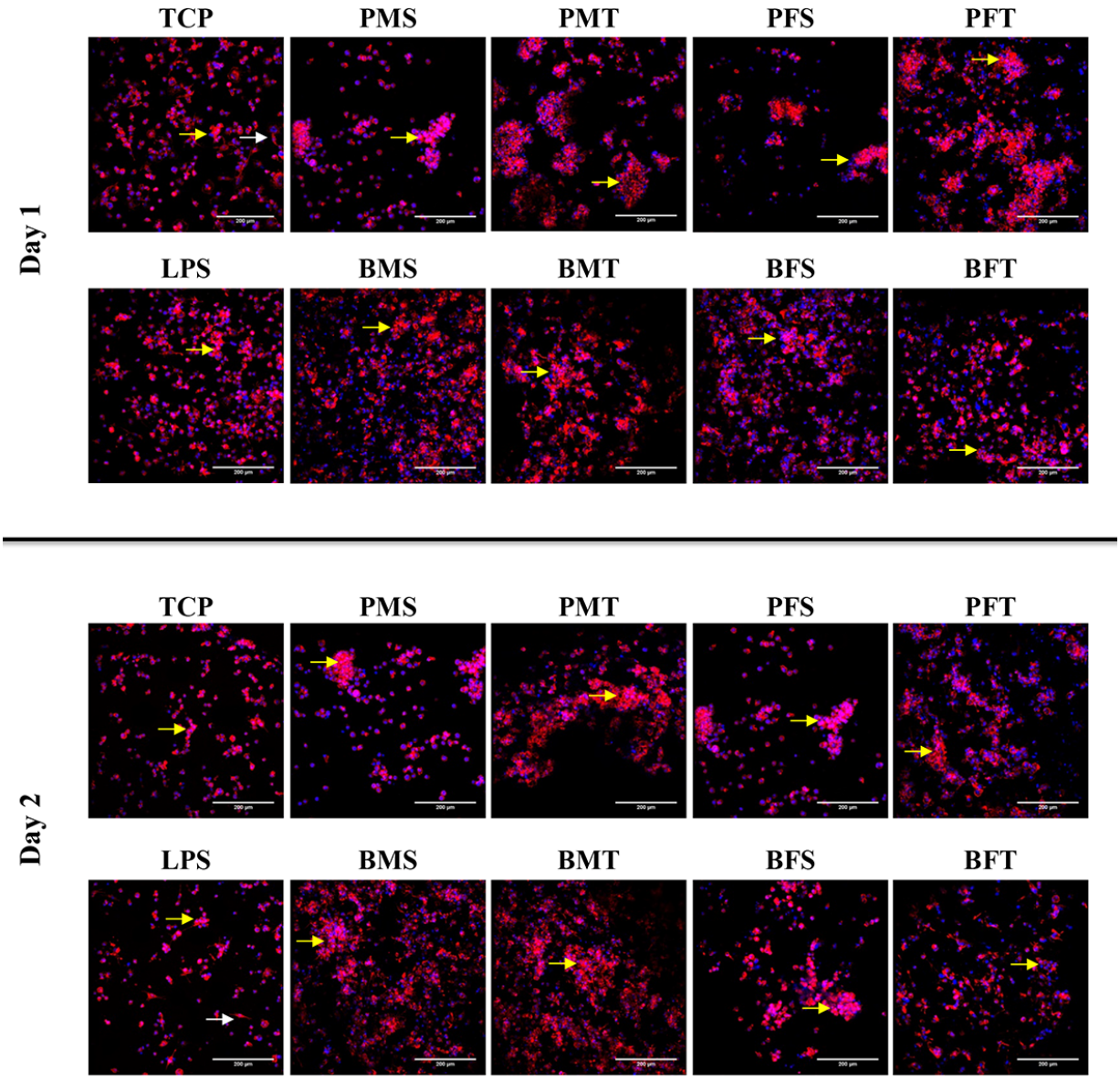

Figure 2.8: Cellular staining (red: cytoskeleton and blue: nuclei) of THP-1 cells at day 1 and 2 revealed that most cells adopted a rounded morphology and formed aggregates on all samples (5 or more cells; yellow arrows), including TCP and LPS controls. Some cells on TCP and LPS also exhibited an elongated morphology (white arrows). Scalebar = 200 µm. N=3.

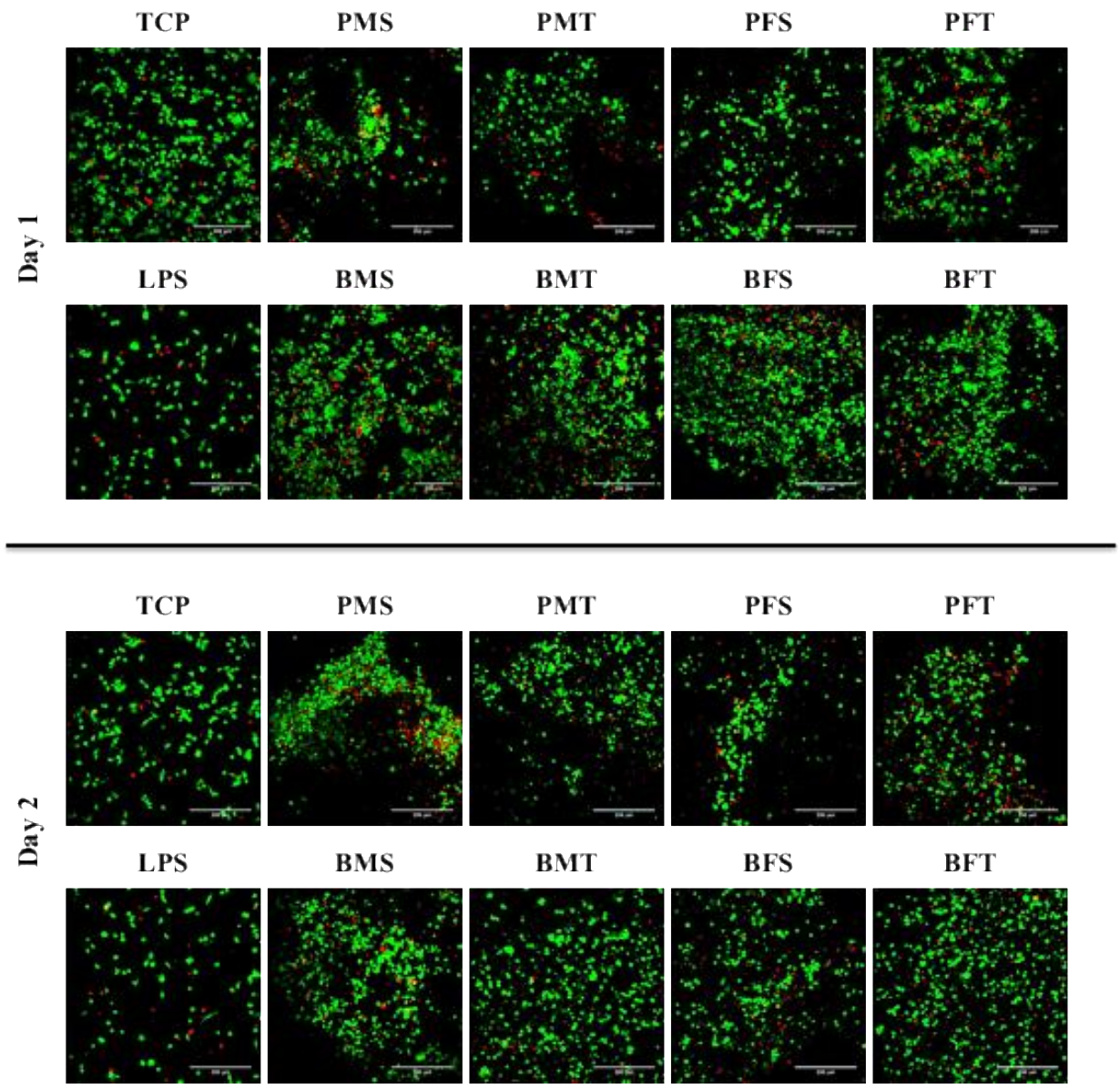

Figure 2.9: At day 2, among the collagen groups, the PMS sponges exhibited the lowest ($p < 0.001$) THP-1 viability (quantification is provided at **Figure 10A**). Green: live cells, Red: dead cells. Scalebar = 200 µm. N=3.

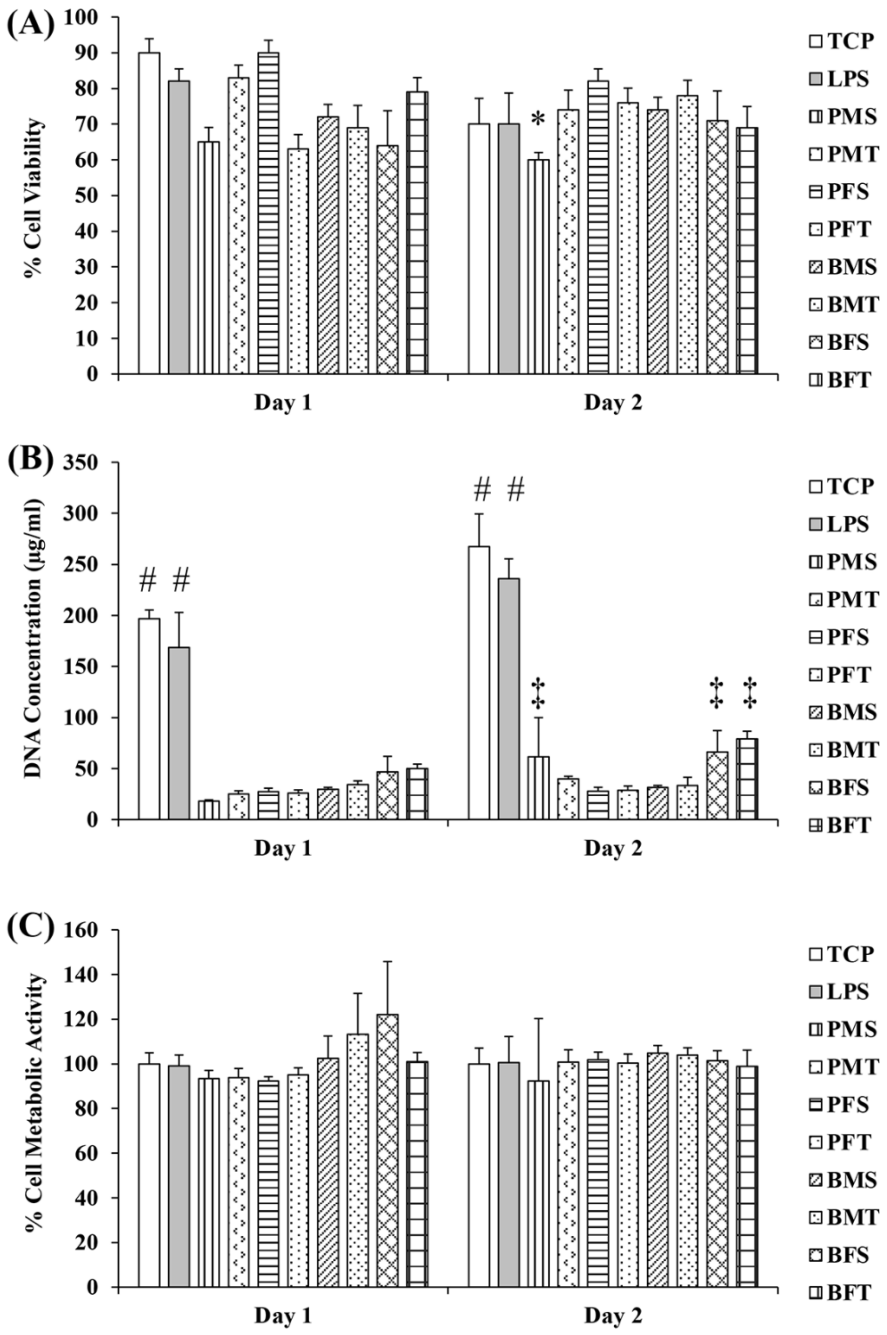

Figure 2.10: (**A**) At day 2, among the collagen groups, the PMS sponges exhibited the lowest ($p < 0.001$) THP-1 viability. (**B**) Add both times point, TCP and LPS has the highest DNA concentration and at day 2, among the collagen groups, the BFT sponges had the highest ($p < 0.001$) THP-1 DNA concentration. (**C**) No significant differences ($p > 0.05$) were observed between all groups in THP-1 metabolic activity. * indicates statistically significant difference from all groups; # indicates statistically significant difference from all groups; ‡ indicates statistically significant difference from collagen groups. N=3.

2.4 Discussion

Collagen is the most abundant protein family in vertebrates. Among the 29 collagen subtypes, collagens type I, type II and type III are more frequently encountered and together comprising around 80-90 % of the total body collagen [4]. This abundance, along with various properties (e.g. tissue-specific structure and mechanical properties, physiological biodegradability, low antigenicity, cell recognition signals) make collagens the materials of choice for various biomedical applications, including skin [31], bone [32], tendon [33] and cartilage [34] repair and regeneration. Although collagen type I can be extracted from various animals and tissues, type I collagens extracted from skin or tendon of close herd porcine or bovine animals represent the lion's share. Considering though that collagen is a biological material, differences in amino acid composition as a function of species, age, gender and tissue may affect the properties of the resultant scaffolds. Although collagen extracted from different species and tissues has been shown to produce scaffolds with different properties [7, 12, 35], no study has compared the properties of collagen-based scaffolds as a function of species, gender and tissue. Thus, herein, we assessed the properties of extracted collagen and subsequently produced collagen sponges, as a function of species (porcine and bovine), tissue (skin and tendon) and gender (male and female).

All collagen preparations were produced following a pepsin digestion and a filtration, double salt precipitation, centrifugation and dialysis protocol, which has been shown to increase yield and purity, respectively [12]. In fact, the produced collagen solutions were as pure as the commercially available standard that was used in this study. With respect to yield, the porcine tendons yielded more collagen than the bovine tendons, which can be attributed to the lower level of activity of the porcine tendons (pigs are slaughtered at 100-120 Kg weight, whilst calves are slaughtered at 460-640 Kg) and thus lower cross-linking density and higher solubility [36, 37]. With respect to skin yield, one would have expected more collagen to be extracted from bovine skin as opposed to porcine skin. To substantiate this, we should consider that domesticated pigs evolved from the wild boar and adapted a thick and tightly interwoven collagen network. Indeed, the collagen fibres within the skin of the pig are arranged in two directions, creating an interwoven dense network of small fibres and fibre bundles. The fibres and fibre bundles cross each other and merge from one bundle to the next, with smaller fibres interweaving in between and in different orientations. This

compact, higher-order network is also interwoven with elastic fibres [38, 39]. Bovine skin, on the other hand, is thinner in comparison to the porcine skin. The collagen fibres in the bovine skin align in a non-uniform order and it is thought that fibres align parallel to the cows' spinal column to allow for the skin movement while grazing and walking [40]. However, in our case, the porcine skin groups yielded more collagen than the bovine skin groups, possibly attributed to the age of the animals (pigs are slaughtered at month 5.0 to 5.5, whilst calves are slaughtered between month 14 and 24). As the animal ages, more mature cross-links are formed that renders collagen solubility [41-44].

Various factors (e.g. freeze-drying parameters, concertation of solution, cross-linking time / density) have been shown to affect pore size and porosity of freeze-dried materials [45-48]. Considering that all freeze-drying parameters and the collagen concentration were kept constant for all collagen preparations, the observed differences may be attributed to the random nature of the process that results in materials with heterogeneous pore structure and with large variations in average pore size throughout the material [49], as opposed to the inherent properties of the collagen preparations. In any case, the produced collagen sponges were highly porous, which is beneficial for cell adhesion, proliferation, migration and differentiation [50-52].

Although no significant differences were observed in free amine content, as a function of species, gender and tissue, in general, sponges produced from porcine collagen exhibited significantly higher resistance to enzymatic degradation and denaturation temperature and significantly lower swelling ratio than bovine collagen sponges of the same gender and tissue. All these suggest a higher in cross-linking density material, which is surprisingly, considering that the porcine tissues yielded the highest amount of collagen, which indicates lower cross-linking density. As all these properties were assessed with freeze-dried sponges, we believe that these differences may be due to freeze-drying-induced intermolecular cross-linking that provided better organisation and stabilisation of the helices through maintenance of the distances between neighbouring molecules and prevention of incorporation of excess water that disrupts hydrogen and electrostatic bond formation between molecules [53-57]. This has been more profound with the porcine collagen preparations possibly due to the lower extend of cross-linking, as the animals were of younger age.

Mechanical properties wise, porcine collagen sponges exhibited significantly lower compression stress and modulus than bovine collagen sponges of the same gender and tissue and tendon derived scaffolds exhibited significantly higher compression stress and modulus than skin derived scaffolds, independently of the species and gender. Both these observations may be attributed to the 'memory' of collagen from the tissue that has been extracted. Bovine (older animals) extracted collagen sponges had higher mechanical properties than porcine (younger animals) extracted collagen sponges and tendon extracted collagen sponges had higher mechanical properties than skin extracted collagen sponges, as previous studies have shown age-related increases in mechanical properties as a function of increased cross-linking density [58] and increased mechanical properties as a function of weight-bearing tasks [59], respectively. The higher in mechanical properties collagen sponges derived from tendon tissues in comparison to collagen sponges derived from skin tissues can also be attributed to the architecture of the collagen fibres in the respective tissues, which, in turn, is responsible for the tissue-specific biomechanical properties. In skin, collagen fibres are more loosely packed and are interwoven with elastin fibres, whilst in tendons collagen fibres are more closely packed along the longitudinal axis of the tissue, as has been revealed by polarised, transmission electron and second harmonic generation microscopy [60-63].

With respect to biological analysis, in general, all collagen sponges supported hDFs attachment, proliferation and growth. The only deviation was observed in (reduced) metabolic activity of hDFs grown on PMS and PFS sponges. It is worth noting though that these sponges had the lowest modulus values and it has been well described in the literature the influence of substrate rigidity on hDFs growth and function [64-66]. THP-1 morphology analysis revealed that most cells adopted a rounded morphology and formed aggregates, whilst some cells on TCP and LPS groups exhibited an elongated morphology. Rounded cell morphology is associated with M1 pro-inflammatory response, elongated morphology is indicative of M2 anti-inflammatory response phenotype and cell aggregates suggest foreign body response [67-69]. The BFT sponges formed the least aggregates and had the highest DNA concentration; this may be due to the fact that these scaffolds had also the highest modulus values, which may be explained considering that previous studies have associated macrophage response to substrate rigidity [70, 71]. Whether though such slight increase in rigidity

is capable of inducing macrophage response has yet to be verified and should be investigated further.

With respect to the influence of gender on the properties of the produced scaffolds, some differences were observed. For example, collagen sponges from porcine female tendon and skin had significantly higher mechanical properties than collagen sponges from porcine male tendon and skin. However, collagen sponges from bovine female tendon had significantly higher mechanical properties than collagen sponges from bovine male tendon and the reverse was the case for skin-derived collagen. Although gender-dependant differences have been documented in the literature for mechanical, structural and compositional properties of tendon [16-21] and skin [22-26], a more detailed investigation (e.g. analysing the properties of the original tissue and the derived scaffolds) is required to safely conclude on the influence of the gender on the properties of the scaffold.

2.5 Conclusions

Collagen type I is the most abundant extracellular matrix protein in vertebrates. This abundance makes collagen the material of choice for scaffold fabrication. Herein we illustrated that although purity, free-amine content and biological (hDFs and THP-1 monocyte cultures) response were not affected as a function of species (porcine versus bovine), gender (female versus male) and tissue (skin versus tendon) from which the collagen was extracted, yield, denaturation temperature, resistance to enzymatic degradation, swelling ratio and biomechanical properties were certainly species and tissue dependent. To safely conclude on the influence of gender, more detailed studies are required. Collectively, these data suggest that all these parameters should be considered in the development of a collagen-based implantable device.

2.6 References

[1] R. Parenteau-Bareil, R. Gauvin, F. Berthod, Collagen-based biomaterials for tissue engineering applications, Materials 3(3) (2010) 1863-1887.

[2] L.T. Smith, K.A. Holbrook, J.A. Madri, Collagen types I, III, and V in human embryonic and fetal skin, Am J Anat 175(4) (1986) 507-521.

[3] P. Kannus, Structure of the tendon connective tissue, Scand J Med Sci Sports 10(6) (2000) 312-320.

[4] A. Sorushanova, L.M. Delgado, Z. Wu, N. Shologu, A. Kshirsagar, R. Raghunath, A. Mullen, Y. Bayon, A. Pandit, M. Raghunath, D.I. Zeugolis, The collagen suprafamily: From biosynthesis to advanced biomaterial development, Adv Mater 31 (2018) e1801651.

[5] S.R. Chowdhury, M.F. Mh Busra, Y. Lokanathan, M.H. Ng, J.X. Law, U.C. Cletus, R. Binti Haji Idrus, Collagen type I: A versatile biomaterial, Adv Exp Med Biol 1077 (2018) 389-414.

[6] C. Dong, Y. Lv, Application of collagen scaffold in tissue engineering: Recent advances and new perspectives, Polymers (Basel) 8(2) (2016) E42.

[7] Y.K. Lin, D.C. Liu, Comparison of physical–chemical properties of type I collagen from different species, Food Chem 99(2) (2006) 244-251.

[8] N. Cozza, W. Bonani, A. Motta, C. Migliaresi, Evaluation of alternative sources of collagen fractions from Loligo vulgaris squid mantle, Int J Biol Macromol 87 (2016) 504-513.

[9] S. Bohm, C. Strauss, S. Stoiber, C. Kasper, V. Charwat, Impact of source and manufacturing of collagen matrices on fibroblast cell growth and platelet aggregation, Materials (Basel) 10(9) (2017) 1086.

[10] J.P. Widdowson, A.J. Picton, V. Vince, C.J. Wright, A. Mearns-Spragg, In vivo comparison of jellyfish and bovine collagen sponges as prototype medical devices, J Biomed Mater Res B 106(4) (2017) 1524-1533.

[11] S.A. Ghodbane, M.G. Dunn, Physical and mechanical properties of cross-linked type I collagen scaffolds derived from bovine, porcine, and ovine tendons, J Biomed Mater Res A 104(11) (2016) 2685-2692.

[12] D.I. Zeugolis, R.G. Paul, G. Attenburrow, Factors influencing the properties of reconstituted collagen fibers prior to self-assembly: Animal species and collagen extraction method, J Biomed Mater Res A 86A(4) (2008) 892-904.

[13] S. Browne, D.I. Zeugolis, A. Pandit, Collagen: Finding a solution for the source, Tissue Eng Part A 19(13-14) (2013) 1491-1494.

[14] L.M. Delgado, N. Shologu, K. Fuller, D.I. Zeugolis, Acetic acid and pepsin result in high yield, high purity and low macrophage response collagen for biomedical applications, Biomed Mater 12(6) (2017) 065009.

[15] A.K. Lynn, I.V. Yannas, W. Bonfield, Antigenicity and immunogenicity of collagen, J Biomed Mater Res B 71(2) (2004) 343-354.

[16] A.S. Lepley, M.F. Joseph, N.R. Daigle, J.E. Digiacomo, J. Galer, E. Rock, S.B. Rosier, P.B. Sureja, Sex differences in mechanical properties of the Achilles tendon: Longitudinal response to repetitive loading exercise, J Strength Cond Res 32(11) (2018) 3070-3079.

[17] D.C. Sarver, Y.A. Kharaz, K.B. Sugg, J.P. Gumucio, E. Comerford, C.L. Mendias, Sex differences in tendon structure and function, J Orthop Res 35(10) (2017) 2117-2126.

[18] K.G. Silbernagel, A. Brorsson, N. Olsson, B.I. Eriksson, J. Karlsson, K. Nilsson-Helander, Sex differences in outcome after an acute Achilles tendon rupture, Orthop J Sports Med 3(6) (2015) 2325967115586768.

[19] K.A. Bonilla, A.M. Pardes, B.R. Freedman, L.J. Soslowsky, Supraspinatus tendons have different mechanical properties across sex, J Biomech Eng 141(1) (2019) doi: 10.1115/1.4041321.

[20] K.M. Hicks, G.L. Onambele-Pearson, K. Winwood, C.I. Morse, Gender differences in fascicular lengthening during eccentric contractions: the role of the patella tendon stiffness, Acta Physiol (Oxf) 209(3) (2013) 235-244.

[21] D. Little, J.W. Thompson, L.G. Dubois, D.S. Ruch, M.A. Moseley, F. Guilak, Proteomic differences between male and female anterior cruciate ligament and patellar tendon, PLoS One 9(5) (2014) e96526.

[22] L. Blom, A. Klingberg, L. Laflamme, L. Wallis, M. Hasselberg, Gender differences in burns: A study from emergency centres in the Western Cape, South Africa, Burns 42(7) (2016) 1600-1608.

[23] N. Skroza, E. Tolino, A. Mambrin, S. Zuber, V. Balduzzi, A. Marchesiello, N. Bernardini, I. Proietti, C. Potenza, Adult acne versus adolescent acne: A retrospective study of 1,167 patients, J Clin Aesthet Dermatol 11(1) (2018) 21-25.

[24] M. Lundin, S. Chawa, A. Sachdev, D. Bhanusali, K. Seiffert-Sinha, A.A. Sinha, Gender differences in alopecia areata, J Drugs Dermatol 13(4) (2014) 409-413.
[25] E.A. Holm, S. Esmann, G.B. Jemec, Does visible atopic dermatitis affect quality of life more in women than in men?, Gend Med 1(2) (2004) 125-130.
[26] C. Phuong, H.I. Maibach, Gender differences in skin in: M. Farage, K. Miller, H. Maibach (Eds.), Textbook of Aging Skin, Springer, Berlin, 2017, pp. 1729-1755.
[27] H. Capella-Monsonís, J.Q. Coentro, V. Graceffa, Z. Wu, D.I. Zeugolis, An experimental toolbox for characterization of mammalian collagen type I in biological specimens, Nat Protoc 13(3) (2018) 507-529.
[28] L.M. Delgado, K. Fuller, D.I. Zeugolis, Collagen cross-linking: Biophysical, biochemical, and biological response analysis, Tissue Eng Part A 23(19-20) (2017) 1064-1077.
[29] A.L. Helling, E.K. Tsekoura, M. Biggs, Y. Bayon, A. Pandit, D.I. Zeugolis, In vitro enzymatic degradation of tissue grafts and collagen biomaterials by matrix metalloproteinases: Improving the collagenase assay, ACS Biomat Sc Eng 3(9) (2017) 1922-1932.
[30] D.I. Zeugolis, M. Raghunath, The physiological relevance of wet versus dry differential scanning calorimetry for biomaterial evaluation: A technical note, Polym Int 59(10) (2010) 1403-1407.
[31] E. Davison-Kotler, W.S. Marshall, E. García-Gareta, Sources of collagen for biomaterials in skin wound healing, Bioengineering (Basel) 6(3) (2019) E56.
[32] D. Zhang, X. Wu, J. Chen, K. Lin, The development of collagen based composite scaffolds for bone regeneration, Bioact Mater 3(1) (2017) 129-138.
[33] S.J. Kew, J.H. Gwynne, D. Enea, M. Abu-Rub, A. Pandit, D. Zeugolis, R.A. Brooks, N. Rushton, S.M. Best, R.E. Cameron, Regeneration and repair of tendon and ligament tissue using collagen fibre biomaterials, Acta Biomater 7(9) (2011) 3237-3247.
[34] V. Irawan, T.C. Sung, A. Higuchi, T. Ikoma, Collagen scaffolds in cartilage tissue engineering and relevant approaches for future development, Tissue Eng Regen Med 15(6) (2018) 673-697.
[35] P. Angele, J. Abke, R. Kujat, H. Faltermeier, D. Schumann, M. Nerlich, B. Kinner, C. Englert, Z. Ruszczak, R. Mehrl, R. Mueller, Influence of different collagen

species on physico-chemical properties of crosslinked collagen matrices, Biomaterials 25(14) (2004) 2831-2841.

[36] E.A. Makris, D.J. Responte, N.K. Paschos, J.C. Hu, K.A. Athanasiou, Developing functional musculoskeletal tissues through hypoxia and lysyl oxidase-induced collagen cross-linking, Proc Natl Acad Sci U S A 111(45) (2014) E4832-E4841.

[37] M. Kaku, J.M. Rosales Rocabado, M. Kitami, T. Ida, Y. Akiba, M. Yamauchi, K. Uoshima, Mechanical loading stimulates expression of collagen cross-linking associated enzymes in periodontal ligament, J Cell Physiol 231(4) (2016) 926-933.

[38] D. Moyo, M. Gomes, K.H. Erlwanger, Comparison of the histology of the skin of the windsnyer, kolbroek and large white pigs, J S Afr Vet Assoc 89(0) (2018) e1-e10.

[39] W. Meyer, K. Neurand, B. Radke, Collagen fibre arrangement in the skin of the pig, J Anat 134(Pt 1) (1982) 139-148.

[40] S. Osaki, Distribution map of collagen fiber orientation in a whole calf skin, 1999.

[41] J.G. Snedeker, A. Gautieri, The role of collagen crosslinks in ageing and diabetes - The good, the bad, and the ugly, Muscles Ligaments Tendons J 4(3) (2014) 303-308.

[42] S.L. Schnider, R.R. Kohn, Effects of age and diabetes mellitus on the solubility and nonenzymatic glucosylation of human skin collagen, J Clin Invest 67(6) (1981) 1630-1635.

[43] T. Miyahara, A. Murai, T. Tanaka, S. Shiozawa, M. Kameyama, Age-related differences in human skin collagen: solubility in solvent, susceptibility to pepsin digestion, and the spectrum of the solubilized polymeric collagen molecules, J Gerontol 37(6) (1982) 651-655.

[44] R.B. Svensson, K.M. Heinemeier, C. Couppé, M. Kjaer, S.P. Magnusson, Effect of aging and exercise on the tendon, J Appl Physiol 121(6) (1985) 1237-1246.

[45] L. Yang, K. Tanabe, T. Miura, M. Yoshinari, S. Takemoto, S. Shintani, M. Kasahara, Influence of lyophilization factors and gelatin concentration on pore structures of atelocollagen/gelatin sponge biomaterial, Dent Mater J 36(4) (2017) 429-437.

[46] A.M. Haparanta, J. Koivurinta, E.R. Hamalainen, M. Kellomaki, The effect of cross-linking time on a porous freeze-dried collagen scaffold using 1-ethyl-3-(3-dimethylaminopropyl)carbodiimide as a cross-linker, J Appl Biomater Biomech 6(2) (2008) 89-94.

[47] Y. Zhang, C. Wang, W. Jiang, W. Zuo, G. Han, Influence of stage cooling method on pore architecture of biomimetic alginate scaffolds, Sci Rep 7(1) (2017) 16150.
[48] H. Schoof, J. Apel, I. Heschel, G. Rau, Control of pore structure and size in freeze-dried collagen sponges, J Biomed Mater Res 58(4) (2001) 352-357.
[49] F.J. O'Brien, B.A. Harley, I.V. Yannas, L.J. Gibson, Influence of freezing rate on pore structure in freeze-dried collagen-GAG scaffolds, Biomaterials 25(6) (2004) 1077-1086.
[50] C.M. Murphy, M.G. Haugh, F.J. O'Brien, The effect of mean pore size on cell attachment, proliferation and migration in collagen-glycosaminoglycan scaffolds for bone tissue engineering, Biomaterials 31(3) (2010) 461-466.
[51] F.J. O'Brien, B.A. Harley, I.V. Yannas, L.J. Gibson, The effect of pore size on cell adhesion in collagen-GAG scaffolds, Biomaterials 26(4) (2005) 433-441.
[52] S. Pina, V.P. Ribeiro, C.F. Marques, F.R. Maia, T.H. Silva, R.L. Reis, J.M. Oliveira, Scaffolding strategies for tissue engineering and regenerative medicine applications, Materials (Basel) 12(11) (2019) 1824.
[53] R.N. Chen, H.O. Ho, M.T. Sheu, Characterization of collagen matrices crosslinked using microbial transglutaminase, Biomaterials 26(20) (2005) 4229-4235.
[54] C.J. Mentink, M. Hendriks, A.A. Levels, B.H. Wolffenbuttel, Glucose-mediated cross-linking of collagen in rat tendon and skin, Clin Chim Acta 321(1-2) (2002) 69-76.
[55] M.C. Wang, G.D. Pins, F.H. Silver, Collagen fibres with improved strength for the repair of soft tissue injuries, Biomaterials 15(7) (1994) 507-512.
[56] M.J. Wissink, R. Beernink, J.S. Pieper, A.A. Poot, G.H. Engbers, T. Beugeling, W.G. van Aken, J. Feijen, Immobilization of heparin to EDC/NHS-crosslinked collagen. Characterization and in vitro evaluation, Biomaterials 22(2) (2001) 151-163.
[57] I. Rault, V. Frei, D. Herbage, N. Abdul-Malak, A. Huc, Evaluation of different chemical methods for cros-linking collagen gel, films and sponges, J Mater Sci: Mater Med 7 (1996) 215-221.
[58] N.C. Avery, A.J. Bailey, Enzymic and non-enzymic cross-linking mechanisms in relation to turnover of collagen: Relevance to aging and exercise, Scand J Med Sci Sports 15(4) (2005) 231-240.
[59] C.M. Waugh, A.J. Blazevich, F. Fath, T. Korff, Age-related changes in mechanical properties of the Achilles tendon, J Anat 220(2) (2012) 144-155.

[60] M. Franchi, A. Trirè, M. Quaranta, E. Orsini, V. Ottani, Collagen structure of tendon relates to function, Sci World J 7 (2007) 404-420.

[61] M. Benjamin, E. Kaiser, S. Milz, Structure-function relationships in tendons: A review, J Anat 212(3) (2008) 211-228.

[62] J.F. Ribeiro, E.H. dos Anjos, M.L. Mello, B. de Campos Vidal, Skin collagen fiber molecular order: A pattern of distributional fiber orientation as assessed by optical anisotropy and image analysis, PLoS One 8(1) (2013) e54724.

[63] D.I. Zeugolis, S.T. Khew, E.S. Yew, A.K. Ekaputra, Y.W. Tong, L.Y. Yung, D.W. Hutmacher, C. Sheppard, M. Raghunath, Electro-spinning of pure collagen nano-fibres - just an expensive way to make gelatin?, Biomaterials 29(15) (2008) 2293-2305.

[64] I. Hopp, A. Michelmore, L.E. Smith, D.E. Robinson, A. Bachhuka, A. Mierczynska, K. Vasilev, The influence of substrate stiffness gradients on primary human dermal fibroblasts, Biomaterials 34(21) (2013) 5070-5077.

[65] V.F. Achterberg, L. Buscemi, H. Diekmann, J. Smith-Clerc, H. Schwengler, J.J. Meister, H. Wenck, S. Gallinat, B. Hinz, The nano-scale mechanical properties of the extracellular matrix regulate dermal fibroblast function, J Invest Dermatol 134(7) (2014) 1862-1872.

[66] M.E. Smithmyer, L.A. Sawicki, A.M. Kloxin, Hydrogel scaffolds as in vitro models to study fibroblast activation in wound healing and disease, Biomater Sci 2(5) (2014) 634-650.

[67] A. Yahyouche, X. Zhidao, J.T. Czernuszka, A.J. Clover, Macrophage-mediated degradation of crosslinked collagen scaffolds, Acta Biomater 7(1) (2011) 278-286.

[68] F.Y. McWhorter, T. Wang, P. Nguyen, T. Chung, W.F. Liu, Modulation of macrophage phenotype by cell shape, Proc Natl Acad Sci U S A 110(43) (2013) 17253-17258.

[69] F.Y. McWhorter, C.T. Davis, W.F. Liu, Physical and mechanical regulation of macrophage phenotype and function, Cell Mol Life Sci 72(7) (2015) 1303-1316.

[70] N.R. Patel, M. Bole, C. Chen, C.C. Hardin, A.T. Kho, J. Mih, L. Deng, J. Butler, D. Tschumperlin, J.J. Fredberg, R. Krishnan, H. Koziel, Cell elasticity determines macrophage function, PLoS One 7(9) (2012) e41024.

[71] A.K. Blakney, M.D. Swartzlander, S.J. Bryant, The effects of substrate stiffness on the in vitro activation of macrophages and in vivo host response to poly(ethylene glycol)-based hydrogels, J Biomed Mater Res A 100(6) (2012) 1375-1386.

Chapter 3 - Maintenance of tenogenic phenotype on tendon and not skin collagen derived devices

This chapter has been published:

Tissue origin matters: Maintenance of tenogenic phenotype on tendon and not skin collagen derived devices. **A. Sorushanova**, D. Tsiapalis, I. Skoufos, A. Tzora, U. FitzGerald, A.M. Mullen, D.I. Zeugolis. MedComm - Biomaterials and Applications. 2022.

3.1 Introduction

Collagen is the most abundant extracellular matrix (ECM) protein that provides tissues with tensile strength and host cells with a framework that regulates their attachment, migration, proliferation and differentiation [1-3]. These properties have made extracted collagen the building block of choice in the development of medical devices for a diverse range of clinical indications. Over the years, collagen type I and collagen type II have been extracted from various tissues of terrestrial [4-8] and aquatic [9-13] animals. Porcine and bovine tendon and skin tissues are by far the main source of collagen type I used in biomedicine. Acid / pepsin treatment followed by salt-precipitation is the favoured extraction method for the production of high yield and purity and low antigenicity and immunogenicity collagen preparations [14-16]. Numerous cross-linking methods have also been assessed to further modulate antigenicity and immunogenicity and to provide an effective balance between mechanical resilience, enzymatic stability, cytocompatibility and functional tissue remodelling [17-22], with data advocating the use of natural (e.g. genipin [22-24]) and chemical [e.g. poly(ethylene glycol) derivatives [24, 25] agents. Despite all these significant advancements in the field, clinical data have yielded contradictory outcomes for collagen-based devices. For example, both tissue grafts [26-31] and extracted collagen devices [32-40] have shown both positive and negative clinical outcomes, suggesting that other factors than the extraction or cross-linking methods are at play.

In this context, previous studies suggest that collagen retains memory of the tissue that derives from, affecting the physicochemical and the biological properties of the final product / device. For example, tendon tissues with large diameter collagen fibres (e.g. Achilles, quadriceps) are exposed to heavy mechanical loads, whilst tendon tissues with small diameter collagen fibres (e.g. biceps brachii, extensor pollicis longus) are exposed to low mechanical loads, but carry functions of high specificity [41]. This observation is also translated to collagen-based devices; acid-soluble bovine Achilles (high load bearing tissue) tendon-derived reconstituted collagen fibres had higher diameter than acid-soluble rat tail (high function tissue) tendon-derived reconstituted collagen fibres [4]. With respect to biological response, articular cartilage, as opposed to tracheal and auricular cartilage, collagen type II scaffolds have been shown to stimulate the highest sulphated glycosaminoglycans synthesis and aggrecan and

collagen type II mRNA expression in chondrogenically induced human adipose derived stem cell cultures [42].

Considering the above, herein we ventured to compare the influence of the tissue origin (skin and tendon) on the biophysical, biochemical and biological properties of pepsin extracted bovine collagen type I scaffolds. Pepsin extraction was chosen as it has been shown to increase yield and to reduce immune response [4, 43]. The 4-arm polyethylene glycol succinimidyl glutarate (4SG-PEG) was selected to cross-link the produced scaffolds, as its stabilisation and cytocompatibility efficiency have been repeatedly reported in the literature [44, 45]. The optimal 4SG-PEG concertation was identified using human adult dermal fibroblasts (hDFs). Subsequently, detailed *in vitro* biological analysis was conducted using human tenocytes (hTCs), as they are known to readily lose their phenotype *ex vivo* [46-49] and therefore it is imperative to develop appropriate culture and carrier systems to maintain their function.

3.2 Materials and methods

3.2.1 Materials

Bovine tissues were obtained from a slaughterhouse. Quant-iT™ PicoGreen® dsDNA Reagent was purchased from Invitrogen (Bio Sciences Ltd., Ireland). 4SG-PEG, 10,000 kDa molecular weight, was purchased from JenKem Technology (USA). All chemical, reagents, laboratory consumables and cell culture media were purchased from Sigma-Aldrich (Ireland) unless otherwise stated. Human adult dermal fibroblasts were purchased from ATCC (Donor number: PCS-201-012™, UK; Gender: Lot specific; Age: Adult). Human tenocytes were purchased from DV Biologics (USA) (Gender: Female; Age: 29). Collagen extraction protocol has been standardised in the group. Each step of the extraction has been followed according to the protocol for collagen type I extraction.

3.2.2 Collagen extraction and characterisation

Collagen type I was extracted following established protocols [4, 43]. Briefly, bovine female skin and tendon tissues were subjected to acid solubilisation, pepsin digestion (3,200-4,500 units per mg protein, cat. no. P6887, Sigma-Aldrich) and collagen type I was purified by repeated (twice) salt precipitation (0.9 M NaCl) and acetic acid (1 M) solubilisation. The final collagen solutions were dialysed against 1 mM acetic acid and their concentration was adjusted to 5 mg/ml. The purity of the collagen preparations was assessed by sodium dodecyl sulphate-polyacrylamide gel electrophoresis (SDS-PAGE) under non-reducing conditions [50]. Briefly, collagen samples were freeze dried, suspended in 0.5 M acetic acid in 1 mg/ml concertation, neutralised with 1 N NaOH, mixed with 5x sample buffer (bromophenol blue / SDS), denatured (95 ºC for 5 min) and run in a Mini-Protean 3 electrophoresis system (Bio-Rad Laboratories, UK) loaded with a 3 % stacking gel (run for ~ 30 min at 50 V) and 5 % separation gel (run for ~ 60 min at 120 V). The gels were stained using the SilverQuest™ kit (Invitrogen, UK) according to the manufacturer's protocol (**Figure 3.1**).

3.2.3 Fabrication of collagen sponges

Collagen solutions (5 mg/ml) were dissolved in phosphate buffered saline (PBS) 4SG-PEG at a final concentration of 0.5 mM, 1 mM, 2.5 mM and 5 mM, pipetted into well

plates, frozen at -80 ºC overnight and freeze-dried (Freezone 4.5L, Labconco, USA) for 24 h. 24 well plates were used to fabricate sponges for stability analysis with 2 ml per well collagen / 4SG-PEG solutions and 48 well plates were used to fabricate sponges for biological analysis with 250 µl per well collagen / 4SG-PEG solutions. Non-cross-linked collagens were also prepared using PBS only. Note: The values of the non-crosslinked samples (i.e. 0 mM 4SG-PEG) have been reported previously in this manuscript of the group [51].

3.2.4 Structural characterisation

The structure of produced sponges was visualised using scanning electron microscopy (SEM, Hitachi S-4700, Japan). Adhesive carbon tabs were used on top of SEM specimen stubs. Collagen sponges were cut horizontally and stuck onto carbon tabs. Collagen sponges were gold coated (Emitech K-550X Sputter Coater, Emitech, UK) prior to SEM imaging at 25 mA current for 5 minutes. Pore diameter was measured using ImageJ software (National Institutes of Health, USA).

3.2.5 Quantification of free amines

Free amine groups were determined using the ninhydrin assay [50]. Briefly, 3 mg of freeze-dried samples were added to 1 ml ninhydrin buffer and incubated at 100 ºC for 10 minutes. After the samples were cooled down at room temperature, 50 % of isopropanol was added and the absorbance was measured at 570 nm (Varioskan Flash Multimode Reader, Thermo Fisher Scientific, Ireland). Free amine groups were quantified by interpolating values from a linear standard curve of known concentrations of glycine.

3.2.6 Enzymatic stability analysis

Enzymatic degradation of collagen sponges was assessed using collagenase type I assay [52]. Briefly, 5 mg of freeze-dried samples were added to 1 ml of collagenase solution. The samples were incubated for 3, 6, 9, 12 and 24 h at 37 ºC. The supernatants were then collected, the samples were freeze dried overnight and weighed. The degree of enzymatic degradation was quantified using the weight difference approach [(Wo-Wt)/ Wo] x 100, where Wo is the original weight and Wt is the remaining weight.

3.2.7 Thermal stability and swelling analysis

The denaturation temperature of the collagen sponges was determined using differential scanning calorimetry (DSC-60, Shimadzu, Japan) [53]. The collagen sponges were hydrated overnight at room temperature in 0.01 M PBS. The sponges were then removed from the PBS and quickly blotted on a filter paper to remove non-bound PBS. The sponges were then hermetically sealed in aluminium pans. Heating was carried out at a rising temperature rate of 10 ºC/min within a temperature range of 20 ºC to 70 ºC. An empty aluminium pan was used as reference. The endothermic transition was recorded as a typical peak and the peak temperature (the temperature of maximum power of absorption during denaturation) was noted.

For degree of swelling determination, collagen sponges were weighed and then incubated in 0.01 M PBS overnight. The next day collagen sponges were quickly blotted using filter paper to remove surface PBS and weighed. Swelling ratio was calculated using the following equation: Swelling (%) = [(Ww - Wd) / (Wd)] x 100, where Ww and Wd refer to the average wet weight and dry weight of the sponges, respectively.

3.2.8 Mechanical stability analysis

Compression test was carried out in dry state using an electromechanical testing machine (Z2.5, Zwick, Germany). Compression stress and modulus values were calculated as follows: compressive stress was defined as the force at 70 % compression divided by the original cross-sectional area and modulus was defined as the slope of the stress-strain (deformation) curve at the elastic deformation region (Young's modulus).

3.2.9 Dermal fibroblast culture and analysis

Human adult dermal fibroblasts (hDFs) (PCS-201-012™, ATCC, UK) were used between passages 3 and 5. Collagen sponges (0, 0.5, 1, 2.5 and 5 mM 4SG-PEG) were sterilised with UV for 2 h prior to seeding. The cells were seeded onto collagen sponges at a density of 30,000 cells per cm^2 in 48 well plates. The cells were cultured for 3, 7 and 14 days in Dulbecco's Modified Eagle Medium (DMEM), supplemented with 1 % penicillin streptomycin and 10 % foetal bovine serum (FBS) at 37 ºC and 5 % CO_2. Media were changed every 2 days. For cell morphology assessment, media

were removed after 3, 7 and 14 days in culture and the sponges were washed three times with Hank's Balanced Salt Solution (HBSS). Cells were fixed with 2 % paraformaldehyde (PFA), permeabilised with 0.2 % Triton X-100 and then nuclei were stained with 4′,6-diamidino-2-phenylindole (DAPI) and cytoskeleton was stained with rhodamine phalloidin. The sponges were imaged using Andor Revolution Spinning Disk Confocal Microscope (Olympus IX81, Japan). Cell proliferation was assessed using PicoGreen® dsDNA assay kit after 3, 7 and 14 days in culture, according to manufacturer's protocol. Metabolic activity was assessed using the alamarBlue® assay (Thermo Fisher Scientific, UK) after 3, 7 and 14 days in culture, according to manufacturer's protocol. Cell viability was assessed using the Live/Dead® assay (Thermo Fisher Scientific, UK) after 3, 7 and 14 days in culture, according to the manufacturer's protocol.

3.2.10 Tenocytes culture and analysis

Human tenocytes (hTCs) (Cambridge Bioscience, UK) were used between passages 3 and 5. Collagen sponges (0 and 1 mM 4SG-PEG) were sterilised with UV for 2 h prior to seeding. Cell culture and cell morphology, proliferation, metabolic activity and viability analyses were conducted as described above.

3.2.11 Tenocytes immunocytochemistry analysis

hTCs were fixed with 2 % PFA and blocked with 3 % bovine serum albumin (BSA) in PBS for 30 min. Cells were then incubated for 90 min at room temperature with the primary antibodies (Abcam, UK) for collagen types I (Ab90395), II (Ab185430), III (Ab7778), IV (Ab6586), V (Ab6586) and VI, fibronectin (Ab2413), scleraxis (Ab58655), tenomodulin (Ab81328), aggrecan (Ab36861), osteocalcin (Ab13418) and osteopontin (Ab69498), washed with PBS and subsequently with secondary antibody for 30 min (Alexa Fluor® 488 goat anti-rabbit A11034 and Alexa Fluor® 488 goat anti-mouse A11001, Thermo Fisher Scientific, UK). Nuclei were counterstained with DAPI for 5 min. Fluorescent images were captured using Andor Revolution Spinning Disk Confocal Microscope (Olympus IX81). Cells on three sponges were analysed by taking five images per sponge (fifteen images in total were analysed per experimental group). To determine matrix composition at each time-point the area of fluorescence per image was quantified and DAPI count was carried

out per image using ImageJ. The area of fluorescence was divided by the cell number of the same image (National Institutes of Health, USA).

3.2.12 Tenocytes gene expression

Gene analysis was performed using a RealTime ready Custom Panel (Roche, Germany) after 3, 7 and 14 days in culture to assess the expression of tenogenic, chondrogenic and osteogenic markers (**Appendices Table B.10**). Briefly, skin- and tendon- derived collagen type I sponges were placed in 2 ml Eppendorf™ tubes containing TRI Reagent® (Sigma Aldrich, Ireland) and were broken down using iron oxide beads under shaking conditions at 4 °C for 5 min to lyse the cells. Then, the TRI Reagent® was collected, chloroform was added and samples were vortexed and then incubated at ambient temperature for 5 min. The solution was then centrifuged and the upper aqueous phase containing the RNA was collected and mixed with 70 % ethanol. The solution was then purified using the High Pure isolation kit (Roche, Germany). RNA concentration and quality were analysed using the NanoDrop 1000 (ThermoFisher Scientific, UK) and the Agilent 2100 Bioanalyser (Agilent Technologies, Ireland). RNA was transcribed to cDNA using the Transcriptor First Strand cDNA synthesis kit (Roche, Germany) and 1 μg of RNA sample was used in all the groups. After cDNA synthesis, 1 μl of cDNA was added to 9 μl of probes master into a RealTime ready custom 384 well plate (Roche, Germany). Negative controls of empty wells and untranscribed RNA were added in the study and the plate was run in the LightCycler® 480 Instrument (Roche, Germany). Genes were normalised to the housekeeper β-actin and fold-change was obtained using the 2-ΔΔCT. Z-scores of fold-change were calculated and relevant up- and down- regulation were accepted when the score was at least two standard deviations away from the mean value of fold-change for each gene.

3.2.13 Statistical analysis

Statistical analysis was performed using SPSS (version 20.0, IBM SPSS Statistics, IBM Corporation, USA). All values are expressed as mean values ± standard deviation (SD). One-way analysis of variance (ANOVA) for multiple comparisons was employed, after confirming the following assumptions: (a) the distribution from which each of the samples was derived was normal; (b) and the variances of the population

of the samples were equal to one another. Nonparametric statistics were used when either or both of the above assumptions were violated and consequently Kruskal-Wallis test for multiple comparisons was carried out. Independent *t*-test was employed to evaluate the means of two independent groups for immunocytochemistry ranking analysis. Statistical significance was accepted at $p < 0.05$.

3.3 Results

3.3.1 Structural characterisation

SEM analysis (**Figure 3.2**) revealed that all collagen sponges had a porous structure, with the skin-derived collagen sponges having circular shaped pores and the tendon-derived collagen sponges having elliptical shaped pores. Among the skin-derived collagen sponges, the 1 mM 4SG-PEG sponges exhibited the highest ($p < 0.05$) pore diameter and among the tendon-derived collagen sponges, the 2.5 mM and 5 mM 4SG-PEG sponges exhibited significantly ($p < 0.05$) longer pore diameter than the other groups. All 4SG-PEG concentrations significantly ($p < 0.05$) reduced % porosity of both skin- and tendon- derived collagen sponges.

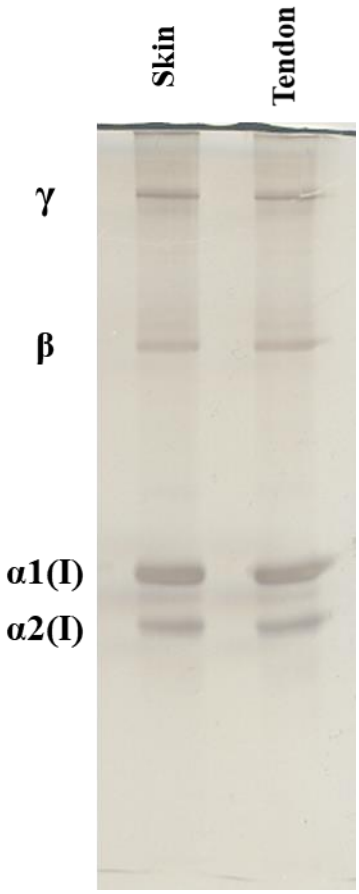

Figure 3.1: SDS-PAGE of skin and tendon collagen preparations.

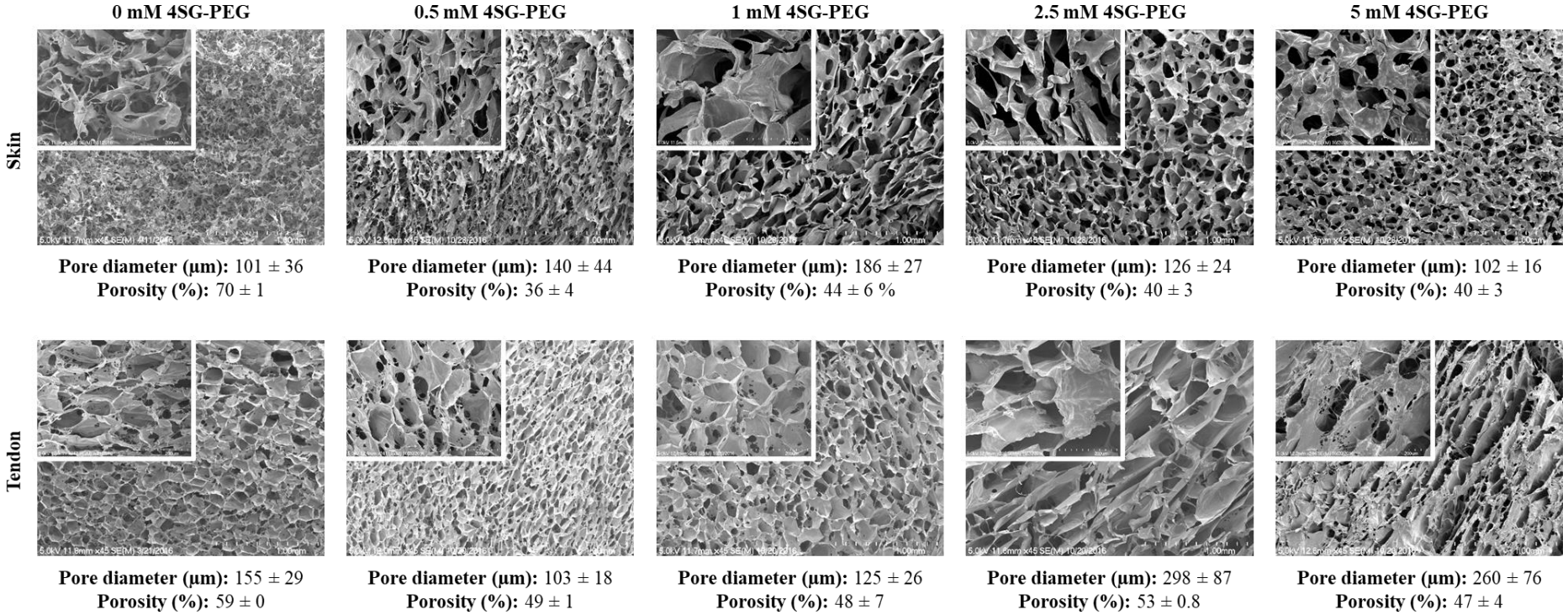

Figure 3.2: Scanning electron microscopy (SEM) and complementary pore size (µm) and porosity (%) of non-cross-linked and cross-linked with 4-arm polyethylene glycol succinimidyl glutarate (4SG-PEG) skin- and tendon- derived collagen sponges.

3.3.2 Cross-linking characterisation

Ninhydrin (**Figure 3.3**) and collagenase digestion (**Figure 3.4**) analyses revealed for both skin- and tendon- derived collagen scaffolds that as the 4SG-PEG cross-linking density was increased, the % of free amine groups was significantly ($p < 0.05$) reduced and the resistance to collagenase digestion was significantly ($p < 0.05$) increased. In general, denaturation temperature, mechanical properties and swelling analyses (**Table 3.1**) revealed for both skin- and tendon- derived collagen scaffolds that as the 4SG-PEG cross-linking density was increased, the denaturation temperature, compressive stress and compressive modulus were significantly ($p < 0.05$) increased and the % swelling was significantly ($p < 0.05$) reduced. It is interesting to note that the tendon-derived collagen scaffolds exhibited significantly ($p < 0.05$) higher compressive stress and compressive modulus values at a given 4SG-PEG cross-linking density than their skin-derived collagen scaffolds counterparts.

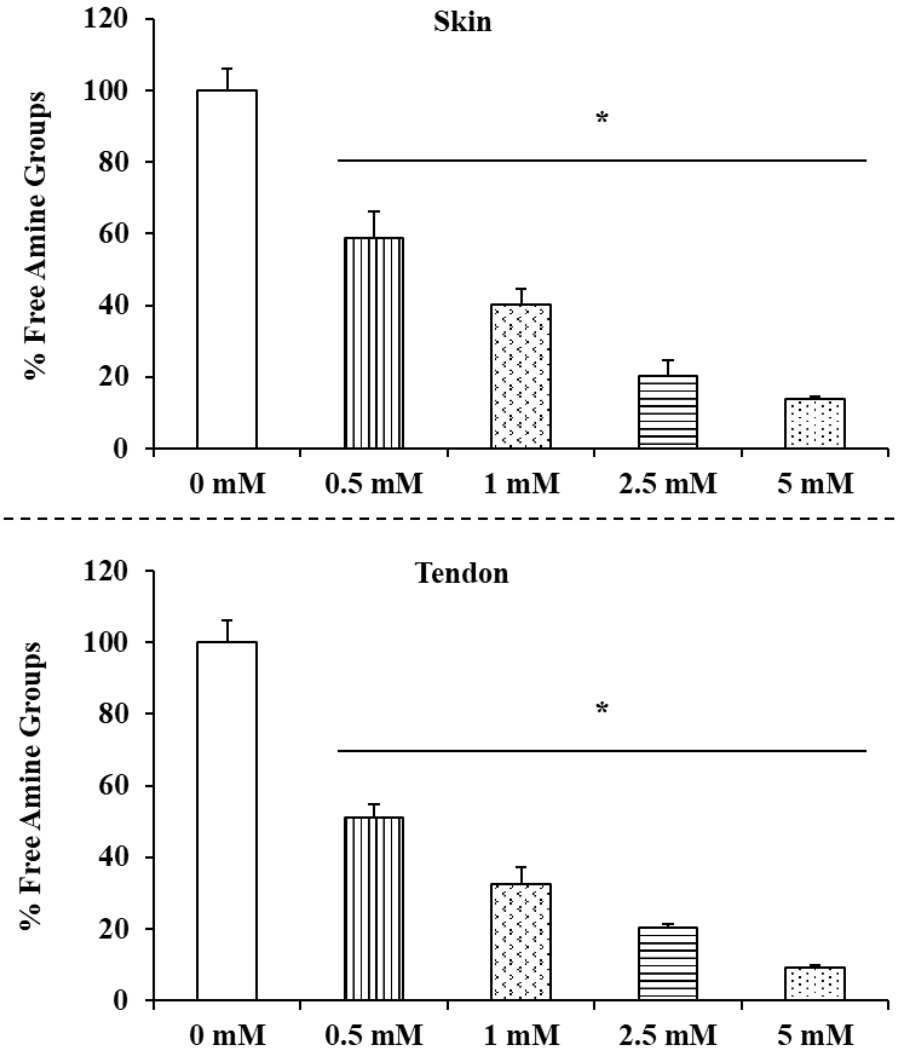

Figure 3.3: Quantitative analysis of free amine groups of skin- and tendon-derived collagen sponges cross-linked with 0 mM, 1 mM, 2.5 mM and 5 mM 4SG-PEG. * indicates statistically significant ($p < 0.05$) difference in comparison to the 0 mM 4SG-PEG. N = 6.

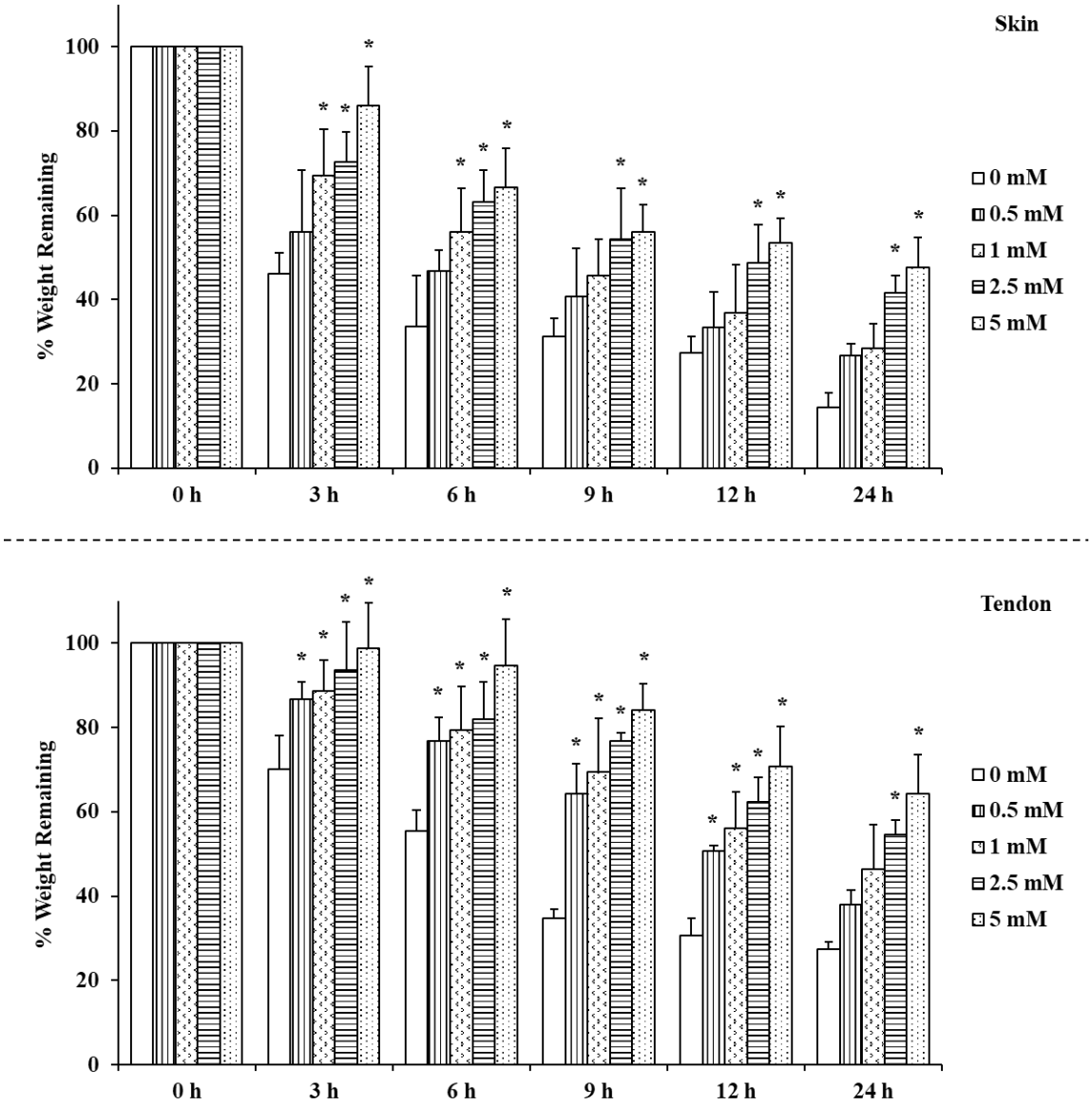

Figure 3.4: Quantitative analysis of resistance to enzymatic degradation of skin- and tendon-derived collagen sponges cross-linked with 0 mM, 1 mM, 2.5 mM and 5 mM 4SG-PEG. * indicates statistically significant ($p < 0.05$) difference in comparison to the 0 mM 4SG-PEG. N = 6.

Table 3.1: Peak temperature, swelling, compressive stress and modulus analyses of skin- and tendon- derived collagen sponges as a function of different 4-arm polyethylene glycol succinimidyl glutarate (4SG-PEG) cross-linking concentrations. * indicates significant ($p < 0.05$) difference to the respective tissue-derived 0 mM 4SG-PEG collagen sponge. Denaturation temperature: N = 5; Swelling: N = 6; Mechanical properties: N = 7.

Tissues	4SG-PEG (mM)	Peak temperature ± SD (ºC)	Swelling ± SD (%)	Compressive stress at 70 % deformation ± SD (kPa)	Compressive modulus (Young's modulus) ± SD (kPa)
Skin	**0**	50.55 ± 1.14	2,502 ± 529	1.03 ± 0.21	1.29 ± 0.27
	0.5	54.48 ± 0.67 *	2,914 ± 4,219	2.32 ± 0.33	3.78 ± 1.03 *
	1.0	55.51 ± 0.40 *	653 ± 97 *	2.77 ± 1.24	4.31 ± 0.99 *
	2.5	57.96 ± 0.44 *	434 ± 49 *	4.13 ± 1.13 *	6.31 ± 0.66 *
	5.0	61.46 ± 0.48 *	289 ± 47 *	13.19 ± 4.06 *	14.01 ± 0.73 *
Tendon	**0**	49.63 ± 1.06	12,031 ± 1,900	3.18 ± 0.66	4.67 ± 1.61
	0.5	52.89 ± 1.00 *	2,993 ± 760 *	4.22 ± 1.88	6.03 ± 0.82 *
	1.0	52.87 ± 0.53 *	945 ± 90 *	10.92 ± 1.46 *	27.93 ± 0.74 *
	2.5	56.47 ± 0.32 *	473 ± 52 *	19.02 ± 8.01 *	39.08 ± 1.15 *

	5.0	56.27 ± 0.53 *	301 ± 78 *	38.04 ± 2.36 *	48.36 ± 0.62 *

3.3.3 Cross-linking cytotoxicity characterisation using dermal fibroblasts

Qualitative hDF morphology analysis (**Figure 3.5**) revealed that the cells attached and spread well only on 0 mM, 0.5 mM and 1 mM 4SG-PEG cross-linked skin- and tendon- derived collagen sponges. Quantitative hDF DNA concentration (**Figure 3.6A**) and metabolic activity (**Figure 3.6B**) analyses showed that the 2.5 mM and 5 mM 4SG-PEG cross-linked skin- and tendon- derived collagen sponges consistently induced significantly ($p < 0.05$) lower than the other groups cell DNA concentration and metabolic activity at all time points. Qualitative hDF viability analysis (**Figure 3.7**) made apparent that the 2.5 mM and 5 mM 4SG-PEG cross-linked skin- and tendon- derived collagen sponges reduced cell viability.

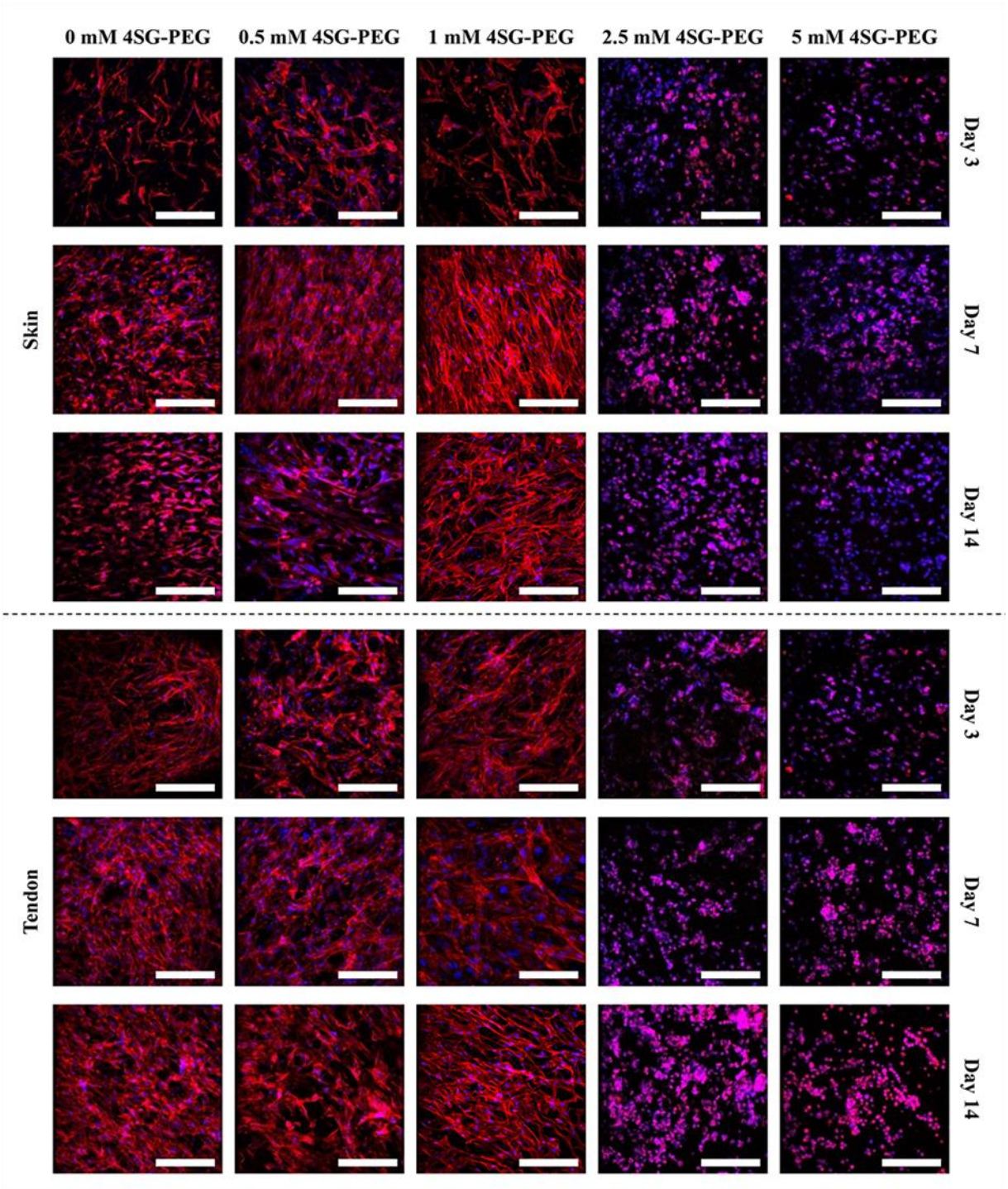

Figure 3.5: hDF morphology after 3, 7 and 14 days in culture on skin- and tendon-derived collagen sponges cross-linked with 0 mM, 1 mM, 2.5 mM and 5 mM 4SG-PEG. Scalebar: 200 µm. N = 3. Blue: DAPI. Red: rhodamine phalloidin.

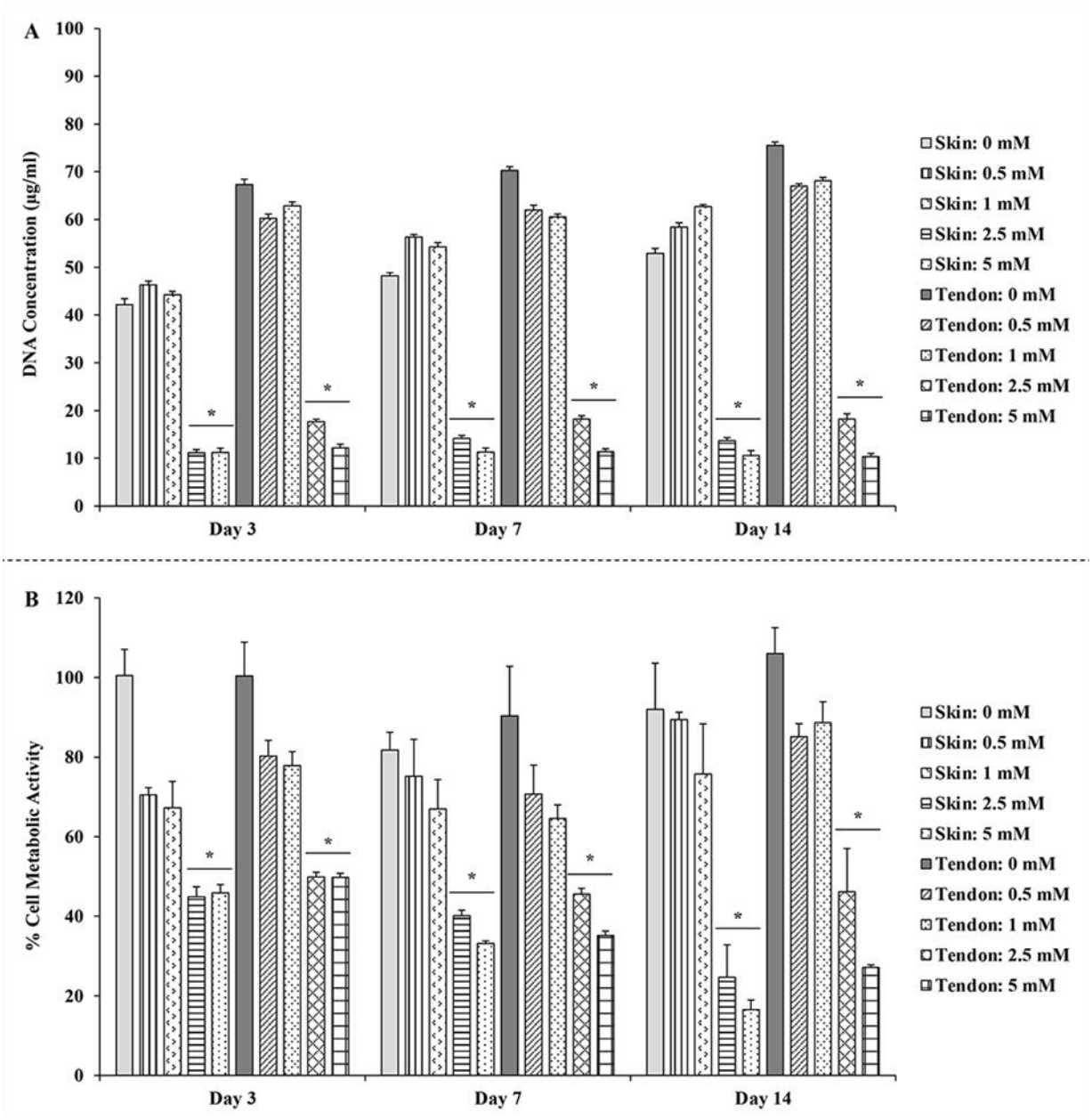

Figure 3.6: hDF **(A)** proliferation and **(B)** metabolic activity after 3, 7 and 14 days in culture on skin- and tendon-derived collagen sponges cross-linked with 0 mM, 1 mM, 2.5 mM and 5 mM 4SG-PEG. * indicates statistically significant ($p < 0.05$) difference from the 0 mM, 0.5 mM and 1 mM 4SG-PEG cross-linked groups. N = 3.

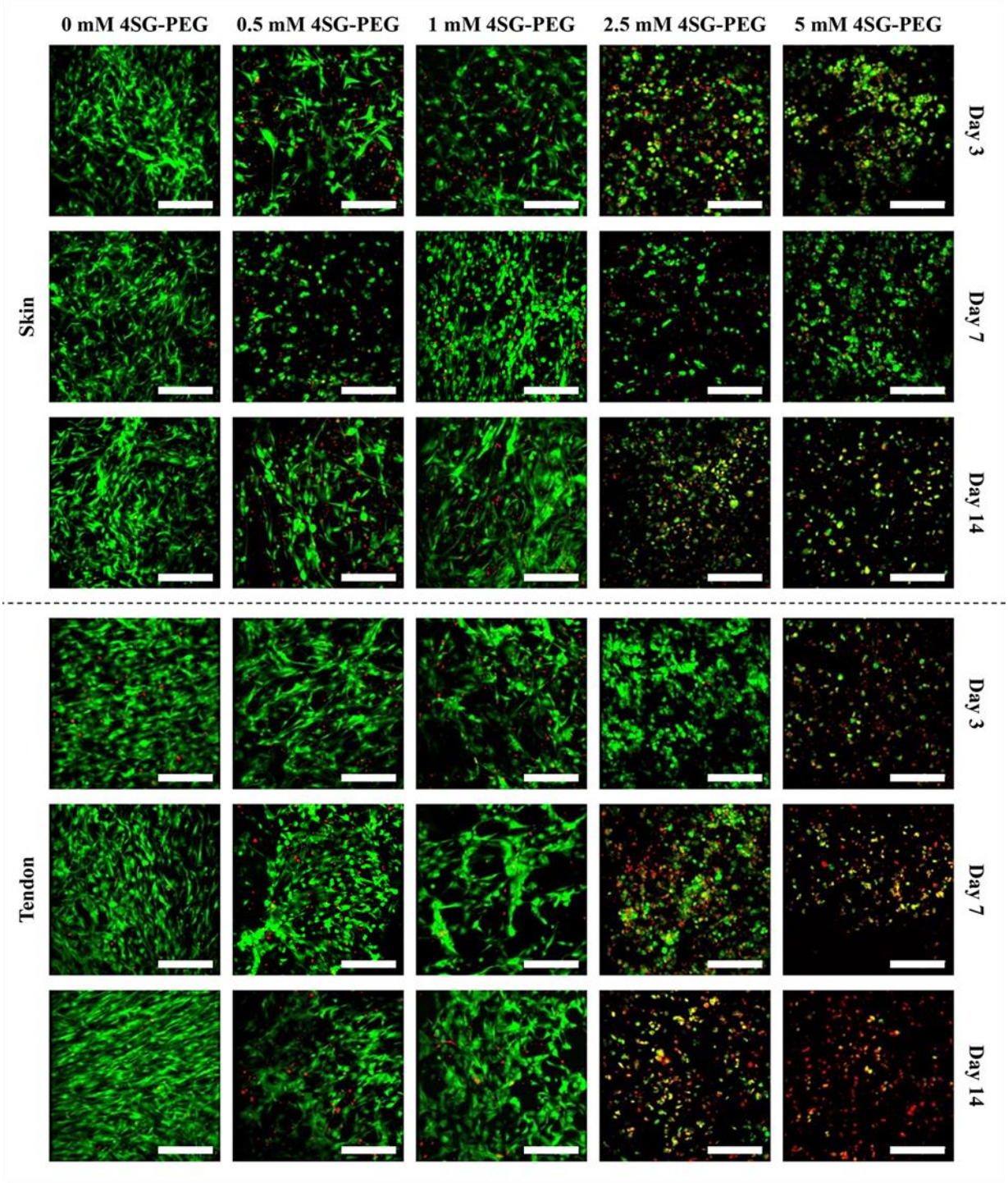

Figure 3.7: hDF viability after 3, 7 and 14 days in culture on skin- and tendon-derived collagen sponges cross-linked with 0 mM, 1 mM, 2.5 mM and 5 mM 4SG-PEG. Scalebar: 200 µm. N = 3. Green: live cells. Red: dead cells.

3.3.4 Tenocyte basic cellular function analysis

Qualitative hTC morphology (**Figure 3.8**) and viability (**Figure 3.10**) analysis revealed that the cells attached, spread and grew well on the 0 mM and 1 mM 4SG-PEG crosslinked skin- and tendon- derived collagen sponges. Quantitative hTC DNA concentration analysis (**Figure 3.9A**) made apparent that at all time points, the 0 mM and 1 mM 4SG-PEG crosslinked skin-derived collagen sponges induced significantly ($p < 0.05$) lower than the 0 mM and 1 mM 4SG-PEG crosslinked tendon-derived collagen sponges, respectively, cell DNA concentration. With respect to hTC metabolic activity (**Figure 3.9B**), only at day 14, the 0 mM and 1 mM 4SG-PEG crosslinked skin-derived collagen sponges induced significantly ($p < 0.05$) lower metabolic activity than the 0 mM and 1 mM 4SG-PEG crosslinked tendon-derived collagen sponges, respectively [at day 3 and day 7, they induced lower, albeit not significant ($p > 0.05$), metabolic activity].

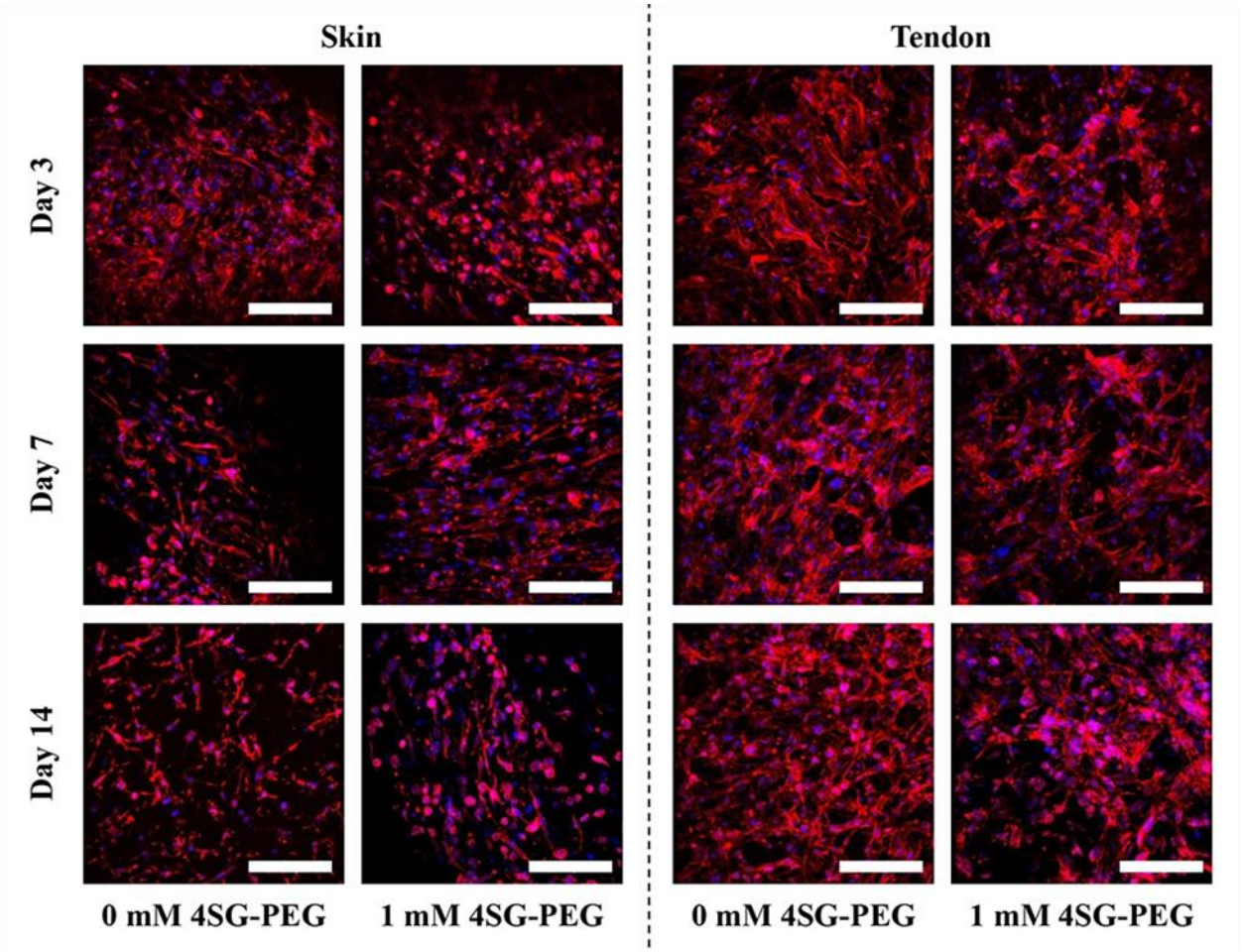

Figure 3.8: hTCs morphology after 3, 7 and 14 days in culture on skin- and tendon-derived collagen sponges cross-linked with 0 mM and 1 mM 4SG-PEG. Scalebar: 200 µm. N = 3. Blue: DAPI. Red: rhodamine phalloidin.

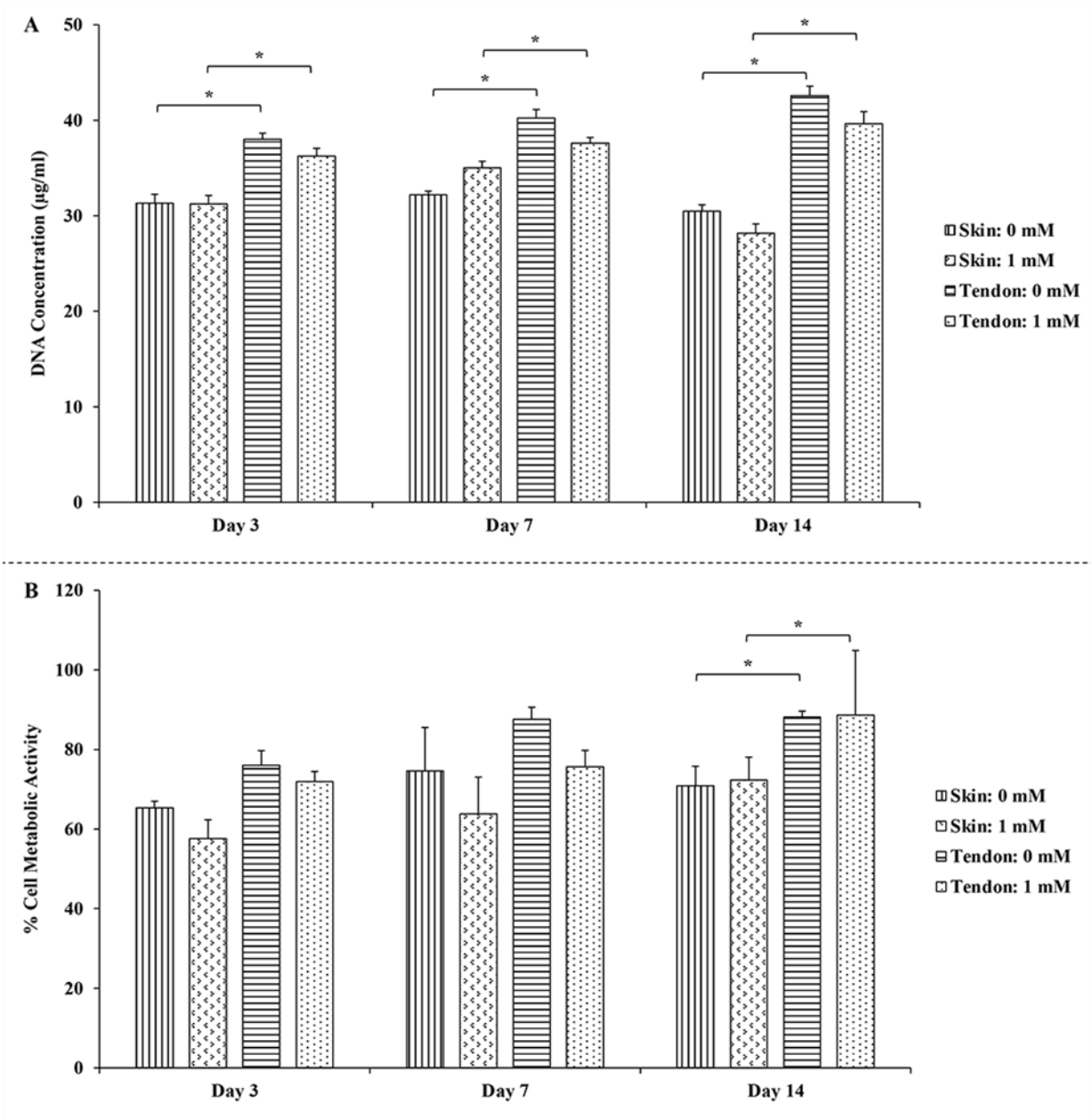

Figure 3.9: hTCs **(A)** proliferation and **(B)** metabolic activity after 3, 7 and 14 days in culture on skin- and tendon-derived collagen sponges cross-linked with 0 mM and 1 mM 4SG-PEG. * indicates statistically significant ($p < 0.05$) difference. N = 3.

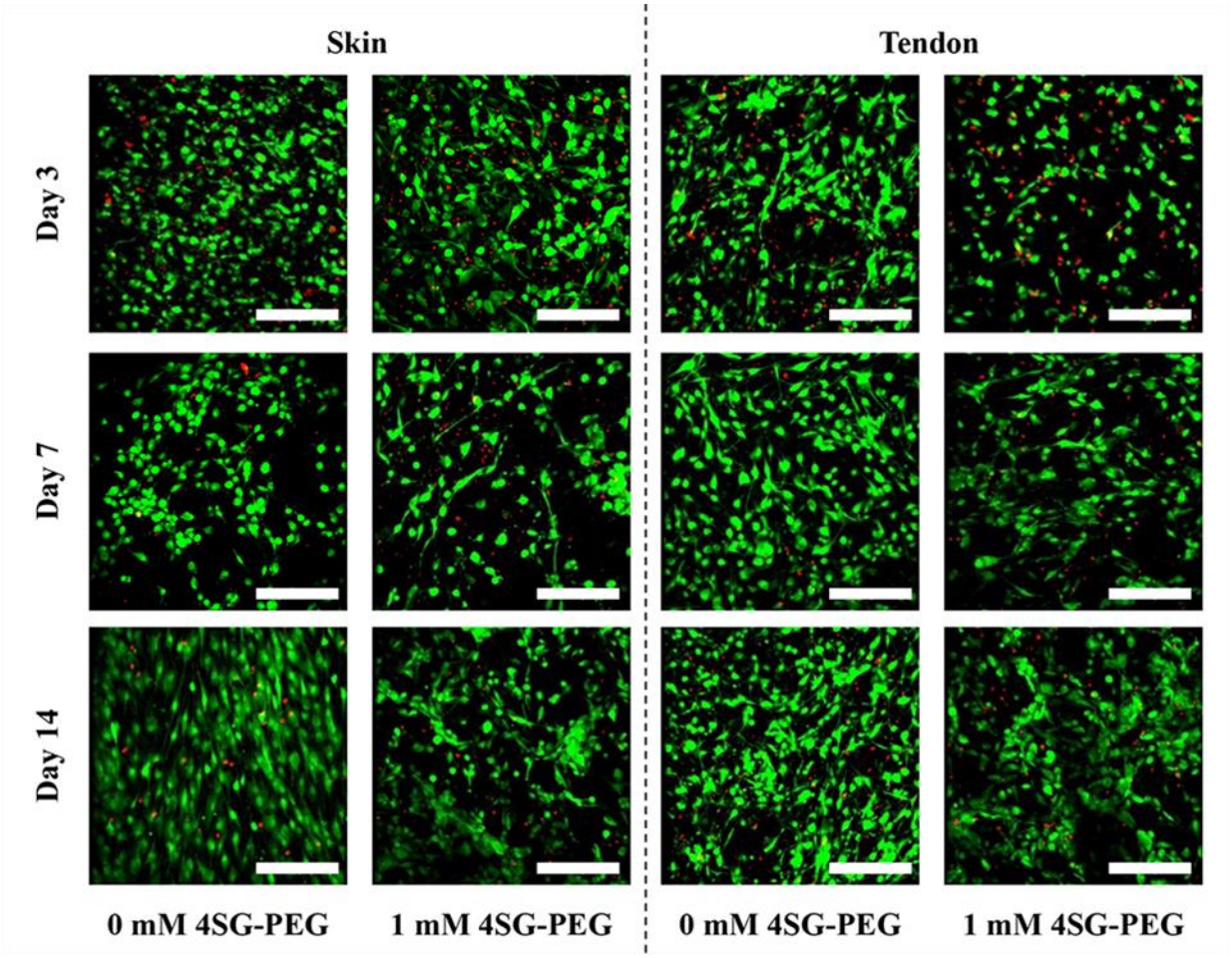

Figure 3.10: hTC viability after 3, 7 and 14 days in culture on skin- and tendon-derived collagen sponges cross-linked with 0 mM and 1 mM 4SG-PEG. Scalebar: 200 µm. N = 3. Green: live cells. Red: dead cells.

3.3.5 Tenocyte immunocytochemistry analysis

Table 3.2 summarises immunocytochemistry and complementary matrix area deposited per cell (μm²) analyses for collagen type I, collagen type III, collagen type IV, collagen type V, collagen type VI, fibronectin, scleraxis, tenomodulin, collagen type II, aggrecan, osteocalcin and osteopontin (**Figure 3.11-3.22**) synthesis on 0 and 1 mM 4SG-PEG concentration skin- and tendon- derived collagen scaffolds at day 3, day 7 and day 14. At day 3 and at 0 mM 4SG-PEG concentration, the skin-derived collagen scaffolds induced significantly ($p < 0.05$) higher collagen IV, collagen type V, collagen type VI and tenomodulin synthesis and the tendon-derived collagen scaffolds induced significantly ($p < 0.05$) higher fibronectin and scleraxis synthesis. At day 3 and at 1 mM 4SG-PEG concentration, the skin-derived collagen scaffolds induced significantly ($p < 0.05$) higher collagen type I, collagen type III, collagen type VI and tenomodulin synthesis and the tendon-derived collagen scaffold induced significantly ($p < 0.05$) higher collagen type IV synthesis. At day 7 and at 0 mM 4SG-PEG concentration, only the tendon-derived collagen scaffolds induced significantly ($p < 0.05$) higher fibronectin, scleraxis and tenomodulin synthesis. At day 7 and at 1 mM 4SG-PEG concentration, the skin-derived collagen scaffolds induced significantly ($p < 0.05$) higher scleraxis synthesis and the tendon-derived collagen scaffolds induced significantly ($p < 0.05$) higher collagen type V and collagen type VI synthesis. At day 14 and at 0 mM 4SG-PEG concentration, the skin-derived collagen scaffolds induced significantly ($p < 0.05$) higher collagen type IV, collagen type V, collagen type VI and fibronectin synthesis and the tendon-derived collagen scaffolds induced significantly ($p < 0.05$) higher scleraxis and tenomodulin synthesis. At day 14 and at 1 mM 4SG-PEG concentration, the skin-derived collagen scaffolds induced significantly ($p < 0.05$) higher collagen type IV synthesis and the tendon-derived collagen scaffolds induced significantly ($p < 0.05$) higher collagen type III synthesis. None of the scaffolds induced synthesis of chondrogenic (collagen type II and aggrecan) and osteogenic (osteocalcin and osteopontin) molecules (**Look at Appendices C.1.3 for hDFs immunocytochemistry results).**

Table 3.2: Summary of immunocytochemistry analysis. ND indicates not detected. NS indicates no significance. Sin / Tendon indicates which tissue derived collagen preparation induced significantly ($p < 0.05$) higher matrix area deposited per cell (μm²).

	Day 3		**Day 7**		**Day 14**	
	Skin Vs Tendon		**Skin Vs Tendon**		**Skin Vs Tendon**	
4SG-PEG	**0 mM**	**1 mM**	**0 mM**	**1 mM**	**0 mM**	**1 mM**
Col I	ND	Skin	NS	NS	NS	NS
Col III	NS	Skin	NS	NS	NS	Tendon
Col IV	Skin	Tendon	NS	NS	Skin	Skin
Col V	Skin	NS	NS	Tendon	Skin	NS
Col VI	Skin	Skin	NS	Tendon	Skin	NS
Fibronectin	Tendon	NS	Tendon	NS	Skin	NS
Scleraxis	Tendon	NS	Tendon	Skin	Tendon	NS
Tenomodulin	Skin	Skin	Tendon	NS	Tendon	NS
Col II	ND	ND	ND	ND	ND	ND
Aggrecan	ND	ND	ND	ND	ND	ND
Osteocalcin	ND	ND	ND	ND	ND	ND
Osteopontin	ND	ND	ND	ND	ND	ND

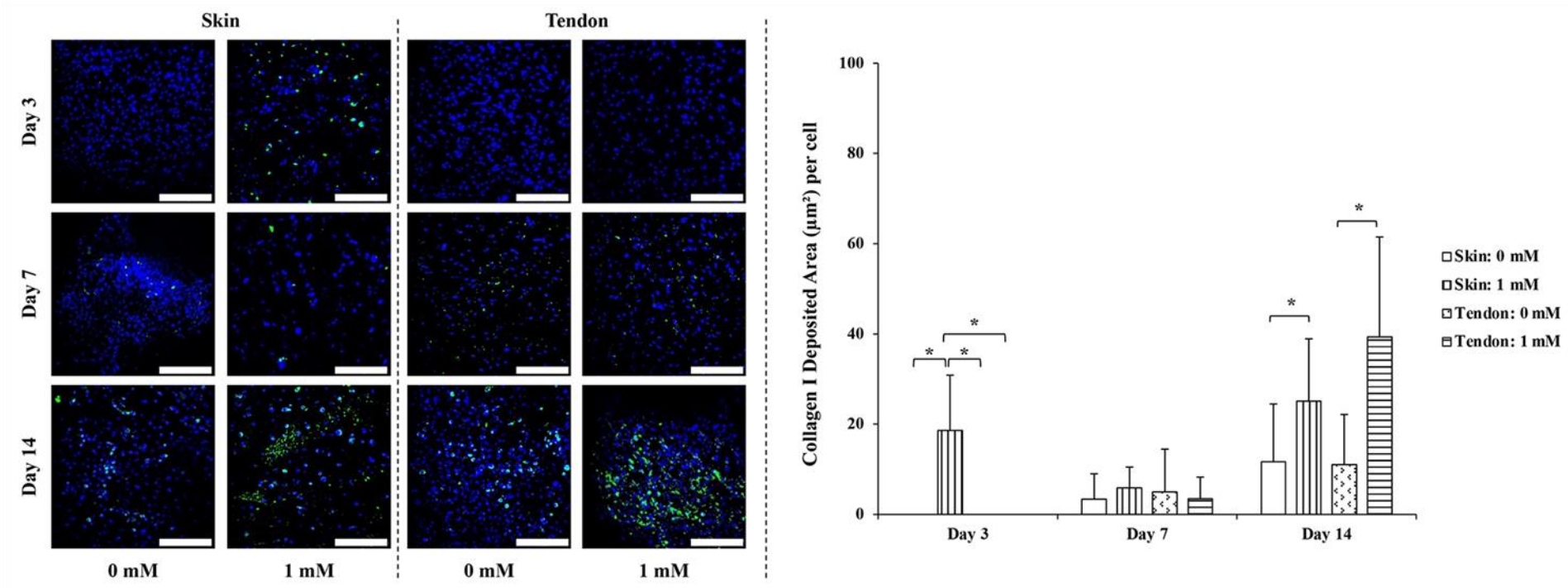

Figure 3.11: hTC deposited collagen type I (green) after 3, 7 and 14 days in culture on skin- and tendon-derived collagen sponges cross-linked with 0 mM and 1 mM 4SG-PEG. * indicates statistically significant ($p < 0.05$) difference. Scalebar: 200 µm. N = 3. Blue: DAPI.

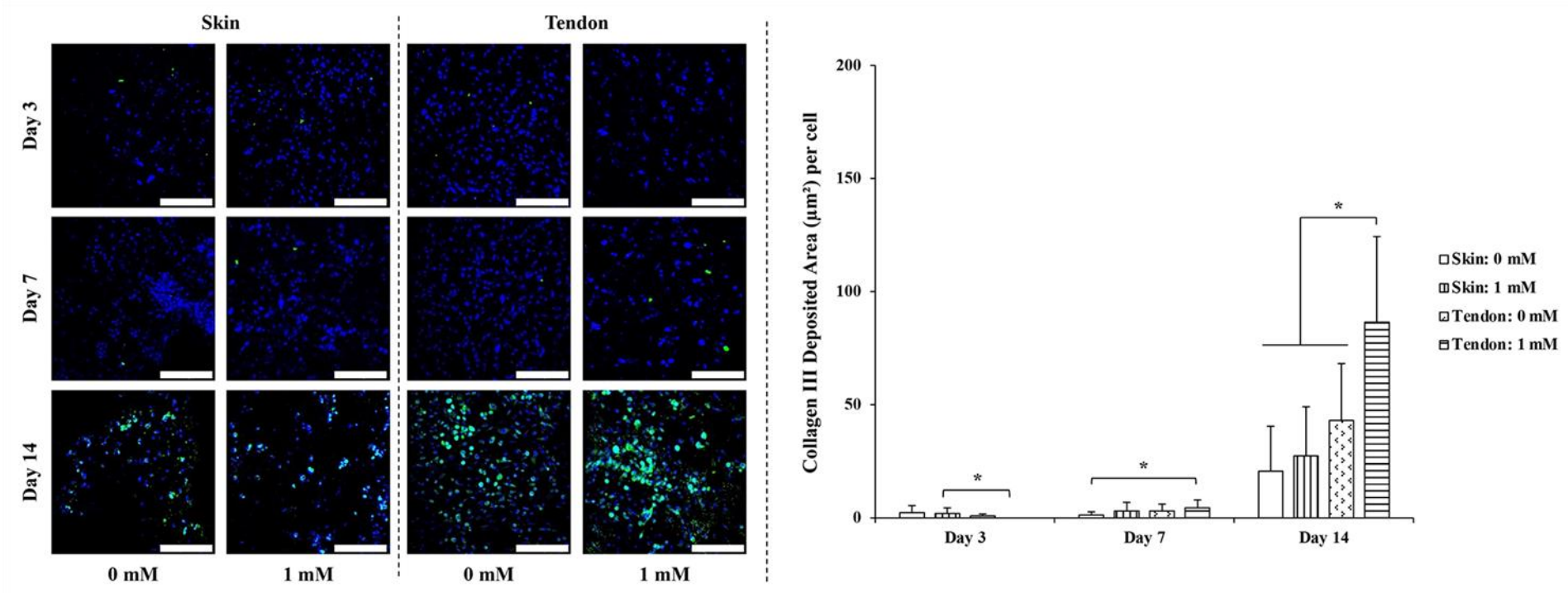

Figure 3.12: hTC deposited collagen type III (green) after 3, 7 and 14 days in culture on skin- and tendon-derived collagen sponges cross-linked with 0 mM and 1 mM 4SG-PEG. * indicates statistically significant ($p < 0.05$) difference. Scalebar: 200 µm. N = 3. Blue: DAPI.

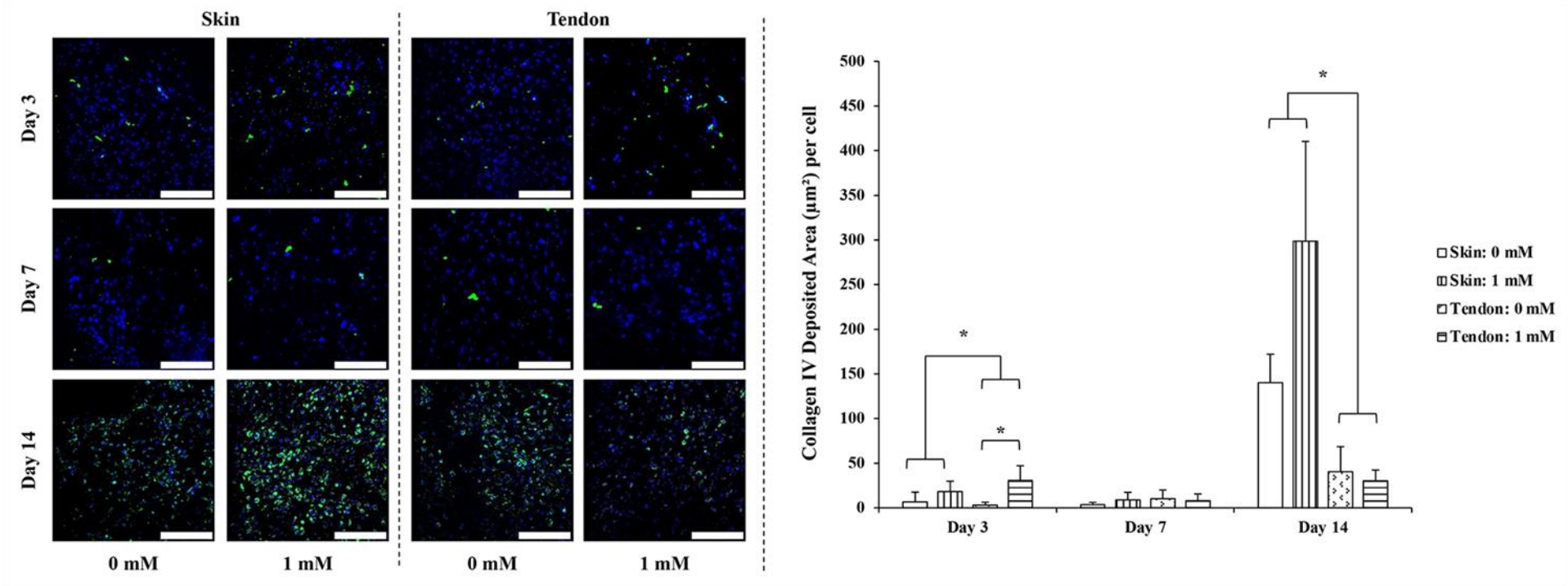

Figure 3.13: hTC deposited collagen type IV (green) after 3, 7 and 14 days in culture on skin- and tendon-derived collagen sponges cross-linked with 0 mM and 1 mM 4SG-PEG. * indicates statistically significant ($p < 0.05$) difference. Scalebar: 200 µm. N = 3. Blue: DAPI.

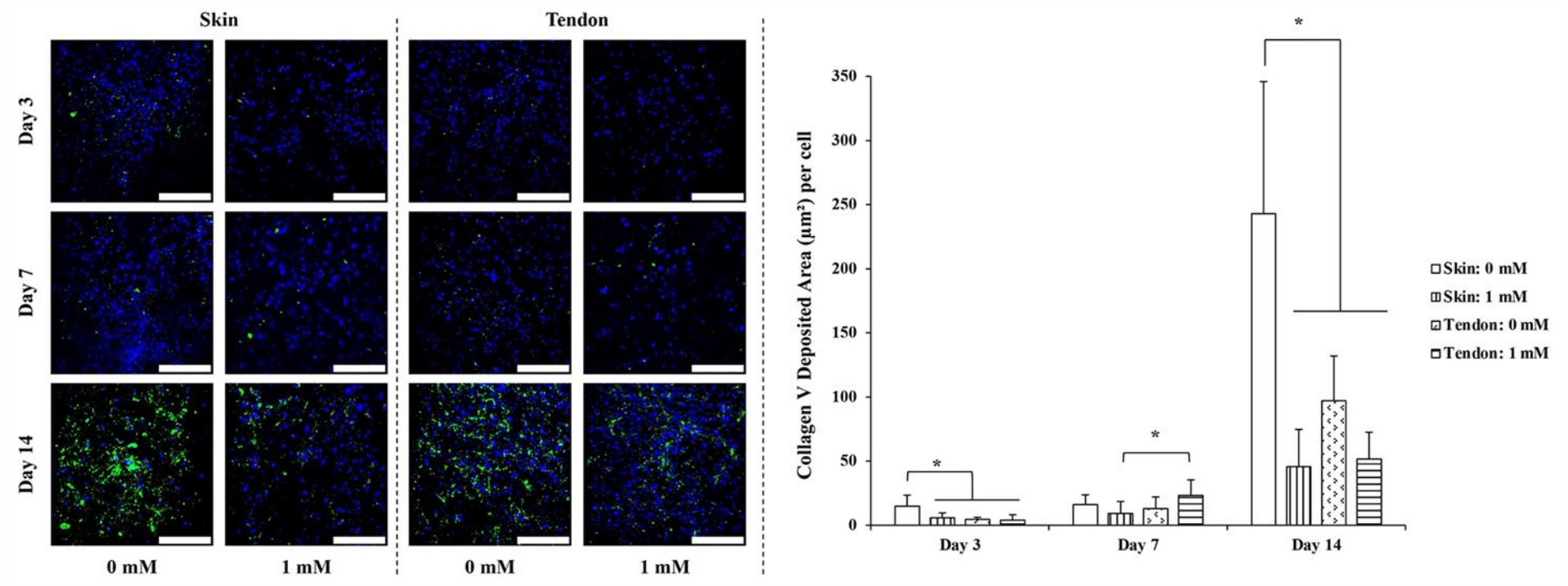

Figure 3.14: hTC deposited collagen type V (green) after 3, 7 and 14 days in culture on skin- and tendon-derived collagen sponges cross-linked with 0 mM and 1 mM 4SG-PEG. * indicates statistically significant ($p < 0.05$) difference. Scalebar: 200 µm. N = 3. Blue: DAPI.

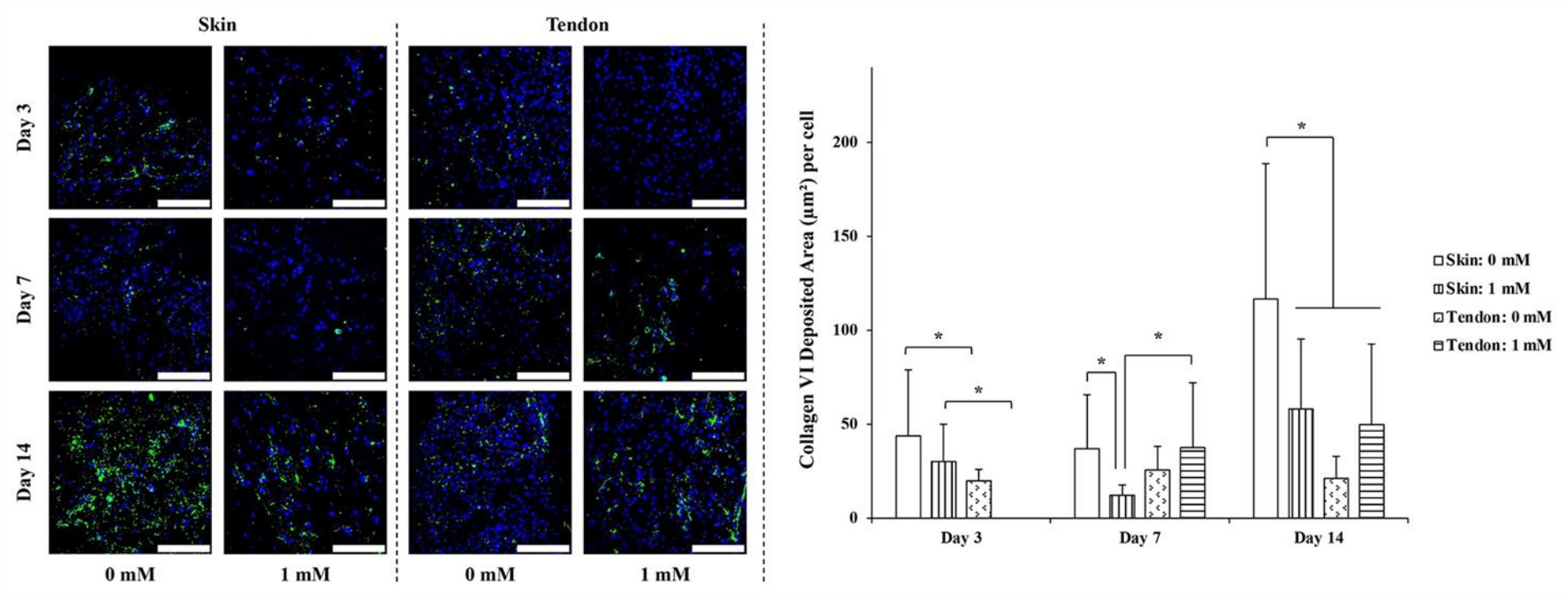

Figure 3.15: hTC deposited collagen type VI (green) after 3, 7 and 14 days in culture on skin- and tendon-derived collagen sponges cross-linked with 0 mM and 1 mM 4SG-PEG. * indicates statistically significant ($p < 0.05$) difference. Scalebar: 200 µm. N = 3. Blue: DAPI.

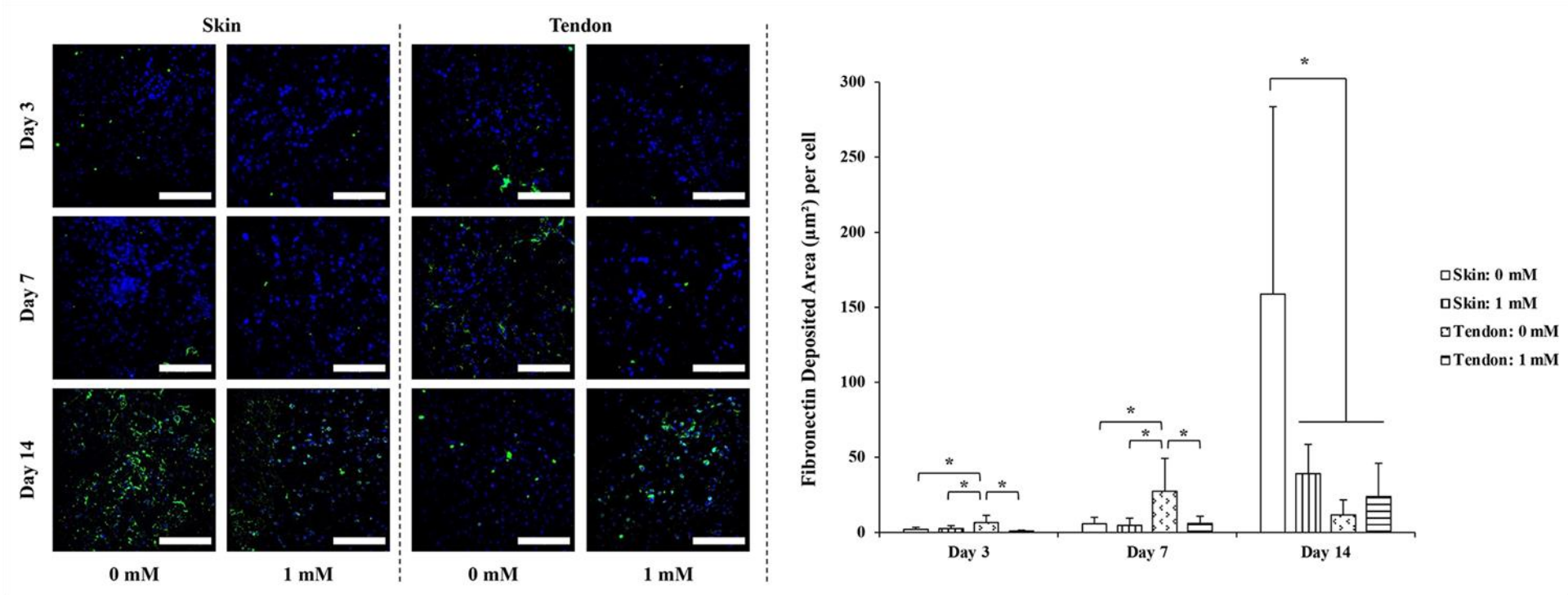

Figure 3.16: hTC deposited fibronectin (green) after 3, 7 and 14 days in culture on skin- and tendon-derived collagen sponges cross-linked with 0 mM and 1 mM 4SG-PEG. * indicates statistically significant ($p < 0.05$) difference. Scalebar: 200 µm. N = 3. Blue: DAPI.

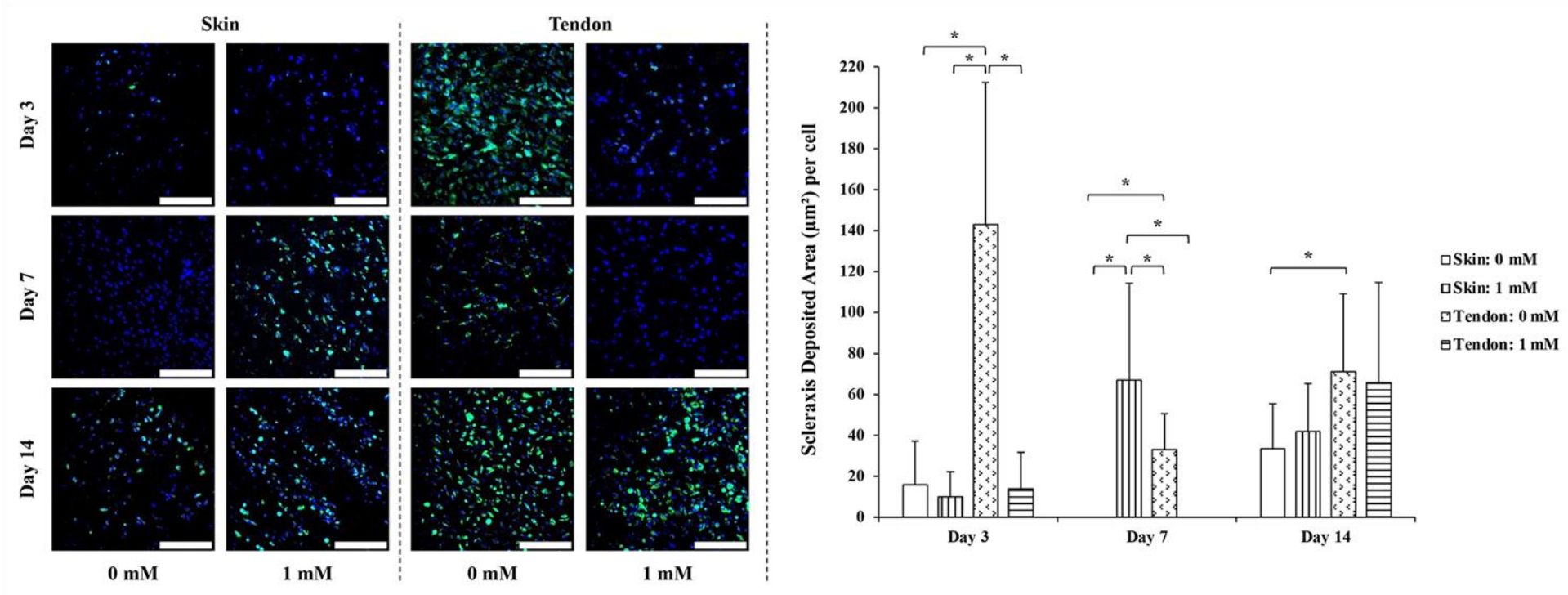

Figure 3.17: hTC deposited scleraxis (green) after 3, 7 and 14 days in culture on skin- and tendon-derived collagen sponges cross-linked with 0 mM and 1 mM 4SG-PEG. * indicates statistically significant ($p < 0.05$) difference. Scalebar: 200 µm. N = 3. Blue: DAPI.

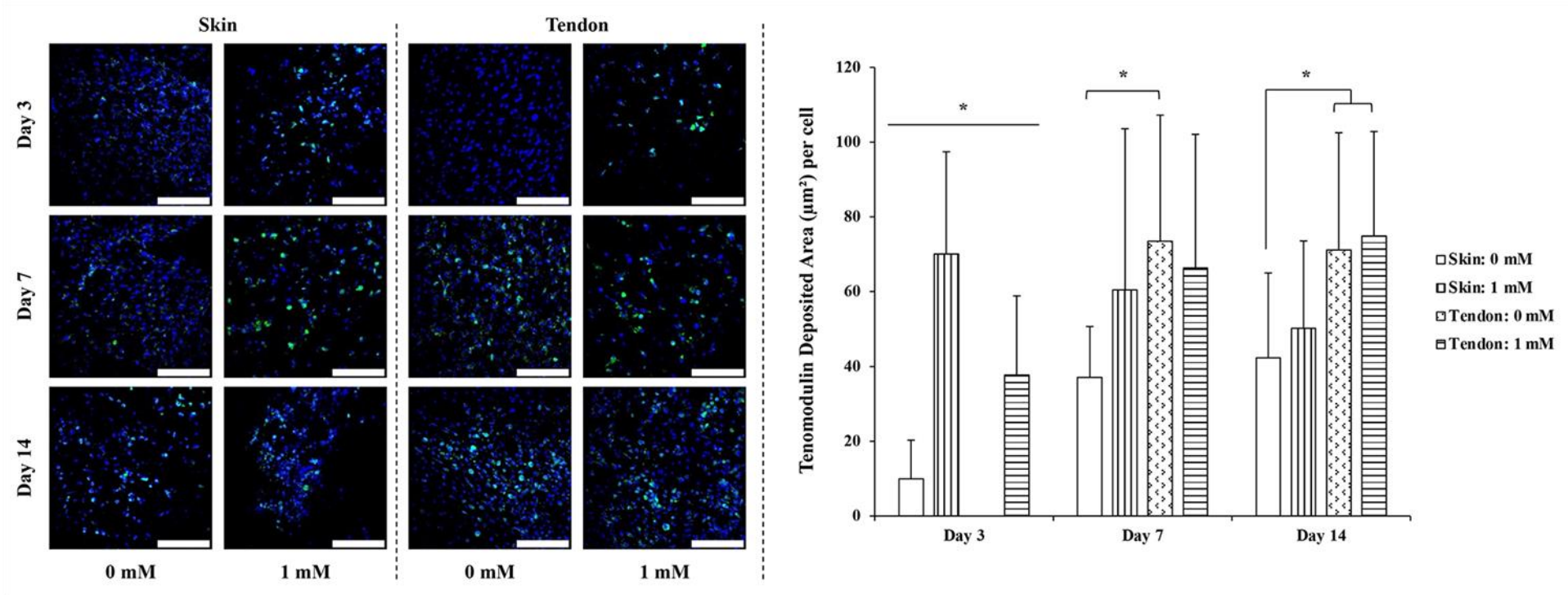

Figure 3.18: hTC deposited tenomodulin (green) after 3, 7 and 14 days in culture on skin- and tendon-derived collagen sponges cross-linked with 0 mM and 1 mM 4SG-PEG. * indicates statistically significant ($p < 0.05$) difference. Scalebar: 200 µm. N = 3. Blue: DAPI.

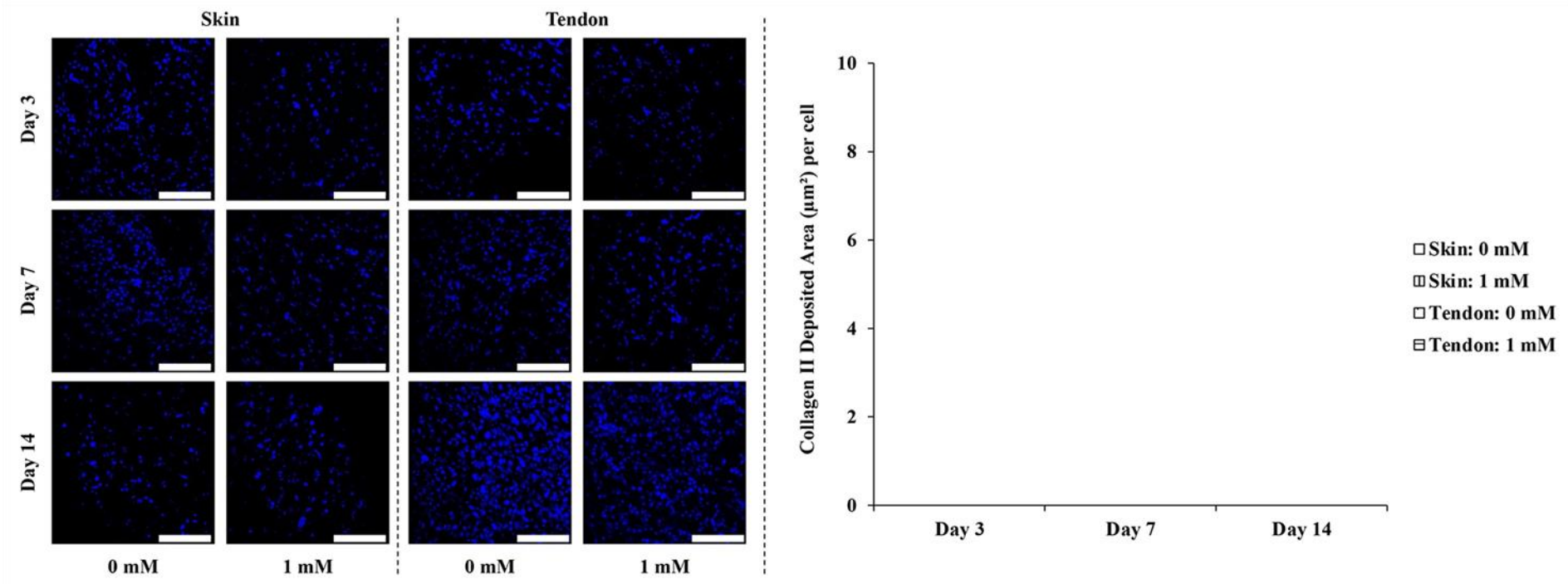

Figure 3.19: hTC deposited collagen type II (green) after 3, 7 and 14 days in culture on skin- and tendon-derived collagen sponges cross-linked with 0 mM and 1 mM 4SG-PEG. Scalebar: 200 µm. N = 3. Blue: DAPI.

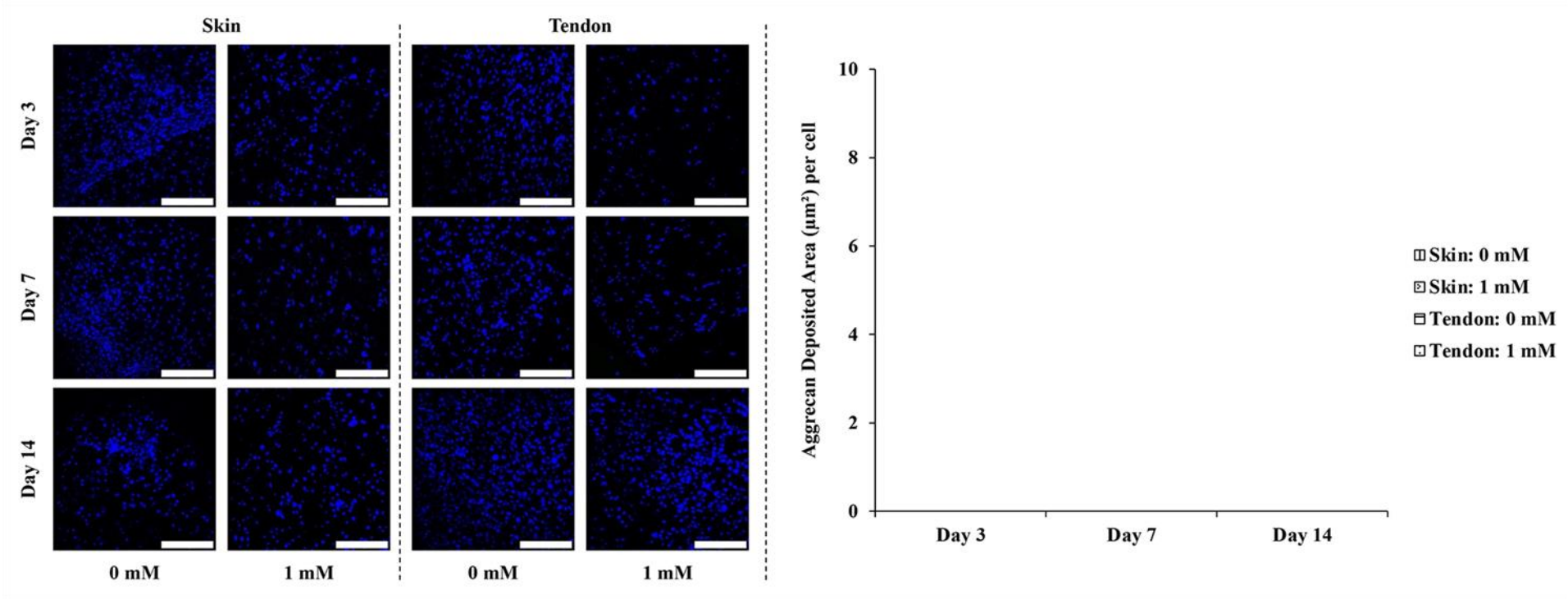

Figure 3.20: hTC deposited aggrecan (green) after 3, 7 and 14 days in culture on skin- and tendon-derived collagen sponges cross-linked with 0 mM and 1 mM 4SG-PEG. Scalebar: 200 µm. N = 3. Blue: DAPI.

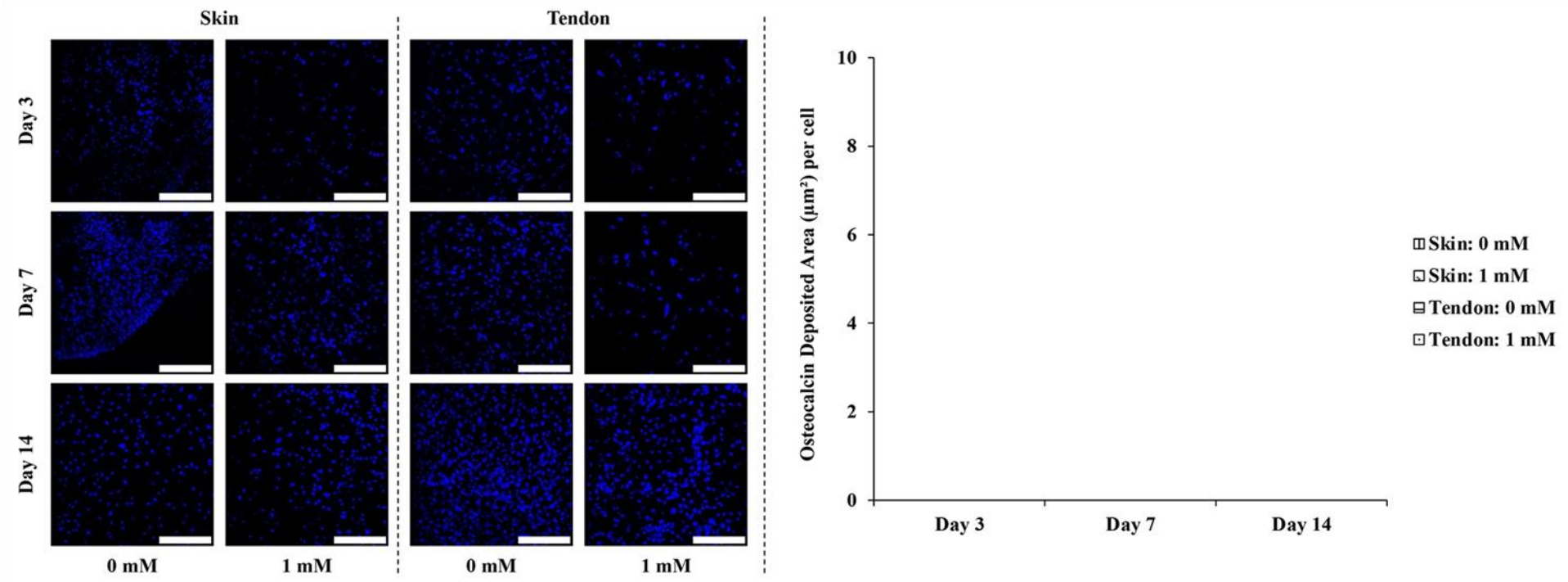

Figure 3.21: hTC deposited osteocalcin (green) after 3, 7 and 14 days in culture on skin- and tendon-derived collagen sponges cross-linked with 0 mM and 1 mM 4SG-PEG. Scalebar: 200 µm. N = 3. Blue: DAPI.

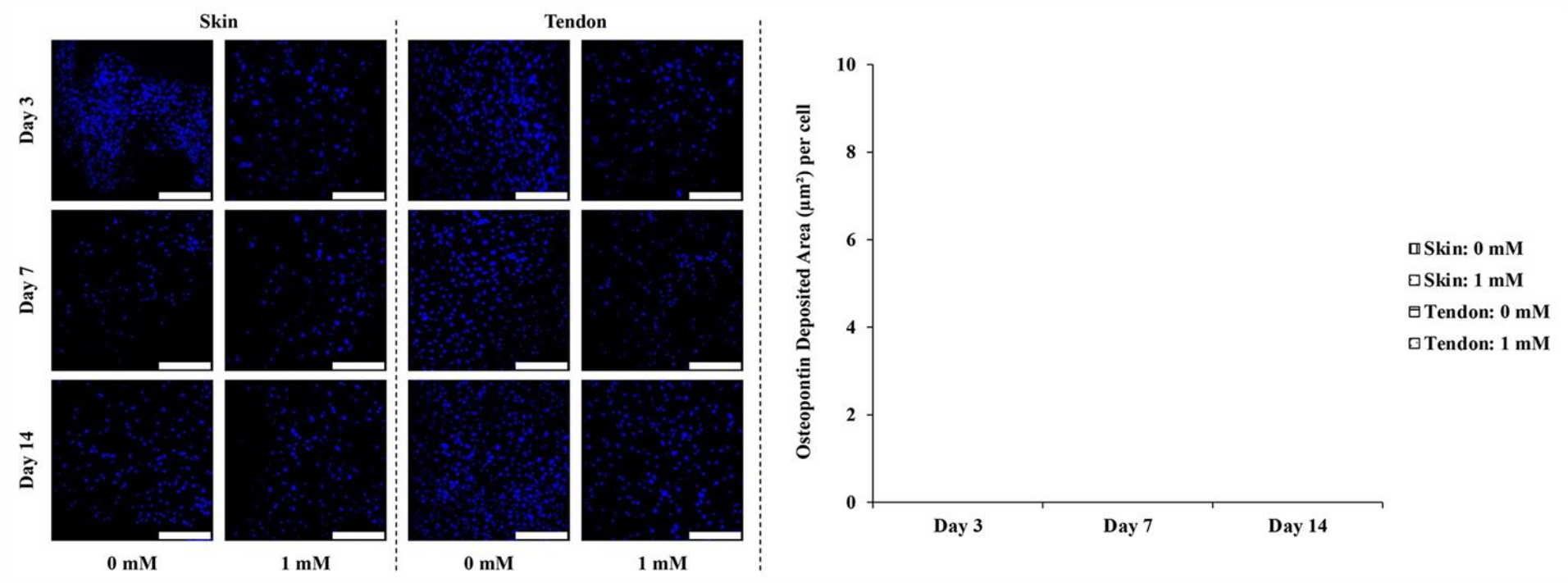

Figure 3.22: hTC deposited osteopontin (green) after 3, 7 and 14 days in culture on skin- and tendon-derived collagen sponges cross-linked with 0 mM and 1 mM 4SG-PEG. Scalebar: 200 µm. N = 3. Blue: DAPI.

3.3.6 Tenocyte gene expression analysis

Gene expression analysis (**Figure 3.23**) revealed that at day 3, hTCs seeded on 1 mM 4SG-PEG concentration skin-derived collagen scaffolds upregulated P4HA2 and SPP1 and downregulated VCAN and THBS4 and hTCs seeded on 1 mM 4SG-PEG concentration tendon-derived collagen scaffolds upregulated P4HA2, PLOD1, ELN and ACTA2 and downregulated VCAN and THBS4. At day 7, hTCs seeded on 1 mM 4SG-PEG concentration skin-derived collagen scaffolds upregulated P4HA2, COL3, SCXA, TNMD, MKX, DCN, BGN, THBS4, SPP1, BGLAP, SERPINH1 and downregulated COL1 and VCAN and hTCs seeded on 1 mM 4SG-PEG concentration tendon-derived collagen scaffolds upregulated PLOD1, SCXA, TNMD, BGN, THBS4, BGLAP, SERPINH1 and FABP4 and downregulated DCN, VCAN, ELN and SPP1. At day 14, hTCs seeded on 1 mM 4SG-PEG concentration skin-derived collagen scaffolds upregulated P4HA1, P4HA2, PLOD1, PLOD2, SCXA, TNC, BGN, ELN and SERPINH1 and downregulated VCAN and hTCs seeded on 1 mM 4SG-PEG concentration tendon-derived collagen scaffolds upregulated P4HA2, PLOD1, PLOD2, SCXA, TNC, BGN, ELN and SERPINH1 and downregulated VCAN and ACTA2. It is interesting to note that at day 14, the longest time point assessed, only two differences were observed: the 1 mM 4SG-PEG concentration skin-derived collagen scaffolds upregulated P4HA1 and the 1 mM 4SG-PEG concentration tendon-derived collagen scaffolds downregulated ACTA2.

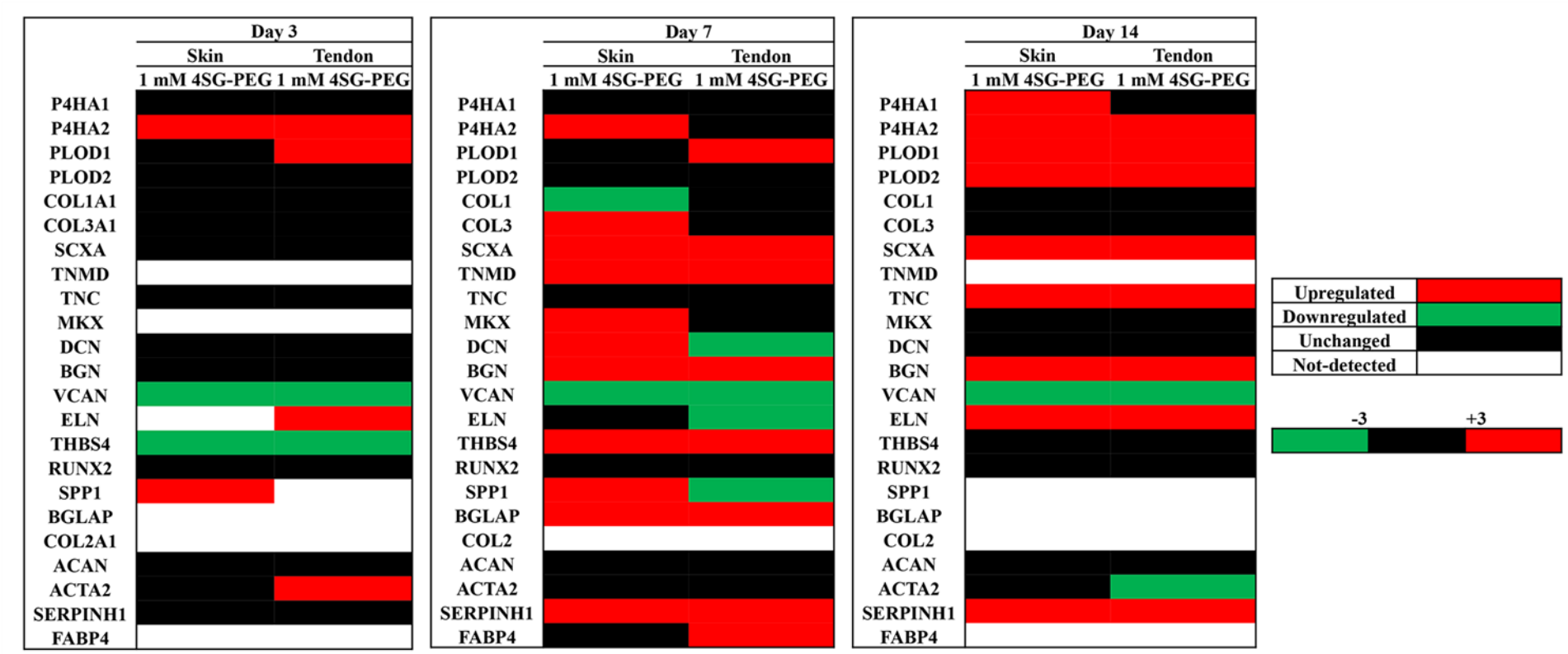

Figure 3.23: Gene expression analysis of hTCs seeded on skin- and tendon- derived collagen scaffolds cross-linked with 1 mM 4-arm polyethylene glycol succinimidyl glutarate (4SG-PEG).

3.4 Discussion

Collagen has many favourable properties as building block for scaffold fabrication, including high cytocompatibility, acceptable biodegradability, low immunogenicity, low antigenicity and ability to be processed in structural conformations that closely match the structural and physical properties of the tissue to be replaced. Despite the significant advancement in collagen extraction, purification, cross-linking and sterilisation methods, commercially available collagen devices still yield inconsistent therapeutic efficiency in clinical setting, suggesting that other factors should also be considered in the design of a collagen-based medical device. Herein, we ventured to assess whether the tissue from which the collagen is extracted (skin versus tendon) could influence cell response, in particular hTCs that readily lose their phenotype and function *ex vivo*.

Starting with purity assessment, SDS-PAGE analysis revealed a typical collagen type I electrophoretic mobility [4, 43]. Further, no particular differences between the skin- and tendon- derived collagen preparations were identified, which is expected considering that the tissues were obtained from the same animals (therefore similar level of age-related cross-linking [54-58]) and processed (pepsin extracted and purified via repeated salt precipitation) in the same way.

We subsequently fabricated collagen sponges and proceeded to identify the optimal 4SG-PEG cross-linking concentration via structural, biochemical, biomechanical and biological analyses. Ultrastructural analysis revealed that both collagen preparations, independently of the 4SG-PEG concentration, yielded porous scaffolds (pore diameter range 101-186 μm and 103-298 μm for the skin- and tendon- derived scaffolds, respectively) and that the % porosity was reduced after 4SG-PEG cross-linking [from 70 % to 36-44 % (depending on the 4SG-PEG concertation) and from 59 % to 47-53 % (depending on the 4SG-PEG concertation) porosity for the skin- and tendon-derived scaffolds, respectively]. Over the years, collagen scaffolds with a diverse range of pore size values have been obtained (e.g. from 20-40 μm [59] to > 800 μm [60]), subject to the freeze-drying protocol and cross-linking method employed. In general, pore size > 40 μm is required for soft tissue replacement [61] to allow for cell and neo-tissue infiltration and nutrient / waste and oxygen diffusion. Cross-linking with 4SG-PEG increased denaturation temperature, resistance to enzymatic degradation and mechanical properties and reduced free amine content and %

swelling, as has been shown before for various collagen preparations using a diverse range of cross-linking approaches [22-25, 62]. All these observations are interconnected and are associated with the extent of cross-linking. Indeed, intermolecular cross-links are responsible for increased thermal stability and resistance to collagenase digestion and reduced % of free amines, due to the increased energy of crystallisation derived from the interaction between the closely packed molecules [63-67]. Previous studies have also shown that the water holding capacity of collagen is cross-linking-dependent [68, 69], as the water binding sites are occupied or removed by the formation of cross-links, which explains the reduced swelling ratio [70-73]. This reduction in water content as a function of cross-linking is also responsible for the increase in mechanical properties, as the higher the cross-linking density, the lower the water binding capacity, which promotes intermolecular stiffening and prevents slippage between neighbouring molecules [22, 70, 74, 75]. It is very interesting to note that a profound difference in mechanical properties between skin- and tendon- derived collagen sponges was observed. We believe that tissue origin is responsible for the higher mechanical properties of the tendon-derived collagen scaffolds, in accordance to previously published works, where bovine Achilles tendon-derived collagen scaffolds had higher force at break than rat tail tendon-derived collagen scaffolds [4] and porcine and bovine tendon-derived collagen scaffolds had higher mechanical properties than porcine and bovine skin-derived collagen scaffolds [51]. A 4SG-PEG concentration-dependent cytotoxicity was observed in hDF cultures, as has been repeatedly reported in the literature (e.g. genipin [76, 77]; carbodiimide [78]) indicating once more the need to find an optimal balance between stability and cytocompatibility [17]. As the 1 mM 4SG-PEG concentration did not induce any cytotoxic effect and resulted in collagen sponges with significantly higher thermal and mechanical properties and significantly lower free amines and % swelling than the 0 mM 4SG-PEG collagen sponges, we considered this concentration as the minimum effective concentration, which is also in agreement with a previous study that have shown the 1 mM 4SG-PEG to induce adequate collagen scaffold stability and cytocompatibility [44].

Similar to hDF cultures, basic cellular function analysis using hTC morphology, proliferation metabolic activity and viability revealed no apparent differences between the skin- and tendon- derived collagen scaffolds and, again, the 1 mM 4SG-PEG did

not induce any cytotoxicity. This is in accordance to previous publications, where 4SG-PEG has shown acceptable levels of cytocompatibility (e.g. collagen type I hydrogels [79], collagen type I films [24, 62], collagen type I fibres [25, 80], collagen type II hydrogels [44], collagen type II sponges [42, 81]).

Immunocytochemistry analysis (the function of each molecule assessed is provided in **Supplementary Table S2**) made apparent that at day 14 (the longest time point assessed), the 0 mM 4SG-PEG skin-derived collagen scaffolds significantly increased (over the tendon-derived collagen scaffolds) the synthesis of collagen type IV, collagen type V, collagen type VI and fibronectin. Collagen type IV is a basement membrane collagen that is primarily found in the lamina densa of the dermal-epidermal junction of skin [82] and it has also been detected in the basement membrane that overlies the keratinised epithelium of tendons [83]. Collagen type V is critical at the early stages of fibril nucleation and plays crucial role in fibril diameter and mechanical properties of tendons, dermis and cornea [84-87]. Collagen type VI is a non-fibrillar collagen expressed in many connective tissues, including skin and tendon [88-90]. Fibronectin is primarily associated with physiological skin development and healing [91-93], whilst in normal tendons is found primarily in epitenon and sheath synovium, as opposed to endotenon and collagen fibres, and in injured / ruptured tendons on the tear surface and in the collagen fibres [94-96]. It is also interesting to note that our data correlate well with a preclinical work with equine tendons, where fibronectin was evidenced only at the first month post-injury, whilst collagen type III was detectable for the duration of the study (three months post-injury) [97]. At day 14 on the other hand, the 0 mM 4SG-PEG tendon-derived collagen scaffolds significantly increased (over the skin-derived collagen scaffolds) the synthesis of scleraxis and tenomodulin. Scleraxis [98-101] and tenomodulin [102-105] are extensively used and considered as tenogenic markers, as they play crucial role in embryonic and foetal cell differentiation towards tenocyte, tenocyte proliferation and tendon development, healing, physiological function and maturation. Also at day 14, the 1 mM 4SG-PEG skin-derived collagen scaffolds significantly increased (over the tendon-derived collagen scaffolds) the synthesis of collagen type IV (found primarily in the skin within the basement membrane zone [82, 106]), whilst the 1 mM 4SG-PEG tendon-derived collagen scaffolds significantly increased (over the skin-derived collagen scaffolds) the synthesis of collagen type III. The increased collagen type III

synthesis may be attributed to the site from which the cells were obtained, as increased collagen type III is detected at the rupture side of tendons [107], or the donor, as some people may produce increased quantities of collagen type III [108] and ageing is associated with increased synthesis of collagen type III in tendon [109, 110]. Another plausible explanation is that the day 14 is still an early time point in tendon healing and the cells are still primed to produce high amounts of collagen type III. Indeed, in physiological tendon healing, collagen type III is the major constituent, which is replaced later by collagen type I [111, 112]. Neither the skin- nor the tendon- derived collagen scaffolds induced synthesis of chondrogenic (collagen type II, aggrecan) and osteogenic (osteocalcin, osteopontin) markers, despite the documented influence of substrate rigidity in hTC trans-differentiation [113]. This is not surprising, considering that the mechanical properties of the produced scaffolds were within the reported values of native tendon tissues (ranging from 10 KPa to 2,000 MPa, subject to species, tendon, location, age, disease state [114-118]). Although the following markers have been previously used and validated in the lab, and are widely used in the literature, non-specific staining or autofluorescence is a possibility. For future studies that will use the same markers in the lab, should carry out controlled staining for validation of marker expression. A positive control is crucial to determine whether the staining has been successful. This method involves staining a tissue or a cell where the marker of interest is expressed in abundance. Immunofluorescent staining should be observed with the positive control, otherwise this indicates that the staining did not work. Another method that can be carried out to validate the success of the immunofluorescent staining is to incubate the sample without the primary antibody. This method will reveal if the staining was due to a non-specific binding of the secondary antibody. This can happen due to the formation of aggregates by the secondary antibody if the storage conditions were not correct. Therefore, appropriate storage conditions of immunofluorescent markers are critical to avoid false positive staining. To dismiss the background autofluorescence, incubation of the sample can be carried out without the secondary antibody. A tissue sample or a cell type that is high in fluorescence such as lungs, brain or colon cells can be used for this method. Using a negative control, which involves staining a tissue or a cell that does not express the marker of interest to determine the specificity of the chosen antibody.

These control methods can be used in the future studies to further validate the chosen markers

Gene expression analysis (the function of each molecule assessed is provided in **Supplementary Table S2**) revealed 4 differences (PLOD1, ELN and ACTA2 upregulation on tendon-derived collagen scaffolds and SPP1 upregulation on skin-derived collagen scaffolds) at day 3; 9 differences (PLOD1 and FABP4 upregulation on tendon-derived collagen scaffolds; P4HA2, COL3 and MKX upregulation on skin-derived collagen scaffolds; COL1 downregulation on skin-derived collagen scaffolds; DCN and SPP1 upregulation on skin-derived collagen scaffolds and downregulation on tendon-derived collagen scaffolds; and ELN downregulation on tendon-derived collagen scaffolds) at day 7; and 2 differences (P4HA1 upregulation on skin-derived collagen scaffolds and ACTA2 downregulation on tendon-derived collagen scaffolds) at day 14 in gene expression as a function of the tissue from which the collagen was extracted (skin and tendon). If we consider the day 14 as the most critical timepoint (longest time point assessed), it appears that only P4HA1 and ACTA2 separate the skin- from the tendon- derived collagen scaffolds (both scaffolds upregulated P4HA2, PLOD1, PLOD2, SXCA, TNC, BGN, ELN and SERPINH1 and downregulated VCAN). This upregulation of P4HA1 on skin-derived collagen scaffolds and this downregulation of ACTA2 on tendon-derived collagen scaffolds may indicate that the tendon-derived collagen scaffolds did not drive the cells towards fibrotic lineage. To substantiate this one should consider that although prolyl 4 hydroxylase plays an important role in collagen biosynthesis [119], it also constitutes a main target for antifibrotic compounds [120, 121]. Suppression of smooth muscle α actin expression, which is associated with myofibroblast differentiation [122, 123], also supports the notion the tendon-derived collagen scaffolds inhibited fibrotic trans-differentiation.

Table 3.3: List of assessed via immunocytochemistry and gene expression molecules and their function.

Molecule	Function
Collagen I	Collagen I is a major component of tendon ECM [124, 125]. Collagen I is produced by tenocytes and plays a role in stebalising the tendon, by providing structural and mechanical support [126, 127].
Collagen II	Important component of articular cartilage ECM and is synthesised by chondrocytes. Collagen II is used as a marker of chondrogenic phenotype [124, 128-130].
Collagen III	Collagen III is found in skin at a high concentration, while in the tendon the concentration is much lower [131, 132]. Collagen III has been shown to play a role in early tendon healing, as well as provide tissues with support and elasticity [133, 134]. Collagen III regulates the size of collagen I fibrils in tendon ECM depending on the ratio of collagen type III to type I [124, 133]. Elevated collagen III content is associated with the wound healing process and inflammation of tendon [107, 134, 135].
Collagen IV	Literature indicates the importance of collagen IV in cell adhesion, migration, growth and differentiation [136, 137]. Collagen IV has been shown to have a role in wound healing [82]. It is not found in tendon tissue, however it has been shown to be present in the basement membrane at the surface of tendon, which prevents adhesion formation [138].
Collagen V	Fibrillar collagen that is present in minor amounts in tissues that express collagen I, and is essential for collagen I and III fibrillation [139-143]. Collagen V is part of fibrillar-forming collagen that co-assembles with collagen I into heterotypic fibrils, where the triple-helical domain is buried within the fibrils [143, 144]. Collagen V also plays a role in forming a bridge between interstitial collagen IV and VI in the skin, while creating an interwoven network with collagen VI [141,

	145]. Collagen V found in the dermis, while creating connections with other collagen fibrils and elastin [145].
Collagen VI	Non-fibrillar collagen and it has been shown to colocalise with collagen I on cell surface in tendon and influencing fibril assembly, while interacting with receptors on the cell membrane and ECM components [146, 147]. Collagen VI plays a role in early fibrillogenesis and studies indicate its role in cellular behaviour and migration [146]. Collagen VI is an important component of pericellular matrix in cartilage and plays a role in cell function and mechanotransduction [147].
Fibronectin	Glycoprotein that is widely found in the ECM and expressed by a large variety of cells [148, 149]. Fibronectin plays a major role in cell migration, adhesion, differentiation and growth, and is essential for cellular interactions with the ECM [148, 150, 151]. It is also important for ECM organisation and the maintenance of collagen type I and III [152, 153]. The binding of fibronectin to collagens is essential for the appropriate collagen deposition and organisation to form fibrillar matrix, as fibronectin fibrils act as a template for collagen I and III [154, 155]. Fibronectin matrix and its ability to interact with collagen is dependent on the contractility of cells, which governs cell migration [155]. Fibronectin also impacts the deposition of non-collagenous ECM, that can bind to collagens [152, 156, 157]. Deposition of collagen I and III has been shown to be dependent on fibronectin fibrillar matrix [158].
Scleraxis	Specific marker for tendon lineage and is part of early tendon development [124, 159, 160]. Expression of collagen I and tenomodulin is regulated by scleraxis in tenocytes [160].
Tenomodulin	Expressed in mature tendons and ligaments [124, 161]. Its expression is exclusive to tension-specific tissues, indicating a role in mechano-regulation [104].

Aggrecan	Important component of articular cartilage ECM and is synthesised by chondrocytes. Aggrecan is used as a marker of chondrogenic phenotype [124, 128, 162].
Osteocalcin	Present in the bone matrix and is secreted by osteoblasts and osteocytes, and plays a role in bone mineralisation and endocrine system. BGLAP is also known as osteocalcin [163-166].
Osteopontin	Present in the bone matrix and is secreted by osteoblasts and plays a role in their differentiation, adhesion and attachment [163, 167-171]. Osteopontin occurs in the early development stages of bone formation and is involved in remodelling of bone [169, 171, 172]. SPP1 is also known as osteopontin and is involved in bone remodelling and formation [167].
Decorin	Part of small leucine-rich proteoglycans (SLRPs) family and are expressed by tendon tissue and play a role in fibrillogenesis by binding to collagen fibrils [173, 174]. Decorin is present during tendon development and maintains homeostasis of collagen, peaking in expression during lateral growth of collagen fibrils and maintaining expressing through maturation and aging [174-177]. Decorin has been shown to bind collagen I with greater affinity compared to biglycan, however both share a binding site for collagen [177, 178]. Decorin has been shown to regulate assembly of matrix by limiting formation of collagen fibrils and thus playing a role in remodelling of tendon [179, 180].
Biglycan	Part of small leucine-rich proteoglycans (SLRPs) family that is expressed by tendon tissue, and plays a role in fibrillogenesis by binding to collagen fibrils [173]. Studies show that fibrillar diameter and architecture varies in the absence of biglycan [173, 181]. Biglycan has been shown to induce differentiation of tendon-derived stem cells and maintain tissue homeostasis [182]. The expression of

	biglycan peaks during post-natal development, following with a rapid decline [175].
Tenascin C	Glycoprotein that is expressed in tendon and found abundantly in the ECM [183-186]. Tenascin C is mostly expressed during embryogenesis and tissue regeneration, as well as aiding ECM organisation and cell migration [185, 187, 188].
Thrombospondin 4	Glycoprotein that is expressed in tendon and found abundantly in the ECM [183, 184]. THBS4 is necessary for ECM deposition and appropriate collagen fibril organisation [184, 189].
Mohawk homeobox	Transcription factor that is involved in tendon development during embryogenesis, tenogenic differentiation, and plays an important role in maturation of tendon [190-193]. MKX has also been shown to play a role in expression of SCXA, DCN, TNM and TNC [190]. Collagen I production and regulation of fibril growth is regulated by MKX. Studies demonstrated that MKX is efficient at promoting tenogenesis [190, 194, 195].
Prolyl 4-hydroxylase subunit alpha-1	Isoform of prolyl 4-hydroxylases (P4Hs) that are essential for the appropriate collagen biosynthesis. It is responsible for newly synthesised procollagen polypeptides to be folded into a stable triple helical structure [196, 197].
Prolyl 4-hydroxylase subunit alpha-2	Isoform of prolyl 4-hydroxylases that are essential for the appropriate collagen biosynthesis. It is responsible for newly synthesised procollagen polypeptides to be folded into a stable triple helical structure [196, 197].
Procollagen-lysine,2-oxoglutarate 5-dioxygenase	Responsible for lysyl hydroxylation of procollagen, which is critical for collagen biosynthesis. Mechanical stability of collagen fibrils is dependent on intermolecular crosslinks that are initiated by PLODs. Following peptide formation, PLODs catalyse lysine hydroxylation and thus inducing formation of

	crosslinks [194, 197, 198]. PLOD1 carries out hydroxylation in the helical domain [199].
Procollagen-lysine,2-oxoglutarate 5-dioxygenase 2	Responsible for lysyl hydroxylation of procollagen, which is critical for collagen biosynthesis. Mechanical stability of collagen fibrils is dependent on intermolecular crosslinks that are initiated by PLODs. Following peptide formation, PLODs catalyse lysine hydroxylation and thus inducing formation of crosslinks [194, 197, 198]. PLOD2 carries out hydroxylation in the telopeptide region of procollagen [199].
Serpin family E member 1	Known as heat-shock protein, is a chaperone that assists collagen folding in the endoplasmic reticulum (ER). It is essential for the stabilisation of folded collagen triple helix and protects it from unfolding due to temperature and proteases. SERPIN1 binds to collagen type I to IV and is expressed by collagen-synthesising cells [200, 201].
Actin alpha 2	Gene that encodes α-smooth muscle actin that are expressed by vascular smooth muscle cells that is used as a hallmark for tendinopathy lesions. ACTA2 expression has also been linked to remodelling of collagen matrix [202].
Fatty acid binding protein 4	Intracellular lipid chaperone and is expressed by adipose cells. It is involved in uptake of fatty acids, metabolism and transport [203, 204].
Versican	Chondroitin sulfate proteoglycan that binds to hyaluronan and is expressed in a variety of tissues such as dermis. It plays a role in cell adhesion, migration and proliferation, as well as managing migration of embryonic cells during development. Studies have shown its role in wound healing and patellar tendinosis, as well as remodelling of ECM [173, 205-207].
Elastin	Found in skin, tendon, lungs and cartilage, and provides the tissues with the required elasticity and support. Elastin is found in ECM space in the form of fibres. It provides skin and tendon with mechanical resilience and the ability to withstand

	deformations, as well as regulating intercations between ECM and cells [208-213].
Runt-related transcription factor 2	Transcription factor that plays a role in differentiation of osteoblasts and is crucial for skeletal development. RUNX2 induces osteoblasts and promotes differentiation during early stages, while the expression in reduced at later stages of bone formation [214, 215]. Studies have also shown the role of RUNX2 in chondrocyte maturation [216].

3.5 Conclusions

Although collagen has a long-standing history in biomedicine, clinical data show mixed results with respect to efficacy and efficiency of collagen-based devices. Thus, herein we probed whether the tissue from which the collagen is extracted could be responsible for the observed deviations in clinical setting. Collagen, extracted from bovine skin and tendon tissues, sponges with different cross-linking densities of 4-arm polyethylene glycol succinimidyl glutarate were fabricated and their structural, chemical, physical and biological properties were assessed. Although broadly speaking similar tendencies between the two different collagen preparations were observed as a function of cross-linking with respect to structural, biochemical and resistance to enzymatic degradation, profound differences in mechanical properties and cell response were observed as a function of tissue origin (i.e. tendon-derived collagen scaffolds more effectively supported human tenocyte growth than skin-derived collagen scaffolds). Our data suggest that the tissue from which collagen is extracted should be considered in the development of medical devices.

3.6 References

[1] A. Sorushanova, L.M. Delgado, Z. Wu, N. Shologu, A. Kshirsagar, R. Raghunath, A.M. Mullen, Y. Bayon, A. Pandit, M. Raghunath, D.I. Zeugolis, The collagen suprafamily: From biosynthesis to advanced biomaterial development, Adv Mater 31(1) (2019) 1801651.

[2] K.M. Pawelec, S.M. Best, R.E. Cameron, Collagen: A network for regenerative medicine, J Mater Chem B 4(40) (2016) 6484-6496.

[3] A.J. Minor, K.L.K. Coulombe, Engineering a collagen matrix for cell-instructive regenerative angiogenesis, J Biomed Mater Res B Appl Biomater 108(6) (2020) 2407-2416.

[4] D.I. Zeugolis, R.G. Paul, G. Attenburrow, Factors influencing the properties of reconstituted collagen fibers prior to self-assembly: Animal species and collagen extraction method, J Biomed Mater Res A 86(4) (2008) 892-904.

[5] E. Strawich, M.E. Nimni, Properties of a collagen molecule containing three identical components extracted from bovine articular cartilage, Biochemistry 10(21) (1971) 3905-3911.

[6] F. Beghé, C. Menicagli, P. Neggiani, A. Zampieri, L. Trallori, E. Teta, S. Rosini, Lyophilized non-denatured type-I collagen (Condress) extracted from bovine Achilles' tendon and suitable for clinical use, Int J Tissue React 14 Suppl (1992) 11-19.

[7] S.R. Chowdhury, M.F. Mh Busra, Y. Lokanathan, M.H. Ng, J.X. Law, U.C. Cletus, R. Binti Haji Idrus, Collagen type I: A versatile biomaterial, Adv Exp Med Biol 1077 (2018) 389-414.

[8] S.A. Ghodbane, M.G. Dunn, Physical and mechanical properties of cross-linked type I collagen scaffolds derived from bovine, porcine, and ovine tendons, J Biomed Mater Res A 104(11) (2016) 2685-2692.

[9] M.H. Cumming, B. Hall, K. Hofman, Isolation and characterisation of major and minor collagens from hyaline cartilage of Hoki (Macruronus novaezelandiae), Mar Drugs 17(4) (2019) 223.

[10] R.O. Sousa, A.L. Alves, D.N. Carvalho, E. Martins, C. Oliveira, T.H. Silva, R.L. Reis, Acid and enzymatic extraction of collagen from Atlantic cod (Gadus Morhua) swim bladders envisaging health-related applications, J Biomater Sci Polym Ed 31(1) (2020) 20-37.

[11] M. Akita, Y. Nishikawa, Y. Shigenobu, D. Ambe, T. Morita, K. Morioka, K. Adachi, Correlation of proline, hydroxyproline and serine content, denaturation temperature and circular dichroism analysis of type I collagen with the physiological temperature of marine teleosts, Food Chem 329 (2020) 126775.

[12] M. Dai, X. Liu, N. Wang, J. Sun, Squid type II collagen as a novel biomaterial: Isolation, characterization, immunogenicity and relieving effect on degenerative osteoarthritis via inhibiting STAT1 signaling in pro-inflammatory macrophages, Mater Sci Eng C Mater Biol Appl 89 (2018) 283-294.

[13] W.K. Song, D. Liu, L.L. Sun, B.F. Li, H. Hou, Physicochemical and biocompatibility properties of type I collagen from the skin of nile tilapia (oreochromis niloticus) for biomedical applications, Mar Drugs 17(3) (2019) 137.

[14] A.K. Lynn, I.V. Yannas, W. Bonfield, Antigenicity and immunogenicity of collagen, J Biomed Mater Res B Appl Biomater 71(2) (2004) 343-354.

[15] D.D. Stefania, G. De Rinaldis, M. Paulmery, S. Piraino, A. Leone, Barrel jellyfish (Rhizostoma pulmo) as source of antioxidant peptides, Mar Drugs 17 (2019) md17020134.

[16] X. Zhang, S. Xu, L. Shen, G. Li, Factors affecting thermal stability of collagen from the aspects of extraction, processing and modification, J Leather Sci Eng 2(1) (2020) 19.

[17] L.M. Delgado, Y. Bayon, A. Pandit, D.I. Zeugolis, To cross-link or not to cross-link? Cross-linking associated foreign body response of collagen-based devices, Tissue Eng Part B Rev 21(3) (2015) 298-313.

[18] L. Gu, T. Shan, Y.X. Ma, F.R. Tay, L. Niu, Novel biomedical applications of crosslinked collagen, Trends Biotechnol 37(5) (2019) 464-491.

[19] C.H. Gagnieu, P.O. Forest, In vivo biodegradability and biocompatibility of porcine type I atelocollagen newly crosslinked by oxidized glycogen, Biomed Mater Eng 17(1) (2007) 9-18.

[20] K.R. Meade, F.H. Silver, Immunogenicity of collagenous implants, Biomaterials 11(3) (1990) 176-180.

[21] A. Oryan, A. Kamali, A. Moshiri, H. Baharvand, H. Daemi, Chemical crosslinking of biopolymeric scaffolds: Current knowledge and future directions of crosslinked engineered bone scaffolds, Int J Biol Macromol 107 (2018) 678-688.

[22] D.I. Zeugolis, G.R. Paul, G. Attenburrow, Cross-linking of extruded collagen fibers -- A biomimetic three-dimensional scaffold for tissue engineering applications, J Biomed Mater Res A 89(4) (2009) 895-908.

[23] A. Satyam, G.S. Subramanian, M. Raghunath, A. Pandit, D.I. Zeugolis, In vitro evaluation of Ficoll-enriched and genipin-stabilised collagen scaffolds, J Tissue Eng Regen Med 8(3) (2014) 233-241.

[24] L.M. Delgado, K. Fuller, D.I. Zeugolis, Collagen cross-linking: Biophysical, biochemical, and biological response analysis, Tissue Eng Part A 23(19-20) (2017) 1064-1077.

[25] M. Sanami, I. Sweeney, Z. Shtein, S. Meirovich, A. Sorushanova, A.M. Mullen, M. Miraftab, O. Shoseyov, C. O'Dowd, A. Pandit, D.I. Zeugolis, The influence of poly(ethylene glycol) ether tetrasuccinimidyl glutarate on the structural, physical, and biological properties of collagen fibers, J Biomed Mater Res B Appl Biomater 104(5) (2016) 914-922.

[26] F. Catena, L. Ansaloni, F. Gazzotti, S. Gagliardi, S. Di Saverio, L. D'Alessandro, A.D. Pinna, Use of porcine dermal collagen graft (Permacol) for hernia repair in contaminated fields, Hernia 11(1) (2007) 57-60.

[27] M.M. Abdelfatah, N. Rostambeigi, E. Podgaetz, M.G. Sarr, Long-term outcomes (>5-year follow-up) with porcine acellular dermal matrix (Permacol™) in incisional hernias at risk for infection, Hernia 19(1) (2015) 135-140.

[28] A. Adeel, B. Tyler, R. Brian, Repair of complete atrioventricular septal defects with decellularized extracellular matrix: Initial and midterm outcomes, World J Pediatr Congenit Heart Surg 8(3) (2017) 310-314.

[29] T.M. Kelley, M. Kashem, H. Wang, J. McCarthy, N.D. Carroll, G.W. Moser, T.S. Guy, Anterior leaflet augmentation with CorMatrix porcine extracellular matrix in twenty-five patients: Unexpected patch failures and histologic analysis, Ann Thorac Surg 103(1) (2017) 114-120.

[30] N.S. Hillberg, P.I. Ferdinandus, R.E.G. Dikmans, B. Winkens, J. Hommes, R.R.W.J. van der Hulst, Is single-stage implant-based breast reconstruction (SSBR) with an acellular matrix safe?: Strattice™ or Meso Biomatrix® in SSBR, Eur J Plast Surg 41(4) (2018) 429-438.

[31] C.A. Salzberg, C. Dunavant, N. Nocera, Immediate breast reconstruction using porcine acellular dermal matrix (Strattice®): Long-term outcomes and complications, J Plast Reconstr Aesthet Surg 66(3) (2013) 323-328.

[32] A. Flynn, D. Kilmartin, S. Phelan, M. McMenamin, J. Kelly, M.E. Laing, Delayed immunological reaction to Integra™ skin graft, Clin Exp Dermatol 44(6) (2019) 714-716.

[33] G. Vithlani, P. Santos Jorge, E. Brizman, K. Mitsimponas, Integra(®) as a single-stage dermal regeneration template in reconstruction of large defects of the scalp, Br J Oral Maxillofac Surg 55(8) (2017) 844-846.

[34] L. Rúa Gonzálvez, L. de Villalaín Álvarez, A. Novoa Gómez, J.C. de Vicente Rodríguez, I. Peña González, Use of Integra in oral reconstruction: A case series, Oral Surg Oral Med Oral Pathol Oral Radiol 125(3) (2018) e72-e75.

[35] B. De Angelis, F. Orlandi, M. Fernandes Lopes Morais D'Autilio, M.G. Scioli, A. Orlandi, V. Cervelli, P. Gentile, Long-term follow-up comparison of two different bi-layer dermal substitutes in tissue regeneration: Clinical outcomes and histological findings, Int Wound J 15(5) (2018) 695-706.

[36] P. Lohana, S. Hassan, S.B. Watson, Integra™ in burns reconstruction: Our experience and report of an unusual immunological reaction, Ann Burns Fire Disasters 27(1) (2014) 17-21.

[37] K. Kara, P. Kahlert, A.A. Mahabadi, B. Plicht, A.Y. Lind, D. Longwitz, M. Bollow, R. Erbel, Comparison of collagen-based vascular closure devices in patients with vs. without severe peripheral artery disease, J Endovasc Ther 21(1) (2014) 79-84.

[38] K.H. Park, J.B. Kwon, J.H. Park, J.C. Shin, S.H. Han, J.W. Lee, Collagen dressing in the treatment of diabetic foot ulcer: A prospective, randomized, placebo-controlled, single-center study, Diabetes Res Clin Pract 156 (2019) 107861.

[39] I.P. Sharma, R. Bakshi, M. Chaudhry, Corneal collagen cross-linking with and without simultaneous intrastromal corneal ring segment implantation: One-year pilot study, Eur J Ophthalmol 31(1) (2021) 61-68.

[40] G.E. Djavid, S.M. Tabaie, S.B. Tajali, M. Totounchi, A. Farhoud, M. Fateh, M. Ghafghazi, M. Koosha, S. Taghizadeh, Application of a collagen matrix dressing on a neuropathic diabetic foot ulcer: A randomised control trial, J Wound Care 29(Sup3) (2020) S13-S18.

[41] T.A. Järvinen, T.L. Järvinen, P. Kannus, L. Józsa, M. Järvinen, Collagen fibres of the spontaneously ruptured human tendons display decreased thickness and crimp angle, J Orthop Res 22(6) (2004) 1303-1309.
[42] Z. Wu, S.H. Korntner, A.M. Mullen, I. Skoufos, A. Tzora, D.I. Zeugolis, In the quest of the optimal tissue source (porcine male and female articular, tracheal and auricular cartilage) for the development of collagen sponges for articular cartilage, Biomedical Engineering Advances 1 (2021) 100002.
[43] L.M. Delgado, N. Shologu, K. Fuller, D.I. Zeugolis, Acetic acid and pepsin result in high yield, high purity and low macrophage response collagen for biomedical applications, Biomed Mater 12(6) (2017) 065009.
[44] E.C. Collin, S. Grad, D.I. Zeugolis, C.S. Vinatier, J.R. Clouet, J.J. Guicheux, P. Weiss, M. Alini, A.S. Pandit, An injectable vehicle for nucleus pulposus cell-based therapy, Biomaterials 32(11) (2011) 2862-2870.
[45] J. Wang, F. Zhang, W.P. Tsang, C. Wan, C. Wu, Fabrication of injectable high strength hydrogel based on 4-arm star PEG for cartilage tissue engineering, Biomaterials 120 (2017) 11-21.
[46] C.N.M.R. Ryan, D.I. Zeugolis, Engineering the tenogenic niche in vitro with microenvironmental tools, Adv Ther 3(2) (2020) 1900072.
[47] D. Gaspar, K. Spanoudes, C. Holladay, A. Pandit, D.I. Zeugolis, Progress in cell-based therapies for tendon repair, Adv Drug Deliv Rev 84 (2015) 240-256.
[48] A.J. Lomas, C.N. Ryan, A. Sorushanova, N. Shologu, A.I. Sideri, V. Tsioli, G.C. Fthenakis, A. Tzora, I. Skoufos, L.R. Quinlan, G. O'Laighin, A.M. Mullen, J.L. Kelly, S. Kearns, M. Biggs, A. Pandit, D.I. Zeugolis, The past, present and future in scaffold-based tendon treatments, Adv Drug Deliv Rev 84 (2015) 257-277.
[49] K. Spanoudes, D. Gaspar, A. Pandit, D.I. Zeugolis, The biophysical, biochemical, and biological toolbox for tenogenic phenotype maintenance in vitro, Trends Biotechnol 32(9) (2014) 474-482.
[50] H. Capella-Monsonís, J.Q. Coentro, V. Graceffa, Z. Wu, D.I. Zeugolis, An experimental toolbox for characterization of mammalian collagen type I in biological specimens, Nat Protoc 13(3) (2018) 507-529.
[51] A. Sorushanova, I. Skoufos, A. Tzora, A.M. Mullen, D.I. Zeugolis, The influence of animal species, gender and tissue on the structural, biophysical, biochemical and biological properties of collagen sponges, J Mater Sci Mater Med 32(1) (2021) 12.

[52] A.L. Helling, E.K. Tsekoura, M. Biggs, Y. Bayon, A. Pandit, D.I. Zeugolis, In vitro enzymatic degradation of tissue grafts and collagen biomaterials by matrix metalloproteinases: Improving the collagenase assay, ACS Biomat Sc Eng 3(9) (2017) 1922-1932.

[53] D.I. Zeugolis, M. Raghunath, The physiological relevance of wet versus dry differential scanning calorimetry for biomaterial evaluation: A technical note, Polym Int 59(10) (2010) 1403-1407.

[54] D.R. Eyre, I.R. Dickson, K. Van Ness, Collagen cross-linking in human bone and articular cartilage. Age-related changes in the content of mature hydroxypyridinium residues, Biochem J 252(2) (1988) 495-500.

[55] M. Stammers, I.M. Ivanova, I.S. Niewczas, A. Segonds-Pichon, M. Streeter, D.A. Spiegel, J. Clark, Age-related changes in the physical properties, cross-linking, and glycation of collagen from mouse tail tendon, J Biol Chem 295(31) (2020) 10562-10571.

[56] T. Moriguchi, D. Fujimoto, Age-related changes in the content of the collagen crosslink, pyridinoline, J Biochem 84(4) (1978) 933-935.

[57] S.P. Robins, M.S. Shimokomaki, A.J. Bailey, The chemistry of the collagen cross-links. Age-related changes in the reducible components of intact bovine collagen fibres, Biochem J 131(4) (1973) 771-780.

[58] A.J. Bailey, M.S. Shimokomaki, Age related changes in the reducible cross-links of collagen, FEBS Lett 16(2) (1971) 86-88.

[59] H. Schoof, J. Apel, I. Heschel, G. Rau, Control of pore structure and size in freeze-dried collagen sponges, J Biomed Mater Res 58(4) (2001) 352-357.

[60] Y.G. Ko, S. Grice, N. Kawazoe, T. Tateishi, G. Chen, Preparation of collagen-glycosaminoglycan sponges with open surface porous structures using ice particulate template method, Macromol Biosci 10(8) (2010) 860-871.

[61] M. Kuberka, D. von Heimburg, H. Schoof, I. Heschel, G. Rau, Magnification of the pore size in biodegradable collagen sponges, Int J Artif Organs 25(1) (2002) 67-73.

[62] L.M. Delgado, K. Fuller, D.I. Zeugolis, Influence of cross-linking method and disinfection/sterilization treatment on the structural, biophysical, biochemical, and biological properties of collagen-based devices, ACS Biomater Sci Eng 4(8) (2018) 2739-2747.

[63] W. Friess, G. Lee, Basic thermoanalytical studies of insoluble collagen matrices, Biomaterials 17(23) (1996) 2289-2294.

[64] B. Chevallay, N. Abdul_Malak, D. Herbage, Mouse fibroblasts in long-term culture within collagen three-dimensional scaffolds: influence of crosslinking with diphenylphosphorylazide on matrix reorganization, growth, and biosynthetic and proteolytic activities., J Biomed Mater Res 49(4) (2000) 448-459.

[65] A. Sionkowska, Thermal denaturation of UV-irradiated wet rat tail tendon collagen, Int J Biol Macromol 35(3-4) (2005) 145-149.

[66] J.M. Orban, L.B. Wilson, J.A. Kofroth, M.S. El-Kurdi, T.M. Maul, D.A. Vorp, Crosslinking of collagen gels by transglutaminase, J Biomed Mater Res 68A (2004) 756-762.

[67] I. Rault, V. Frei, D. Herbage, N. Abdul-Malak, A. Huc, Evaluation of different chemical methods for cross-linking collagen gel, films and sponges, J Mater Sci Mater Med 7 (1996) 215-221.

[68] M.F. Cote, C.J. Doillon, Wettability of cross-linked collagenous biomaterials: *In vitro* study, Biomaterials 13(9) (1992) 612-616.

[69] J.S. Pieper, A. Oosterhof, P.J. Dijkstra, J.H. Veerkamp, T.H. van Kuppevelt, Preparation and characterization of porous crosslinked collagenous matrices containing bioavailable chondroitin sulphate, Biomaterials 20 (1999) 847-858.

[70] M.C. Wang, G.D. Pins, F.H. Silver, Collagen fibres with improved strength for the repair of soft tissue injuries, Biomaterials 15(7) (1994) 507-512.

[71] Y.P. Kato, F.H. Silver, Formation of continuous collagen fibres: Evaluation of biocompatibilily and mechanical properties, Biomaterials 11(3) (1990) 169-175.

[72] G.A. Hutcheon, C. Messiou, R.M. Wyre, M.C. Davies, S. Downes, Water absorption and surface properties of novel poly(ethylmethacrylate) polymer systems for use in bone and cartilage repair, Biomaterials 22(7) (2001) 667-676.

[73] V. Charulatha, A. Rajaram, Influence of different crosslinking treatments on the physical properties of collagen membranes, Biomaterials 24(5) (2003) 759-767.

[74] C.R. Lee, A.J. Grodzinsky, M. Spector, The effects of cross-linking of collagen-glycosaminoglycan scaffolds on compressive stiffness, chondrocyte-mediated contraction, proliferation and biosynthesis, Biomaterials 22(23) (2001) 3145-3154.

[75] R.N. Chen, H.O. Ho, M.T. Sheu, Characterization of collagen matrices crosslinked using microbial transglutaminase, Biomaterials 26(20) (2005) 4229-4235.

[76] C. Wang, T.T. Lau, W.L. Loh, K. Su, D.A. Wang, Cytocompatibility study of a natural biomaterial crosslinker--Genipin with therapeutic model cells, J Biomed Mater Res B Appl Biomater 97(1) (2011) 58-65.
[77] G. Fessel, J. Cadby, S. Wunderli, R. van Weeren, J.G. Snedeker, Dose- and time-dependent effects of genipin crosslinking on cell viability and tissue mechanics – Toward clinical application for tendon repair, Acta Biomater 10(5) (2014) 1897-1906.
[78] J.Y. Lai, Y.T. Li, Influence of cross-linker concentration on the functionality of carbodiimide cross-linked gelatin membranes for retinal sheet carriers, J Biomater Sci Polym Ed 22(1-3) (2011) 277-295.
[79] J.Q. Coentro, A. di Nubila, U. May, S. Prince, J. Zwaagstra, T.A.H. Järvinen, D.I. Zeugolis, Dual drug delivery collagen vehicles for modulation of skin fibrosisin vitro, Biomed Mater 17(2) (2022) 025017.
[80] M. Sanami, Z. Shtein, I. Sweeney, A. Sorushanova, A. Rivkin, M. Miraftab, O. Shoseyov, C. O'Dowd, A.M. Mullen, A. Pandit, D.I. Zeugolis, Biophysical and biological characterisation of collagen/resilin-like protein composite fibres, Biomed Mater 10(6) (2015) 065005.
[81] Z. Wu, S.H. Korntner, A.M. Mullen, D.I. Zeugolis, In the quest of the optimal chondrichthyan for the development of collagen sponges for articular cartilage, Journal of Science: Advanced Materials and Devices 6(3) (2021) 390-398.
[82] A.M. Abreu-Velez, M.S. Howard, Collagen IV in normal skin and in pathological processes, N Am J Med Sci 4(1) (2012) 1-8.
[83] S.H. Taylor, S. Al-Youha, T. Van Agtmael, Y. Lu, J. Wong, D.A. McGrouther, K.E. Kadler, Tendon is covered by a basement membrane epithelium that is required for cell retention and the prevention of adhesion formation, PLoS One 6(1) (2011) e16337.
[84] B.K. Connizzo, B.R. Freedman, J.H. Fried, M. Sun, D.E. Birk, L.J. Soslowsky, Regulatory role of collagen V in establishing mechanical properties of tendons and ligaments is tissue dependent, J Orthop Res 33(6) (2015) 882-888.
[85] F. Segev, E. Héon, W.G. Cole, R.J. Wenstrup, F. Young, A.R. Slomovic, D.S. Rootman, D. Whitaker-Menezes, I. Chervoneva, D.E. Birk, Structural abnormalities of the cornea and lid resulting from collagen V mutations, Invest Ophthalmol Vis Sci 47(2) (2006) 565-573.

[86] R.J. Wenstrup, S.M. Smith, J.B. Florer, G. Zhang, D.P. Beason, R.E. Seegmiller, L.J. Soslowsky, D.E. Birk, Regulation of collagen fibril nucleation and initial fibril assembly involves coordinate interactions with collagens V and XI in developing tendon, J Biol Chem 286(23) (2011) 20455-20465.

[87] R.J. Wenstrup, J.B. Florer, E.W. Brunskill, S.M. Bell, I. Chervoneva, D.E. Birk, Type V collagen controls the initiation of collagen fibril assembly, J Biol Chem 279(51) 53331-53337.

[88] P. Sabatelli, S.K. Gara, P. Grumati, A. Urciuolo, F. Gualandi, R. Curci, S. Squarzoni, A. Zamparelli, E. Martoni, L. Merlini, M. Paulsson, P. Bonaldo, R. Wagener, Expression of the collagen VI α5 and α6 chains in normal human skin and in skin of patients with collagen VI-related myopathies, J Invest Dermatol 131(1) (2011) 99-107.

[89] G. Theocharidis, Z. Drymoussi, A.P. Kao, A.H. Barber, D.A. Lee, K.M. Braun, J.T. Connelly, Type VI collagen regulates dermal matrix assembly and fibroblast motility, J Invest Dermatol 136(1) (2016) 74-83.

[90] Y. Izu, H.L. Ansorge, G. Zhang, L.J. Soslowsky, P. Bonaldo, M.L. Chu, D.E. Birk, Dysfunctional tendon collagen fibrillogenesis in collagen VI null mice, Matrix Biol 30(1) (2011) 53-61.

[91] R.A. Clark, Fibronectin in the skin, J Invest Dermatol 81(6) (1983) 475-479.

[92] F. Grinnell, Fibronectin and wound healing, J Cell Biochem 26(2) (1984) 107-116.

[93] J. Patten, K. Wang, Fibronectin in development and wound healing, Adv Drug Deliv Rev 170(353-368) (2021).

[94] M. Lehto, L. Jozsa, M. Kvist, M. Järvinen, B.J. Balint, A. Reffy, Fibronectin in the ruptured human Achilles tendon and its paratenon. An immunoperoxidase study, Ann Chir Gynaecol 79(2) (1990) 72-77.

[95] L. Jozsa, M. Lehto, P. Kannus, M. Kvist, A. Reffy, T. Vieno, M. Järvinen, S. Demel, E. Elek, Fibronectin and laminin in Achilles tendon, Acta Orthop Scand 60(4) (1989) 469-471.

[96] B.E. Brigman, P. Hu, H. Yin, M. Tsuzaki, W.T. Lawrence, A.J. Banes, Fibronectin in the tendon-synovial complex: quantitation in vivo and in vitro by ELISA and relative mRNA levels by polymerase chain reaction and northern blot, J Orthop Res 12(2) (1994) 253-261.

[97] I.F. Williams, K.G. McCullagh, I.A. Silver, The distribution of types I and III collagen and fibronectin in the healing equine tendon, Connect Tissue Res 12(3-4) (1984) 211-227.

[98] C. Shukunami, A. Takimoto, Y. Nishizaki, Y. Yoshimoto, S. Tanaka, S. Miura, H. Watanabe, T. Sakuma, T. Yamamoto, G. Kondoh, Y. Hiraki, Scleraxis is a transcriptional activator that regulates the expression of tenomodulin, a marker of mature tenocytes and ligamentocytes, Sci Rep 8(1) (2018) 3155.

[99] A.E.C. Nichols, R.E. Settlage, S.R. Werre, L.A. Dahlgren, Novel roles for scleraxis in regulating adult tenocyte function, BMC Cell Biol 19(1) (2018) 14.

[100] Y.Z. Paterson, N. Evans, S. Kan, A. Cribbs, F.M.D. Henson, D.J. Guest, The transcription factor scleraxis differentially regulates gene expression in tenocytes isolated at different developmental stages, Mech Dev 163 (2020) 103635.

[101] E.P. Bavin, F. Atkinson, T. Barsby, D.J. Guest, Scleraxis is essential for tendon differentiation by equine embryonic stem cells and in equine fetal tenocytes, Stem Cells Dev 26(6) (2017) 441-450.

[102] D. Docheva, E.B. Hunziker, R. Fässler, O. Brandau, Tenomodulin is necessary for tenocyte proliferation and tendon maturation, Mol Cell Biol 25(2) (2005) 699-705.

[103] D. Lin, P. Alberton, M.D. Caceres, E. Volkmer, M. Schieker, D. Docheva, Tenomodulin is essential for prevention of adipocyte accumulation and fibrovascular scar formation during early tendon healing, Cell Death Dis 8(10) (2017) e3116.

[104] S. Dex, P. Alberton, L. Willkomm, T. Söllradl, S. Bago, S. Milz, M. Shakibaei, A. Ignatius, W. Bloch, H. Clausen-Schaumann, C. Shukunami, M. Schieker, D. Docheva, Tenomodulin is required for tendon endurance running and collagen I fibril adaptation to mechanical load, EBioMedicine 20 (2017) 240-254.

[105] P. Alberton, S. Dex, C. Popov, C. Shukunami, M. Schieker, D. Docheva, Loss of tenomodulin results in reduced self-renewal and augmented senescence of tendon stem/progenitor cells, Stem Cells Dev 24(5) (2015) 597-609.

[106] N. Tanaka, S. Tajima, A. Ishibashi, T. Izumi, S. Nishina, N. Azuma, Y. Sado, Y. Ninomiya, Expression of the alpha1-alpha6 collagen IV chains in the dermoepidermal junction during human foetal skin development: temporal and spatial expression of the alpha4 collagen IV chain in an early stage of development, Br J Dermatol 139(3) (1998) 371-374.

[107] H.A. Eriksen, A. Pajala, J. Leppilahti, J. Risteli, Increased content of type III collagen at the rupture site of human Achilles tendon, J Orthop Res 20(6) (2002) 1352-1357.

[108] R.P. Nirschl, Elbow tendinosis/tennis elbow, Clin Sports Med 11 (1992) 851-870.

[109] E. Ippolito, P.G. Natali, F. Postacchini, L. Accinni, C. De Martino, Morphological, immunochemical, and biochemical study of rabbit Achilles tendon at various ages, J Bone Joint Surg Am 62(4) (1980) 583-598.

[110] Y. Sugiyama, K. Naito, K. Goto, Y. Kojima, A. Furuhata, M. Igarashi, I. Nagaoka, K. Kaneko, Effect of aging on the tendon structure and tendon-associated gene expression in mouse foot flexor tendon, Biomed Rep 10(4) (2019) 238-244.

[111] L. Józsa, B.J. Bálint, A. Réffy, Z. Demel, Fine structural alterations of collagen fibers in degenerative tendinopathy, Arch Orthop Trauma Surg (1978) 103(1) (1984) 47-51.

[112] J. Kumagai, H.K. Uhthoff, K. Sarkar, J.P. Murnaghan, Collagen type III in rotator cuff tears: An immunohistochemical study, J Shoulder Elbow Surg 1(4) (1992) 187-192.

[113] A. English, A. Azeem, K. Spanoudes, E. Jones, B. Tripathi, N. Basu, K. McNamara, S.A.M. Tofail, N. Rooney, G. Riley, A. O'Riordan, G. Cross, D. Hutmacher, M. Biggs, A. Pandit, D.I. Zeugolis, Substrate topography: A valuable in vitro tool, but a clinical red herring for in vivo tenogenesis, Acta Biomater 27 (2015) 3-12.

[114] L.N. Williams, S.H. Elder, J.L. Bouvard, M.F. Horstemeyer, The anisotropic compressive mechanical properties of the rabbit patellar tendon, Biorheology 45(5) (2008) 577-586.

[115] R.F. Ker, Mechanics of tendon, from an engineering perspective, Int J Fatigue 29(6) (2007) 1001-1009.

[116] M.E. Zobitz, Z.P. Luo, K.N. An, Determination of the compressive material properties of the supraspinatus tendon, J Biomech Eng 123(1) (2001) 47-51.

[117] I. Bah, S.T. Kwak, R.L. Chimenti, M.S. Richards, J. P Ketz, A. Samuel Flemister, M.R. Buckley, Mechanical changes in the Achilles tendon due to insertional Achilles tendinopathy, J Mech Behav Biomed Mater 53 (2016) 320-328.

[118] R.H. Shin, C. Zhao, M.E. Zobitz, P.C. Amadio, K.N. An, Mechanical properties of intrasynovial and extrasynovial tendon fascicles, Clin Biomech (Bristol, Avon) 23(2) (2008) 236-241.

[119] T. Pihlajaniemi, R. Myllylä, K.I. Kivirikko, Prolyl 4-hydroxylase and its role in collagen synthesis, J Hepatol 13(Suppl 3) (1991) S2-S7.

[120] M. Bickel, K.H. Baringhaus, M. Gerl, V. Günzler, J. Kanta, L. Schmidts, M. Stapf, G. Tschank, K. Weidmann, U. Werner, Selective inhibition of hepatic collagen accumulation in experimental liver fibrosis in rats by a new prolyl 4-hydroxylase inhibitor, Hepatology 28(2) (1998) 404-411.

[121] J.P. Gumucio, M.D. Flood, A. Bedi, H.F. Kramer, A.J. Russell, C.L. Mendias, Inhibition of prolyl 4-hydroxylase decreases muscle fibrosis following chronic rotator cuff tear, Bone Joint Res 6(1) (2017) 57-65.

[122] S.G. Roy, Y. Nozaki, S.H. Phan, Regulation of alpha-smooth muscle actin gene expression in myofibroblast differentiation from rat lung fibroblasts, Int J Biochem Cell Biol 33(7) (2001) 723-734.

[123] A.M. Sousa, T. Liu, O. Guevara, J. Stevens, B.L. Fanburg, M. Gaestel, D. Toksoz, U.S. Kayyali, Smooth muscle alpha-actin expression and myofibroblast differentiation by TGFbeta are dependent upon MK2, J Cell Biochem 100(6) (2007) 1581-1592.

[124] M. Benjamin, J.R. Ralphs, Fibrocartilage in tendons and ligaments-an adaptation to compressive load, J Anat 193 (Pt 4) (1998) 481-494.

[125] A.R. McCluskey, K.S.W. Hung, B. Marzec, J.O. Sindt, N. Sommerdijk, P.J. Camp, F. Nudelman, Disordered filaments mediate the fibrillogenesis of type I collagen in solution, Biomacromolecules 21(9) (2020) 3631-3643.

[126] Z. Ge, H. Tang, W. Chen, Y. Wang, C. Yuan, X. Tao, B. Zhou, K. Tang, Downregulation of type I collagen expression in the Achilles tendon by dexamethasone: A controlled laboratory study, J Orthop Surg Res 15(1) (2020) 70.

[127] M. Tang, T. Li, N.S. Gandhi, K. Burrage, Y. Gu, Heterogeneous nanomechanical properties of type I collagen in longitudinal direction, Biomech Model Mechanobiol 16(3) (2017) 1023-1033.

[128] A. Frazer, R.A. Bunning, M. Thavarajah, J.M. Seid, R.G. Russell, Studies on type II collagen and aggrecan production in human articular chondrocytes in vitro and

effects of transforming growth factor-beta and interleukin-1beta, Osteoarthr Cartilage 2(4) (1994) 235-245.

[129] Z. Wu, S.H. Korntner, A.M. Mullen, I. Skoufos, A. Tzora, D.I. Zeugolis, In the quest of the optimal tissue source (porcine male and female articular, tracheal and auricular cartilage) for the development of collagen sponges for articular cartilage, Biomed Eng Adv 1 (2021) 100002.

[130] G.T.H. Nham, X. Zhang, Y. Asou, T. Shinomura, Expression of type II collagen and aggrecan genes is regulated through distinct epigenetic modifications of their multiple enhancer elements, Gene 704 (2019) 134-141.

[131] P.B. Voleti, M.R. Buckley, L.J. Soslowsky, Tendon healing: Repair and regeneration, Annu Rev Biomed Eng 14 (2012) 47-71.

[132] M.R. Buckley, E.B. Evans, P.E. Matuszewski, Y.L. Chen, L.N. Satchel, D.M. Elliott, L.J. Soslowsky, G.R. Dodge, Distributions of types I, II and III collagen by region in the human supraspinatus tendon, Connect Tissue Res 54(6) (2013) 374-379.

[133] N. Juncosa-Melvin, K.S. Matlin, R.W. Holdcraft, V.S. Nirmalanandhan, D.L. Butler, Mechanical stimulation increases collagen type I and collagen type III gene expression of stem cell-collagen sponge constructs for patellar tendon repair, Tissue Eng 13(6) (2007) 1219-1226.

[134] M. Makuszewska, T. Bonda, M. Cieślińska, I. Bialuk, M.M. Winnicka, K. Niemczyk, Expression of collagen type III in healing tympanic membrane, Int J Pediatr Otorhinolaryngol 136 (2020) 110196.

[135] C.H. Chen, S.H. Chen, C.Y. Kuo, M.L. Li, J.P. Chen, Response of dermal fibroblasts to biochemical and physical cues in aligned polycaprolactone/silk fibroin nanofiber scaffolds for application in tendon tissue engineering, Nanomaterials (Basel) 7(8) (2017).

[136] M. Aumailley, R. Timpl, Attachment of cells to basement membrane collagen type IV, J Cell Biol 103(4) (1986) 1569-1575.

[137] S.P. Boudko, N. Danylevych, B.G. Hudson, V.K. Pedchenko, Basement membrane collagen IV: Isolation of functional domains, Methods Cell Biol 143 (2018) 171-185.

[138] S. H Taylor, S. Al Youha, T. Van Agtmael, Y. lu, J. Wong, D. A McGrouther, K. Kadler, Tendon is covered by a basement membrane epithelium that is required for cell retention and the prevention of adhesion formation, PloS one 6 (2011) e16337.

[139] D.J. Leeming, M. Karsdal, Type V collagen, 2016, pp. 43-48.
[140] D. Schuppan, J. Becker, H. Boehm, E.G. Hahn, Immunofluorescent localization of type-V collagen as a fibrillar component of the interstitial connective tissue of human oral mucosa, artery and liver, Cell Tissue Res 243(3) (1986) 535-543.
[141] K.M. Mak, C.Y. Png, D.J. Lee, Type V collagen in health, disease, and fibrosis, Anat Rec 299(5) (2016) 613-629.
[142] P. Martin, W.R. Teodoro, A.P. Velosa, J. de Morais, S. Carrasco, R.B. Christmann, C. Goldenstein-Schainberg, E.R. Parra, M.L. Katayama, M.N. Sotto, V.L. Capelozzi, N.H. Yoshinari, Abnormal collagen V deposition in dermis correlates with skin thickening and disease activity in systemic sclerosis, Autoimmun Rev 11(11) (2012) 827-835.
[143] S.M. Smith, G. Zhang, D.E. Birk, Collagen V localizes to pericellular sites during tendon collagen fibrillogenesis, Matrix Biol 33 (2014) 47-53.
[144] D.E. Birk, Type V collagen: Heterotypic type I/V collagen interactions in the regulation of fibril assembly, Micron 32(3) (2001) 223-237.
[145] T. Kobayasi, T. Karlsmark, Type V and VI collagen for cohesion of dermal fibrillar structures, J Submicrosc Cytol Pathol 38(2-3) (2006) 103-108.
[146] F. Sardone, S. Santi, F. Tagliavini, F. Traina, L. Merlini, S. Squarzoni, M. Cescon, R. Wagener, N.M. Maraldi, P. Bonaldo, C. Faldini, P. Sabatelli, Collagen VI–NG2 axis in human tendon fibroblasts under conditions mimicking injury response, Matrix Biol 55 (2016) 90-105.
[147] R.J. Leiphart, H. Pham, T. Harvey, T. Komori, T.M. Kilts, S.S. Shetye, S.N. Weiss, S.M. Adams, D.E. Birk, L.J. Soslowsky, M.F. Young, Coordinate roles for collagen VI and biglycan in regulating tendon collagen fibril structure and function, Matrix Biol Plus 13 (2022) 100099.
[148] S.S. Roh, M.H. Lee, Y.L. Hwang, H.H. Song, M.H. Jin, S.G. Park, C.K. Lee, C.D. Kim, T.J. Yoon, J.H. Lee, Stimulation of the extracellular matrix production in dermal fibroblasts by velvet antler extract, Ann Dermatol 22(2) (2010) 173-179.
[149] E.L. George, E.N. Georges-Labouesse, R.S. Patel-King, H. Rayburn, R.O. Hynes, Defects in mesoderm, neural tube and vascular development in mouse embryos lacking fibronectin, Development 119(4) (1993) 1079-1091.
[150] R. Pankov, K.M. Yamada, Fibronectin at a glance, J Cell Sci 115(Pt 20) (2002) 3861-3863.

[151] J. Sottile, F. Shi, I. Rublyevska, H.Y. Chiang, J. Lust, J. Chandler, Fibronectin-dependent collagen I deposition modulates the cell response to fibronectin, Am J Physiol Cell Physiol 293(6) (2007) C1934-1946.

[152] J. Sottile, D.C. Hocking, Fibronectin polymerization regulates the composition and stability of extracellular matrix fibrils and cell-matrix adhesions, Mol Biol Cell 13(10) (2002) 3546-3559.

[153] T. Velling, J. Risteli, K. Wennerberg, D.F. Mosher, S. Johansson, Polymerization of type I and III collagens is dependent on fibronectin and enhanced by integrins alpha 11beta 1 and alpha 2beta 1, J Biol Chem 277(40) (2002) 37377-37381.

[154] J.A. McDonald, D.G. Kelley, T.J. Broekelmann, Role of fibronectin in collagen deposition: Fab' to the gelatin-binding domain of fibronectin inhibits both fibronectin and collagen organization in fibroblast extracellular matrix, J Cell Biol 92(2) (1982) 485-492.

[155] J. Sottile, F. Shi, I. Rublyevska, H.Y. Chiang, J. Lust, J. Chandler, Fibronectin-dependent collagen I deposition modulates the cell response to fibronectin, Am J Physiol Cell Physiol 293 (2008) C1934-1946.

[156] C.Y. Chung, L. Zardi, H.P. Erickson, Binding of tenascin-C to soluble fibronectin and matrix fibrils, J Biol Chem 270(48) (1995) 29012-29017.

[157] M. Pereira, B.J. Rybarczyk, T.M. Odrljin, D.C. Hocking, J. Sottile, P.J. Simpson-Haidaris, The incorporation of fibrinogen into extracellular matrix is dependent on active assembly of a fibronectin matrix, J Cell Sci 115(Pt 3) (2002) 609-617.

[158] J.D. Humphrey, E.R. Dufresne, M.A. Schwartz, Mechanotransduction and extracellular matrix homeostasis, Nat Rev Mol Cell Biol 15(12) (2014) 802-812.

[159] N.D. Murchison, B.A. Price, D.A. Conner, D.R. Keene, E.N. Olson, C.J. Tabin, R. Schweitzer, Regulation of tendon differentiation by scleraxis distinguishes force-transmitting tendons from muscle-anchoring tendons, Development 134(14) (2007) 2697-2708.

[160] Y. Yoshimoto, A. Takimoto, H. Watanabe, Y. Hiraki, G. Kondoh, C. Shukunami, Scleraxis is required for maturation of tissue domains for proper integration of the musculoskeletal system, Sci Rep 7 (2017) 45010.

[161] H. Yin, M.D. Caceres, Z. Yan, M. Schieker, M. Nerlich, D. Docheva, Tenomodulin regulates matrix remodeling of mouse tendon stem/progenitor cells in an ex vivo collagen I gel model, Biochem Biophys Res Commun 512(4) (2019) 691-697.

[162] M.T. Bayliss, S. Howat, C. Davidson, J. Dudhia, The organization of aggrecan in human articular cartilage. Evidence for age-related changes in the rate of aggregation of newly synthesized molecules, J Biol Chem 275(9) (2000) 6321-6327.

[163] O. Nikel, A.A. Poundarik, S. Bailey, D. Vashishth, Structural role of osteocalcin and osteopontin in energy dissipation in bone, J Biomech 80 (2018) 45-52.

[164] S.C. Moser, B.C.J. van der Eerden, Osteocalcin-a versatile bone-derived hormone, Front Endocrinol 9 (2019) 794-794.

[165] O. Berezovska, G. Yildirim, W.C. Budell, S. Yagerman, B. Pidhaynyy, C. Bastien, M.C.H. van der Meulen, T.L. Dowd, Osteocalcin affects bone mineral and mechanical properties in female mice, Bone 128 (2019) 115031.

[166] M. Tavakol, T.J. Vaughan, The structural role of osteocalcin in bone biomechanics and its alteration in Type-2 Diabetes, Sci Rep 10(1) (2020) 17321.

[167] J.H. Chen, Y.C. Chen, C.L. Mao, J.M. Chiou, C.K. Tsao, K.S. Tsai, Association between secreted phosphoprotein-1 (SPP1) polymorphisms and low bone mineral density in women, PloS one 9(5) (2014) e97428-e97428.

[168] B. Depalle, C.M. McGilvery, S. Nobakhti, N. Aldegaither, S.J. Shefelbine, A.E. Porter, Osteopontin regulates type I collagen fibril formation in bone tissue, Acta Biomater 120 (2021) 194-202.

[169] C. Lin, Z. Chen, D. Guo, L. Zhou, S. Lin, C. Li, S. Li, X. Wang, B. Lin, Y. Ding, Increased expression of osteopontin in subchondral bone promotes bone turnover and remodeling, and accelerates the progression of OA in a mouse model, Aging (Albany NY) 14(1) (2022) 253-271.

[170] J. Qian, L. Xu, X. Sun, Y. Wang, W. Xuan, Q. Zhang, P. Zhao, Q. Wu, R. Liu, N. Che, F. Wang, W. Tan, M. Zhang, Adiponectin aggravates bone erosion by promoting osteopontin production in synovial tissue of rheumatoid arthritis, Arthritis Res Ther 20(1) (2018) 26.

[171] K. Terai, T. Takano-Yamamoto, Y. Ohba, K. Hiura, M. Sugimoto, M. Sato, H. Kawahata, N. Inaguma, Y. Kitamura, S. Nomura, Role of osteopontin in bone remodeling caused by mechanical stress, J Bone Miner Res 14(6) (1999) 839-849.

[172] I. Jankovska, M. Pilmane, I. Urtane, Osteopontin and osteocalcin in maxilla tissue of skeletal Class III patients, Stomatologija 11(4) (2009) 125-128.
[173] J.H. Yoon, J. Halper, Tendon proteoglycans: Biochemistry and function, J Musculoskelet Neuronal Interact 5(1) (2005) 22-34.
[174] M.Y. Pechanec, T.N. Boyd, K. Baar, M.J. Mienaltowski, Adding exogenous biglycan or decorin improves tendon formation for equine peritenon and tendon proper cells in vitro, BMC Musculoskelet Disord 21(1) (2020) 627.
[175] G. Zhang, B.B. Young, Y. Ezura, M. Favata, L.J. Soslowsky, S. Chakravarti, D.E. Birk, Development of tendon structure and function: Regulation of collagen fibrillogenesis, J Musculoskelet Neuronal Interact 5(1) (2005) 5-21.
[176] A.A. Dunkman, M.R. Buckley, M.J. Mienaltowski, S.M. Adams, S.J. Thomas, L. Satchell, A. Kumar, L. Pathmanathan, D.P. Beason, R.V. Iozzo, D.E. Birk, L.J. Soslowsky, Decorin expression is important for age-related changes in tendon structure and mechanical properties, Matrix Biol 32(1) (2013) 3-13.
[177] K.A. Robinson, M. Sun, C.E. Barnum, S.N. Weiss, J. Huegel, S.S. Shetye, L. Lin, D. Saez, S.M. Adams, R.V. Iozzo, L.J. Soslowsky, D.E. Birk, Decorin and biglycan are necessary for maintaining collagen fibril structure, fiber realignment, and mechanical properties of mature tendons, Matrix Biol 64 (2017) 81-93.
[178] G. Zhang, Y. Ezura, I. Chervoneva, P. Robinson, D. Beason, E. Carine, L.J. Soslowsky, R.V. Iozzo, D.E. Birk, Decorin regulates assembly of collagen fibrils and acquisition of biomechanical properties during tendon development, J Cell Biochem 98 (2006) 1436-1449.
[179] R.J. McCormick, Extracellular modifications to muscle collagen: Implications for meat quality, Poult Sci 78(5) (1999) 785-791.
[180] K.G. Danielson, H. Baribault, D.F. Holmes, H. Graham, K.E. Kadler, R.V. Iozzo, Targeted disruption of decorin leads to abnormal collagen fibril morphology and skin fragility, J Cell Biol 136(3) (1997) 729-743.
[181] A. Corsi, T. Xu, X.D. Chen, A. Boyde, J. Liang, M. Mankani, B. Sommer, R.V. Iozzo, I. Eichstetter, P.G. Robey, P. Bianco, M.F. Young, Phenotypic effects of biglycan deficiency are linked to collagen fibril abnormalities, are synergized by decorin deficiency, and mimic Ehlers-Danlos-like changes in bone and other connective tissues, J Bone Miner Res 17(7) (2002) 1180-1189.

[182] Y.J. Zhang, Q. Qing, Y.J. Zhang, L.J. Ning, J. Cui, X. Yao, J.C. Luo, W. Ding, T.W. Qin, Enhancement of tenogenic differentiation of rat tendon-derived stem cells by biglycan, J Cell Physiol (2019).

[183] G.P. Riley, R.L. Harrall, T.E. Cawston, B.L. Hazleman, E.J. Mackie, Tenascin-C and human tendon degeneration, Am J Pathol 149(3) (1996) 933-943.

[184] E.G. Frolova, J. Drazba, I. Krukovets, V. Kostenko, L. Blech, C. Harry, A. Vasanji, C. Drumm, P. Sul, G.J. Jenniskens, E.F. Plow, O. Stenina-Adognravi, Control of organization and function of muscle and tendon by thrombospondin-4, Matrix Biol 37 (2014) 35-48.

[185] K. Xu, Y. Shao, Y. Xia, Y. Qian, N. Jiang, X. Liu, L. Yang, C. Wang, Tenascin-C regulates migration of SOX10 tendon stem cells via integrin-α9 for promoting patellar tendon remodeling, Biofactors 47(5) (2021) 768-777.

[186] C.H. Jo, H.J. Lim, K.S. Yoon, Characterization of tendon-specific markers in various human tissues, tenocytes and mesenchymal stem cells, Tissue Eng Regen Med 16(2) (2019) 151-159.

[187] T. Järvinen, L. Józsa, P. Kannus, T. Järvinen, T. Hurme, M. Kvist, M. Pelto-Huikko, H. Kalimo, M. Järvinen, Mechanical loading regulates the expression of tenascin-C in the myotendinous junction and tendon but does not induce de novo synthesis in the skeletal muscle, J Cell Sci 116 (2003) 857-866.

[188] R. Kluger, K.R. Huber, P.G. Seely, C.E. Berger, F. Frommlet, Novel tenascin-C haplotype modifies the risk for a failure to heal after rotator cuff repair, Am J Sports Med 45(13) (2017) 2955-2964.

[189] E.G. Frolova, J. Drazba, I. Krukovets, V. Kostenko, L. Blech, C. Harry, A. Vasanji, C. Drumm, P. Sul, G.J. Jenniskens, E.F. Plow, O. Stenina-Adognravi, Control of organization and function of muscle and tendon by thrombospondin-4, Matrix biology : journal of the International Society for Matrix Biology 37 (2014) 35-48.

[190] H. Liu, C. Zhang, S. Zhu, P. Lu, T. Zhu, X. Gong, Z. Zhang, J. Hu, Z. Yin, B.C. Heng, X. Chen, H.W. Ouyang, Mohawk promotes the tenogenesis of mesenchymal stem cells through activation of the TGFbeta signaling pathway, Stem Cells 33(2) (2015) 443-455.

[191] Y. Ito, N. Toriuchi, T. Yoshitaka, H. Ueno-Kudoh, T. Sato, S. Yokoyama, K. Nishida, T. Akimoto, M. Takahashi, S. Miyaki, H. Asahara, The Mohawk homeobox

gene is a critical regulator of tendon differentiation, Proc Natl Acad Sci 107(23) (2010) 10538.

[192] N. Onizuka, Y. Ito, M. Inagawa, H. Nakahara, S. Takada, M. Lotz, Y. Toyama, H. Asahara, The Mohawk homeobox transcription factor regulates the differentiation of tendons and volar plates, J Orthop Sci 19(1) (2014) 172-180.

[193] H. Liu, C. Zhang, S. Zhu, P. Lu, T. Zhu, X. Gong, Z. Zhang, J. Hu, Z. Yin, B.C. Heng, X. Chen, H.W. Ouyang, Mohawk promotes the tenogenesis of mesenchymal stem cells through activation of the TGFβ signaling pathway, Stem Cells 33(2) (2015) 443-455.

[194] R.A.F. Gjaltema, S. de Rond, M.G. Rots, R.A. Bank, Procollagen lysyl hydroxylase 2 expression is regulated by an alternative downstream transforming growth factor β-1 activation mechanism, J Biol Chem 290(47) (2015) 28465-28476.

[195] Y. Ito, N. Toriuchi, T. Yoshitaka, H. Ueno-Kudoh, T. Sato, S. Yokoyama, K. Nishida, T. Akimoto, M. Takahashi, S. Miyaki, H. Asahara, The Mohawk homeobox gene is a critical regulator of tendon differentiation, Proc Natl Acad Sci U S A 107 (2010) 10538-10542.

[196] D.M. Gilkes, P. Chaturvedi, S. Bajpai, C.C. Wong, H. Wei, S. Pitcairn, M.E. Hubbi, D. Wirtz, G.L. Semenza, Collagen prolyl hydroxylases are essential for breast cancer metastasis, Cancer Res 73(11) (2013) 3285-3296.

[197] D.M. Gilkes, S. Bajpai, P. Chaturvedi, D. Wirtz, G.L. Semenza, Hypoxia-inducible factor 1 (HIF-1) promotes extracellular matrix remodeling under hypoxic conditions by inducing P4HA1, P4HA2, and PLOD2 expression in fibroblasts, J Biol Chem 288(15) (2013) 10819-10829.

[198] Y. Qi, R. Xu, Roles of PLODs in collagen synthesis and cancer progression, Front Cell Dev Biol 6 (2018) 66.

[199] D.M. Gilkes, S. Bajpai, C.C. Wong, P. Chaturvedi, M.E. Hubbi, D. Wirtz, G.L. Semenza, Procollagen lysyl hydroxylase 2 is essential for hypoxia-induced breast cancer metastasis, Mol Cancer Res 11(5) (2013) 456-466.

[200] C. Widmer, J.M. Gebauer, E. Brunstein, S. Rosenbaum, F. Zaucke, C. Drögemüller, T. Leeb, U. Baumann, Molecular basis for the action of the collagen-specific chaperone Hsp47/SERPINH1 and its structure-specific client recognition, Proc Natl Acad Sci USA 109(33) (2012) 13243-13247.

[201] T. Natsume, T. Koide, S. Yokota, K. Hirayoshi, K. Nagata, Interactions between collagen-binding stress protein HSP47 and collagen. Analysis of kinetic parameters by surface plasmon resonance biosensor, J Biol Chem 269(49) (1994) 31224-31228.
[202] G. Fong, L.J. Backman, D.A. Hart, P. Danielson, B. McCormack, A. Scott, Substance P enhances collagen remodeling and MMP-3 expression by human tenocytes, J Orthop Res 31(1) (2013) 91-98.
[203] Y.S. Lee, J.Y. Kim, K.S. Oh, S.W. Chung, Fatty acid-binding protein 4 regulates fatty infiltration after rotator cuff tear by hypoxia-inducible factor 1 in mice, Journal of cachexia, sarcopenia and muscle 8(5) (2017) 839-850.
[204] M. Furuhashi, S. Saitoh, K. Shimamoto, T. Miura, Fatty acid-binding protein 4 (FABP4): pathophysiological insights and potent clinical biomarker of metabolic and cardiovascular diseases, Clin Med Insights Cardiol 8(Suppl 3) (2015) 23-33.
[205] F. Sotoodehnejadnematalahi, B. Burke, Structure, function and regulation of versican: The most abundant type of proteoglycan in the extracellular matrix, Acta Med Iran 51(11) (2013) 740-750.
[206] A. Scott, O. Lian, C.R. Roberts, J.L. Cook, C.J. Handley, R. Bahr, T. Samiric, M.Z. Ilic, J. Parkinson, D.A. Hart, V. Duronio, K.M. Khan, Increased versican content is associated with tendinosis pathology in the patellar tendon of athletes with jumper's knee, Scand J Med Sci Sports 18(4) (2008) 427-435.
[207] S. Islam, K. Chuensirikulchai, S. Khummuang, T. Keratibumrungpong, P. Kongtawelert, W. Kasinrerk, S. Hatano, A. Nagamachi, H. Honda, H. Watanabe, Accumulation of versican facilitates wound healing: Implication of its initial ADAMTS-cleavage site, Matrix Biol 87 (2020) 77-93.
[208] T.M. Grant, M.S. Thompson, J. Urban, J. Yu, Elastic fibres are broadly distributed in tendon and highly localized around tenocytes, J Anat 222(6) (2013) 573-579.
[209] A.C. Weihermann, M. Lorencini, C.A. Brohem, C.M. de Carvalho, Elastin structure and its involvement in skin photoageing, Int J Cosmet Sci 39(3) (2017) 241-247.
[210] A.J. Bailey, Collagen and elastin fibres, J Clin Pathol Suppl (R Coll Pathol) 12 (1978) 49-58.

[211] A. Svärd, M. Hammerman, P. Eliasson, Elastin levels are higher in healing tendons than in intact tendons and influence tissue compliance, Faseb j 34(10) (2020) 13409-13418.
[212] X. Pang, J.P. Wu, G.T. Allison, J. Xu, J. Rubenson, M.H. Zheng, D.G. Lloyd, B. Gardiner, A. Wang, T.B. Kirk, Three dimensional microstructural network of elastin, collagen, and cells in Achilles tendons, J Orthop Res 35(6) (2017) 1203-1214.
[213] J.D. Eekhoff, F. Fang, L.G. Kahan, G. Espinosa, A.J. Cocciolone, J.E. Wagenseil, R.P. Mecham, S.P. Lake, Functionally distinct tendons from elastin haploinsufficient mice exhibit mild stiffening and tendon-specific structural alteration, J Biomech Eng 139(11) (2017) 1110031-1110039.
[214] T. Komori, Runx2, a multifunctional transcription factor in skeletal development, J Cell Biochem 87(1) (2002) 1-8.
[215] T. Komori, Regulation of osteoblast differentiation by Runx2, Adv Exp Med Biol 658 (2010) 43-49.
[216] T. Komori, Roles of Runx2 in skeletal development, Adv Exp Med Biol 962 (2017) 83-93.

Chapter 4 - Collagen type I fibres for tendon repair

Sections of this chapter have been published:

The influence of poly(ethylene glycol) ether tetrasuccinimidyl glutarate on the structural, physical, and biological properties of collagen fibers. M. Sanami, I. Sweeney, Z. Shtein, S. Meirovich, **A. Sorushanova**, A.M. Mullen, M. Miraftab, O. Shoseyov, C. O'Dowd, A. Pandit, D.I. Zeugolis. 2016, 104(5):914-922.

4.1 Introduction

The use of self-assembled collagen fibres in tissue engineering and regenerative medicine has been advocated, as they most closely recapitulate the composition and architecture of the intertwined network of the native extracellular matrix. Further, self-assembled collagen fibres have been shown to induce directional cell growth *in vitro* and to promote directional neotissue formation *in vivo* [1-3].

However, through self-assembly, molecules with chemical complementarity form supramolecular structures, which are hold together by weak reversible and non-covalent bonds. For this reason, exogenous cross-links are often required to produce stable constructs. Specifically to collagen stability, numerous chemical, physical and biological cross-linking methods have been assessed over the years [4-6]. Unfortunately, both biological and physical methods are not suitable for load-bearing tissues, due to the weak-induced stability and the chemical stabilisation methodologies, on the other hand, are often associated with foreign body response [7]. Hence, there is an urgent need to develop suitable stabilisation methods for collagen that will not only bring about sufficient mechanical resilience, but will also be cytocompatible.

Multi-functional poly(ethylene glycol systems) have been used extensively in regenerative medicine either as medical devices on their own right or to add functionality to medical devices [8-11]. Although their potential as stabilisation agents for tissue grafts [12] and collagen hydrogels [13] has been shown, it is still unclear whether such agents can induce proportional stability to traditional cross-linking methods, without associated cytotoxicity. Thus, in this study, we hypothesise that 4-star poly(ethylene glycol) ether tetrasuccinimidyl glutarate can produce cytocompatible collagen fibres with adequate mechanical properties, superior to customarily used chemical approaches.

4.2 Materials and methods

4.2.1 Materials and reagents

Pepsin soluble bovine Achilles tendon collagen (3 mg/ml) was provided from Vornia Biomaterials Ltd (Ireland). 4-arm poly(ethylene glycol) ether tetrasuccinimidylglutarate, Mw10,000, was purchased from JenKem Technology (USA). Quant-iT™ PicoGreen® dsDNA reagent and alamarBlue™ were purchased from Invitrogen (Ireland). Adult human dermal fibroblasts (Cat. Number: C- 013-5C) and low serum growth supplement kit (Cat. Number: S-003-K) were purchased from Gibco® (Life Technologies, Ireland) and ATCC (Donor number: PCS-201-012™, UK; Gender: Lot specific; Age: Adult). Human tenocytes were purchased from DV Biologics (USA) (Gender: Female; Age: 29). Calcein AM and ethidium homodimer I were purchased from Thermo Fisher Scientific, UK. All chemicals, unless otherwise stated, were purchased from Sigma-Aldrich (Ireland).

4.2.2 Cross-linking of collagen type I fibres with 0.0475 mM 4SG-PEG

This work has been carried out in Vornia Biomaterials Ltd. Collagen type I fibres were cross-linked with 0.0475 mM 4SG-PEG, 0.625% glutaraldehyde (GTA) and 60 mM ethyl-3-[3-dimethylamino-propyl] carbodiimide (EDC).

4.2.2.1 Fibre fabrication

Collagen fibres were produced and cross-linked as has been described previously [4, 14]. Briefly, a 20mL syringe (BD) containing the collagen solution was loaded on a syringe pump (KD-Scientific Inc., USA), which was set to extrude the collagen solution through a 1.5 mm internal diameter silicone tube (Samco Silicone Products Ltd., UK) at 0.4 ml/min. The fibres were formed upon contact with the fibre formation buffer (118 mM phosphate buffer, containing 20% polyethylene glycol Mw 8K; pH 7.80, 37 °C). After 3 min, the fibres were transferred into the fibre incubation buffer (6.0 mM phosphate buffer, containing 75 mM sodium chloride; pH 7.1, 37 °C). After 3 min, the fibres were either incubated overnight in phosphate buffer saline (PBS; CTRL) or were incubated overnight with the various cross-linking solutions. The following day, all fibres were washed three times, for 5 min each time, in double distilled water and they were then air-dried at room temperature (RT). The following cross-linking solutions were used as follows: 0.625 % glutaraldehyde (GTA) in 0.01

M PBS; 1.731 g 1-ethyl-3-[3-dimethylaminopropyl] carbodiimide (EDC) and 0.415 g N-hydroxysulfosuccinimide in 215 ml 0.05 M 2-(N-morpholino) ethanesulfonic acid buffer; and 0.0475 mM solution of 4-arm poly(ethylene glycol) ether tetrasuccinimidyl glutarate (4SG-PEG) in 0.01M PBS.

4.2.2.2 Structural characterisation

Gross visual analysis was conducted on dry fibres using an Olympus optical stereo microscope (SZX16, Olympus, UK). More detailed structural analysis was carried out on dry fibres using a Hitachi scanning electron microscope (S-400, Hitachi-Hisco Europe GmbH, Germany), after gold coating (Emitech K550 Sputter Coater, Emitech Limited, UK) of the fibres.

4.2.2.3 Thermal stability analysis

The hydrothermal stability of the fibres was assessed as has been described previously [15]. Briefly, a DSC-60 differential scanning calorimeter (Shimadzu Scientific Instruments, Japan) was used. Dry collagen fibres were hydrated overnight at RT in 0.01 M PBS at pH 7.4. The fibres were then removed from the PBS and quickly blotted on a filter paper to remove excess PBS. The fibres were then hermetically sealed in aluminium pans. Heating was carried out at a constant temperature ramp (5 °C/min) in the temperature range of 20 – 120 °C, with an empty aluminium pan as reference probe. The endothermic transition was recorded as a typical peak and denaturation temperature was defined as the temperature of maximum power absorption during denaturation (peak temperature). Five fibres per group were analysed.

4.2.2.4 Mechanical stability analysis

Dry collagen fibres were hydrated overnight at RT in 0.01 M PBS at pH 7.4. The fibres were then removed from the PBS and quickly blotted on a filter paper to remove excess PBS. Swelling was calculated as following: Swelling (%) = $[(W_w - W_d) / (W_d)] \times 100$, where W_w and W_d refer to the average wet diameter and average dry diameter of the fibres respectively. Stress-strain curves were obtained in uniaxial tension (5 mm/min extension rate, gauge length 3 cm), using an Instron 3369 Universal testing machine (UK). Stress at break was defined as the load at failure divided by the original cross-sectional area; strain at break was defined as the increase in length at maximum load

divided by the original length; and modulus was calculated as the gradient of the linear region between the point of origin and 0.02 % strain. Seven fibres per group were analysed.

4.2.2.5 Dermal fibroblast culture and analysis

20 fibers (1cm long each) were aligned parallel to each other along their longitudinal axis. The ends of the fibers were held together using a minute amount of adhesive (Silastic® Silicone Type A, Dow Corning, MI). After applying the adhesive, the scaffolds were left to dry for 24 hours. Subsequently, the fiber bundles were washed three times in Hank's Balanced Salt Solution (HBSS) for 15 minutes, were left overnight in 70 % (v/v) ethanol, were washed three times with HBSS for 15 minutes and were left under UV light for 1 hour. Human adult dermal fibroblasts (hDFs) were expanded and grown, as per manufacturer's protocols. 15,000 human adult dermal fibroblasts (passage 3-4) were seeded per fiber bundle and were maintained at 37 ºC, 5 % CO2 and 95 % relative humidity. Cells were allowed to grow for 1, 4, and 7 days changing the media (low serum growth supplement kit: 2 % v/v foetal bovine serum, 1 mg/mL hydrocortisone, 10 ng/ml human epidermal growth factor, 3 ng/ml basic fibroblast growth factor, and 10 mg/ml heparin; Gibco®, Life Technologies, Ireland) every two days. The well plates were coated with sterile 1 % (w/v) agarose before cell seeding.

Metabolic activity of human dermal fibroblasts was assessed using the alamarBlue® assay (Invitrogen) after 1, 4 and 7 days of culture according to manufacturer's procedure. Briefly, at the end of each culture time point, cells were washed with HBSS and diluted by a factor of 10 with alamarBlue®. After 3 hours of incubation at 37 ºC, 5 % CO2 and 95 % relative humidity, absorbance was measured at 550 and 595 nm using a BioTek™ ELx800™ absorbance microplate reader (BioTek Instruments). Cell metabolic activity was expressed in terms of reduction in the percentage of alamarBlue®. alamarBlue® assay was carried out in three replicates (33 bundles of 20 fibers each) per group per time point. DNA quantification was carried out using Quant-iT™ PicoGreen® dsDNA assay kit after 1, 4 and 7 days in culture according to the manufacturer's protocol. Briefly, DNA was extracted using three freeze-thaw cycles after addition of 200 ml of nucleic acid free water per well. The cell suspension was subsequently transferred to cold eppendorf tubes and was centrifuged for 5 min

at 12,000 rpm. 25 ml were then transferred into 96 well plate containing 75 ml of 1x Tris EDTA buffer. A standard curve was then generated using various DNA concentrations. 100 ml of a 1:200 dilution of Quant-iT™ PicoGreen® reagent was added to each sample and the plate was read using a BioTek™ ELx800™ absorbance microplate reader (BioTek Instruments) with an excitation wavelength of 480 nm and an emission wavelength of 525 nm. PicoGreen® assay was carried out in three replicates (33 bundles of 20 fibres ers each) per group per time point. Cytoskeleton and nuclei were stained with rhodamine phalloidin and ethidium at each time point. The bundles were washed twice with HBSS for 5 minutes, were fixed for 1 hour in 2.5 % (v/v) GTA and washed twice with HBSS for 5 minutes; 1 ml of permeabilizing solution [5 % (v/v) Triton-X 100, 0.9 % (w/v) NaCl, 0.02 % (w/v) MgCl2, 5.5 % (w/v) sucrose] was then added for 15 minutes at 0 ºC. The bundles were then washed twice in HBSS for 10 minutes; 200 ml of both stains was then added to each bundle for 30 minutes at room temperature. The stains were then removed and the bundles were washed further four times with HBSS for 5 minutes. The bundles were then mounted onto microscope slides and imaged using an inverted confocal laser scanning microscope (LSM510, Zeiss, Germany). Nuclei morphometric analysis was quantified using ImageJ software (National Institutes of Health). Only cells that had adhered onto the fibers were processed. The total area, aspect ratio (the ratio of the major axis divided by the minor axis of each nuclei based on a fitted ellipse), circularity ($4*\pi*area/perimeter^2$, a value of 1 represents a circle) and the specific angle of orientation of nuclei to the longitudinal fibre axis were measured. Nuclei were considered aligned, when the angle of nuclei to longitudinal fibre axis was within 10 degrees of being parallel to fibre axis. At least 10 cells per group and per time point were used for cell morphometric analysis.

4.2.3 4SG-PEG optimisation

Collagen type I fibres were cross-linked with 4SG-PEG of different concentrations: 0.5 mM, 1 mM, 2.5 mM and 5 mM, and 0.625% glutaraldehyde (GTA).

4.2.3.1 Fibre fabrication

Bovine collagen type I was used to fabricate the fibres. The collagen was loaded into a 5ml syringe with a fitted precision tip and extruded through a 1.5 mm in internal

diameter silicone tubing into fibre formation buffer using a syringe pump (New era NE-1000). The collagen was extruded at a controlled rate of 0.4 ml/min. Once extrusion was started, with air flow guidance, the collagen was self-assembled into a fibre in the formation buffer (118 mM phosphate buffer, containing 20% polyethylene glycol Mw58 K; pH57.80, 37 ºC). After 5 minutes, the fibre was transferred into incubation buffer for 5 minutes (6.0 mM phosphate buffer, containing 75 mM sodium chloride; pH 7.1, 37 ºC). The fibres were either incubated in a cross-linker for 2 hours for cross-linked fibres, or were washed three times for 5 minutes each time in double distilled water and then air-dried at room temperature (RT) for non cross-linked fibres. Collagen fibre bundles were fabricated by gathering four fibres being 1cm long and suturing them together on both ends with another fibre, hence 4 fibres per bundle.

4.2.3.2 Polarised microscopy

The alignment of the collagen fibres was assessed with Polarised Microscopy. Randomly aligned collagen film was used as a control. At 90º the collagen fibres reached instinction phase where the fibre did not light up. The fibres were turned 45º angle and all of the regions on the fibre lit up, which indicates alignment.

4.2.3.3 Structural characterisation

Surface characteristics of the cross-linked and non cross-linked collagen fibres were analysed using Scanning Electron Microscopy (Hitachi S-4700 SEM). Adhesive carbon tabs were used on top of SEM specimen stubs. The collagen fibres were gold coated prior to SEM imaging at 25 milliamps at current of 25 mA for 5 minutes. The fibres were visualised at 10 µm and 300 µm.

4.2.3.4 Quantification of free amines

Residual primary amine groups of type I collagen fibres were determined using a ninhydrin assay. Briefly, appropriate amount of samples were weighed out and 1 ml of prepared ninhydrin buffer was added to the samples. The samples were incubated at 100 ºC for 30 minutes and then cooled down, after which 50 % of isopropanol was added. The absorbance was measured at 570 nm and the free amine groups quantified by interpolating values from a linear standard curve of known concentrations of glycine.

4.2.3.5 Enzymatic stability analysis

Enzymatic degradation of collagen fibre was assessed using collagenase assay. Samples were weighed out and 1ml of buffer and collagenase solution was added. The samples were incubated for 9 hours, the supernatant was removed and the samples were freeze dried overnight. Following freeze drying, the samples were weighed.

4.2.3.6 Thermal stability analysis

DSC-60 differential scanning calorimeter (Shimadzu Scientific Instruments, Japan) was used. Dry collagen fibres were hydrated over night at RT in 0.01 M PBS at pH 7.4. The fibres were then removed from the PBS and quickly blotted on a filter article to remove excess PBS. The fibres were then hermetically sealed in aluminium pans. Heating was carried out at a constant temperature ramp (10 ºC/min) in the temperature range of 30 ºC to 90 ºC, with an empty aluminium pan as reference probe. The endothermic transition was recorded as a typical peak and denaturation temperature was defined as the temperature of maximum power absorption during denaturation (peak temperature). Five fibres per group were analysed.

4.2.3.7 Mechanical stability analysis

Uniaxial tensile test using an electromechanical testing machine (Z2.5, Zwick, Germany) was carried out to assess mechanical properties. The collagen fibres were left in PBS overnight and were tested in wet state. It was assumed that the fibres were circular for determination of engineering stress-strain curves from the load-extension graphs. The stress at break was defined as the load at failure divided by the original cross-sectional area. The strain at break was defined as the increase in length in maximum load divided by the original length and modulus will be calculated at 2 %. Modulus was calculated as the gradient of the linear region between the point of origin and 0.02 % strain. Collagen fibres were incubated in PBS overnight and blotted using filter paper to remove excess surface water. Swelling ratio was calculated as following: Swelling (%) = [(Ww - Wd)/ (Wd)] x 100, where Ww and Wd refer to the average wet diameter and average dry diameter of the fibres respectively.

4.2.4 Cross-linking of collagen type I fibres with different cross-linkers

Collagen type I fibres were cross-linked with 1 mM 4SG-PEG, 0.625% glutaraldehyde (GTA) and 60 mM ethyl-3-[3-dimethylamino-propyl] carbodiimide (EDC).

4.2.4.1 Fibre fabrication

Bovine collagen type I was used to fabricate the fibres. The collagen was loaded into a 5ml syringe with a fitted precision tip and extruded through a 1.5 mm in internal diameter silicone tubing into fibre formation buffer using a syringe pump (New era NE-1000). The collagen was extruded at a controlled rate of 0.4 ml/min. Once extrusion was started, with air flow guidance, the collagen was self-assembled into a fibre in the formation buffer (118 mM phosphate buffer, containing 20 % polyethylene glycol Mw58 K; pH57.80, 37 ºC). After 5 minutes, the fibre was transferred into incubation buffer for 5 minutes (6.0 mM phosphate buffer, containing 75 mM sodium chloride; pH 7.1, 37 ºC). The fibres were either incubated in a cross-linker for 2 hours for cross-linked fibres, or were washed three times for 5 minutes each time in double distilled water and then air-dried at room temperature (RT) for non-crosslinked fibres. Collagen fibre bundles were fabricated by gathering four fibres being 1cm long and suturing them together on both ends with another fibre, hence 4 fibres per bundle. For biological studies with human adult dermal fibroblasts, the following cross-linking solutions were used as follows for: 0.625 % glutaraldehyde (GTA) in 0.01 M PBS; 1.731 g 1-ethyl-3-[3-dimethylamino-propyl] carbodiimide (EDC) and 0.415 g N-hydroxysulfosuccinimide in 215 ml 0.05M 2-(N-morpho- lino) ethanesulfonic acid buffer; and 0.0475 mM solution of 4-arm poly(- ethylene glycol) ether tetrasuccinimidylglutarate (4SG-PEG) in 0.01 M PBS. For biological studies with human adult tenocytes, the following cross-linking solutions were used as follows for: 0.625 % glutaraldehyde (GTA) in 0.01 M PBS; 1.731 g 1-ethyl-3-[3-dimethylamino-propyl] carbodiimide (EDC) and 0.415 g N- hydroxysulfosuccinimide in 215 ml 0.05M 2-(N-morpho- lino) ethanesulfonic acid buffer; and 1 mM solution of 4-arm poly(- ethylene glycol) ether tetrasuccinimidylglutarate (4SG-PEG).

4.2.4.2 Structural characterisation

Surface characteristics of the cross-linked and non cross-linked collagen fibres were analysed using Scanning Electron Microscopy (Hitachi S-4700 SEM). Adhesive

carbon tabs were used on top of SEM specimen stubs. The collagen fibres were gold coated prior to SEM imaging at 25 milliamps at current of 25 mA for 5 minutes. The fibres were visualised at 10 µm and 300 µm.

4.2.4.3 Quantification of free amines

Residual primary amine groups of type I collagen fibres were determined using a ninhydrin assay. Briefly, appropriate amount of samples were weighed out and 1 ml of prepared ninhydrin buffer was added to the samples. The samples were incubated at 100 ºC for 30 minutes and then cooled down, after which 50 % of isopropanol was added. The absorbance was measured at 570 nm and the free amine groups quantified by interpolating values from a linear standard curve of known concentrations of glycine.

4.2.4.4 Enzymatic stability analysis

Enzymatic degradation of collagen fibres was assessed using collagenase assay. Samples were weighed out and 1ml of buffer and collagenase solution was added. The samples were incubated for 9 hours, the supernatant was removed and the samples were freeze dried overnight. Following freeze drying, the samples were weighed.

4.2.4.5 Thermal stability analysis

DSC-60 differential scanning calorimeter (Shimadzu Scientific Instruments, Japan) was used. Dry collagen fibres were hydrated over night at RT in 0.01M PBS at pH 7.4. The fibres were then removed from the PBS and quickly blotted on a filter article to remove excess PBS. The fibres were then hermetically sealed in aluminium pans. Heating was carried out at a constant temperature ramp (10 ºC/min) in the temperature range of 30 ºC to 90 ºC, with an empty aluminium pan as reference probe. The endothermic transition was recorded as a typical peak and denaturation temperature was defined as the temperature of maximum power absorption during denaturation (peak temperature). Five fibres per group were analysed.

4.2.4.6 Mechanical stability analysis

Uniaxial tensile test using an electromechanical testing machine (Z2.5, Zwick, Germany) was carried out to assess mechanical properties. The collagen fibres were

left in PBS overnight and were tested in wet state. It was assumed that the fibres were circular for determination of engineering stress-strain curves from the load-extension graphs. The stress at break was defined as the load at failure divided by the original cross-sectional area. The strain at break was defined as the increase in length in maximum load divided by the original length and modulus will be calculated at 2 %. Modulus was calculated as the gradient of the linear region between the point of origin and 0.02 % strain. Collagen fibres were incubated in PBS overnight and blotted using filter paper to remove excess surface water. Swelling ratio was calculated as following: Swelling (%) = [(Ww - Wd)/ (Wd)] x 100, where Ww and Wd refer to the average wet diameter and average dry diameter of the fibres respectively.

4.2.4.7 Tenocyte culture and analysis

Human tenocytes (hTCs) were seeded onto non cross-linked and cross-linked collagen fibres at a density of 25,000 cells per bundle. Collagen fibre bundles were sterilised prior to seeding in IMS for 1 hour and washed with Hank's Balanced Salt Solution (HBSS) three times. The bundles were then incubated overnight at 37 ºC in the suitable media and afterwards, bundles were incubated in 100 % FBS for 1 hour. After incubation, the bundles were allowed to air dry but not dry out. 25, 000 cells per bundle were seeded with a minimum media and the cells were left to attach for 1 hour at 37 ºC. Suitable media was added carefully to the bundles and left at 37 ºC until 7, 14 and 21 day time points. Cell viability of tenocytes was assessed using LIVE/DEAD® assay after 7, 14 and 21 days of culture according to manufacturer's procedure. Briefly, cells were washed with Hank's Balanced Salt Solution (HBSS; Sigma) and the staining solution was added. The cells were incubated at 37 ºC for 30minutes. The cells were imaged under confocal microscope. Live cells were distinguished by the enzymatic conversion of the non-fluorescent calcein AM to fluorescent calcein that stained the cells green. Ethidium homodimer-1 can enter cells with damaged membranes and binds to nucleic acids producing a red fluorescence. Ethidium homodimer-1 cannot enter cells with intact membranes. Nucleus and the cytoskeleton of tenocytes was visualised by DAPI and Rhodamine Phalloidin staining at day 21. The media was removed, and the bundles were washed three times with HBSS prior to staining. Cells were permeabilised with 0.2 % Triton for 5 minutes and then washed with HBSS. Rhodamine Phalloidin was added to the bundles for 1 hour, afterwards the stain was

removed and DAPI was added for 5 minutes. HBSS was added to the bundles after the removal of DAPI stain, to prevent the fibres from drying out. The bundles were imaged using a confocal microscope. Nuclei morphometric analysis was quantified using ImageJ software (National Institutes of Health). Only cells that had adhered onto the fibers were processed. The total area, aspect ratio (the ratio of the major axis divided by the minor axis of each nuclei based on a fitted ellipse), circularity ($4*\pi*area/perimeter^2$, a value of 1 represents a circle) and the specific angle of orientation of nuclei to the longitudinal fibre axis were measured. Nuclei were considered aligned, when the angle of nuclei to longitudinal fibre axis was within 10 degrees of being parallel to fibre axis. At least 10 cells per group and per time point were used for cell morphometric analysis.

4.2.5 Statistical analysis

Statistical analysis was performed using SPSS (version 20.0, IBM SPSS Statistics, IBM Corporation, USA). All values are expressed as mean values ± standard deviation (SD). One-way analysis of variance (ANOVA) for multiple comparisons was employed, after confirming the following assumptions: (a) the distribution from which each of the samples was derived was normal; (b) and the variances of the population of the samples were equal to one another. Nonparametric statistics were used when either one or both of the above assumptions were violated and consequently Kruskal-Wallis test for multiple comparisons was carried out. Statistical significance was accepted at $p<0.05$.

4.3 Results

4.3.1 Cross-linking of collagen type I fibres with 0.0475 mM 4SG-PEG

4.3.1.1 Structural analysis

Optical analysis (**Figure 4.1**) revealed that GTA fibres became yellow. Scanning electron micrographs (**Figure 4.1**) revealed crevices and ridges running along the longitudinal axis of all fibres. CTRL fibres exhibited the smoothest surface topography, whilst the GTA exhibited the roughest surface topography; EDC and 4SG-PEG fibres were of intermedium smoothness / roughness.

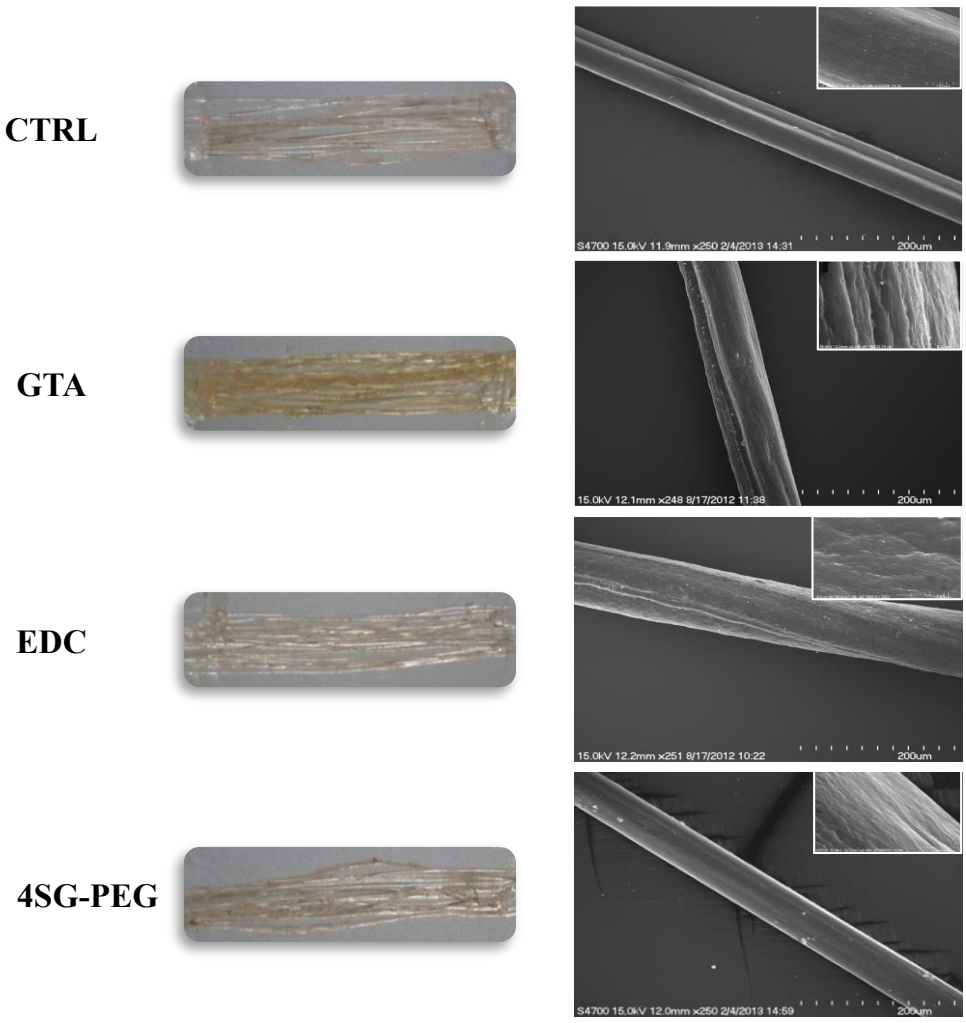

Figure 4.1: Visual analysis indicated that GTA fibres became yellow. Scanning electron micrographs made apparent that crevices and ridges were running parallel to the longitudinal axis of all fibres. CTRL fibres exhibited the smoothest surface topography, GTA exhibited the roughest surface topography and EDC and 4SG-PEG fibres were of intermediate smoothness/ roughness.

4.3.1.2 Mechanical properties and thermal stability analysis

All cross-linked fibres exhibited significantly ($p < 0.001$) lower swelling than the CTRL fibres (**Table 4.1**). GTA fibres exhibited significantly ($p < 0.001$) lower swelling than the EDC and 4SG-PEG fibres (**Table 4.1**). Uniaxial tensile testing revealed that all cross-linked fibres exhibited significantly ($p < 0.001$) higher stress at break than the CTRL fibres (**Table 4.1**). GTA fibres exhibited significantly ($p < 0.001$) higher stress at break than the EDC and 4SG-PEG fibres, with 4SG-PEG fibres having significantly ($p < 0.001$) higher stress at break than the EDC fibres (**Table 4.1**). CTRL fibres exhibited significantly ($p < 0.001$) lower strain at break than the cross-linked fibres (**Table 4.1**) and no significant ($p > 0.05$) difference was observed among the cross-linked fibres (**Table 4.1**). GTA fibres exhibited significantly higher modulus at 2 % strain than the CTRL, EDC and 4SG-PEG fibres. All cross-linked fibres exhibited significantly ($p < 0.001$) higher denaturation temperature than the CTRL fibres (**Table 4.1**). GTA fibres exhibited significantly ($p < 0.001$) higher denaturation temperature than the EDC and 4SG-PEG fibres (**Table 4.1**)

Table 4.1: Physical analysis and denaturation temperature of the produced fibres. * indicates significant ($p < 0.05$) difference to the respective tissue-derived 0 mM 4SG-PEG collagen fibres. Physical properties: N=7; Denaturation temperature: N=5.

Treatment	Swelling %	Stress at Break ± SEM (MPa)	Strain at Break ± SEM	E-modulus at 2 % Strain ± SEM (MPa)	Denaturation Temperature ± SEM (°C)
CTRL	315	1.4 ± 0.2	0.06 ± 0.01	22.4 ± 2.1	47.7 ± 0.2
GTA	13 *	58.9 ± 9.6 *	0.12 ± 0.03 *	688.4 ± 26.1 *	74.3 ± 0.4 *
EDC	204 *	2.8 ± 0.3 *	0.10 ± 0.01 *	18.7 ± 1.7	56 ± 0.3 *
4SG-PEG	68 *	18.8 ± 1.3 *	0.08 ± 0.01 *	230.4 ± 8.2 *	54.4 ± 0.1 *

4.3.1.3 Dermal fibroblast biological analysis

4SG-PEG fibres exhibited significantly higher cell metabolic activity **(Figure 4.2A)** and DNA concentration **(Figure 4.2B)** that all other treatments at all time points ($p < 0.001$). Cellular (cytoskeleton and nuclei) staining (**Figure 4.3**) demonstrated than only a few cells were attached on GTA fibres, even after 7 days in culture, whilst CTRL, EDC and 4SG-PEG fibres supported cell growth (**Figure 4.3**). Qualitative visual analysis (due to cell over-lapping, quantitative analysis was not possible) indicates that CTRL and 4SG-PEG fibres promoted consistently cytoskeleton elongation along the longitudinal fibre axis, whilst some cells on EDC fibres adopted round morphology (**Figure 4.3**). By day 7, only the 4SG-PEG fibres were completely covered by cells (**Figure 4.3**). Quantitative morphometric analysis demonstrates that by day 7, 80% of the cells had aligned parallel to the longitudinal axis of CTRL fibres, whilst 100% of the cells had aligned parallel to the longitudinal axis of EDC and 4SG-PEG fibres (**Figure 4.4A**). No significant difference in nuclei elongation (**Figure 4.4B**) and area (**Figure 4.4C**) was observed between CTRL, EDC and 4SG-PEG treated fibres (GTA fibres were excluded from this analysis, given the low number of adherent cells).

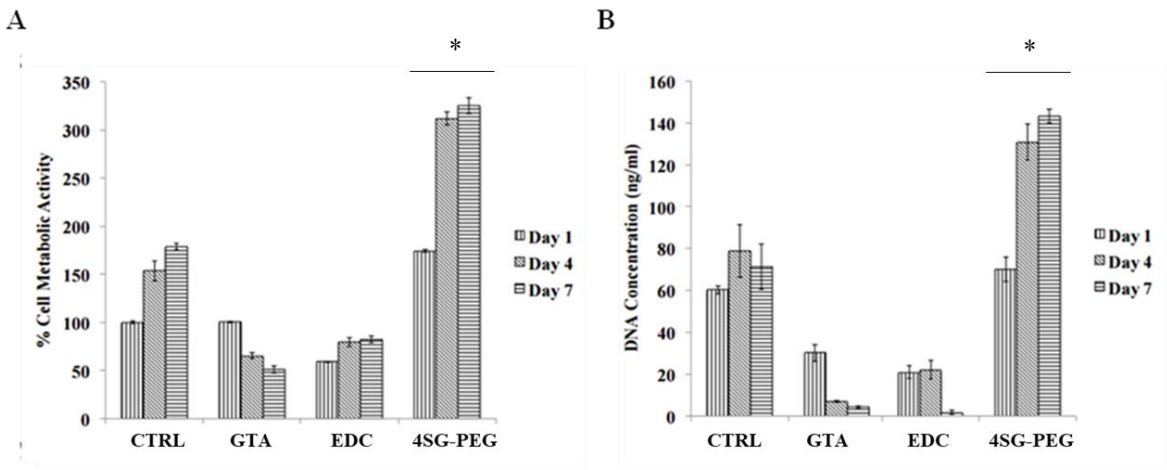

Figure 4.2: 4SG-PEG fibres exhibited significantly higher cell metabolic activity (left) and DNA concentration (right) than all other treatments at all time points (number of replicates: x3 bundles of 20 fibres each). * indicates statistically significant ($p < 0.05$) difference in comparison to other treatments.

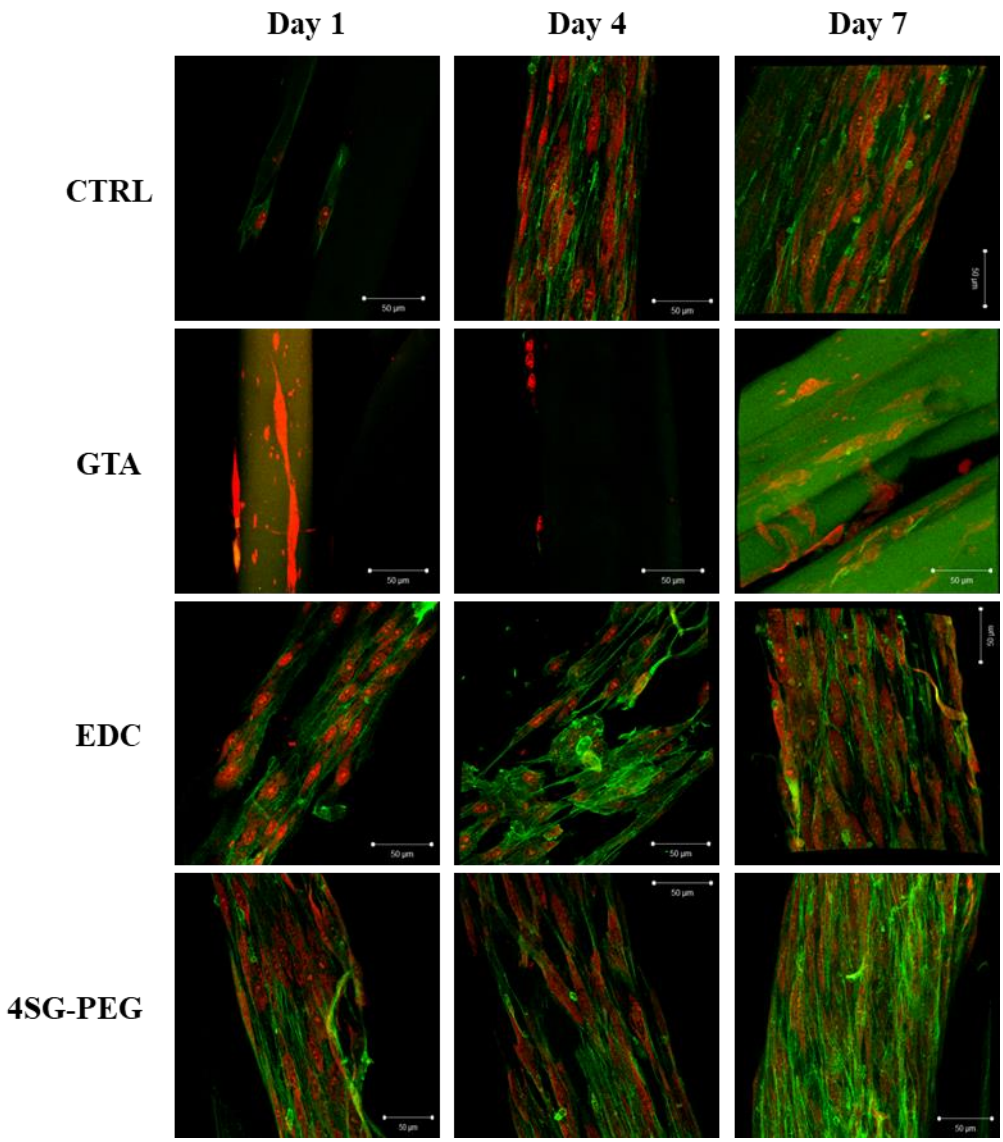

Figure 4.3: CTRL, EDC and 4SG-PEG fibres supported cell growth, whilst only a few cells were attached on GTA and GEN fibres. CTRL and 4SG-PEG fibres promoted consistently cellular elongation along the longitudinal fibre axis. Scalebar = 50 µm. N=3.

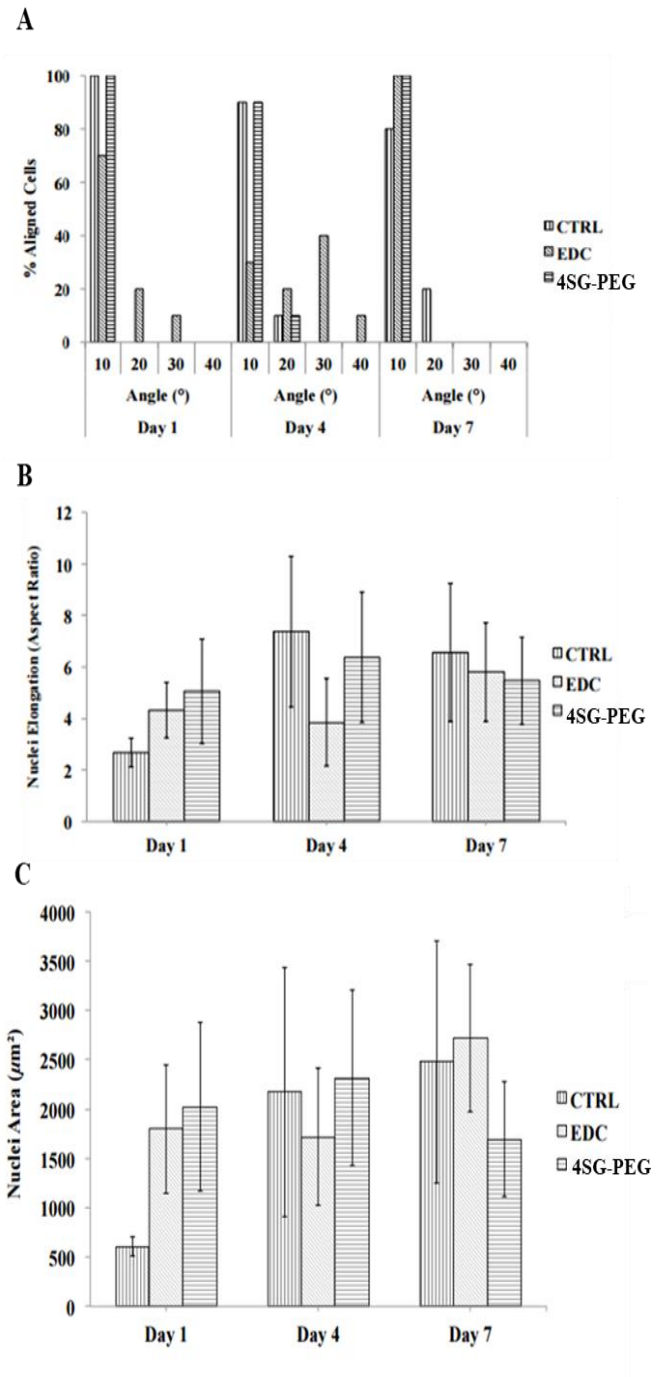

Figure 4.4: Quantitative morphometric analysis demonstrates (**A**) that by day 7, 80% of the cells had aligned parallel to the longitudinal axis of CTRL fibres, whilst 100% of the cells had aligned parallel to the longitudinal axis of EDC and 4SG-PEG fibres. (**B**) No significant difference in nuclei elongation and (**C**) area was observed between CTRL, EDC and 4SG-PEG treated fibres (number of replicates: at least 20 cells per groups per time point).

4.3.2 4SG-PEG optimisation

4.3.2.1 Polarised microscopy and structural analysis

Polarised microscopy revealed that collagen type I fibres were aligned independent of the group. Collagen type I fibres reached distinction after polars were rotated on the optical axis of the microscope from 45º to 90º, indicating alignment **(Figure 4.5B)**. Collagen type I film was used as a control. Collagen type I film did not reach distinction and therefore did not show alignment, as polars were rotated on the optical axis of the microscope every 45º **(Figure 4.5A)**. Optical analysis revealed that GTA fibers became yellow. SEM revealed micro-grooves and crevices on the CTRL fibres that run parallel to the fibres longitudinal axis, while GTA has changed the surface structure **(Figure 4.6)**. 4SG-PEG has maintained the grooves and crevices on fibre surface. **(Figure 4.6)**. EDC fibers exhibited the smoothest surface topography, whilst the GTA exhibited the roughest surface topography.

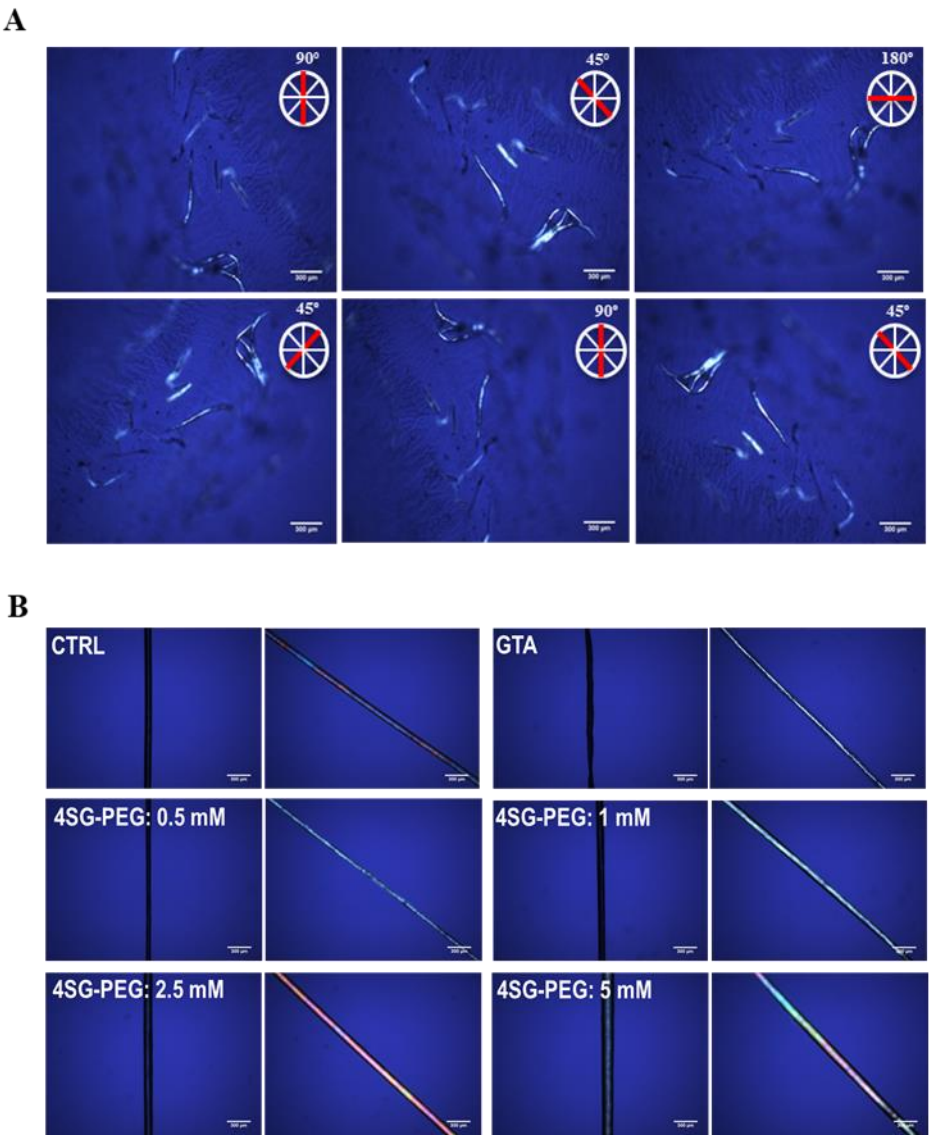

Figure 4.5: Polarised microscopy of collagen type I films (control) and collagen type I fibres cross-linked with GTA and different concentrations of 4SG-PEG. **(A)** Collagen type I film did not reach distinction and therefore did not show alignment, as polars were rotated on the optical axis of the microscope every 45º. **(B)** Collagen type I fibres reached distinction after polars were rotated on the optical axis of the microscope from 45º to 90º, indicating alignment.

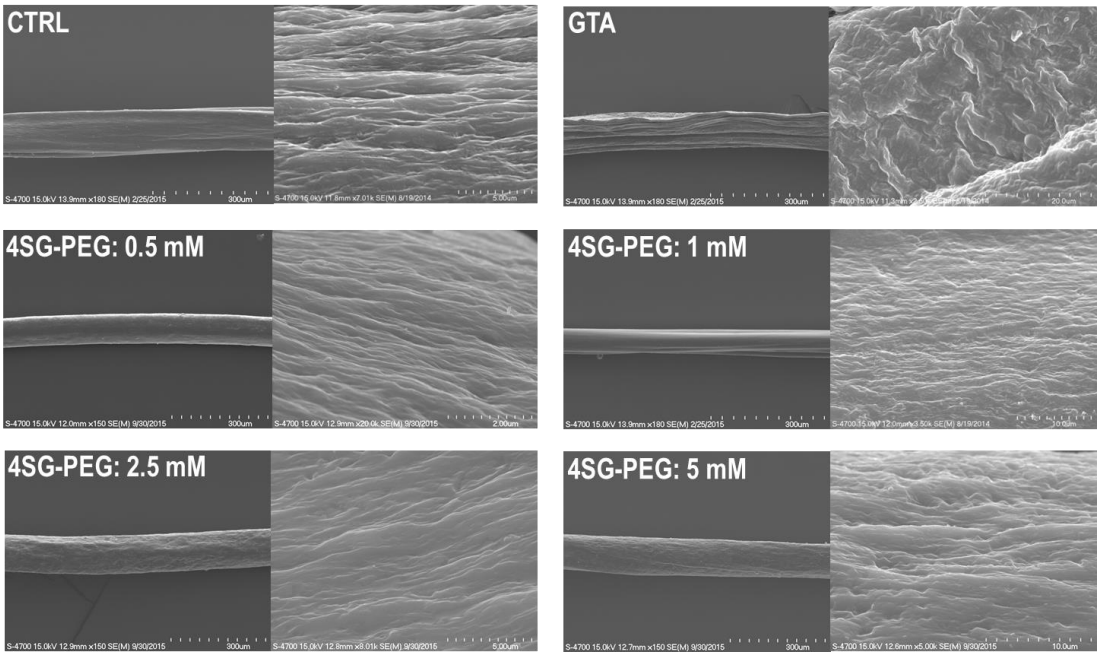

Figure 4.6: Scanning electron microscope (SEM) analysis of cross-linked collagen type I fibres with GTA and different concentrations of 4SG-PEG. Micro-grooves are evident on the CTRL fibres that run parallel to the fibres longitudinal axis while GTA has changed the surface structure. 4SG-PEG has maintained the grooves and crevices on fibre surface.

4.3.2.2 Free amines and resistance to enzymatic degradation analysis

Amount of free amine groups was assessed with ninhydrin assay as an indicator for cross-linking efficiency. A significant ($p < 0.001$) reduction in the free amine groups was observed by all 4SG-PEG and GTA cross-linked fibres. Lowest concentration of 4SG-PEG at 0.5 mM reduced the amount of free amine groups by nearly 50 %, whilst GTA induced a 93 % reduction of free amine groups **(Figure 4.7A)**. *In vitro* enzymatic degradation analysis revealed that after 9 hours of incubation, 0.5 mM 4SG-PEG and GTA significantly ($p < 0.001$) increased resistance of collagen type I fibres to degradation by collagenase type I, whilst CTRL degraded by 80 % **(Figure 4.7B)**.

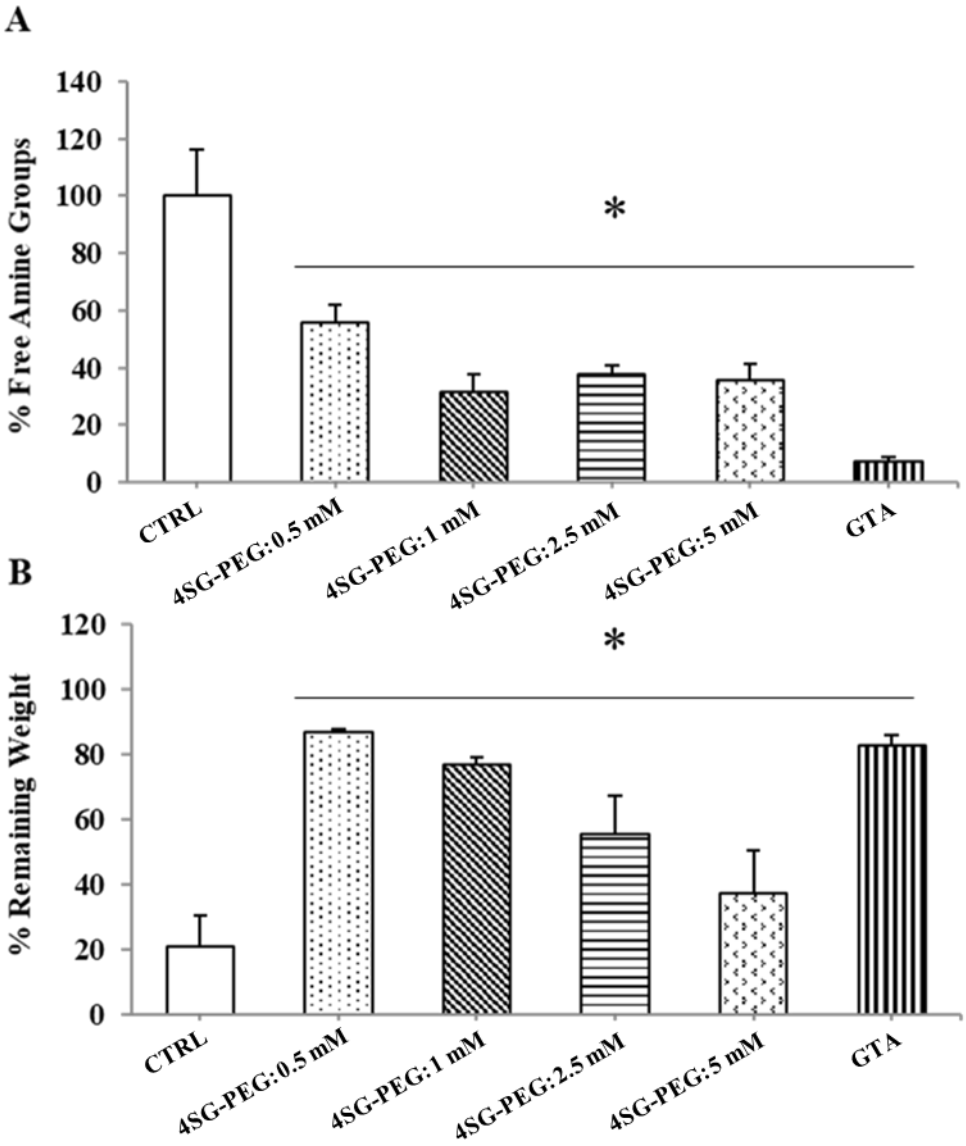

Figure 4.7: (A) Quantification of free amine groups of collagen type I fibres cross-linked with different concentrations of 4SG-PEG, GTA and non cross-linked collagen type I fibres (CTRL) were used as a control. **(B)** Degradation by collagenase after 9 hours of incubation of collagen type I fibres cross-linked with different concentrations of 4SG-PEG, GTA and non cross-linked collagen type I fibres (CTRL) were used as a control. * indicates statistically significant ($p < 0.05$) difference in comparison to the 0 mM 4SG-PEG. N=3.

4.3.2.3 Mechanical properties and thermal stability analysis

Uniaxial tensile testing revealed that the mechanical properties were also found to be subject to different concentrations and cross-linking treatments and extent of swelling, as it has been shown previously that crosslinking density and water content influences the tensile properties. CTRL exhibited significantly ($p < 0.001$) higher force at break. Stress at break was significantly ($p < 0.001$) increased after 4SG-PEG treatment from 0.5mM to 5mM compared to CTRL and GTA. Also, the strain at break was significantly ($p < 0.001$) increased after 4SG-PEG treatment. CTRL and GTA exhibited significantly ($p < 0.001$) higher E-modules inducing stiffer material, whilst 4SG-PEG treatment induced more elastic properties. Different concentrations of 4SG-PEG and GTA exhibited lower swelling ratio than the control fibres. 4SG-PEG at 2.5 mM and GTA showed the greatest swelling capacity while the lowest concentration of 4SG-PEG at 0.5 mM and 1mM reduced water absorbance significantly ($p < 0.001$) compared to CTRL **(Table 4.2)**. DSC analysis revealed that all cross-linked fibers, but 4SG-PEG 2.5 mM, exhibited significantly ($p < 0.001$) higher denaturation temperature than the CTRL fibers. Different concentrations of 4SG-PEG and GTA brought about denaturation temperature higher than the body temperature. 4SG-PEG 0.5 mM induced thermal stability of collagen fibres comparative to GTA **(Table 4.2)**.

Table 4.2: Physical and thermal analysis of collagen type I fibres cross-linked with GTA and different concentrations of 4SG-PEG. Mechanical properties: N=7; Swelling: N=7; Thermal properties: N=5.

Treatment	Force (N) ± SD	Stress at Break (MPa) ± SD	Strain at Break % ± SD	E-modulus at 2 % ± SD	Dry Diameter (µm) ± SD	Swelling %	Peak Temperature ± SD (°C)
CTRL	0.75 ± 0.13	0.61 ± 0.13	9.50 ± 2.33	0.59 ± 0.15	38.93 ± 12.94	245	43.91± 1.05
4SG-PEG: 0.5 mM	0.45 ± 0.16	10.79 ± 5.29	21.38 ± 9.31	0.03 ± 0.01	39.07 ± 13.19	4	73.79 ± 4.53
4SG-PEG: 1 mM	0.46 ± 0.11	7.68 ± 2.21	20.59 ± 5.24	0.05 ± 0.01	37. 65 ± 9.62	3	77.79 ± 8.26
4SG-PEG: 2.5 mM	0.47 ± 0.22	3 ± 1.34	21.64 ± 8.56	0.12 ± 0.05	49.16 ± 16.34	17	60.67 ± 4.90
4SG-PEG: 5 mM	0.29 ± 0.08	8.87 ± 5.39	13. 08 ± 5.96	0.03 ± 0.01	57.81 ± 11.52	0	73.42 ± 3.15
GTA	0.33 ± 0.17	1.05 ± 0.54	6.56 ± 3.39	0.24 ± 0.10	84.88 ± 26.57	11	74.53 ± 0.77

4.3.3 Cross-linking of collagen type I fibres with different cross-linkers

4.3.3.1 Structural analysis

SEM revealed crevices and ridges running parallel to the fibres longitudinal axis on the CTRL fibres. GTA and EDC have changed the fibres surface structure, while 4SG-PEG has maintained the fibres hierarchical structure **(Figure 4.8)**.

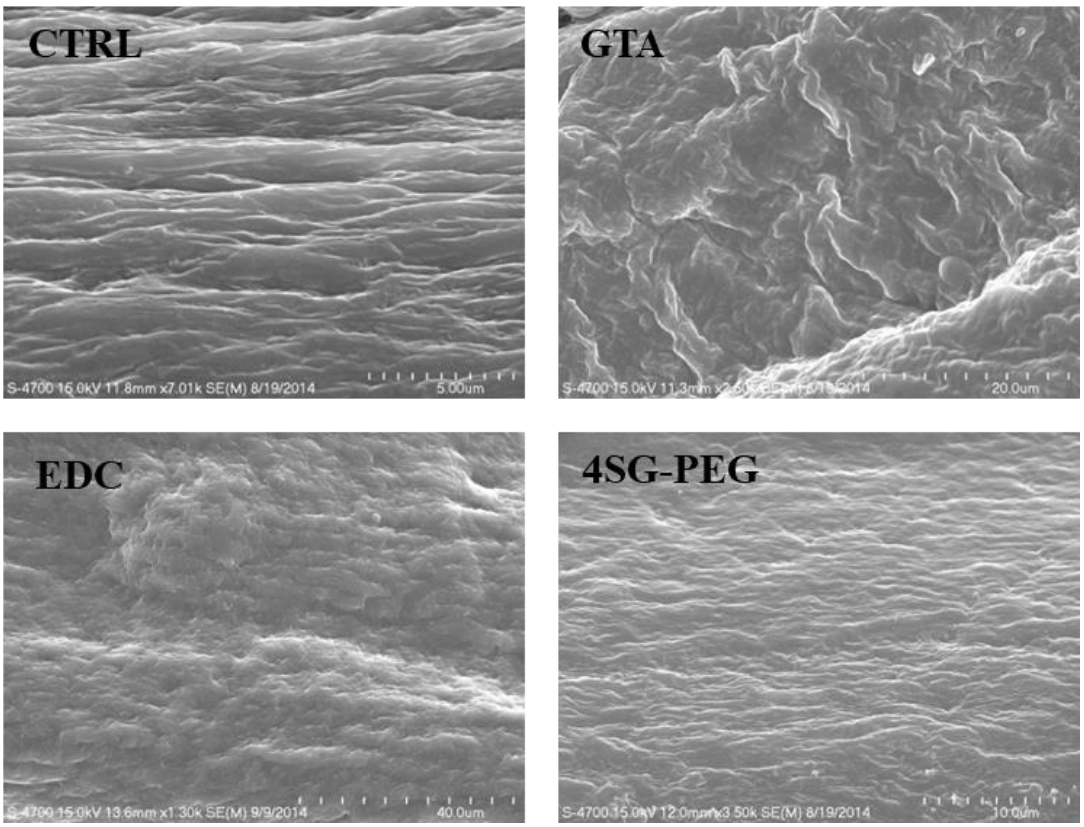

Figure 4.8: Scanning electron microscope (SEM) analysis of collagen type I fibres cross-linked with GTA, EDC, 4SG-PEG and non cross-linked collagen type I fibres (CTRL) were used as control.

4.3.3.2 Free amines and resistance to enzymatic degradation analysis

Amount of free amine groups was assessed with ninhydrin assay as an indicator for cross-linking efficiency. GTA and 4SG-PEG significantly ($p < 0.01$) reduced the amount of free amine groups compared to the CTRL and EDC. Among the cross-linked groups, GTA brought about an approximate 90 % reduction in free amine groups and 4SG-PEG brought about an approximate 55 % reduction in free amine groups **(Figure 4.9A)**. *In vitro* enzymatic degradation analysis revealed that after 9 hours of incubation, GTA and 4SG-PEG have induced significantly ($p < 0.001$) higher resistance to enzymatic degradation, compared to EDC and CTRL (76 % was degraded) **(Figure 4.9B)**.

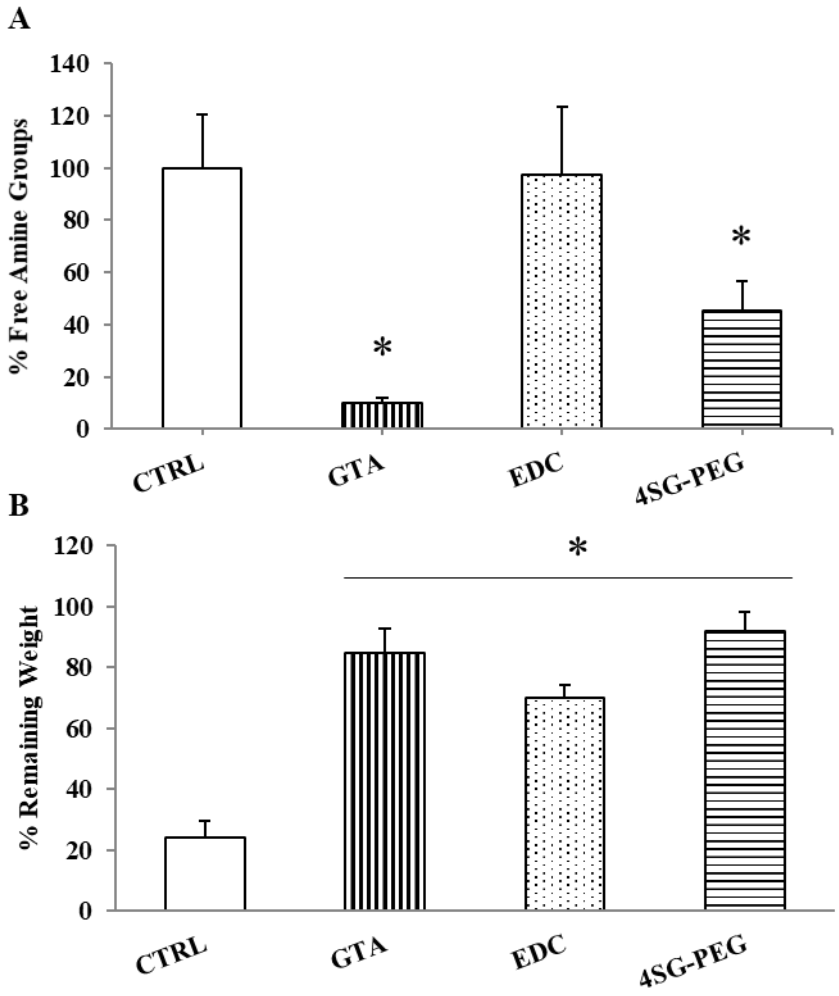

Figure 4.9: (A) Quantification of free amine groups of collagen type I fibres cross-linked with GTA, EDC, 4SG-PEG and non cross-linked collagen type I fibres (CTRL) were used as control. **(B)** Degradation by collagenase after 9 hours of incubation of collagen type I fibres cross-linked with GTA, EDC, 4SG-PEG and non cross-linked collagen type I fibres (CTRL) were used as control. * indicates statistically significant ($p < 0.05$) difference in comparison to the 0 mM 4SG-PEG. N=3.

4.3.3.3 Mechanical properties and thermal stability analysis

Uniaxial tensile testing revealed that GTA exhibited significantly ($p < 0.05$) higher stress at break compared to CTRL and 4SG-PEG. CTRL exhibited significantly ($p < 0.01$) higher force at break, whilst 4SG-PEG exhibited the lowest ($p < 0.01$) force at break. 4SG-PEG exhibited significantly ($p>0.001$) lower E-modulus, whilst GTA exhibited the highest ($p > 0.001$) E-modulus. No significant ($p > 0.05$) change was revealed for strain at break among the cross-linked groups and CTRL. Cross-linking of collagen type I fibres significantly ($p < 0.001$) reduced the swelling ratio compared to the CTRL. Within the cross-linked groups, EDC significantly ($p < 0.001$) reduced the swelling ratio **(Table 4.3)**. DSC analysis revealed that the denaturation temperature of the produced collagen type I fibres was significantly ($p < 0.001$) increased among all cross-linking groups, compared to CTRL. 4SG-PEG exhibited significantly ($p < 0.001$) higher denaturation temperature than the GTA and EDC fibres **(Table 4.3)**.

Table 4.3: GTA exhibited significantly ($p < 0.05$) higher stress at break. CTRL exhibited significantly ($p < 0.01$) higher force at break, whilst 4SG-PEG exhibited the lowest ($p < 0.01$) force at break. 4SG-PEG exhibited significantly ($p > 0.001$) lower E-modulus, whilst GTA exhibited the highest ($p > 0.001$) E-modulus. Cross-linking of collagen type I fibres significantly ($p < 0.001$) reduced the swelling ratio compared to the CTRL. 4SG-PEG exhibited significantly ($p < 0.001$) higher denaturation temperature than the GTA and EDC fibres. Mechanical properties: N=7; Swelling: N=7; Thermal properties: N=5.

Treatment	Force (N) ± SD	Stress at Break (MPa) ± SD	Strain at Break % ± SD	E-modulus at 2 % ± SD	Dry Diameter (µm) ± SD	Swelling %	Peak Temperature ± SD (°C)
CTRL	0.68 ± 0.34	17.54 ± 11.01	7.10 ± 2.30	403.43 ± 209.01	313.07 ± 53.24	174	43.91 ± 1.04
GTA	0.51 ± 0.21	20.28 ± 12.04	9.02 ± 4.17	622.65 ± 423.65	391.29 ± 97.90	17	74.52 ± 0.76
EDC	0.29 ± 0.18	12.56 ± 10.64	7.58 ± 2.96	309.73 ± 272.95	331.45 ± 70.36	9	60.68 ± 4.41
4SG-PEG	0.14 ± 0.09	3.14 ± 2.11	7.97 ± 5.56	74.93 ± 63.86	432.38 ± 112.04	43	77.78 ± 8.25

4.3.3.4 Tenocyte biological analysis

Cellular staining (cytoskeleton and nuclei) has demonstrated that after 21 days in culture, CTRL, EDC and 4SG-PEG fibres supported cell growth **(Figure 4.10A)**. Qualitative visual analysis (due to cell over-lapping, quantitative analysis was not possible) indicates that CTRL, EDC and 4SG-PEG promoted cytoskeleton elongation along the longitudinal fibre axis **(Figure 4.10A)**. GTA was not included due to the red fluorescence of the fibre. LIVE/DEAD® assay demonstrated that 4SG-PEG fibres maintained cell viability up to day 21 **(Figure 4.10B)**. Quantitative morphometric analysis demonstrated that by day 21, 64 % of the cells had aligned parallel to the longitudinal axis of EDC fibres, whilst 82 % of cells aligned parallel to the longitudinal axis of CTRL fibres and 90 % of cells had aligned parallel to the longitudinal axis of 4SG-PEG fibres **(Figure 4.11A)**. Cells on EDC fibres exhibited significantly lower ($p < 0.001$) nuclei elongation compared to CTRL and 4SG-PEG **(Figure 4.11B)**. No significant difference ($p > 0.05$) in nuclei area was observed between CTRL, EDC and 4SG-PEG treated fibres **(Figure 4.11C)**.

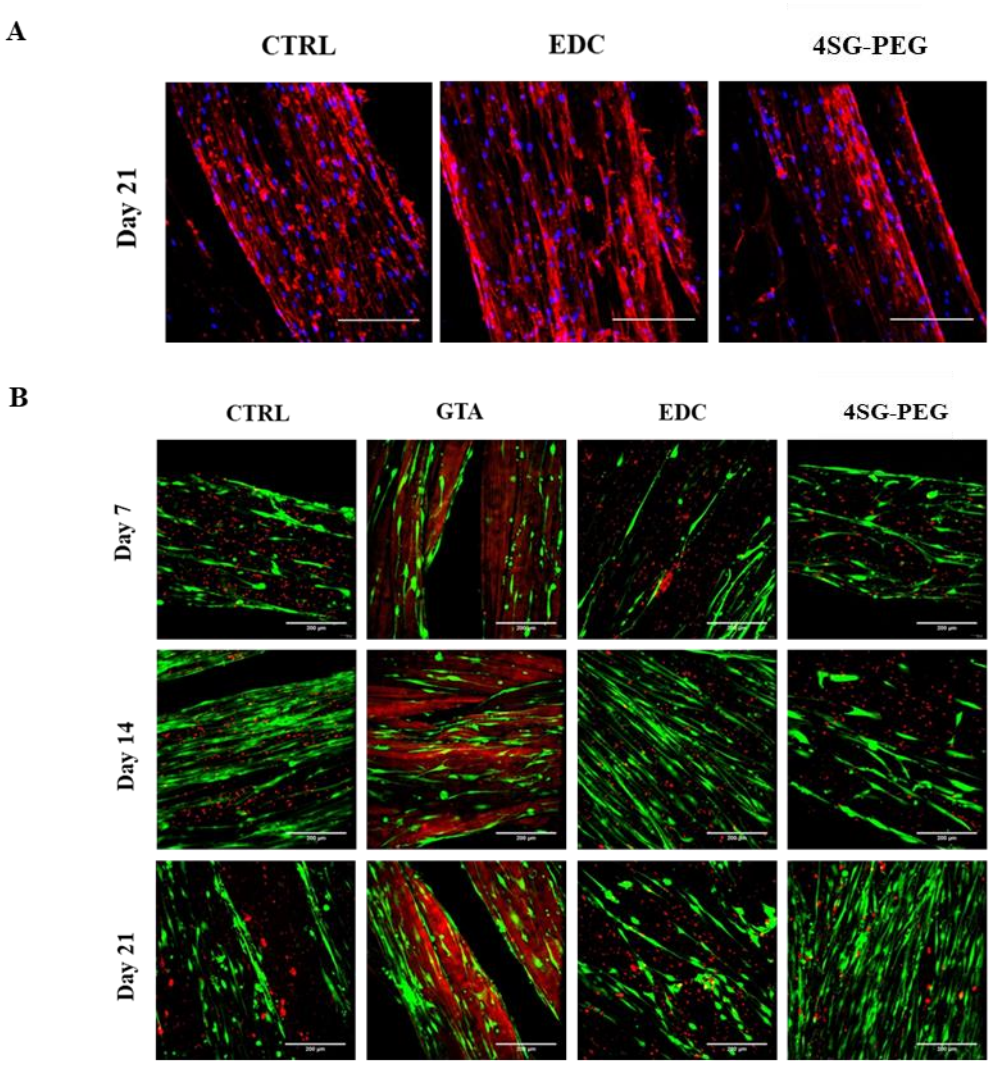

Figure 4.10: (A) Cellular morphology and **(B)** viability of human adult tenocytes at day 21 on collagen type I fibres cross-linked with GTA, EDC, 4SG-PEG and non cross-linked collagen type I fibres (CTRL) were used as control (green cells: live, dead cells: red). Scalebar = 200 µm. N=3.

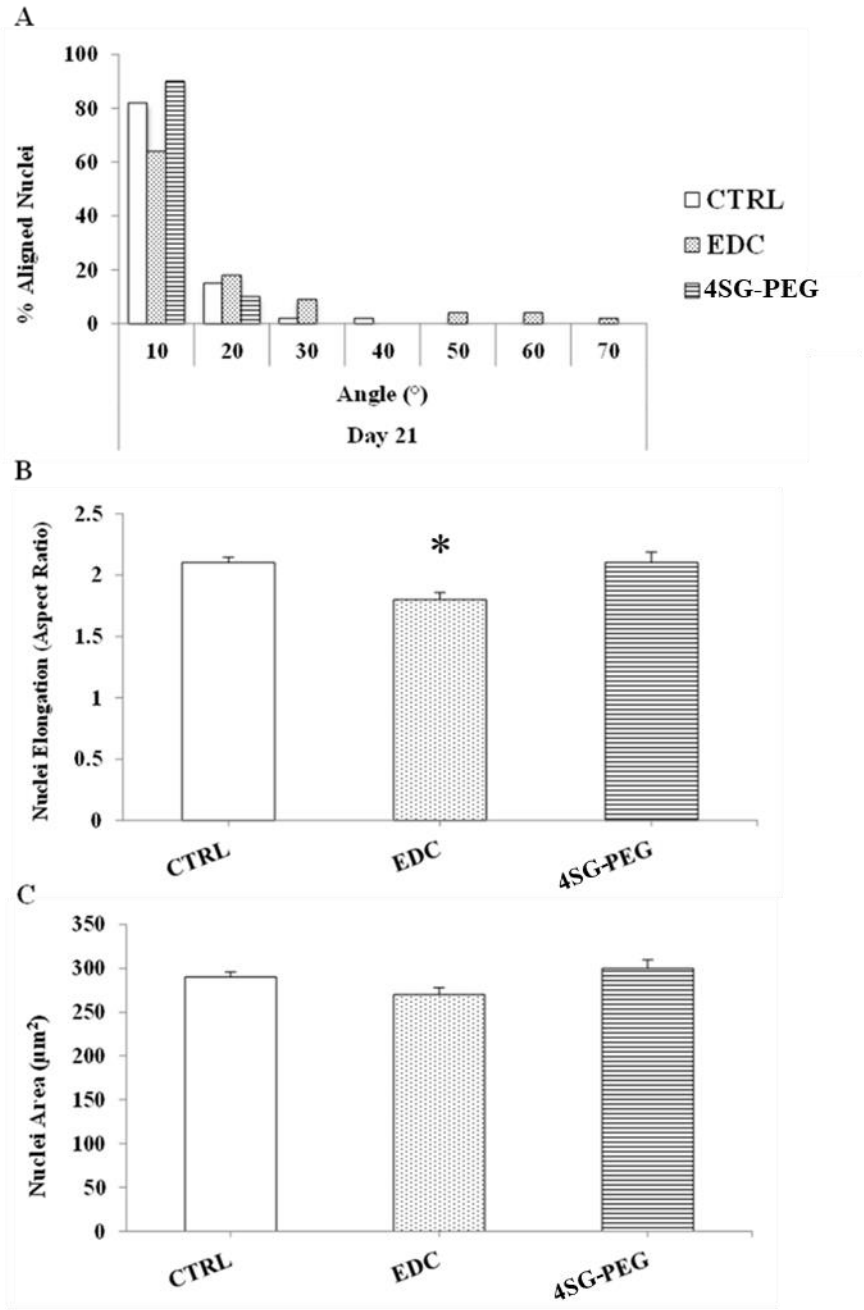

Figure 4.11: Alignment of human adult tenocytes, nuclear area and elongation of cross-linked collagen type I fibres. **(A)** 90 % of cells had aligned parallel to the longitudinal axis of 4SG-PEG fibres. **(B)** Cells on EDC fibres exhibited significantly lower ($p < 0.001$) nuclei elongation compared to CTRL and EDC. **(C)** No significant difference ($p > 0.05$) in nuclei area was observed between the treated fibres and CTRL. N=3.

4.4 Discussion

The natural cross-linking pathway of lysyl oxidase, responsible for mechanical and proteolytic resilience of tissues, does not occur *in vitro*. Therefore, cross-linking is introduced to enhance the properties of the collagen-based scaffolds, to prevent long rod-like collagen molecules from sliding. This involves the formation of bonds between collagen molecules [16]. Further, the harsh extraction, purification and sterilisation methods [17, 18] necessitate the introduction of exogenous cross-links to enhance the mechanical stability and to control the degradation rate of collagen devices. However, customarily used chemical cross-linking approaches are associated with cytotoxicity [19, 20], calcification [21-23] and foreign body response [24, 25], imposing the need for development of new cross-linking approaches. GTA and EDC are the most commonly used chemical cross-linkers. Despite not attaching molecules that can be harmful, EDC cross-linked biomaterials must be thoroughly washed due to the production of a toxic by-product from the cross-linking reaction. GTA has been shown to have great potential as a cross-linker for biomaterials but due to the leaching out as the scaffold degrades, studies have shown GTA to have cytotoxic affect [16]. 4SG-PEG has been used as an alternative to the limiting chemical cross-linkers due to its low toxicity. 4SG-PEG has been FDA approved for a variety of medical applications and has been shown to increase mechanical properties and facilitate infiltration of cells [8]. Herein, we ventured to assess the potential of 4-star poly(ethylene glycol) ether tetrasuccinimidyl glutarate as collagen cross-linker and to assess its structural, thermal, physical and biological consequences on collagen type I fibres in comparison to traditional cross-linking methods.

Starting with visual characterisation, we observed that GTA induced colour changes to the collagen fibres. This evidenced colour change is attributed to the reaction of the cross-linking agent with the amino acid residues [26-28] and it is in accordance with previous data with tissue grafts and collagen-based biomaterials [26-32]. The observed crevices and ridges that run parallel to the longitudinal axis in all treatments is due to the substructure of the collagen type I fibres [33]. Surface smoothness / roughness was also cross-linking method employed dependant, as has been shown previously [34-36]. Polarised microscopy is a useful tool to assess the anisotropic organisation of collagen-based materials and hence, determine the alignment of collagen type I fibres due to its sensitivity to orientation of the collagen. Optically anisotropic collagen type I materials are birefringent, meaning that they can change the direction of polarised

light. Therefore, the regions on collagen materials that are capable of altering the polarised light are said to be anisotropic or orientated. As the collagen type I film was rotated on the optical axis, the polarised light was evident at every angle. This indicated that the collagen film was not anisotropic but had random alignment. Produced collagen type I fibres showed alignment, independent of concentration and method of cross-linking. Collagen type I fibres reached distinction, as they were rotated on the optical axis from 45° to 90° [37-39].

All 4SG-PEG concentrations and GTA reduced the amount of free amine groups and increased the resistance to enzymatic degradation by collagenase. Between different cross-linkers, GTA, EDC and 4SG-PEG increased the resistance to degradation. However, EDC did not show an improvement in reducing the amine groups. Due to the limiting factors of GTA, EDC has been used as an alternative [40-42], however the reduction of amine groups and resistance to degradation was significantly lower compared to 4SG-PEG.

Denaturation temperature was also subject to the 4SG-PEG concentration and cross-linking methods employed, largely attributed to the stabilisation chemistry of the cross-linking method employed. For example, GTA is a self-polymerising aldehyde that reacts with either hydroxyl groups and then condenses to form heterocyclic compounds, which subsequently undergo oxidation to a pyridinium ring or with amine groups to form Schiff bases [26, 43, 44]. Further, GTA can cross-link a great number of molecules that can even be far apart [45, 46], forming large units with slow kinetics and therefore higher denaturation temperature [47, 48]. 4SG-PEG concentration of 1 mM brought about higher denaturation temperature compared to GTA EDC had lower denaturation temperature than GTA, nonetheless, all concentrations and cross-linking methods brought about denaturation temperature higher than the body temperature and therefore they are all suitable for biomedical applications.

The water holding capacity of the produced scaffold was also subject to the cross-linking method used, with all 4SG-PEG concentrations and cross-linking treatments exhibiting significantly lower swelling ratio than the CTRL fibres. This is not surprising, given that cross-linking reduces the free-water binding sites, affecting the equilibrium water content [49-54] and therefore swelling can be used to assess the cross-linking efficiency [34, 55]. Significant lower swelling ratio of some cross-linking methods and concentrations is attributed once more to the chemistries of the

cross-linking method [26, 43, 44, 56] and the density of cross-linking, the higher the cross-linking density, the less water can be bound [57].

The mechanical properties were also found to be subject to the cross-linking method extent of swelling, as it has been shown previously that cross-linking density [58] and water content [59] influences the tensile properties. The stress at break was increased following the cross-linking of collagen type I fibres with different concentrations of 4SG-PEG, due to the reaction of the cross-linking agents with the free amino acids of collagen [49, 60-62]. The strain at break was increased after cross-linking; the fibres retained water within their structure, which acted as plasticiser [63, 64]. GTA exhibited the highest stiffness values, which again can be attributed to the cross-linking efficiency of these agents to bind collagen molecules together [50].

With respect to biological analysis, 4SG-PEG was clearly the more cytocompatible cross-linking agent, as judged by cell metabolic activity, DNA content analysis, cell attachment and morphology. Cytotoxicity drawbacks of GTA have been repeatedly documented in the literature [56, 65-69], as non-reacted GTA or degradation products of GTA introduce cytotoxic derivatives [43, 58]. Although EDC supported cell growth, rounded cell morphology is of concern. 4SG-PEG fibres, at all instances, maintained physiological elongated cell morphology and by day 7 were completely covered by human adult dermal fibroblasts. 4SG-PEG treated fibres were also found to be the most cytocompatible for human adult tenocytes, as 4SG-PEG maintained cell viability up to day 21 and had the highest number of aligned cells along the fibre axis, and therefore 4SG-PEG clearly demonstrated the biological superiority of this cross-linker.

4.5 Conclusions

Herein, we investigated the influence of different concentrations of 4-star poly(ethylene glycol) ether tetrasuccinimidyl glutarate (4SG-PEG) and of various chemical cross-linking methods such as glutaraldehyde (GTA) and carbodiimide (EDC) on structural, thermal, physical, and biological properties of collagen type I fibres. All 4SG-PEG concentrations reduced free amine groups. Resistance to collagenase, denaturation temperature and mechanical properties were cross-linking method and concentration dependent. Among the cross-linking methods assessed, only the 4-star poly(ethylene glycol) ether tetrasuccinimidyl glutarate induced acceptable thermal and mechanical properties. Further, it was the only cross-linker that comprehensively supported growth of human adult dermal fibroblasts and human adult tenocytes, clearly demonstrating its superiority as compared with GTA and carbodiimide fixation.

4.6 References

[1] Y.P. Kato, M.G. Dunn, J.P. Zawadsky, A.J. Tria, F.H. Silver, Regeneration of Achilles tendon with a collagen tendon prosthesis. Results of a one-year implantation study, J Bone Joint Surg Am 73(4) (1991) 561-574.

[2] J.F. Cavallaro, P.D. Kemp, K.H. Kraus, Collagen fabrics as biomaterials, Biotechnol Bioeng 43(8) (1994) 781-791.

[3] K.G. Cornwell, B.R. Downing, G.D. Pins, Characterizing fibroblast migration on discrete collagen threads for applications in tissue regeneration, J Biomed Mater Res Part A 71A(1) (2004) 55-62.

[4] D.I. Zeugolis, G.R. Paul, G. Attenburrow, Cross-linking of extruded collagen fibres - A biomimetic three-dimensional scaffold for tissue engineering applications, J Biomed Mater Res Part A 89(4) (2009) 895-908.

[5] D.I. Zeugolis, P.P. Panengad, E.S. Yew, C. Sheppard, T.T. Phan, M. Raghunath, An *in situ* and *in vitro* investigation for the transglutaminase potential in tissue engineering, J Biomed Mater Res Part A 92(4) (2010) 1310-1320.

[6] D.I. Zeugolis, R.G. Paul, G. Attenburrow, The influence of a natural cross-linking agent (Myrica rubra) on the properties of extruded collagen fibres for tissue engineering applications, Materials Science and Engineering - Part C 30(1) (2010) 190-195.

[7] L. Delgado, Y. Bayon, A. Pandit, D.I. Zeugolis, To cross-link or not to cross-link? Cross-linking associated foreign body response of collagen-based devices, Tissue Eng Part B Rev (In Press).

[8] J. Ward, J. Kelly, W. Wang, D.I. Zeugolis, A. Pandit, Amine functionalization of collagen matrices with multifunctional polyethylene glycol systems, Biomacromolecules 11(11) (2010) 3093-3101.

[9] L. Baumann, S. Prokoph, C. Gabriel, U. Freudenberg, C. Werner, A.G. Beck-Sickinger, A novel, biased-like SDF-1 derivative acts synergistically with starPEG-based heparin hydrogels and improves eEPC migration in vitro, J Control Release 162(1) (2012) 68-75.

[10] P.B. Welzel, M. Grimmer, C. Renneberg, L. Naujox, S. Zschoche, U. Freudenberg, C. Werner, Macroporous starPEG-heparin cryogels, Biomacromolecules 13(8) (2012) 2349-2358.

[11] M.V. Tsurkan, K. Chwalek, S. Prokoph, A. Zieris, K.R. Levental, U. Freudenberg, C. Werner, Defined polymer-peptide conjugates to form cell-instructive starPEG-heparin matrices in situ, Adv Mater 25(18) (2013) 2606-2610.

[12] X.J. Hu, N.G. Dong, J.W. Shi, C. Deng, H.D. Li, C.F. Lu, Evaluation of a novel tetra-functional branched poly(ethylene glycol) crosslinker for manufacture of crosslinked, decellularized, porcine aortic valve leaflets, J Biomed Mater Res B Appl Biomater 102(2) (2014) 322-336.

[13] E.C. Collin, S. Grad, D.I. Zeugolis, C.S. Vinatier, J.R. Clouet, J.J. Guicheux, P. Weiss, M. Alini, A.S. Pandit, An injectable vehicle for nucleus pulposus cell-based therapy, Biomaterials 32(11) (2011) 2862-2870.

[14] D.I. Zeugolis, R.G. Paul, G. Attenburrow, The influence of a natural cross-linking agent (Myrica rubra) on the properties of extruded collagen fibres for tissue engineering applications, Mater Sci Eng C 30(1) (2010) 190-195.

[15] D.I. Zeugolis, M. Raghunath, The physiological relevance of wet versus dry differential scanning calorimetry for biomaterial evaluation: A technical note, Polym Int 59(10) (2010) 1403-1407.

[16] M.G. Haugh, C.M. Murphy, R.C. McKiernan, C. Altenbuchner, F.J. O'Brien, Crosslinking and mechanical properties significantly influence cell attachment, proliferation, and migration within collagen glycosaminoglycan scaffolds, Tissue Eng Part A 17(9-10) (2011) 1201-1208.

[17] D.I. Zeugolis, S.T. Khew, E.S.Y. Yew, A.K. Ekaputra, Y.W. Tong, L.Y.L. Yung, D.W. Hutmacher, C. Sheppard, M. Raghunath, Electro-spinning of pure collagen nano-fibres - Just an expensive way to make gelatin?, Biomaterials 29(15) (2008) 2293-2305.

[18] L.M. Delgado, A. Pandit, Z.D. I., Influence of sterilisation methods on collagen-based devices stability and properties, Expert Rev Med Devices 11(3) (2014) 305-314.

[19] P.B. van Wachem, R. Zeeman, P.J. Dijkstra, J. Feijen, M. Hendriks, P.T. Cahalan, M.J. van Luyn, Characterization and biocompatibility of epoxy-crosslinked dermal sheep collagens, J Biomed Mater Res 47(2) (1999) 270-277.

[20] J.E. Gough, C.A. Scotchford, S. Downes, Cytotoxicity of glutaraldehyde crosslinked collagen/poly(vinyl alcohol) films is by the mechanism of apoptosis, J Biomed Mater Res 61(1) (2002) 121-130.

[21] R.J. Levy, F.J. Schoen, F.S. Sherman, J. Nichols, M.A. Hawley, S.A. Lund, Calcification of subcutaneously implanted type I collagen sponges. Effects of formaldehyde and glutaraldehyde pretreatments, Am J Pathol 122(1) (1986) 71-82.
[22] J.M. McPherson, S. Sawamura, R. Armstrong, An examination of the biologic response to injectable, glutaraldehyde cross-linked collagen implants, J Biomed Mater Res 20(1) (1986) 93-107.
[23] S.C. Vasudev, T. Chandy, Effect of alternative crosslinking techniques on the enzymatic degradation of bovine pericardia and their calcification, J Biomed Mater Res 35(3) (1997) 357-369.
[24] Q. Ye, M.C. Harmsen, M.J. van Luyn, R.A. Bank, The relationship between collagen scaffold cross-linking agents and neutrophils in the foreign body reaction, Biomaterials 31(35) (2010) 9192-9201.
[25] B.N. Brown, R. Londono, S. Tottey, L. Zhang, K.A. Kukla, M.T. Wolf, K.A. Daly, J.E. Reing, S.F. Badylak, Macrophage phenotype as a predictor of constructive remodeling following the implantation of biologically derived surgical mesh materials, Acta Biomater 8(3) (2012) 978-987.
[26] H.W. Sung, R.N. Huang, L.L.H. Huang, C.C. Tsai, C.T. Chiu, Feasibility study of a natural crosslinking reagent for biological tissue fixation, J Biomed Mater Res 42(4) (1998) 560-567.
[27] L.L. Huang, H.W. Sung, C.C. Tsai, D.M. Huang, Biocompatibility study of a biological tissue fixed with a naturally occurring crosslinking reagent, J Biomed Mater Res 42(4) (1998) 568-576.
[28] H.C. Liang, Y. Chang, C.K. Hsu, M.H. Lee, H.W. Sung, Effects of crosslinking degree of an acellular biological tissue on its tissue regeneration pattern, Biomaterials 25(17) (2004) 3541-3552.
[29] R.H. Nagaraj, V.M. Monnier, Protein modification by the degradation products of ascorbate: Formation of a novel pyrrole from the Maillard reaction of L-threose with proteins, Biochim Biophys Acta 1253(1) (1995) 75-84.
[30] P.B. van Wachem, R. Zeeman, P.J. Dijkstra, J. Feijen, M. Hendriks, P.T. Cahalan, M.J. van Luyn, Characterization and biocompatibility of epoxy-crosslinked dermal sheep collagens., J Biomed Mater Res A 47(2) (1999) 270-277.
[31] S.B. Hong, K.W. Lee, J.T. Handa, C.K. Joo, Effect of advanced glycation end products on lens epithelial cells in vitro, Biochem Biophys Res Commun 275(1) (2000) 53-59.

[32] G.K. Reddy, Glucose-mediated in vitro glycation modulates biomechanical integrity of the soft tissues but not hard tissues, J Orthop Res 21(4) (2003) 738-743.
[33] D.L. Christiansen, F.H. Silver, Mineralization of an axially aligned collagenous matrix: A morphological study, Eur Cells Mater 3(2) (1993) 177-188.
[34] M.F. Cote, C.J. Doillon, Wettability of cross-linked collagenous biomaterials: *In vitro* study, Biomaterials 13(9) (1992) 612-616.
[35] Y. Nomura, S. Toki, Y. Ishii, K. Shirai, Effect of transglutaminase on reconstruction and physicochemical properties of collagen gel from shark type I collagen, Biomacromolecules 2(1) (2001) 105-110.
[36] A. Sionkowska, T. Wess, Mechanical properties of UV irradiated rat tail tendon (RTT) collagen, Intern J Biolog Macromol 34(1-2) (2004) 9-12.
[37] A. Changoor, N. Tran-Khanh, S. Methot, M. Garon, M.B. Hurtig, M.S. Shive, M.D. Buschmann, A polarized light microscopy method for accurate and reliable grading of collagen organization in cartilage repair, Osteoarthritis Cartilage 19(1) (2011) 126-135.
[38] M. Wolman, F.H. Kasten, Polarized light microscopy in the study of the molecular structure of collagen and reticulin, Histochemistry 85(1) (1986) 41-49.
[39] S. Bancelin, A. Nazac, B.H. Ibrahim, P. Dokladal, E. Decenciere, B. Teig, H. Haddad, H. Fernandez, M.C. Schanne-Klein, A. De Martino, Determination of collagen fiber orientation in histological slides using Mueller microscopy and validation by second harmonic generation imaging, Opt Express 22(19) (2014) 22561-22574.
[40] D.L. Scheffel, L. Bianchi, D.G. Soares, F.G. Basso, C. Sabatini, C.A. de Souza Costa, D.H. Pashley, J. Hebling, Transdentinal cytotoxicity of carbodiimide (EDC) and glutaraldehyde on odontoblast-like cells, Oper Dent 40(1) (2015) 44-54.
[41] L. Salvatore, M. Madaghiele, C. Parisi, F. Gatti, A. Sannino, Crosslinking of micropatterned collagen-based nerve guides to modulate the expected half-life, J Biomed Mater Res A 102(12) (2014) 4406-4414.
[42] A.M. Haaparanta, J. Koivurinta, E.R. Hamalainen, M. Kellomäki, The effect of cross-linking time on porous freeze-dried collagen scaffold using 1-ethyl-3-(3-dimethylaminopropyl)carbodiimide as a cross-linker, 2008.
[43] L.H.H.O. Damink, P.J. Dijkstra, M.J.A. van Luyn, P.B. van Wachem, P. Nieuwenhuis, J. Feijen, Crosslinking of dermal sheep collagen using hexamethylene diisocyanate, J Mater Sci Mater Med 6(7) (1995) 429-434.

[44] L.H.H.O. Damink, P.J. Dijkstra, M.J.A. van Luyn, P.B. van Wachem, P. Nieuwenhuis, J. Feijen, *In vitro* degradation of dermal sheep collagen cross-linked using a water-soluble carbodiimide, Biomaterials 17(7) (1996) 679-684.

[45] D. Chachra, P.F. Gratzer, C.A. Pereira, J.M. Lee, Effect of applied uniaxial stress on rate and mechanical effects of cross-linking in tissue-derived biomaterials, Biomaterials 17(19) (1996) 1865-1875.

[46] B. Madhan, C. Muralidharan, R. Jayakumar, Study on the stabilisation of collagen with vegetable tannins in the presence of acrylic polymer, Biomaterials 23(14) (2002) 2841-2847.

[47] K.H. Rajini, R. Usha, V. Arumugam, R. Sanjeevi, Fracture behaviour of cross-linked collagen fibres, J Materials Science 36(23) (2001) 5589-5592.

[48] R. Usha, T. Ramasami, Structure and conformation of intramolecularly cross-linked collagen, Colloids Surf B Biointerfaces 41(1) (2005) 21-24.

[49] Y.P. Kato, F.H. Silver, Formation of continuous collagen fibres: Evaluation of biocompatibilily and mechanical properties, Biomaterials 11(3) (1990) 169-175.

[50] M.C. Wang, G.D. Pins, F.H. Silver, Collagen fibres with improved strength for the repair of soft tissue injuries, Biomaterials 15(7) (1994) 507-512.

[51] K. Vizarova, D. Bakos, M. Rehakova, V. Macho, Modification of layered atelocollagen by ultraviolet irradiation and chemical cross-linking: Structure stability and mechanical properties, Biomaterials 15(13) (1994) 1082-1086.

[52] M. Rehakova, D. Bakos, K. Vizarova, M. Soldan, M. Jurickova, Properties of collagen and hyaluronic acid composite materials and their modification by chemical crosslinking, J Biomed Mater Res 30(3) (1996) 369-372.

[53] G.A. Hutcheon, C. Messiou, R.M. Wyre, M.C. Davies, S. Downes, Water absorption and surface properties of novel poly(ethylmethacrylate) polymer systems for use in bone and cartilage repair, Biomaterials 22(7) (2001) 667-676.

[54] V. Charulatha, A. Rajaram, Influence of different crosslinking treatments on the physical properties of collagen membranes, Biomaterials 24(5) (2003) 759-767.

[55] J.S. Pieper, A. Oosterhof, P.J. Dijkstra, J.H. Veerkamp, T.H. van Kuppevelt, Preparation and characterization of porous crosslinked collagenous matrices containing bioavailable chondroitin sulphate, Biomaterials 20(9) (1999) 847-858.

[56] M.A. Moore, W.M. Chen, R.E. Phillips, I.K. Bohachevsky, B.K. McIlroy, Shrinkage temperature versus protein extraction as a measure of stabilization of photooxidized tissue, J Biomed Mater Res 32(2) (1996) 209-214.

[57] R.N. Chen, H.O. Ho, M.T. Sheu, Characterization of collagen matrices crosslinked using microbial transglutaminase, Biomaterials 26(20) (2005) 4229-4235.
[58] C.R. Lee, A.J. Grodzinsky, M. Spector, The effects of cross-linking of collagen-glycosaminoglycan scaffolds on compressive stiffness, chondrocyte-mediated contraction, proliferation and biosynthesis, Biomaterials 22(23) (2001) 3145-3154.
[59] V. Arumugam, M.D. Naresh, N. Somanathan, R. Sanjeevi, Effect of strain rate on the fracture behaviour of collagen, J Materials Science 27(10) (1992) 2649-2652.
[60] Y.P. Kato, D. Christiansen, R.A. Hahn, S.J. Shieh, J.D. Goldstein, F.H. Silver, Mechanical properties of collagen fibres: A comparison of reconstituted and rat tail tendon fibres, Biomaterials 10(1) (1989) 38-42.
[61] H.W. Sung, Y. Chang, C.T. Chiu, C.N. Chen, H.C. Liang, Mechanical properties of a porcine aortic valve fixed with a naturally occurring crosslinking agent, Biomaterials 20(19) (1999) 1759-1772.
[62] K. Madhavan, D. Belchenko, A. Motta, W. Tan, Evaluation of composition and crosslinking effects on collagen-based composite constructs, Acta Biomater 6(4) (2010) 1413-1422.
[63] M.N. Taravel, A. Domard, Collagen and its interactions with chitosan: III. Some biological and mechanical properties, Biomaterials 17(4) (1996) 451-455.
[64] C. Menard, S. Mitchell, M. Spector, Contractile behavior of smooth muscle actin-containing osteoblasts in collagen-GAG matrices in vitro: implant-related cell contraction, Biomaterials 21(18) (2000) 1867-1877.
[65] H. Petite, V. Frei, A. Huc, D. Herbage, Use of diphenylphosphorylazide for cross-linking collagen-based biomaterials, J Biomed Mater Res 28(2) (1994) 159-165.
[66] E. Jorge-Herrero, P. Fernandez, J. Turnay, N. Olmo, P. Calero, R. Garcia, I. Freile, J.L. Castillo-Olivares, Influence of different chemical cross-linking treatments on the properties of bovine pericardium and collagen, Biomaterials 20(6) (1999) 539-545.
[67] A.K. Adams, E.A. Talman, L. Campbell, B.K. McIlroy, M.A. Moore, Crosslink formation in porcine valves stabilized by dye-mediated photooxidation, J Biomed Mater Res 57(4) (2001) 582-587.
[68] V. Charulatha, A. Rajaram, Dimethyl 3,3'-dithiobispropionimidate: A novel crosslinking reagent for collagen, J Biomed Mater Res 54(1) (2001) 122-128.

[69] C.F. Rousseau, C.H. Gagnieu, In vitro cytocompatibility of porcine type I atelocollagen crosslinked by oxidized glycogen, Biomaterials 23(6) (2002) 1503-1510.

Chapter 5 - Summary and future directions

5.1 Summary

Collagen type I is the most abundant extracellular matrix protein in vertebrates and plays a vital role in providing tissues with tensile strength and the necessary framework for the growth of cells by regulating and promoting cell adhesion, migration, proliferation and differentiation [1-8]. The ability of tailoring the physical properties of collagen to the properties of the target tissue via cross-linking methods has been an attractive aspect of this material [9-11]. Although collagen has a long-standing history in biomedicine, clinical data show mixed results with respect to efficacy and efficiency of collagen-based devices, suggesting that other factors than cross-linking are at play when assessing the properties of collagen-based devices. The aim of this work was to assess the influence of collagen source (e.g. species, tissue, gender) as well as cross-linking [e.g. 4-star poly(ethylene glycol) ether tetrasuccinimidyl glutarate, glutaraldehyde, carbodiimide] on the properties (structural, chemical and physical) of collagen-based devices, and evaluate their effect on different cell types (human dermal fibroblasts and human tenocytes).

Firstly, the properties of the isolated collagen from different species (porcine and bovine), tissue (skin and tendon) and genders (male and female) were assessed, and whether the source of collagen influences free-amine content, denaturation temperature, resistance to enzymatic degradation, mechanical properties and biological responses. Collagen type I was successfully isolated and porous sponges were fabricated independent of species, tissue or gender. Collagen type I purity and free-amine content were not affected as a function of species (porcine versus bovine), gender (female versus male) and tissue (skin versus tendon) from which the collagen was extracted. However, yield, denaturation temperature, resistance to enzymatic degradation, swelling ratio and biomechanical properties were evidently species- and tissue- dependent. Independent of species, tissue or gender, sponges did not affect biological (human dermal fibroblast and THP-1 monocyte cultures) response. These data indicate that the source of collagen should be considered for the development of collagen-based implantable devices.

Continuing with the use of the optimum collagen source, sponges from bovine female tendon and skin were fabricated and their structural, chemical, physical and biological properties with different cross-linking densities of 4-arm polyethylene glycol succinimidyl glutarate were assessed. It was demonstrated that porous collagen sponges were produced independent of collagen source. The tendon-derived collagen

scaffolds exhibited significantly higher compressive stress and compressive modulus values and provided a more suitable environment for human tenocyte growth than the skin-derived collagen scaffolds. These data clearly illustrate that when developing medical devices, the tissue from which collagen is extracted from should be considered in the context of the intended application.

Finally, collagen type I fibres were developed to assess the influence of different concentrations of 4-arm polyethylene glycol succinimidyl glutarate and various chemical cross-linking methods, such as glutaraldehyde and carbodiimide on the structural, thermal, physical and biological properties of collagen type I fibres. Resistance to collagenase, denaturation temperature and mechanical properties were cross-linking method and concentration dependent. Treatment of collagen fibres with 4-arm polyethylene glycol succinimidyl glutarate resulted in maintenance of their micro-grooved surface, reduction of free-amine content and increased resistance to enzymatic degradation, denaturation temperature and mechanical properties. 4-arm polyethylene glycol succinimidyl glutarate collagen fibres also supported cellular growth, demonstrating superiority over commonly used glutaraldehyde and carbodiimide cross-linkers.

Overall, we provide evidence that prior to developing collagen-based implantable medical devices, collagen source should be taken into consideration. Cross-linker and concentration also plays a major role, as their properties and chemical structure can compromise cellular responses. This work demonstrates a new perspective on collagen source and relatively novel cross-linker for tissue engineering applications.

5.2 Future directions

Collagen has been a material of choice for decades for a large variety of applications such as drug delivery, wound healing, tissue engineering and repair, bone, neural regeneration and many more, as collagen is a natural found substance, with high distribution within the tissues and plays an important role it tissue and cell function. Collagen has been fabricated into many biomedical devices ranging from sponges, hydrogels, spheres, films, fibers and conduits. The attractive aspect of collagen is the ability to fabricate devices in different shapes and sizes, that will be appropriate for the specific clinical target. Other advantages that make collagen a material of choice is the ability to modify the collagen properties with cross-linkers to suit the application of interest. Addition of such cross-linkers can improve mechanical properties, reduce

enzymatic degradation and increase thermal properties. In addition, functionalisation of collagen with varies agents to achieve the desired surface properties for cell interaction or to stimulate cellular response has also been an area of interest. Collagen has been used for controlled drug delivery to promote tissue regeneration and repair, as well as administration of antibiotics to the site of infection. Functionalisation of collagen allows for the optimum release of therapeutic agents into the site of interest without jeopardising cellular function.

As collagen is used for a large variety of applications and clinical targets, it is important to match the properties of the biomaterial as closely as possible to the properties of the tissue of interest. Therefore, it is important to understand your clinical target, tissue properties and to select suitable agent for collagen functionalisation to improve its properties. Prior to this, standardisation of protocols of collagen extraction is important to make sure that collagen is of the same quality across different laboratories and companies. This will also ensure that collagen quality and its properties are reproducible, with very little to none batch to batch variation. Improving on the tools and equipment that are used for collagen extraction can also reduce the variability among the extractions.

This work indicates the importance of collagen source due to the difference in its properties that can impact the regeneration or failure of the tissue. Commercial collagen, although indicates the species where it is sourced from such as bovine, porcine or rat, it does not indicate further details such as the sex and age of the animal, which can impact the properties of the collagen. As the source impacts the collagen properties, data on the mechanical, biochemical and biological properties should be provided commercially.

It has been shown in the literature the affect that collagen source has on the properties of collagen. This work has also indicated the impact collagen source has on the physiochemical and biological activity of the collagen sponges. The age of the animal plays an important part in determining the physiomechanical proprieties of the sponges due to the level of cross-linking in the tissue, where higher levels are found in the older animal compared to a younger animal. The higher in mechanical properties collagen sponges derived from tendon tissues in comparison to collagen sponges derived from skin tissues can also be attributed to the architecture of the collagen fibres in the respective tissues, which, in turn, is responsible for the tissue-specific physiomechanical properties. From the results it is clear, that the acid from the

collagen extraction protocol is able to break down the cross-links in the tissue but yet, the stronger covalent bonds are retained in the collagen from the older animal. Physiomechanical properties have been shown to affect biological properties of the sponges. This work clearly displayed that stiffness and rigidity of the sponges can influence the migration and proliferation of cells, as well as their viability. Furthermore, cellular morphology has been shown to be affected by sponge stiffness. It is well established in the literature that materials with higher mechanical modulus and therefore stiffer, promote cellular connection with the extracellular matrix and establish focal adhesions that allow the cells to migrate. Equally, this work shows the importance of tissue type and the differences in properties between tendon and skin. Given that tendon is a load bearing tissue, and some level of native cross-linking is retained post extraction, the physiomechanical properties of the sponges will be higher compared to skin. Skin is a thermoregulating tissue, and therefore the properties of collagen sponges extracted from skin tissue will be higher compared to tendon tissue, as seen with the results of this work. Overall, many factors are to be considered when choosing a collagen source as it can have an impact on the physiomechanical and biological properties of the biomaterial.

Considering the limitations and other questions that have surfaced throughout the course of this work, some research areas of further interest are outlined below.

5.2.1 Influence of collagen type I fibres in tenogenic phenotype maintenance and induction

Collagen type I fibres have been used in tissue engineering and tendon repair applications due to the fibrillary structure that resembles native tendon structure [12, 13]. The micro-grooves and crevices have been shown to enhance cell adhesion and growth, while regenerating tendon tissue *in vivo* [14-16]. The alignment of collagen fibres induces cell elongation, migration and tenogenic phenotype [16-18]. Furthermore, cross-linker and cross-linking concentrations affect cellular responses and phenotype. Cross-linking affects the stiffness of collagen fibres and therefore induces changes in cellular behaviour. The changes to the surface structure of collagen fibres by cross-linkers have also been noted [19]. Therefore, detailed cellular response (i.e. tenocyte phenotype maintenance and tenogenic induction of stem cells) on collagen type I fibres should be assessed.

5.2.2 Influence of sex hormone-loaded scaffolds in human engineering

Hormones play a major role in the cellular functions and gender differences have been shown to affect receptor activation, immune system and disease onset [20-23]. Hormones, such as oestrogen, have been shown to affect collagen production and thus tendon structure and function. As oestrogen levels decline, collagen production declines and collagen fibrils reduce in diameter. Increased oestrogen levels protect tendons from rupture and injury, compared to males and menopausal women [24-26]. Oestrogen has been shown to directly impact cellular proliferation and synthesis of collagen [27-29]. Tendon has been shown to respond to oestrogen level as hormone specific receptors are located on tenocytes and tendon tissue [30, 31]. Testosterone affects collagen turnover and deposition levels by enhancing stiffness of tendons [32]. The effects of sex hormones on tendon mechanical properties and morphological structure are known, however, to date, they are not well understood [33, 34]. Therefore, sex hormones should be incorporated into collagen scaffolds of appropriate gender and their effect in tenocyte and stem cell (of appropriate gender as well) cultures should be assessed.

5.2.3 Influence of mechanical stimulation, sex hormones and collagen type I fibres in tenogenic phenotype maintenance and induction

Tendon is a load bearing tissue that transmits large tensile forces. It is a fibrillar tissue that consists of multiple aligned fibres. Tenocytes are mechanosensitive cells and therefore response to the mechanical cues [35-37]. Anisotropic structure has been shown to promote cell elongation, while mechanical cues have been shown to alter stem cell differentiation and tendon specific markers [38]. Furthermore, the biophysical cues from mechanical stimulation are known to cause changes in the gene regulation of cells [39]. Cyclic strain of 5 % on bone marrow stem cells induces expression of tenogenic markers such as collagen I, III, scleraxis and Mohawk that are responsible for tissue development. Moreover, micro-grooves play a role in alteration of gene expression during mechanical stimulation [40]. Sex hormones, especially oestrogen can increase collagen turnover [41]. Therefore, a multifactorial approach based on collagen type I fibres loaded with sex hormones and subjected to appropriate mechanical loading regimes should be assessed in both tenocyte and stem cell cultures (particular attention should be paid in the gender aspect, i.e. gender of the animal from

which the collagen was extracted from, gender-specific hormones and gender of the cell donors).

5.3 References

[1] C.A. Fleck, D. Chakravarthy, Understanding the mechanisms of collagen dressings, Adv Skin Wound Care 20(5) (2007) 256-259.

[2] W. Friess, Collagen-biomaterial for drug delivery, Eur J Pharm Biopharm 45(2) (1998) 113-136.

[3] C.H. Lee, A. Singla, Y. Lee, Biomedical applications of collagen, Int J Pharm 221(1-2) (2001) 1-22.

[4] J.P. McAleer, S. Sharma, E.M. Kaplan, G. Persich, Use of autologous platelet concentrate in a nonhealing lower extremity wound, Adv Skin Wound Care 19(7) (2006) 354-363.

[5] M. Yamauchi, M. Sricholpech, M. Terajima, K.B. Tomer, I. Perdivara, Glycosylation of type I collagen, Methods Mol Biol 1934 (2019) 127-144.

[6] Z. Ge, H. Tang, W. Chen, Y. Wang, C. Yuan, X. Tao, B. Zhou, K. Tang, Downregulation of type I collagen expression in the Achilles tendon by dexamethasone: A controlled laboratory study, J Orthop Surg Res 15(1) (2020) 70.

[7] M.G. McCoy, J.M. Wei, S. Choi, J.P. Goerger, W. Zipfel, C. Fischbach, Collagen fiber orientation regulates 3D vascular network formation and alignment, ACS Biomater Sci Eng 4(8) (2018) 2967-2976.

[8] H. Fujisaki, S. Futaki, K. Mizuno, S. Hattori, Evaluation of keratinocyte proliferation on two- and three-dimensional type I collagen substrates, J Vis Exp (146) (2019).

[9] D. Brett, A review of collagen and collagen-based wound dressings, Wounds 20(12) (2008) 347-356.

[10] M.M. Islam, D.B. AbuSamra, A. Chivu, P. Argüeso, C.H. Dohlman, H.K. Patra, J. Chodosh, M. González-Andrades, Optimization of collagen chemical crosslinking to restore biocompatibility of tissue-engineered scaffolds, Pharmaceutics 13(6) (2021).

[11] D.V. Bax, N. Davidenko, D. Gullberg, S.W. Hamaia, R.W. Farndale, S.M. Best, R.E. Cameron, Fundamental insight into the effect of carbodiimide crosslinking on cellular recognition of collagen-based scaffolds, Acta Biomater 49 (2017) 218-234.

[12] A. Sorushanova, L.M. Delgado, Z. Wu, N. Shologu, A. Kshirsagar, R. Raghunath, A. M Mullen, Y. Bayon, A. Pandit, M. Raghunath, D. Zeugolis, The collagen suprafamily: From biosynthesis to advanced biomaterial development, Adv Mater 31 (2018) e1801651.

[13] J.L. Puetzer, T. Ma, I. Sallent, A. Gelmi, M.M. Stevens, Driving hierarchical collagen fiber formation for functional tendon, ligament, and meniscus replacement, Biomaterials 269 (2021) 120527.
[14] D. Enea, J. Gwynne, S. Kew, M. Arumugam, J. Shepherd, R. Brooks, S. Ghose, S. Best, R. Cameron, N. Rushton, Collagen fibre implant for tendon and ligament biological augmentation. In vivo study in an ovine model, Knee Surg Sports Traumatol Arthrosc 21(8) (2013) 1783-1793.
[15] K.G. Cornwell, B.R. Downing, G.D. Pins, Characterizing fibroblast migration on discrete collagen threads for applications in tissue regeneration, J Biomed Mater Res A 71(1) (2004) 55-62.
[16] M. Sanami, I. Sweeney, Z. Shtein, S. Meirovich, A. Sorushanova, A.M. Mullen, M. Miraftab, O. Shoseyov, C. O'Dowd, A. Pandit, D. Zeugolis, The influence of poly(ethylene glycol) ether tetrasuccinimidyl glutarate on the structural, physical, and biological properties of collagen fibers: Multibranched PEG crosslinked collagen fibeRs, J Biomed Mater Res Part B Appl Biomater 104 (2015).
[17] W. Wang, J. He, B. Feng, Z. Zhang, W. Zhang, G. Zhou, Y. Cao, W. Fu, W. Liu, Aligned nanofibers direct human dermal fibroblasts to tenogenic phenotype in vitro and enhance tendon regeneration in vivo, Nanomedicine (Lond) 11(9) (2016) 1055-1072.
[18] T.L. Jenkins, D. Little, Synthetic scaffolds for musculoskeletal tissue engineering: cellular responses to fiber parameters, NPJ Regen Med 4 (2019) 15-15.
[19] W.K. Grier, E.M. Iyoha, B.A.C. Harley, The influence of pore size and stiffness on tenocyte bioactivity and transcriptomic stability in collagen-GAG scaffolds, J Mech Behav Biomed Mater 65 (2017) 295-305.
[20] V. Muller, A. Szabo, O. Viklicky, I. Gaul, S. Portl, T. Philipp, U.W. Heemann, Sex hormones and gender-related differences: their influence on chronic renal allograft rejection, Kidney Int 55(5) (1999) 2011-2020.
[21] R. Panchanathan, H. Shen, M.G. Bupp, K.A. Gould, D. Choubey, Female and male sex hormones differentially regulate expression of Ifi202, an interferon-inducible lupus susceptibility gene within the Nba2 interval, J Immunol 183(11) (2009) 7031-7038.
[22] G. Pinna, Sex and COVID-19: A protective role for reproductive steroids, Trends Endocrinol Metab 32(1) (2021) 3-6.

[23] A. Villa, P. Gelosa, L. Castiglioni, M. Cimino, N. Rizzi, G. Pepe, F. Lolli, E. Marcello, L. Sironi, E. Vegeto, A. Maggi, Sex-specific features of microglia from adult mice, Cell Rep 23(12) (2018) 3501-3511.

[24] P.A. Moalli, L.C. Talarico, V.W. Sung, W.L. Klingensmith, S.H. Shand, L.A. Meyn, S.C. Watkins, Impact of menopause on collagen subtypes in the arcus tendineous fasciae pelvis, Am J Obstet Gynecol 190(3) (2004) 620-627.

[25] J.L. Cook, K.M. Khan, P.R. Harcourt, Z.S. Kiss, M.W. Fehrmann, L. Griffiths, J.D. Wark, Patellar tendon ultrasonography in asymptomatic active athletes reveals hypoechoic regions: a study of 320 tendons. Victorian Institute of Sport Tendon Study Group, Clin J Sport Med 8(2) (1998) 73-77.

[26] D.R. Leblanc, M. Schneider, P. Angele, G. Vollmer, D. Docheva, The effect of estrogen on tendon and ligament metabolism and function, J Steroid Biochem Mol Biol 172 (2017) 106-116.

[27] M. Hansen, M. Kongsgaard, L. Holm, D. Skovgaard, S.P. Magnusson, K. Qvortrup, J.O. Larsen, P. Aagaard, M. Dahl, A. Serup, J. Frystyk, A. Flyvbjerg, H. Langberg, M. Kjaer, Effect of estrogen on tendon collagen synthesis, tendon structural characteristics, and biomechanical properties in postmenopausal women, J Appl Physiol 106(4) (2009) 1385-1393.

[28] S.H. Liu, R.A. Al-Shaikh, V. Panossian, G.A. Finerman, J.M. Lane, Estrogen affects the cellular metabolism of the anterior cruciate ligament. A potential explanation for female athletic injury, Am J Sports Med 25(5) (1997) 704-709.

[29] D. Iwańska, A. Kęska, E. Dadura, A. Wójcik, A. Mastalerz, C. Urbanik, The effect of the menstrual cycle on collagen metabolism, growth hormones and strength in young physically active women, Biol Sport 38(4) (2021) 721-728.

[30] D.A. Hart, J.M. Archambault, A. Kydd, C. Reno, C.B. Frank, W. Herzog, Gender and neurogenic variables in tendon biology and repetitive motion disorders, Clin Orthop Relat Res (351) (1998) 44-56.

[31] X. Bian, T. Liu, M. Yang, C. Gu, G. He, M. Zhou, H. Tang, K. Lu, F. Lai, F. Wang, Q. Yang, J. Gustafsson, X. Fan, K. Tang, The absence of oestrogen receptor beta disturbs collagen I type deposition during Achilles tendon healing by regulating the IRF5-CCL3 axis, J Cell Mol Med 24(17) (2020) 9925-9935.

[32] M. Hansen, M. Kjaer, Sex hormones and tendon, Adv Exp Med Biol 920 (2016) 139-149.

[33] C. Ganderton, A. Semciw, J. Cook, T. Pizzari, The effect of female sex hormone supplementation on tendon in pre and postmenopausal women: A systematic review, J Musculoskelet Neuronal Interact 16(2) (2016) 92-104.
[34] K.A. Bonilla, A.M. Pardes, B.R. Freedman, L.J. Soslowsky, Supraspinatus tendons have different mechanical properties across sex, J Biomech Eng 141(1) (2019) 0110021-0110028.
[35] M.T. Galloway, A.L. Lalley, J.T. Shearn, The role of mechanical loading in tendon development, maintenance, injury, and repair, J Bone Joint Surg AM 95(17) (2013) 1620-1628.
[36] A. Scott, P. Danielson, T. Abraham, G. Fong, A.V. Sampaio, T.M. Underhill, Mechanical force modulates scleraxis expression in bioartificial tendons, J Musculoskelet Neuronal Interact 11(2) (2011) 124-132.
[37] Y. Kubo, B. Hoffmann, K. Goltz, U. Schnakenberg, H. Jahr, R. Merkel, G. Schulze-Tanzil, T. Pufe, M. Tohidnezhad, Different frequency of cyclic tensile strain relates to anabolic/catabolic conditions consistent with immunohistochemical staining intensity in tenocytes, Int J Mol Sci 21(3) (2020).
[38] W.G. Grier, A.S. Moy, B.A. Harley, Cyclic tensile strain enhances human mesenchymal stem cell Smad 2/3 activation and tenogenic differentiation in anisotropic collagen-glycosaminoglycan scaffolds, Eur Cell Mater 33 (2017) 227-239.
[39] D. Kessler, S. Dethlefsen, I. Haase, M. Plomann, F. Hirche, T. Krieg, B. Eckes, Fibroblasts in mechanically stressed collagen lattices assume a "synthetic" phenotype, J Biol Chem 276(39) (2001) 36575-36585.
[40] Y. Morita, T. Sato, K. Higashiura, Y. Hirano, F. Matsubara, K. Oshima, K. Niwa, Y. Toku, G. Song, Q. Luo, Y. Ju, The optimal mechanical condition in stem cell-to-tenocyte differentiation determined with the homogeneous strain distributions and the cellular orientation control, Biol Open 8(5) (2019) bio039164.
[41] P. Torricelli, F. Veronesi, S. Pagani, N. Maffulli, S. Masiero, A. Frizziero, M. Fini, In vitro tenocyte metabolism in aging and oestrogen deficiency, Age 35(6) (2013) 2125-2136.

Appendices - Protocols and supplementary information

A. List of reagents

Table A.1: List of reagents and respective suppliers

Reagent	Supplier
alamarBlue®	Life Technologies, Ireland
4',6-diamidino-2-phenylindole (DAPI)	Sigma Aldrich, Ireland
4arm PEG Succinimidyl Glutarate MW 10,000 (4S-StarPEG)	Jenkem Technology, USA
Agilent RNA 6000 Nano kit	Agilent Technologies, Ireland
Acetic acid glacial	Fischer Chemical, Ireland
Acrylamide/bis-acrylamide 30 % solution	Sigma Aldrich, Ireland
Bovine serum albumin	Sigma Aldrich, Ireland
Bovine tendons	Local abattoirs, Ireland
Bovine skin	Local abattoirs, Ireland
Calcein AM	Life Technologies, Ireland
Calcium chloride	Sigma Aldrich, Ireland
Collagen type I standard	Symatese Biomateriaux, France
Collagen type I	Vornia Biomaterials Ltd, Ireland
Collagenase type I from Clostridium histolyticum	Sigma Aldrich, Ireland
DAPI (4’,6-diamidino-2-phenylindole)	Sigma Aldrich, Ireland
Dialysis tubing cellulose membrane	Sigma Aldrich, Ireland
Dimethyl sulfoxide	Sigma Aldrich, Ireland
Dulbecco’s Modified Eagle’s Medium high glucose	Sigma Aldrich, Ireland
Ethanol absolute	Lennox, Ireland
Ethidium homodimer I	Sigma Aldrich, Ireland
Foetal bovine serum	Sigma Aldrich, Ireland
Glacial acetic acid	Fisher Scientific, Ireland
Glycine	Fisher Chemicals, Ireland
Glutaraldehyde	Sigma Aldrich, Ireland
Hank’s balanced salt solution	Sigma Aldrich, Ireland

High Pure RNA Isolation kit	Roche, Germany
Human adult dermal fibroblasts	ATCC, LGC Standards, UK
Human tenocytes	DV Biologics, USA
Human derived leukemic monocyte cells (THP1)	ATCC, LGC Standards, UK
Hydrochloric acid 37 %	Sigma Aldrich, Ireland
Isopropanol	Sigma Aldrich, Ireland
Lipopolysaccharides	Sigma Aldrich, Ireland
Live/Dead® reagent	Invitrogen, Thermo Fisher Scientific, Ireland
N-(3-Dimethylaminopropyl)-N'-ethylcarbodiimide (EDC)	Sigma Aldrich, Ireland
N,N,N\'N\'-Tetramethyl-ethylenediamine (TEMED)	Bio-Rad, UK
N-hydroxysuccinimide (NHS)	Sigma Aldrich, Ireland
Ninhydrin	Sigma Aldrich, Ireland
Paraformaldehyde	Sigma Aldrich, Ireland
PEG	Sigma Aldrich, Ireland
Penicillin streptomycin	Sigma Aldrich, Ireland
Pepsin from gastric mucosa 3200 – 4500 units/mg protein	Sigma Aldrich, Ireland
Phenol red	Sigma Aldrich, Ireland
Picric acid-saturated solution 0.3 %	Sigma Aldrich, Ireland
Phosphate buffered saline tablets	Sigma Aldrich, Ireland
Porcine tendons	Local abattoirs, Ireland
Porcine skin	Local abattoirs, Ireland
Potassium phosphate monobasic	Sigma Aldrich, Ireland
Quant-iT™ PicoGreen® dsDNA assay	Life Technologies, Ireland
RPMI-1640 medium	Sigma Aldrich, Ireland
Rhodamine Phalloidin	Sigma Aldrich, Ireland
RIPA buffer	Sigma Aldrich, Ireland
SilverQuest™ Silver staining kit	Life Technologies, Ireland
Sodium dodecyl sulphate 20 % solution	Sigma Aldrich, Ireland

Sodium hydroxide	Sigma Aldrich, Ireland
Sodium phosphate dibasic	Sigma Aldrich, Ireland
Sodium phosphate monobasic	Sigma Aldrich, Ireland
Sodium chloride	Sigma Aldrich, Ireland
Tin(II) chloride	Sigma Aldrich, Ireland
Transcriptor First Strand cDNA synthesis kit	Roche, Germany
TRI Reagent ®	Sigma Aldrich, Ireland
Tris base	Fisher Chemicals, Ireland
Triton® X-100	Sigma Aldrich, Ireland
Trypsin / EDTA	Sigma Aldrich, Ireland

Table A.2: List of primary antibodies and respective suppliers

Antibody	Supplier
Fibronectin	Sigma Aldrich, Ireland
Collagen I	Abcam, United Kingdom
Collagen III	
Collagen IV	
Collagen V	
Collagen VI	
Scleraxis	
Tenomodulin	
Collagen II	
Aggrecan	
Osteocalcin	
Osteopontin	

Table A.3: List of secondary antibodies

Antibody	Supplier
Alexa Fluor® 488 Goat anti-mouse	Life Technologies, Ireland
Alexa Fluor® 488 Goat anti-rabbit	Life Technologies, Ireland

B. List of protocols

B.1 Collagen type I extraction

B.1.1 Material preparation and equipment

1. Frozen Bovine/Porcine Tendons.
2. 3.7 mM Na_2HPO_4 (Sodium phosphate dibasic).
3. 0.35 mM KH_2PO_4 (Potassium phosphate monobasic).
4. 51 mM NaCl (Sodium chloride).
5. Sodium Chloride.
6. Glacial Acetic Acid.
7. Pepsin (activity 3200-4500 U/mg of protein, stored at -20 ºC).
8. Filter.
9. Sieve.
10. Surgical scalpel.
11. Blender.
12. Magnetic stirrer and magnetic stirring bar.
13. Centrifuge, 500 ml centrifuge bottles
14. Weighing scales.

B.1.2 Extraction process

1. Wash skin to remove blood and the hair was removed with a scalpel.
2. Cut skin and tendon into small pieces using scalpel (1x1x1 cm^3).
3. Weigh out 200 g of each tissue.
4. Wash cut pieces in salt solutions (3.7 mM Na_2HPO_4, 0.35 mM KH_2PO_4, 51 mM NaCl) and stir gently at 4 ºC. Wash pieces three times for 2 hours each.
5. Suspend washed tendon and skin pieces in 0.5 M acetic acid for 48 hours and leave stirring at 4 ºC (50 ml acetic acid/g tissue).
6. Sieve the collagen solution and collect the swollen pieces of skin and tendon.
7. Blend the swollen pieces with a hand blender and suspend the gel-like solution in the original solution of acetic acid.
8. Allow the collagen solution to reach 20 ºC and add pepsin at a ratio of 1g pepsin:100 g tissue. Leave the collagen solution for 1 hour and then put under stirring at 4 ºC for 48 hours.
9. Filter the collagen solution through a sieve and 250 µm mesh to remove the insoluble pieces.

10. Add 0.9 M NaCl to the filtered solution and stir. Leave the collagen solution to precipitate overnight.

11. Collect the precipitated collagen at the top of the solution with a sieve and a mesh.

12. Squeeze the water out of the collagen using a mesh and record the dry weight of collagen.

13. Re-suspend the dry collagen in 1 M acetic acid and lightly stir at 4 ºC until it comes into solution for 24 hours.

14. Centrifuge the collagen solution at 8,000 rpm for 2 minutes at 4 ºC. Collect only the top liquid and discard any precipitate.

15. Add 0.9 M NaCl to the re-suspended collagen solution and stir. Leave the collagen solution to precipitate overnight.

16. Collect the precipitated collagen at the top of the solution with a sieve and a mesh.

17. Squeeze the water out of the collagen using a mesh and record the dry weight of collagen.

18. Re-suspend collagen in minimum volume of 1 M acetic acid to produce highly concentrated collagen solution.

19. Once fully suspended, dialyse collagen against 1mM acetic acid 4 times changing the acetic acid every 2 hours. Last dialysis is overnight.

20. Check the purity with SDS-PAGE.

B.2 Sodium dodecyl sulphate polyacrylamide gel electrophoresis (SDS-PAGE)

B.2.1 Material preparation

1. 1.875 M Tris-HCl, pH 8.8. Dissolve 22.70 g Tris-base (Bio-Rad, 161-0716) in 80 ml ddH_2O; add 2 ml concentrated HCl (37%), leave it overnight to equilibrate, adjust pH to 8.8 with a few drops concentrated HCl, make it up to 100 ml with ddH_2O. Keep it at 4-8 ºC
2. 1.25 M Tris-HCl, pH 6.8. Dissolve 15.14 g Tris-base in 70 ml ddH2O; add 7 ml concentrated HCl (37 %), leave it overnight to equilibrate, adjust pH to 6.8 with a few drops concentrated HCl, make it up to 100 ml with ddH_2O. Keep it at 4-8 ºC
3. 5x sample buffer. Dissolve completely 0.25 g SDS (Bio-Rad 161-0301) in 0.625 ml 1.25 M Tris-HCl, pH 6.8 and 2 ml ultrapure water. Leave it overnight for the foam to settle. Top up with glycerol (Bio-Rad) to 5 ml (approximately 2.3 ml). Add 2.5 mg bromophenol blue (Bio-Rad 161-0404) per 10 ml buffer.
4. 5x running buffer. Dissolve 15.1 g Tris-base (Bio-Rad 161-0716), 72 g glycine (Bio-Rad 161-0718) and 5 g SDS (Bio-Rad 161-0301) in 1 l ddH_2O. Store at 4 ºC. 1x running buffer is made to run the gel from 5x running buffer by diluting in ddH_2O. Alternatively, 10x Tris-Glycine-SDS 5lt tube can be purchased (Bio-Rad 161-0772). 1x running buffer is made to run the gel from 10x running buffer by diluting in ddH_2O.
5. 30 % Acrylamide/Bis (37.5:1) (Bio-Rad, 161-0158)
6. 10 % SDS (Bio-Rad, 161-0416)
7. 100 mg/ml Ammonium Persulphate (Bio-Rad, 161-0700) in ddH_2O. Dissolve 500 mg APS in 5 ml ddH_2O, aliquot it in Eppendorf tubes and keep it at – 20 ºC. The solution is active for a few months.
8. TEMED (Bio-Rad, 161-0800)
9. 10 % and 70 % Ethanol in dH_2O
10. Phenol Red Solution: Dissolve 10 mg of phenol red in 40 ml of ddH_2O, then dilute to 50 ml.

B.2.2 Sample collection

1. Freeze dry the extracted collagen into a sponge.
2. Dissolve the sponges in 0.5 M acetic acid to a concentration of 1 mg/ml.

B.2.3 Sample preparation

1. Take the collagen sponge samples and collagen standard in a fresh 1.5 ml centrifuge tube (24 µl each).
2. Add 24 µl of double distilled water in these samples.
3. Add 12 µl of 5X sample buffers to get 5:1 dilution.
4. Vortex the samples and centrifuge them briefly. Store them at 4 °C.
5. Prior to SDS-PAGE, denature the samples and standard by heating at 95 °C for 5 minutes.
6. Vortex and then centrifuge the samples briefly.
7. Load 15 µl per well in Mini gel (for 10-well: 15 µl and for 15-well: 10 µl).
8. Empty well: 15 µl of 1x sample buffer (diluted from 5x sample buffer with water)

Table B.1: Detailed sample preparation for SDS-PAGE

Sample	Total volume on the well	Collagen standard/ sample composition
Mini gel; 10-well	15 μl (1 μg of sample per well)	4 μl sample 4 μl NaOH 1N 34 μl dH2O 18 μl 5x sample buffer

B.2.4 Gel preparation

1. Clean glass plates with 70 % ethanol and wipe dry with tissue paper.
2. Set the gel making apparatus ensuring that the glass plates fit snugly to the platform (mini gel: 1mm space using appropriate spacers).
3. Check for any leaks by pouring water prior to making the gels.
4. Add the gel ingredients to make the 5 % resolving gel according to Table B.5.
5. Make sure to add the APS and TEMED last, right before the gels are to be poured.
6. Using a Pasteur pipette, pour the prepared mixture carefully into the space between the 2 glass plates to reach about 1 cm (mini gel) from the bottom of the wells etched out by the comb (keep the excess solution to check how quickly the gels will be polymerised).
7. Overlay the gel with 10 % Ethanol to cut off oxygen in contact with the gels.

8. Leave it aside for approximately 30 minutes until set (check with the excess solution remained).
9. During the setting period, prepare the 3 % stacking gel according to the Table B.6 (do not add the APS and TEMED until the gel is ready for pouring).
10. A line at the ethanol-gel interface that initially had disappeared will reappear when polymerization is complete.
11. Carefully aspirate the ethanol out of the glass plates using a syringe and imbibe any traces using filter paper.
12. Now add the APS and TEMED to the stacking gel and carefully pour it on top of the polymerised resolving gel. Immediately insert the comb taking care to avoid trapping any air bubbles (keep the excess solution to check how quickly the gels will be polymerised).
13. Allow it to set for 10-15 minutes and, in the meantime, denature samples and standards at 95 °C as described above.
14. After the gels have been set (10 - 15 minutes, check it with the excess solution), remove the combs slowly.
15. Assemble the electrophoresis apparatus, for small gel apparatus, fit the gel plates on the electrode bar and fit the set into the inner chamber and clamp them.
16. Fill the upper/inner chamber with 1x running buffer.
17. Wash the wells by squirting buffer into the wells with a hypodermal needle syringe to remove all air bubbles.
18. Load the standards, samples and markers using Hamilton syringe. Wash the syringe in between using the running buffer in the chamber (at least 5-times).
19. Put the upper chamber on the main chamber, close the lid and run the gel(s).
20. For the mini gel: run at constant voltage (50 V) until the front reaches the end of the stacking gel (± 30 - 40 min), then increase voltage to 120 V until the front reaches the end of the separating gel (± 1 hour).
21. Remove the glass using the wonder wedge, cut the lower right hand corner and release the gel slowly into dH2O.

Table B.2: 5 % Separation Gel (1mm thickness) for collagen for mini gel (Protean II Bio-Rad)

	1 Gel	**2 Gels**

30 % Acrylamide/Bis (37.5:1)	830 μl	1660 μl
1.875 M Tris-HCl pH 8.8	1000 μl	2000 μl
10 % SDS	50 μl	100 μl
ddH2O	3070 μl	6140 μl
APS (100 mg/ml)	42 μl	84 μl
TEMED	5 μl	10 μl
Total	5000 μl	10000 μl

Table B.3: 3 % Stacking Gel (1mm thickness) for collagen for mini gel (Protean II Bio-Rad)

	1 Gel	**2 Gels**
30 % Acrylamide/Bis (37.5:1)	200 μl	400 μl
1.25 M Tris-HCl pH 6.8	200 μl	400 μl
10 % SDS	33 μl	66 μl
ddH2O	1550 μl	3100 μl
APS (100 mg/ml)	17 μl	33 μl
TEMED	3 μl	6 μl
Total	2000 μl	4000 μl

B.2.5 Silver staining

To stain the gels obtained in the previous steps the SilverQuest™ Silver Staining kit was used. The procedure for the Basic Protocol is detailed in Table B.7.

Table B.4: Detailed procedure for silver staining

Step	**Reagent**	**Total volume**	**Incubation time**
Fix	40 ml ethanol 10 ml acetic acid 50 ml water	100 ml	20 minutes
Wash	30 ml ethanol 70 ml water	100 ml	10 minutes
Sensitise	30 ml ethanol	100 ml	10 minutes

	10 ml sensitiser 60 ml water		
First wash	30 ml ethanol 70 ml water	100 ml	10 minutes
Second wash	100 ml water	100 ml	10 minutes
Stain	1 ml stainer 99 ml water	100 ml	15 minutes
Develop	10 ml developer 1 drop developer enhancer 90 ml water	100 ml	5-8 minutes
Stop	10 ml Stopper (add directly to the developing solution)	100 ml	10 minutes
Wash	100 ml water	100 ml	10 minutes

B.3 Lyophilisation: Freeze drying

Freeze-drying (also known as ice crystal templating or lyophilisation or ice-segregation-induced self-assembly) was used to fabricate the collagen sponges. 24 well plates were used to fabricate sponges for stability analysis and 48 well plates were used to fabricate sponges for biological analysis.

B.3.1 Material preparation and equipment

1. Well plate(s).
2. Collagen
3. Multipette® plus
4. Freeze dryer (Labconco)

B.3.2 Freeze drying process

1. Pipette collagen type I (Multipette® plus) in 24 and 48 well plates.
2. Freeze collagen at -80 ^{o}C overnight.
3. Place the plates in the freeze dryer (Labconco) for 24 hours.

B.4 Extrusion of collagen fibres

B.4.1 Material preparation and equipment

1. 5 ml syringe.
2. Gauge needle/ precision tip.
3. Silicone tubing.
4. Weight.
5. Syringe pump.
6. Water bath.
7. Fibre formation buffer (20 % PEG, 94 mM sodium phosphate dibasic, 24 mM sodium phosphate monobasic, pH 7.8).
8. Fibre incubation buffer (5.5 mM sodium phosphate dibasic, 1.5 mM potassium phosphate monobasic, 75 mM sodium chloride, pH 7.1).

B.4.2 Fibre formation buffer preparation

1. Weigh out 94 mM sodium phosphate dibasic and 24 mM sodium phosphate monobasic.
2. Transfer to a large beaker, add 1000ml of water and add a stir bar.
3. Allow to stir until dissolved.
4. Weigh out 20 % PEG and add in small amounts to the centre of the solution.
5. Allow to stir until dissolved.
6. Bring up the solution to the required volume by adding water.
7. Adjust the pH by using a pH meter.
8. Rinse pH meter with water and calibrate the pH meter with pH 7 and pH 9.2.
9. Place the pH meter into the solution.
10. Add NaOH 10M drop by drop, to neutralise the solution to pH 7.8.
11. Transfer to a bottle.

B.4.3 Fibre incubation buffer preparation

1. Transfer to a large beaker, add 2000 ml of water and add a stir bar.
2. Allow to stir until dissolved.
3. Adjust the pH by using a pH meter.
4. Rinse pH meter with water and calibrate the pH meter with pH 7 and pH 9.2.
5. Place the pH meter into the solution.
6. Slowly add HCL 6 M drop by drop, to acidify the solution to pH 7.1

7. Transfer to a bottle.

B.4.4 Extrusion method

1. Heat fibre formation buffer and fibre incubation buffer to 37 °C in incubator.
2. While water bath is heating fill 5 cc syringe with required amount of collagen (5ml of collagen = approximately 12 fibres).
3. Place the filled syringe onto the syringe pump and secure with the required clamp.
4. Turn on the pump and input the following parameters:
    - Chart
    - BD Plastics syringes (5 cc)
    - Volume = 0 (continuous)
    - Rate = 0.4 ml/min
5. Connect the silicone tubing to the FFB container, via the silicone tubing, to the free end of the syringe.
6. Confirm tubing is secured to the syringe.
7. Begin extrusion of collagen solution.
8. Allow air bubbles to clear.
9. Start air flow to guide extrusion of collagen fibre.
10. Stop the pump once the end of the container has been reached.
11. Leave for 5-10 minutes in fibre formation buffer.
12. Transfer by securing to free end of stainless steel rod and leave for 5-10 minutes in fibre incubation buffer.
13. Transfer to either to distilled water, cross-linker or PBS and leave for 2 hours
14. After 2 hours rinse 5 times in distilled water and dry the fibres under the tension of their own weight.

B.5 Cross-linking methods

1. 4-StarPEG (4-arm polyethylene glycol succinimidyl glutarate MW 10,000): Concentrations of 0.5 mM, 1 mM, 2.5 mM and 5 mM.
2. EDC/NHS (1-ethyl-3-(3-dimethylaminopropyl)carbodiimide and N-Hydroxy-succinimide): 60 mM (Ratio 5:5:1, RDC: NHS: COOH (MES)).
3. GTA (Glutaraldehyde): 0.625 %.

B.5.1 Cross-linking method: Collagen I fibres

1. Make up the cross-linker to the desired concentration.
2. Transfer the cross-linking solution into a container.
3. Add the collagen fibres into the container and cross-link for 2 hours.
4. For non-crosslinked fibres, wash the fibres in double distilled water for 5 minutes.
5. After washing step, air dry the fibres at room temperature.

B.5.2 Cross-linking method: Collagen I sponges

1. Add the cross-linking solution to collagen I to the desired final concentration.
2. Add the desired amount of collagen into 24 or 48 well plate(s) and freeze at -80 ^{o}C overnight.
3. Place the plates in the freeze dryer (Labconco) for 24 hours.

B.6 Scanning electron microscopy (SEM)

Surface characteristics of the cross-linked collagen fibres were analysed by SEM imaging.

1. Gold coat the collagen fibres prior to SEM imaging.
2. Gold coat at current of 25 milliamps (mA) for 5 minutes.
3. Visualise the fibres at 10 µm and 300 µm.

B.7 Polarised microscopy

The alignment of the collagen fibres was assessed with Polarised Microscopy. Randomly aligned collagen film was used as a control.

1. At 90 º the collagen fibres reached distinction phase where the fibre did not light up.
2. The fibres were turned 45 º angle and all of the regions on the fibre lit up, which indicates alignment.

B.8 Ninhydrin assay for free amine quantification

B.8.1 Material preparation

1. Collagen samples.
2. 4 % ninhydrin powder.
3. Glysine (stock solution).
4. 2 ethoxy ethan
5. 200 mM citric acid
6. Trin II chloride

B.8.2 Sample preparation and method

1. Weight the samples 2.5 to 3 mg.
2. Place into a labelled Eppendorf tube.
3. Add 200 µl dH2O to each sample.
4. Prepare a standard curve of glycine at 0, 0.01, 0.05, 0.1, 0.2 and 0.5 mg/ml.
5. Prepare one tube of 4 % ninhydrin powder in 2-ethoxyethanol and protect from light.
6. Prepare a second tube of 200 mM citric acid, 0.16 w/v % Tin II Chloride, pH 5.0.
7. Mix both solutions together.
8. Add 1 ml Ninhydrin solution to each tube.
9. Incubate tubes at 95-100 ºC for 30-35 minutes, protecting from light.
10. Allow tubes to cool to room temperature.
11. Add 250 µl of 50 % isopropanol and vortex.
12. Read using plate reader at 570 nm.

B.9 Collagenase: Degradation/ enzymatic resistance assay

The enzymatic degradation is a process that occurs during the remodelling process when a collagen scaffold is implanted in the body. Different enzymes (mainly proteases and more specifically matrix metalloproteases (MMPs) are responsible for the material degradation.

B.9.1 Material preparation

1. Tris buffer: 0.1 M TrisHCl + 500 mM $CaCl_2$
    - Dilute 6.207 g of Tris-base in 400 ml of dH_2O
    - Adjust the pH to 7.4 with HCl and make up the volume to 500 ml with dH_2O
    - Add 3.55 g of $CaCl_2$
2. Collagenase I (MMP-I): Activity 50 U (sponges) (Sigma ref C0130)
3. Collagen samples (sponges or fibres)

B.9.2 Sample preparation and method

1. Weigh out 5 mg of sample and place in Eppendorf tubes (sample was weighed with Eppendorf tube).
2. Prepare collagenase type I in tris buffer of 50U/ml.

x samples $*$ 1 $ml/_{sample}$ $*$ (x) $U/_{ml}$ $*$ $\frac{1}{125}$ mg/U = (x) mg of collagenase

3. Add 1ml of collagenase and buffer solution to the samples.
4. Incubate the samples at 37 ºC for the required time-points (3, 6, 9, 12 and 24 hours).
5. After the time-points, centrifuge the samples at 1200 rpm for 10 minutes.
6. Remove the supernatant carefully, make a hole in each of the Eppendorfs and place the samples in the freeze dryer overnight.
7. Weigh out the Eppendorf and calculate the weight loss.

$$\Delta W = \frac{Wo - WT}{Wo} \times 100$$

Wo = initial weight, Wt = weight of the sample after degradation

B.10 Differential scanning calorimetry (DSC): Thermal stability

B.10.1 Method

1. Immerse sample in 1x PBS overnight.
2. Roughly dry off samples with whatman or blotting paper.
3. Tare scale with pan on it.
4. Place sample in the pan and weigh out 15-20 mg.
5. Record weight of samples.
6. Place the lid on the pan and seal using a crimper.
7. Make a reference pan (empty sealed pan).
8. Place in DSC stage (Equipment: DSC-60 (Shimdzy)).
9. Close the door of stage.
10. Set up temperature programme and sampling parameters (20 ºC to 70 ºC at a rate of 10 ºC/min.
11. Run the programme.
12. Analyse the peaks.

B.11 Compression: Mechanical properties of collagen type I sponges

Compression test was carried out to assess mechanical properties of collagen type I sponges. The collagen sponges were tested in dry state as the sponges were collapsing in wet state and the testing was not successful. The height of the sponges was recorded for determination of engineering stress-strain curves from the load- extension graphs. Deformation of the sponges was recorded at 70% deformation.

B.11.1 Method

1. Set up programme for compression test.
2. Mark auto tool separation.
3. Select appropriate specimen shape (round shape).
4. Set up the test parameters (Maximum deformation: 70 %, Test speed: 10 mm/min, Load cell: 10 N).
5. Select the desired output data and parameters for the report.
6. Load the sample.
7. Input the thickness and work out 70 % deformation and input the value.
8. Zero the force and start the test.
9. Once the sample breaks in the middle, press stop and save the data.
10. Use raw data to work out force, stress and modulus.

B.12 Uniaxial tensile testing: Mechanical properties of collagen type I fibres

Uniaxial tensile test was carried out to assess mechanical properties. The collagen fibres were left in PBS overnight and were tested in wet state. It was assumed that the fibres were circular for determination of engineering stress-strain curves from the load- extension graphs. The stress at break was defined as the load at failure divided by the original cross-sectional area. The strain at break was defined as the increase in length in maximum load divided by the original length and modulus will be calculated at 2 %.

B.12.1 Material preparation and equipment

1. Zwick/Roell (Leominster, Herefordshire, UK) Z005 testing machine (10 N load cell).
2. Digital callipers Scienceware®, Digi-Max™, Sigma-Aldrich, Ireland.
3. 1 X PBS
4. Sample.
5. Blotting paper.

B.12.2 Method

1. Immerse samples in PBS overnight.
2. Before testing, blot the excess off.
3. Measure fibre diameter using callipers.
4. Place the fibre between the clamps at the top and bottom.
5. Set the parameters and run the machine.

B.13 Swelling

1. Image fibres dry.
2. Incubate collagen fibres in PBS overnight.
3. Blot using filter paper to remove excess surface water.
4. Image fibres wet.
5. Measure the width of the fibres.
6. Calculate swelling ratio as following: Swelling (%) = [(Ww - Wd)/ (Wd)] x 100, where Ww and Wd refer to the average wet diameter and average dry diameter of the fibres respectively.

B.14 Scaffold sterilisation

B.14.1 UV sterilisation: Collagen type I sponges

1. Remove the 48 well plate from the freezer dryer.
2. Place the well plate, with the lid open, into a laminar hood.
3. Turn on the UV for 2 hours.

B.14.2 Ethanol sterilisation: Collagen type I fibres

1. Place the fibre bundles into a petri dish.
2. Spray down the petri dish and place into a laminar hood.
3. Wash fibres with Hanks Balance Salt Solution (HBSS) three times for 15 minutes each.
4. Prepare 70 % IMS.
5. Add 1 ml of IMS to each scaffold.
6. Leave to sterilise for overnight.
7. Remove IMS and wash the scaffolds with HBSS three time, 15 minutes each.
8. Leave fibres under UV for 1 hour

B.15 Cell culture

B.15.1 Culture media preparation for human adult dermal fibroblasts and tenocytes

1. Dulbecco's Modified Eagle's Medium (DMEM) high glucose (45000 mg/l)
3. 10 % Foetal bovine serum (FBS)
4. 1 % Penicillin streptomycin

B.15.2 Cell culture and culture media preparation for THP1 cells (macrophages)

Expansion

1. RPMI 1640 medium supplemented with 10 % FBS, 1 % P/S and 1 % glutamine.
2. Seed at 300,000 cells/ml.
3. Daily observation in the optical microscope for morphology check.
4. Top up with fresh media every second day or when cell concentration reaches 800,000 cells/ml (Do not allow the cell concentration to exceed 1,000,000 cells/ml).
5. Spin down and use fresh media every 7 days.

Differentiation

1. Use THP-1 cells when their density reaches 800,000-1,000,000 cells/ml.
2. Dilute PMA in DMSO at 5 μg/ml.
3. Add 100 μl PMA at 5 μg/ml for each 50 ml supplemented RPMI 1640 medium (10 ng/ml).
4. Spin down the cells and re-suspend them with the medium of differentiation.
5. Count the THP-1 cells with haematocytometer.
6. Seed cells at a density of 50,000 cells per sponge in a 48 well plate.
7. Incubate cells at 37 °C for 24 hours.
8. Check the differentiation by observation at the microscope. If you see floating cells (undifferentiated), incubate for 24 hours more.
9. Then, remove the media and replace it by normal medium or activation medium (1ml/well). Activation medium is supplemented RPMI 1640 medium with 100 ng/ml LPS (2.5 μl of LPS stock solution at 2 mg/ml for 50 ml medium).
10. Incubate the cells for 48 hours at 37 °C.

B.15.3 Cell thawing and passaging

1. Remove vial from liquid nitrogen container and thaw in water bath at 37 ºC.
2. Transfer contents to culture flask of appropriate size and add pre-warmed culture medium.
3. Change medium every 2-3 days and monitor cell proliferation with a phase contrast microscope.
4. When cells cover more than 80 % of the culture flask, remove culture medium, wash cell layer with Hank's Balanced Salt Solution (HBSS) and add 5 ml of trypsin / EDTA. Incubate at 37 ºC for 5 minutes until cells start detaching.
5. Add 5ml of culture medium to neutralise the action of trypsin / EDTA and transfer flask contents into a tube and centrifuge at 1200 rpm for 5 minutes.
6. Discard the supernatant and re-suspend cells in desired amount of medium.

B.15.4 Cell freezing

1. Aspirate culture medium and wash cell layer with HBSS.
2. Add trypsin / EDTA and incubate at 37 ºC for 5 minutes.
3. Add culture medium to neutralise the action of trypsin, collect flask contents into a tube and centrifuge at 1200 rpm for 5 minutes.
4. Re-suspend supernatant in 1 ml of medium and count cells using a Neubauer chamber.
5. Re-suspend cells in necessary amount of freezing medium (90 % growth medium with 10 % of DMSO) to have 1 million cells per millilitre of medium.
6. Add 1 ml of cell suspension per cryogenic vial and place in Mr. Frosty overnight at -80 ºC.
7. Move to liquid nitrogen for long term storage.

B.15.5 Cell seeding

1. When cells have become ~80 % confluent in tissue culture flask remove from incubator.
2. Remove cell media and discard.
3. Add 5 ml of pre-warmed Hanks balanced salt solution.
4. Gently agitate the cell culture flask.
5. Remove Hanks balanced salt solution and discard.

6. Add 3 ml of pre-warmed trypsin EDTA. Note: 3ml is sufficient for T-75 flasks. Use 5 ml for T-175 flasks.
7. Place in incubator for 5 minutes.
8. Upon removal from incubator view the cells under light microscope. If cells have not detached gently tap the base of the flask to dislodge the remaining cells.
9. Return to laminar flow hood and add 7 ml of cell media.
10. Gently agitate flask.
11. Remove contents of flask and deposit in a 15 ml tube.
12. Centrifuge the tube at 1200 rpm for 5 minutes.
13. Remove supernatant and discard taking care not to disturb the cell pellet at the base of the tube.
14. Add media (1-5 ml) to resuspend the pellet. Aspirate the media to homogenise the cells.
15. Remove 10 µl for use with the haemocytometer.
16. Place under the light microscope and count the number of cells in the centre square on opposing sides of the haemocytometer.
17. Calculate the average cell number on opposing sides.
18. Multiply by 10,000 to calculate the number of cells/ml in 15 ml tube. Depending on the number of ml in the tube the total cell number can be calculated.
19. Dilute the cells as per number required per well.
20. Place sterile scaffolds at the base of the well.
21. Add appropriate amount of cell media containing appropriate number of cells.
22. Place well plate in incubator at 37 °C and 5 % CO_2 until the time point.

B.16 alamarBlue® assay

1. Prepare a 10 % alamarBlue® solution in HBSS.
2. Remove culture medium from the cells and wash with HBSS.
3. If using a scaffold, move scaffold to new well plate.
4. Add 1 ml of the diluted alamarBlue® solution to the cells and a negative control of alamarBlue® at 10 % alone
5. To obtain the background absorbance, add HBSS to empty wells.
6. Incubate for 3 hours at 37 ºC, 5 % CO_2.
7. Transfer 100 µl of the alamarBlue® solution and of the negative control and background to a clear 96 well plate.
8. Measure the absorbance at 550 nm and at 595 nm.
9. Subtract the values of HBSS to the values of alamarBlue® alone from both absorbances to obtain the absorbance of alamarBlue®. For 550 nm this value is called
10. absorbance of the oxidised form at lower wavelength (AOLW) and for 595 nm it is called absorbance of the oxidised form at higher wavelength (AOHW).
11. Calculate the correlation factor:
    Ro=AOLW/AOHW
12. To calculate the percentage of alamarBlue® reduced (AR) by the cells use the
13. following:
    AR=ALW-(AHW*Ro)*100

B.17 Live / Dead assay

1. Prepare staining solution by diluting calcein AM to 4 μM and ethidium homodimer-1 to 2 μM in HBSS.
1. To prepare a negative control, sample can be immersed in dimethyl sulfoxide (DMSO) to kill all cells before staining.
2. Remove culture medium from the cells and wash cells with HBSS.
3. Add staining solution to cells (enough volume to cover completely the sample).
4. Incubate at 37 ºC, 5 % CO_2 for 30 minutes.
5. Image under inverted fluorescence microscope:
    - Calcein AM: use FITC filter
    - Ethidium homodimer-1: use Texas Red filter

B.18 Cytoskeleton and nuclei staining

1. At each time point remove culture medium and wash cell layer with HBSS.
2. Fix the cell layer with 2 % paraformaldehyde (PFA) for 15 minutes at room temperature.
3. Remove PFA and wash briefly with HBSS.
4. Add 0.2 % of Triton-X100 (enough to cover the sample) and incubate for 5 minutes at room temperature.
5. Remove Triton-X100 and wash with phosphate buffered saline (PBS).
6. Add Rhodamine-phalloidin diluted in PBS (1:500) and incubate at room temperature for 1 hour.
7. Wash samples briefly with PBS.
8. Incubate with DAPI in 1x PBS for 5 minutes at room temperature.
9. Image under the inverted fluorescence microscope.

B.19 Cell morphometric analysis

1. Open ImageJ software.
2. File > Open > Select Image
3. For merged images: Image > Colour > Split channels
4. Image > Colour > Channels tools > More > select appropriate colour for each channel.
5. Select freehand tool and trace around the nucleus / cytoskeleton of the cell.
6. Analyse > Set measurements > Select Area, Shape descriptors, Feret's diameter.
7. Analyse > Measure (or Ctr M) to take measurement of selected area.
8. Measured parameters will appear in a separate screen.
9. Press Ctr D to mark the outline of measured area.
10. Repeat for each cell.

B.20 PicoGreen®

B.20.1 Material preparation

1. 96-well white opaque plates.
2. Falcon tubes (50 ml).
3. Micro-pipettes and tips.
4. Microplate reader.
5. Vortex.
6. Ultra-pure water.
7. Pico Green Kit (Molecular Probes, P-7589) (PicoGreen dsDNA quantification reagent, 20X TE and DNA standard).

B.20.2 Sample preparation

Scaffold

1. Remove media.
1. Wash samples with HBSS.
2. Transfer samples into fresh Eppendorf tubes.
3. Add 1 ml of ultra-pure water.
4. Freeze at - 80 °C until use.

TCP

1. Remove media.
2. Wash samples with HBSS.
3. Add ultra-pure water.
4. Scrape with a tip.
5. Pipette solution into a fresh Eppendorf tube.
6. Freeze at - 80 °C until use.

B.20.3 Method

1. Prepare TE by diluting 20x TE 20-fold in sterile ultra-pure water.
2. Prepare the DNA standard for the standard curve in ultra-pure water (concentrations of 0 µg/ml, 0.2 µg/ml, 0.5 µg/ml, 1 µg/ml and 2 µg/ml).
3. Dilute 200-fold the PicoGreen dsDNA quantification kit with 1x TE.
4. Remove samples from the freezer and heat up at 60 °C.
5. Vortex the samples.

6. Remove the required amount of sample (21.7 µl).
7. In each well of the 96-well white opaque plate add 21.7 µl of sample, 71.3 µl of PicoGreen solution and 100 µl of 1x TE (make triplicates of samples or standard).
8. Incubate the plate in the dark for 10 minutes.
9. Read fluorescence: Excitation of 485/20 nm and Emission of 528/20 nm.
10. Read of DNA concentration from standard graph.

B.21 Immunocytochemistry

1. At the end of culture time points, aspirate the medium and was cell layer with HBSS.
2. Fix with 2 % PFA (pre-cooled at 4 °C) for 15 minutes.
3. To make 2 % PFA (in glass bottle with magnetic stirrer): Weight 0.2 g of PFA and add 10 ml of PBS. Put on a magnetic stirrer with heater. Leave it for around 1 hour (put the cap on, but loosen it). Cool it and keep it at 4 °C.
4. Drain away fixative and wash 3x with PBS, 5 minutes each.
5. Block with 3 % (w/v) BSA in 1x PBS for 30 minutes at room temperature (RT).
6. To make 3 % BSA: weight 0.3 g of BSA and add 10 ml of PBS. Put on a magnetic stirrer and leave it for around 1 hour. Store it at 4 °C.
7. Incubate with primary antibody in 1x PBS for 90 minutes at room temperature or overnight at 4 °C. List of primary antibodies used can be found in Table B.8.
8. Wash 3x with 1x PBS, 5 minutes each.
9. Incubate with secondary antibody in 1x PBS for 30 minutes at room temperature.
10. List of secondary antibodies can be found in Table B.9.
11. Wash 3x with 1x PBS, 5 minutes each.
12. Incubate with DAPI in 1x PBS for 5 minutes at room temperature.
13. Wash 3x with PBS, 5 minutes each.
14. Image samples under Confocal microscope (Andor Revolution Spinning Disk Confocal Microscope (Olympus IX81).

Table B.5: Primary antibody source and dilution

Antibody	Source	Dilution
Fibronectin	Mouse monoclonal	1:200
Collagen I	Mouse monoclonal	1:200
Collagen III	Rabbit polyclonal	1:200
Collagen IV	Rabbit polyclonal	1:200
Collagen V	Rabbit polyclonal	1:200

Collagen VI	Rabbit polyclonal	1:200
Scleraxis	Rabbit polyclonal	1:200
Tenomodulin	Rabbit polyclonal	1:200
Collagen II	Mouse monoclonal	1:200
Aggrecan	Rabbit polyclonal	1:200
Osteocalcin	Mouse monoclonal	1:200
Osteopontin	Rabbit polyclonal	1:200

Table B.6: Secondary antibody source and dilution

Antibody	**Source**	**Dilution**
Alexa Fluor® 488	Goat anti – rabbit	1:200
Alexa Fluor® 488	Goat anti - mouse	1:200

B.22 Gene array

B.22.1 Total RNA isolation using High Pure RNA isolation kit (Roche, Germany)

1. At each time point remove media from cells.
2. Place the scaffold in a fresh Eppendorf.
3. Add 1 ml of TRI Reagent® with iron oxide beads to lyse the cells.
4. Incubate under shaking conditions at 4 ºC for 5 minutes.
5. Remove all lysed cells into Eppendorf tubes.
6. Centrifuge at top speed to remove sediments and transfer supernatant into a clean Eppendorf.
7. Add 200 µl of chloroform (without isoamyl alcohol) for every 1 ml of TRI Reagent® used.
8. Vortex for 15 seconds.
9. Incubate at room temperature for 5 minutes.
10. Centrifuge at 13,000 rpm at 4 ºC for 15 minutes.
11. Transfer aqueous phase (colourless top layer) to a clean tube containing the same volume of 70 % ethanol and mix with pipette.
12. Transfer the entire volume to a filter column.
13. Centrifuge at 8.000 g for 15 seconds and discard flow through.
14. Add 500 µl of Wash 1 (black cap) and centrifuge at 8.000 g for 15 seconds and discard flow through.
15. Add 500 µl of Wash 2 (blue cap) and centrifuge at 8.000 g for 15 seconds and discard flow through.
16. Add 200 µl of Wash 2 (blue cap) and centrifuge at 13.000 g for 2 minutes and discard flow through.
17. Place filter in a new tube and add 50 µl of elution buffer and centrifuge at 8.000 g for 1 minute.
18. Take the 50 µl and put them again in the filter column and centrifuge at 8.000 g for 1 minute.
19. Aliquot 45 µl for cDNA synthesis and 5 µl for RNA quantity and quality testing.

B.22.2 Assessment of RNA quantity and quality

RNA quantity

1. Blank NanoDrop 1000 by using 1 µl of DNase free water.
2. Add 1 µl of sample and measure concentration.
3. Use A260/A280 and A260/A230 to conclude about sample purity.
    a. For A260/A280: samples are accepted above 1.8 (ratio of ~2 is considered pure), lower than that it might indicate presence of protein, phenol or other contaminants.
    b. For A260/A230: values higher then A260/A280 indicate pure nuclei acid. Expected values are in the range of 2.0 - 2.2. values lower than this indicate contaminants which absorb at 230 nm.

RNA quality (Agilent Technologies, Ireland)

1. Prepare Nano gel matrix by placing 550 µl of the gel matrix in the receptacle of a spin filter. Centrifuge at 1.500 g for 10 minutes. Aliquot 65 µl of gel matrix intro 0.5 ml tubes and store them at 4 ºC.
2. Vortex Nano dye concentrate for 10 seconds and spin down.
3. Add 1 µl of Nano dye to 65 µl of gel matrix, vortex and spin tube for 10 minutes at 13.000 g.
4. Take a Nano chip and place it in the priming station.
5. Add 9 µl of gel – dye mix to the well marked G.
6. Set a timer for 30 seconds and close the priming station making sure the plunger of the syringe is at 1 ml position.
7. Press the plunger until it is held down by the clip and start timer.
8. Release the plunger and wait 5 seconds and confirm the plunger has moved back at least to the 0.3 ml mark.
9. Pipette 9 µl of the gel - dye mix in remaining wells marked G.
10. Load 5 µl of Nano marker into the well with the ladder symbol and then on all other 12 wells.
11. Pipette 1 µl of ladder into the well marked with the ladder symbol.
12. Pipette 1 µl of each sample into each of the 12 sample wells.
13. Vortex at 2.400 rpm in IKA vortex mixer for 60 seconds.
14. Decontaminate electrodes of Agilent Bioanalyzer using RNase ZAP and DNase free water.

15. Samples with a RNA integrity number (RIN) lower than 8 were not used for further experiments.

B.22.3 RealTime ready Custom Panel

1. Thaw the solutions and briefly spin vials in a microcentrifuge before opening. To compensate for pipetting losses prepare mixes with 10% overdosage (one extra sample for every 10).
2. Prepare a tube with the water and Probes Master as detailed in table below (PCR mix). Mix carefully by pipetting up and down. Do not vortex.
3. Pull the foil from the Custom Multiwell Plate
4. Pipette 9 µl of PCR mix into each well of the plate.
5. Add 1 µl of cDNA template (sample) into each well for a total volume of 10 µl.
6. When using negative controls, add 1 µl of untranscribed RNA to the corresponding wells.
7. Seal the well plate with sealing foil.
8. Centrifuge plate for 2 minutes at 1,500 g in a standard swing bucket centrifuge.
9. Transfer the plate to the LightCycler® 480 Instrument.
10. Table B.10 shows the Gene sequence.

Table B.7: List of genes and sequence of their primers.

Gene Name	Gene Symbol	Forward Sequence	Reverse Sequence
Prolyl-4-hydroxylase subunit alpha 1	P4HA1	TGAAATCGTCAAAGACCTAGCA	TGTTATTGGGTTTGAAATGGTG
Prolyl-4-hydroxylase subunit alpha 2	P4HA2	AAACTGGTGAAGCGGCTAAA	GAGAGGTTGGCGATAAAACCT
Procollagen-lysine,2-oxoglutarate 5-dioxygenase 1	PLOD1	GCTGCCGTATCTTCCAGAAC	TTTCAAACTTGAGCACGACCT
Procollagen-lysine,2-oxoglutarate 5-dioxygenase 2	PLOD2	AAGGACTTTAAAAATTTTGATTGAACA	GACTCAATGCTCCCCAGAAAT
Collagen type I alpha 1	COL1	AGGTGAAGCAGGCAAACCT	CTCGCCAGGGAAACCTCT
Collagen type III alpha 1	COL3	ACTGGAGCACGGGGTCTT	TCCTGGTTTCCCACTTTCAC
Scleraxis homolog A	SCXA	CCCAAACAGATCTGCACCTT	TCTTTCTGTCGCGGTCCTT
Tenomodulin	TNMD	TCCTCTGGCATCTGTTAGCC	TCCTTGCTTTGAGAGGACTGA
Tenascin C	TNC	CCTTGCTGTAGAGGTCGTCA	CCAACCTCAGACACGGCTA

Mohawk homeobox	MKX	GGATCCAATAAGGGTGAAAGC	TAAGGCCATAGCTGCGTTG
Decorin	DCN	GGCAAATTCCCGGATTAAAA	CAGGAAACTTGTGCAAGCAG
Biglycan	BGN	CTACAGCGCCATGTGTCCT	TCTTTGGGCACAGACTTCAG
Versican	VCAN	CTTCCCTCCCCCTGATAGC	CGATGGTTGTAGCCTCTTTAGG
Elastin	ELN	CACTGGGGTATCCCATCAAG	GTGGTGTAGGGCAGTCCATAG
Thrombospondin 4	THBS4	CTACCGCTGGTTCCTACAGC	GAGCCTTCATAAAATCGTACCC
Runt related transcription factor 2	RUNX2	TGCCACCTCTGACTTCTGC	AAAGGGCCCAGTTCTGAAG
Alkaline phosphatase, placental	ALPP	ACGCAGCTCATCTCCAACAT	CCCACCTTGGCTGTAGTCAT
Secreted phosphoprotein 1	SSP1	CGCAGACCTGACATCCAGTA	GGCTGTCCCAATCAGAAGG
Bone gamma carboxyglutamate protein	BGLAP	CCAGCCCTATGGATGTGG	TTTTCAGATTCCTCTTCTGGAGTT
Collagen type II alpha 1	COL2	CTGGTCCTCAAGGCAAAGTT	GAGGTCCAGGACGACCATC

Aggrecan	ACAN	GAACGACAGGACCATCGAA	AAAGTTGTCAGGCTGGTTGG
Smooth muscle alpha (α)-2 actin	ACTA2	CTGTTCCAGCCATCCTTCAT	TCATGATGCTGTTGTAGGTGGT
Serpin H1 precursor (heat shock protein 47)	SERPINH1	ATGCAGAAGAAGGCTGTTGC	CTTGTCAATGGCCTCAGTCA
Fatty acid binding protein 4	FABP4	CCTTTAAAAATACTGAGATTTCCTTCA	AGGACACCCCCATCTAAGGT
Transforming growth factor beta 1	TGFB1	ACTACTACGCCAAGGAGGTCAC	TGCTTGAACTTGTCATAGATTTCG
Early growth response 1	EGR1	AGCACCTGACCGCAGAGT	GGCAGTCGAGTGGTTTGG
Cartilage oligomeric matrix protein	COMP	GGAGATCGTGCAGACAATGA	GTCATCCGTGACCGTGTTC
Housekeeping genes			
Glyceraldehyde-3-phosphate dehydrogenase	GAPDH	AGCCACATCGCTCAGACAC	GCCCAATACGACCAAATCC

Actin beta	ACTB	TCCTCCCTGGAGAAGAGCTA	CGTGGATGCCACAGGACT
18S ribosomal RNA	RN18S1	GACGGACCAGAGCGAAAG	CGTCTTCGAACCTCCGACT

C. Results

C.1 Biological analysis

C.1.1 Nuclei area and nuclei elongation of hDFs at day 3, 7 and 14

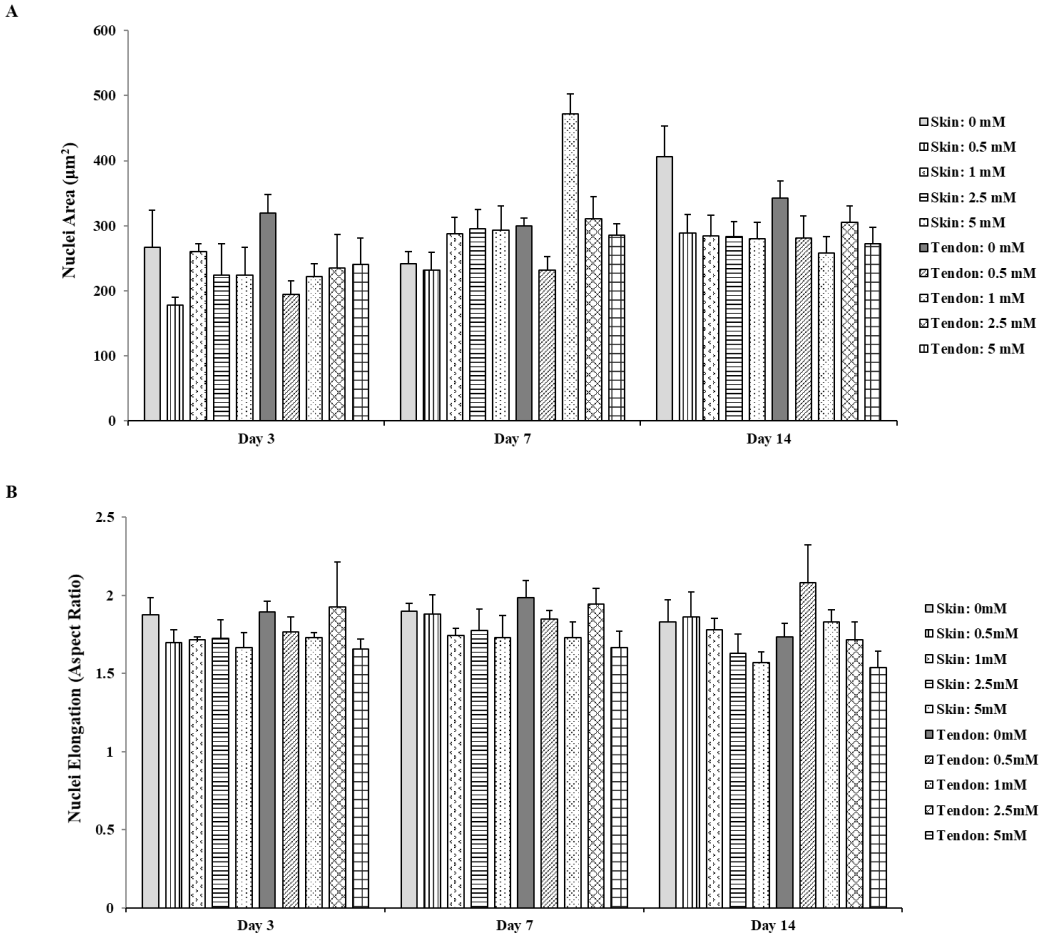

Figure C.1: Quantitative morphometric analysis of hDFs at day 3, 7 and 14 on non-crosslinked and crosslinked skin- and tendon- derived collagen sponges. **(A)** Quantitative morphometric analysis of nuclei area demonstrated that at day 14, cells that grew on non-crosslinked skin- and tendon- derived collagen sponges, had significantly higher ($p < 0.001$) nuclei area. **(B)** At day 14, tendon-derived collagen sponges crosslinked with 0.5 mM 4SG-PEG had significantly higher ($p<0.001$) nuclei elongation.

C.1.2 Nuclei area and nuclei elongation of hTCs at day 3, 7 and 14.

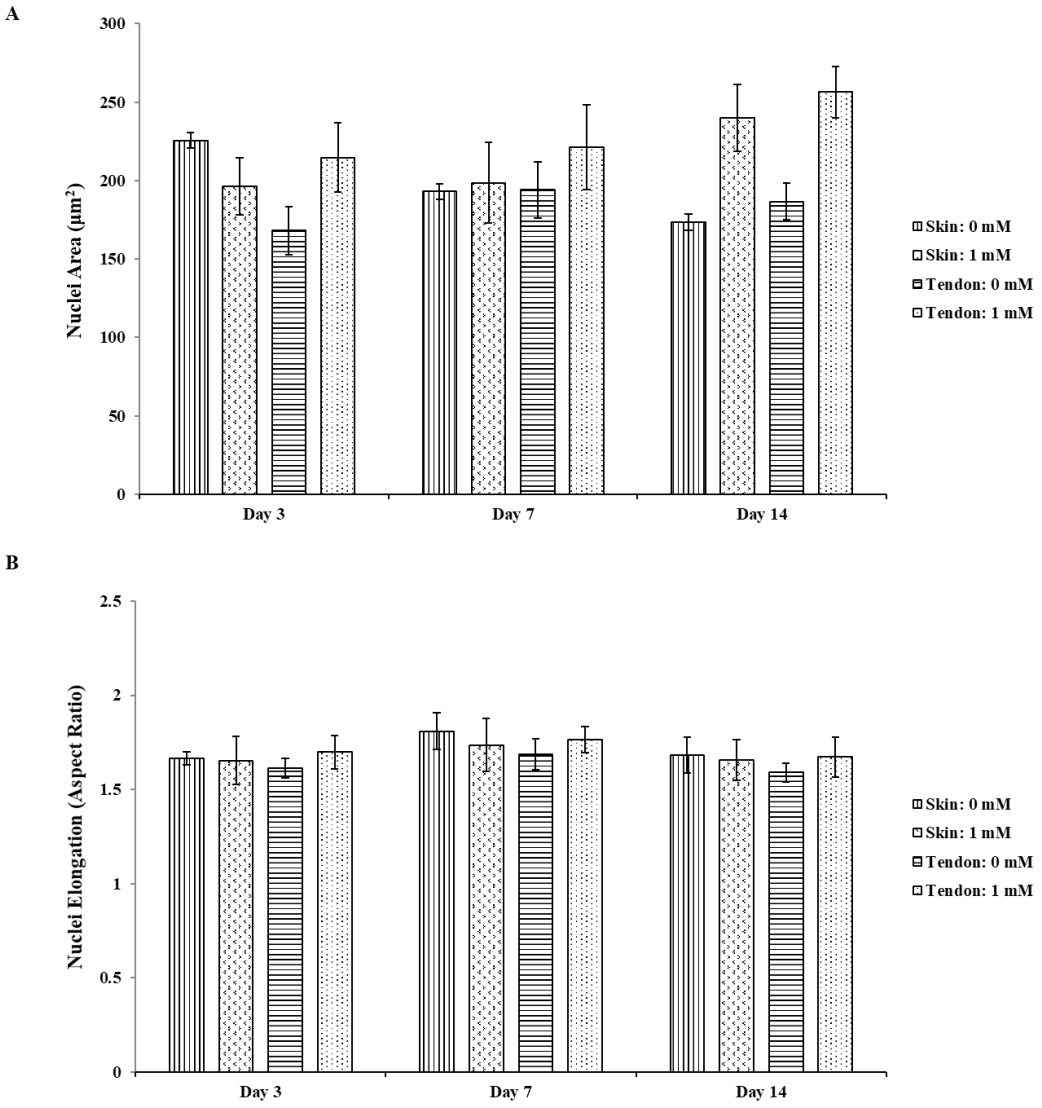

Figure C.2: Quantitative morphometric analysis of hTCs at day 3, 7 and 14 on non-crosslinked and crosslinked skin- and tendon- derived collagen sponges. **(A)** Nuclei area was significantly increased ($p < 0.001$) on crosslinked sponges by day 14. **(B)** At day 14, nuclei elongation was significantly lower ($p<0.001$) on tendon-derived collagen 0 mM 4SG-PEG sponges compared to skin-derived 0 mM 4SG-PEG collagen sponges at day 14.

C.1.3 Immunocytochemistry of hDFs at day 3, 7 and 14.

Extensive immunocytochemistry analysis of collagen type I, II, III, IV, V, VI, fibronectin, scleraxis, tenomodulin, aggrecan, osteocalcin and osteopontin deposition by hDFs was carried out at day 3, 7 and 14 on skin- and tendon-derived collagen type I sponges with 0 mM and 1 mM 4SG-PEG

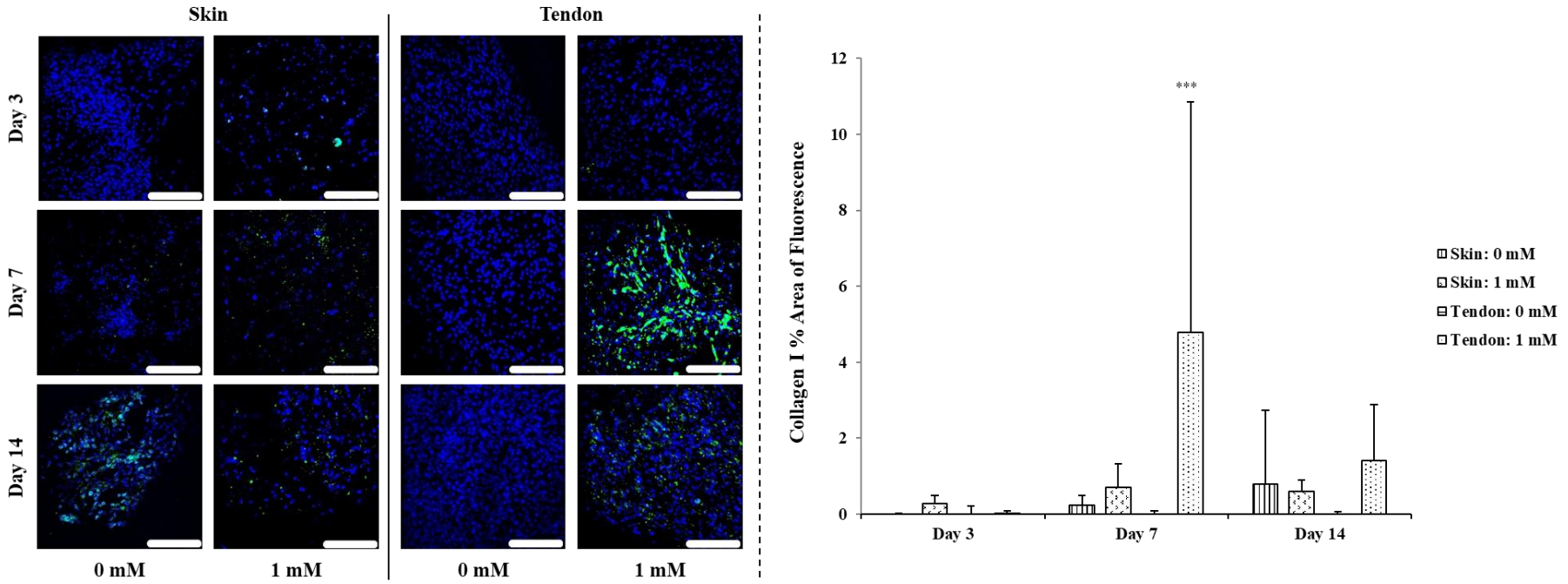

Figure C.3: hDFs deposited collagen type I on skin- and tendon-derived 0 mM and 1 mM 4SG-PEG collagen sponges for up to 14 days. Collagen type I is represented in green and DAPI is represented in blue. *** indicates statistically significant difference from all groups. Scalebar = 200 µm. N=3.

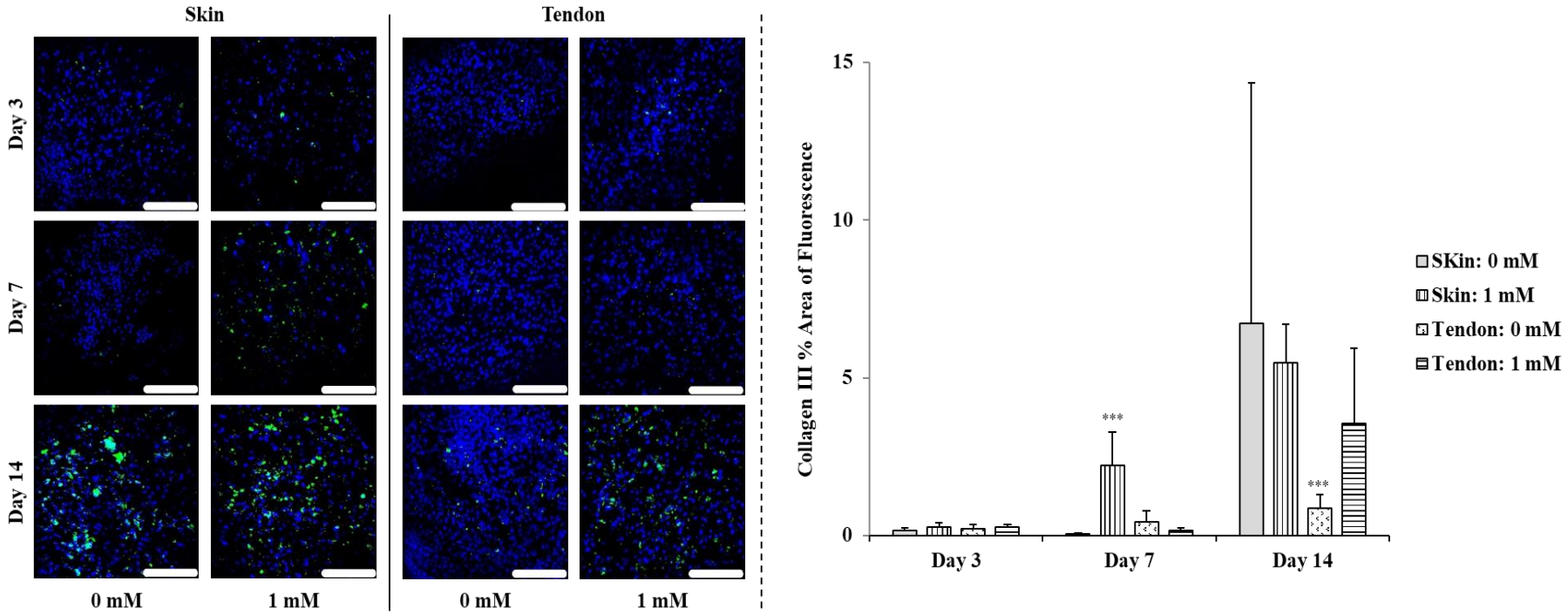

Figure C.4: hDFs deposited collagen type III on skin- and tendon-derived 0 mM and 1 mM 4SG-PEG collagen sponges for up to 14 days. Collagen type III is represented in green and DAPI is represented in blue. *** indicates statistically significant difference from all groups. Scalebar = 200 µm. N=3.

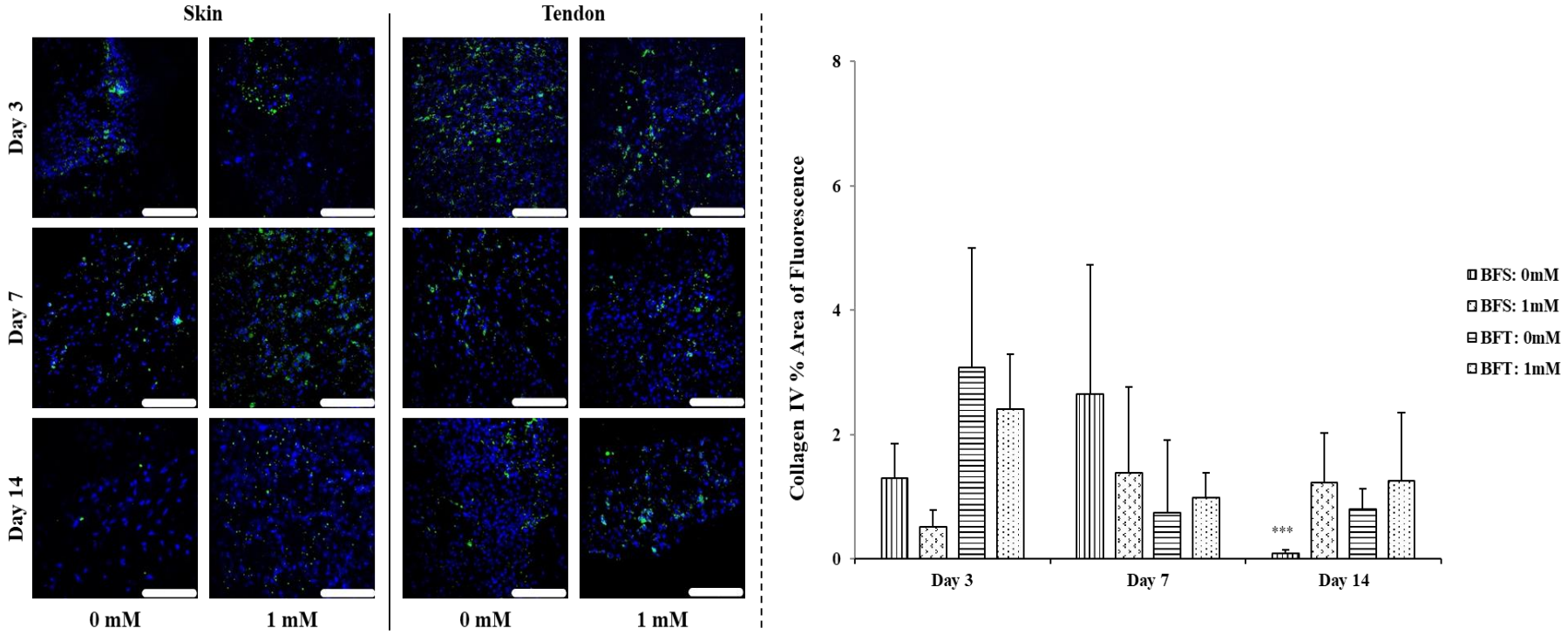

Figure C.5: hDFs deposited collagen type IV on skin- and tendon-derived 0 mM and 1 mM 4SG-PEG collagen sponges for up to 14 days. Collagen type IV is represented in green and DAPI is represented in blue. *** indicates statistically significant difference from all groups. Scalebar = 200 µm. N=3.

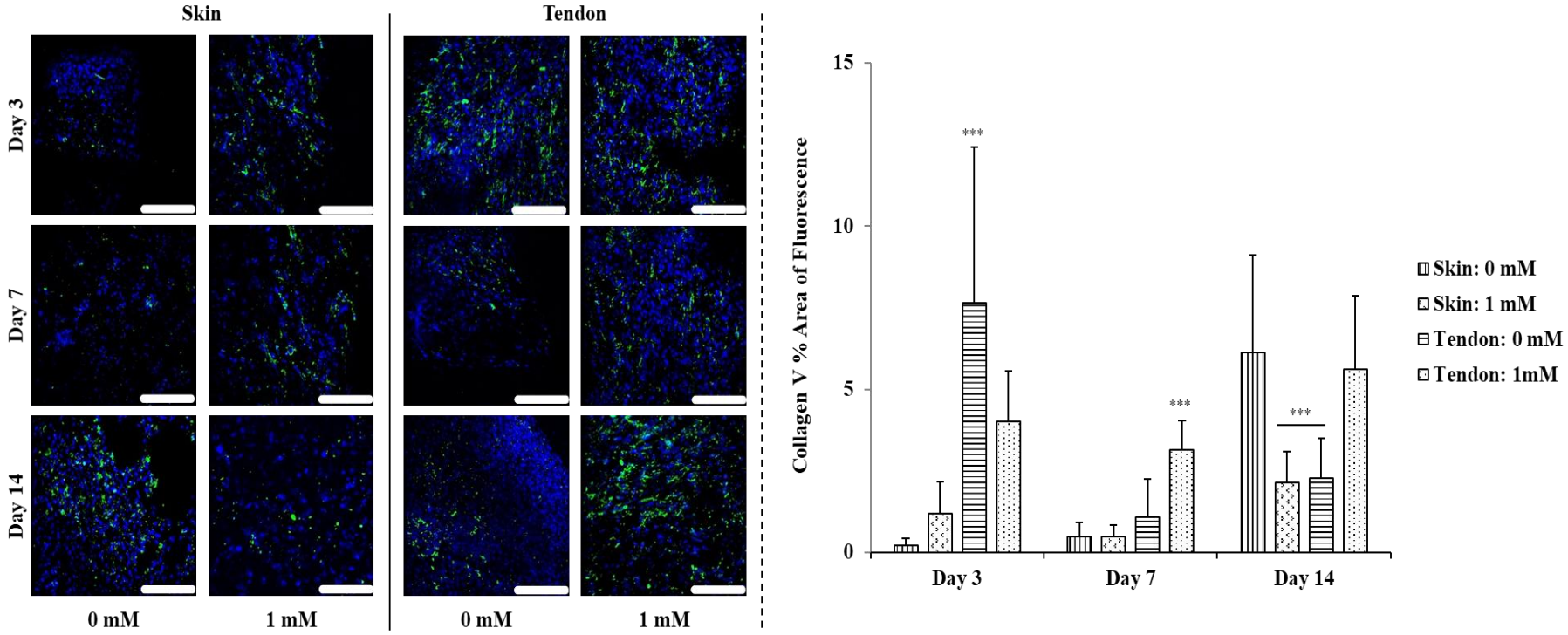

Figure C.6: hDFs deposited collagen type V on skin- and tendon-derived 0 mM and 1 mM 4SG-PEG collagen sponges for up to 14 days. Collagen type V is represented in green and DAPI is represented in blue. *** indicates statistically significant difference from all groups. Scalebar = 200 µm. N=3.

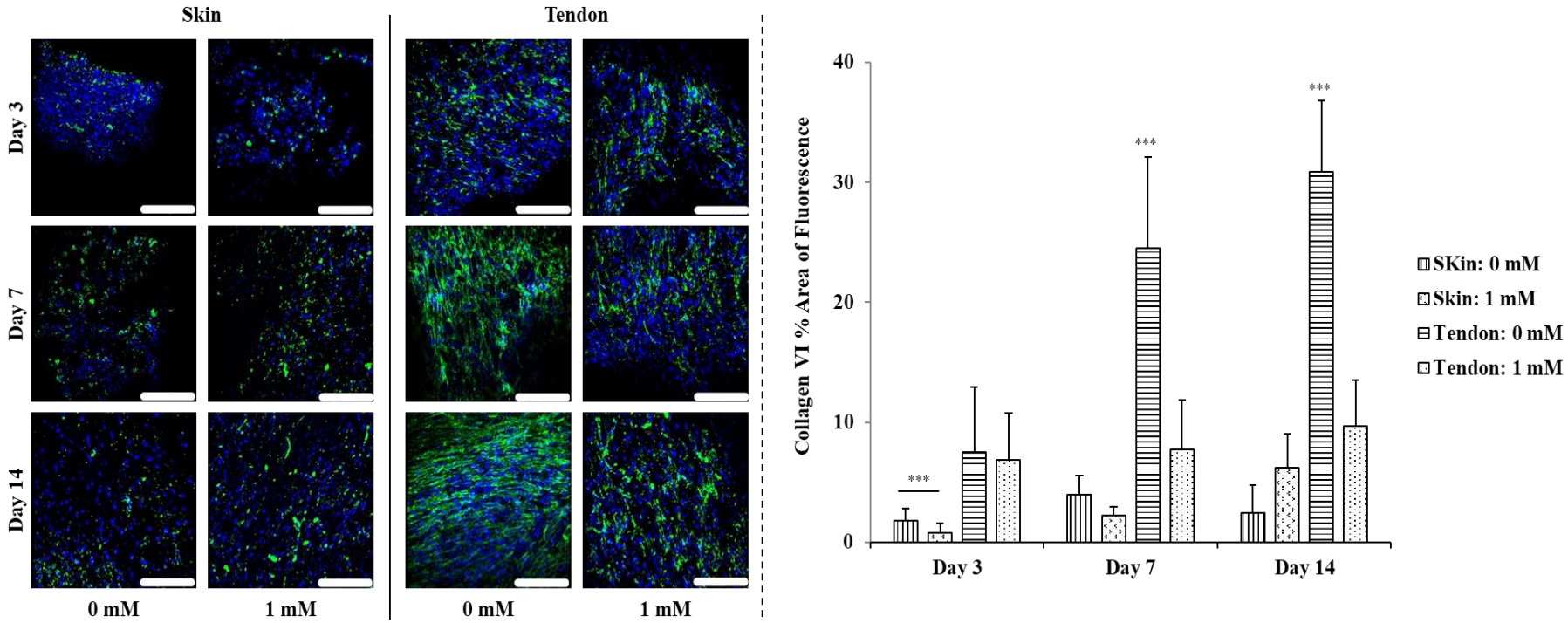

Figure C.7: hDFs deposited collagen type VI on skin- and tendon-derived 0 mM and 1 mM 4SG-PEG collagen sponges for up to 14 days. Collagen type VI is represented in green and DAPI is represented in blue. *** indicates statistically significant difference from all groups. Scalebar = 200 µm. N=3.

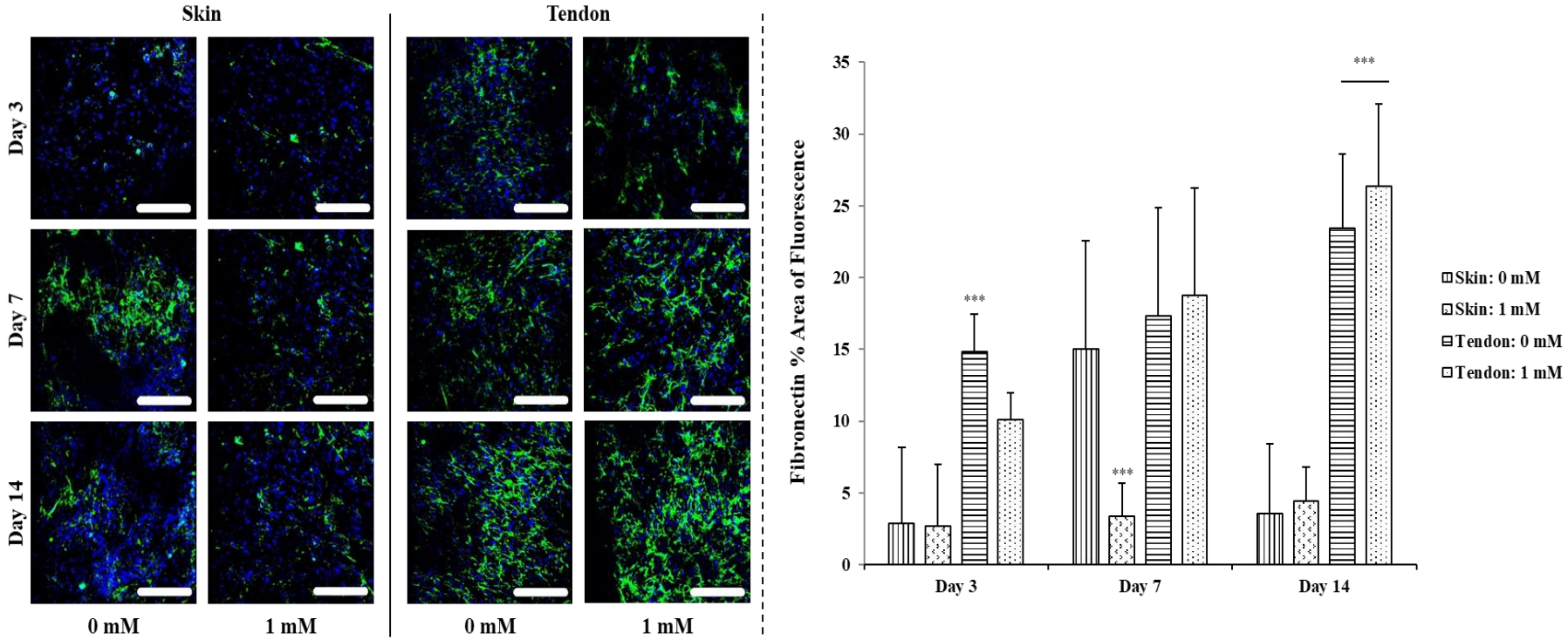

Figure C.8: hDFs deposited fibronectin on skin- and tendon-derived 0 mM and 1 mM 4SG-PEG collagen sponges for up to 14 days. Fibronectin is represented in green and DAPI is represented in blue. *** indicates statistically significant difference from all groups. Scalebar = 200 µm. N=3.

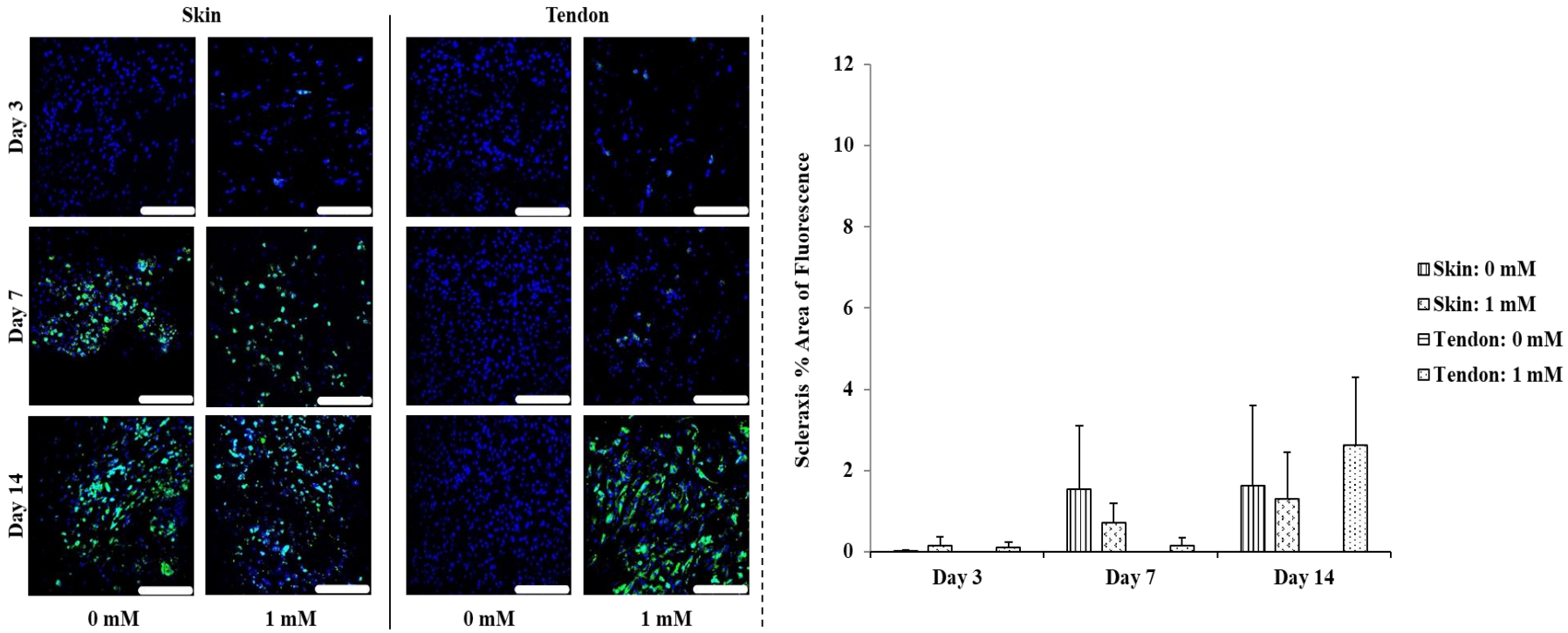

Figure C.9: hDFs deposited scleraxis on skin- and tendon-derived 0 mM and 1 mM 4SG-PEG collagen sponges for up to 14 days. Scleraxis is represented in green and DAPI is represented in blue. Scalebar = 200 µm. N=3.

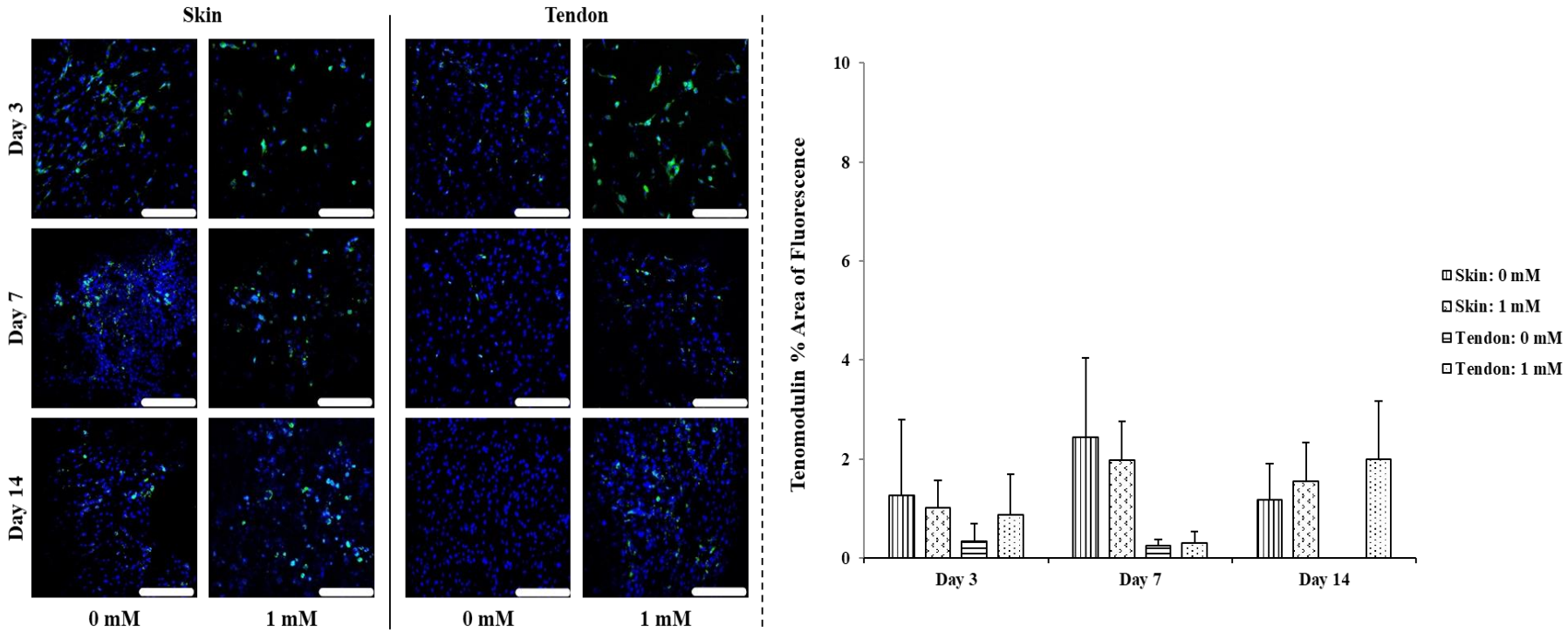

Figure C.10: hDFs deposited tenomodulin on skin- and tendon-derived 0 mM and 1 mM 4SG-PEG collagen sponges for up to 14 days. Tenomodulin is represented in green and DAPI is represented in blue. Scalebar = 200 µm. N=3.

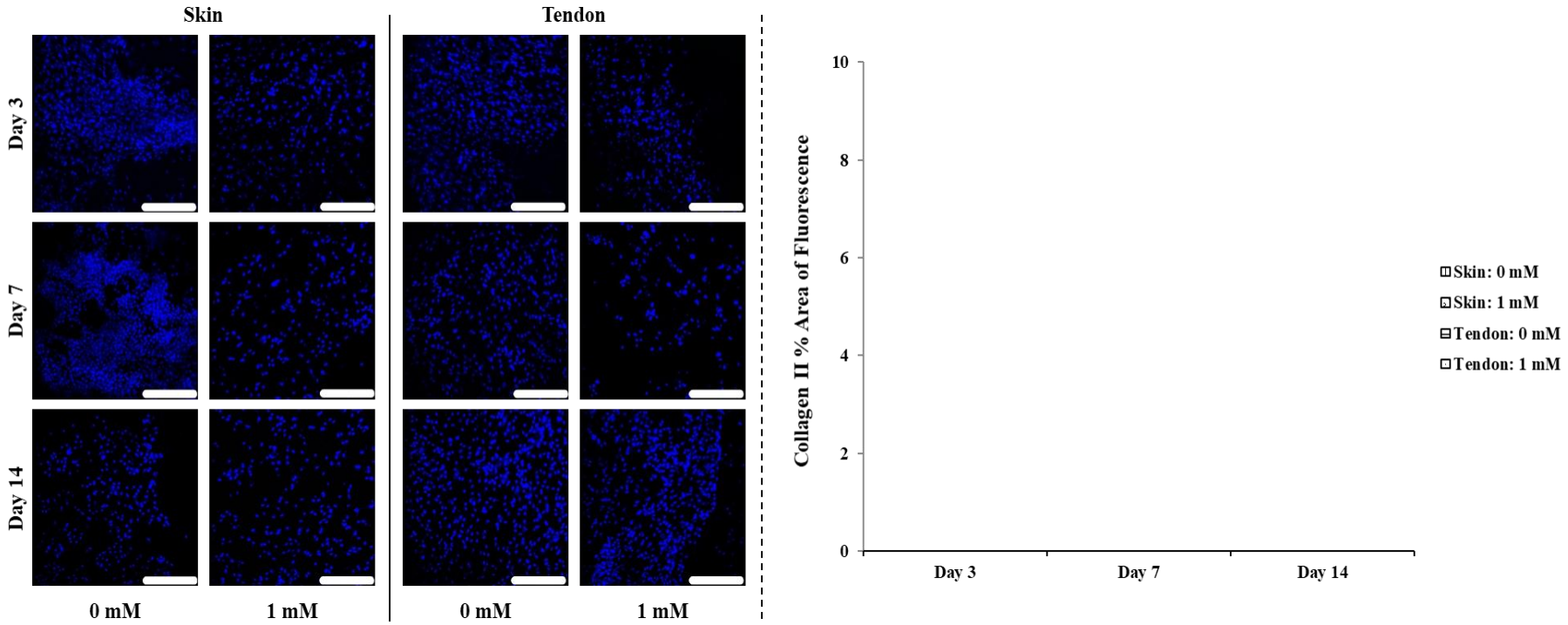

Figure C.11: hDFs deposited collagen type II on skin- and tendon-derived 0 mM and 1 mM 4SG-PEG collagen sponges for up to 14 days. Collagen type II deposition was not observed. Scalebar = 200 µm. N=3.

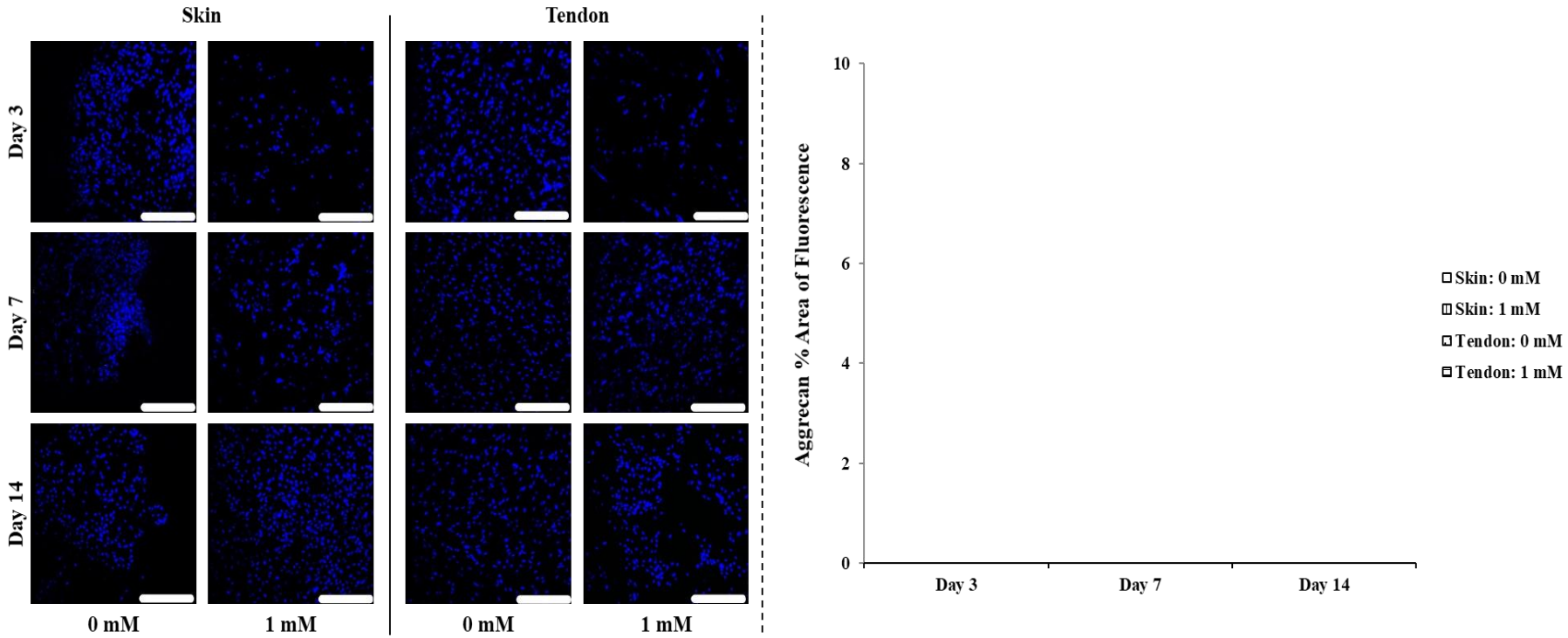

Figure C.12: hDFs deposited aggrecan on skin- and tendon-derived 0 mM and 1 mM 4SG-PEG collagen sponges for up to 14 days. Aggrecan deposition was not observed. Scalebar = 200 µm. N=3.

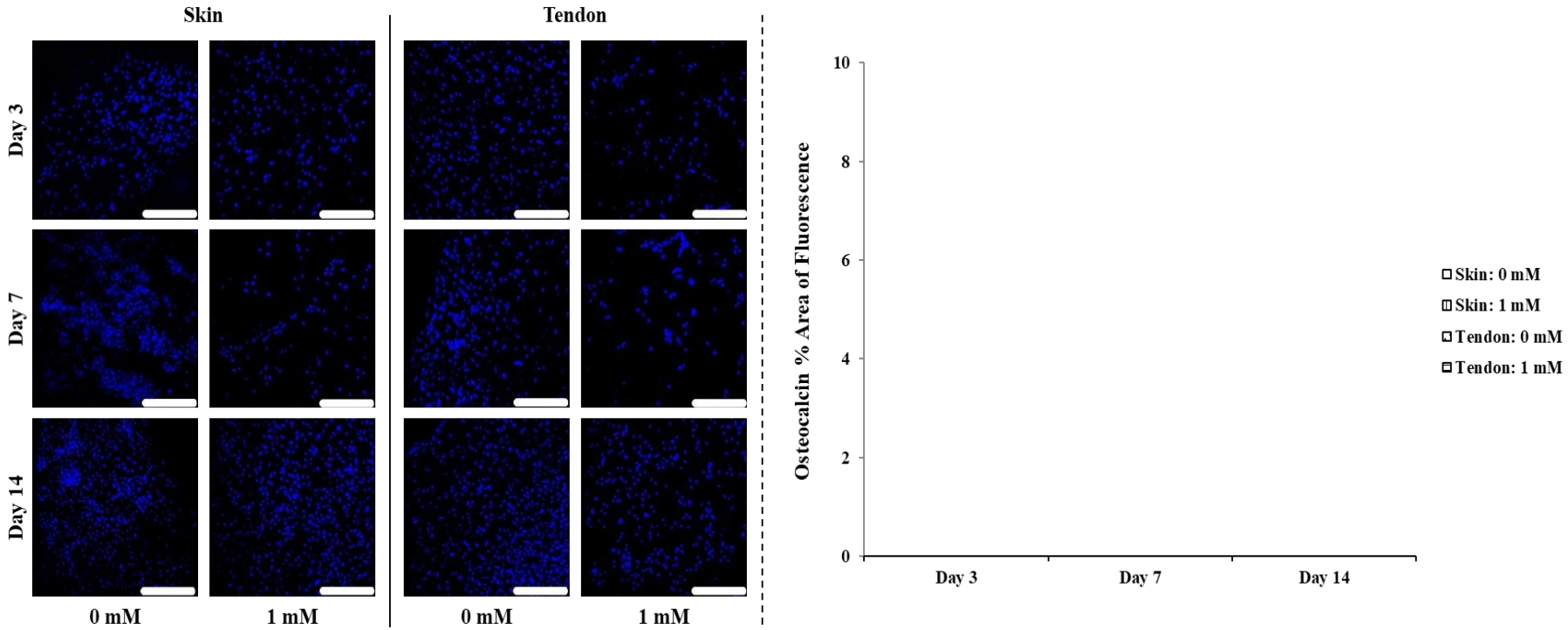

Figure C.13: hDFs deposited osteocalcin on skin- and tendon-derived 0 mM and 1 mM 4SG-PEG collagen sponges for up to 14 days. Osteocalcin deposition was not observed. Scalebar = 200 µm. N=3.

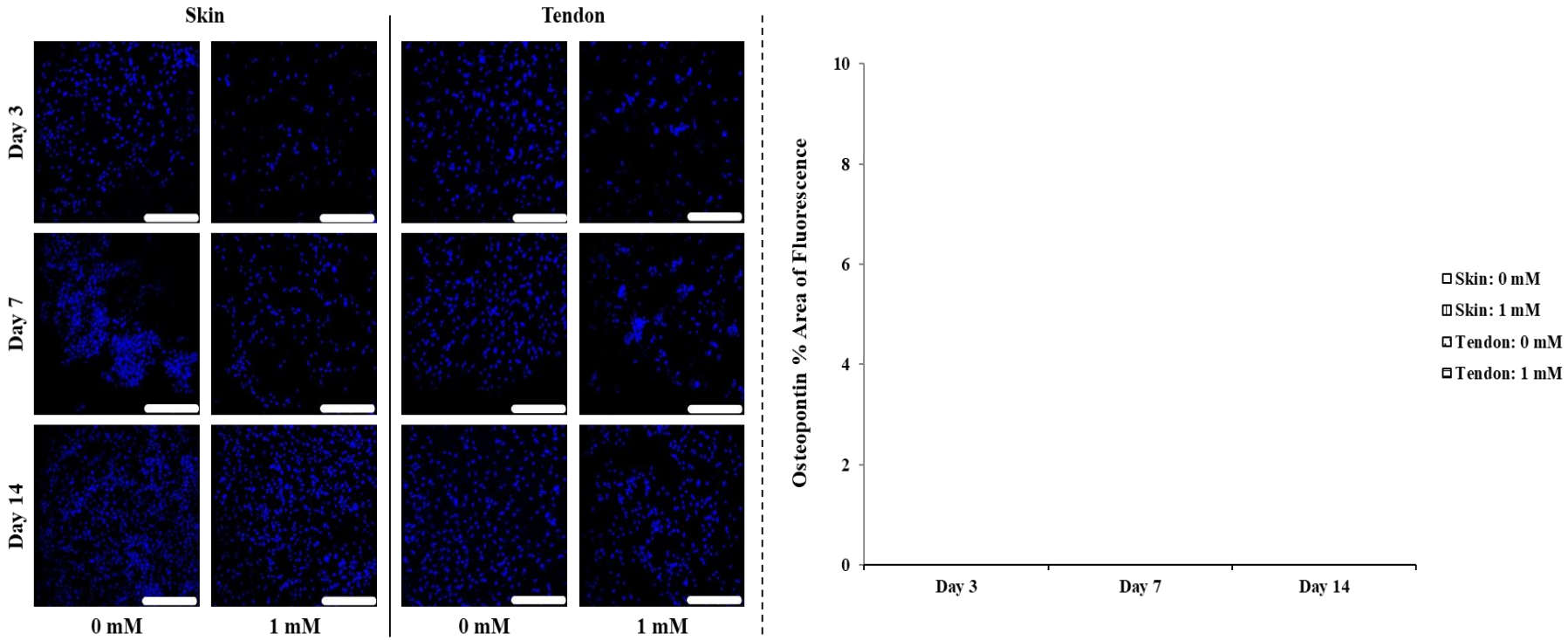

Figure C.14: hDFs deposited osteopontin on skin- and tendon-derived 0 mM and 1 mM 4SG-PEG collagen sponges for up to 14 days. Osteopontin deposition was not observed. Scalebar = 200 µm. N=3.

C.2 Mechanical properties

C.2.1 Stress-strain curves

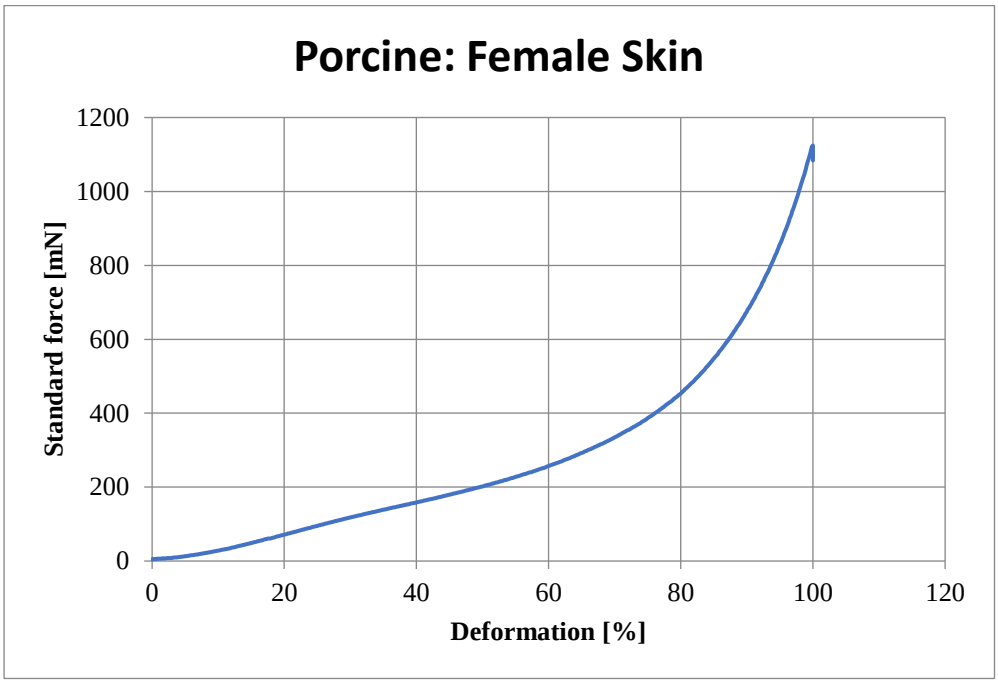

Figure C.15: Stress-strain curve for collagen sponge extracted from porcine female skin.

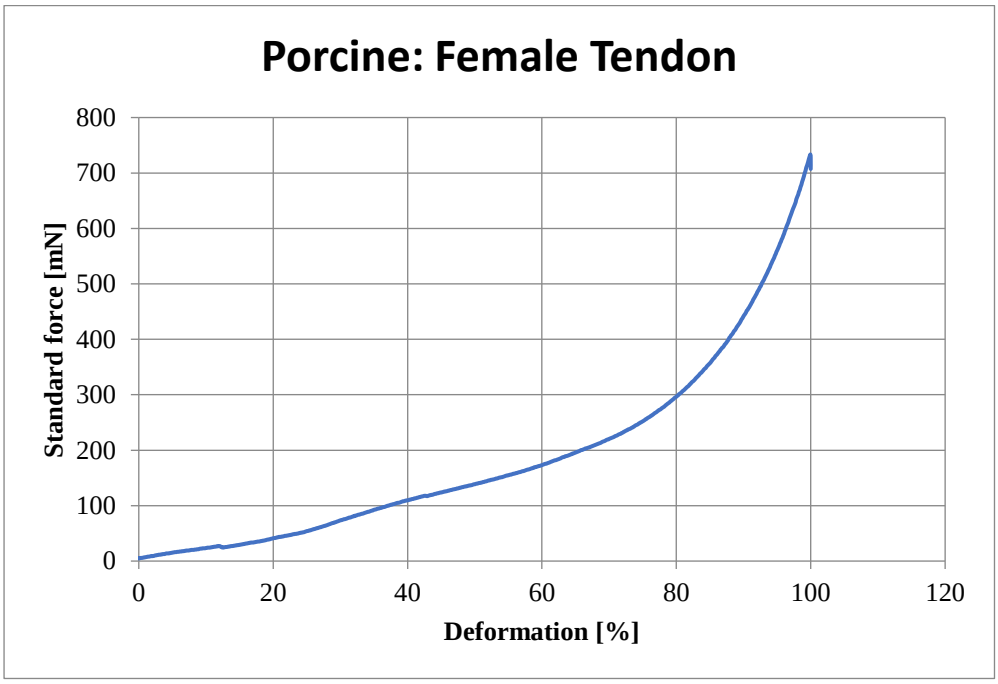

Figure C.16: Stress-strain curve for collagen sponge extracted from porcine female tendon.

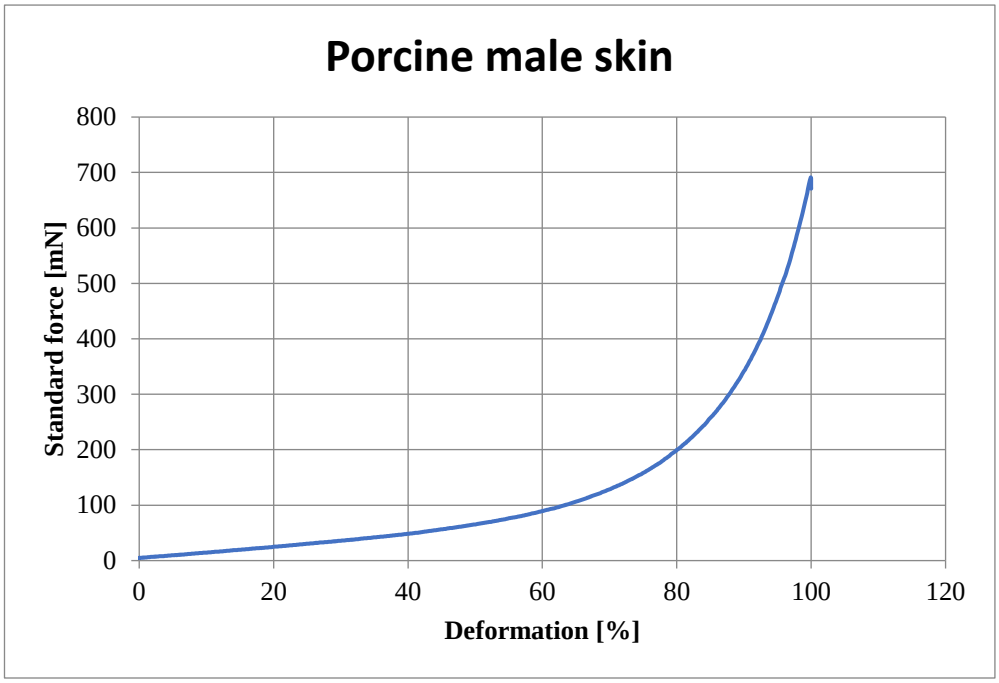

Figure C.17: Stress-strain curve for collagen sponge extracted from porcine male skin.

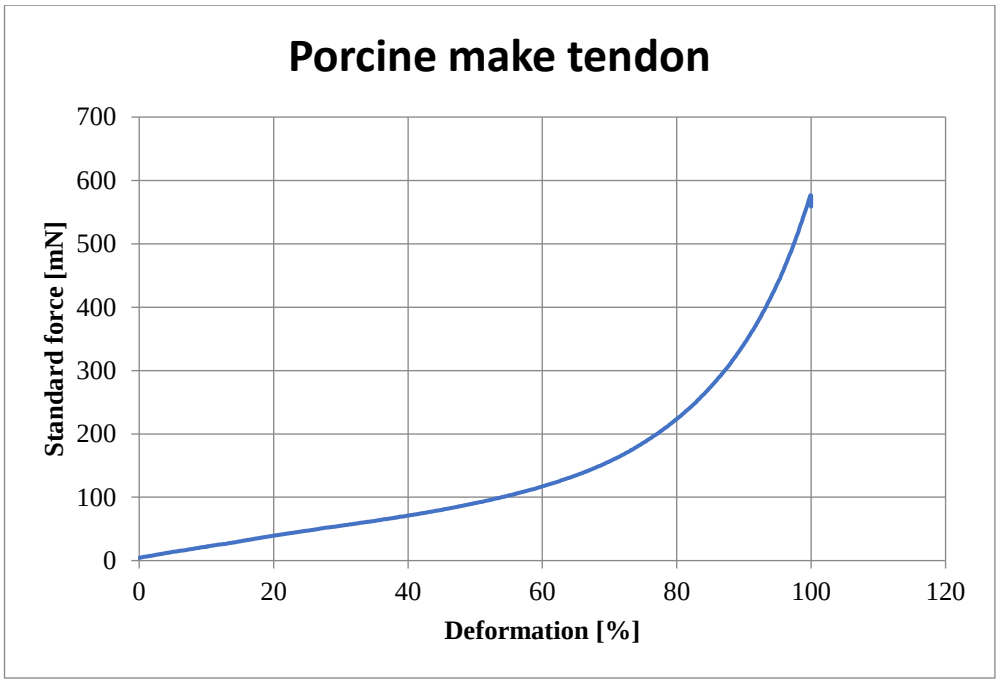

Figure C.18: Stress-strain curve for collagen sponge extracted from porcine male tendon.

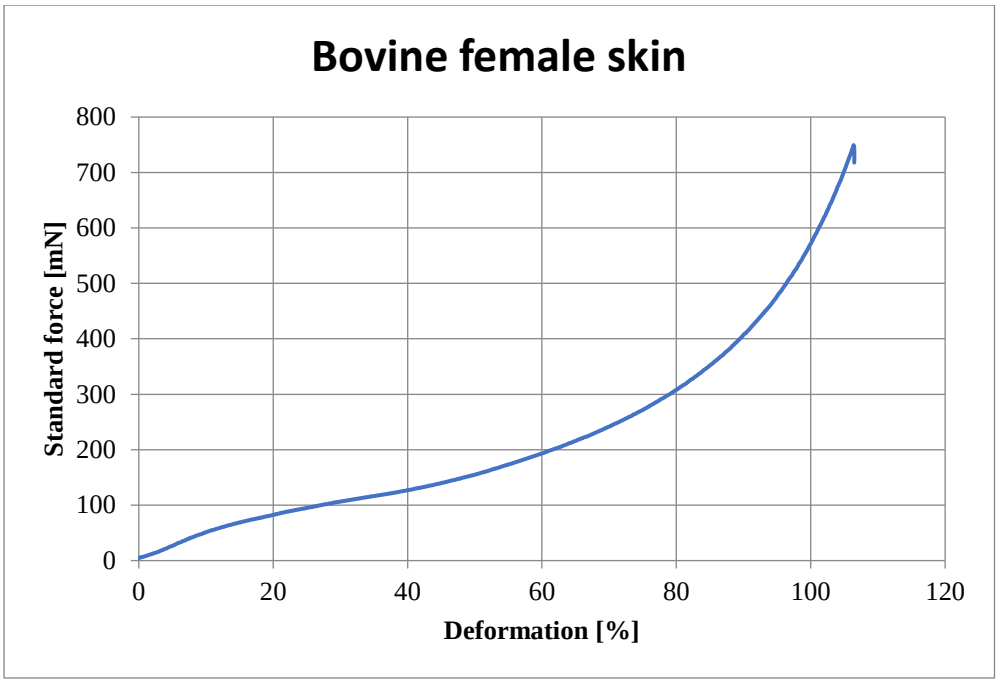

Figure C.19: Stress-strain curve for collagen sponge extracted from bovine female skin.

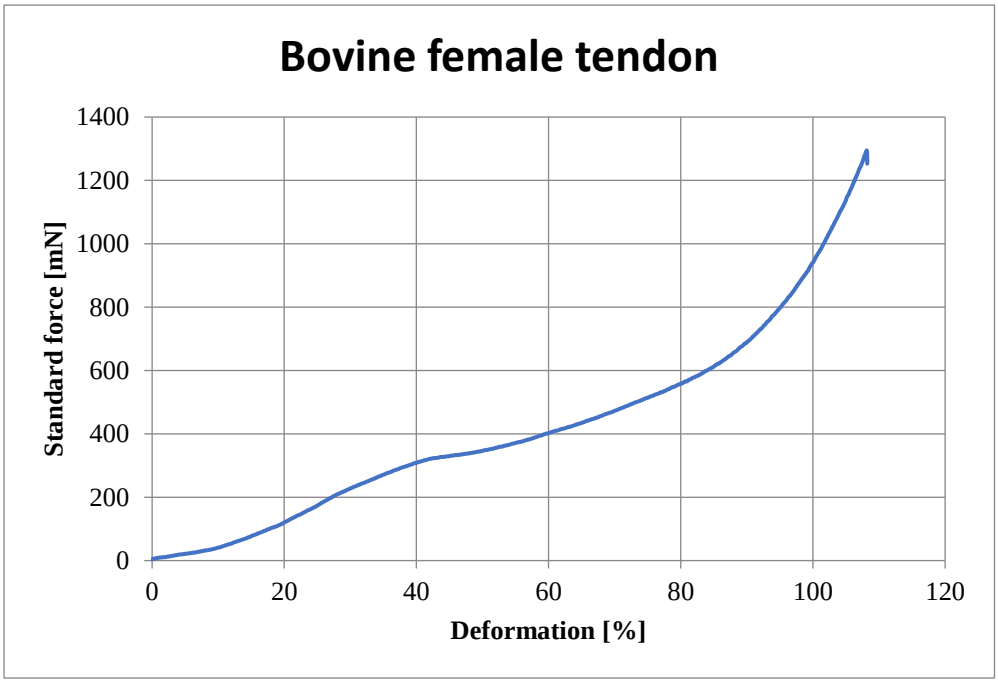

Figure C.20: Stress-strain curve for collagen sponge extracted from bovine female skin.

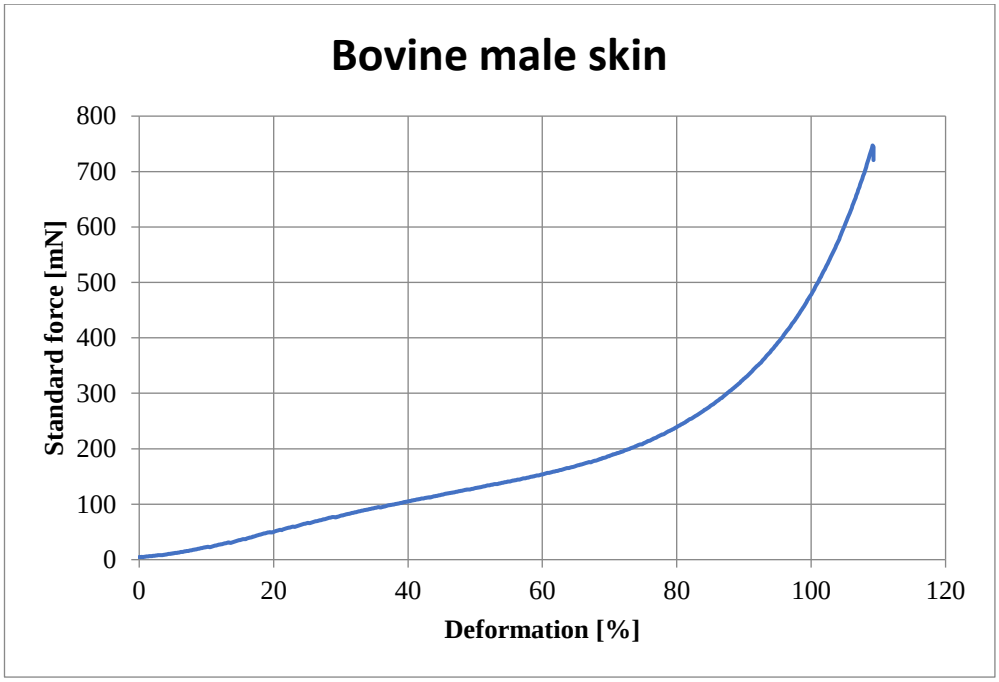

Figure C.21: Stress-strain curve for collagen sponge extracted from bovine male skin.

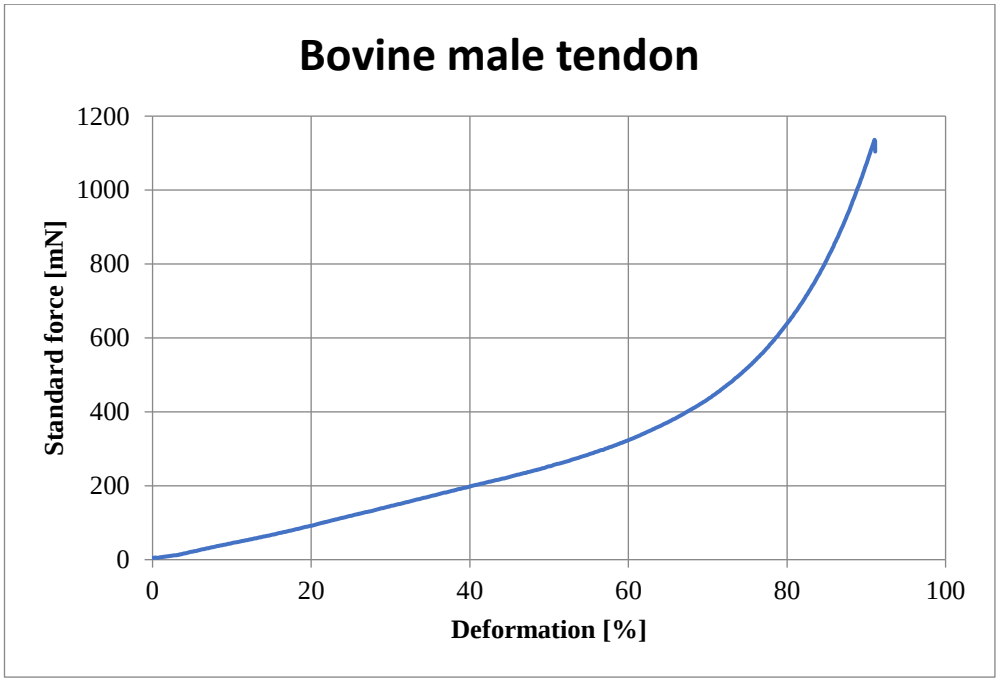

Figure C.22: Stress-strain curve for collagen sponge extracted from bovine male tendon.

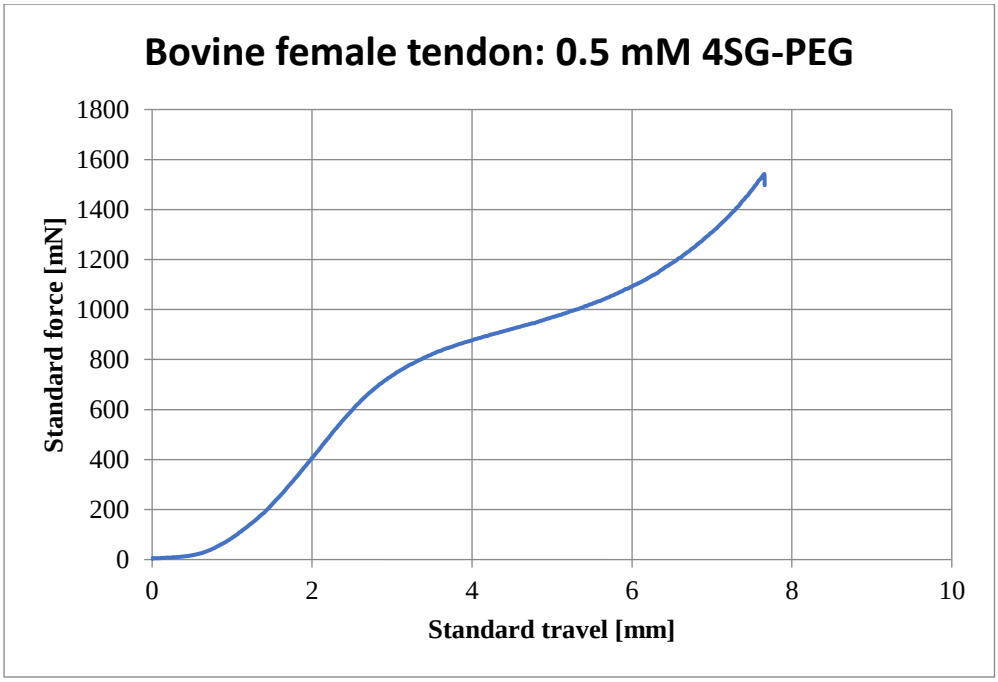

Figure C.23: Stress-strain curve for collagen sponge extracted from bovine female tendon, cross-linked with 0.5 mM 4SG-PEG.

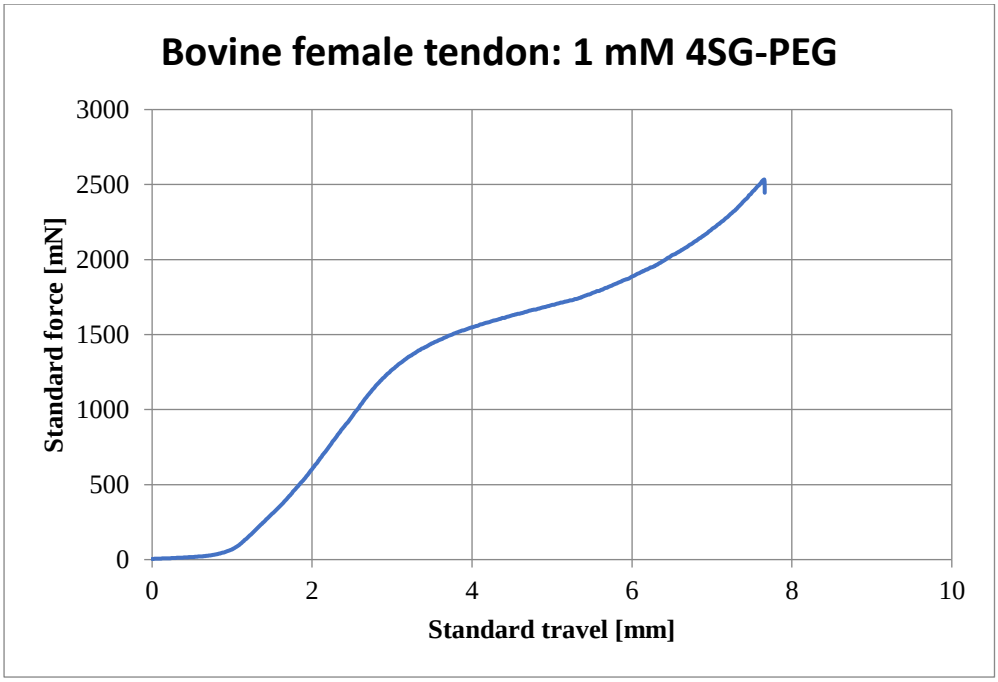

Figure C.24: Stress-strain curve for collagen sponge extracted from bovine female tendon, cross-linked with 1 mM 4SG-PEG.

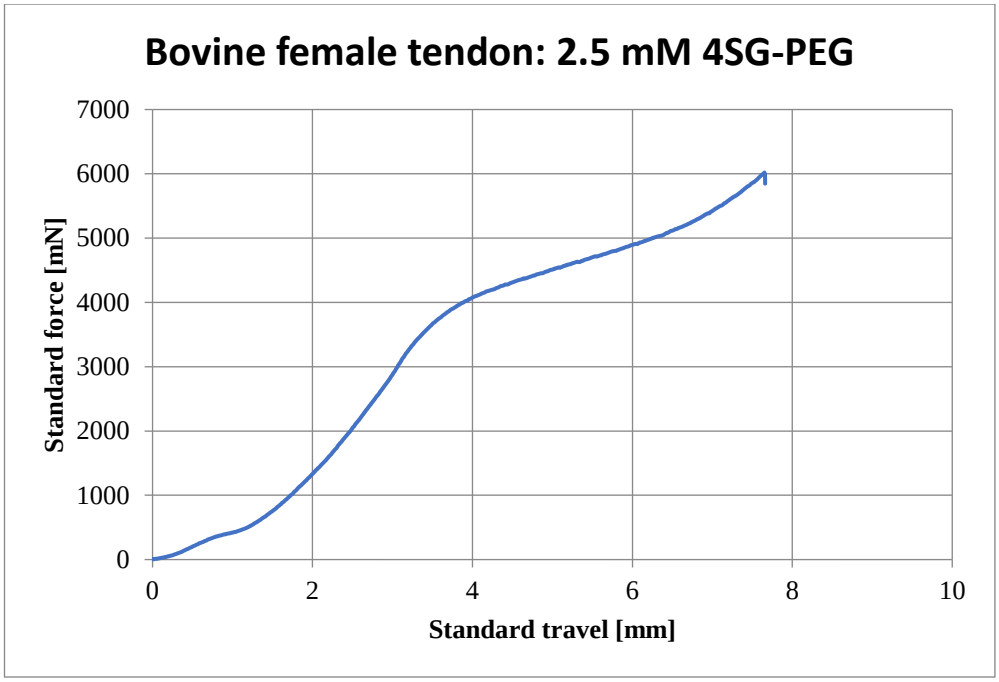

Figure C.25: Stress-strain curve for collagen sponge extracted from bovine female tendon, cross-linked with 2.5 mM 4SG-PEG.

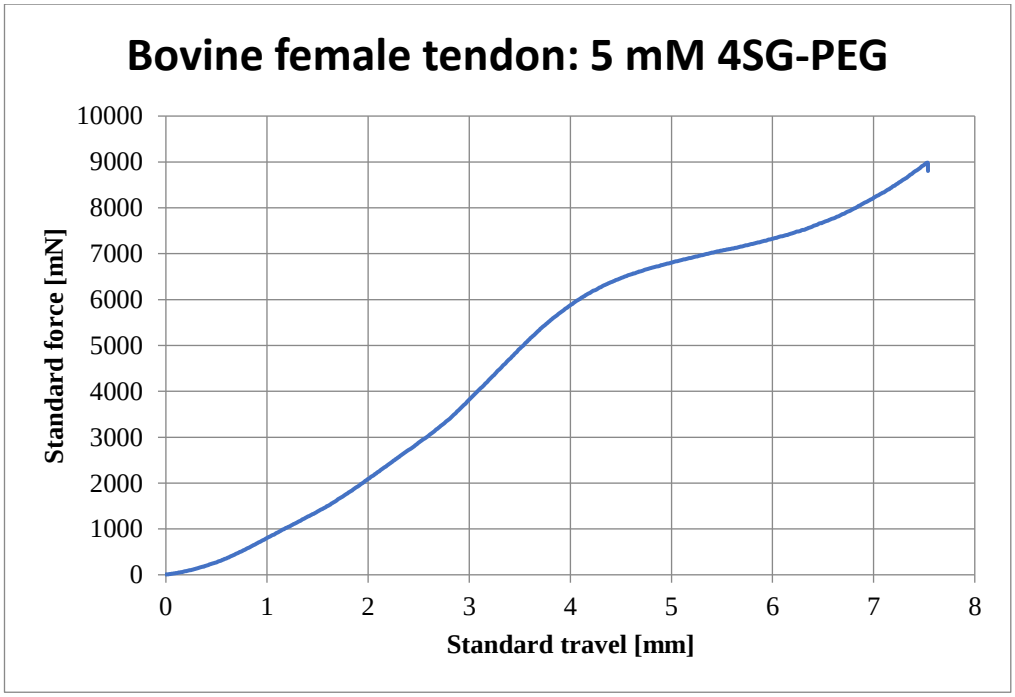

Figure C.26: Stress-strain curve for collagen sponge extracted from bovine female tendon, cross-linked with 5 mM 4SG-PEG.

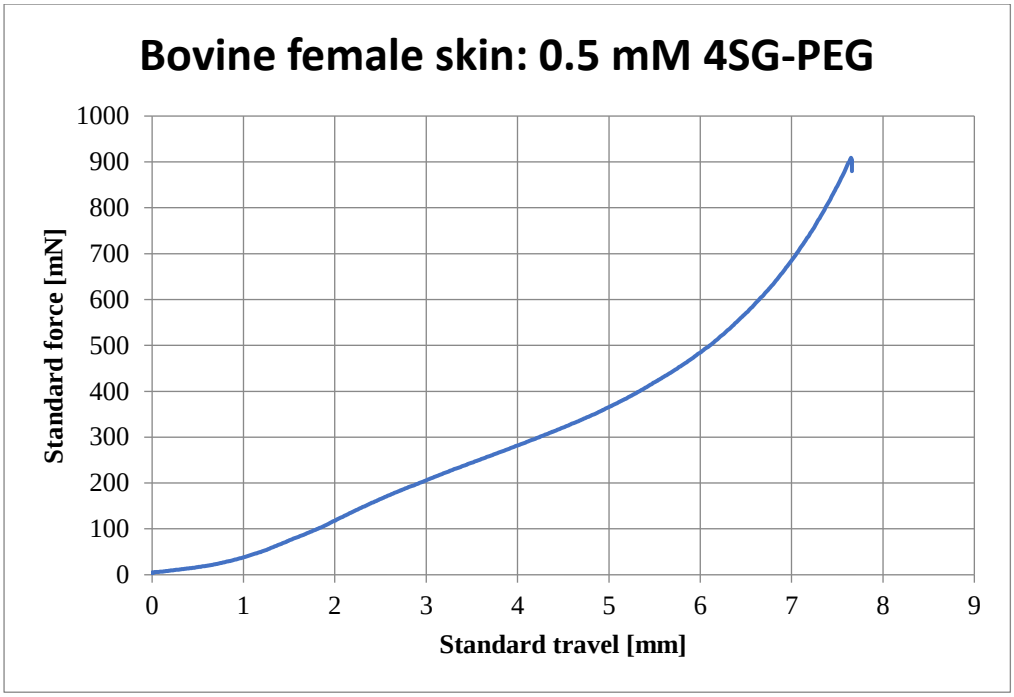

Figure C.27: Stress-strain curve for collagen sponge extracted from bovine female skin, cross-linked with 0.5 mM 4SG-PEG.

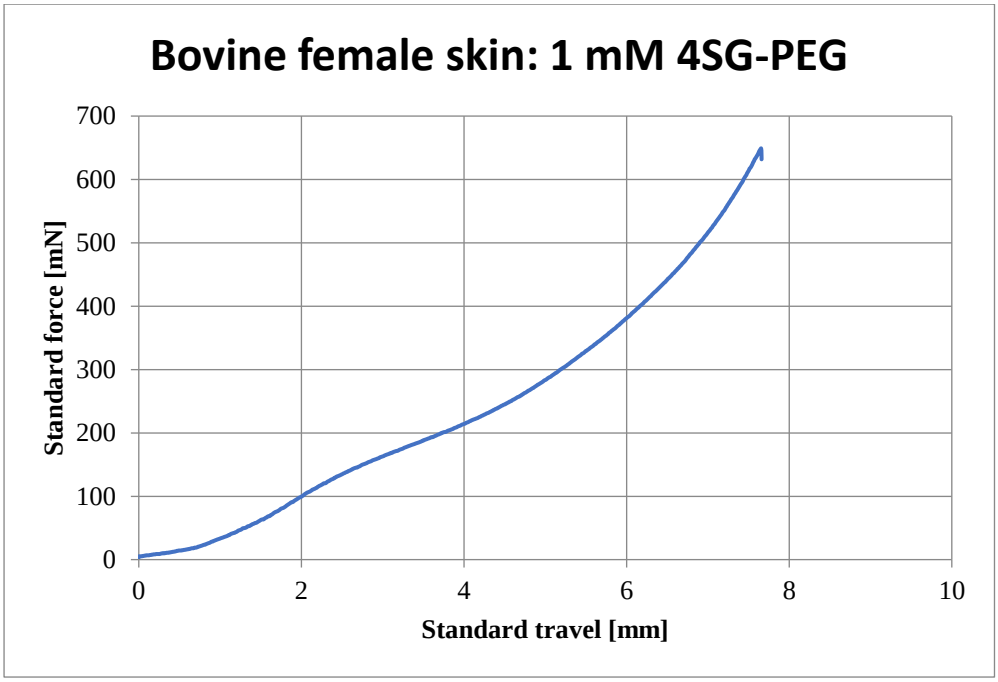

Figure C.28: Stress-strain curve for collagen sponge extracted from bovine female skin, cross-linked with 1 mM 4SG-PEG.

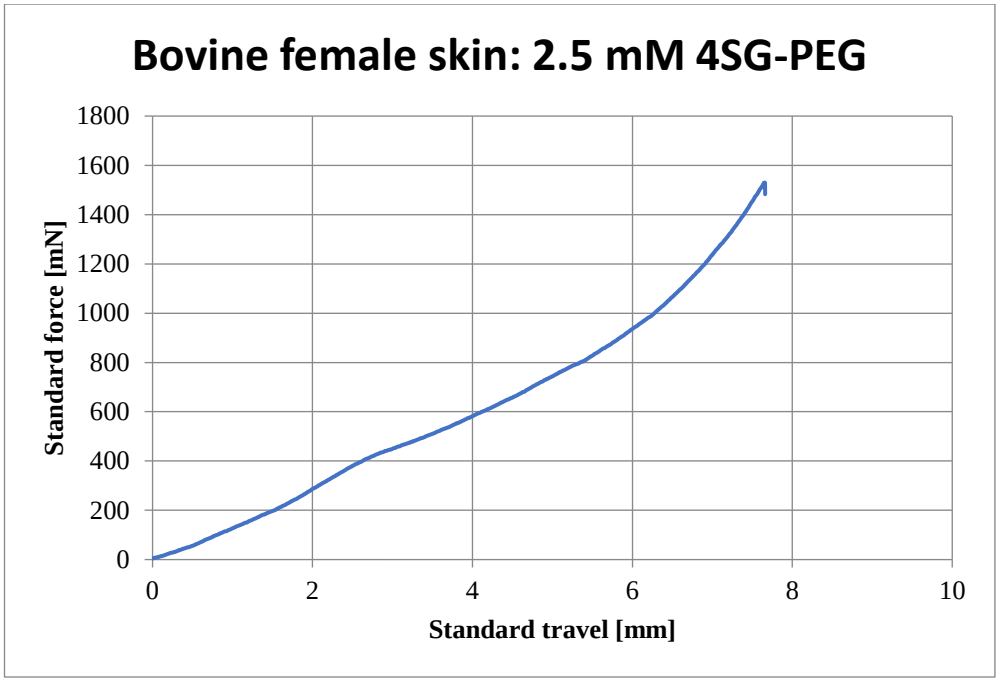

Figure C.29: Stress-strain curve for collagen sponge extracted from bovine female skin, cross-linked with 2.5 mM 4SG-PEG.

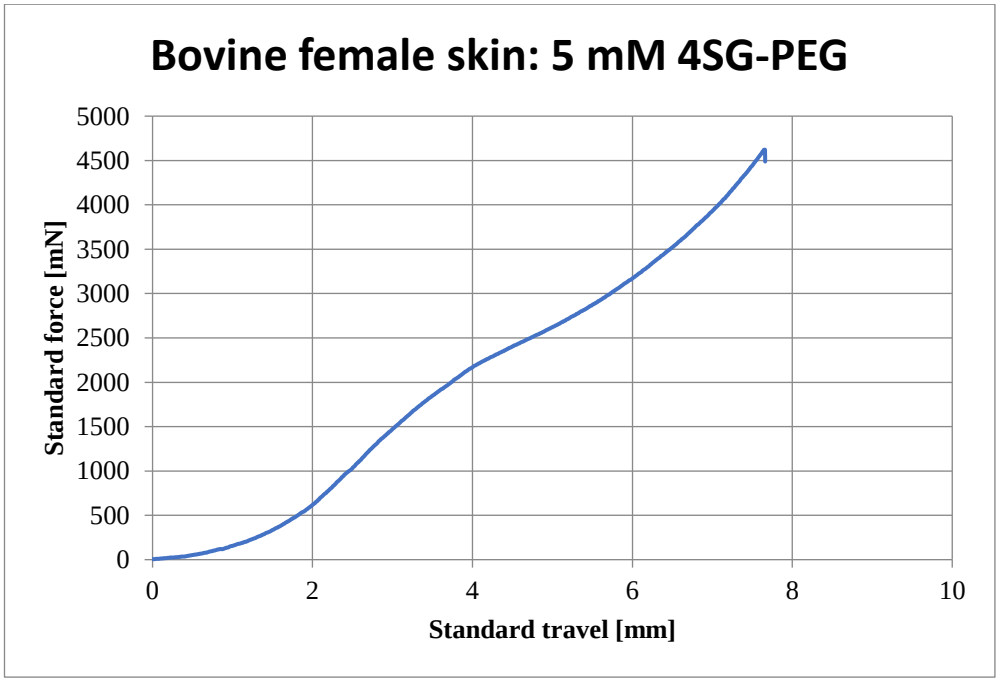

Figure C.30: Stress-strain curve for collagen sponge extracted from bovine female skin, cross-linked with 5 mM 4SG-PEG.

D. Research outputs

D.1 Publications

Accepted manuscripts

1. **Anna Sorushanova**, Ioannis Skoufos, Athina Tzora, Anne Maria Mullen, Dimitrios Zeugolis. The influence of animal species, gender and tissue on the structural, biophysical, biochemical and biological properties of collagen sponges. Journal of Materials Science: Materials in Medicine. 2021 Jan 21;32(1):12. doi: 10.1007/s10856-020-06485-4. PMID: 33475864; PMCID: PMC7819930.
2. Alex Lomas, Christina Ryan, **Anna Sorushanova**, Naledi Shologu, Aikaterini Sideri, Vassiliki Tsioli, G.C. Fthenakis, Athina Tzora, Ioannis Skoufos, Leo Quinlan, Gearóid O'laighin, Anne Marie Mullen, Jack Kelly, Stephen Kearns, Manus Biggs, Abhay Pandit, Dimitrios Zeugolis. The past, present and future in scaffold-based tendon treatments. Advanced Drug Delivery. 2015 Apr;84:257-77. doi: 10.1016/j.addr.2014.11.022. Epub 2014 Dec 10. PMID: 25499820.
3. Christina Ryan, **Anna Sorushanova**, Alex Lomas, Anne Maria Mullen, Abhay Pandit, Dimitrios Zeugolis. Glycosaminoglycans in tendon physiology, pathophysiology and therapy. Bioconjugate chemistry. 2015 Jul 15;26(7):1237-51. doi: 10.1021/acs.bioconjchem.5b00091. Epub 2015 May 26. PMID: 25970130.
4. Mohammad Sanami, Zvi Shtein, India Sweeney, **Anna Sorushanova**, Amit Rivkin, Mohsen Miraftab, Oded Shoseyov, Colm O'Dowd, Anne Marie Mullen, Abhay Pandit, Dimitrios Zeugolis. Biophysical and biological characterisation of collagen / resilin composites. Biomedical Materials. 2015 Nov 6;10(6):065005. doi: 10.1088/1748-6041/10/6/065005. PMID: 26541078.
5. Mohammad Sanami, India Sweeney, Zvi Shtein, Sigal Meirovich, **Anna Sorushanova**, Anne Maria Mullen, Mohsen Miraftab, Oded Shoseyov, Colm O'Dowd, Abhay Pandit, Dimitrios Zeugolis. The influence of poly (ethylene glycol) ether tetrasuccinimidyl glutarate on the structural, physical, and biological properties of collagen fibers. Journal of Biomedical Materials Research Part B: Applied Biomaterials. 2016 Jul;104(5):914-22. doi: 10.1002/jbm.b.33445. Epub 2015 May 7. PMID: 25952265.

6. Dilip Thomas, Diana Gaspar, **Anna Sorushanova**, Gesmi Milcovich, Kyriakos Spanoudes, Anne Maria Mullen, Timothy O'Brien, Abhay Pandit, Dimitrios I Zeugolis. Scaffold and scaffold-free self-assembled systems in regenerative medicine. Biotechnology and Bioengineering. 2016 Jun;113(6):1155-63. doi: 10.1002/bit.25869. Epub 2015 Nov 10. PMID: 26498484.
7. Arwa Bazaid, Sabine Neumayer, **Anna Sorushanova**, Jill Guyonnet, Dimitrios Zeugolis, Brian Rodriguez. Non-destructive determination of collagen fibril width in extruded collagen fibres by piezoresponse force microscopy. Biomedical Physics & Engineering Express. 2017 Sept; 3(5):055004 DOI:10.1088/2057-1976/aa85ec.
8. **Anna Sorushanova**, Luis Delgado, Zhuning Wu, Naledi Shologu, Aniket Kshirsagar, Rufus Raghunath, Anne Marie Mullen, Yves Bayon, Abhay Pandit, Michael Raghunath, Dimitrios Zeugolis. The Collagen Suprafamily: From Biosynthesis to Advanced Biomaterial Development. Advanced Materials. 2019 Jan;31(1):e1801651. doi: 10.1002/adma.201801651. Epub 2018 Aug 20. PMID: 30126066.

Submitted manuscripts

1. **Anna Sorushanova**, Dimitrios Tsiapalis, Ioannis Skoufos, Athina Tzora, Una FitzGerald, Anne Maria Mullen, Dimitrios I. Zeugolis. Tissue origin matters: Maintenance of tenogenic phenotype on tendon and not skin collagen derived devices. MedComm - Biomaterials and Applications. 2022.

D.2 Book chapters

1. **Anna Sorushanova**, João Coentro, A Pandit, Dimitrios Zeugolis, Michael Raghunath. Collagen: Materials analysis and implant uses. Comprehensive Biomaterials. 2011 Oct; DOI:10.1016/B978-0-08-055294-1.00074-X.

D.3 Conference presentations

1. **Sorushanova, A**., Sweeny, I., Skoufos, I., Mullen, A.M., Pandit, A., Zeugolis, D. Optimally stabilised starPEG collagen fibres increase stability and maintain tenocyte function. **Poster presentation** at European Materials Research

Society 2014 Fall Meeting (E-MRS 2014), 15th to 18th of September 2014, Warsaw, Poland.

2. **Sorushanova, A**., Sweeny, I., Pandit, A., Zeugolis, D.I. Mechanical stabilisation of non-toxic collagen fibres for tendon repair. **Poster Presentation** at ESB 2014 Meeting, 31 August to 3 September 2014, Liverpool, UK.
3. Fthenakis, G.C., Tsioli, V., Sideri, K.I., Gouletsou, P.G., Barbagianni, M.S., Vasileiou, N.G.C., Gelasakis, A., Gougoulis, D.A., Spanos, S.A., Kormpou, F.F., Mpalatsouka, M.C.N, Balasi, E.G., Naskou, M.C., Skoufos, I., Tzora, A., Sweeney I.R., **Sorushanova, A**., Zeugolis D.I. Regenerative medicine prototypes in a sheep model. Biomaterials for Achilles tendon repair. **Podium Presentation** at 3rd Greek Congress for Farm Animal Medicine, 2nd to 4th of May 2014, Ioannina, Greece.
4. Sideri, K.I., Tsioli, V., Gelasakis, A., Gougoulis, D.A., Spanos, S.A., Vasileiou, N.G.C., Kormpou, F.F., Mpalatsouka, M.C.N, Gouletsou, P.G., Barbagianni, M.S., Balasi, E.G., Naskou, M.C., Skoufos, I., Tzora, A., Sweeney I.R., **Sorushanova, A**., Zeugolis D.I., Fthenakis, G.C. Biomaterial assessment in sheep Achilles tendon model. Experimental design and clinical mobility analysis. **Podium Presentation** at 3rd Greek Congress for Farm Animal Medicine, 2nd to 4th of May 2014, Ioannina, Greece.
5. Tsioli, V., Sideri, K.I., Kormpou, F.F., Gelasakis, A., Gougoulis, D.A., Vasileiou, N.G.C., Balasi, E.G., Gouletsou, P.G., Mpalatsouka, M.C.N, Naskou, M.C., Spanos, S.A., Barbagianni, M.S., Skoufos, I., Tzora, A., Sweeney I.R., **Sorushanova, A**., Zeugolis D.I., Fthenakis, G.C. Biomaterial assessment in sheep Achilles tendon model. Biomechanical analysis. **Podium Presentation** at 3rd Greek Congress for Farm Animal Medicine, 2nd to 4th of May 2014, Ioannina, Greece.
6. Vasileiou, N.G.C., Sideri, K.I., Tsioli, V., Balasi, E.G., Gouletsou, P.G., Kormpou, F.F., Mpalatsouka, M.C.N, Naskou, M.C., Spanos, S.A., Barbagianni, M.S., Gelasakis, A., Gougoulis, D.A., Skoufos, I., Tzora, A., Sweeney I.R., **Sorushanova, A**., Zeugolis D.I., Fthenakis, G.C. Biomaterial assessment in sheep Achilles tendon model. Functional analysis. **Podium**

Presentation at 3rd Greek Congress for Farm Animal Medicine, 2nd to 4th of May 2014, Ioannina, Greece.

7. **Sorushanova, A**., Mullen, A.M., Pandit, A., Zeugolis, D. Biophysical, biochemical and biological properties of nano-textured collagen fibres. **Oral presentation** at Matrix Biology Ireland 2015, 2nd to 4th December 2015, Dublin, Ireland.
8. **Sorushanova, A**., Mullen, A.M., Pandit, A., Zeugolis, D. Biophysical, biochemical and biological properties of nano-textured collagen fibres. **Oral presentation** at Bioengineering in Ireland 2016. 22nd to 23rd January 2016, Galway, Ireland.
9. **Sorushanova, A**., Mullen, A.M., Pandit, A., Zeugolis, D. Biophysical, biochemical and biological properties of nano-textured collagen fibres. **Oral presentation** at European Materials Research Society 2016, 2nd to 6th May 2016, Lille, France.
10. **Sorushanova, A**., Skoufos, I., Tzora, A., Mullen, A.M., Zeugolis, D. Collagen characterisation for biomedical applications. **Oral presentation** at Matrix Biology Ireland 2016, 16th to 18th November 2016, Galway, Ireland.
11. **Sorushanova, A**., Mullen, A.M., Pandit, A., Zeugolis, D. Biophysical, biochemical and biological properties of nano-textured collagen fibres. **Poster presentation** at World Biomaterials Congress 2016, 17th to 22nd May 2016, Montreal, Canada.
12. **Sorushanova, A**., Mullen, A.M., Pandit, A., Zeugolis, D. Biophysical, biochemical and biological properties of nano-textured collagen fibres. **Poster presentation** at TERMIS 2016, 28th June to 1st July 2016, Uppsala, Sweden.
13. **Sorushanova, A**., Skoufos, I., Tzora, A., A., Mullen, A.M., Zeugolis, D. Collagen characterisation for biomedical applications. **Poster presentation** at TERMIS 2017, 26th June to 30th June 2017, Davos, Switzerland.